

APPENDIX A: SUBSTANTIVE FILE DOCUMENTS

Blue Ribbon Commission on America's Nuclear Future. (2012). Report to the Secretary of Energy. PDF.

https://www.energy.gov/sites/default/files/2013/04/f0/brc_finalreport_jan2012.pdf.

California Coastal Commission. (2001). W15a Revised Findings for Application No. E-00-014. Attached.

California Coastal Commission. (2015). Tu14a Adopted Findings: Regular Permit for Application No. 9-15-0228. Attached.

Coastal Environments, Inc. (2022a). Coastal Hazard Analysis at San Onofre Nuclear Generating Station – Part 2: Geological Hazards. Attached

Coastal Environments, Inc. (2022b). Coastal Hazard Analysis at San Onofre Nuclear Generating Station – Part 3: Tsunami Hazards. Attached

Coastal Environments, Inc. (2022c). Coastal Hazards Analysis at San Onofre Nuclear Generating Station – Part 1: Coastal Hazards

Hinkle, D. (2011). Third-party Review – Slope Evaluation, Independent Fuel Storage Installation. Attached [included as an attachment to Coastal Environments 2022a].

Jennings, C.W., and W.A. Bryant. (2010). Fault activity map of California. California Geological Survey. Sacramento, California, 2010.

<https://maps.conservation.ca.gov/cgs/fam/>

Kuhn, G.G. (2005). Paleoseismic features as indicators of earthquake hazards in North Coastal San Diego County, California, USA. *Engineering Geology*.

<https://fddocuments.net/document/paleoseismic-features-as-indicators-of-earthquake-features-as-indicators-of.html?page=5>

Nuclear Regulatory Commission. (2021). Interim Storage Partners, Issuance of Materials License SNM-2515, WCS Consolidated Interim Storage Facility ISFSI. Webpage. <https://www.nrc.gov/docs/ML2118/ML21188A096.html>.

Ocean Protection Council. (2018). State of California Sea Level Rise Guidance. http://www.opc.ca.gov/webmaster/ftp/pdf/agenda_items/20180314/Item3_Exhibit-A OPC SLR Guidance-rd3.pdf

Petersen, M.D., Bryant, W.A., Cramer, C.H., Cao, T., Reichle, M.S., Frankel, A.D., Leinkaemper., J.J., McCrory, P.A., and Schwarta, D.P. (1996). *Probabilistic seismic hazard assessment for the state of California*. California Division of Mines and Geology, Sacramento, CA 1996.

<https://pubs.usgs.gov/of/1996/0706/report.pdf>

Powers, M.B., Rubin D.K. (2022). State-Fed fight heats up over building private nuclear disposal sites. *Engineering News-Record*. <https://www.enr.com/articles/54456-state-fed-fight-heats-up-over-building-private-nuclear-disposal-sites>. (attached)

E-00-014-A2 (Southern California Edison)

Southern California Edison. (2022a). SCE Responses to August 18 Questions from Coastal Commission Staff. Attached.

State of California. (2009). Tsunami Inundation Map for Emergency Planning – San Onofre Bluff Quadrangle.

https://www.conservation.ca.gov/cgs/Documents/Publications/Tsunami-Maps/Tsunami_Inundation_SanOnofreBluff_Quad_SanDiego.pdf

CALIFORNIA COASTAL COMMISSION

45 FREMONT, SUITE 2000
SAN FRANCISCO, CA 94105-2219
VOICE AND TDD (415) 904-5200



RECORD PACKET COPY

W15a

Date Filed: 10/11/00
Hearing held
and continued: 11/14/00
Staff: DAC/MJJ-SF
Hearing Date: 03/13/01
Commission
Action: Conditional
Approval (10-0)

Revised Findings: 05/24/01
Hearing Date on
Revised Findings: 06/13/01

REVISED FINDINGS

APPLICATION FILE NO.:

E-00-014

APPLICANTS:

**Southern California Edison Company, San
Diego Gas and Electric Company, City of
Anaheim, and City of Riverside**

PROJECT DESCRIPTION:

Construction of San Onofre Nuclear Generating Station
(SONGS) Units 2 and 3 temporary spent nuclear fuel
storage facility.

PROJECT LOCATION:

5000 Pacific Coast Highway (unincorporated San Diego
County). (Exhibit 1)

**SUBSTANTIVE FILE
DOCUMENTS:**

See Appendix B

**COMMISSIONERS ON THE
PREVAILING SIDE:**

Dettloff, Estolano, Hart, Kruer, McCoy, Orr, Weinstein,
Rose, Woolley, Wan

STAFF NOTE

On November 14, 2000, the Coastal Commission held a public hearing on this application but continued consideration of it, requesting that staff analyze the geologic stability of the proposed project, including, but not limited to, potential hazards from earthquakes, tsunamis, and landslides, consistent with Section 30253 of the Coastal Act. At a public hearing on March 13, 2001, the Commission approved the proposed project, as conditioned, and added special conditions #3, 4, and 5.

SYNOPSIS

Southern California Edison Company, San Diego Gas and Electric Company, the City of Anaheim, and the City of Riverside (hereinafter, applicants) propose to construct a temporary spent nuclear fuel storage facility at the San Onofre Nuclear Generating Station (SONGS), located in an unincorporated portion of northern San Diego County. The facility will house spent fuel used to generate electricity at SONGS Units 2 and 3. It will be located on an existing, developed industrial site at Unit 1.

The applicants propose to construct three separate steel-reinforced concrete pads (covering an approximate area of 25,550 square feet) and approximately 104 steel-reinforced concrete fuel storage modules that will be placed on top of the pads. The facility will be designed and constructed in accordance with the SONGS 2 and 3 Nuclear Regulatory Commission (NRC) operating licenses and NRC regulations. The fuel storage facility will be constructed in three separate phases from approximately 2002 to 2015.

According to the applicants, additional storage capacity is necessary to store SONGS 2 and 3 spent fuel until their NRC operating licenses expire in 2022. The SONGS 2 and 3 spent fuel storage pools currently provide the capacity to store all fuel that will be used by both units through roughly 2007. The applicants are proposing dry storage, as opposed to a new pool storage facility, because the method is more economical and it places the fuel into containers that can be removed from the SONGS site by the Department of Energy when its permanent repository becomes available. Some fuel currently stored in water-filled pools will be transferred to the proposed storage facility until the U.S. Department of Energy (DOE), under obligation pursuant to the Nuclear Waste Policy Act of 1982, accepts the fuel for final disposal at a federal repository. The applicants will continue to use the existing SONGS 2 and 3 pool spent fuel storage facility. Spent fuel will be stored in these pools for a minimum of five years before it is transferred to dry storage.

The U.S. Nuclear Regulatory Commission has sole jurisdiction over the regulation of nuclear power plants, including radioactive hazards, safety issues, and spent fuel handling and storage. **The State of California is preempted from imposing upon nuclear power plant operators any regulatory requirements concerning radiation hazards and nuclear safety.** The possession, handling, storage, and transportation of spent nuclear fuel similarly are precluded from state regulation. The applicants' SONGS 2 and 3 operating licenses require them to comply with all NRC regulations that apply to the operations and activities conducted at those units,

including the possession, use, and storage of nuclear fuel. The applicants will control and monitor radioactive releases from the proposed project using the same programs and procedures currently implemented for the commercial operation of the plant.

Coastal Act Issues

The San Onofre bluffs, site of the SONGS facility, are an area of high geologic, flood and fire hazard. The Commission has identified the following geologic issues that must be considered to find that the proposed development will minimize risk to life and property (including the proposed development), and to assure stability and structural integrity at the site: seismic safety (including ground shaking, fault rupture, liquefaction, and tsunami runup), bearing capacity of the foundation elements, safety from coastal bluff retreat and shoreline erosion, and stability of slopes adjacent to the proposed development. As proposed, the project will minimize risk to life and property and will not create nor contribute significantly to erosion, geologic instability, or destruction of the site or surrounding area.

Because the proposed project will take place on an existing, industrial site currently occupied by SONGS 1, no on-site biological resources exist. Potential lighting and noise impacts to nearby environmentally sensitive habitat areas will be avoided. Recreation on and public access to the adjacent San Onofre State Beach will not be restricted during project operations. All relevant air quality permits, if required, will be obtained through the San Diego County Air Pollution Control District.

Commission Action

On March 13, 2001, by a vote of 10-0, the Commission granted subject to conditions Coastal Development Permit (CDP) No. E-00-014 for the proposed project. In doing so the Commission adopted the following resolution:

The Commission hereby approves Coastal Development Permit E-00-014 on grounds that the development as conditioned will be in conformity with the policies of Chapter 3 of the Coastal Act and will not prejudice the ability of the local government having jurisdiction over the area to prepare a Local Coastal Program conforming to the provisions of Chapter 3. Approval of the permit complies with the California Environmental Quality Act because either 1) feasible mitigation measures and/or alternatives have been incorporated to substantially lessen any significant adverse effects of the development on the environment, or 2) there are no further feasible mitigation measures or alternatives that would substantially lessen any significant adverse impacts of the development on the environment.

1.0 STAFF RECOMMENDATION ON APPROVAL OF REVISED FINDINGS

Motion:

I move that the Commission adopt the revised findings set forth in this staff report dated May 24, 2001, in support of the Commission's conditional approval on March 13, 2001, of CDP No. E-00-014.

Staff recommends a **YES** vote on the foregoing motion. Pursuant to section 30315.1 of the Coastal Act, adoption of findings requires a majority vote of the members of the prevailing side present at the March 13, 2001 hearing, with at least three of the prevailing members voting. Only those Commissioners on the prevailing side of the Commission's action on the permit are eligible to vote. See the list on page 1. Approval of the motion will result in the adoption of revised findings as set forth in this staff report.

2.0 STANDARD CONDITIONS See Appendix A

3.0 SPECIAL CONDITIONS

The Commission grants this permit subject to the following special conditions:

1. **Construction Debris.** Construction debris generated as part of the proposed project shall at the earliest practicable opportunity be disposed of at an appropriate offsite facility. Any construction debris or material present on-site, including construction debris or material subject to removal in accordance with the preceding requirement, that could potentially contribute to increased sediment loading shall be covered and/or contained during precipitation events.
2. **Sump Monitoring and Maintenance.** Sediment and other material that collects in the on-site sump from the project site's yard (storm water) drains shall be monitored and removed before such sediment or material reach quantities sufficient to pose a risk to the proper functioning of the sump.
3. **Sump Maintenance Fund.** To assure that sufficient financial resources are available to monitor and maintain the sump and yard drains in working order, prior to commencement of project construction, the applicants shall enter into an agreement, in substantially the same form and content as the draft "SONGS ISFSI Yard Sump Maintenance Trust Account" attached hereto as Exhibit 19 and incorporated herein by reference, with a state or federally chartered financial institution of the applicant's choice for the purpose of establishing a sump maintenance fund. The applicant shall deposit into the fund \$136,000, which represents the present value of the full costs of monitoring and maintaining the sump for the life of the project. The sump maintenance fund shall be reviewed and approved by the Executive Director, in coordination with the applicants. Prior to commencement of project construction, the applicant shall provide a copy of the fully executed agreement and evidence that the funds were deposited as described above to the Executive Director.

4. **Permit Expiration.** Unless extended by action of the Commission pursuant to an application submitted prior thereto, this permit shall terminate and be of no further force and effect on November 15, 2002.
5. **Future Development Restriction.** This permit is only for the development described in the project description set forth in this staff report dated May 24, 2001. Pursuant to Title 14 California Code of Regulations Section 13253(b)(6), the exemptions otherwise provided in Public Resources Code Section 30610(b) shall not apply to the project. Accordingly, any future improvements to the permitted structure, including but not limited to any structural or physical modifications to the Independent Spent Fuel Storage Installation, an increase in storage capacity of spent nuclear fuel, the storage of spent nuclear fuel from nuclear power plants other than the San Onofre Nuclear Generating Station Units 2 and 3, and the storage of anything other than spent nuclear fuel which are proposed within the restricted area shall require an amendment to coastal development permit E-00-014 from the Commission or shall require an additional coastal development permit from the Commission or from the applicable certified local government.

4.0 FINDINGS AND DECLARATIONS

The Commission finds and declares the following:

4.1 PROJECT DESCRIPTION

Project Location

The San Onofre Nuclear Generating Station (SONGS) is located in an unincorporated area of northern San Diego County on the United States Marine Corps Base, Camp Pendleton (Exhibit 1).

Background and Preemption of State Regulation

SONGS Units 2 and 3 have operated as 1127-megawatt commercial nuclear power plants since 1983 and 1984, respectively. Both units were constructed on land leased from the U.S. Department of the Navy, U.S. Marine Corp Base, Camp Pendleton. SONGS Unit 1, currently non-operational and in the process of being decommissioned, is located adjacent to and immediately north of Unit 2. The entire SONGS site covers 83.6 acres. SONGS 2 and 3 are collectively owned by Southern California Edison (75.05% interest), San Diego Gas and Electric Company (20%), the City of Anaheim (3.16%), and the City of Riverside (1.79%).

A power plant that uses radioisotopes in the production of energy is required to comply with the federal Atomic Energy Act (Act) (42 U.S.C. Sect. 2011). The Nuclear Regulatory Commission (NRC) was created to issue operating licenses under the Act and to enforce the requirements of the Act and a plant's operating license. Federal regulations (e.g., 10 CFR Parts 20, 50, 71 and 72) also govern the possession, handling, storage, and transportation of radioactive materials from a nuclear power plant. **The State of California is preempted from imposing upon the**

operators any regulatory requirements concerning radiation hazards and nuclear safety. In Pacific Gas and Electric Company v. State Energy Commission, 461 U.S. 190, 103 S.Ct. 1713 (1983), the U.S. Supreme Court held that the federal government has preempted the entire field of "...radiological safety aspects involved in the construction and operation of a nuclear plant, but that the states retain their traditional responsibility in the field of regulating electrical utilities for determining questions of need, reliability, costs and other related state concerns."

The possession, handling, storage, and transportation of spent nuclear fuel similarly are precluded from state regulation. The applicants' SONGS 2 and 3 operating licenses require them to comply with all NRC regulations that apply to the operation of both units, including the possession, use, and storage of spent nuclear fuel. The applicants will control and monitor radioactive releases from the proposed project using the same programs and procedures currently implemented for the commercial operation of the units.

On February 15, 2000, the Commission approved CDP E-00-001, authorizing the demolition of the structures comprising SONGS Unit 1 and the construction of the SONGS 1 spent fuel storage facility (19 fuel storage modules) that the applicants will undertake in connection with the decommissioning of Unit 1. The proposed project will be constructed adjacent to and integrated into the SONGS 1 storage facility, adding 104 fuel storage modules to house SONGS 2 and 3 spent fuel (Exhibit 3).

Project Purpose

According to the applicants, additional storage capacity is necessary to store SONGS 2 and 3 spent fuel until their NRC operating licenses expire in 2022. The SONGS 2 and 3 spent fuel storage pools currently provide the capacity to store all fuel that will be used by both units through roughly 2007. The applicants are proposing dry storage, as opposed to a new pool storage facility, because the method is more economical and it places the fuel into containers that can be removed from the SONGS site by the Department of Energy when its permanent repository becomes available. Some fuel currently stored in water-filled pools will be transferred to the proposed storage facility until the U.S. Department of Energy (DOE), under obligation pursuant to the Nuclear Waste Policy Act of 1982, accepts the fuel for final disposal at a federal repository. The applicants will continue to use the existing SONGS 2 and 3 pool spent fuel storage facility. Spent fuel will be stored in these pools for a minimum of five years before it is transferred to dry storage.

According to the applicants, the DOE does not expect to start accepting SONGS 2 and 3 spent fuel or spent fuel from any U.S commercial nuclear power plant until 2010, at the earliest. Until then, the applicants are required by NRC regulations to safely monitor and maintain the SONGS 2 and 3 fuel.

Temporary Spent Nuclear Fuel Storage Facility

As stated above, until the U.S. Department of Energy accepts SONGS spent fuel for final disposal at a federal repository, the applicants are required by NRC regulations and their

operating licenses to safely store and maintain it. The proposed project, an "Independent Spent Fuel Storage Installation" (ISFSI) is comprised of an array of concrete fuel storage modules (FSMs) located on a reinforced concrete pad. A stainless steel canister containing the spent fuel assemblies is secured inside the FSMs. The proposed project will be located within the existing Unit 1 boundaries on a generally flat area at an approximate elevation of 20 feet above sea level. It will be a minimum of 180 feet away from the beach/seawall and a minimum of 150 feet from the slopes surrounding the plant.

Approximately 104 steel-reinforced FSMs that will be placed on top of three steel-reinforced concrete pads, covering an approximate area of 25,550 square feet (Exhibit 2). The concrete pads will be a minimum of three feet thick (with the top being at the existing grade elevation) and will be approximately 43 feet wide and long enough to accommodate the module array. It will contain 7/8" diameter reinforcing bar (rebar) spaced on 12" centers running the length of the pad (top and bottom) and 1-1/8" diameter rebar spaced on 12" centers across the width of the pad. The minimum compressive strength of concrete is 4000 lbs./inch². The pad will be designed in accordance with the requirements of American Concrete Institute (ACI-349), "Code Requirements for Nuclear Safety Related Concrete Structures".

A FSM is shaped like a rectangular box and will be no more than 22 feet in height above the existing grade by 9 feet wide and 23 feet long. The FSMs are constructed of reinforced concrete and weigh over 400,000 lbs. each. Generally, rebar within the FSM will range in size from 1/2" to 1" in diameter with spacing ranging from 6" to 18". The FSMs are tied together in arrays with a combination of 1.5" bolts and 1" rebar. The minimum compressive strength of concrete is 5000 lbs./inch². The design and construction of the FSMs will be in accordance with ACI-349 and ACI-318, "Building Code Requirements for Reinforced Concrete".

Each FSM will house a NRC-licensed steel cask or canister that may contain up to 24 fuel assemblies. A fuel assembly consists of 236 zircalloy metal tubes approximately 12.8 feet long and 3/8" in diameter, in which ceramic uranium dioxide fuel pellets are placed. Known as fuel pins, the tubes are completely sealed with welded end plugs. Each fuel assembly has an overall length of about 15 feet and weighs approximately 1,500 lbs.

As indicated above, the proposed project will consist of three separate reinforced concrete pads, to be constructed in three separate phases. The first pad will be constructed adjacent to and integrated into the construction schedule of the SONGS 1 spent fuel storage facility. This phase is proposed to commence in November 2002. The second pad is anticipated to be constructed in 2008 after the SONGS 1 decommissioning is complete and as additional capacity is needed. The third pad is to be constructed sometime between 2011 and 2015 as the need arises.

The proposed fuel storage facility will be constructed within the existing, developed SONGS 1 site (Exhibit 3). The construction process will involve: (1) minor grading without breaking new ground; (2) placing the flat, reinforced concrete pad at ground level; (3) installing a chain-link security fence, perimeter lighting, and cameras and; (4) lifting and setting the free-standing spent FSMs, to be fabricated offsite, on the pad. This work will involve customary grading equipment (such as a front-end loader and a compaction roller) and concrete construction equipment (such

as forms, concrete tooling, and a mobile crane). Concrete will be delivered pre-mixed from local suppliers. Construction activities are scheduled to be performed during daylight hours. However, the applicants state that some tasks, completion of which cannot be delayed, such as a large concrete pour or finishing, could occasionally continue until after daylight hours.

The entire facility will be designed and constructed in accordance with NRC regulations (10 C.F.R. Part 72, Subpart K, "General License for Storage of Spent Fuel at Power Reactor Sites," as published in the Federal Register on July 18, 1990, 55 FR 29191) and the SONGS 2 and 3 operating licenses. The applicants maintain that the proposed project will be undertaken in accordance with the existing programs that implement and comply with NRC and Occupational Safety and Health Administration regulations. Existing lighting, telephone, and drainage infrastructure may be modified to accommodate the storage facility. However, the project will not change the existing drainage pattern from the site. All liquid discharges from the construction project will be regulated under the current SONGS 1 National Pollution Discharge Elimination System (NPDES) permit. There will be no liquid discharges or gaseous emissions from the storage facility.

4.2 PRIOR COMMISSION APPROVALS

In 1974, the Commission conditionally approved the construction of SONGS Units 2 and 3 (6-81-330). In 1991, the Commission further conditioned the same permit to require the applicants to implement a compensatory mitigation program. In 1997, the Commission, among other things, approved an amendment (6-81-330-A) to the SONGS 2 and 3 permit to amend the condition that required mitigation for adverse impacts to the marine environment caused by SONGS Units 2 and 3.

On February 15, 2000, the Commission approved coastal development permit E-00-001 authorizing Southern California Edison and San Diego Gas and Electric Company to decommission Unit 1 and construct a temporary spent fuel storage facility for Unit 1. The facility, slated for construction in November 2002, will consist of 19 fuel storage modules and cover an area approximately 4067 sq. ft. and reach 38 feet high.

4.3 OTHER AGENCY APPROVALS

U.S. Nuclear Regulatory Commission

The U.S. Nuclear Regulatory Commission (NRC) has three principal regulatory functions: (1) establish standards and regulations, (2) issue licenses for nuclear facilities and users of nuclear materials, and (3) inspect facilities and users of nuclear materials to ensure compliance with the requirements. The applicants are required to possess, use, and store radioactive waste streams in accordance with federal regulations (*e.g.*, 10 CFR Parts 20, 50, and 72) and their SONGS 2 and 3 NRC Operating License. NRC regulations allow licensees to store spent nuclear fuel either in a wet (pool storage) or dry (cask storage) method. However, they require an applicant to obtain

either a specific or seek coverage under a general license¹. Under a specific licensing process, the NRC conducts site-specific review of the proposed storage site. A general license allows persons authorized to possess or operate nuclear power plants to contract with an NRC-approved supplier of spent fuel storage casks. The supplier has the obligation to obtain NRC approval (*i.e.*, a Certificate of Compliance) of its casks pursuant to 10 C.F.R. 72, Subpart L.

In a letter dated October 4, 2000 to the NRC, the applicants informed the NRC that they will pursue a general license and that they have contracted with Transnuclear West Inc. to furnish storage casks. Transnuclear West Inc. submitted an application for a Certificate of Compliance (COC) to the NRC on September 29, 2000. A COC expires 20 years after the date that the cask is first used by the general licensee to store spent fuel, unless the cask's COC is renewed.

In order to seek coverage under a general license, the applicants are required to comply with the general license conditions pursuant to 10 C.F.R. 72.212 and others as indicated in 10 C.F.R. 72.13(c). Among other requirements, the former section requires the applicants to:

1. Formally notify the NRC at least 90 days prior to the initial storage of spent fuel.
2. Register use of each cask with the NRC no later than 30 days after using that cask to store spent fuel.
3. Perform written evaluations, prior to use, that establish that conditions set forth in the COC have been met and cask storage pads and areas have been designed to adequately support the static load of the stored casks.
4. Review the Safety Analysis Report (SAR) referenced in the Certificate of Compliance and the related NRC Safety Evaluation Report, prior to use of the general license, to determine whether or not the reactor site parameters, including analyses of earthquake intensity and tornado missiles, are enveloped by the cask design bases considered in these reports.
5. Protect the spent fuel against the design basis threat of radiological sabotage in accordance with the same provisions and requirements as are set forth in the licensee's physical security plan.
6. Review the reactor emergency plan, quality assurance program, training program, and radiation protection program to determine if their effectiveness is decreased and, if so, prepare the necessary changes and seek and obtain the necessary approvals.

Additionally, 10 C.F.R. 72.122 specifies overall requirements the proposed project must meet. Major requirements include:

¹ In issuing 10 C.F.R. 72.210, a general license for the storage of spent fuel in an independent spent fuel storage installation was effectively granted to persons authorized to possess or operate nuclear power reactors. Applicants wishing to seek coverage under this license must comply with the general license conditions pursuant to 10 C.F.R. 72.212 and others as indicated in 10 C.F.R. 72.13(c).

- (a) *Quality Standards.* Structures, systems, and components important to safety must be designed, fabricated, erected, and tested to quality standards commensurate with the importance to safety of the function to be performed.
- (b) *Protection against environmental conditions and natural phenomena.*
 - (1) Structures, systems, and components important to safety must be designed to accommodate the effects of, and to be compatible with, site characteristics and environmental conditions associated with normal operation, maintenance, and testing of the ISFSI [independent spent fuel storage installation] or MRS [monitored retrievable storage installation] and to withstand postulated accidents.
 - (2) Structures, systems, and components important to safety must be designed to withstand the effects of natural phenomena such as earthquakes, tornadoes, lighting, hurricanes, floods, tsunamis, and seiches, without impairing their capability to perform safety functions. The design bases for these structures, systems, and components must reflect:
 - (i) Appropriate consideration of the most severe of the natural phenomena reported for the site and surrounding area, with appropriate margins to take into account the limitations of the data and the period of time in which the data have accumulated, and
 - (ii) Appropriate combinations of the effects of normal and accident conditions and the effects of natural phenomena. The ISFSI or MRS should also be designed to prevent massive collapse of building structures or the dropping of heavy objects as a result of building structural failure on the spent fuel or high-level radioactive waste or on to structures, systems, and components important to safety.
 - (3) Capability must be provided for determining the intensity of natural phenomena that may occur for comparison with design bases of structures, systems, and components important to safety.
- (c) *Protection against fires and explosions.* Structures, systems, and components important to safety must be designed and located so that they can continue to perform their safety functions effectively under credible fire and explosion exposure conditions. Noncombustible and heat-resistant materials must be used wherever practical throughout the ISFSI or MRS, particularly in locations vital to the control of radioactive materials and to the maintenance of safety control functions. Explosion and fire detection, alarm, and suppression systems shall be designed and provided with sufficient capacity and capability to minimize the adverse effects of fires and explosions on structures, systems, and components important to safety. The design of the ISFSI or MRS must include provisions to protect against adverse effects that might result from either the operation or the failure of the fire suppression system.

...

- (e) *Proximity of sites.* An ISFSI or MRS located near other nuclear facilities must be designed and operated to ensure that the cumulative effects of their combined operations will not constitute an unreasonable risk to the health and safety of the public.

...

- (g) *Emergency capability.* Structures, systems, and components important to safety must be designed for emergencies. The design must provide for accessibility to the equipment of onsite and available offsite emergency facilities and services such as hospitals, fire and police departments, ambulance service, and other emergency agencies.

- (h) *Confinement barriers and systems.*

- (1) The spent fuel cladding must be protected during storage against degradation that leads to gross ruptures or the fuel must be otherwise confined such that degradation of the fuel during storage will not pose operational safety problems with respect to its removal from storage. This may be accomplished by canning of consolidated fuel rods or unconsolidated assemblies or other means as appropriate.

...

- (3) Ventilation systems and off-gas systems must be provided where necessary to ensure the confinement of airborne radioactive particulate materials during normal or off-normal conditions.
- (4) Storage confinement systems must have the capability for continuous monitoring in a manner such that the licensee will be able to determine when corrective action needs to be taken to maintain safe storage conditions. For dry spent fuel storage, periodic monitoring is sufficient provided that periodic monitoring is consistent with the dry spent fuel storage cask design requirements. The monitoring period must be based upon the spent fuel storage cask design requirements.
- (5) The high-level radioactive waste must be packaged in a manner that allows handling and retrievability without the release of radioactive materials to the environment or radiation exposures in excess of part 20 limits. The package must be designed to confine the high-level radioactive waste for the duration of the license.

Other requirements the proposed project must comply with specify criteria for nuclear criticality safety (10 C.F.R. 124), criteria for radiological protection (10 C.F.R. 126), quality assurance (10 C.F.R. 140-176), and operator requirements (10 C.F.R. 190, 194).

Construction of the SONGS 2 and 3 dry storage facility will not require further NRC approval. NRC staff may, however, inspect the construction of the fuel storage modules and the process of loading and moving the spent fuel to the storage facility.

San Diego Air Pollution Control District (APCD)

The San Diego Air Pollution Control District (APCD) has permit authority under the California Clean Air Act (CCAA) over direct emission sources in the project area. The APCD has not established California Environmental Quality Act emission thresholds for construction activity and instead relies on district rules to determine whether permit requirements are triggered by construction-related emissions.

Since the proposed project's emission sources will be construction equipment brought on the site temporarily, the APCD will require permits, if necessary, for these individual sources of emissions. The applicants will either obtain or contractually require vendors supplying the equipment to obtain necessary permits from the APCD. Mobile construction equipment (e.g., cranes) used in connection with the project may be permit exempt, as determined by the APCD.

4.4 COASTAL ACT ISSUES

4.4.1 Geologic Hazards

Section 30253 of the Coastal Act states, in part, that:

New development shall:

- (1) Minimize risks to life and property in areas of high geologic, flood, and fire hazard.*
- (2) Assure stability and structural integrity, and neither create nor contribute significantly to erosion, geologic instability, or destruction of the site or surrounding area or in any way require the construction of protective devices that would substantially alter natural landforms along bluffs and cliffs.*

...

The San Onofre bluffs, site of the SONGS facility, are an area of high geologic, flood and fire hazard. Accordingly, the Commission's Senior Geologist has reviewed the documents submitted by both the applicants and the opponents to the project, and has conducted his own literature research. This section (4.4.1) contains his conclusions, which the Commission hereby incorporates as findings.

As described above, in section 4.1, the Commission is proscribed from applying section 30253—or any section of the California Coastal Act—to issues related to nuclear or radiation safety. Nevertheless, proposed development must assure geologic stability in order to conform to the Coastal Act. The analysis that follows relates to the safety of the proposed development from geologic hazard; it does not address the consequence of structural failure in terms of nuclear safety. Such consequences are under the jurisdiction of the Nuclear Regulatory Commission (NRC). The findings in this section relate only to issues of geologic stability pursuant to the California Coastal Act.

The Commission has identified the following geologic issues that must be considered to find that the proposed development will minimize risk to life and property (including the proposed development), and to assure stability and structural integrity at the site: seismic safety (including ground shaking, fault rupture, liquefaction, and tsunami runup), bearing capacity of the foundation elements, safety from coastal bluff retreat and shoreline erosion, and stability of slopes adjacent to the proposed development.

4.4.1.1. Geologic Setting

The SONGS site lies in the Peninsular Ranges geomorphic province of southern California. Bedrock at the site is the San Mateo Formation, a dense well lithified sandstone of Pliocene to Pleistocene age. Borings indicate that this formation extends to at least a depth of 900 feet below grade at the site. This bedrock unit is overlain by a series of marine and nonmarine terrace deposits approximately 50 feet thick, which have been dated by correlation with similar deposits containing mollusk fossils that are well dated at 80,000 to 180,000 years old (Fugro, 1975a; Fugro, 1975b). The bedrock at the SONGS site is nearly flat-lying, dipping 10-15 degrees to the northeast (Ehlig, 1977).

At the SONGS facility itself, the terrace deposits and the upper 10-20 feet of the San Mateo Formation have been removed by grading, and the finished grade of the facility is set well below the top of the coastal cliffs at an elevation of approximately 20 feet MLLW. The excavated material was placed on the beach as sand nourishment, greatly increasing the width of the beach in this area. Much of this material has now been removed by longshore drift, but a narrow beach still exists seaward of the facility.

The Cristianitos fault, an apparently inactive low-angle normal fault (Shlemon, 1987), lies south and east of the site, intersecting the seacliff approximately one mile south of the SONGS facility. South of the fault, bedrock consists of the Miocene Monterey Formation, which is underlain by the San Onofre breccia, well exposed in the San Onofre hills to the east. The marine and nonmarine terrace deposits overlie the Monterey Formation as well as the San Mateo Formation. In addition to the Cristianitos fault, which will be described in more detail below, four minor faults have been mapped on the northwest flank of the San Onofre hills to the east of the site. None show evidence of movement during the past two million years (U.S. Nuclear Regulatory Commission, 1981). Several sets of shears in the San Mateo Formation were uncovered during excavation for SONGS Units 2 and 3. These shears show displacements of 3 to 6 inches, but do not offset overlying terrace deposits (Fugro, 1974a; Fugro, 1974b) (Fugro, 1976), and the NRC concluded that they do not represent recent faulting at the site (U.S. Nuclear Regulatory Commission, 1975).

More distant geologic structures include the Newport-Inglewood-Rose Canyon fault zone (variously referred to during NRC review as the "Offshore Zone of Deformation," or the "Southern California Offshore Zone of Deformation"), which passes approximately 8 km offshore. Further offshore, in the region known as the California Borderland, lie several poorly understood northwest-southeast trending strike-slip and/or thrust faults including the Coronado Bank Fault Zone, San Diego Trough Fault Zone, Thirtymile Bank Fault Zone, and Oceanside

Thrust. Onshore, the northwest-southeast trending Elsinore, San Jacinto, and San Andreas Fault Zones pass 38, 73, and 93 km from the site, respectively. Despite the proximity to these active faults, the area is one of the most seismically quiet areas in coastal California, and historically has experienced severe ground shaking relatively rarely.

4.4.1.2. Earthquakes and seismic hazards

Like most of coastal California, the SONGS site lies in an area subject to earthquakes. The site lies approximately 8 km from the Newport-Inglewood-Rose Canyon fault system, 38 km from the Elsinore Fault, 73 km from the San Jacinto Fault, and 93 km from the San Andreas Fault, all of which have been designated "active" (evidence of movement in the past 11,000 years) by the California Division of Mines and Geology (Jennings, 1994). Several relatively nearby offshore faults, including the Coronado Bank Fault Zone, the San Diego Trough Fault Zone, the Thirty-Mile Bank Fault, and the Oceanside Thrust also may be active faults by this definition. Nevertheless, seismicity here has historically been relatively quiet compared to much of the rest of southern California (Exhibit 4), probably because of the relatively great distance of the San Andreas fault, which accommodates most of the plate motion in the area, and the relatively low slip rates of the closer faults (Peterson et al., 1996). A magnitude (M_L) 5.4 earthquake, associated with an unusually large swarm of aftershocks, occurred near the offshore San Diego Trough Fault Zone in 1986, but no other moderate or large (M_w 5.0) earthquake has occurred within 50 km in historic time (Exhibit 4).

Seismic hazards at the site include ground shaking, surface rupture, liquefaction, slope instability, and tsunami runup. All of these issues are addressed in these findings, but ground shaking deserves special attention as it is the seismic hazard most likely to affect the proposed development. To fully discuss the ground shaking hazard, an understanding of the means geologists use to quantify ground shaking is necessary.

Ground shaking

Many different measures have been used over the years to assess earthquake magnitude. The familiar Richter, or local, magnitude (M_L) is based on the ground shaking observed on a particular type of seismograph that is most sensitive to short period (0.8 second) seismic waves. These waves die out with distance, and so this measure is inappropriate when applied over long distances ($> \sim 500$ km) to measure distant earthquakes. Moreover, for large earthquakes, the Richter magnitude "saturates," and fails to accurately reflect differences between large earthquakes of different magnitudes. The surface wave magnitude (M_S) was developed to measure shaking of long period (20 second) waves, and is more suited to larger earthquakes. This scale, like its counterpart the body wave magnitude (M_B) also saturates in large earthquakes and, like the Richter magnitude, is based solely on ground shaking, not the amount of energy released by an earthquake. Currently, most seismologists prefer the moment magnitude (M_w) for measuring large earthquakes. This measure is based on the strength of the rocks, the area of fault rupture, and the amount of slip during an earthquake, and is a better measure of the amount of energy released by an earthquake.

An earthquake of a given magnitude will produce different levels of ground shaking at different locations, depending on the distance of the location from the earthquake hypocenter, the nature of the soil or rock between the location and the earthquake, and soil and rock conditions at the site. The level of shaking is expressed by a term called "intensity," and is quantified by the Modified Mercalli Index, whereby intensities ranging from I (not felt) through XII (near total destruction) are assigned based on the level of damage sustained by structures. Better quantification of the level of shaking also is possible; and the standard measure is peak ground acceleration (PGA), usually expressed as a fraction of the acceleration due to gravity (9.81 m/s^2 , or 1.0 g). Peak ground acceleration is typically measured in horizontal and vertical directions. It can be expressed deterministically ("a given earthquake can be expected to produce a peak horizontal ground accelerations at the site of X g"), or probabilistically ("given the seismic environment at the site, there is a 10% chance that a peak ground acceleration of X g will be exceeded in 50 years"). The current trend is to express seismic risk in probabilistic terms. The State of California has defined ground accelerations with a 10% chance of exceedance in 50 years as corresponding to the "maximum probable earthquake" for the site. Ground shaking with a 10% chance of exceedance in 100 years is defined as the "maximum credible earthquake." Peak ground accelerations depend not only on the intensity of the causative earthquake and the distance of the site from the hypocenter of the earthquake, but also on site characteristics. Most important is the depth and firmness of the soil and/or bedrock underlying the site. All of these parameters are evaluated in producing a seismic shaking hazard assessment of a site.

In evaluating the response of structures to ground shaking, the frequency (cycles per second) of that shaking is important—higher frequency shaking is more damaging to smaller, more rigid structures, whereas lower frequency shaking is more damaging to larger, or more flexible structures. The proposed ISFSI facility fits into the latter category. Different ground acceleration values apply to seismic waves with different frequencies. The inverse of the frequency of a seismic wave is its period. Thus, an earthquake with a peak ground acceleration of 0.7 g may have a peak "spectral acceleration" (SA) of 1.1 g for waves of 0.3 second period, but only 0.5 g for waves with periods of 1 second. A typical earthquake produces seismic waves with many different periods, and a plot of spectral accelerations for an earthquake shows the ground accelerations for waves of all periods. In addition, the duration of shaking appears to be important in determining the amount of damage caused by ground shaking. The duration of shaking correlates reasonably well with earthquake magnitude, but there are no currently accepted means of estimating the expected duration of ground shaking from a given earthquake.

The SONGS Seismic Design Criteria

The applicant maintains that the seismic safety of the site has been assured through review by the U.S. Nuclear Regulatory Commission, most recently the licensing review for Units 2 and 3. Accordingly, it is appropriate to evaluate the SONGS seismic design criteria when considering the safety of the proposed project, which would be located immediately adjacent to Units 2 and 3 on the site of the decommissioned Unit 1.

The recently-released seismic shaking hazard map of California (Peterson et al., 1999) portrays the San Onofre area as a region of "low" seismic shaking potential, with a 10% chance of

exceeding approximately 0.3 g in 50 years. For comparison, the Big Sur coast is the only other part of coastal California having a comparably low ground shaking potential according to this assessment. The U.S. Geologic Survey's latitude-longitude earthquake ground motion hazard look-up page (<http://geohazards.cr.usgs.gov/eqint/html/lookup.shtml>) similarly reports an expected peak ground acceleration of 0.32 g (10% chance of exceedance in 50 years). The probabilistic peak ground accelerations and spectral accelerations for the San Onofre area, assuming firm bedrock conditions, are as follows (determined from the USGS lookup page):

| | 10% in 50 yr | 5% in 50 yr | 2% in 50 yr |
|------------|--------------|-------------|-------------|
| PGA | 0.32 g | 0.47 g | 0.67 g |
| 0.2 sec SA | 0.74 | 1.12 | 1.50 |
| 0.3 sec SA | 0.64 | 1.06 | 1.36 |
| 1.0 sec SA | 0.28 | 0.38 | 0.54 |

This assessment, however, is based only on current understanding of the likelihood of earthquakes of varying intensities on nearby faults. A deterministic study undertaken at the time of the licensing permit application for SONGS Units 2 and 3 (U.S. Nuclear Regulatory Commission, 1981) identified an earthquake on the Newport-Inglewood-Rose Canyon fault system, centered on the portion of the fault nearest to the SONGS site, to be the seismic event with the greatest potential ground shaking for the SONGS site. Other faults, such as the San Andreas Fault, although capable of producing larger earthquakes than the Newport-Inglewood-Rose Canyon fault system, are so far distant from the site that ground shaking would be less than an earthquake on the Newport-Inglewood-Rose Canyon fault system. Because the applicant refers to this assessment to assure the stability of the proposed project, analysis of how this assessment was performed follows.

The 1981 NRC document reviewed several methods put forth by the applicant to arrive at an estimate for the expected magnitude of a design basis earthquake (the "safe shutdown earthquake" of the NRC). One method is the evaluation of historical seismicity on the Newport-Inglewood-Rose Canyon fault system. Three historic earthquakes are known on this system, or its possible extension into Baja California. Only the most recent, which occurred on March 11, 1933, can be accurately assigned a magnitude. That earthquake, the damaging Long Beach earthquake, had a magnitude (M_w) of 6.4 (SCEC, 2001; the NRC (1981) reports both M_s and M_L of 6.3). The locations of the two other earthquakes are not accurately known, but may be related to this system. The first occurred near San Diego on November 22, 1800, and may have had a magnitude of about 6.5 (U.S. Nuclear Regulatory Commission, 1981). The other earthquake, the December 8, 1812 San Juan Capistrano earthquake, likely actually occurred on the San Andreas Fault (SCEC, 2001) and may have had a moment magnitude of about 7.5. The NRC assumed in 1981 that the earthquake was centered on San Juan Capistrano, placing it on the Newport-Inglewood-Rose Canyon fault, and estimated its magnitude as about 6.5 (Toppozada et al., 1979). An 1892 earthquake in Baja California (Laguna Salada earthquake), with an estimated magnitude of 6.9 (M_s ; Toppozada et al., 1979; $M_w = 7.0$ according to SCEC, 2001) probably is not related to the Newport-Inglewood-Rose Canyon fault system (Gastil et al., 1979). From these data, the

NRC concluded that "the largest historical earthquakes which have an impact upon the assessment of the maximum earthquake on the OZD [the Newport-Inglewood-Rose Canyon fault system] are $M_s = 6.3$, 6.5 , and 6.5 in southern coastal California and possibly $M_s = 6.8$ [sic] in Baja California." Earthquakes in southern California that have taken place since the NRC report was published in 1981, including the 1992 Landers ($M_w = 7.3$; SCEC, 2001), 1994 Northridge ($M_w = 6.7$; SCEC, 2001), and 1999 Hector Mine ($M_w = 7.1$; SCEC, 2001) earthquakes were not associated with the Newport-Inglewood-Rose Canyon fault system. Shaking from each of these events was minimal ($< 0.1g$) at the SONGS site (Collins, 1997).

A second approach to estimating the maximum earthquake likely to be produced by movement along a fault is based on estimates of fault parameters, especially the long-term rate of slip on the fault, estimates of the length of the fault that would rupture during an earthquake, and the amount of displacement that would occur during an earthquake. David Slemmons, consultant to the NRC, put forth over ten different estimates for the maximum magnitude of an earthquake on the Newport-Inglewood-Rose Canyon fault system using various estimates of these parameters. His analysis resulted in estimates of M_s ranging from 6.6 to 7.3 (U.S. Nuclear Regulatory Commission, 1981). These estimates used a long-term slip rate of 0.5 mm/year, and rupture lengths of up to 44 km (22 percent of the 200-km long system). Based on its own review, and a limited review by the U.S. Geological Survey, the NRC concluded "that $M_s = 7.0$ is a reasonable, yet conservative estimate of maximum earthquake potential based upon fault parameter evaluation" (U.S. Nuclear Regulatory Commission, 1981).

Estimating the amount of ground shaking expected at a particular location from a nearby earthquake is challenging. At the time of the licensing of SONGS 2 and 3, the applicant combined empirical data from recent earthquakes (especially the 1979 Imperial Valley earthquake) and theoretical models to estimate the ground shaking expected at the SONGS site as a result of the design basis earthquake ($M_s = 7.0$ at 8 km from the site). The theoretical estimate was arrived at by 1) characterizing the nature of the fault slip in terms of fault type, rupture velocity, dynamic stress release, and duration of slip; 2) propagating the energy released in (1) through the earth structure between the fault and the site; and 3) calculating actual ground motion by mathematically combining (1) and (2). The NRC and its consultants reviewed this procedure, and required some modifications to the model. The applicants responded with a model that assumes a rupture distance of 40 km, maximally focused at the site, with a fault offset of 130 cm and a rupture velocity equal to 90% of the shear wave velocity. The mean spectra has a peak acceleration of 0.31 g. After comparison with empirical models, and in order to build in conservatism for inaccuracies in the model, the NRC approved the calculated spectra multiplied by a factor of about 2. The NRC approved spectra thus is pegged at a high-frequency peak acceleration of 0.67 g (Exhibit 5) (U.S. Nuclear Regulatory Commission, 1981). Also shown in exhibit 5 are spectral accelerations expected at the site from the design-basis earthquake according to several newer models for the attenuation of seismic energy with distance.

The approach outlined above is deterministic in nature: a design basis earthquake was established, and that earthquake was used to calculate expected ground acceleration. In 1995 a probabilistic study was undertaken. Three independent sets of consultants contributed to this product: Geomatrix (1994; 1995a; 1995b) determined the seismic source models; Woodward-

Clyde (1995a; 1995b) determined the seismic wave propagation (attenuation) models; and Risk Engineering (1995) integrated these results and performed hazard assessment. The results represent the annual frequency of exceedance of various ground motions at SONGS, shown as a family of seismic hazard curves and as seismic spectra corresponding to the "safe shutdown earthquake," (annual probability of occurrence of 0.00014, or recurrence interval of 7,143 years). This spectra peaks at somewhat higher accelerations than the deterministic spectra (Exhibit 6).

Recent studies and implications to seismic potential at the site

Some opponents to the proposed project indicate that, as a result of research undertaken since the licensing of SONGS 2 and 3, new information is available on the geologic environment offshore of the SONGS site that indicate that the design basis earthquake ($M_S = 7.0$ at 8 km; with high-frequency ground accelerations pegged at 0.67 g) may underestimate the seismic risk at the site. This is not the first time that the seismic safety of the SONGS facility has been formally challenged. On September 22, 1996, Stephen Dwyer, a geologist from southern California, petitioned the NRC to shut down the SONGS facility "as soon as possible" pending a complete review of the "new seismic risk." Mr. Dwyer asserted that the design criteria are "fatally flawed" on the basis of new information gathered at the Landers and Northridge earthquakes. In particular, he cited 1) ground accelerations as high as 1.8 g that were recorded during the $M_W = 6.7$ Northridge earthquake; 2) horizontal offsets of up to 20 feet in the Landers earthquake, and 3) the fact that the Northridge fault was a "blind thrust and not mapped or assessed." These issues were addressed by the NRC in "Director's Decision-97-23" (Collins, 1997). The high ground acceleration associated with the Northridge earthquake appears to be due to characteristics (still poorly understood) of one particular instrumented site (Rial, 1996). Nevertheless, as the record from strong motion instrumentation improves, geologists are obtaining more and more records showing high ground accelerations from even modest earthquakes (e.g., 0.48 g from the M_W 5.0 Napa earthquake of 3 September 2000; L. Jones, USGS, pers. comm., 2001). What is equally or more important than ground acceleration, however, is the spectral frequency at which the acceleration occurs and the duration of shaking. Most of these high acceleration values are of very short duration and occur at high spectral frequencies. The horizontal offset at the Landers earthquake is not germane to an earthquake on the Newport-Inglewood-Rose Canyon fault system as the fault dynamics are very different in the two cases. The NRC similarly dismissed the fact that the Northridge fault was a blind thrust as not being germane to the SONGS site in that the Newport-Inglewood-Rose Canyon system is known to be a strike-slip fault, not a blind thrust (Collins, 1997). There is, however, evidence (presented below) that a thrust component may contribute to this fault system. To summarize, the NRC found in 1997 that there was no basis for the Dwyer petition, that the design basis earthquake was adequate, and that the SONGS seismic design criteria exceed the expected seismic spectra from such an earthquake.

Dr. Mark Legg has expressed several concerns related to the proposed project (Exhibit 7). Like Mr. Dwyers, he is concerned with information gained by seismologists since the SONGS Units 2 and 3 licensing review:

Newer attenuation relations based upon recent large earthquake activity including the 1989 Loma Prieta, California; 1992 Landers, California; 1999 Chi-Chi, Taiwan; 1999 Izmit, Turkey; and

1995 Kobe, Japan, and moderate earthquakes including the 1994 Northridge, California; 1987 Whittier Narrows, California; 1983 Coalinga, California; and 1984 Morgan Hill, California are more accurate in estimating ground motions than the relationships used for the Safety Evaluation conducted in the late 1970s (Abrahamson and Silva, 1997; Boore et al., 1997; Campbell, 1997; Sadigh et al., 1997).

This statement is true, and is in fact born out by similar data from even smaller earthquakes such as the 2000 Napa earthquake. However, as shown in Director's Decision 97-23 (Collins, 1997), the SONGS design spectra exceeds the spectral accelerations expected at the site from the design-basis earthquake according to the attenuation models cited by Dr. Legg (Exhibit 5). Even these attenuation models, as well as that by Spudich and others (1997), failed to predict the 0.48 g acceleration measured from the Napa earthquake of 2000—by a factor of four (Miranda and Aslani, 2001). Nevertheless, irrespective of the attenuation models adopted during the licensing review, the design spectra for the ISFSI facility is sufficiently conservative to allow for much larger ground accelerations than might be predicted by the newer attenuation models.

Dr. Legg also points out in his communication to Commission staff (Exhibit 7) that:

it is now recognized that major detachment fault systems in the region are reactivated as thrust faults, some blind (not reaching the surface). The major Oceanside detachment/thrust system underlies the San Onofre Nuclear Generating Station (SONGS). Consequently, large thrust or oblique-reverse earthquakes on this system may generate shaking levels in excess of the design level of SONGS units 2 and 3 (Bohannon et al., 1990; Bohannon and Geist, 1998; Crouch and Suppe, 1993; Grant et al., 1999; Legg et al., 1992; Nicholson et al., 1993; Rivero et al., 2000).

He goes on to indicate that:

...the reverse fault character of microearthquakes recorded along the Cristianitos fault trend in the mid-1970s and reactivation of minor faulting uncovered during site excavations is consistent with overall reactivation of ancient normal fault structures by a new stress regime involving northeast-directed shortening or transpression. This assertion has now been confirmed by recent geologic studies in the neighboring offshore region...

and that, because of the dipping nature of these thrust faults, in an earthquake involving them

... the SONGS site would not be 5-7 km from the epicentral zone, but instead directly above the potential fault rupture plane. Estimation of strong motion should use an epicentral distance of zero (0).

The studies cited by Dr. Legg, as well as other studies, do suggest that a complex system of low-angle faults, which appear to be old normal faults (related to crustal extension) reactivated as thrust faults (related to crustal shortening) lie offshore of the SONGS site. The thrust character of these faults may be related to the bend in the Newport-Inglewood-Rose Canyon fault system offshore of Carlsbad. In this area Kuhn and others (Kuhn et al., 2000; Shlemon, 2000) have documented complex fault features that appear to be related to thrusting. It is probably significant that the 1986 Oceanside earthquake (M_L 5.4, which was centered on one of these low-angle faults, showed a thrust fault mechanism.

Thus, there appears to be credible evidence that, in addition to the strike-slip faulting recognized at the time of the SONGS licensing review, thrust faults exist in the area offshore of the SONGS site which might interact with the Newport-Inglewood-Rose Canyon fault system in a complex way during an earthquake. If these faults are active or potentially active, the increase in potential fault rupture area has, at a minimum, the potential to increase the magnitude of an earthquake on the integrated fault system. Geologists' understanding of this area is rapidly evolving, and there are few constraints on the parameters needed to assess the increase in earthquake risk (such as slip rate on each of the potentially active faults, segmentation of the faults, and potential for cascading failure between fault segments). One of the few published estimates is that of Shaw and his students (Rivero et al., 2000), who hypothesize that the combined system may be capable of an earthquake ranging from M_w 7.1 to 7.6, depending on which sets of faults are involved in the earthquake (Exhibit 8). Shaw's tectonic model for the area is, however, quite controversial (Jones, USGS, pers. comm., 2001). Commission staff consulted with seismologists and geologists at the U.S. Geological Survey, California Division of Mines and Geology, California Seismic Safety Commission, within academia, and at private consulting firms. Although there was near unanimous recognition that there is an increased earthquake risk given our emerging understanding of the complexities of the region relative to a simple strike-slip model used in the SONGS seismic hazard assessments, no one could assess the potential ground shaking that might be expected at the SONGS site.

The Commission thus finds that there is credible reason to believe that the design basis earthquake approved by the NRC at the time of the licensing of SONGS 2 and 3—a magnitude 7.0 earthquake on the Newport-Inglewood-Rose Canyon fault system 8 km from the site, resulting in ground shaking with a high frequency component peaking at 0.67 g—may underestimate the seismic risk at the site. This does not mean that the facility is unsafe—although the design basis earthquake may have been undersized, the plant was engineered with very large margins of safety, and would very likely be able to attain a safe shutdown even given the larger ground accelerations that might occur during a much larger earthquake. Assessing the safety of the SONGS facility is not under consideration with this application. As will be shown, the seismic design of the proposed project, which is under consideration, so far exceeds the ground accelerations anticipated from the design basis earthquake that it is reasonable to believe that it will be safe from even a much larger earthquake whose focus is even closer than the design basis earthquake.

ISFSI seismic design

Exhibit 9 shows the horizontal (X and Y) and vertical seismic spectra for which the proposed project is designed, together with spectra corresponding to SONGS seismic design, derived from the design basis earthquake described above. Superimposed on each is the Commission staff's calculation for the maximum spectra that would be required at the site according to the Uniform Building Code (Seismic Source A, epicentral distance <2 km, soil profile type S_C). The spectra labeled "SONGS" is derived from the NRC-approved "free-field" spectra and takes into account the interaction of the proposed structure with ground motions, which tends to amplify shaking. The design spectra corresponds to NRC Regulatory Guide 1.60, "Design response spectra for seismic design of nuclear power plants." Comparison of the design spectra with the calculated

spectra corresponding to the design basis earthquake show a very large factor of safety. The design spectra greatly exceeds that of the design basis earthquake at all frequencies. It is accordingly reasonable to conclude that even a much larger earthquake, a much lower epicentral distance, or both, will not produce ground shaking exceeding the design of the proposed project.

Accordingly, the Commission finds that the proposed project has been designed to assure seismic stability, consistent with section 30253 of the Coastal Act.

Surface Rupture and the Cristianitos Fault

No active faults were found at the SONGS site despite concerted efforts during geologic studies related to construction and licensing permits before the NRC (Fugro, 1977; Shlemon, 1977; 1979). Several faults were encountered, but without exception they are truncated by the overlying marine terrace deposits, whose age has been established as approximately 120,000 years (1975a; Fugro, 1975b), thus indicating that there has been no movement on those faults since at least that time. Hence, the risk of surface rupture at the SONGS site is very low.

The largest fault near the SONGS site is the Cristianitos fault, which passes less than one mile south of the site (Exhibit 10). This fault, which appears to be a low-angle normal fault, is similarly overlain by undisturbed terrace deposits (Exhibit 11), indicating that there has been no movement on it for at least 120,000 years (Shlemon, 1987). Green and others (1979) did indicate that the fault may connect with the Newport-Inglewood-Rose Canyon system, based on limited seismic data. Despite this potential connection, and the occurrence of two small (magnitude 3.3 and 3.8) earthquakes that occurred near (but not on) the fault trace 30 km north of SONGS in January 1975, the NRC and its USGS consultants concluded that the Cristianitos fault is inactive (U.S. Nuclear Regulatory Commission, 1981). Without more compelling evidence to the contrary, the Commission concurs with this assessment.

Commission staff received a letter from Aladdin Masry, a geologist from Hemet, California, dated 26 June 2000 and originally addressed to "USGS" (Exhibit 12). In this letter, Mr. Masry states that a "recent visit to camp San Onofre indicated that the San Cristianitos [sic] fault has moved and ruptures the ground." Mr. Masry goes on to express concern for the safety of the plant. Movement along a fault generally occurs through earthquakes. Movement sufficient to produce surface rupture should produce a substantial earthquake. Commission staff reviewed the earthquake database from the Southern California Earthquake Center for the period January 1998 through July 2000 and found no earthquake that could have been associated with movement of the Cristianitos fault. Commission staff visited the site on 10 January 2001, and found no evidence for surface rupture at the site. There has been recent landslide activity approximately ¼ mile south of the intersection of the Cristianitos fault and the sea cliff, and associated with the landslide are active ground fissures, some of them quite deep. It is possible that Mr. Masry mistook this activity for surface rupture of the Cristianitos fault. Fissures associated with landslides in the area have been previously mistaken for deep-seated faulting (Fugro, 1977).

Accordingly, the Commission finds that the stability of the site with respect to surface rupture can be assured consistent with section 30253 of the Coastal Act.

4.4.1.3. Liquefaction

As discussed below, under "bearing capacity," the SONGS site is underlain by dense sands of the San Mateo Formation. The upper terrace deposits which formerly overlaid the San Mateo formation were removed during construction of SONGS units 1, 2, and 3. Although the water table is very shallow at the site (+5 feet MSL; Southern California Edison Company, 1998), cyclic triaxial tests, field density tests, and very high blow counts during standard penetrometer tests show that liquefaction during the design basis earthquake should not occur. The minimum factor-of-safety against liquefaction in the plant area was calculated at 1.5 to 2.0 (Southern California Edison Company, 1998). The NRC concurred with the applicant's assessment that these calculated factors-of-safety against liquefaction of the San Mateo Formation at the site, for the design basis earthquake loading, are ample (U.S. Nuclear Regulatory Commission, 1981).

The applicant submitted a geotechnical investigation (Southern California Edison Company, 1995) in which liquefaction at the proposed project site itself was specifically addressed. They used the empirical approach of Seed and others (1985) relating Standard Penetration Test (SPT) blow count data from sites that have experienced liquefaction and at sites that have not experienced liquefaction for specific cyclic stress ratios. Using empirical data appropriate to the site characteristics (design basis earthquake, percent fines in the San Mateo Formation), the SPT blow count data indicate that the sands will not liquefy during the design basis earthquake (Exhibit 13).

Several geologists working in southern California have identified features in the San Onofre-Carlsbad area that they interpret to be the results of liquefaction that has occurred at various times in recent geologic history (Franklin and Kuhn, 2000; Kuhn et al., 1996; Kuhn et al., 2000; Shlemon, 2000). These features, including sand dikes, lenses, and disturbed bedding, were also mentioned by Dr. Mark Legg in his communication with Commission staff (Exhibit 7). Because these features appear to disturb Native American middens (Kuhn et al., 2000), it can be inferred that some of them, at least, are younger than about 10,000 years old, and perhaps as young as 2000-3000 years. Some such features occur in areas where the only likely source for the sand injected into higher layers of the soil is well-consolidated sandstones of Eocene age (Franklin and Kuhn, 2000). Kuhn (1996; Kuhn et al., 2000) cites these features as evidence for very large earthquakes in the area in the past.

Although these features are suggestive, the Commission does not consider them indicative of a serious liquefaction hazard at the site of the proposed project. Liquefaction in sands as dense as those encountered at the SONGS site have not previously been documented in even very large earthquakes; it is far more common for unconsolidated sands or artificial fills to fail by liquefaction. While it is possible that an earthquake much larger than the design basis earthquake might be capable of causing liquefaction of the San Mateo formation sands, no estimates have been provided by any of the cited studies as to the required ground shaking needed to induce such cyclic stresses. In light of the high factor of safety evident on Exhibit 13, and without credible data to the contrary, the Commission finds that the applicant has adequately addressed the liquefaction hazard at the site.

Accordingly, the Commission finds that the stability of the site with respect to liquefaction can be assured consistent with section 30253 of the Coastal Act.

4.4.1.4. Tsunamis

Several studies have been undertaken to address the potential for tsunami runup at the SONGS site. The most recent are summarized in the Safety Evaluation Report prepared by the NRC at the time of licensing hearings for SONGS 2 and 3 (Southern California Edison Company, 1998; U.S. Nuclear Regulatory Commission, 1981). Both local- and distant-sourced tsunamis were considered; the local-source tsunami (resulting from a magnitude 7.5 earthquake occurring 8 km offshore along the Newport-Inglewood-Rose Canyon fault system) was specifically modeled by Dr. Basil Wilson, consultant for Southern California Edison, at the time of original licensing review. By assuming that the vertical ground movement associated with this earthquake would be 7.1 feet, he calculated that a tsunami of 7.6 feet would result. By superimposing this tsunami on a 7-foot high tide (the 10% exceedance Spring high tide for the site) and a one-foot storm surge, the maximum "still" water level was found to be 15.6 feet MLLW. In its review, the NRC generally agreed with this model, arriving at a maximum still water level of 15.83 feet MLLW. In these calculations, the presence of the seawall was ignored.

The applicant submitted a geotechnical investigation (Southern California Edison Company, 1995) in which tsunami runup at the project site itself was specifically addressed. This evaluation made use of the tsunami calculations prepared for the SONGS 2 and 3 licensing application summarized above. Noting that the elevation of the proposed project's foundation pad is 20 feet MLLW, and the maximum still water level calculated by their consultant, the report notes that the foundation pad would be about 4.4 feet higher than proposed wave runup. To address the effects of breaking storm waves superimposed on this tsunami-generated still water runup, a wave uprush study used in the design of the seawall at the time of the SONGS Unit 1 design was applied. Again assuming that the seawall is not present, the wave would break at the riprap revetment protecting the walkway along the beach. The maximum breaking wave was found during the seawall study to be 8.8 feet high. If the seawall were not present, this wave would disperse as a wedge of water as it moved inland from the walkway. Volumetric calculations show that this wedge of water would fill the area between the riprap and the ISFSI site up to elevation 18.8 feet MLLW; 1.2 feet below the pad grade. The velocity of this wave would be low and the major impact to the site would be from flooding. Inundation of the pad itself would not harm either the pad or the casks (T. Yee, SCE, pers. comm., 2001).

For the initial examination of SONGS Units 2 & 3, the only tsunamis considered were those generated by earthquakes. Several recent tsunamis have been generated by massive submarine landslides (e.g., Kulikov et al., 1996; Rabinovich et al., 1999, Tappin et al., 2001[in press]). These tsunamis are often localized, but very large events. There have been a number of studies in recent years which appear to demonstrate that massive underwater landslides have occurred off the southern California coast, particularly in Santa Monica Bay, in the recent geologic past. As described by Dr. Legg in his letter (Exhibit 7):

It is likely that large **underwater landslides** would be triggered by severe earthquakes, and the possibility of both tectonic **displacement** and landslide inducement of tsunamis exists. Maximum expected run-up maps for locally generated tsunami are currently being prepared for coastal San Diego County (Bohannon and Gardner, 2001 (in press); Field and Edwards, 1993; Kuhn et al., 1994; Legg and Kamerling, 2001 (in press); Legg et al., 1995; Locat et al., 2001 (in press); Tappin et al., 2001 (in press); Watts and Raichlen, 1994).

These studies suggest that large local-source tsunamis could be generated by mechanisms other than those considered during licensing for SONGS 2 and 3, the basis for the 1995 SCE report. However, there have been no local runup studies based on this mechanism that are widely agreed upon, and certainly none for the SONGS site itself. As Dr. Legg indicates, tsunami runup maps are currently being prepared for San Diego County by individuals at the University of Southern California in conjunction with the Office of Emergency Services, but they are not currently available.

Commission staff accordingly concludes that although the proposed project may be threatened by tsunami, the major effect from an earthquake-generated tsunami would be site inundation. Possible inundation has been factored into the project design, and it would not adversely effect the stability of the site. There is also a potential for a submarine landslide to generate a tsunami that could threaten this site; however, current mapping and modeling do not provide any information of how the site would be effected by such an event. Even if the current models for locally-generated tsunami are insufficient, inundation of the pad by up to several feet of water should not damage the foundation pads or the storage casks.

Accordingly, the Commission finds that the stability of the site with respect to tsunami hazard can be assured consistent with section 30253 of the Coastal Act.

4.4.1.5. Bearing Capacity

The proposed ISFSI facility is a massive structure. The ISFSI facility for Unit 1, approved by the Commission in February 2000, will consist of a concrete pad 43 feet 6 inches wide by 188 feet long by 3 feet thick; the proposed pads for Units 2 and 3 will be of similar width, but may be longer as necessary to accommodate the module array. Assuming a unit weight of 145 pounds per cubic foot, the pad for Unit 1 will weigh approximately 3.5 million pounds. Each module consists of reinforced concrete shaped like a rectangular box 20 feet high, 9 feet wide and 23 feet long and weighs approximately 400,000 pounds. Into each module will be placed a stainless steel canister containing the spent fuel assemblies, weighing approximately 80,000 pounds. Thus, the 19 modules and pad approved for Unit 1 decommissioning will weigh approximately 12.6 million pounds. When completed, the complete project, which would consist of 104 modules, would weigh approximately 70 million pounds.

For perspective, this figure may be compared with the weight of the terrace deposits and the upper part of the San Mateo Formation formerly overlying the site. Since these deposits were approximately 70 feet thick, and had a unit weight of approximately 102-117 pounds per cubic foot, the volume formerly occupying the space above the Unit 1 pad weighed approximately 65

million pounds. Thus, even after the construction of the project, the weight applied to the San Mateo Formation at the site will be only about 20% of the pre-development weight.

More germane to the question of the ability of the site materials to support the ISFSI is a calculation of the bearing capacity of the San Mateo Formation relative to general or local shear failure. The applicant has supplied a calculation of static ultimate bearing capacity (Exhibit 14) indicating that, assuming a 67-foot square footing, the bearing capacity for the San Mateo Formation is 449,000 pounds per square foot. Commission staff has checked these calculations, and finds that the applicant may overestimate bearing capacity because (1), the project design specifications are for a rectangular (not square) pad only 43 feet six inches wide and (2), the effects of ground water, typically located at about elevation 5 MLLW (15 feet below grade), were not considered. Nonetheless, because the foundation will only be loaded to approximately 1750 pounds per square foot (Exhibit 15), a sufficient factor of safety exists to conclude that the static bearing capacity of the San Mateo Formation sands will not be exceeded.

The applicant also has submitted a dynamic analysis, SCE Calculation No. C-296-01.04, Rev. A (Exhibit 16), which demonstrates the capacity of the pad design under seismic loading, and an analysis of soil response to ground shaking using two bounding cases for estimates of soil properties (Exhibit 17). These calculations, which make use of 1.5 g horizontal and 1.0 g vertical ground accelerations (considerably higher than the NRC-approved SONGS criteria), demonstrates not only the adequacy of the foundation, but also shows that with the recommended steel reinforcement, the concrete pads will not fail during an earthquake with the specified ground accelerations.

Accordingly, the Commission finds that the materials at the site have sufficient bearing capacity to assure stability of the proposed development, consistent with section 30253 of the Coastal Act.

4.4.1.6. Coastal Erosion and Bluff Retreat

The proposed development lies within an industrial site, protected by a seawall, and has been protected from coastal erosion and bluff retreat for more than 25 years. To the south of the site, in the footwall of the Cristianitos fault, bedrock is the Monterey formation. This rock unit is known to be susceptible to landsliding throughout the state, and the seacliff in this area is collapsing through a series of large, ongoing landslides. This process appears to be the primary mechanism of bluff retreat in this region. To the north of the Cristianitos fault, bedrock consists of the relatively dense San Mateo Formation, a sandstone that is not highly susceptible to landsliding. Although no large landslides comparable to those to the south occur, the overall rate of seacliff retreat, measurable over geologic time (hundreds of thousands of years) would appear to be comparable, as no "point" or "embayment" in the coastline occurs where the bedrock types change. The mechanism for seacliff retreat in the San Mateo Formation are unclear, but the shape of the seacliff suggests dominantly marine process, such as undercutting, block collapse, and slumping of poorly consolidated upper bluff (terrace) materials.

The rate of bluff retreat in the San Onofre area is somewhat difficult to assess, due both to its episodic nature and to the varying mechanisms of retreat along the coast. There is no doubt that

active bluff retreat is occurring south of the site, at San Onofre State Beach where bedrock is the Monterey Formation and where runoff has been concentrated through the creation of new drainage systems associated with the construction of Interstate 5 (Kuhn, 2000). In the vicinity of the proposed project, however, there has been little appreciable bluff retreat or headward erosion of the terrace deposits for at least the last 120 years. The U.S. Army Corps of Engineers reviewed U.S. Coast and Geodetic Surveys (USCGS) along the San Diego Coast and, based on their ability to locate all of the triangulation monuments installed by the USCGS, concluded that "the bluff line had, between 1889 and 1934, remained unchanged" (U.S. Army Corps of Engineers, 1960). The monuments also were located in 1954, indicating no measurable retreat of the bluff line at that time as well. Although no data are available since that time, comparison of aerial photographs and maps indicate that there has been little measurable bluff retreat through 1998 (Kuhn, 2000).

There is, however, substantial subaerial erosion of the terrace deposits and the Monterey Formation south of the SONGS site (Kuhn, 2000). This erosion takes the form of headward erosion of gullies, slumping of the face of bluffs, and deep-seated landslides. These landslides are seated in the Monterey Formation south of the Cristianitos Fault, and do not affect the SONGS site, which is underlain by the dense sandstones of the San Mateo Formation.

In any case, any bluff erosion has been severely retarded over natural rates at the SONGS site because: 1) armoring of exposed natural and artificial cliff exposures in gunite, and 2) the installation of a seawall protecting the entire site. The former tends to protect the affected cliffs from subaerial erosion, and the latter effectively prevents marine erosion. The seawall consists of a sheet pile wall driven 18 feet below finish grade of the SONGS facility (to a depth of approximately 2 feet MLLW), a 2.5 inch layer of gunite secured by wire mesh, and a rock revetment extending seaward 12 feet from the seawall. Documents furnished by the applicant indicate that the sheet pile wall is subject to corrosion, including through-going holes. This, together with the shallow depth of emplacement, lack of foundation elements, and the lack of an engineered key to the rip-rock revetment, suggest that continued maintenance of the seawall may be necessary for its continued function. Nonetheless, the low bluff retreat rates indicate that it is not needed to guard against bluff retreat at the SONGS site.

The applicants indicate further that the seawall is not necessary for the protection of the proposed project; in particular the evaluation of tsunami hazard described above assumes that the seawall is not present. Given that section 30253 of the Coastal Act requires that new development not depend on shoreline protection devices, it is necessary to evaluate whether the proposed project would be safe from coastal erosion and bluff retreat without the seawall. No expected economic life of the development is available, but the site is intended as a temporary facility awaiting licensing of a Federal high-level nuclear waste depository, which will probably not be available for at least ten years. The SONGS Units 2 and 3 operating licenses expire in 2022.

Given the setback of the proposed pad, at least 180 feet from the seawall, and its elevation at approximately 20 feet MLLW, and the low rate of coastal bluff retreat where bedrock is the San Mateo Formation, the Commission finds that facility should be safe from coastal erosion for its anticipated useful life. Sea level rise that might occur over the expected life of the facility

likewise is not expected to effect the site, given its elevation of 20 feet MLLW and its setback from the seawall.

Accordingly, the Commission finds that the proposed development will be safe from coastal erosion and bluff retreat and will not require the construction of protective devices that would substantially alter natural landforms along bluffs and cliffs, as required by section 30253 of the Coastal Act.

4.4.1.7. Slope Stability

The proposed project is located approximately 200 feet south of a cut slope approximately 70 feet high, and approximately 170 feet west of a somewhat lower cut slope. Both slopes are covered in gunite, although a small portion (approximately 1/3) of the slope to the north is not. During studies for the SONGS Unit 1 ISFSI facility (Southern California Edison Company, 1995), the applicant produced slope stability analyses to determine the minimum factor of safety of these slopes during seismic shaking corresponding to the design basis earthquake (described above). These analyses, performed using the method of Makdisi and Seed (1977), are for four cross sections through the cut slopes (Exhibit 18), and demonstrate minimum factors of safety ranging from 1.77 to over 3. The study concluded that:

The small displacements estimated using the Makdisi-Seed procedure suggest that only minor sloughing of the near slope surface material is likely to occur during design basis earthquake ground shaking. Minor sloughing will not adversely affect the ISFSI which is located at distances greater than about 60 feet [sic] from the toe of the slopes. Therefore, slope stability will not be a concern for the ISFSI facility since the 60 feet offset provides a sufficient standoff distance.

Despite this conclusion, the applicant performed an additional evaluation to determine, if a slope failure were to occur, what distance the soil could be expected to travel (Hadidiafarnj, 2000). The concern was whether landslide material could bury the dry storage casks, blocking their cooling vents (a nuclear safety issue). This calculation indicated that the maximum distance the soil would travel would be 120 feet, and the site for the ISFSI was moved accordingly to isolate the site from the potential runout zone.

The Commission finds that these analyses adequately address the stability of the cut slopes adjacent to the proposed project. Concern has been raised that ground shaking during the maximum possible earthquake at the site may, in light of recent discoveries, exceed the design basis earthquake (see discussion above, under "ground shaking"). Nevertheless, the high factors of safety demonstrated by the calculations cited above suggest that it is reasonable to believe that the cut slopes will remain stable even during a much larger earthquake whose focus is even closer than the design basis earthquake.

South of the site, at San Onofre State Beach, several coalescing large active landslides affect the coastal bluff (Kuhn, 2000; Kuhn and McArthur, 2000). These slides are each seated within the Monterey Formation, which is known to contain weak layers and to be prone to landsliding throughout California. The Monterey Formation is not known to occur near the surface north of the Cristianitos fault, and landslides of the character occurring south of the fault have not been

observed to the north of it. The SONGS site, lying north of the Cristianitos fault, is underlain by the San Mateo Formation to depths of at least 900 feet as confirmed through boreholes undertaken prior to development of SONGS Unit 1. Accordingly, there is very little risk that a landslide similar to those in San Onofre State Beach south of the SONGS site could involve the SONGS site itself. If the site is, nevertheless, subject to a slow-moving, deep seated landslide similar to those south of the site, this should be manifested by differential vertical movement across the site. Commission staff asked for, and received, settlement records from throughout the SONGS site. These records show the elevation of over 100 survey monuments as determined by repeated surveys extending from 1975 to 1999. Very little settlement occurred at the site, probably due primarily to the overconsolidation of the finish grade due to removal of the overlying terrace deposits. The maximum settlement observed is less than 0.1 inch, and there is no indication of differential settlement across the site, as might be expected during a rotational landslide.

Accordingly, the Commission finds that the stability of the slopes adjacent to and underlying the proposed project is assured consistent with section 30253 of the Coastal Act.

4.4.1.8. Conclusions

For all of the reasons described above, the Commission finds that the proposed project will minimize risk to life and property pursuant to section 30253(1) and, pursuant to section 30253(2), will not create nor contribute significantly to erosion, geologic instability, or destruction of the site or surrounding area. Further, the proposed project will not require the construction of protective devices, and does not depend on the existing seawall installed at the site.

4.4.2 Public Access and Recreation

Coastal Act Section 30211 states:

Development shall not interfere with the public's right of access to the sea where acquired through use or legislative authorization, including, but not limited to, the use of dry sand and rocky coastal beaches to the first line of terrestrial vegetation.

Coastal Act Section 30220 states:

Coastal areas suited for water-oriented recreational activities that cannot be readily provided at inland water areas shall be protected for such uses.

The nearest public access to coastal waters or recreation areas is at San Onofre State Beach, directly to the north and south of SONGS. A pathway directly in front of the SONGS site connects these two beach areas. There is no public access to the beach through the SONGS site.

Public access to and recreation on San Onofre State Beach will not be restricted in any way by the proposed project. Additionally, the pathway in front of the SONGS site will remain

accessible for pedestrian passage. The project will take place entirely within the SONGS 1, 2, and 3 boundaries. No development will extend onto or adjoin San Onofre State Beach.

4.4.2.1 Conclusion

Because the proposed project will not affect public access or recreation areas, the Commission finds that the proposed project is consistent with Coastal Act Sections 30211 and 30220.

4.4.3 Marine Resources, Water Quality, and Environmentally Sensitive Habitat Areas

Coastal Act Section 30230 states:

Marine resources shall be maintained, enhanced, and where feasible, restored. Special protection shall be given to areas and species of special biological or economic significance. Uses of the marine environment shall be carried out in a manner that will sustain the biological productivity of coastal waters and that will maintain healthy populations of all species of marine organisms adequate for long-term commercial, recreational, scientific, and educational purposes.

Coastal Act Section 30231 states in part:

The biological productivity and the quality of coastal waters... appropriate to maintain optimum populations of marine organisms and for the protection of human health shall be maintained and, where feasible, restored....

Coastal Act Section 30240 states in part:

Environmentally sensitive habitat areas shall be protected against any significant disruption of habitat values, and only uses dependent on those resources shall be allowed within those areas.

4.4.3.1 Marine Resources and Water Quality

According to the applicants, there will be no liquid discharges from the spent fuel storage facility. Existing drainage infrastructure may be modified to accommodate the new facility but the project will not change the existing drainage pattern from the site. The existing storm or yard drains, water treatment facilities, and sump will not be altered. However, during construction of the proposed project, stormwater may be generated and could contribute to sediment loading of receiving waters.

Currently, stormwater and other non-radioactive liquid waste streams generated by SONGS 1 are discharged under an existing industrial National Pollutant Discharge Elimination System (NPDES) permit (#CA0001228), renewed by the San Diego Regional Water Quality Control Board on February 11, 2000. The proposed project will be covered under this NPDES permit. The permit contains specific numeric effluent limits for all suspected pollutants associated with

industrial activities at SONGS 1 and runoff from the site. Stormwater flows are co-mingled with other industrial discharges and monitored for effluent limit exceedances at several stages prior to final discharge through the SONGS 1 outfall. The applicants are required to report any exceedances to the RWQCB within 24 hours and propose remedies for immediate compliance with the effluent limits. During the construction of the proposed project, the applicants will continue to perform routine sampling of liquid effluents consistent with the SONGS 1 NPDES permit and NRC effluent control procedures.

Best Management Practices contained in the applicants' Storm Water Pollution Prevention Plan (prepared as a condition to the NPDES permit) specifically assess the potential for discharges of hazardous waste and material to the ocean through plant site runoff, sludge and waste disposal, spillage or leaks, and drainage from material storage areas. In addition, training for good housekeeping practices and emergency response is provided to personnel, and regular site inspections are performed. Water used for dust suppression will be collected and either filtered or treated at the wastewater treatment plant prior to discharge. Stormwater runoff will be collected, co-mingled with other discharges, monitored, and treated when necessary, prior to discharge through the SONGS 1 outfall.

However, during precipitation events, exposed debris or soil materials can runoff into the SONGS 1 yard drains and potentially contribute to increased sediment loading to receiving waters. This increased sediment loading can potentially increase turbidity of coastal waters, resulting in decreased water clarity, and over the long-term, can impact epifaunal organisms. **Special Condition 1** requires the applicants dispose of construction debris, at the earliest practicable opportunity, generated as part of the proposed project at an appropriate offsite facility. The condition also requires the applicants to cover or contain any debris or material left on-site that could potentially contribute to increased sediment loading to receiving waters during precipitation events.

Special Condition 2 requires the applicants to monitor and remove sediment and other material collected in an on-site sump before such sediment or material reach quantities sufficient to pose a risk to the proper functioning of the sump. This sump has a nominal capacity of 10,000 gallons and collects stormwater flowing into yard drains from the SONGS 1 site. The sump has a weir configuration designed to trap and settle sediment. As mentioned above, these waste discharges are sampled and treated, if necessary, prior to discharge to receiving waters. However, if the sump is not properly monitored and maintained, its ability to effectively remove sediment can be compromised, resulting in additional sediment loading and turbidity to receiving waters, as discussed above.

In addition to regulating runoff from SONGS 1 essentially as a point source pollutant under the existing NPDES permit, SONGS 1 is currently covered under a general stormwater NPDES permit for industrial activities. However, because the effluents limits contained in the individual NPDES permit, as described above, are more specific and stringent than the general stormwater NPDES permit, compliance with the former provides a higher level of protection to receiving waters.

To assure that the applicants have sufficient financial resources to implement Special Condition 2 for the life of the project, **Special Condition 3** requires that, prior to project construction, the applicant shall establish a sump maintenance fund similar in form and content as the draft "SONGS ISFSI Yard Sump Maintenance Trust Account" (Exhibit 19). The fund shall provide for the full costs of monitoring and maintaining the sump for the life of the project (through November 15, 2022) and shall represent the present value of the full cost of all monitoring and maintenance costs that the applicants will incur over the life of the permit. The maintenance fund shall be reviewed and approved by the Executive Director, in coordination with the applicants.

Based on at least 15 years of operating history, the applicants estimate total annual sump maintenance and monitoring costs of \$7,364.00, including labor costs. These costs are itemized in the table below. In addition to chemical analyses of sump discharges, as required by the NPDES permit, it is visually inspected periodically for the presence of significant amounts of oils or sediments. When visual inspection indicates a significant accumulation of sediment or oil in the sump, a vacuum truck is contracted to pump out the sump contents, clean the sump if necessary, and dispose of the contents at a permitted offsite disposal facility.

Table 1. SONGS Units 2 and 3 Sump Maintenance and Monitoring Costs

| Task | Cost |
|---|------------------|
| Required inspections | \$1535.00 |
| Sampling and chemical analysis | \$1044.00 |
| Removal of sand and debris from yard sump | \$3991.00 |
| Sub-total | \$6570.00 |
| Contingency | \$794.00 |
| Total | \$7364.00 |

The attached draft "SONGS ISFSI Yard Sump Maintenance Trust Account" Agreement (Trust Account), prepared by the applicant in coordination with Commission staff, provides that all funds deposited in the Trust Account are to be held in trust and shall be disbursed only for expenditures for storm water sump monitoring and maintenance, consistent with Special Condition 2. A deposit of \$136,000 will be made by the applicants to the Trust Account at its inception, which is the estimated present value of the sump monitoring and maintenance costs plus the estimated present value of the expenses of the trustee for the life of the project through December 31, 2022. Over its life, the account balance is assumed to grow at an average annual percentage rate of 6.0% (in a federally insured certificate of deposit or U.S. Treasury Bill), while the cost of sump maintenance, estimated at \$7,500/year, is assumed to inflate at an average annual rate of 3.0%. Using a more conservative growth rate of 5.5% and inflation rate of 3.5%, the principal amount would be sufficient to cover sump monitoring and maintenance costs for the life of the project. The account will be debited \$2,000 each year for bank administrative fees.

The assumptions for sump maintenance cost inflation and trust fund growth are derived from the applicants' Economic Assumptions Manual, dated July 1, 1999, which is part of the applicants' standard accounting practices that are independently audited periodically pursuant to federal regulations.

The Commission recognizes that Special Conditions 2 and 3 will substantially minimize any impacts to water quality and coastal resources caused during project construction or operation. However, there is still a possibility that residual or other impacts due to, for example, untimely sump maintenance or stormwater flows that overwhelm the capacity of the sump could adversely affect water quality and coastal resources. Additionally, according to the applicants and the NRC, a federal repository for permanent spent fuel storage may be established by the U.S. Department of Energy and begin accepting transfers of spent nuclear fuel generated by the nation's commercial nuclear facilities, including the SONGS, as early as 2010. Thus, the proposed project may become unnecessary after this date. The Commission finds that under a circumstance in which it is foreseeable that the underlying rationale for a project may change or even disappear, it is reasonable place a finite limit on the term of the permit that authorizes that project. In this connection the Commission notes that the SONGS Units 2 and 3 NRC operating licenses expire on February 16, 2022 and November 22, 2022, respectively. Accordingly, **Special Condition 4** limits the term of this coastal development permit to November 15, 2022, the later of the two above-identified expiration dates, thus eliminating any potential residual or other impacts to coastal resources or water quality that may occur after this date.

However, according to the applicants, decommissioning Units 2 and 3 may take upwards of 20 years after they cease operating, which may require onsite storage of spent fuel during this time. Additionally, the transfer of spent fuel from Units 2 and 3 to the federal repository may not take place immediately after it begins accepting transfers of spent fuel as fuel from other nuclear power plants may have priority given their older age. Thus, the Commission acknowledges that the applicants may need to amend CDP No. E-00-014 to extend its term beyond November 15, 2022. To do so the applicants must prior to this expiration date submit to the Commission an application for an extension of the term of the permit supported by: 1) evidence that additional storage time beyond November 15, 2022 is needed during the decommissioning of Units 2 and 3; 2) evidence that a federal repository will not become operational or available to accept Units 2 and 3 spent fuel during the term of this permit or; 3) other newly discovered material information, which they could not, with reasonable diligence, have discovered and produced before the permit was granted and which justifies an extension of the term of the permit.

Finally, **Special Condition 5** states that this coastal development permit is only for the development described in the project description. Pursuant to Title 14 California Code of Regulations Section 13253(b)(6), the exemptions otherwise provided in Public Resources Code Section 30610(b) shall not apply to the project. Accordingly, any future improvements to the permitted structure, including but not limited to any structural or physical modifications to the Independent Spent Fuel Storage Installation, an increase in storage capacity of spent nuclear fuel, the storage of spent nuclear fuel from nuclear power plants other than the San Onofre Nuclear Generating Station Units 2 and 3, and the storage of anything other than spent nuclear fuel which are proposed within the restricted area shall require an amendment to coastal development permit

E-00-014 from the Commission or shall require an additional coastal development permit from the Commission or from the applicable certified local government. This condition ensures that the Commission will have an opportunity to review changes to the project and identify any potential impacts to marine resources or water quality not considered or mitigated in this staff report.

4.4.3.2 Environmentally Sensitive Habitat Areas ("ESHA")

The proposed project will take place on land that is currently occupied by SONGS Unit 1, an existing, disturbed industrial site with no on-site biological resources. The entire SONGS site is situated upcoast and downcoast from the San Onofre State Beach and is bordered on the west by the Pacific Ocean and beach area. According to the resource ecologist overseeing the San Onofre State Beach, high-quality gnatcatcher coastal sage habitat exists in the state beach approximately 1.5 miles north of SONGS 1 and 0.5 mile south of the SONGS Units 2 and 3 (Pryor, 2000). Gnatcatchers have been observed in this habitat. The U.S. Fish and Wildlife Service listed the gnatcatcher in 1993 as a federal threatened species.

The proposed project will involve the installation of lighting as required by NRC federal regulations. The U.S. Fish and Wildlife Service has previously required that artificial lighting from development be shielded or angled away from gnatcatcher habitat to minimize potential threats such as predation, collision, and decreased breeding success (Miller, 2000). Current lighting requirements for the SONGS 1, 2, and 3 site are specified by NRC federal regulations. After SONGS 1 is fully decommissioned, the existing perimeter lighting will be removed. New lighting will be installed, consistent with NRC federal regulations, for the SONGS 1, 2, and 3 fuel storage facility. However, the new lighting will not be more intense than the existing SONGS 1 perimeter lighting. Thus, there is no potential for project-related lighting to adversely impact nearby environmental sensitive habitat areas or the gnatcatcher.

The U.S. Fish and Wildlife Service has established a 60 dbA (decibel) threshold or criterion for analyzing noise impacts to the gnatcatcher or when assessing the level of a take of this species (Hays, 2000). Noise levels at or above this threshold are assumed to indirectly affect the reproductive success of songs birds, including the gnatcatcher, increase stress levels, and interfere with predator avoidance, among other impacts (Miller, 2000). Thus, if project-related noise reached beyond the SONGS site and into the gnatcatcher habitat, which includes Units 1, 2, and 3, the gnatcatcher may be impacted, especially during nesting season (February 1 to July 15). However, according to the applicants, any noise generated from project-related activities will be short-term and is not expected to result in any noticeable change in noise levels beyond the entire SONGS site.² Furthermore, the entire SONGS site is physically sited 50-70 feet below the surrounding geography, providing a noise buffer. Any project-related noise extending beyond the SONGS site is expected to attenuate to undetectable levels before reaching nearby gnatcatcher habitat. Thus, the proposed project will not disrupt the resources of the adjacent ESHA.

² It should be noted that a railroad line and Interstate Highway 5 lies directly to the east of SONGS and the San Onofre State Beach.

4.4.3.3 Conclusion

The Commission finds that with the imposition of **Special Conditions 1, 2, 3, 4, and 5** the proposed project will be carried out in a manner that will sustain the biological productivity of coastal waters, maintain healthy populations of all potentially affected species of marine organisms, and protect environmentally sensitive habitat areas in conformity with the requirements of Coastal Act Sections 30230, 30231, and 30240.

4.4.4 Visual Quality

Coastal Act Section 30251 states in part:

The scenic and visual qualities of coastal areas shall be considered and protected as a resource of public importance. Permitted development shall be sited and designed to protect views to and along the ocean and scenic coastal areas, to minimize the alteration of natural land forms, to be visually compatible with the character of surrounding areas, and, where feasible, to restore and enhance visual quality in visually degraded areas.

The SONGS site is situated directly on the Pacific Ocean and bordered on the east by Interstate 5. With the exception of the SONGS 1 sphere enclosure building (scheduled for demolition in 2006), which is partially visible from Old Highway 101 and Interstate 5, current views of the SONGS 1 site are generally obscured or blocked. Looking south from the bluff north of SONGS, the bluff blocks any view of the project area. From south of the SONGS site, Units 2 and 3 block views of the project area. From the beach looking landward, an existing SONGS seawall blocks most views into the project area.

The proposed fuel storage facility is estimated to reach 42 feet or 22 feet above the existing grade, but will not be visible from areas accessible to the public. Similarly, construction equipment, including a mobile crane, will not be visible from outside the SONGS site.

4.4.4.1 Conclusion

Since the proposed project will not be visible from areas accessible to the public, the Commission finds that the proposed project is consistent with the requirements of Coastal Act section 30251.

4.4.5 Air Quality

Coastal Act Section 30253(3) requires that:

New development shall:

...

(3) Be consistent with requirements imposed by an air pollution control district or the State Air Resources Control Board as to each particular development.

Since the proposed project's emission sources will be construction or other equipment brought on the project site temporarily, the San Diego County APCD will require permits, if necessary, for these individual sources of emissions. Internal combustion (IC) engines powering, for example, generators and pumps, portable diesel generators, cranes and other construction equipment brought on the SONGS 1 site will either have individual APCD permits, California registration³, or be permit exempt (drive engines that power construction equipment are exempted by the APCD).

4.4.5.1 Conclusion

The Commission finds that the project will be carried out consistent with the requirements of the San Diego APCD and thus is consistent with Coastal Act Section 30253(3).

4.5 THE CALIFORNIA ENVIRONMENTAL QUALITY ACT (CEQA)

Section 13096 of the Commission's administrative regulations requires Commission approval of CDP applications to be supported by a finding showing the application, as modified by any conditions of approval, to be consistent with any applicable requirements of the California Environmental Quality Act (CEQA). Section 21080.5(d)(2)(A) of the CEQA prohibits approval of a proposed development if there are feasible alternatives or feasible mitigation measures available that would substantially lessen any significant impacts that the activity may have on the environment.

The project as conditioned herein incorporates measures necessary to avoid any significant environmental effects under the Coastal Act, and there are no less environmentally damaging feasible alternatives. Therefore, the Commission finds that the proposed project is consistent with the resource protection policies of the Coastal Act and with the CEQA.

³ Portable equipment can be registered with a local air district or the state Air Resources Board. The registration process imposes emission limits on certain portable equipment (e.g., internal combustion engines, abrasive blast booths) but is considered a more expeditious permitting process.

APPENDIX A STANDARD CONDITIONS

1. Notice of Receipt and Acknowledgment. The permit is not valid and development shall not commence until a copy of the permit, signed by the permittee or authorized agent, acknowledging receipt of the permit and acceptance of the terms and conditions, is returned to the Commission office.
2. Expiration. If development has not commenced, the permit will expire two years from the date on which the Commission voted on the application. Development shall be pursued in a diligent manner and completed in a reasonable period of time. Application for extension of the permit must be made prior to the expiration date.
3. Interpretation. Any questions of intent of interpretation of any condition will be resolved by the executive director or the Commission..
4. Assignment. The permit may be assigned to any qualified person, provided assignee files with the Commission an affidavit accepting all terms and conditions of the permit.
5. Terms and Conditions Run with the Land. These terms and conditions shall be perpetual, and it is the intention of the Commission and the permittee to bind all future owners and possessors of the subject property to the terms and conditions.

APPENDIX B

SUBSTANTIVE FILE DOCUMENTS

Coastal Development Permit Application Materials

Application for Coastal Development Permit E-00-014, as amended.

Agency Permits and Orders

Order No. 2000-04, NPDES Permit No. CA0001228, Waste Discharge Requirements for the Southern California Edison Company San Onofre Nuclear Generating Station, Unit 1, San Diego County.

Environmental Documents and Reports

"Final Environmental Statement Related to the Operation of the San Onofre Nuclear Generating Station Unit 1", Southern California Edison Company and San Diego Gas and Electric Company, Docket No. 50-206, approved by the U.S. Atomic Energy Commission, October 1973.

"Final Generic Environmental Impact Statement on Decommissioning of Nuclear Facilities-NUREG-0586", prepared by the U.S. Nuclear Regulatory Commission, August 1988.

"Environmental Assessment by the Office of Nuclear Reactor Regulation Relating to the Conversion of the Provisional Operating License to a Full-Term Operating License", Southern California Edison Company and San Diego Gas and Electric Company, San Onofre Nuclear Generating Station Unit 1, Docket Number 50-206, approved by the U.S. Nuclear Regulatory Commission September 16, 1991.

Post Shutdown Decommissioning Activities Report for San Onofre Nuclear Generating Station Unit 1, submitted to the U.S. Nuclear Regulatory Commission, December 1998.

Storm Water Pollution Prevention Plan, as amended, submitted to the California Regional Water Quality Control Board, San Diego Region, September 27, 2000.

Lease Documents

Grant of Easement to Southern California Edison Company and San Diego Gas and Electric Company by United States Department of the Navy, May 12, 1964.

References cited in section 4.4.1

Abrahamson, N. A., and Silva, W. J., 1997, Empirical response spectra attenuation relations for shallow crustal earthquakes: Seismological Research Letters, v. 68, p. 94-127.

Bohannon, R., Eittreim, S., Childs, J., Geist, E., Legg, M., Lee, C., Sorlien, C., and Busch, L., 1990, A seismic-reflection study of the California continental borderland [abs]: Eos, Transactions of the American Geophysical Union, v. 71, p. 1631.

- Bohannon, R. G., and Gardner, J., 2001 (in press), Submarine landslides of San Pedro Sea Valley, southwest Los Angeles basin, *in* Watts, P., Synolakis, C. E., and Bardet, J. P., eds., Prediction of underwater landslide hazards: Rotterdam, Balkema.
- Bohannon, R. G., and Geist, E., 1998, Upper crustal structure and Neogene tectonic development of the California continental borderland: Geological Society of America Bulletin, v. 110, no. 6, p. 779-800.
- Boore, D. M., Joyner, W. B., and Fumal, T. E., 1997, Equations for estimating horizontal response spectra and peak acceleration from western North American earthquakes: Seismological Research Letters, v. 68, p. 128-153.
- Campbell, K. W., 1997, Empirical near-source acceleration relationships for horizontal and vertical components of peak ground acceleration, peak ground velocity, and pseudo-absolute acceleration response spectra: Seismological Research Letters, v. 68, p. 154-179.
- Collins, S. J., 1997, Director's Decision Under 10 CFR Section 2.206: U.S. Nuclear Regulatory Commission, Office of Nuclear Reactor Regulation, 28 p.
- Crouch, J. K., and Suppe, J., 1993, Late Cenozoic tectonic evolution of the Los Angeles basin and inner California borderland: A model for core complex-like crustal extension: Geological Society of America Bulletin, v. 105, no. 11, p. 1415-1434.
- Ehlig, P. L., 1977, Geologic report on the area adjacent to the San Onofre Nuclear Generating Station, northwestern San Diego County, California unpublished geologic report for Southern California Edison Company, 26 p.
- Field, M. E., and Edwards, B. D., 1993, Submarine landslides in a basin and ridge setting, southern California, *in* Schwab, W. C., Lee, H. J., and Twichell, D. C., eds., Submarine landslides: Selected studies in the U.S. Exclusive Economic Zone, U.S. Geological Survey Bulletin 2002, p. 176-183.
- Franklin, J. P., and Kuhn, G. G., 2000, Paleoseismic features exposed by trenching the lowest coastal terrace at Carlsbad, California, *in* Legg, M. R., Kuhn, G. G., and Shlemon, R. J., eds., Neotectonics and coastal instability: Orange and northern San Diego Counties, California: Long Beach, California, AAPG-Pacific Section and SPE-Western Section, p. 1-13.
- Fugro, Inc., 1974a, Analysis of C and D type features at the San Onofre Nuclear Generating Station: Fugro, Inc. unpublished geologic report for Southern California Edison Company, 19 p.
- Fugro, Inc., 1974b, Analysis of geologic features at the San Onofre Nuclear Generating Station: Fugro, Inc. unpublished geologic report for Southern California Edison Company, 32 p.
- Fugro, Inc., 1975a, Geomorphic analysis of terraces in San Juan and Bell Canyons, Orange County, California: Fugro, Inc. unpublished geologic report for Southern California Edison Company 74-069-01, 11 p.
- Fugro, Inc., 1975b, Summary of geomorphic and age data for the first emergent terrace (QT₁) at the San Onofre Nuclear Generating Station: Fugro, Inc. unpublished geologic report for Southern California Edison Company 74-069-02, 30 p.

- Fugro, Inc., 1976, Final report on geologic features at the San Onofre Nuclear Generating Station, Units 2 and 3: Fugro, Inc. unpublished geologic report for Southern California Edison Company, 24 p.
- Fugro, Inc., 1977, Geologic investigation of offsets in Target Canyon, Camp Pendleton, California: Fugro, Inc. unpublished geologic report for Southern California Edison Company 77-206-03, 19 p.
- Gastil, R. G., Kies, R., and Melius, D. J., 1979, Active and potentially active faults; San Diego County and north-western-most Baja California, *in* Abbott, P. K., and Elliott, W. J., eds., Earthquakes and other perils, San Diego region, San Diego Association of Geologists Field Trip Guidebook, p. 47-60.
- Geomatrix Consultants Inc., 1994, Seismic Source Characterization: Geomatrix Consultants, Inc., unpublished report, 86 p.
- Geomatrix Consultants Inc., 1995a, Earthquake recurrence relationships: Geomatrix Consultants, Inc., unpublished report, 9 p.
- Geomatrix Consultants Inc., 1995b, Maximum magnitude distributions: Geomatrix Consultants, Inc., unpublished report, 4 p.
- Grant, L. B., Mueller, K. J., Gath, E. M., Cheng, H., Edwards, R., Lawrence, Munro, R., and Kennedy, G. L., 1999, Late Quaternary uplift and earthquake potential of the San Joaquin Hills, southern Los Angeles basin, California: *Geology*, v. 27, no. 11, p. 1031-1034.
- Greene, H. G., Bailey, K. A., Clarke, S. H., Ziony, J. I., and Kennedy, M. P., 1979, Implications of fault patterns of the inner Continental Borderland between San Pedro and San Diego, *in* Abbott, P. L., and Elliott, W. J., eds., Earthquakes and other perils -- San Diego Region, San Diego Association of Geologists Guidebook, p. 21-27.
- Hadidiafarnj, H., 2000, ISFSI Pad Slope Stability Evaluation: Southern California Edison Company engineering calculations C-296-01.03, 60 p.
- Jennings, C. W., 1994, Fault activity map of California and adjacent areas: California Division of Mines and Geology, Geologic Data Map No. 6, scale 1:750,000.
- Kuhn, G., Legg, M. R., and Frost, E., 1994, Large pre-historic earthquake(s) in coastal San Diego County, California, Paleoseismology Workshop Proceedings, September 1994: Marshall, California, U.S. Geological Survey Open-File Report 94-568, p. 100-103.
- Kuhn, G. G., 2000, Sea cliff, canyon, and coastal terrace erosion between 1887 and 2000: San Onofre State Beach, Camp Pendleton Marine Corps Base, San Diego County, California, *in* Legg, M. R., Kuhn, G. G., and Shlemon, R. J., eds., Neotectonics and coastal instability: Orange and northern San Diego Counties, California: Long Beach, California, AAPG-Pacific Section and SPE-Western Section, p. 31-87.
- Kuhn, G. G., Legg, M. R., Johnson, A., Shlemon, R. J., and Frost, E. G., 1996, Paleoliquefaction evidence for large pre-historic earthquake(s) in north-coastal San Diego County, California, *in* Munasinghe, T., and Rosenberg, P., eds., *Geology and natural resources of*

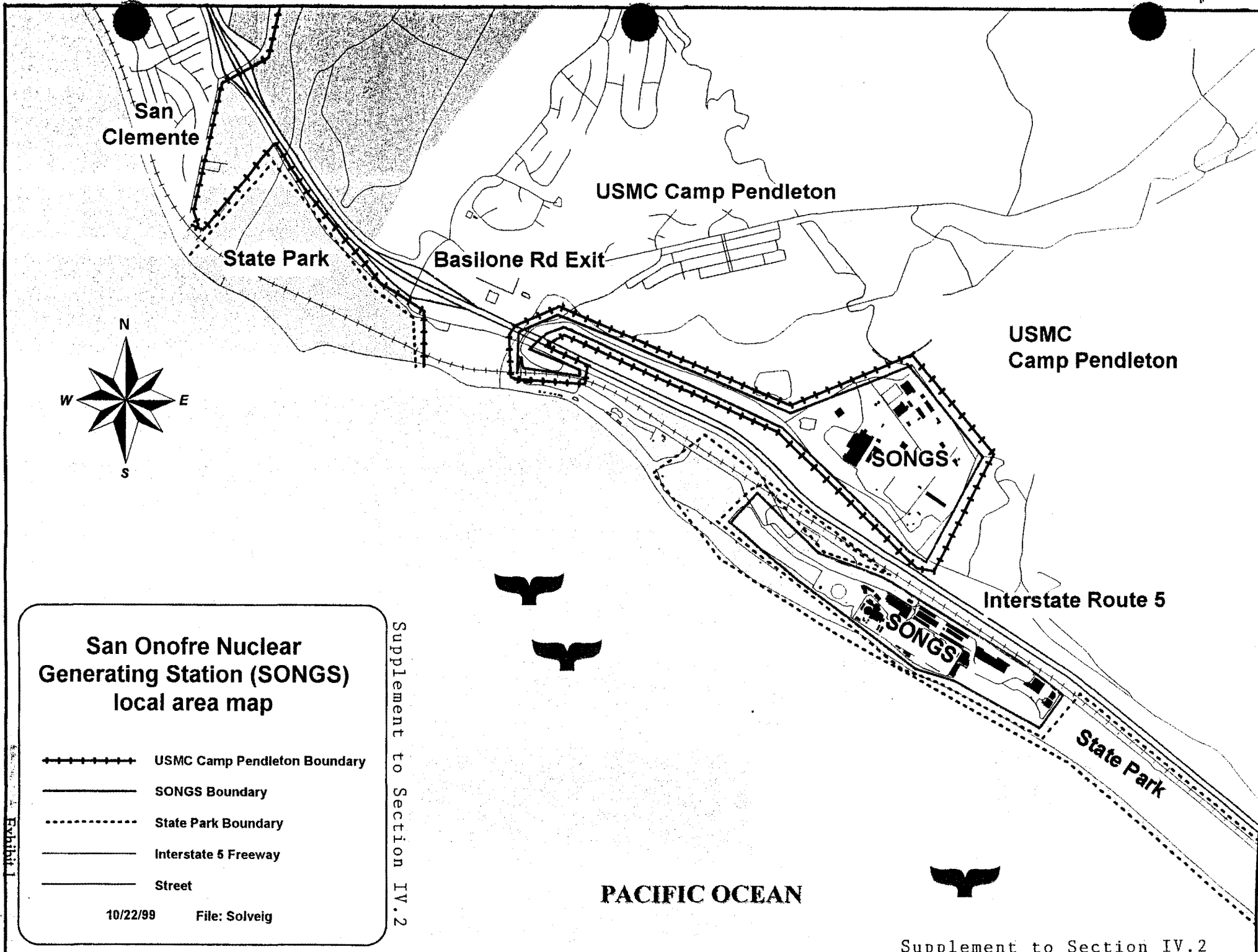
- coastal San Diego county, California, San Diego Association of Geologists Field Trip Guidebook, p. 16-24.
- Kuhn, G. G., Legg, M. R., and Shlemon, R. J., 2000, Neotectonics in the north coastal area, San Diego County, California, *in* Legg, M. R., Kuhn, G. G., and Shlemon, R. J., eds., Neotectonics and coastal instability: Orange and northern San Diego Counties, California: Long Beach, California, AAPG-Pacific Section and SPE-Western Section, p. 88-104.
- Kuhn, G. G., and McArthur, D. S., 2000, Beaches and sea cliffs of central and northern San Diego County, *in* Legg, M. R., Kuhn, G. G., and Shlemon, R. J., eds., Neotectonics and coastal instability: Orange and northern San Diego Counties, California: Long Beach, California, AAPG-Pacific Section and SPE-Western Section, p. 104-122.
- Kulikov, E. A., Rabinovich, A. B., Thomson, R. E., et al., 1996, The landslide tsunami of November 3, 1994, Skagway Harbor, Alaska: *Journal of Geophysical Research*, v. 101, no. C3, p. 6609-6615.
- Legg, M. R., and Kamerling, M. J., 2001 (in press), Large-scale basement-involved landslides, *in* Watts, P., Synolakis, C. E., and Bardet, J. P., eds., Prediction of underwater landslide hazards: Rotterdam, Balkema.
- Legg, M. R., Kuhn, G., Johnson, J., and Frost, E. G., 1995, Prehistoric tsunami investigations in southern California [expanded abstract], *Proceedings, Tsunami Deposits: Geologic Warnings of Future Inundation: Workshop at University of Seattle, Washington*, p. 33-34.
- Legg, M. R., Nicholson, C., and Sorlien, C., 1992, Active faulting and tectonics of the inner California Continental Borderland [abs]: *Eos, Transactions of the American Geophysical Union*, v. 73, p. 588.
- Locat, J., Locat, P., and Lee, H. J., 2001 (in press), Numerical modeling of the mobility of the Palos Verdes debris avalanche, California and its implication for the generation of tsunamis, *in* Watts, P., Synolakis, C. E., and Bardet, J. P., eds., Prediction of underwater landslide hazards: Balkema, Rotterdam.
- Makdisi, F., and Seed, H. B., 1977, Simplified procedure for estimating dams and embankment earthquake-induced deformations: *Journal of Soil Mechanics and Foundation Engineering*, v. 104, p. 849-867.
- Miranda, E., and Aslani, H., 2001, Brief report on the September 3, 2000 Yountville/Napa, California earthquake: Berkeley Earth Engineering Research Laboratory, on line report <http://www.eerc.berkeley.edu/yountville/>.
- Nicholson, C., Sorlien, C. C., and Legg, M. R., 1993, Crustal imaging and extreme Miocene extension of the Inner Continental Borderland [abs]: *Geological Society of America Abstracts with Programs*, v. 25, p. 418.
- Peterson, M., Beeby, D., Bryant, W., Cao, C., Cramer, C., Davis, J., Reichle, M., Saucedo, G., Tan, S., Taylor, G., Topozada, T., Treiman, J., and Wills, C., 1999, Seismic shaking hazard maps of California: California Division of Mines and Geology, Seismic Shaking Hazard Maps, Map Sheet 48, scale various.

- Peterson, M. D., Byrant, W. A., Cramer, C. H., Cao, T., Reichle, M. S., Frankel, A. D., Leinkaemper, J. J., McCrory, P. A., and Schwarta, D. P., 1996, Probabilistic seismic hazard assessment for the state of California: California Division of Mines and Geology Open File Report 96-08, 33 p.
- Rabinovich, A. B., Thomson, R. E., Kulikov, E. A., et al., 1999, The landslide-generated tsunami of November 3, 1994 in Skagway Harbor, Alaska: A case study: Geophysical Research Letters, v. 26, no. 19, p. 3009-3012.
- Rial, J. A., 1996, The anomalous seismic response of the ground motion at the Tarzana Hill site during the Northridge 1994 southern California earthquake: A resonant, sliding block?: Bulletin of the Seismological Society of America, v. 86, p. 1714-1723.
- Risk Engineering, Inc., 1995, Seismic Hazard at San Onofre Nuclear Generating Station: Risk Engineering, Inc., unpublished report.
- Rivero, C., Shaw, J. H., and Mueller, K., 2000, Oceanside and Thirtymile Bank blind thrusts: Implications for earthquake hazards in southern California: Geology, v. 28, no. 10, p. 891-894.
- Sadigh, K., Chang, C.-Y., Egan, M. A., Makdisi, F., and Youngs, R. R., 1997, Attenuation relationships for shallow crustal earthquakes based on California strong motion data: Seismological Research Letters, v. 68, p. 180-189.
- SCEC, 2001, Southern California Earthquake Data Center: Southern California Earthquake Center, <http://www.scecdc.scec.org/>
- Seed, H. B., Tokimatsu, K., Harder, L. F., Jr., and Chung, R. M., 1985, Influence of SPT procedures in soil liquefaction resistance evaluations: Journal of Geotechnical Engineering, v. 111, no. 12, p. 1425-1445.
- Shlemon, R. J., 1977, Geomorphic analysis of Fault "E" Camp Pendleton, California: Roy J. Shlemon and Associates, Inc., unpublished geologic report for Southern California Edison Company, 20 p.
- Shlemon, R. J., 1979, Age of "Dana Point," "Vaciadero," and "Carr" Faults Capistrano Embayment coastal area, Orange County, California: Roy J. Shlemon and Associates, Inc. unpublished geologic report for Southern California Edison Company, 19 p.
- Shlemon, R. J., 1987, The Cristianitos fault and Quaternary geology, San Onofre State Beach, California, Geological Society of America Centennial Field Guide--Cordilleran Section: Boulder, CO, Geological Society of America, p. 171-174.
- Shlemon, R. J., 2000, State-of-the-art to standard-of-practice: Active faults, paleoliquefaction and tsunamis in the Carlsbad area, San Diego County, California: Geological Society of America Abstracts with Programs, v. 32, no. 7, p. A-121.
- Southern California Edison Company, 1995, Final report, geotechnical investigation of alternate independent spent fuel storage installation (ISFSI) unpublished geotechnical report .

- Southern California Edison Company, 1998, Final safety analysis report (UFSAR), San Onofre Nuclear Generating Station, Units 2 and 3, Docket numbers 50-361 and 50-362, Southern California Edison Company, et al.: Southern California Edison Company, version 13.
- Spudich, P., and al., e., 1997, Sea96 -- a new predictive relation for earthquake ground motions in extensional tectonic regimes: *Seismological Research Letters*, v. 68, no. 1, p. 190-198.
- Tappin, D. R., Watts, P., McMurtry, G. M., Lafoy, Y., and Matsumoto, T., 2001 (in press), Prediction of slump-generated tsunamis: The July 17, 1998 Papua New Guinea tsunami, in Watts, P., Synolakis, C. E., and Bardet, J. P., eds., *Prediction of underwater landslide hazards*: Balkema, Rotterdam.
- Toppozada, T. R., Real, C. R., Bezore, S. P., and Parke, D. L., 1979, Compilation of pre-1900 California earthquake history; annual technical report -- fiscal year 1978-79: California Division of Mines and Geology Open-File Report 79-6.
- U.S. Army Corps of Engineers, 1960, Beach erosion control report on cooperative study of San Diego County, California: U.S. Army Corps of Engineers W004-193-ENG-5196.
- U.S. Nuclear Regulatory Commission, 1975, Safety evaluation of the geologic features at the site of the San Onofre Nuclear Generating Station, Units 2 and 3: U.S. Nuclear Regulatory Commission, Office of Nuclear Reactor Regulation Report Docket Numbers 50-206, 50-361, 50-362, 24 p.
- U.S. Nuclear Regulatory Commission, 1981, Safety evaluation report related to the operation of San Onofre Nuclear Generating Station, Units 2 and 3, Docket numbers 50-361 and 50-362, Southern California Edison Company, et al.: U.S. Nuclear Regulatory Commission, Office of Nuclear Reactor Regulation, NUREG-0712.
- Watts, P., and Raichlen, F., 1994, Water waves generated by underwater landslides [abs]: *Seismological Research Letters*, v. 65, p. 25.
- Woodward-Clyde Consultants, 1995a, Attenuation relationships: Woodward-Clyde Consultants unpublished report, 100 p.
- Woodward-Clyde Consultants, 1995b, Time histories for fragility analysis: Woodward-Clyde Consultants unpublished report, 18 p.

Other

- Pryor, David. California Department of Parks and Recreation, Orange Coast District. Personal Communication. October 11, 2000.
- Miller, Will. U.S. Fish and Wildlife Service, Carlsbad District. Personal Communication. January 26, 2000.
- Spear, Dan. San Diego Air Pollution Control District. Personal Communication. October 25, 2000.



**San Onofre Nuclear
Generating Station (SONGS)
local area map**

- USMC Camp Pendleton Boundary
- SONGS Boundary
- State Park Boundary
- Interstate 5 Freeway
- Street

10/22/99

File: Solveig

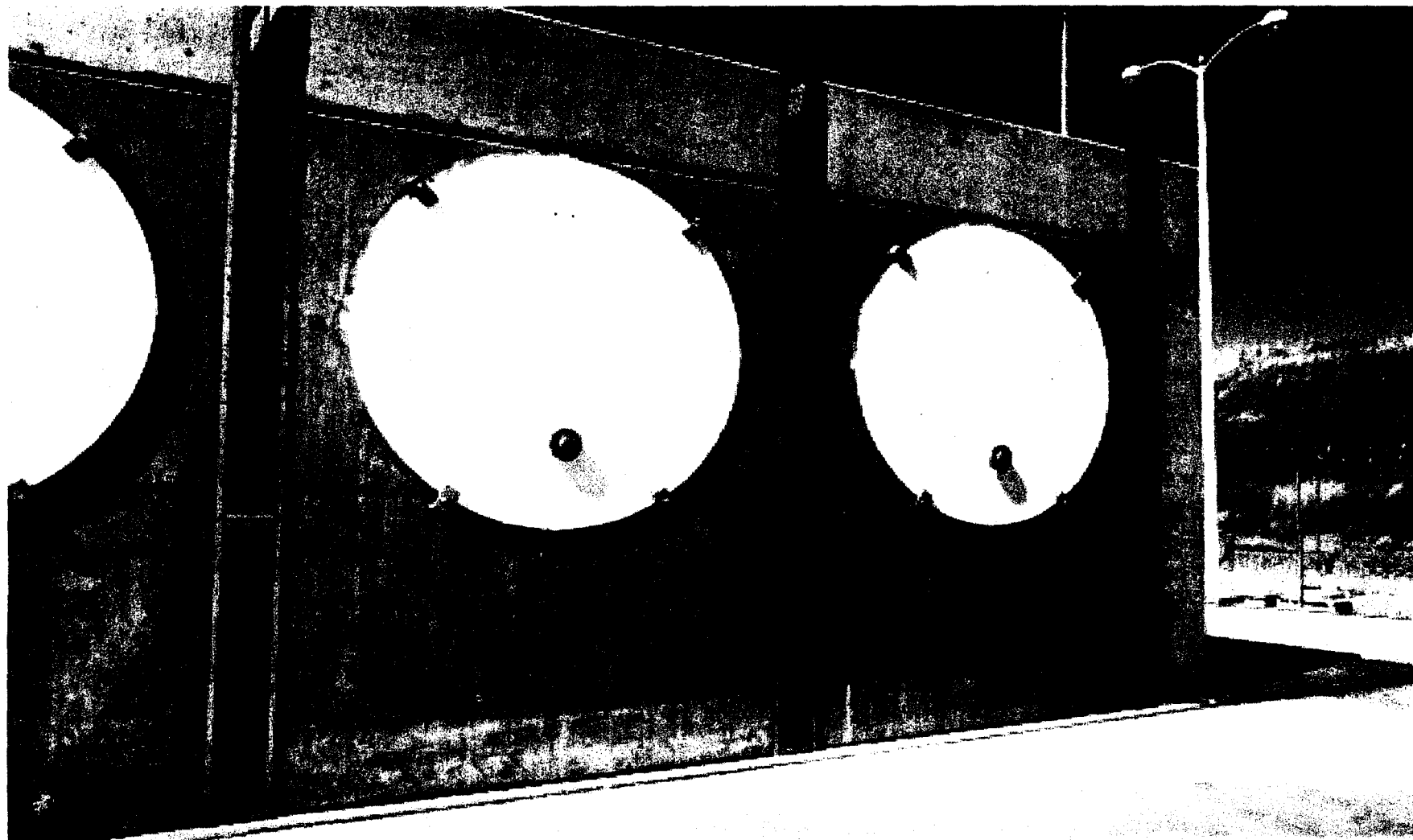
Supplement to Section IV.2

PACIFIC OCEAN

Supplement to Section IV.2

1
2
3
4
5
6
7
8
9
10
11
12
13
14
15
16
17
18
19
20
21
22
23
24
25
26
27
28
29
30
31
32
33
34
35
36
37
38
39
40
41
42
43
44
45
46
47
48
49
50
51
52
53
54
55
56
57
58
59
60
61
62
63
64
65
66
67
68
69
70
71
72
73
74
75
76
77
78
79
80
81
82
83
84
85
86
87
88
89
90
91
92
93
94
95
96
97
98
99
100

Temporary Fuel Storage Modules



Supplement to Section II.2
Attachment B-4
(See Sections II.4-6 and
IV.7 for dimensions.)

Exhibit 2
E-00-014

Supplement to Section II.2
Attachment B-4

N-41/42

AWS

SONGS 1 Temp. Fuel Storage Facility
Permit No E-00-001

SONGS 2/3 Temp. Fuel Storage Facility

SONGS 2/3 Temp. Fuel Storage Facility

SONGS 2/3 Temp. Fuel Storage Facility

SPF

Tank

Structures remaining after
SONGS 1 Decommissioning

Sewage
Treatment

Sea Wall

Not to Scale

Temporary Fuel Storage Facility
SONGS 1 Project Area

Supplement to Section II.2
Attachment B

Supplement to Section II.2
Attachment B

Exhibit 3
E-00-014

[illegible]

FAULTS THAT DISPLACE VOLCANES & 10 mi OR LARGER
ALTI-TUDINE & 20 mi DEPTHS OR GEOSYNCLINAL SURFACES.

FAULTS THAT DISPLACE LATE QUATERNARY & 700 ft DEPOSITS
ON GEOSYNCLINAL SURFACES.

QUATERNARY FAULTS 6.5 MA.

FAULTS THAT DISPLACE PRE-QUATERNARY DEPOSITS.
RECORD OF LAST DISPLACEMENT FOR OFFSHORE FAULTS
IS 1000 YEARS AGO. ONLY SELECTED FAULTS FROM JEROME
1930 ARE SHOWN.

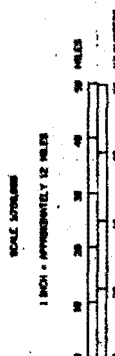
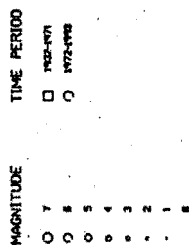


Exhibit 4
E-00-014

Ground Motion Response Spectra

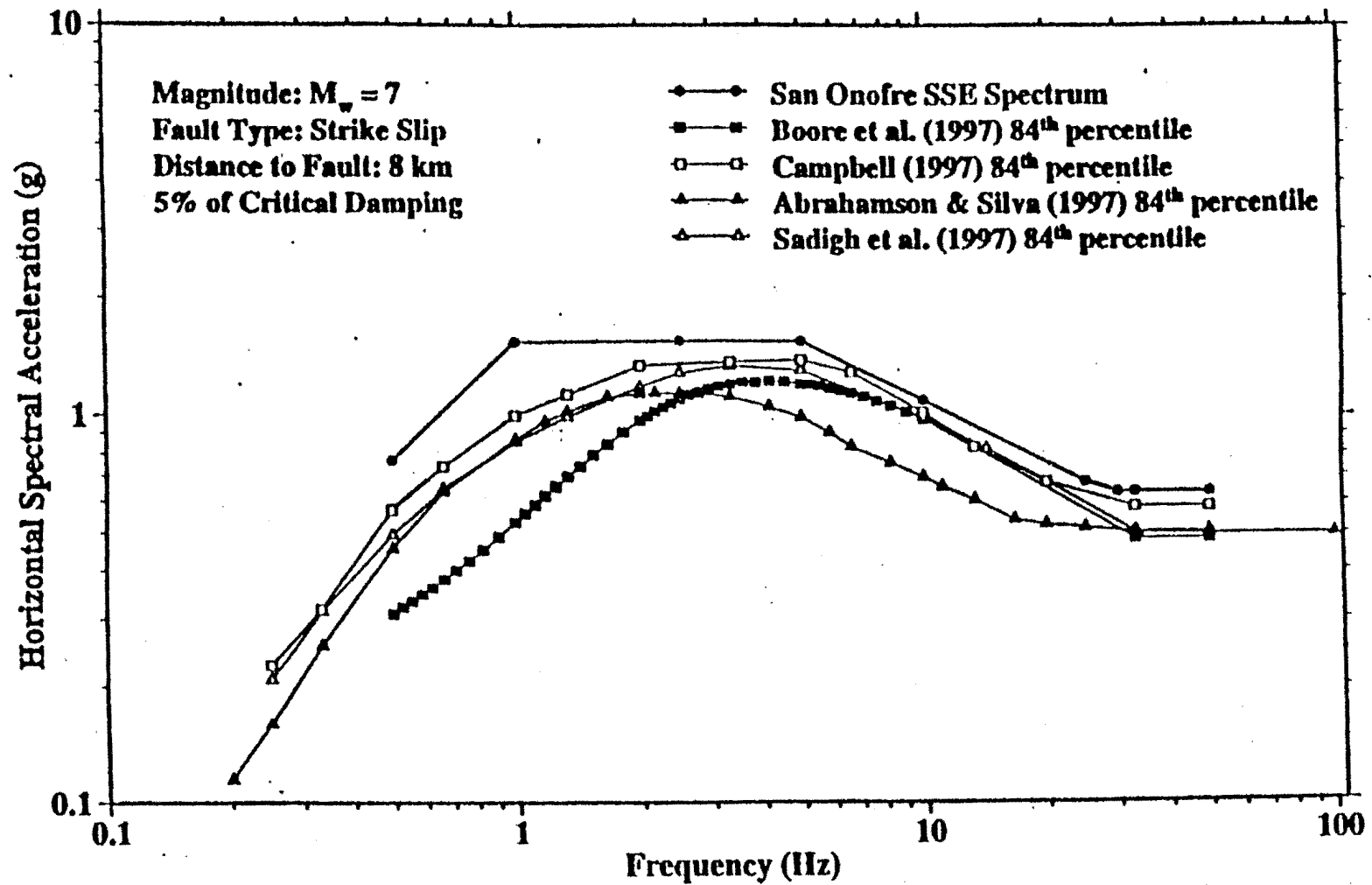


Figure 3

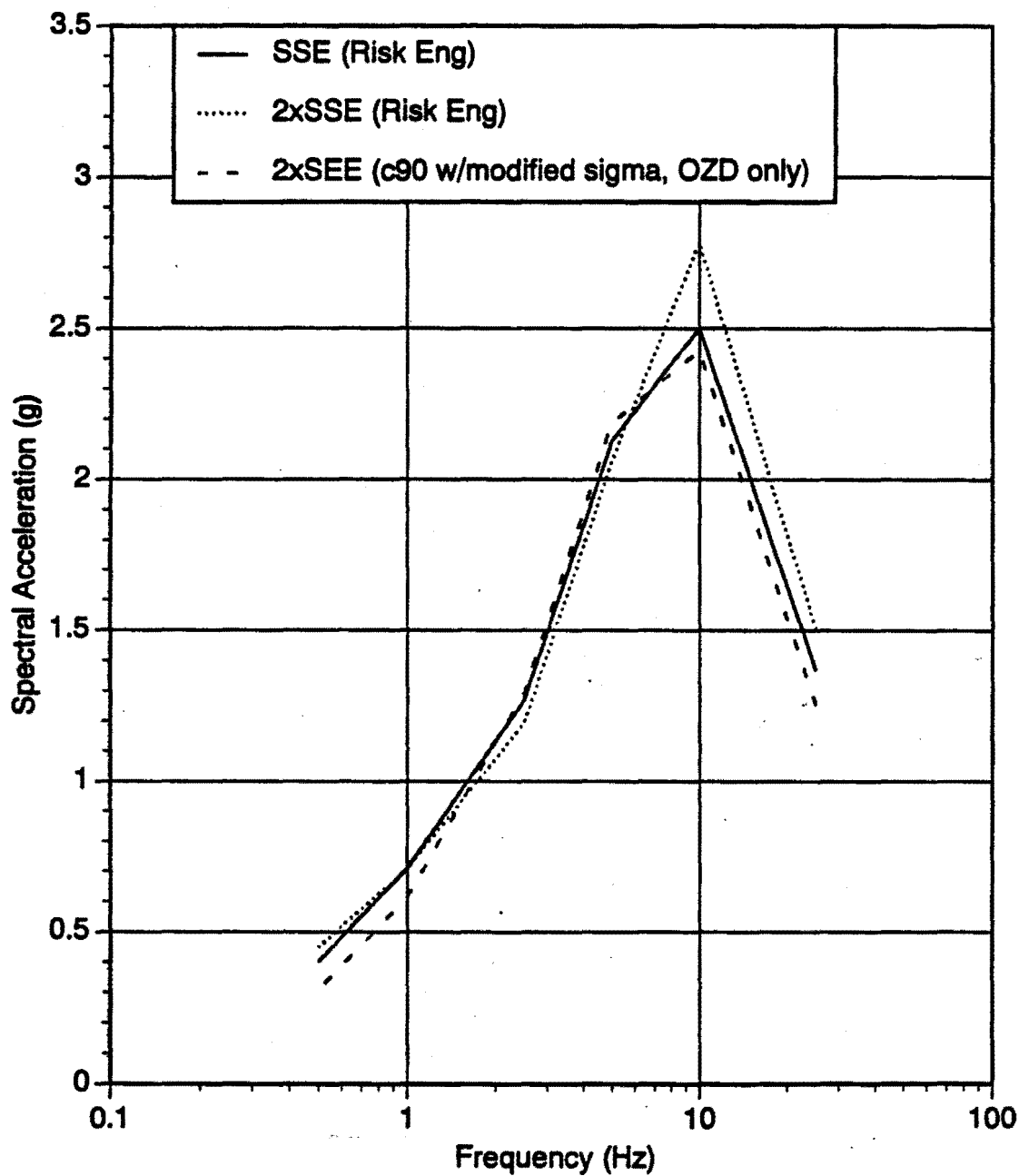


Exhibit 6
E-00-014

Figure 6-34. Comparison of vertical spectral shapes at the SSE and 2xSSE levels.

Comments on the Faulting and Seismic Hazard at San Onofre, San Diego County, California
Submitted by Mark R. Legg, PhD, California Reg. Geologist #6463, Reg. Geophysicist #948.
President, Legg Geophysical, Huntington Beach, California

1. It is now well established that the Rose Canyon and Newport-Inglewood fault zones are continuous, via the South Coast Offshore Zone of Deformation. Consequently, the combined fault system is capable of large earthquakes ($M > 7$). [Fischer and Mills, 1991]
2. It is now recognized that major detachment fault systems in the region are reactivated as thrust faults, some blind (not reaching the surface). The major Oceanside detachment/thrust system underlies the San Onofre Nuclear Generating Station (SONGS). Consequently, large thrust or oblique-reverse earthquakes on this system may generate shaking levels in excess of the design level of SONGS units 2 and 3. [Bohannon and others, 1990; Legg and others, 1992; Nicholson and others, 1993; Crouch and Suppe, 1993; Bohannon and Geist, 1998; Mueller and others, 1998; Grant and others, 1999; Rivero and others, 2000]
 - a. The SONGS site would not be 5-7 km from the epicentral zone, but instead directly above the potential fault rupture plane. Estimation of strong motion should use an epicentral distance of zero (0).
 - b. Newer attenuation relations based upon recent large earthquake activity including the 1989 Loma Prieta, California; 1992 Landers, California; 1999 Chi-Chi, Taiwan; 1999 Izmit, Turkey; and 1995 Kobe, Japan, and moderate earthquakes including the 1994 Northridge, California; 1987 Whittier Narrows, California; 1983 Coalinga, California; and 1984 Morgan Hill, California are more accurate in estimating ground motions than the relationships used for the Safety Evaluation conducted in the late 1970s. [Abrahamson and Silva, 1997; Boore and others, 1997; Campbell, 1997; Sadigh and others, 1997]
 - c. The recent earthquake experience has shown that near source effects are substantial, resulting in strong amplification of ground motions. The SONGS site lies directly above the detachment/thrust system, and therefore is subject to such effects. These effects include focusing of energy due to the rupture propagation and hanging wall effects wherein the seismic energy is trapped and amplified in the wedge of crust above the fault plane.
 - d. As stated during my testimony during the NRC hearings in 1981, the reverse fault character of microearthquakes recorded along the Cristianitos fault trend in the mid-1970s and reactivation of minor faulting uncovered during site excavations is consistent with overall reactivation of ancient normal fault structures by a new stress regime involving northeast-directed shortening or transpression. This assertion has now been confirmed by recent geologic studies in the neighboring offshore region, and in fact, may have been deduced from the proprietary exploration industry data available to the Safety Evaluators in the late 1970s.
3. Geologic investigations along the coast in the Carlsbad and Camp Pendleton areas to the south of the SONGS site have identified numerous paleoseismic features indicative of prehistoric large earthquakes along the north San Diego County coastline. [Kuhn and others, 1996; Franklin and Kuhn, 2000; Kuhn and others, 2000]
 - a. Abundant evidence of paleoliquefaction has been identified at numerous sites in the Carlsbad and Camp Pendleton area. This liquefaction involved Pleistocene terrace deposits, and in some

cases, older Eocene siltstone bedrock. It is rare that such older and densified, but not lithified, materials liquefy. Consequently, the recognition of such liquefaction in Holocene time, as evident by involvement of Native American midden deposits, implies that the strong motion (shaking) was very severe. Reasons to expect such severe shaking were outlined above.

- b. Some of the ground deformation features identified with the paleoliquefaction include sand blow deposits and craters, low-angle slip surfaces associated with lateral spreading, and numerous shallow sand filled fissures, sand injection dikes, and polygonal structures. Some of these features look remarkably similar to features uncovered during the excavation of the building pads for SONGS units 2 and 3; the nature of these features was unrecognized or unknown at the time of the Safety Evaluations.
4. Large active landslides along the coast immediately south of the SONGS site, at San Onofre State Beach, may have been considered ancient for the Safety Evaluation during the 1970s. The reactivation, and continued movement for more than two (2) years demonstrates that the coastal bluffs are highly unstable along the north San Diego County coastline. Although the surficial lithology and structure are somewhat different at San Onofre, being in the hanging wall of the Cristianitos fault, the relative straight or smoothly curving character of the shoreline and coastal bluff suggests that some active coastal erosion mechanisms, possibly landsliding or block falls, have acted in the past in the San Onofre area to keep pace with the active landslide headward erosion of the coast to the south. This process needs to be investigated to determine what threat exists to the San Onofre site, and whether seawall installed provide adequate protection for such processes. [Ehlig, 1977; Kuhn, 2000]
5. Locally generated tsunami, from large nearby offshore earthquake or submarine landslide, is now recognized as a serious threat to coastal southern California. With the recognition of major oblique components to offshore faulting, including blind thrusts, restraining bend uplifts and transtensional sags along strike-slip faults, major seafloor displacement during large ($M_{ag} > 6.5$) submarine earthquakes are likely to generate tsunami that attack the southern California coast with destructive force. Indeed, long term uplift of coastal marine terraces may attest to infrequent, but large tectonic displacements of the southern California coast. Furthermore, the steep slopes in unstable geologic materials on offshore ridges, banks, and basins, may generate large amplitude tsunami that can be locally destructive to the nearby coast, as occurred in Papua New Guinea. It is likely that large underwater landslides would be triggered by severe earthquakes, and the possibility of both tectonic displacement and landslide inducement of tsunamis exists. Maximum expected run-up maps for locally generated tsunami are currently being prepared for coastal San Diego County. The presence of steep coastal bluffs, like those near SONGS, also tend to amplify the wave so that narrow coastal valleys or lowlands may expect even higher wave run-up than broader low-lying coastal areas. [Field and Edwards, 1993; Lander and others, 1993; McCarthy and others, 1993; Kuhn and others, 1994, 1995; Legg, 1994; Watts and Raichlen, 1994; Bohannon and Gardner, 2001; Legg and Kamerling, 2001; Locat and others, 2001; Tappin and others, 2001]

Abrahamson, N.A., and Silva, W.J., 1997, Empirical response spectral attenuation relations for shallow crustal earthquakes: *Seismological Research Letters*, v. 68, p. 94-127.

Bohannon, R., Eittreim, S., Childs, J., Geist, E., Legg, M., Lee, C., Sorlien, C., and Busch, L., 1990, A seismic-reflection study of the California Continental Borderland, [abstract] in *Trans. American Geophysical Union*, v. 71, p. 1631.

Bohannon, R. and Geist, E., 1998, Upper crustal structure and Neogene tectonic development of the California continental borderland: *Geological Society of America Bulletin*, v. 110, p. 779-800.

- Bohannon, R.G., and Gardner, 2001, Submarine landslides of San Pedro Sea Valley, southwest Los Angeles basin: in Watts, P., Synolakis, C.E., and Bardet, J.P., eds., *Prediction of Underwater Landslide Hazards*, Balkema, Rotterdam, in press.
- Boore, D.M., Joyner, W.B., and Fumal, T.E., 1997, Equations for estimating horizontal response spectra and peak acceleration from western North American earthquakes: *Seismological Research Letters*, v. 68, p. 128-153.
- Campbell, K.W., 1997, Empirical near-source acceleration relationships for horizontal and vertical components of peak ground acceleration, peak ground velocity, and pseudo-absolute acceleration response spectra: *Seismological Research Letters*, v. 68, p. 154-179.
- Clarke, S. H., Greene, H. G., Kennedy, M. P., and Vedder, J. G., 1987, Geologic map of the inner-southern California continental margin: California Division of Mines and Geology, California Continental Margin Geologic Map Series, Area 1 of 7, sheet 1 of 4, scale 1:250,000.
- Crouch, J.K., and Suppe, J., 1993, Late Cenozoic tectonic evolution of the Los Angeles basin and Inner California Borderland: A model for core complex-like extension: *Geological Society of America Bulletin*, v. 105, p. 1415-1434.
- Davis, T. L., Namson, J., and Yerkes, R. F., 1989, A cross-section of the Los Angeles area: Seismically active fold-and-thrust belt, the 1987 Whittier Narrows earthquake, and earthquake hazard: *Journal of Geophysical Research*, v. 94, p. 9644-9664.
- Ehlig, P.L., 1977, Geologic report on the area adjacent to the San Onofre Nuclear Generating Station, northwestern San Diego County, California: unpublished report prepared for Southern California Edison Company (Rosemead), 38 p., 10 figs.
- Field, M.E., and Edwards, B.D., 1993, Submarine landslides in a basin and ridge setting, southern California: in Schwab, W.C., Lee, H.J., and Twichell, D.C., eds., *Submarine Landslides; Selected Studies in the U.S. Exclusive Economic Zone*, U.S. Geological Survey Bulletin 2002, p. 176-183.
- Fischer, P. J., and Mills, G. I., 1991, The offshore Newport-Inglewood - Rose Canyon fault zone, California: Structure, segmentation, and tectonics: in Abbott, P.L., and W.J. Elliott, eds., *Environmental Perils of the San Diego Region*. San Diego Association of Geologists Guidebook, p. 17-36.
- Franklin, J.P., and Kuhn, G.G., 2000, Paleoseismic features exposed by trenching the lowest coastal terrace at Carlsbad, California: in *Neotectonics and Coastal Instability*, Orange and northern San Diego Counties, California, Joint Field Conference guidebook, v. 1., AAPG Pacific Section, Long Beach, California, p. 1-13.
- Grant, L.B., Mueller, K.J., Gath, E.M., Cheng, H., Edwards, R.L., Munro, R., and Kennedy, G., 1999, Late Quaternary uplift and earthquake potential of the San Joaquin Hills, southern Los Angeles basin, California: *Geology*, v. 27, p. 1031-1034.
- Greene, H. G., Bailey, K. A., Clarke, S. H., Ziony, J. I., and Kennedy, M. P., 1979, Implications of fault patterns of the inner California Continental Borderland between San Pedro and San Diego: in Abbott, P. L., and Elliott, W. J., eds., *Earthquakes and other perils - San Diego Region*: San Diego Association of Geologists Guidebook, p. 21-27.
- Ingersoll, R.V., and Rumelhart, P.E., 1999, Three-stage evolution of the Los Angeles basin, southern California: *Geology*, v. 27, p. 593-596.
- Kuhn, G., M.R. Legg, and E. Frost, 1994, Large pre-historic earthquake(s) in coastal San Diego County, California: in *Paleoseismology Workshop Proceedings*, Sept. 1994, Marshall, CA, U.S. Geological Survey Open-File Report 94-568, p. 100-103.
- Kuhn, G.G., Legg, M.R., Johnson, A., Shlemon, R.J., and Frost, E.G., 1996, Paleoliquefaction evidence for large pre-historic earthquake(s) in north-coastal San Diego County, California: in Munasinghe, T. and Rosenberg, P., eds., *Geology and natural resources of coastal San Diego County, California*, Field-trip guidebook, San Diego Association of Geologists, p. 16-24.
- Kuhn, G.G., 2000, Sea cliff, canyon, and coastal terrace erosion between 1997 and 2000: San Onofre

- State Beach, Camp Pendleton Marine Corps Base, San Diego County, California: in *Neotectonics and Coastal Instability, Orange and northern San Diego Counties, California, Joint Field Conference guidebook*, v. 1., AAPG Pacific Section, Long Beach, California, p. 31-87.
- Kuhn, G.G., Legg, M.R., Shlemon, R.J., and Bauer, J.L., 2000, Neotectonics in the North Coastal Area, San Diego County, California: in *Neotectonics and Coastal Instability, Orange and northern San Diego Counties, California, Joint Field Conference guidebook*, v. 1., AAPG Pacific Section, Long Beach, California, p. 88-103.
- Lander, J.F., Lockridge, P.A., and Kozuch, M.J., 1993, Tsunamis affecting the west coast of the United States, 1806-1992: U.S. Dept. Commerce, NOAA, Boulder, Colorado.
- Legg, M.R., and M.P. Kennedy, 1991, Oblique divergence and convergence in the California Continental Borderland. in Abbott, P.L., and W.J. Elliott, eds., *Environmental Perils of the San Diego Region*. San Diego Association of Geologists Guidebook, p. 1-16.
- Legg, M.R., Nicholson, C., and Sorlien, C., 1992, Active faulting and tectonics of the inner California Continental Borderland: [abstract] *EOS Trans. American Geophysical Union*, v. 73, p. 588.
- Legg, M. R., G. Kuhn, J. Johnson, and E. G. Frost, 1995, Prehistoric tsunami investigations in southern California [expanded abstract]: in *Proceedings, Tsunami Deposits: Geologic Warnings of Future Inundation: Workshop at University of Washington, Seattle*, p. 33-34.
- Legg, M.R., and Kamerling, M.J., 2001, Large-scale basement-involved landslides, California Continental Borderland: in Watts, P., Synolakis, C.E., and Bardet, J.P., eds., *Prediction of Underwater Landslide Hazards*, Balkema, Rotterdam, in press.
- Locat, J., Locat, P., and Lee, H.J., 2001, Numerical modeling of the mobility of the Palos Verdes debris avalanche, California, and its implication for the generation of tsunamis: in Watts, P., Synolakis, C.E., and Bardet, J.P., eds., *Prediction of Underwater Landslide Hazards*, Balkema, Rotterdam, in press.
- McCarthy, R.J., Bernard, E.N., and Legg, M.R., 1993, The Cape Mendocino earthquake: A local tsunami wake-up call? in *Proc. 8th Symposium on Coastal and Ocean Management*, New Orleans, Louisiana, p. 2812-2828.
- McCulloch, D.S., 1985, Evaluating tsunami potential: in Ziony, J.I., ed., *Evaluating Earthquake Hazards in the Los Angeles Region: U.S. Geological Survey Professional Paper 1360*, p. 375-413.
- Mueller, K., Grant, L.B., and Gath, E., 1998, Late Quaternary growth of the San Joaquin Hills anticline: A new source of blind thrust earthquakes in the Los Angeles basin: *Seismological Research Letters*, v. 69, p. 161.
- Nicholson, C., Sorlien, C.C. and Legg, M.R., 1993, Crustal imaging and extreme Miocene extension of the Inner California Continental Borderland: [Abstract] in *Geological Society of America Abstracts with Programs*, v. 25, p. 418.
- Nicholson, C., Sorlien, C. C., Atwater, T., Crowell, J. C., and Luyendyk, B. P., 1994, Microplate capture, rotation of the western Transverse Ranges, and initiation of the San Andreas transform as a low-angle fault system: *Geology*, v. 22, p. 491-495.
- Plafker, G., and Galloway, J.P., eds., 1989, Lessons learned from the Loma Prieta, California, earthquake of October 17, 1989: U.S. Geological Survey Circular 1045, 48 p.
- Rivero, C., Shaw, J.H., and Mueller, K., 2000, Oceanside and Thirtymile Bank blind thrusts: Implications for earthquake hazards in coastal southern California: *Geology*, v. 28, p. 891-894.
- Sadigh, K., Chang, C.-Y., Egan, M.A., Makdisi, F., and Youngs, R.R., 1997, Attenuation relationships for shallow crustal earthquakes based on California strong motion data: *Seismological Research Letters*, v. 68, p. 180-189.
- Somerville, P.G., Smith, N.F., Graves, R.W., and Abrahamson, N.A., 1997, Modification of empirical strong ground motion attenuation relations to include the amplitude and duration effects of rupture directivity: *Seismological Research Letters*, v. 68, p. 199-222.
- Tappin, D.R., Watts, P., McMurtry, G.M., Lofoy, Y., and Matsumoto, T., 2001, Prediction of slump

generated tsunamis; The July 17, 1998 Papua New Guinea tsunami: in Watts, P., Synolakis, C.E., and Bardet, J.P., eds., Prediction of Underwater Landslide Hazards, Balkema, Rotterdam, in press.
Watts, P., and Raichlen, F., 1994, Water waves generated by underwater landslides: [abstract]
Seismological Research Letters, v. 65, p. 25.



Oceanside and Thirtymile Bank blind thrusts: Implications for earthquake hazards in coastal southern California

Carlos Rivero
John H. Shaw* } Department of Earth and Planetary Sciences, Harvard University, Cambridge, Massachusetts 02138, USA
Karl Mueller } Department of Geological Sciences, University of Colorado, Boulder, Colorado 80309, USA

ABSTRACT

We define an active blind thrust system in offshore southern California that extends from Los Angeles south to the United States–Mexico international border. These blind thrusts formed by tectonic inversion of Miocene extensional detachments. We attribute the 1986 Oceanside (M_L 5.3) earthquake, local uplift of marine terraces, seafloor fold scarps, and observed geodetic convergence to motion on these faults. Single and multisegment fault rupture scenarios suggest the potential for large (M 7.1–7.6) but infrequent earthquakes that would affect the Los Angeles and San Diego metropolitan areas.

Keywords: blind thrusts, strike-slip faults, tectonic reactivation, earthquakes, Inner California Borderland, Oceanside.

INTRODUCTION

The importance of blind thrust faults as sources of destructive earthquakes in southern California was demonstrated by the 1994 Northridge (M 6.7) event, which caused more than \$35 billion in damage to metropolitan Los Angeles (U.S. Geological Survey and Southern California Earthquake Center Scientists, 1994). Similar blind thrusts have been proposed to underlie much of the Los Angeles basin (Davis et al., 1989; Schneider et al., 1996; Shaw and Suppe, 1996; Shaw and Shearer, 1999). In this paper we show that active thrusting extends to the offshore California Borderlands, on the basis of analysis of more than 10 000 km of seismic reflection data. These thrusts reactivate Miocene extensional detachments (Crouch and Suppe, 1993), and may pose significant hazards to coastal California.

OCEANSIDE AND THIRTYMILE THRUSTS

Recent studies invoke low-angle normal faults in the Neogene formation of the Inner California Borderlands and rotation of the Transverse Ranges (Luyendyk and Hornafius, 1987; Crouch and Suppe, 1993; Nicholson et al., 1994; Bohannon and Geist, 1998; Ingersoll and Rumelhart, 1999). Through detailed mapping and structural modeling, we demonstrate that two of these faults, the Oceanside and Thirtymile Bank detachments, extend south from Laguna Beach and Catalina Island, respectively, to at least the United States–Mexico international border (Fig. 1). The extensional nature of these faults is reflected in the normal separation of basement (Figs. 1 and 2), and in the presence of extensional folds (rollovers) and Miocene growth structures (Crouch and Suppe, 1993; Bohannon and Geist, 1998).

Here we document that large portions of these detachments have been reactivated to form the Oceanside and Thirtymile Bank blind thrusts,

which compose the Inner California Borderlands blind thrust system. Tectonic inversion of the Oceanside detachment is reflected by a submarine fold-and-thrust belt located offshore between Dana Point and Oceanside (Fisher and Mills, 1991) (Fig. 2A). In contrast to the extensional features, these contractional structures deform Pliocene and younger strata, and are commonly associated with pronounced seafloor fold scarps. These structures do not cut or fold the detachment. Thus, we interpret that they sole into the Oceanside thrust.

The Oceanside thrust is mapped over an area of more than 1800 km². In migrated seismic reflection profiles, the thrust is imaged as a coherent set of strong reflections that dip to the northeast between 14° and 25° (Fig. 2). The thrust extends south along the Coronado Banks to the international border near San Diego Bay (Fig. 1). At Coronado Banks, thrusting is reflected by tectonic inversion of the

Coronado Bank detachment (Fig. 2B and 2C) (Nicholson et al., 1993; Sorlien et al., 1993).

The Thirtymile Bank thrust is west of the Oceanside fault, and also originated as an extensional detachment (Legg et al., 1992). The fault defines an almost linear, continuous scarp extending from southwest of Catalina Island to Thirtymile Bank (Fig. 1). The hanging wall of the thrust contains Neogene synrift strata that are gently folded in a manner consistent with thrust inversion of the underlying fault.

Growth strata in contractional folds above the Oceanside and Thirtymile Bank thrusts suggest that thrusting began in the Pliocene. The shallow, east-vergent fold-and-thrust belt above the Oceanside thrust between Dana Point and Oceanside is the most direct evidence for this tectonic inversion. Folds in this belt generate pronounced seafloor scarps that persist for ~30 km. Although these scarps may reflect recent activity of the underlying Oceanside thrust (Fig. 2), they are not definitive; we lack precise age control on seafloor sediments. However, young contractional folds also occur along the coast and involve dated marine terraces. These structures record recent fault activity that may be attributed to the Oceanside thrust.

The San Joaquin Hills are at the southern margin of the Los Angeles basin, where the mapped part of the Oceanside thrust extends onshore. The hills are formed by a northeast-vergent anticline that uplifts and deforms marine terraces. Grant

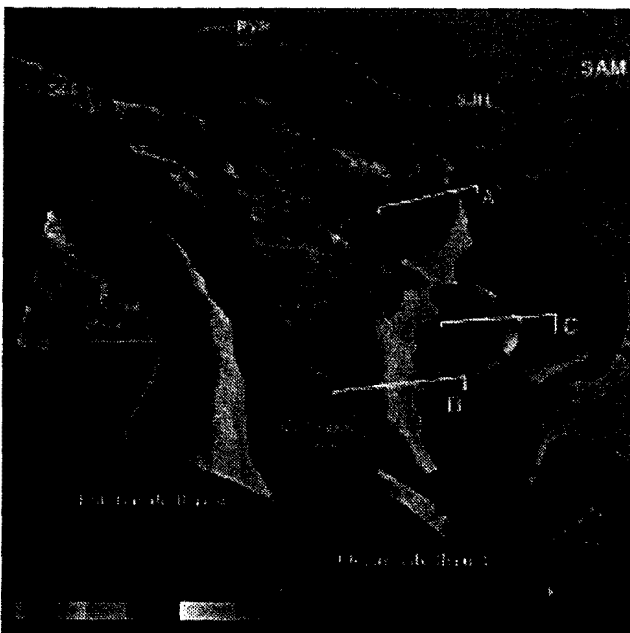


Figure 1. Perspective view of three-dimensional model of Oceanside and Thirtymile Bank blind thrusts. Gray surface is top of basement (Catalina Schist). Small triangles indicate areas of recent uplift (Lajoie et al., 1979, 1992; Barrie and Gath, 1992; Kern and Rockwell, 1992; Grant et al., 1999; Kier and Mueller, 1999). Digital shaded relief map of southern California topography was derived from digital elevation data provided by U.S. Geological Survey. SAM—Santa Ana Mountains; SJH—San Joaquin Hills; PVP—Palos Verdes Peninsula; SCI—Santa Catalina Island.

*Corresponding author.

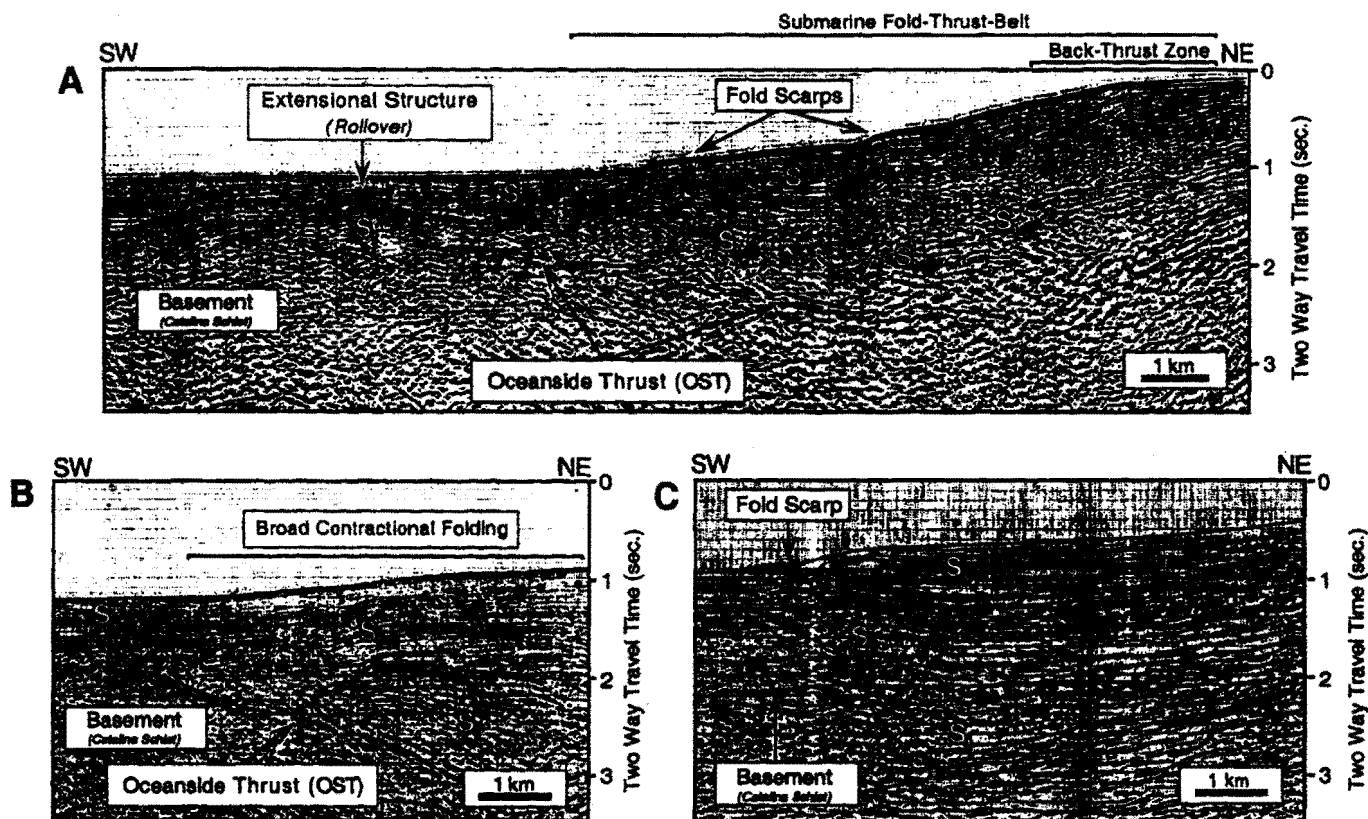


Figure 2. Geometry of Oceanside thrust as imaged in seismic reflection profiles. A: Migrated seismic reflection profile imaging segment of thrust south of Lasuen Knoll. Sharp and continuous reflections dipping to east define location of thrust. Note shallow fold-and-thrust belt above Oceanside thrust that produces seafloor fold scarps. This contractional deformation does not affect thrust; thus, we interpret Oceanside as basal thrust of sequence. Note older (Neogene) extensional rollover structure buried by Pliocene and younger strata preserved on west end of section. B: Migrated seismic image of Oceanside thrust northeast of Coronado Banks. Oceanside thrust motion is reflected by broad, contractional fold involving shallow sedimentary units and forming broad seafloor slope. C: Migrated seismic reflection profile across Carlsbad thrust, which resides in hanging wall of Oceanside thrust east of Crespi Knoll. Fault is defined by offset of top basement reflection, and produces contractional fold with pronounced seafloor scarp. Unit S_1 is Miocene and Oligocene(?) synextensional strata; S_2 is late Miocene–early Pliocene postextensional drape; S_3 is late Pliocene(?)–Holocene syncontractional strata. S_1 and S_2 are grouped where undifferentiated. Vertical scale is $\sim 1:1$; datum is sea level; s—seconds. Section traces are shown in Figure 1.

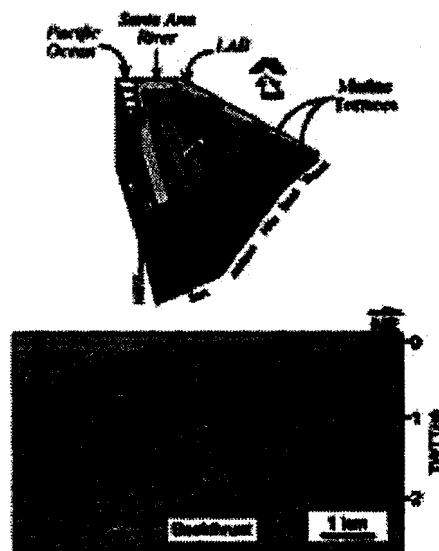
et al. (1999) proposed that the fold is developed above an active, southwest-dipping blind thrust that slips at a rate of ~ 0.42 – 0.79 mm/yr, based on uplift rates of 0.21 – 0.27 mm/yr. Our seismic data image the offshore extension of this structure (Fig. 3), and confirm that it formed above a shallow blind thrust with an average southwest dip value of 23° . However, this shallow fault is restricted to the hanging wall of the Oceanside thrust; at depth, we interpret that this shallow fault soles into the thrust, forming a structural wedge (Medwedeff, 1992; Mueller et al., 1998). We combined the observed dip values for the back-thrust system (23°) and the Oceanside thrust (14° – 25°) with the uplift rate at the San Joaquin Hills into a structural wedge model and calculated a slip rate on the thrust of 0.27 – 0.41 mm/yr. This slip rate yields an uplift rate above the Oceanside thrust, in the absence of the backthrust, of 0.07 – 0.17 mm/yr. This result is compatible with the observed 0.13 – 0.17 mm/yr uplift rate of marine terraces south of the San Joaquin Hills, which extend to San Diego and into northern Mexico (Lajoie et al., 1979, 1992; Barrie and Gath, 1992; Kern and Rockwell, 1992) (Fig. 1). If

the Oceanside blind thrust is responsible for all or part of this coastal uplift, it implies that the thrust is active far to the south of the San Joaquin Hills.

We consider the calculated slip rates for the Oceanside thrust to be minimum values because they are derived from uplift rates, which may be affected by isostatic compensation and/or flexural subsidence that may occur due to crustal thickening (Shaw et al., 1994). To govern maximum slip rates, we use geodetic observations that indicate as much as 2 mm/yr of northeast-southwest ($N43^\circ E$) convergence between Catalina Island and the coast (Kier and Mueller, 1999). Given that shortening produced by the Oceanside thrust should not exceed this value, we calculate a maximum slip rate for the thrust of 2.2 mm/yr. Simi-

larly, the slip rate of the Thirtymile Bank thrust should be no more than 0.96 mm/yr, such that the resultant shortening does not exceed the geodetic convergence rate of 0.86 mm/yr calculated between Catalina Island and San Clemente Island

Figure 3. Top: Kinematic model of blind thrust faulting and terrace uplift beneath San Joaquin Hills (Grant et al., 1999). LAB—Los Angeles basin; NIFZ—Newport-Inglewood fault zone. Bottom: Migrated seismic reflection profile imaging offshore extension of this fold system, which has developed above west-dipping back-thrust. TWTT—two-way traveltimes; s—seconds.



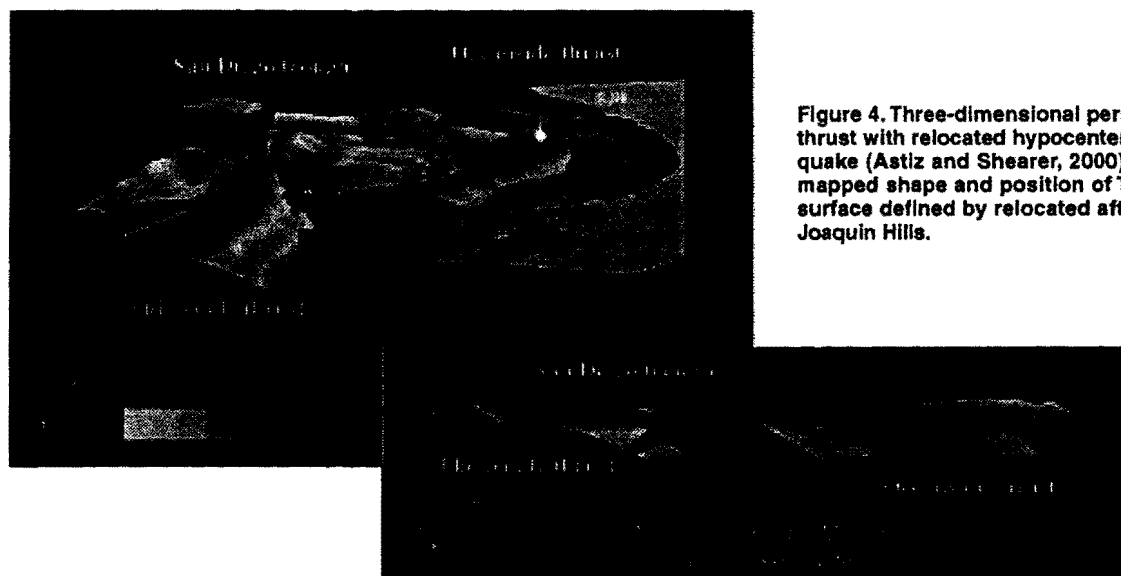


Figure 4. Three-dimensional perspective of Thirtymile Bank thrust with relocated hypocenters of 1986 Oceanside earthquake (Astiz and Shearer, 2000). Note correlation between mapped shape and position of Thirtymile Bank thrust with surface defined by relocated aftershock cluster. SJH—San Joaquin Hills.

(Kier and Mueller, 1999), which is west of the Thirtymile Bank thrust.

To further define activity on the Inner Borderlands thrust system, and to determine if these faults are seismogenic, we sought to establish the origin of the 1986 Oceanside (M_L 5.3) earthquake. The mainshock had a dominant component of thrust movement, whereas many of the aftershocks were strike slip (Hauksson and Jones, 1988). Astiz and Shearer (2000) relocated the mainshock and aftershocks of the Oceanside earthquake by using the L_1 -norm waveform cross-correlation method and quarry blast information from Catalina Island. The relocated earthquake sequence is clustered at ~ 8 km depth, and defines a 25° – 30° east-dipping surface (Fig. 4). The orientation and position of the fault plane are consistent with the downdip projection of the Thirtymile Bank thrust. Thus, we suggest that the earthquake ruptured a small part of the thrust, revealing the activity and seismogenic potential of thrust faults in the Inner California Borderlands.

SEISMIC HAZARDS

We assess the seismic hazard posed by these blind thrusts using fault areas to predict earthquake magnitudes and recurrence intervals based on empirical relations among rupture area, slip rate, and moment magnitude (Wells and Copper-smith, 1994). Lacking direct evidence of fault segmentation, we consider complete ruptures of the faults and thus maximum earthquake magnitudes, although ruptures may occur in smaller and more frequent events.

We defined the seismogenic fault area as the interval between 5 km depth and the base of the seismogenic crust at 20 km depth. If the Oceanside thrust ruptures only along the extent of the San Joaquin Hills (1390 km^2), this would produce an earthquake of M_w 7.1. This magnitude is similar to that proposed for a south-dipping blind

thrust (Grant et al., 1999), but invokes an opposed northeast-dipping seismic source. We contend, however, that the Oceanside and Thirtymile Bank thrusts are active over a region much larger than the extent of the San Joaquin Hills, on the basis of the Oceanside earthquake, coastal uplift, seafloor scarps, and observed geodetic shortening. To define these larger potential rupture areas, we must first address the interaction of these thrusts with active strike-slip faults in the region (Fig. 5). The Newport–Inglewood–Rose Canyon fault system is above or adjacent to the Oceanside thrust. Similarly, the San Diego trough strike-slip fault is above the Thirtymile Bank thrust.

We propose four possible interactions between these two classes of faults, each solution invoking a different fault geometry at depth that influences hazard estimates. One solution would have younger strike-slip faults cutting and precluding further activity on older thrusts (Fig. 5A). We contend that this solution is incompatible with the seismologic, geodetic, and geologic evidence supporting present activity on the thrust system. A second solution would have the thrusts terminate in the strike-slip faults (Fig. 5B). This scenario would dictate that the strike-slip faults cut down through the entire seismogenic crust, as is considered in most current hazard assessments. This solution is plausible for the Oceanside thrust. In this scenario, only the area of the Oceanside thrust west of this Newport–Inglewood–Rose Canyon strike-slip fault system should be considered as a possible earthquake source. In contrast, the location of the Oceanside earthquake indicates that the Thirtymile Bank thrust extends east of the San Diego trough fault (Fig. 4), precluding the type of fault linkage shown in Figure 5B.

Alternatively, the thrusts may cut the strike-slip fault zones (Fig. 5C). This solution would permit coeval activity on both types of faults and would yield two independent sources for each of

the paired thrust and strike-slip systems. In the final scenario, the thrust and strike-slip faults may merge into a single structure at depth (Fig. 5D). In this case, oblique slip on a deep fault would partition into pure thrust and strike-slip motion on the shallow faults. This linkage would imply that the combined areas of the strike-slip and thrust faults should be considered to determine maximum potential rupture areas.

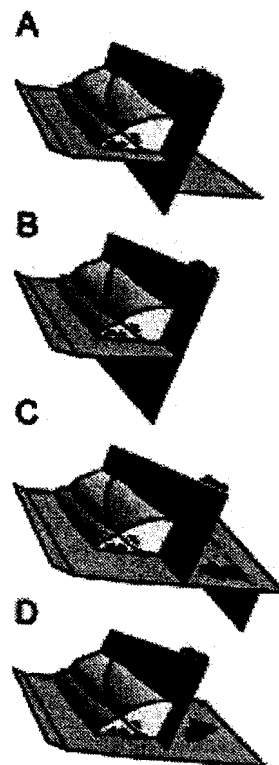


Figure 5. Potential configurations for thrust and strike-slip fault interaction (see text for discussion).

If the Oceanside thrust terminates in the Newport–Inglewood–Rose Canyon fault zone, as dictated in solution two, the thrust would have an area of 1890 km². A rupture of this entire fault would generate an earthquake of M_w 7.3. In contrast, if the Oceanside thrust extends through the Newport–Inglewood–Rose Canyon system, then it would have an area of 3180 km², which could produce an event of M_w 7.5. An estimated seismogenic area of 2516 km² for the Thirtymile Bank thrust would generate similar (M_w 7.4) earthquakes. If the Oceanside thrust and Newport–Inglewood–Rose Canyon system are linked, as described in the last solution (Fig. 5D), then the combined fault area (4393 km²) could produce M_w 7.6 earthquakes. This fault linkage scenario would not affect the magnitude estimate for the Thirtymile Bank thrust, because the San Diego trough fault is confined to sediments in the upper 2 km of the crust.

To estimate average recurrence intervals for these earthquake scenarios, we use minimum slip rates derived from terrace uplift (0.27 mm/yr for the Oceanside thrust), and maximum slip rates governed by the observed geodetic shortening (2.2 mm/yr for the Oceanside thrust; 0.96 mm/yr for Thirtymile Bank thrust). On the basis of these rates, M_w 7.1 events on the Oceanside thrust limited to the extent of the San Joaquin Hills would occur every 600–4600 yr. M_w 7.3 and 7.5 earthquakes on the greater Oceanside thrust would occur every 790–6400 and 1100–8800 yr, respectively. M_w 7.4 events on the Thirtymile Bank thrust would have minimum repeat times of 2100 yr. For the M_w 7.6 rupture scenario linking the Oceanside thrust and Newport–Inglewood–Rose Canyon faults, we must consider the oblique-slip rate that is resolved on the thrust and strike-slip faults. Onshore studies at San Diego Bay provide a slip rate of 1.07 ± 0.03 mm/yr for the Newport–Inglewood–Rose Canyon system (Rockwell et al., 1992). This strike slip combined with the range of dip-slip rates on the Oceanside thrust (0.27–2.2 mm/yr) yields an oblique slip range of 1.19–2.91 mm/yr. On the basis of these ranges of oblique slip rates, M_w 7.6 earthquakes would occur on average every 960–2300 yr. These rupture scenarios predict very large, but infrequent, earthquakes similar to those documented on other thrust faults in southern California (Rubin et al., 1998). Alternatively, stress on the Oceanside and Thirtymile Bank blind thrusts could be released in smaller but more frequent events.

ACKNOWLEDGMENTS

This research was partially funded by Harvard University and the Southern California Earthquake Center (SCEC). Data were provided by Texaco and other industry sponsors. SCEC is funded by the National Science Foundation (NSF) Cooperative Agreement EAR-8920136 and U.S. Geological Survey Cooperative Agreements 14–08-0001–A0899 and 1434–HQ–97AG01718. We thank M.P. Süss and F. Bilotti for contributions to this work.

REFERENCES CITED

- Astiz, L., and Shearer, P.M., 2000, Earthquake location in the Inner Continental Borderland, offshore southern California: *Seismological Society of America Bulletin*, v. 90, p. 425–449.
- Barrie, D., and Gath, E., 1992, Neotectonic uplift and ages of Pleistocene marine terraces, San Joaquin Hills, Orange County, California, in Heath, E., and Lewis, L., eds., *The regressive Pleistocene shoreline in southern California*: Santa Ana, California, South Coast Geological Society Annual Field Trip Guidebook 20, p. 115–121.
- Bohannon, R., and Geist, E., 1998, Upper crustal structure and Neogene tectonic development of the California continental borderland: *Geological Society of America Bulletin*, v. 110, p. 779–800.
- Crouch, J.K., and Suppe, J., 1993, Late Cenozoic tectonic evolution of the Los Angeles basin and Inner California Borderland: A model for core complex-like crustal extension: *Geological Society of America Bulletin*, v. 105, p. 1415–1434.
- Davis, T.L., Namson, J., and Yerkes, R.F., 1989, A cross section of the Los Angeles area: Seismically active fold and thrust belt, the 1987 Whittier Narrows earthquake, and earthquake hazard: *Journal of Geophysical Research*, v. 94, p. 9644–9664.
- Fisher, P.J., and Mills, G.I., 1991, The offshore Newport–Inglewood–Rose Canyon fault zone, California: Structure, segmentation and tectonics, in Abbott, P.L., and Elliott, W.J., eds., *Environmental perils, San Diego region*: San Diego, California, San Diego Association of Geologists, p. 17–36.
- Grant, L.B., Mueller, K.J., Gath, E.M., Cheng, H., Edwards, R.L., Munro, R., and Kennedy, G., 1999, Late Quaternary uplift and earthquake potential of the San Joaquin Hills, southern Los Angeles basin, California: *Geology*, v. 27, p. 1031–1034.
- Hauksson, E., and Jones, L., 1988, The July 1986 Oceanside ($M_L=5.3$) earthquake sequence in the Continental Borderland, southern California: *Seismological Society of America Bulletin*, v. 78, p. 1885–1906.
- Ingersoll, R.V., and Rumelhart, P.E., 1999, Three-stage evolution of the Los Angeles basin, southern California: *Geology*, v. 27, p. 593–596.
- Kern, J.P., and Rockwell, T.K., 1992, Chronology and deformation of Quaternary marine shorelines, San Diego county, California, in Heath, E., and Lewis, L., eds., *The regressive Pleistocene shoreline in southern California*: Santa Ana, California, South Coast Geological Society Annual Field Trip Guidebook 20, p. 1–7.
- Kier, G., and Mueller, K., 1999, Evidence for active shortening in the offshore Borderlands and its implications for blind thrust hazards in the Coastal Orange and San Diego Counties, 1999 Southern California Earthquake Center–SCEC Annual Meeting: Los Angeles, Southern California Earthquake Center, Proceedings and Abstracts, p. 71.
- Lajoie, K.R., Kern, J.P., and Wehmiller, J.F., 1979, Quaternary marine shorelines and crustal deformation, San Diego to Santa Barbara, California, in Abbott, P., ed., *Geologic excursions in the southern California area*: San Diego, California, San Diego State University, p. 3–15.
- Lajoie, K.R., Ponti, D.J., Powell, C.L., Mathieson, S.A., and Sarna-Wojcicki, A.M., 1992, Emergent marine strandlines and associated sediments, coastal California: A record of Quaternary sea-level fluctuations, vertical tectonic movements, climatic changes and coastal processes, in Heath, E., and Lewis, L., eds., *The regressive Pleistocene shoreline in southern California*: Santa Ana, California, South Coast Geological Society Annual Field Trip Guidebook 20, p. 81–104.
- Legg, M., Nicholson, C., and Sorlien, C., 1992, Active faulting and tectonics of the Inner California Continental Borderland: USGS lines 114 and 112: *Eos (Transactions, American Geophysical Union)*, v. 73, p. 588.
- Luyendyk, B.P., and Hornafius, J.S., 1987, Neogene crustal rotations transtension, and transpression in southern California, in Ingersoll, R.V., and Ernst, W.G., eds., *Cenozoic basin development of coastal California*: Englewood Cliffs, New Jersey, Prentice Hall, p. 259–283.
- Medwedeff, D., 1992, Geometry and kinematics of an active, laterally propagating wedge thrust, Wheeler Ridge, California, in Mitra, S., and Fisher, G.W., eds., *Structural geology of fold and thrust belts*: Baltimore, Maryland, Johns Hopkins University Press, p. 3–28.
- Mueller, K., Grant, L.B., and Gath, I., 1998, Late Quaternary growth of the San Joaquin Hills anticline: A new source of blind thrust earthquakes in the Los Angeles basin: *Seismological Research Letters*, v. 69, p. 161.
- Nicholson, C., Sorlien, C., and Legg, M., 1993, Crustal imaging and extreme Miocene extension of the Inner California Continental Borderland: *Geological Society of America Abstracts with Programs*, v. 25, no. 6, p. A-418.
- Nicholson, C., Sorlien, C., Atwater, T., Crowell, J., and Luyendyk, B.P., 1994, Microplate capture, rotation of the western Transverse Ranges, and initiation of the San Andreas transform as a low-angle fault system: *Geology*, v. 22, p. 491–495.
- Rockwell, T.K., Lindvall, S.C., Haraden, C., Kenji, C., and Baker, E., 1992, Minimum Holocene slip rate for the Rose Canyon fault, in Heath, E., and Lewis, L., eds., *The regressive Pleistocene shoreline in southern California*: Santa Ana, California, South Coast Geological Society Annual Field Trip Guidebook 20, p. 55–64.
- Rubin, C.M., Lindvall, S.C., and Rockwell, T.K., 1998, Evidence for large earthquakes in metropolitan Los Angeles: *Science*, v. 281, p. 398–401.
- Schneider, C.L., Hummon, C., Yeats, R.S., and Huftile, G.L., 1996, Structural evolution of the northern Los Angeles basin, California, based on growth strata: *Tectonics*, v. 15, p. 341–355.
- Shaw, J.H., and Shearer, P.M., 1999, An elusive blind thrust fault beneath metropolitan Los Angeles: *Science*, v. 283, p. 1516–1518.
- Shaw, J.H., and Suppe, J., 1996, Earthquake hazards of active blind thrust faults under the central Los Angeles basin, California: *Journal of Geophysical Research*, v. 101, p. 8623–8642.
- Shaw, J.H., Bischke, R.E., and Suppe, J., 1994, Relations between folding and faulting in the Loma Prieta epicentral zone: Strike-slip fault-bend folding, in Simpson, R.W., ed., *The Loma Prieta, California, earthquake of October 17, 1989*: U.S. Geological Survey Professional Paper 1550-F, p. F3–F21.
- Sorlien, C., Nicholson, C., and Luyendyk, B., 1993, Miocene collapse of the California continental margin: *Geological Society of America Abstracts with Programs*, v. 25, no. 6, p. A-311.
- U.S. Geological Survey and Southern California Earthquake Center Scientists, 1994, The magnitude 6.7 Northridge, California, earthquake of 17 January 1994: *Science*, v. 266, p. 389–397.
- Wells, D.L., and Coppersmith, K.J., 1994, New empirical relationships among the magnitude, rupture length, rupture width, rupture area, and surface displacement: *Seismological Society of America Bulletin*, v. 84, p. 974–1002.

Manuscript received March 10, 2000

Revised manuscript received July 5, 2000

Manuscript accepted July 14, 2000

SONGS vs ISFSI Design 4% Horiz. Spectra

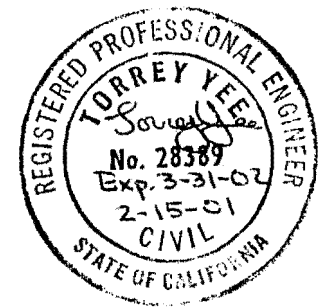
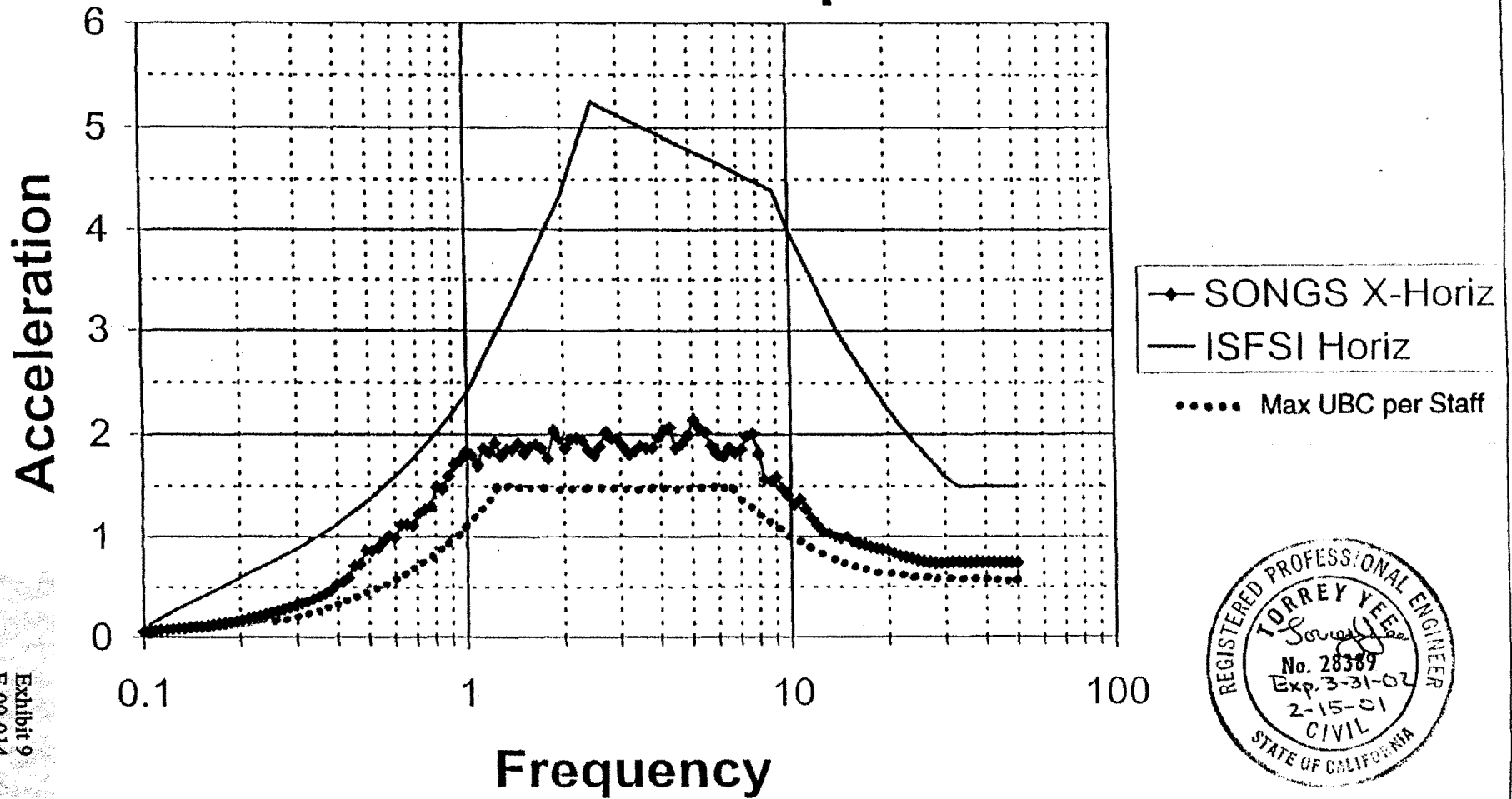


Exhibit 9
E-00-014

Figure 1

SONGS vs ISFSI Design 4% Horiz. Spectra

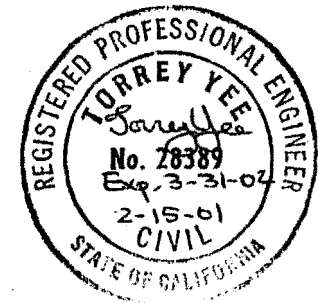
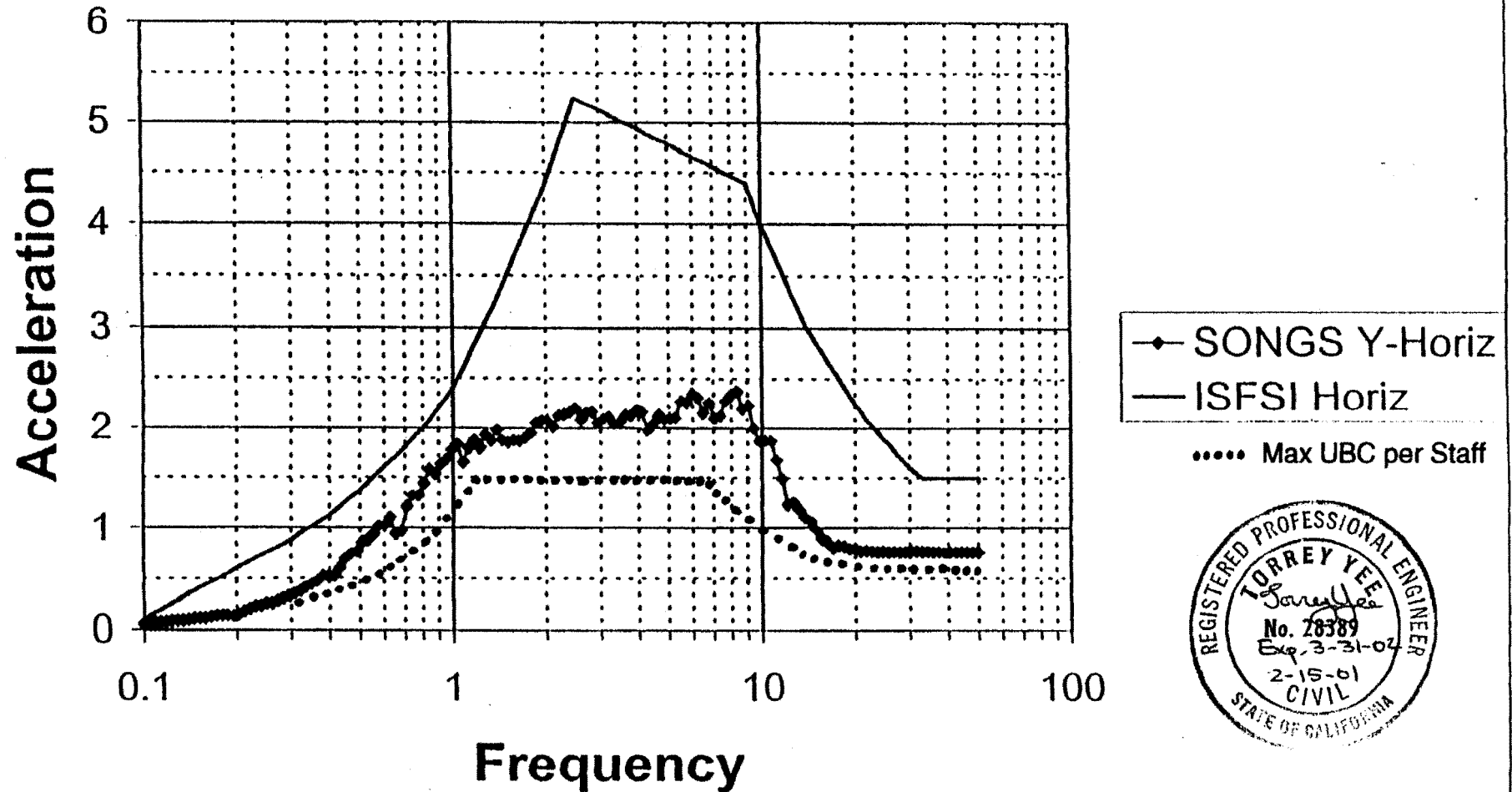


Figure 2

SONGS vs ISFSI Design 4% Vertical Spectra

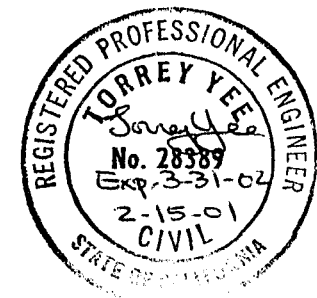
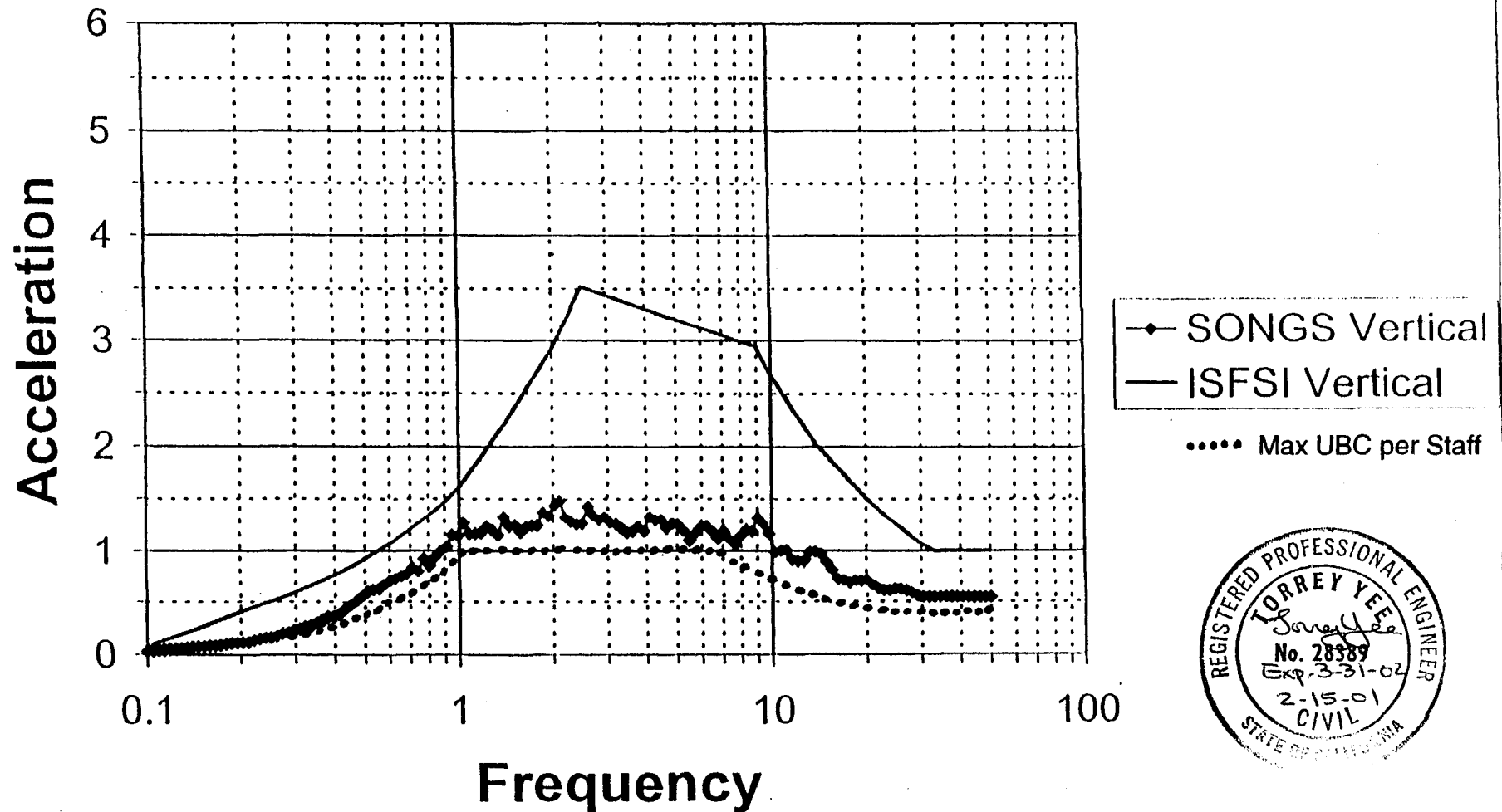


Figure 3

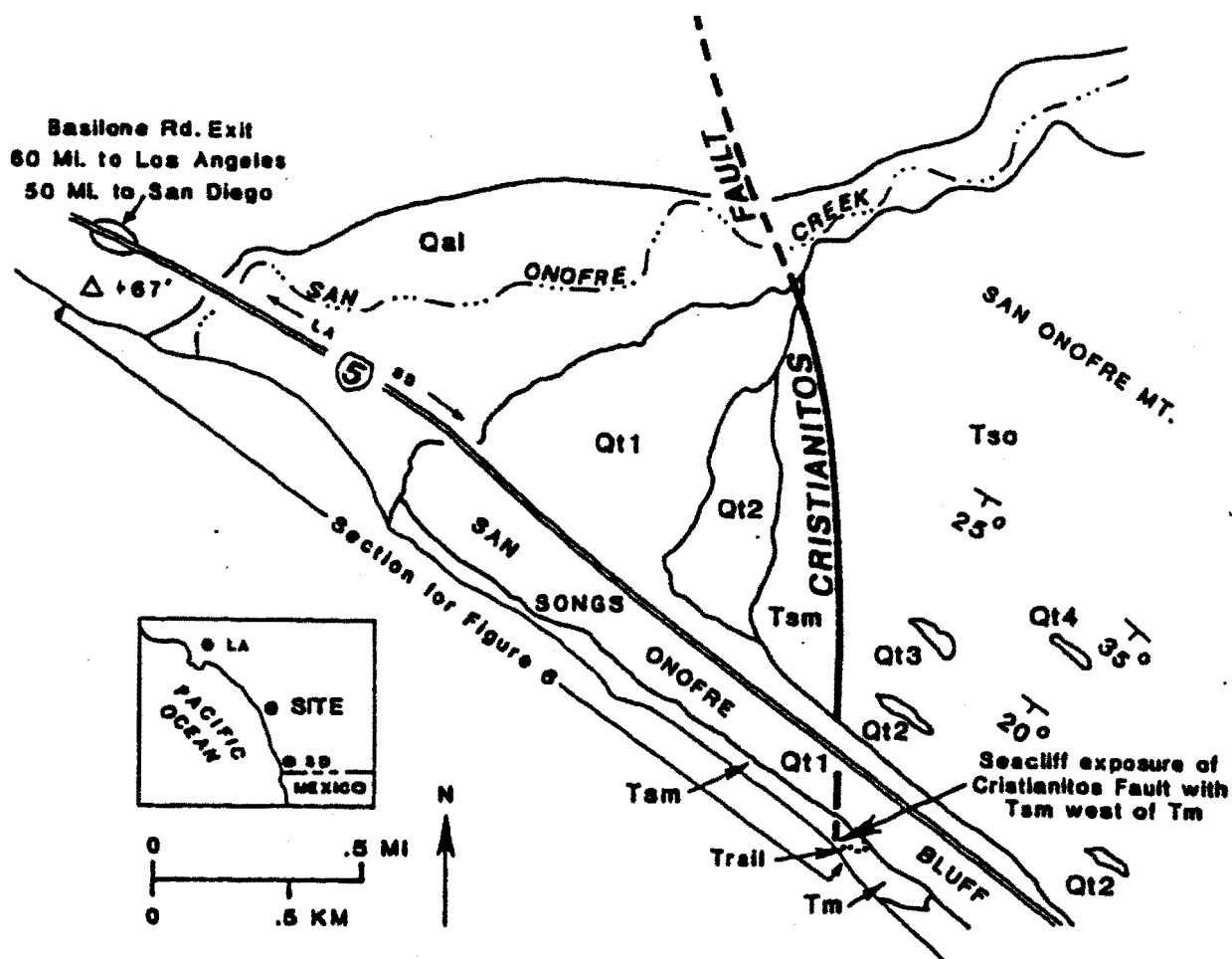


Figure 1. Generalized location and geologic map of the San Onofre State Beach and adjacent area. Geographic symbols: LA = Los Angeles; SD = San Diego; SONGS = San Onofre Nuclear Generating Stations. Geologic symbols: Qal = alluvium; Qt1 (younger), Qt2, etc. = marine terraces and fluvial terraces of San Onofre Creek; Tm = Tertiary Monterey Formation; Tsm = Tertiary San Mateo Formation; Tso = Tertiary San Onofre Breccia; + 67' = Medio triangulation station (modified from Moyle, 1973; Hunt and Hawkins, 1975).

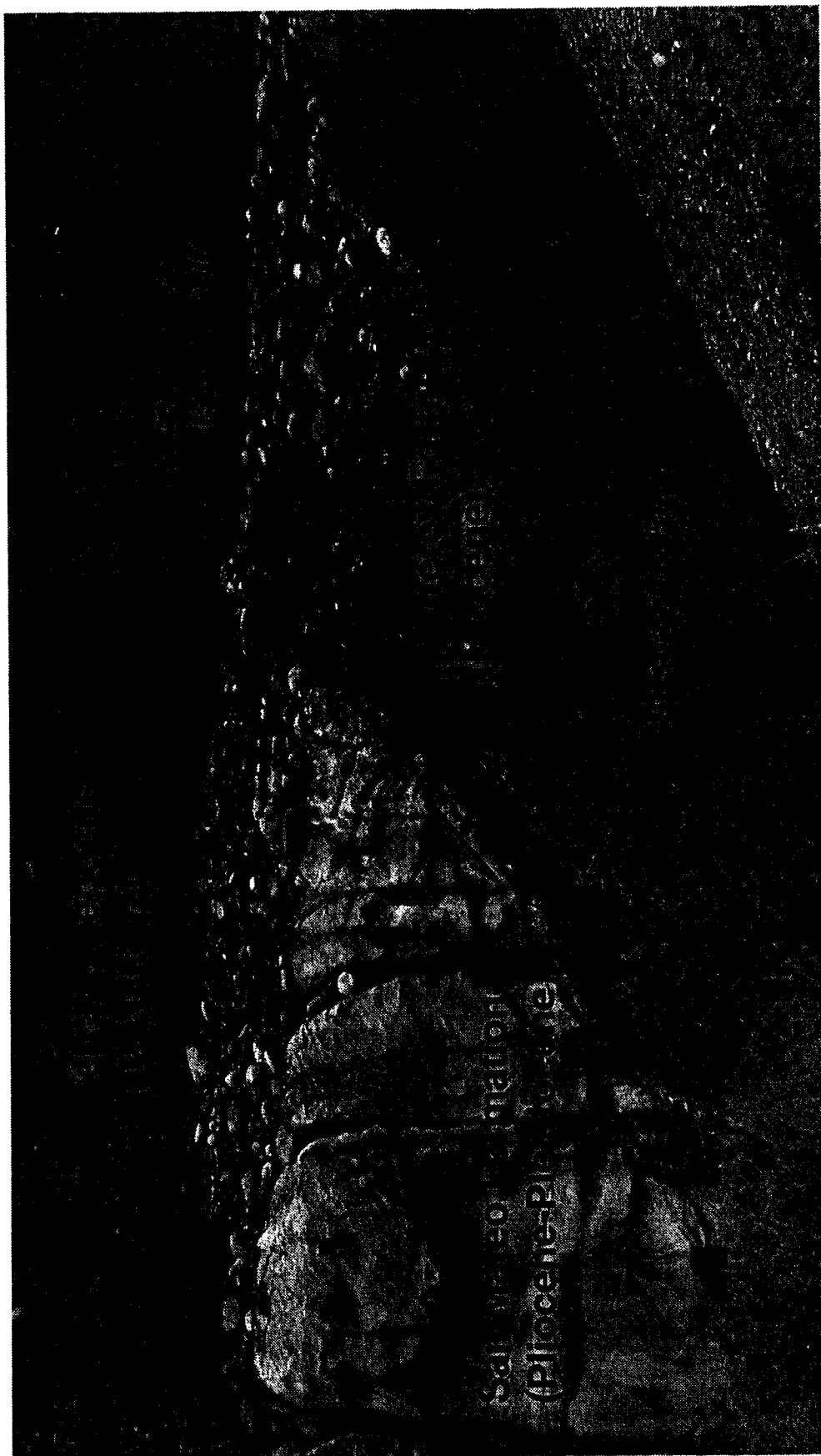


Exhibit 11
E-00-014

June 26, 2000

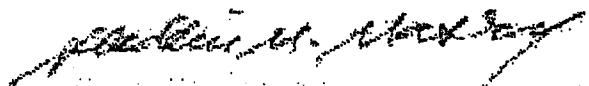
USGS:

Dear Gentlemen:

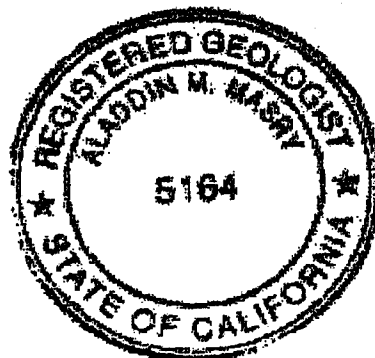
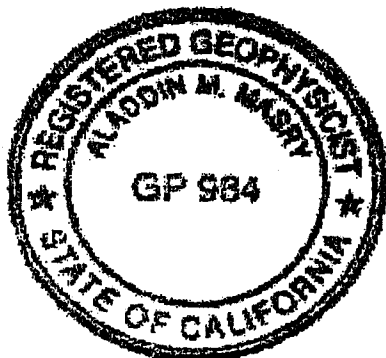
URGENT MESSAGE REGARDING PUBLIC SAFETY FROM GEOLOGIC
HAZARD

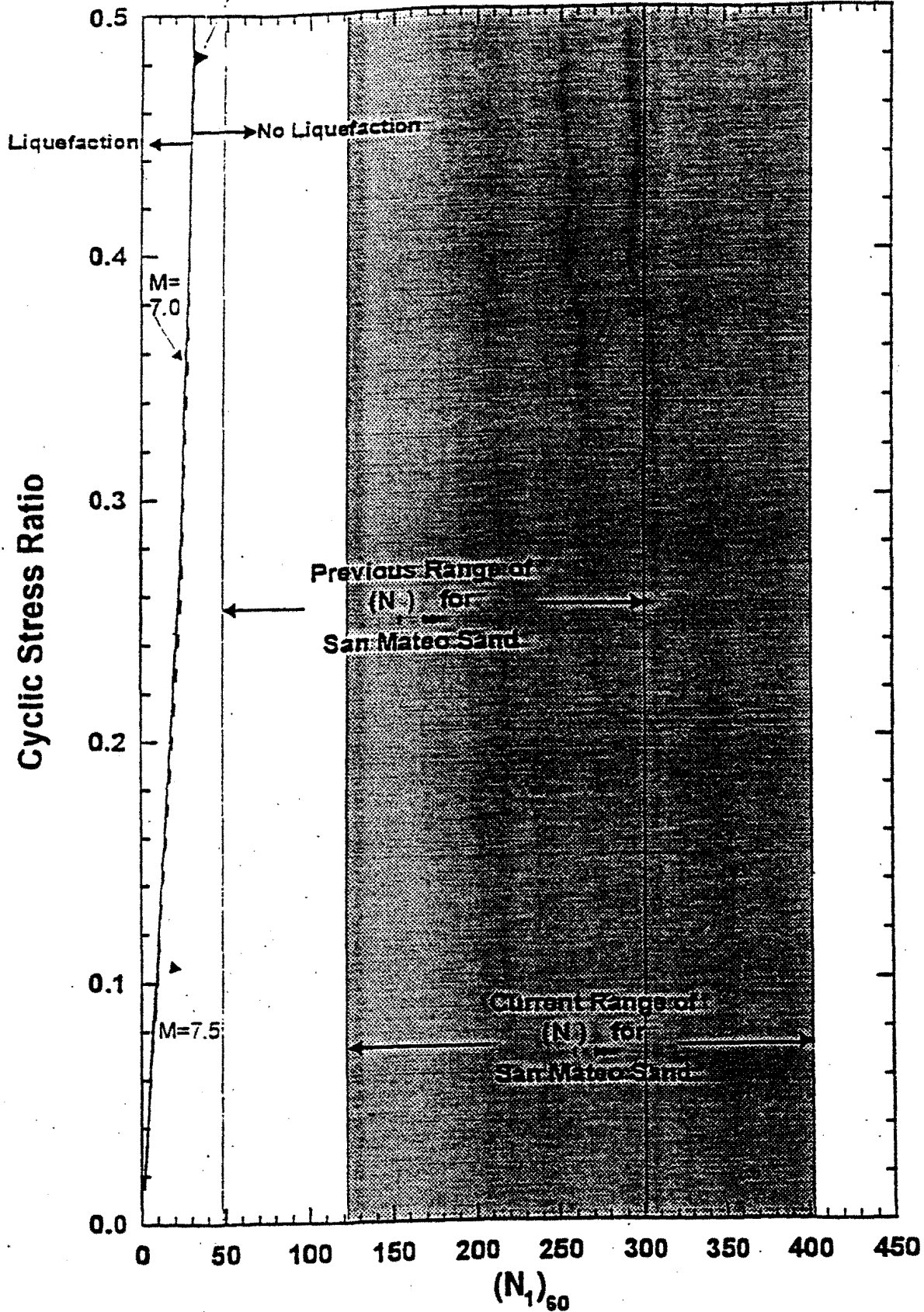
Recent visit to camp San Onofre indicated that the San Christianitos Fault has moved and ruptures the ground. The fault runs in juxtaposition to San Onofre nuclear power plant and its movement endangers the plant structural integrity and possibly results in a nuclear disaster in the Southland of California, San Diego County.

The public has the right to know and the government has the obligations to initiate immediate technical investigation to determine the size and nature of the fault's displacement for risk assessment. This is a serious situation that requires immediate response.


ALADDIN M. MASRY, B.S., M.S., M.S.
26473 Cynthia St., Hemet, CA 92544

909-65-6817





Comparison of Cyclic Resistance vs. Liquefaction Threshold for San Mateo Sand

Project No. 954E181

Date: SEPT 1995

Project: SONGS CASK STORAGE

Fig. 5.3

CALCULATION SHEET

| | |
|-----------------|-------------------|
| ICCN NO./ | PAGE ____ OF ____ |
| PRELIM. CCN NO. | CCN CONVERSION: |
| | CCN NO. CCN-- |

Project or DCP/MMP _____ Calc No. _____

Subject CALCULATION OF ULTIMATE BEARING CAPACITY Sheet No. _____

| REV | ORIGINATOR | DATE | IRE | DATE | REV | ORIGINATOR | DATE | IRE | DATE | REV. INDICATOR |
|-----|------------|---------|-----|------|-----|------------|------|-----|------|----------------|
| △ | T.Yee | 2/15/01 | | | △ | | | | | ↓ |
| △ | | | | | △ | | | | | |

ULTIMATE STATIC BEARING CAPACITY

$$q_u = cN_c \zeta_c + qN_q \zeta_q + \frac{1}{2} \gamma B N_\gamma \zeta_\gamma$$

where:

- q_u = ultimate bearing capacity
- c = cohesion = 800 lb/ft² *
- γ = unit weight = 130 lb/ft³ *
- q = overburden. (conservatively ignore)
- N_c, N_q, N_γ = bearing capacity factors = 95.7, 81.3, 100.4 **
- B = foundation width = 67' (minimum SONGS building width)
- $\zeta_c, \zeta_q, \zeta_\gamma$ = shape factors = 1.3, 1, .8 for square footing



* San Mateo sand properties
 $\phi = 41^\circ$

** Factors from J. Bowles, "Foundation Analysis and Design," Third Edition, 1982. (Table 4-2)
Values are for $\phi = 40^\circ$.

Ignore overburden

$$q_u = .800(95.7)1.3 + 0 + \frac{1}{2} (.130)67(100.4)(.8)$$

$$= 449 \text{ ksf}$$

Exhibit 14
E-00-014

Q.1 Although data were provided that address soil properties according to a "Seismic System Analysis" in the document entitled "Foundation and Soil Properties, Independent Spent Fuel Storage Installation, San Onofre Nuclear Generating Station Unit 1," no data were provided that demonstrate the stability of the pad foundation for general or localized shear failure under static conditions. Such data would be useful.

A.1 SCE constructed SONGS Units 1, 2, and 3 in accordance with the seismic standards established by the U.S. Nuclear Regulatory Commission (NRC). The NRC performed a comprehensive evaluation of the soil properties and stability of the site foundation prior to issuing the operating licenses for these units, in part, for the purposes of assuring stability and structural integrity, and assuring that the units do not create or contribute to erosion, geologic instability, or destruction of the site or surrounding area. The results of the NRC's evaluation is NUREG-0712, NUREG-0712 Safety Evaluation Report related to the operation of San Onofre Nuclear Generating Station Units 2 and 3, dated February 1981, which was provided in pertinent part in Enclosure 2 of SCE's December 21, 2000 letter to Mr. Dan Chia.

The uniform static bearing load of the storage modules and pad on the soil will be about 1.75 ksf. The ultimate bearing capacity of San Mateo sand was computed for the most heavily loaded structures at SONGS and is greater than 400 ksf. The ultimate bearing capacity was determined using the soil properties and building parameters given in UFSAR Section 2.5.4.10.3, page 2.5-215 (which was provided in Enclosure 3 of the December 21, 2000 letter and is included in Document 1 of this transmittal).

SCE will construct the temporary spent fuel storage facility on a portion of the site licensed by the NRC for the construction of the nuclear units. SCE will design and construct this facility to meet the NRC seismic standards for such facilities. These standards are included in 10 C.F.R. 72, "Licensing Requirements for the Independent Storage of Spent Nuclear Fuel and High Level Radioactive Waste", Regulatory Guide 1.60, "Design Response Spectra for Seismic Design of Nuclear Power Plants", and NUREG 1536, "Standard Review Plan for Dry Cask Storage Systems". These federal design standards ensure the protection of public health and safety relative to the nuclear fuel and fully bound standards used in industrial construction, including PRC Section 30253.

INFORMATION ONLY

CALCULATION TITLE PAGE

| | | |
|---|---|--|
| ICCN NO./ PRELIM. CCN NO. N/A | | PAGE OF |
| Calc No. <u>C-296- 01. 04</u> DCP/FIDCN/ FCN No. & Rev. _____ | | CCN CONVERSION: CCN NO. CCN- |
| Subject: <u>ISFSI Foundation Design</u> | | Sheet <u>1</u> of <u>10</u> |
| System Number/Primary Station System Designators <u>2126 / XA1</u> | | SONGS Unit <u>1</u> Q-Class <u>II</u> |
| Tech. Spec./LCS Affecting? <input checked="" type="radio"/> NO <input type="radio"/> YES Section No. _____ | | Equipment Tag No. _____ |
| Site Programs/Procedure Impact? <input checked="" type="radio"/> NO <input type="radio"/> YES, AR No. _____ | | |
| CONTROLLED COMPUTER PROGRAM/ DATABASE | <input type="checkbox"/> PROGRAM <input type="checkbox"/> DATABASE <u>N/A</u> According to SO123-XXIV-5.1 | PROGRAM/ DATABASE NAME(S) _____ <input type="checkbox"/> ALSO, LISTED BELOW VERSION/ RELEASE NO. (S) _____ |

RECORD OF ISSUES

| REV. DISC | DESCRIPTION | TOTAL SHTS. LAST SHT | PREPARED (Print name/sign/date) | APPROVED (Signature/date) |
|--------------|---------------------------------------|----------------------------|---|---------------------------------------|
| <u>A</u> | <u>Original Issue for Information</u> | <u>10</u> | ORIG. <u>[Signature]</u> | FLS <u>[Signature]</u> 11-17-00 OTHER |
| <u>CIVIL</u> | | <u>10</u> | IRE <u>John Stoclet</u> <u>John P. Stoclet 9/24/00</u> | OTHER <u>[Signature]</u> OTHER |
| | | | ORIG. | FLS OTHER |
| | | | IRE | OTHER OTHER |
| | | | ORIG. | FLS OTHER |
| | | | IRE | OTHER OTHER |
| | | | ORIG. | FLS OTHER |
| | | | IRE | OTHER OTHER |

Space for RPE Stamp, identify use of an alternate calc., and notes as applicable.



INFORMATION ONLY

This calc. was prepared for the identified DCP/FCN. DCP/FCN completion and turnover acceptance to be verified by receipt of a memorandum directing DCN Conversion. Upon receipt, this calc. represents the as-built condition. Memo date. _____ by _____

CALCULATION CROSS-INDEX

| | |
|------------------------------|---------------------------------|
| ICCN NO./ PRELIM. CCN NO. | PAGE _____ OF _____ |
| Sheet No. <u>2</u> of _____ | CCN CONVERSION: CCN NO. CCN- |

Calculation No. C-296 - 01.04

Sheet No. 2 of

| Calc. rev. number and responsible FLS initials and date | INPUTS These interfacing calculations and/or documents provide input to the subject calculation and if revised may require revision of the subject calculation. | | OUTPUTS Results and conclusions of the subject calculation are used in these interfacing calculations and/or documents. | | Does the out- put interface calc/ document require change? | Identify output interface calc/document CCN, DCN, TCN/Rev., FIDCN, or tracking number. |
|---|---|------------------|--|----------|---|---|
| | Calc / Document No. | Rev. No. | Calc / Document No. | Rev. No. | | |
| 0 | 501-207-1-C11 C-296-1.01 C-296-01.02 501-207-1-M135 | 4 0 0 0 | None | | N/A | |
| | | | | | | |
| | | | | | | |

EC&FS DEPARTMENT
CALCULATION SHEET

| | |
|----------------------------------|-------------------|
| ICCN NO./ PRELIM. CCN NO. | PAGE ____ OF ____ |
| CCN CONVERSION: CCN NO. CCN - | |

Project or DCP/FCN _____ Calc No. C-296-01.04

Subject SPB FOUNDATION DESIGN Sheet 3 of ____

| REV | ORIGINATOR | DATE | IRE | DATE | REV | ORIGINATOR | DATE | IRE | DATE | REV INDICATOR |
|-----|------------|------|-----|---------|-----|------------|------|-----|------|---------------|
| | P. BARN | | JCS | 9/22/00 | | | | | | |
| | | | | | | | | | | |

TABLE OF CONTENTS

SHEET

| | | |
|----|------------------------|---|
| 1. | Introduction / Purpose | 4 |
| 2. | Results / Conclusions | 4 |
| 3. | Assumptions | 4 |
| 4. | Design Inputs | 4 |
| 5. | Methodology | 4 |
| 6. | References | 5 |
| 7. | Nomenclature | 5 |
| 8. | Calculations | 6 |

INFORMATION ONLY

EC&FS DEPARTMENT
CALCULATION SHEET

| | |
|----------------------------------|-------------------|
| ICCN NO./ | PAGE ____ OF ____ |
| PRELIM. CCN NO. | |
| CCN CONVERSION: CCN NO. CCN - | |

Project or DCP/FCN _____ Calc No. C-296-01.04

Project ISFSI FOUNDATION DESIGN

Sheet 4 of ____

| REV | ORIGINATOR | DATE | IRE | DATE | REV | ORIGINATOR | DATE | IRE | DATE | REV INDICATOR |
|-----|------------|------|-----|---------|-----|------------|------|-----|------|---------------|
| | P. BARN | | JCS | 9/22/00 | | | | | | |
| | | | | | | | | | | |

1. Introduction / Purpose

The purpose of this calculation is to design the reinforced concrete pad for the storage modules of Independent Spent Fuel Storage Installation (ISFSI). There are multiple storage modules placed on the concrete pad and they are connected together to form a single structure.

2. Results / Conclusions

Design loads are based on seismic accelerations of 1.5g horizontal and 1.0g vertical.

ISFSI concrete pad : 3'-0 thick

Moment (Capacity) = 268 foot kips > Moment (Design Load) = 260 ft kips

Allowable Soil Bearing = 23.5 ksf > Soil Bearing (Design) = 10.11 ksf

3. Assumptions - Stated in calculation.

4. Design Inputs

Module weight = 400 + 70 = 470 kips with back wall (SO1-207-1-C11, Rev. 4, Table H1 and page H9). Used 471 kips in this calculation which is conservative.

Concrete compressive strength = 4000 psi; F_y = 60 ksi for A615, Grade 60

Seismic load: DBE 1.5g horizontal and 1.0g vertical (Reference TN West design spectra included in C-296-1.01, Rev. 0). SONGS requirements are actually based on a 0.67g seismic event. The higher seismic accelerations were used to be consistent with the TN West design and are not a design basis for SONGS.

5. Methodology

The multiple storage modules are placed in a single row without any separation between them. The modules are not connected to the concrete pad. The ISFSI Pad Other Events Hazard Evaluation, Ref. 6.7, demonstrates that the seismic event bounds the other events applicable to the SONGS site. The configuration of the module array will tend to reduce the bending of the concrete pad in the area under the modules.

INFORMATION ONLY

EC&FS DEPARTMENT
CALCULATION SHEET

| | |
|----------------------------------|-------------------|
| ICCN NO./ PRELIM. CCN NO. | PAGE ____ OF ____ |
| CCN CONVERSION: CCN NO. CCN - | |

Project or DCP/FCN _____ Calc No. C-296-01.04

Subject ISFSI FOUNDATION DESIGN Sheet 5 of ____

| REV | ORIGINATOR | DATE | IRE | DATE | REV | ORIGINATOR | DATE | IRE | DATE | REV INDICATOR |
|-----|------------|------|-----|---------|-----|------------|------|-----|------|---------------|
| | P. BARN | | JCS | 9/22/00 | | | | | | |
| | | | | | | | | | | |

5. Methodology (cont.)

Soil pressure is calculated by using a two-component horizontal seismic load of 1.5g and a vertical component of 1.0 g, and combining them by SRSS method. The reinforcing design is based on the moment calculated for a 10 feet cantilever one-way slab, loaded with the resultant of maximum soil pressure. Reinforced concrete design is in accordance with ACI 349.

The structural design and stability of the storage module are given in Ref. 6.4.

6. References

- 6.1 SO1-207-1-C11, Rev. 4, DSC/AHSM/0S197 Cask Component Weights, Mass Properties, and Lift Weight Calculation and Evaluation by TN West
- 6.2 SCE Calculation C-296-1.01, Rev. 0, Seismic Response of ISFSI Pad
- 6.3 ACI Manual Of Concrete Practice-Code Requirements for Nuclear Safety Related Concrete Structures (ACI-349)
- 6.4 SO1-207-1-M135, Rev. 0, Safety Analysis Report for the Standardized Advanced NUHOMS Horizontal Modular Storage System for Irradiated Nuclear Fuel, by TN West
- 6.5 SONGS 2&3 Preliminary Safety Analysis Report, Appendix 2B, Seismic and Foundation Studies for Proposed Units 2 and 3, San Onofre Nuclear Generating Station - Dames and Moore
- 6.6 Designing Floor Slabs on Grade Design Manual
- 6.7 SCE Calculation C-296-01.02, Rev. 0, ISFSI Pad Other Events Hazard Evaluation

7. Nomenclature

ISFSI - Independent Spent Fuel Storage Installation
 AHSM - Advanced Horizontal Storage Module
 TNW - TransNuclear West
 SRSS- Square Root of the Summation of Squares
 g - Acceleration of Gravity
 q - Soil pressure

INFORMATION ONLY

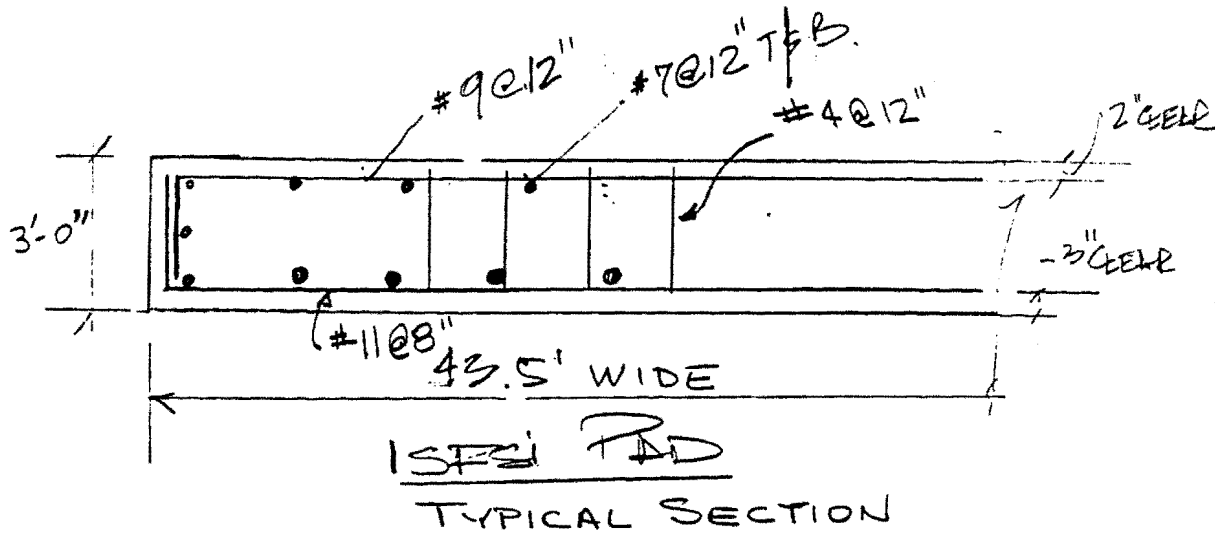
Project or DCP/FCN _____ Calc No. C-246-01.04

Subject ISFC FOUNDATION DESIGN

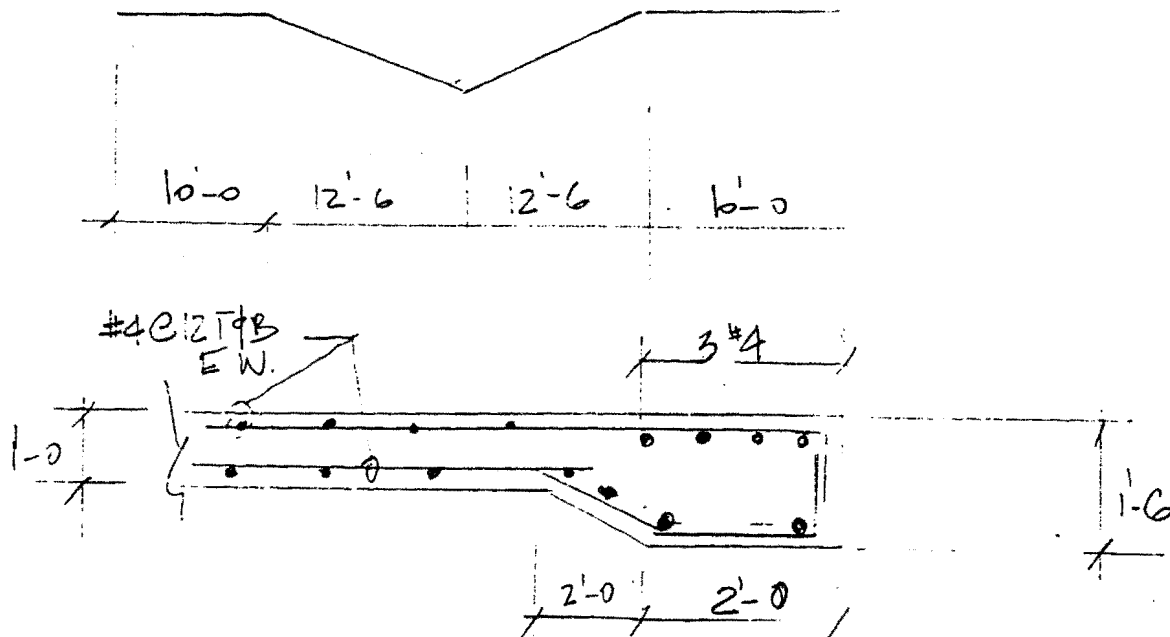
Sheet 6 of

| REV | ORIGINATOR | DATE | I/E | DATE | REV | ORIGINATOR | DATE | I/E | DATE |
|-----|------------|---------|-----|---------|-----|------------|------|-----|------|
| | P.B. MANN | 7/22/00 | JCS | 9/26/00 | | | | | |
| | | | | | | | | | |

REV
↓
INDICATOR



INFORMATION ONLY



SUB ON GRADE

CALCULATION SHEET

Project or DCP/FCN

Calc No.

C-2016-01.04

CCN CONVERSION:
CCN NO. CCN-

Subject ISFSI FOUNDATION DESIGN

Sheet 7 of

| REV | ORIGINATOR | DATE | REV | ORIGINATOR | DATE |
|-----|------------|---------|-----|------------|------|
| | PDN | JCI | | | |
| | | 9/26/00 | | | |

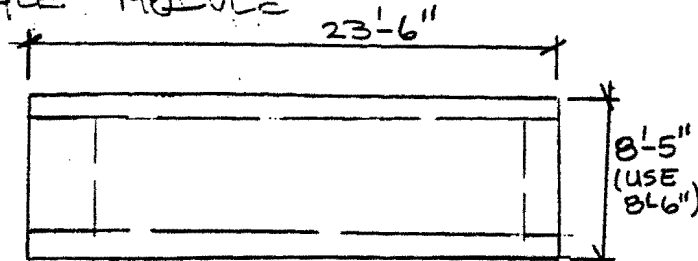
REV
RECORD

ISFSI FOUNDATION DESIGN

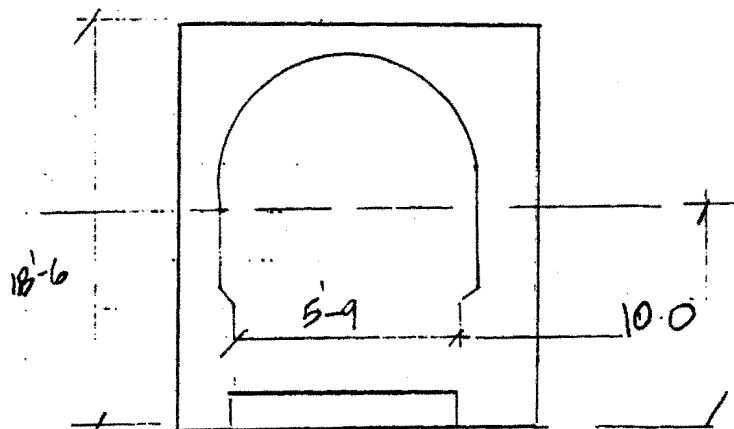
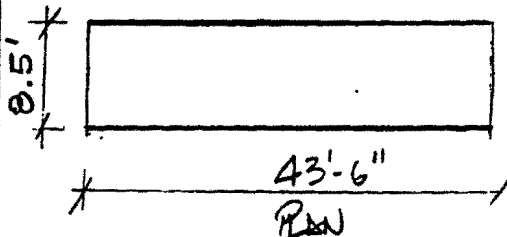
MODULE WEIGHT = 400K → FOR REF COE 501-207-1-C11, TABLE 41

PAD SIZE FOR A SINGLE MODULE

USE 43.5' x 8.5' x 3.0'



MODULE & REAR SHIELD WALL PLAN



MODULE SECTION

REAR SHIELDING WALL WT:

$$18.5 \times 3 \times 8.5 = 71K$$

TOTAL MODULE WT. = 400 + 71 = 471K
(INCLUDING REAR SHIELD WALL)

INFORMATION ONLY

WEIGHT OF PDN = $43.5 \times 3 \times 8.5 \times .15 = 166K$

$$\therefore \sum U = 471 + 166 = 637K \text{ MODULE + PAD}$$

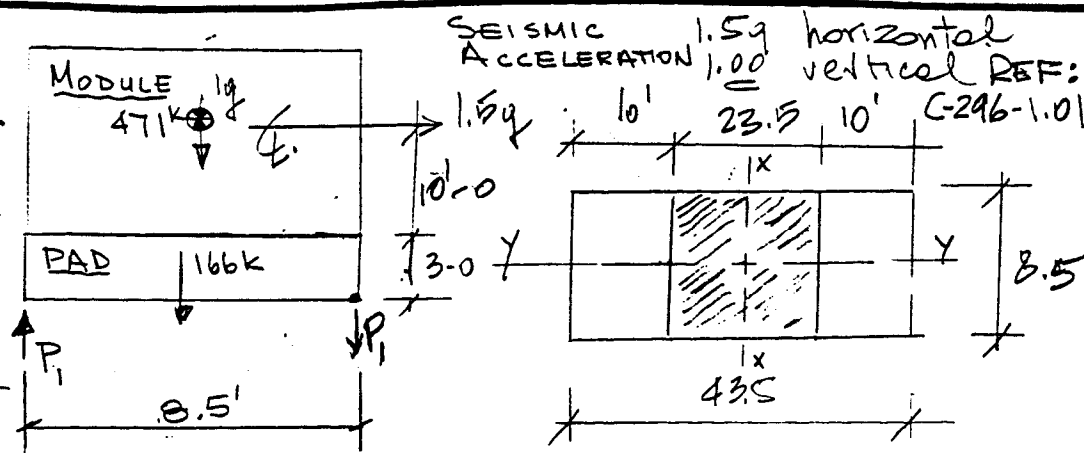
Subject ISPS FOUNDATION DESIGN

Sheet 8 of 10

| REV | ORIGINATOR | DATE | IRE | DATE | REV | ORIGINATOR | DATE | IRE | DATE |
|-----|------------|------|-----|---------|-----|------------|------|-----|------|
| | BARN | | LCI | 9/22/00 | | | | | |
| | | | | | | | | | |

REV
 INDICATOR

DUE TO
SEISMIC
& DEAD
WEIGHT
OF MODULE



DEAD LOAD
SOIL PRESSURE: $q_{DL} = \frac{V}{A} = \frac{637}{8.5 \times 43.5} = 1.72 \text{ ksf}$

SEISMIC VERTICAL: $q_z = 1g \times 1.72 = 1.72 \text{ ksf}$

SEISMIC SOIL PRESSURE ABOUT X-X

$$OTM_x = 1.5g \times 471 \times 13 + 1.5g \times 166 \times 1.5$$

$$= 9558 \text{ k-ft}$$

$$e_x = \frac{\sigma_{TM}}{V} = \frac{9558}{637} = 15.0' > \frac{L}{6} = \frac{43.5}{6} = 7.25'$$

$$q_x = \frac{2V}{3B(\frac{L}{2} - e)} = \frac{2 \times 637}{3(0.5)(\frac{43.5}{2} - 15)} = 7.4 \text{ ksf}$$

SEISMIC SOIL PRESSURE ABOUT 4-4

INFORMATION ONLY

SINCE THE MODULES ARE TIED TOGETHER, THE SOIL PRESSURE WILL BE BASED ON 10 MODULES. ACTUALLY, 19 MODULES ARE PLANNED FOR SONG 1.

$$OTM_y = 10 [1.5 \times 471 \times 13 + 1.5 \times 166 \times 1.5] = 95,580 \text{ k-ft}$$

$$e_y = \frac{95580}{10 \times 637} = 15' > \frac{L}{6} = \frac{10 \times 8.5}{6} = 14.17'$$

$$q_y = \frac{2 \times 637(10)}{3(43.5)\left(\frac{85}{2} - 15\right)} = 3.55 \text{ ksf}$$

EC2FS DEPARTMENT CALCULATION SHEET

| | |
|----------------------------------|-------------------|
| CCN NO. / PRELIM. CCN NO. | PAGE ____ OF ____ |
| CCN CONVERSION: CCN NO. CCN - | |

Project or OCP/FCN _____ Calc No. C-296-01.01

Subject ISPS FOUNDATION DESIGN

Sheet 9 of ____

| REV | ORIGINATOR | DATE | REV | ORIGINATOR | DATE |
|-----|------------|------|-----|------------|---------|
| | J.P. Brown | | JCS | | 9/12/00 |
| | | | | | |

REV
ORIGINATOR

TOTAL SOIL PRESSURE

$$\therefore q_{TOT} = q_{DL} + [q_x^2 + q_y^2 + q_z^2]^{\frac{1}{2}} = 1.72 + [7.4^2 + 3.55^2 + 1.72^2]^{\frac{1}{2}}$$

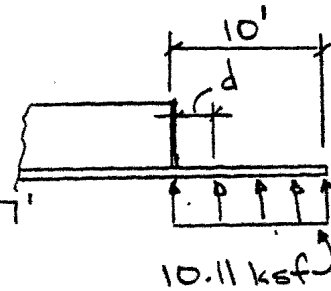
$$= 1.72 + 8.39 = 10.11 \text{ ksf} < 15.63 \times 1.5 = 23.5 \text{ ksf}$$

Allowable soil bearing
at 3' embedment
and 50% increase
for seismic loads.
(SONGS 243 PSAR
Appendix 2B)

CONCRETE DESIGN (ACI 349)

ASSUME 10'-0" PERIOD FROM MODULE
TO THE EDGE CANTILEVER

$$d = \frac{32}{12} = 2.67'$$



$$M_{ed} = \frac{qL^2}{2} = \frac{(10.11 - .45)(10 - 2.67)^2}{2}$$

← pad wt.

$$= 260 \text{ k-ft/ft}$$

INFORMATION ONLY

Based on $A_s = 2.34 \text{ in}^2/\text{ft}$: $M_{CAP} = A_s \text{ and } d = 2.34 / (3.58)^{3/2}$
(see below) $= 268 \text{ k-ft/ft}$

$$V_{shear} = (10.11 - .45)(10 - 2.67) = 70.8 \text{ k/ft}$$

Root

$$A_s = \frac{M}{a_u d} = \frac{260}{3.58(32)} = 2.27 \frac{\text{in}^2}{\text{ft}} \text{ use } \#11 @ 8" \quad A_s = 2.34 \text{ in}^2/\text{ft}$$

$$K_u = \frac{M_u}{F} = \frac{260}{1.024} = 254 \rightarrow a_u = 3.58 F = \frac{b d^2}{12000} \cdot \frac{12 \times 32^2}{12000}$$

(ACI Design Handbook, Flexure 1.2) $= 1.024$

CALCULATION SHEET

SC&FS DEPARTMENT

CCN NO. /
PRELIM. CCN NO.

PAGE ____ OF ____

CCN CONVERSION:
CCN NO. CCN -

Project or OCP/FCN _____ Calc No. C-296-01.04

Subject ISFSI FOUNDATION DESIGN Sheet 10 of 10

| REV | ORIGINATOR | DATE | IRE | DATE | REV | ORIGINATOR | DATE | IRE | DATE | REV INDICATOR |
|-----|------------|------|-----|---------|-----|------------|------|-----|------|---------------|
| | P. BREW | | JU | 9/11/00 | | | | | | |
| | | | | | | | | | | |

$$v_u = 70.8 / (12 \times 32) = .184 \text{ ksi} \approx .108 \text{ ksi}$$

$$v_c = 2 \times .25 \sqrt{4000} \approx .108 \text{ ksi}$$

Provide shear reinforcement:

$$v_s = .184 - .108 = .076 \text{ ksi}$$

Try #4 : $A_v = .20 \text{ in}^2$

Spacing:

$$s = \frac{A_v f_y}{v_s b} = \frac{.20 \times 60}{.076 \times 12}$$

$$= 13.2"$$

\therefore Use #4 @ 12" O.C. shear reinforcing in the area 4' to 10' from the edges of the pad.

INFORMATION ONLY

**Foundation and Soil Properties
Independent Spent Fuel Storage Installation
San Onofre Nuclear Generating Station Unit 1**

Reference: EQE Report No. 201038.02-R-001, "Soil-Structure Interaction of the Independent Spent Fuel Storage Installation for San Onofre Nuclear Generating Station, Unit 1," April 3, 2000.

The location of the Independent Spent Fuel Storage Installation (ISFSI) will be at the existing site of the decommissioned Unit 1 plant at San Onofre. The ISFSI pad size will be about 43'-6" wide by 188 feet long by 3 feet thick. The pad will support 19 spent fuel cask modules and may be expanded in the future to allow for additional modules. The pad will be constructed with reinforced concrete that has a minimum compressive strength of 4000 psi.

The soil beneath the pad is a very dense well graded sand of the San Mateo Formation with a depth of about 900 feet under the plant. The soil properties are given in Tables 1 through 6, and Figures 1 through 6, and represent the parameters used in the soil-structure interaction analysis of the San Onofre ISFSI pad (Reference). Table 1 is the low strain best estimate soil properties. Two bounding cases were defined in accordance with NRC NUREG-0800, Standard Review Plan for the Review of Safety Analysis Reports for Nuclear Power Plants, Section 3.7.2, Seismic System Analysis, to account for possible variations in soil properties. An upper bound case was obtained by scaling the best estimate soil modulus by 2, and a lower bound estimate was obtained by scaling the best estimate soil modulus by 0.5. The P wave velocity for the saturated layers was kept constant since it corresponds to the velocity in water. Table 2 gives the low strain lower and upper bound soil properties. The shear modulus and shear wave velocity profiles for the three low strain soil cases are shown in Figures 1 and 2. Shear modulus and soil damping relationships with shear strain are given in Table 3 and shown in Figure 3.

Since the strain compatible upper bound soil properties were lower than the low strain best estimate properties, a strain compatible soil profile was developed and the shear wave profiles are given in Table 4 and shown in Figure 4. The strain compatible soil damping ratios are given in Table 5 and shown in Figure 5. The strain compatible P wave velocity profiles are given in Table 6 and shown in Figure 6.

Also included are the results of the soil-structure interaction analysis. Figures 7 through 9 show the comparisons of the TN-West design response spectra for the storage modules with the seismic demand of the San Onofre site specific Design

Basis Earthquake (0.67g ZPA) at the pad. The figures demonstrate that the seismic design of the TN-West dry storage system will bound the seismic requirements at San Onofre.

Table 1

LOW STRAIN BEST ESTIMATE SOIL PROPERTIES

| Layer | Thickness (ft) (Surface at 15.75') | Shear Modulus (ksf) | Vs (1) (fps) | Unit Weight (kcf) | Poisson's ratio | Vp (2) (fps) |
|-------|--|---------------------------|-----------------|-------------------------|--------------------|-----------------|
| 1 | 3.50 | 3,599.27 | 930.00 | 0.134 | 0.35 | 1,935.95 |
| 2 | 3.50 | 3,599.27 | 930.00 | 0.134 | 0.35 | 1,935.95 |
| 3 | 3.75 | 3,599.27 | 930.00 | 0.134 | 0.35 | 1,935.95 |
| 4 | 5.00 | 4,337.14 | 1,002.36 | 0.139 | 0.48 | 5,000.00 |
| 5 | 5.00 | 4,991.60 | 1,075.33 | 0.139 | 0.48 | 5,000.00 |
| 6 | 5.00 | 5,605.60 | 1,139.55 | 0.139 | 0.48 | 5,000.00 |
| 7 | 5.00 | 6,187.62 | 1,197.24 | 0.139 | 0.48 | 5,000.00 |
| 8 | 5.00 | 6,743.43 | 1,249.86 | 0.139 | 0.48 | 5,000.00 |
| 9 | 5.00 | 7,277.19 | 1,298.38 | 0.139 | 0.48 | 5,000.00 |
| 10 | 5.00 | 7,792.04 | 1,343.53 | 0.139 | 0.48 | 5,000.00 |
| 11 | 5.00 | 8,290.41 | 1,385.83 | 0.139 | 0.48 | 5,000.00 |
| 12 | 5.00 | 8,774.22 | 1,425.69 | 0.139 | 0.48 | 5,000.00 |
| 13 | 5.00 | 9,245.03 | 1,463.44 | 0.139 | 0.48 | 5,000.00 |
| 14 | 5.00 | 9,704.15 | 1,499.34 | 0.139 | 0.48 | 5,000.00 |
| 15 | 5.00 | 10,152.65 | 1,533.59 | 0.139 | 0.48 | 5,000.00 |
| 16 | 5.00 | 10,591.45 | 1,566.38 | 0.139 | 0.48 | 5,000.00 |
| 17 | 5.00 | 11,021.34 | 1,597.86 | 0.139 | 0.48 | 5,000.00 |
| 18 | 5.00 | 11,443.01 | 1,628.14 | 0.139 | 0.48 | 5,000.00 |
| 19 | 5.00 | 11,857.04 | 1,657.33 | 0.139 | 0.48 | 5,000.00 |
| 20 | 5.00 | 12,263.96 | 1,685.53 | 0.139 | 0.48 | 5,000.00 |
| 21 | 10.00 | 12,862.03 | 1,726.14 | 0.139 | 0.48 | 5,000.00 |
| 22 | 10.00 | 13,638.50 | 1,777.48 | 0.139 | 0.48 | 5,000.00 |
| 23 | 10.00 | 14,393.46 | 1,826.01 | 0.139 | 0.48 | 5,000.00 |
| 24 | 10.00 | 15,129.11 | 1,872.09 | 0.139 | 0.48 | 5,000.00 |
| 25 | 10.00 | 15,847.28 | 1,916.01 | 0.139 | 0.48 | 5,000.00 |
| 26 | 15.00 | 16,722.77 | 1,968.22 | 0.139 | 0.48 | 5,000.00 |
| 27 | H. S. (-160.75' ->) | 17,744.05 | 2,027.43 | 0.139 | 0.48 | 5,000.00 |

(1) Lower limit for Vs = 930 fps

(2) Layers below water table, Vp = 5,000 fps (P wave velocity in water)

Table 2

LOW STRAIN LOWER AND UPPER BOUND SOIL PROPERTIES

| Layer | Thickness (ft) (Surface at 15.75') | L.B. Shear Modulus (ksf) | L.B. Vs (fps) | U.B. Shear Modulus (ksf) | U.B. Vs (fps) |
|-------|--|--------------------------------|------------------|--------------------------------|------------------|
| 1 | 3.50 | 1,799.64 | 657.61 | 7,198.54 | 1,315.22 |
| 2 | 3.50 | 1,799.64 | 657.61 | 7,198.54 | 1,315.22 |
| 3 | 3.75 | 1,799.64 | 657.61 | 7,198.54 | 1,315.22 |
| 4 | 5.00 | 2,168.57 | 708.77 | 8,674.27 | 1,417.55 |
| 5 | 5.00 | 2,495.80 | 760.37 | 9,983.20 | 1,520.74 |
| 6 | 5.00 | 2,802.80 | 805.78 | 11,211.21 | 1,611.56 |
| 7 | 5.00 | 3,093.81 | 846.58 | 12,375.24 | 1,693.16 |
| 8 | 5.00 | 3,371.71 | 883.78 | 13,486.85 | 1,767.57 |
| 9 | 5.00 | 3,638.60 | 918.09 | 14,554.38 | 1,836.19 |
| 10 | 5.00 | 3,896.02 | 950.02 | 15,584.09 | 1,900.03 |
| 11 | 5.00 | 4,145.20 | 979.93 | 16,580.82 | 1,959.85 |
| 12 | 5.00 | 4,387.11 | 1,008.11 | 17,548.44 | 2,016.23 |
| 13 | 5.00 | 4,622.52 | 1,034.81 | 18,490.07 | 2,069.62 |
| 14 | 5.00 | 4,852.07 | 1,060.19 | 19,408.30 | 2,120.38 |
| 15 | 5.00 | 5,076.32 | 1,084.41 | 20,305.30 | 2,168.83 |
| 16 | 5.00 | 5,295.72 | 1,107.60 | 21,182.90 | 2,215.20 |
| 17 | 5.00 | 5,510.67 | 1,129.86 | 22,042.68 | 2,259.71 |
| 18 | 5.00 | 5,721.50 | 1,151.27 | 22,886.01 | 2,302.53 |
| 19 | 5.00 | 5,928.52 | 1,171.91 | 23,714.08 | 2,343.82 |
| 20 | 5.00 | 6,131.98 | 1,191.85 | 24,527.93 | 2,383.70 |
| 21 | 10.00 | 6,431.01 | 1,220.56 | 25,724.05 | 2,441.13 |
| 22 | 10.00 | 6,819.25 | 1,256.87 | 27,276.99 | 2,513.73 |
| 23 | 10.00 | 7,196.73 | 1,291.18 | 28,786.91 | 2,582.37 |
| 24 | 10.00 | 7,564.55 | 1,323.77 | 30,258.21 | 2,647.54 |
| 25 | 10.00 | 7,923.64 | 1,354.82 | 31,694.57 | 2,709.65 |
| 26 | 15.00 | 8,361.39 | 1,391.75 | 33,445.55 | 2,783.49 |
| 27 | H. S. (-160.75' ->) | 8,872.02 | 1,433.61 | 35,488.10 | 2,867.23 |

Table 3

SOIL DEGRADATION CURVES

| Shear Strain (%) | G/GMAX | Soil Damping Ratio (%) |
|------------------|-----------|------------------------|
| 0.0001 | 1.000 | 2.061 |
| 0.0003 | 0.978 | 2.691 |
| 0.001 | 0.852 | 3.568 |
| 0.003 | 0.600 | 4.621 |
| 0.01 | 0.391 | 6.067 |
| 0.03 | 0.258 | 7.496 |
| 0.1 | 0.173 | 10.158 |
| 0.3 | 0.128 | 12.930 |
| 1.0 | 0.095 | 16.442 |
| 2.0 | 0.076 | 19.031 |
| 3.0 | 0.066 | 20.900 |
| 10.0 (1) | 0.063 (1) | 20.900 (1) |

(1) These values were added to allow for larger deformation.

Table 4

STRAIN COMPATIBLE SHEAR WAVE VELOCITY

| Layer | Thickness (ft) | Vs lower bound (strain comp.) (fps) | Vs best est. (strain comp.) (fps) | Vs upper bound (strain comp.) (fps) | Vs best est. (low strain) (fps) |
|-------|-------------------|---|---|---|---------------------------------------|
| 1 | 3.50 | 376.53 | 649.40 | 1096.24 | 930.00 |
| 2 | 3.50 | 282.88 | 468.14 | 815.56 | 930.00 |
| 3 | 3.75 | 258.93 | 420.26 | 706.30 | 930.00 |
| 4 | 5.00 | 272.27 | 435.31 | 711.29 | 1002.36 |
| 5 | 5.00 | 282.29 | 453.55 | 739.86 | 1075.33 |
| 6 | 5.00 | 292.37 | 468.13 | 770.84 | 1139.55 |
| 7 | 5.00 | 303.64 | 484.66 | 802.93 | 1197.24 |
| 8 | 5.00 | 315.25 | 500.19 | 830.44 | 1249.86 |
| 9 | 5.00 | 326.79 | 515.02 | 851.11 | 1298.38 |
| 10 | 5.00 | 335.88 | 530.09 | 870.48 | 1343.53 |
| 11 | 5.00 | 344.06 | 544.96 | 888.00 | 1385.83 |
| 12 | 5.00 | 352.37 | 559.23 | 904.67 | 1425.69 |
| 13 | 5.00 | 360.50 | 572.94 | 920.16 | 1463.44 |
| 14 | 5.00 | 368.44 | 586.32 | 935.52 | 1499.34 |
| 15 | 5.00 | 376.22 | 599.22 | 951.48 | 1533.59 |
| 16 | 5.00 | 382.93 | 609.76 | 967.29 | 1566.38 |
| 17 | 5.00 | 389.23 | 618.62 | 982.74 | 1597.86 |
| 18 | 5.00 | 395.14 | 627.55 | 998.87 | 1628.14 |
| 19 | 5.00 | 401.25 | 636.34 | 1014.40 | 1657.33 |
| 20 | 5.00 | 407.83 | 645.38 | 1029.59 | 1685.53 |
| 21 | 10.00 | 416.82 | 658.88 | 1052.18 | 1726.14 |
| 22 | 10.00 | 426.44 | 676.23 | 1081.71 | 1777.48 |
| 23 | 10.00 | 436.11 | 692.98 | 1110.03 | 1826.01 |
| 24 | 10.00 | 445.82 | 707.37 | 1135.51 | 1872.09 |
| 25 | 10.00 | 455.34 | 720.19 | 1153.43 | 1916.01 |
| 26 | 15.00 | 466.15 | 736.26 | 1173.24 | 1968.22 |
| H.S. | | 480.17 | 758.40 | 1208.53 | 2027.43 |

Table 5

STRAIN COMPATIBLE DAMPING RATIOS

| Layer | Thickness (ft) | Damping Ratio Lower bound (strain comp.) | Damping Ratio Best estimate (strain comp.) | Damping Ratio Upper bound (strain comp.) | Damping Ratio Best estimate (low strain) |
|-------|-------------------|--|--|--|--|
| 1 | 3.50 | 0.067 | 0.054 | 0.042 | 0.021 |
| 2 | 3.50 | 0.098 | 0.076 | 0.061 | 0.021 |
| 3 | 3.75 | 0.113 | 0.092 | 0.072 | 0.021 |
| 4 | 5.00 | 0.117 | 0.097 | 0.077 | 0.021 |
| 5 | 5.00 | 0.123 | 0.100 | 0.082 | 0.021 |
| 6 | 5.00 | 0.127 | 0.104 | 0.084 | 0.021 |
| 7 | 5.00 | 0.129 | 0.107 | 0.085 | 0.021 |
| 8 | 5.00 | 0.130 | 0.110 | 0.087 | 0.021 |
| 9 | 5.00 | 0.130 | 0.111 | 0.088 | 0.021 |
| 10 | 5.00 | 0.131 | 0.112 | 0.090 | 0.021 |
| 11 | 5.00 | 0.132 | 0.113 | 0.091 | 0.021 |
| 12 | 5.00 | 0.133 | 0.113 | 0.093 | 0.021 |
| 13 | 5.00 | 0.133 | 0.114 | 0.094 | 0.021 |
| 14 | 5.00 | 0.134 | 0.114 | 0.095 | 0.021 |
| 15 | 5.00 | 0.134 | 0.114 | 0.095 | 0.021 |
| 16 | 5.00 | 0.135 | 0.115 | 0.096 | 0.021 |
| 17 | 5.00 | 0.135 | 0.116 | 0.097 | 0.021 |
| 18 | 5.00 | 0.136 | 0.117 | 0.097 | 0.021 |
| 19 | 5.00 | 0.136 | 0.117 | 0.097 | 0.021 |
| 20 | 5.00 | 0.136 | 0.118 | 0.097 | 0.021 |
| 21 | 10.00 | 0.136 | 0.118 | 0.098 | 0.021 |
| 22 | 10.00 | 0.137 | 0.119 | 0.098 | 0.021 |
| 23 | 10.00 | 0.138 | 0.119 | 0.098 | 0.021 |
| 24 | 10.00 | 0.138 | 0.120 | 0.098 | 0.021 |
| 25 | 10.00 | 0.139 | 0.121 | 0.099 | 0.021 |
| 26 | 15.00 | 0.139 | 0.122 | 0.100 | 0.021 |
| H.S. | | 0.139 | 0.122 | 0.100 | 0.021 |

Table 6

STRAIN COMPATIBLE P WAVE VELOCITY

| Layer | Thickness (ft) | Vp lower bound (strain comp.) (fps) | Vp best est. (strain comp.) (fps) | Vp upper bound (strain comp.) (fps) | Vp best est. (low strain) (fps) |
|-------|-------------------|---|---|---|---------------------------------------|
| 1 | 3.50 | 783.81 | 1351.84 | 2282.00 | 1935.95 |
| 2 | 3.50 | 588.86 | 974.50 | 1697.73 | 1935.95 |
| 3 | 3.75 | 539.00 | 874.84 | 1470.28 | 1935.95 |
| 4 | 5.00 | 3500.00 | 5000.00 | 5000.00 | 5000.00 |
| 5 | 5.00 | 3500.00 | 5000.00 | 5000.00 | 5000.00 |
| 6 | 5.00 | 3500.00 | 5000.00 | 5000.00 | 5000.00 |
| 7 | 5.00 | 3500.00 | 5000.00 | 5000.00 | 5000.00 |
| 8 | 5.00 | 3500.00 | 5000.00 | 5000.00 | 5000.00 |
| 9 | 5.00 | 3500.00 | 5000.00 | 5000.00 | 5000.00 |
| 10 | 5.00 | 3500.00 | 5000.00 | 5000.00 | 5000.00 |
| 11 | 5.00 | 3500.00 | 5000.00 | 5000.00 | 5000.00 |
| 12 | 5.00 | 3500.00 | 5000.00 | 5000.00 | 5000.00 |
| 13 | 5.00 | 3500.00 | 5000.00 | 5000.00 | 5000.00 |
| 14 | 5.00 | 3500.00 | 5000.00 | 5000.00 | 5000.00 |
| 15 | 5.00 | 3500.00 | 5000.00 | 5000.00 | 5000.00 |
| 16 | 5.00 | 3500.00 | 5000.00 | 5000.00 | 5000.00 |
| 17 | 5.00 | 3500.00 | 5000.00 | 5000.00 | 5000.00 |
| 18 | 5.00 | 3500.00 | 5000.00 | 5000.00 | 5000.00 |
| 19 | 5.00 | 3500.00 | 5000.00 | 5000.00 | 5000.00 |
| 20 | 5.00 | 3500.00 | 5000.00 | 5000.00 | 5000.00 |
| 21 | 10.00 | 3500.00 | 5000.00 | 5000.00 | 5000.00 |
| 22 | 10.00 | 3500.00 | 5000.00 | 5000.00 | 5000.00 |
| 23 | 10.00 | 3500.00 | 5000.00 | 5000.00 | 5000.00 |
| 24 | 10.00 | 3500.00 | 5000.00 | 5000.00 | 5000.00 |
| 25 | 10.00 | 3500.00 | 5000.00 | 5000.00 | 5000.00 |
| 26 | 15.00 | 3500.00 | 5000.00 | 5000.00 | 5000.00 |
| H.S. | | 3500.00 | 5000.00 | 5000.00 | 5000.00 |

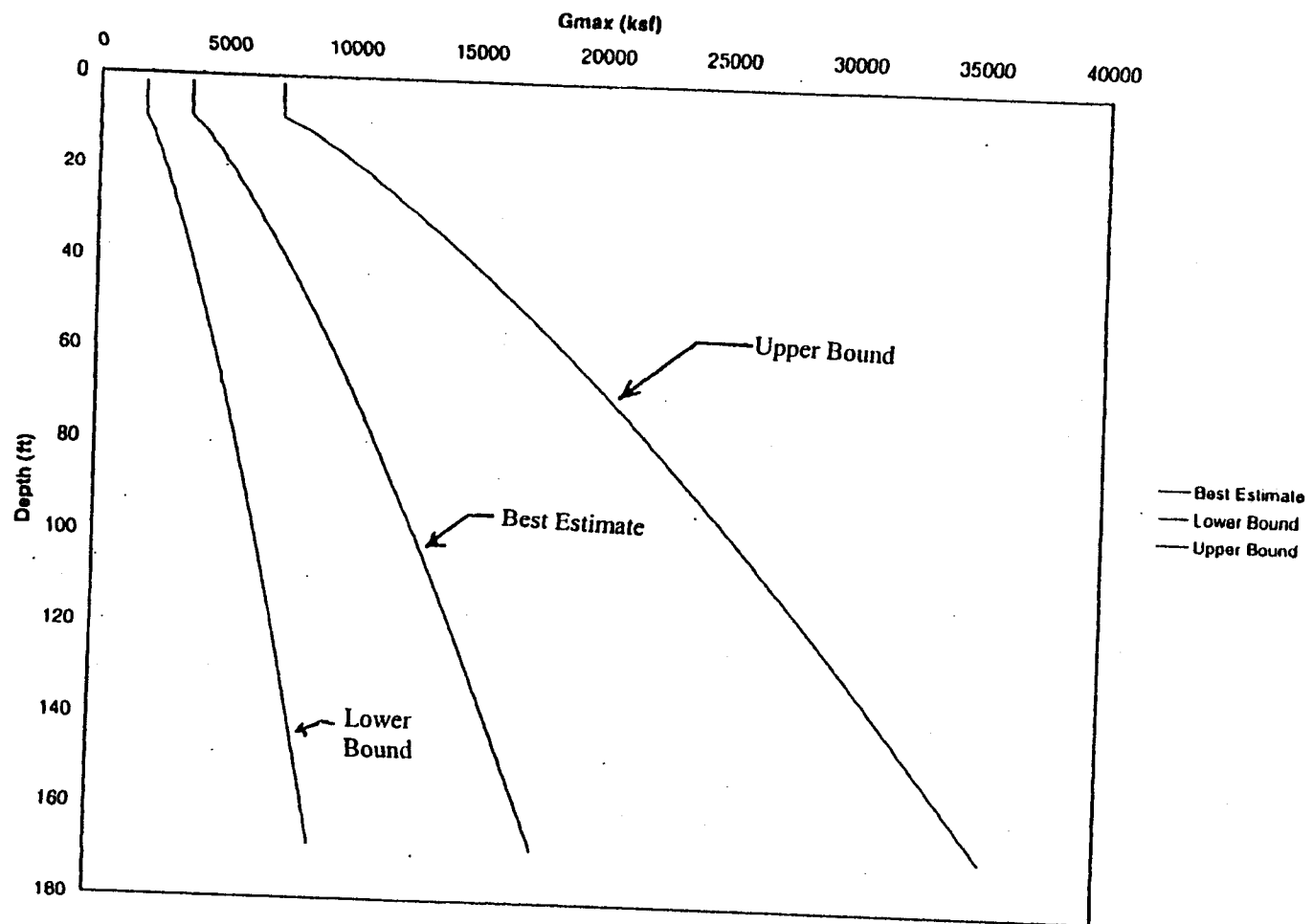


Figure 1: Low Strain Shear Modulus

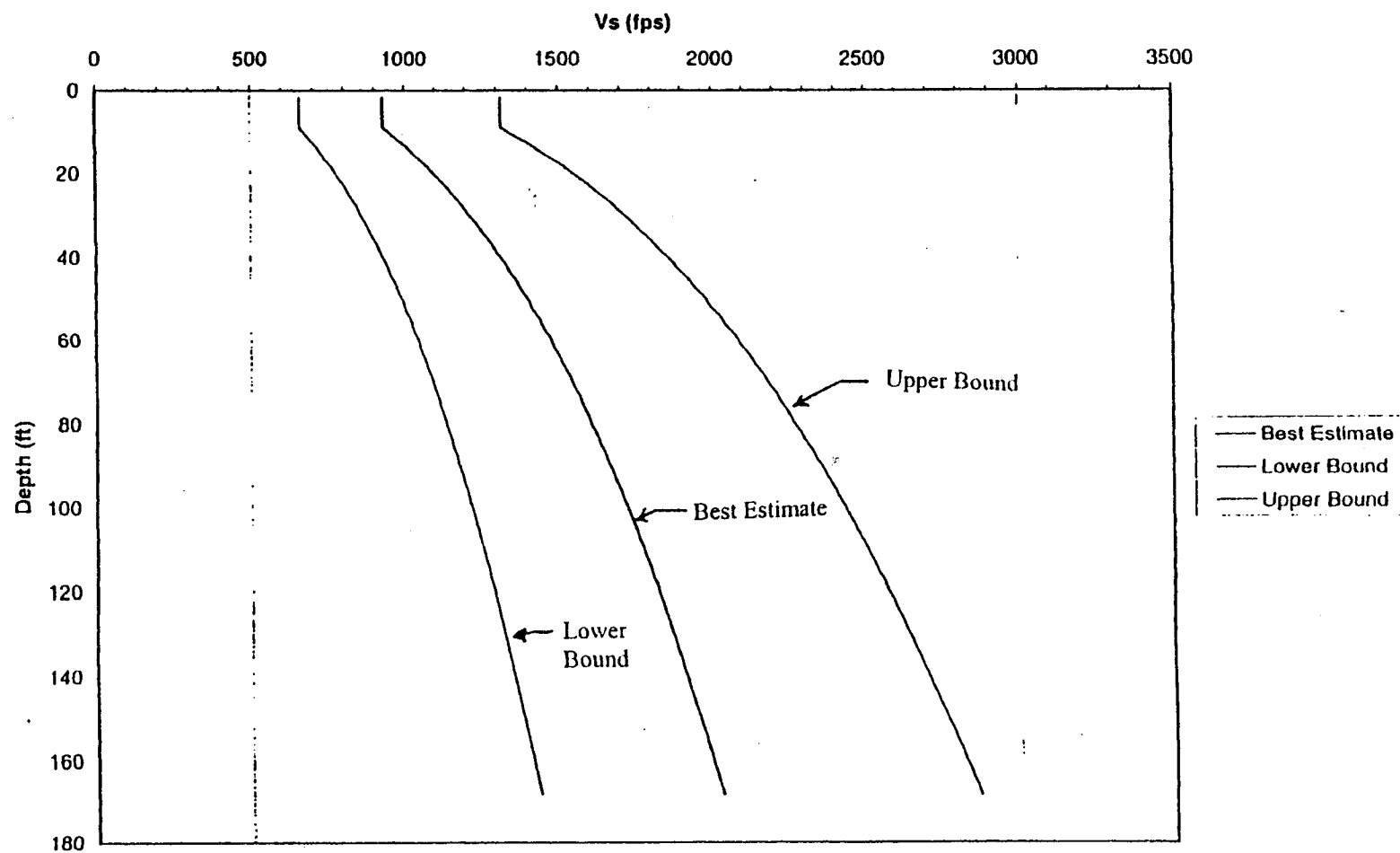


Figure 2: Low Strain Shear Wave Velocity

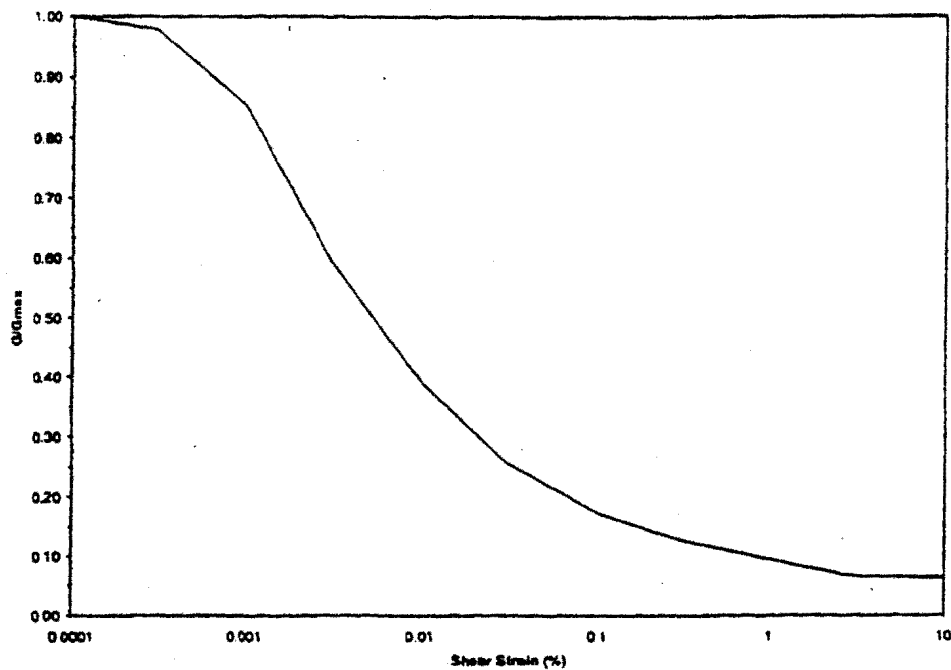


Figure 3a: Soil Shear Modulus Degradation Curve

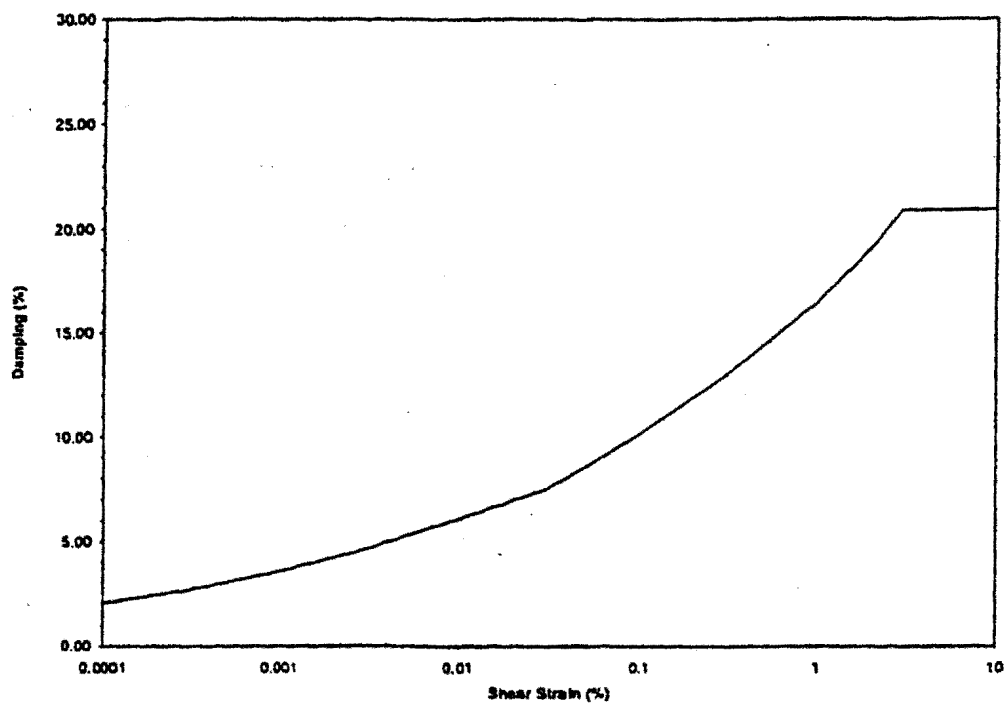


Figure 3b: Soil Material Damping Curve

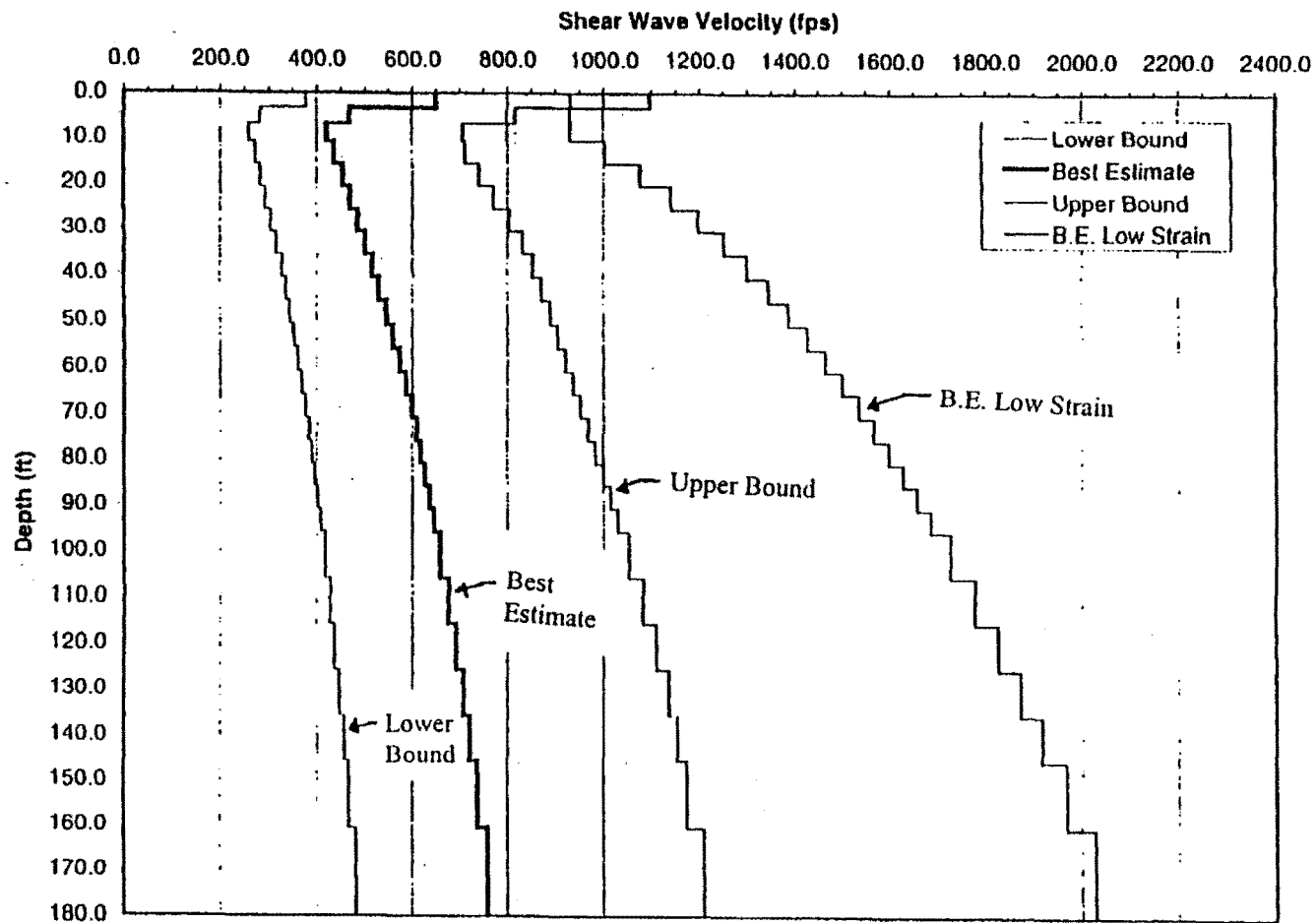


Figure 4: Strain Compatible Shear Wave Velocity

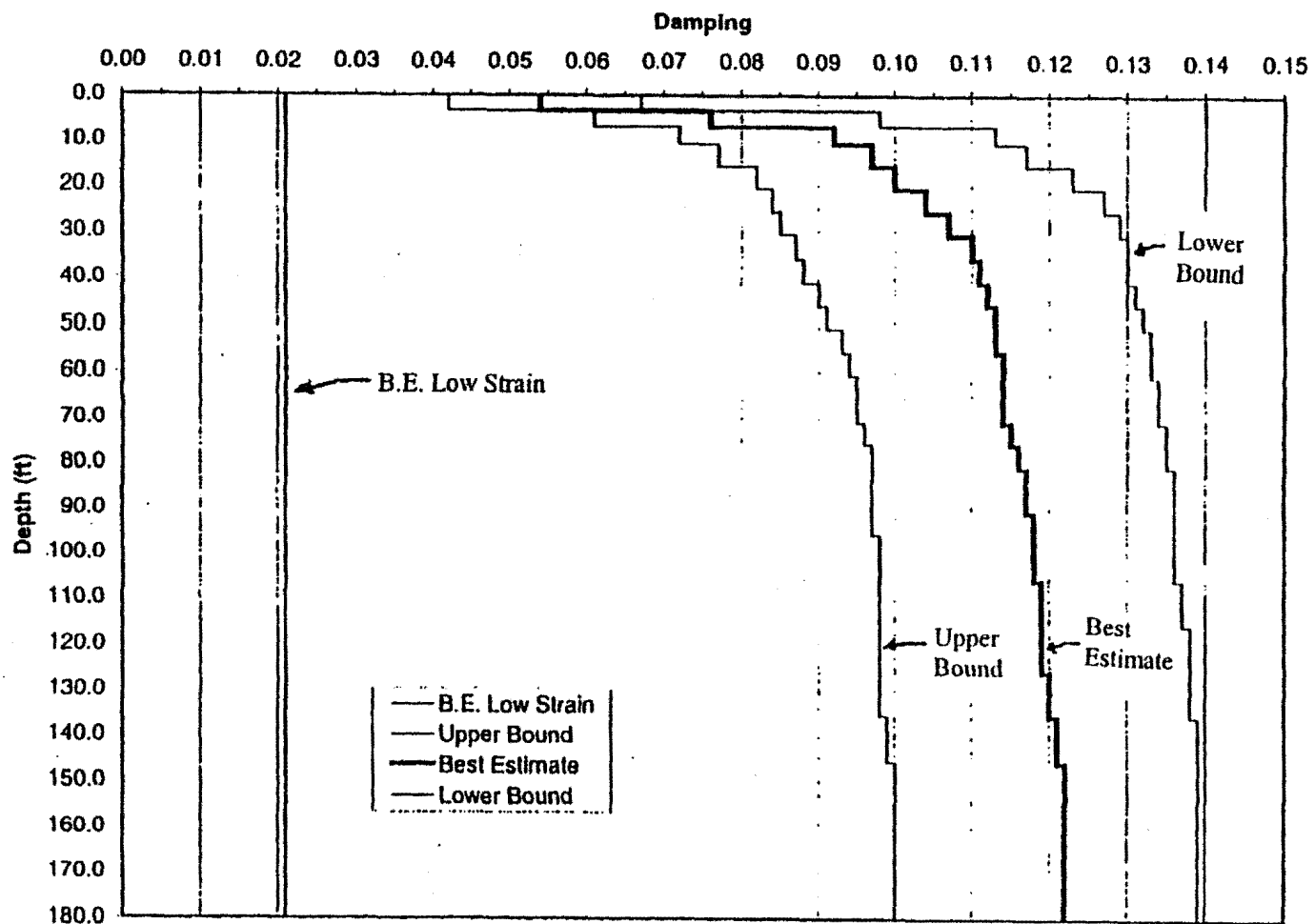


Figure 5: Strain Compatible Damping Ratios

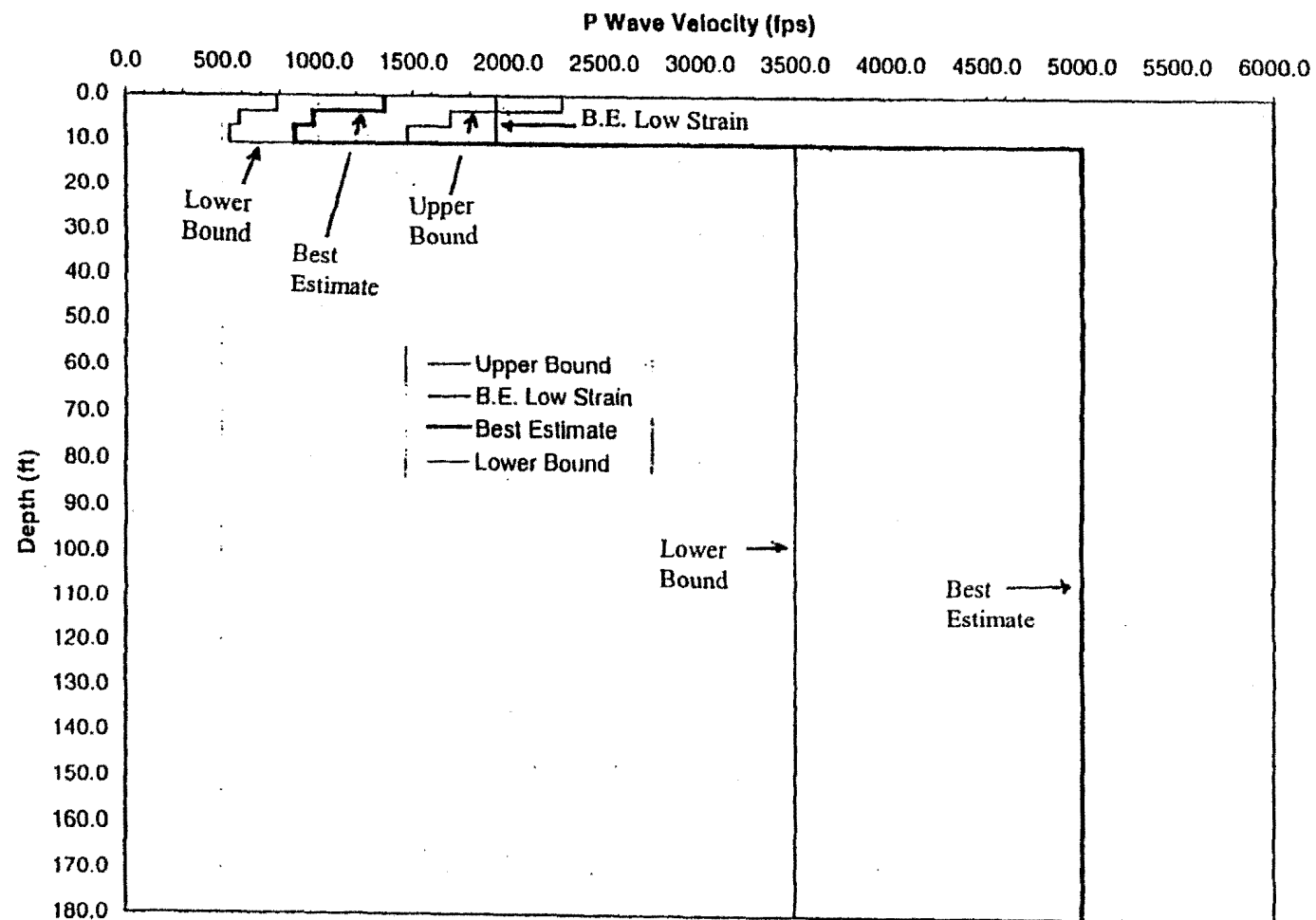


Figure 6: Strain Compatible P Wave Velocity

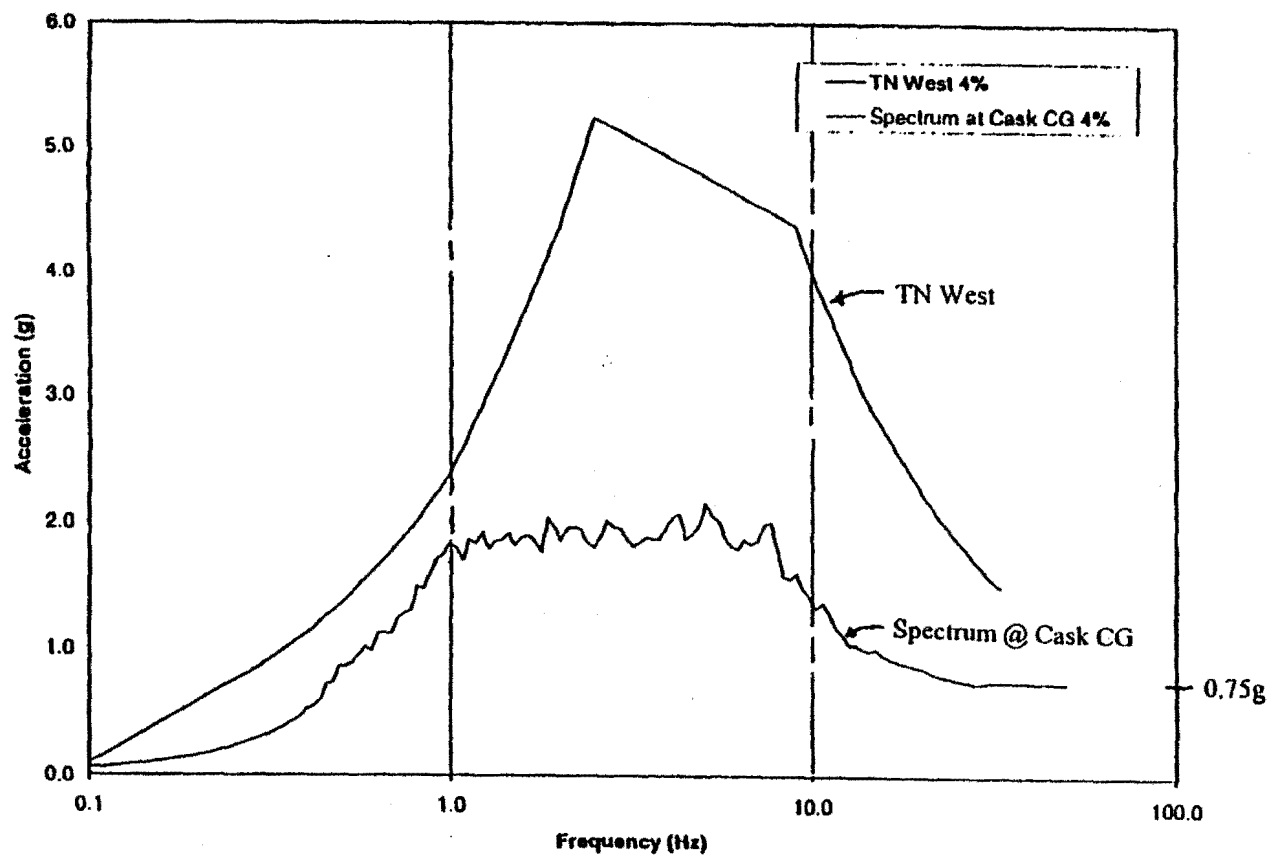


Figure 7: TN West Vs SSE Casks CG Spectra – Horizontal Longitudinal Direction

Frequency, Acceleration values for CG Spectrum contained in SO1-207-1-C31, R1 on sheet 2450

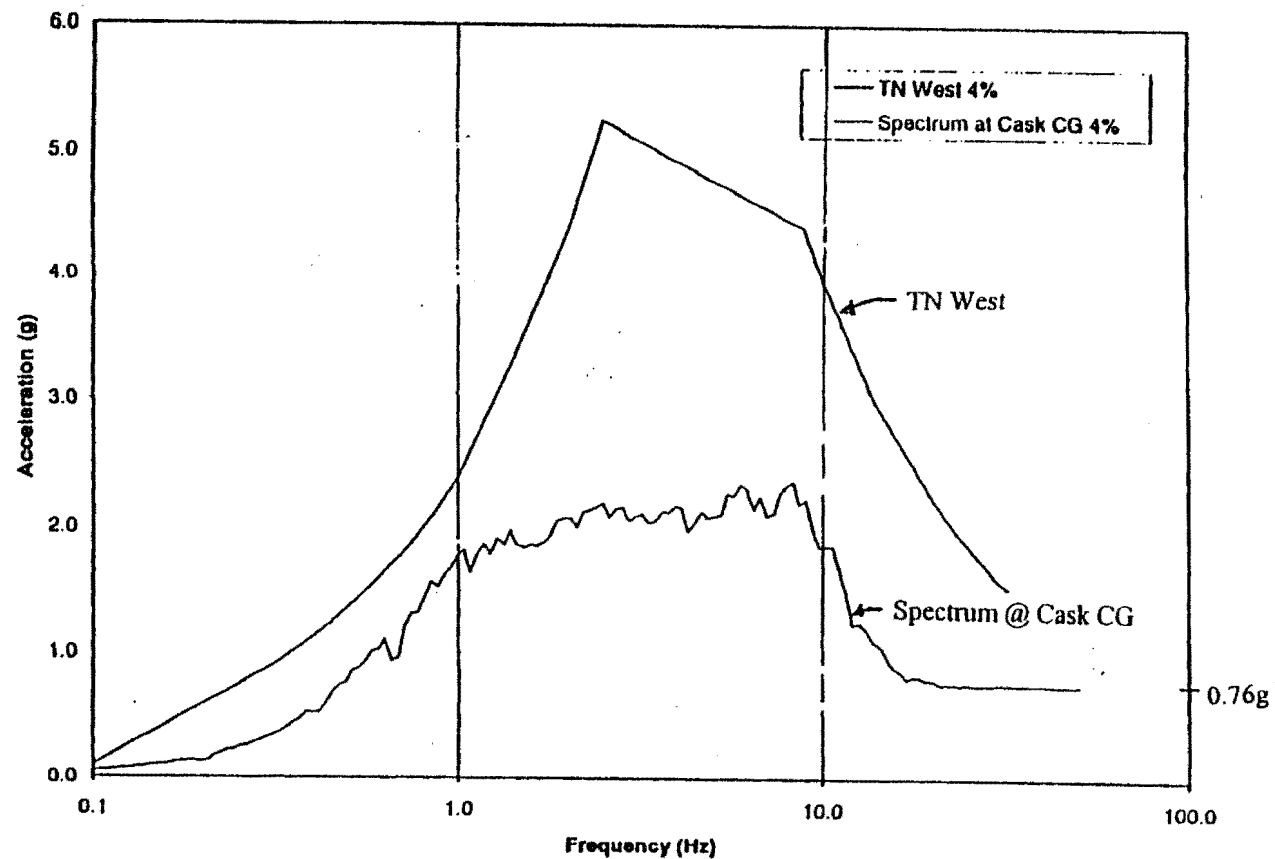


Figure 8: TN West Vs. SSE Casks CG Spectra – Horizontal Transverse Direction

Frequency, Acceleration values for CG Spectrum contained in SO1-207-1-C31, R1 on sheet 2450

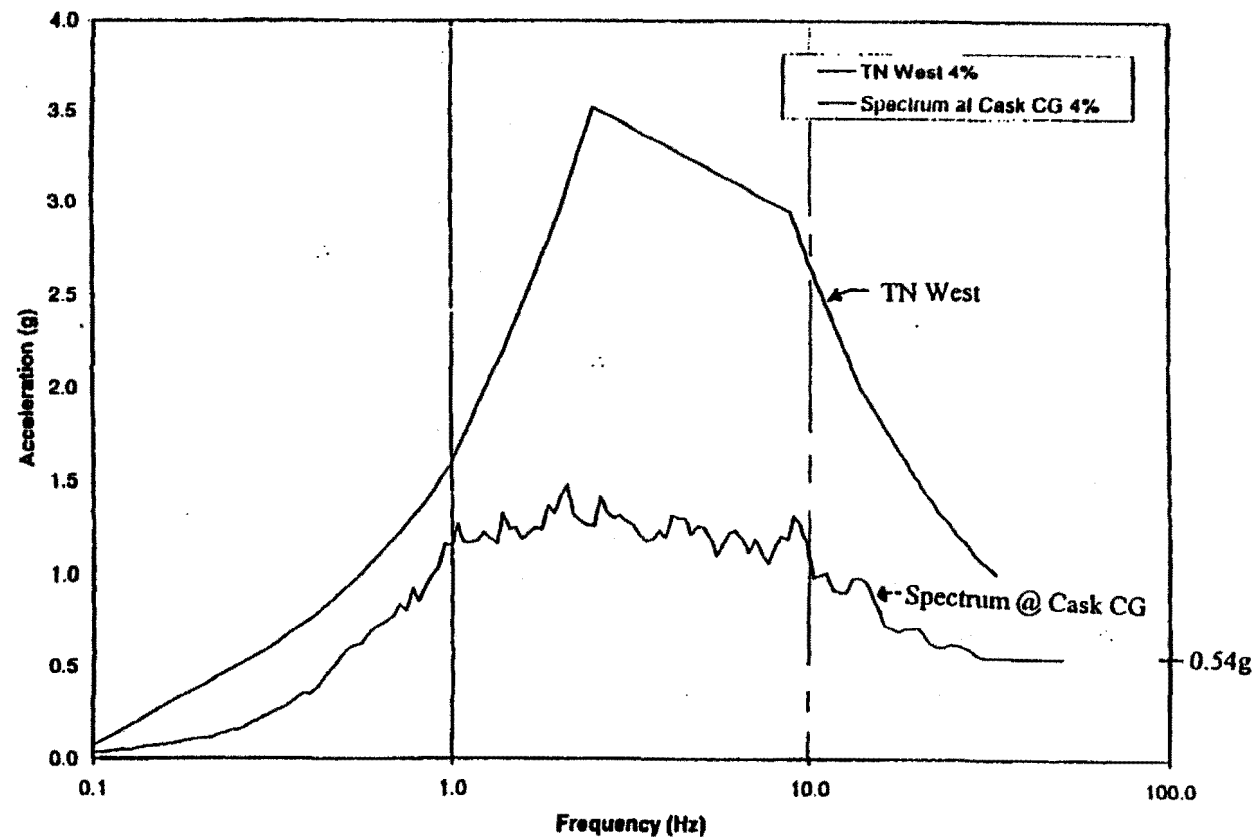
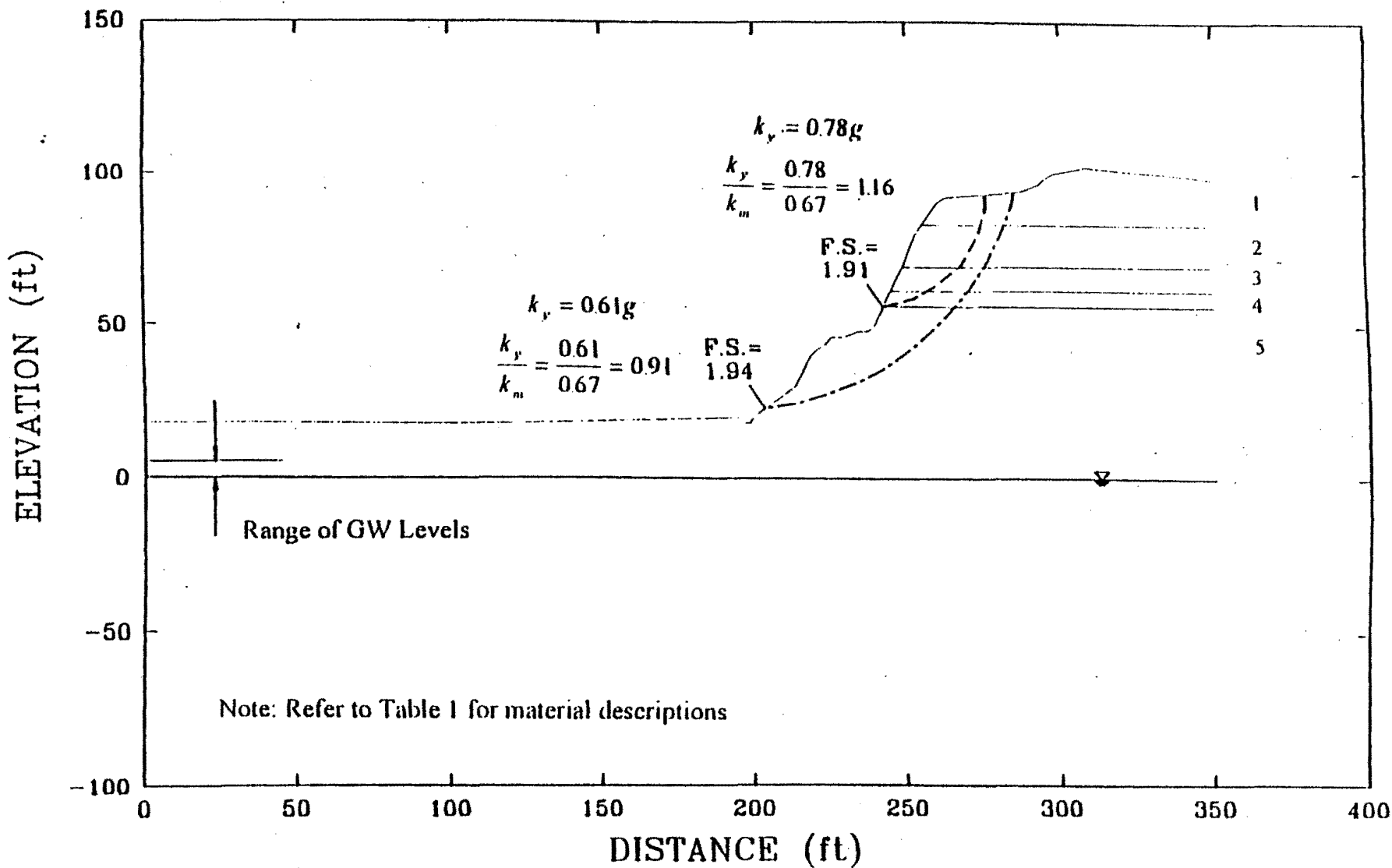


Figure 9: TN West Vs. SSE Casks CG Spectra – Vertical Direction

Frequency, Acceleration values for CG Spectrum contained in SO1-207-1-C31, R1 on sheet 2450



CALC C-296-01.03 SHT A-40
APPENDIX A

File : A-A-F.PLT, 09-28-1995

Run By: P.TAN

SECTION A-A' - SLOPE STABILITY FACTOR OF SAFETY

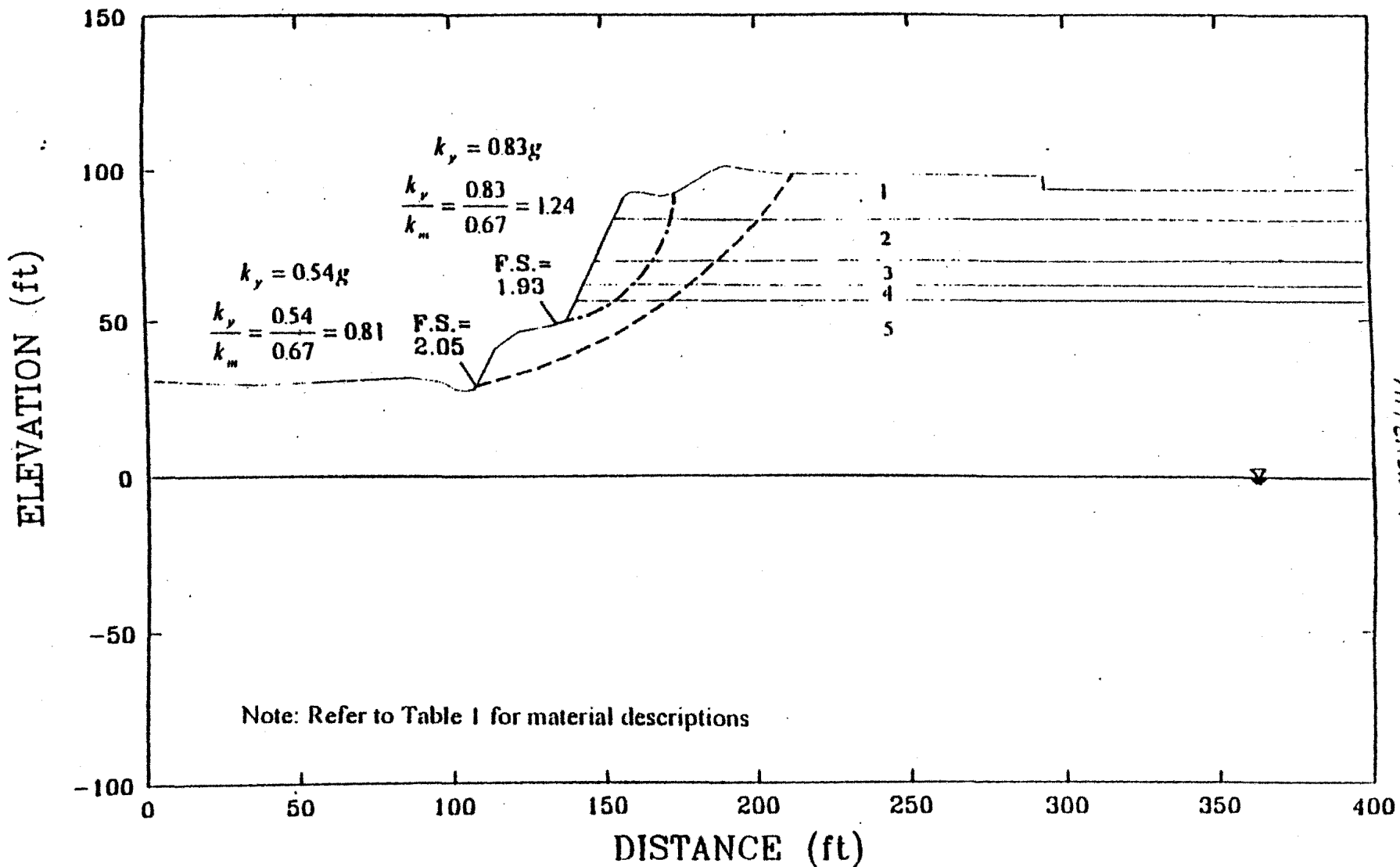
Project No.: 954E181

Date: SEP 95

Project:

SONGS CASK STORAGE

Fig. 4.1



CALC C-296-01.03 SHT A-41
 APPENDIX A

File : B-B2.PLT, 09-28-1995

Run By: P.TAN

SECTION B-B' - SLOPE STABILITY FACTOR OF SAFETY

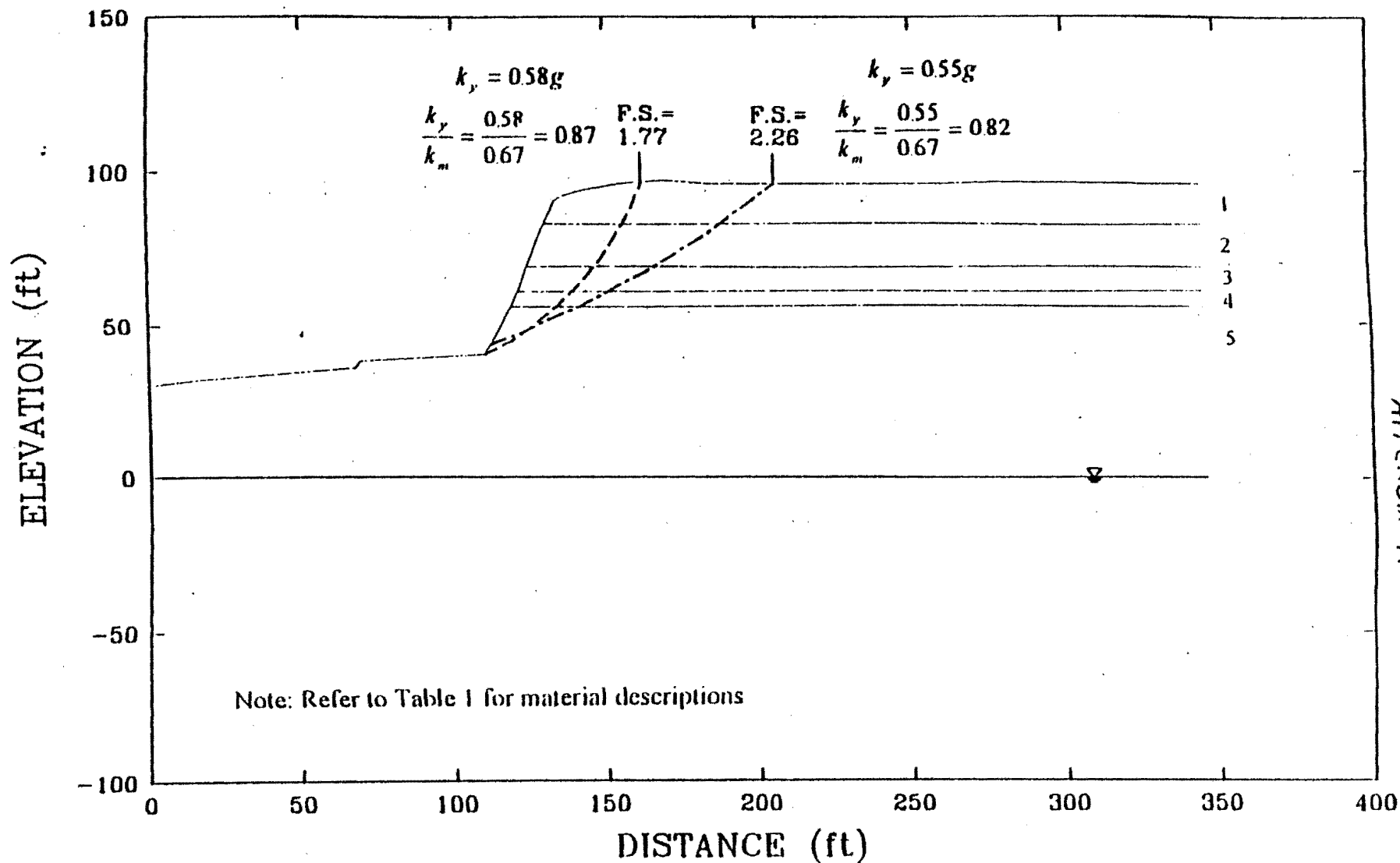
Project No.: 954E181

Date: SEP 95

Project:

SONGS CASK STORAGE

Fig. 4.2



CMC C-296-01.02 SHT A-42
 APPENDIX A

File : C-C1.PLT, 09-28-1995

Run By: P.TAN

SECTION C-C' - SLOPE STABILITY FACTOR OF SAFETY

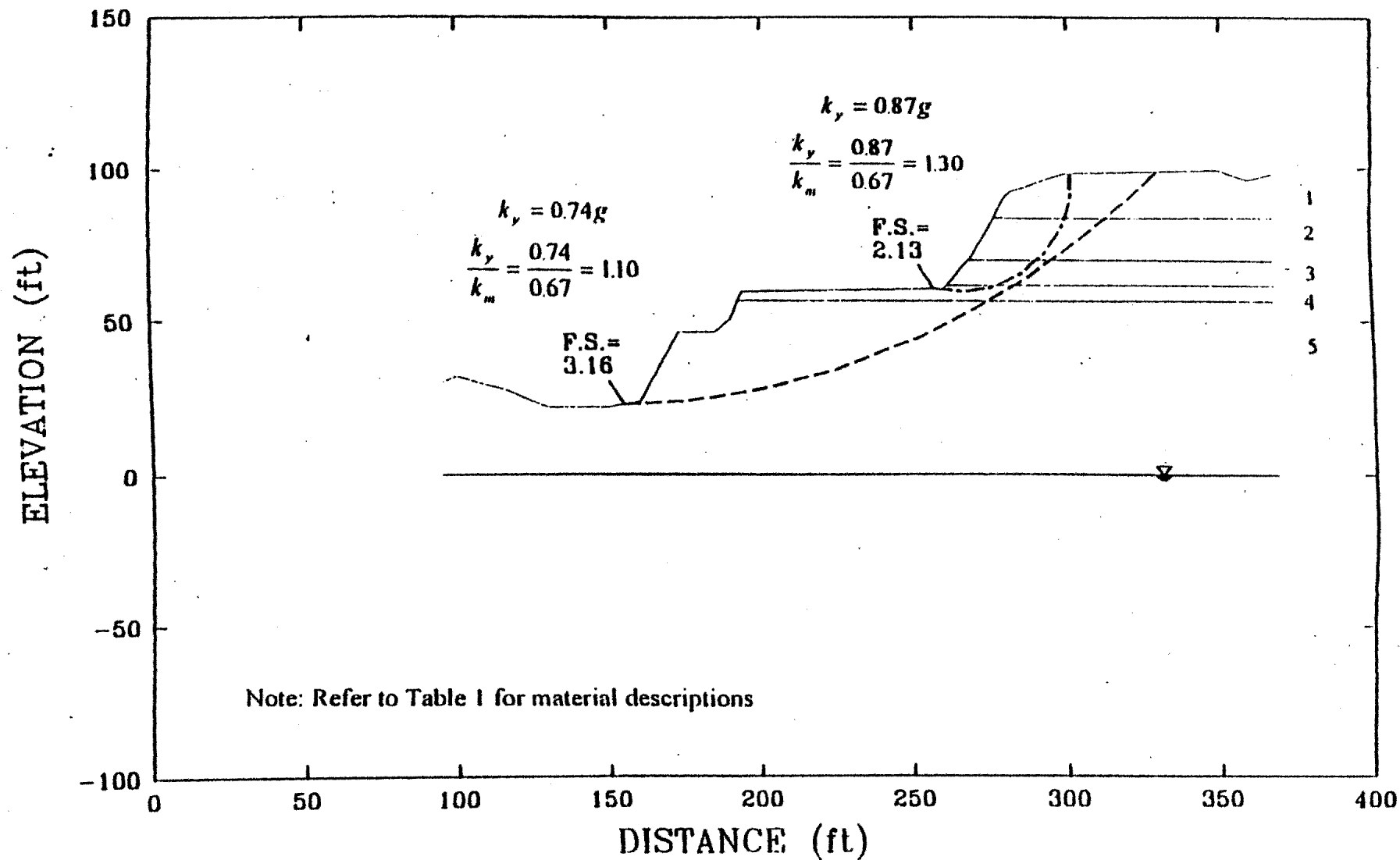
Project No.: 054E181

Date: SEP 95

Project:

SONGS CASK STORAGE

Fig. 4.3



CALC C-296-01.03 SH1 A-43
APPENDIX A

File : D-D4.PLT, 09-28-1995

Run By: P.TAN

SECTION D-D' - SLOPE STABILITY FACTOR OF SAFETY

Project No.: 954E181

Date: SEP 95

Project:

SONGS CASK STORAGE

Fig. 4.4

DRAFT TRUST AGREEMENT

This trust agreement (the "Agreement") is entered into as of _____, 2001 by and between City National Bank, national association (the "Trustee"), and Southern California Edison Company, (the "Company"), also collectively referenced to herein as the "Parties."

ARTICLE I TRUST FUND

- 1.1 Establishment of Trust. This "SONGS ISFSI Yard Sump Maintenance Trust Account" (the "Trust Account") is established by the Company pursuant to the requirements of the California Coastal Commission. All funds deposited in the Trust Account are held in trust and shall be disbursed only for expenditures for storm water sump monitoring and maintenance, consistent with Special Condition 2 of Coastal Development Permit E-00-014, on the project site at the San Onofre Nuclear Generating Station ("SONGS"). The term of the Trust Account will be from _____, 2001 through December 31, 2022 unless terminated sooner as provided in Section 8.2.
- 1.2 Funding of Trust. The Trust Account will be established within thirty (30) days after receipt by the Company of the California Coastal Commission coastal development permit for the SONGS 2 and 3 spent fuel storage facility and prior to commencing construction of said facility. A deposit of \$136,000 will be made by the Company to the Trust Account at its inception, which amount is the estimated present value of the sump monitoring and maintenance costs plus the estimated present value of the expenses of the Trustee for the term of the Trust Account.
- 1.3 Disbursement of Funds. The Company represents that requests by it for disbursement of funds pursuant to Section 2.2.1 herein, shall be made in accordance with Section 1.1 herein. Disbursement requests from the Company to the Trustee will be accompanied by either (i) a vendor invoice if the work has been performed by a third-party, or (ii) documentation of Company costs if the work is performed by the Company. The Company will establish separate accounting mechanisms to identify and capture costs related to the SONGS ISFSI Yard Sump Maintenance project.
- 1.4 Separate Funds of the Trust Account. The Company may direct the Trustee to establish one or more funds to hold such portions of the assets of the Trust Account as the Company shall direct, along with the earnings and profits thereon.

ARTICLE II THE TRUSTEE

- 2.1 Scope of Powers, Duties and Obligations of the Trustee. Subject to the Company's directions, the Trustee has whatever powers are conferred by law and which are required to discharge its obligations and exercise its rights under this Agreement, including but not limited to the powers specified in Section 2.2, and the powers and authority granted to the Trustee under other provisions of this Agreement. The Trustee shall have no duties or obligations except those specifically set forth in this Agreement.
- 2.2 Powers Exercisable by the Trustee, Subject to this Agreement. The Trustee is authorized and empowered to exercise the following powers, subject to the limitations contained in this Agreement:

- 2.2.1 To disburse, distribute or otherwise make payment as requested by the Company pursuant to Instructions given under Section 4.1 herein, provided that unless Company Instructions requesting same-day funding are received by the Trustee, in writing, no later than 9:00 am (California time) of such day, such Instructions will be acted upon by the Trustee on the following business day.
- 2.2.2 To register any investment held in the Trust Account in its own name or in the name of a nominee and to hold any investment in bearer form. The books and records of the Trustee shall show that all such investments are part of the Trust Account. The Trustee shall be liable for all acts of its nominee.
- 2.2.3 To utilize registered securities depositories to hold assets of the Trust Account, provided however that the Trustee shall not be relieved of any fiduciary responsibility with respect to the assets so held.
- 2.2.4 To employ agents, including public accountants and legal counsel (which may be counsel for Company), as it shall determine appropriate, and to pay their reasonable expenses and compensation from Trust Account;
- 2.2.5 To rely on Company to defend and litigate, or settle, at their expense, any suit brought against the Trust Account or any order sought to be satisfied out of the Trust Account, without duty on the Trustee beyond forwarding related papers to Company and complying with any final order to the extent of the Trust Account;
- 2.2.6 To withhold from taking any action until it receives proper written notice of an occurrence of an event affecting this Trust Account;
- 2.2.7 To treat as genuine, sufficient and correct, in form, execution and validity, and as the document it purports to be, and from the party it purports to be from, any notice, instruction, letter, paper, telex or other document purported to be furnished to Trustee by Company and believed by Trustee to be both genuine and to have been transmitted by the proper party or parties, and Trustee shall have no liability with respect to any action taken or foregone by Trustee in good faith in reliance on such document;
- 2.2.8 To deposit the Trust Account assets, after reduction for Trustee's accrued fees and expenses, in an interest bearing passbook savings account with Trustee's commercial department requiring the signatures of Company, should Company not appoint a successor trust holder for the Trust Account within fifteen (15) days following the resignation or removal of Trustee;
- 2.2.9 To be fully released and discharged from any obligation to perform any further duties imposed upon it with respect to this Trust Account following its resignation or removal and the appointment of a successor or the deposit of the Trust Account assets under Paragraph 2.2.8, above; and
- 2.2.10 To be free from any liabilities or change in duties, other than as may be specifically described elsewhere herein, for the action or inaction of a party to this Agreement, or any other party, or the occurrence or non-occurrence of an event outside of this Trust.

ARTICLE III INVESTMENT OF THE TRUST FUND

- 3.1 Permitted Investments. The Trustee shall invest and reinvest the principal and accumulated income of the Trust Account in one or more federally-insured Certificates of Deposit or U.S.

Government Treasury Bills through a federally-insured bank (including the Trustee).

- 3.2 Trustee Not Responsible For Investment Advice. The Trustee assumes no responsibility for advising the Company, or its Representative, with respect to the investment and reinvestment of the Trust Account. The Trustee shall as promptly as possible comply with any direction given by the Company or its Representative; provided, however, that the Trustee shall have no duty to take any action which, in the Trustee's opinion, would expose the Trustee to liability unless and until the Company indemnifies the Trustee to its satisfaction. The Trustee shall neither be liable in any manner nor for any reason for any losses or other unfavorable investment results arising from its compliance with such direction, nor be liable for failing to invest any assets of the Trust Account in the absence of written investment directions regarding such assets.
- 3.3 Delegation of Responsibility and Authority for Investment of Trust Account. The Company may by written resolution delegate its authority over the investments of the Trust Account to its designated representative ("Representative"), and Trustee shall accept Representative's instructions to invest and reinvest the assets of all or any portion of the Trust Account. The Company may revoke the delegation of any such investment responsibility and authority by written notice to the Trustee, and Representative may relinquish such responsibility and authority by written notice to the Company and Trustee.
- 3.4 Notification of Rights Regarding Securities. Following receipt of information, the Trustee will notify the Company of any conversion, redemption, exchange, subscription or other right relating to any securities purchased hereunder of which notice was given after the acquisition of such securities by the Trustee, and the Trustee shall have no obligation to exercise any such right unless it is instructed by the Company or its Representative in writing to exercise such right, within a reasonable time prior to the expiration of such right.
- 3.5 Uninvested Cash. Subject to the directions of the Company, or its Representative, the Trustee may hold any or all of the Trust Account in cash, uninvested and nonproductive of income. The Trustee shall not be required to pay interest on any cash so held uninvested. The Trustee may deposit cash awaiting investment or distribution in any interest-bearing account in any Bank (including the Trustee), subject to the collateral requirements set forth in Section 3.1 above.
- 3.6 Shareholder Communications. The Company directs the Trustee not to disclose to any company requesting shareholder information the name and the address of the Company or the share position of the securities of the inquiring company in the Trust Account.

ARTICLE IV TRUSTEE NOTICES AND INSTRUCTIONS

- 4.1 Instructions; Notices. Except as hereafter provided, any directions, instructions or notices which the Company or any other duly authorized person is required or permitted to give to the Trustee under this Agreement (the "Instructions") shall be in writing and shall be deemed effective upon receipt by the Trustee; provided, however, that the Trustee in its discretion may act upon oral Instructions if it believes them to be genuine, but the Trustee shall not be required to do so. If the Trustee requires, all oral Instructions are to be promptly confirmed in writing, but the Trustee shall not be liable for any action or any failure to act in accordance with oral Instructions, even though it fails to receive written confirmation from the Company. The Trustee shall be provided with specimen signatures of the authorized representatives of the Company. The Trustee shall be entitled to rely in good faith upon any Instructions signed by any authorized representative of the Company, and shall incur no liability for following such directions. Any written notices, affidavits or other communications hereunder shall be deemed to have been duly given if delivered or mailed first class, certified mail, postage prepaid, addressed as follows:

City National Bank, national association
Attn: Sue Behning/VP
1950 Avenue of the Stars, 2nd floor
Los Angeles, CA 90067
Tel: (310) 282-2921
Fax: (310) 282-2936

Southern California Edison Company
Attn: Tim Bint, Cash Manager
2244 Walnut Grove Ave., Quad 2A - 210
Rosemead, CA 91770
Tel: (626) 302-4476
Fax: (626) 302-6823

- 4.2 Photostatic Teletransmission. The transmission of the Instructions by photostatic teletransmission with duplicate or facsimile signatures shall be an authorized method of communication until the Trustee is notified by the Company to the contrary.
- 4.3 Electronic Affirmation. Notwithstanding any other provision of this Article IV, the Trustee may settle securities trades effected by the Company through a securities depository that utilizes an institutional delivery system, in which event the Trustee may deliver or receive securities in accordance with appropriate trade reports or statements given to the Trustee by such depository without having received direct communications or instructions from the Company.
- 4.4 Additional Instructions. In any matter under this Agreement in which the Trustee is permitted or required to act upon Instructions, the Trustee, where it deems necessary, may request further Instructions from the person or entity giving the original instructions, or from the Company, as the case may be, and may defer any and all action pending receipt thereof.

ARTICLE V COMPENSATION AND EXPENSES OF THE TRUSTEE

- 5.1 Trustee's fees will be as set forth on the fee schedule attached hereto, plus actual expenses incurred in performing its duties hereunder, and Trustee is hereby granted a lien on the Trust Account for such amounts. Any setup fee will be payable in advance. In addition, Trustee will receive its usual sweep fee for any Trust Account assets, which are invested in a sweep vehicle selected by the Company. Unless other payment arrangements are set forth herein or are agreed to by Trustee in writing, Trustee may disburse from the Trust Account sufficient funds to pay its compensation and expenses. If at any time cash is not available in the Trust Account to pay the Trustee's compensation and expenses, then Trustee may bill Company for such amounts. The fee schedule will be subject to periodic revision as the Company and the Trustee shall mutually agree.

ARTICLE VI RECORDS AND ACCOUNTS

- 6.1 Accurate Records and Accounts. The Trustee shall keep accurate records and accounts with respect to all cash and other assets held by it in the Trust Account, and all receipts and disbursements and other transactions involving such cash, securities and other assets. The Company shall have access to all such accounts, books and records at all reasonable times. All

such accounts, books and records shall be open for inspection and audit at all reasonable times by the Company or by any person or persons duly authorized by the Company.

- 6.2 Periodic Reports. The Trustee shall furnish the Company and any third party with such periodic reports, as the Company and the Trustee shall mutually agree, setting forth all receipts, disbursements and transactions effected by the Trustee.
- 6.3 Principal and Income. Except as otherwise specifically provided in this Agreement, the determination of all matters with respect to what is principal or income of the Trust Account and the apportionment and allocation of receipts and disbursements between these accounts (if any), shall be governed by the provisions of the California Revised Uniform Principal and Income Act from time to time existing. Any such matter not provided for herein or in the California Revised Uniform Principal and Income Act shall be determined by the Trustee in the Trustee's discretion.
- 6.4 Income Tax Reporting: Company assumes all duty to file any and all tax reports and returns, except as noted below, as well as full responsibility for the payment of all taxes assessed on or with respect to any Trust Property and all taxes due on the income collected for Company on any and all transactions with respect to any Trust Property. For purposes of IRS Form 1099 which Trustee may be required to prepare and file, all reportable income shall be reported to the IRS as being attributable to Company.

ARTICLE VII RESIGNATION AND REMOVAL OF THE TRUSTEE

- 7.1 Resignation and Removal. The Trustee may resign at any time upon thirty- (30) days' written notice to the Company, unless a shorter period is acceptable to the Company. The Company may at any time remove the Trustee upon thirty- (30) days' written notice to the Trustee, unless a shorter period is acceptable to the Trustee.
- 7.2 Appointment of Successor. In the event of the removal or resignation of the Trustee, the Company shall, by the earlier to occur of either (i) 30 days after removal or resignation of the Trustee or (ii) prior to the date of the next disbursement of funds necessary for proper storm water sump monitoring and maintenance, consistent with Special Condition 2 of Coastal Development Permit E-00-014, appoint a successor which, upon its acceptance in writing of such appointment delivered to the Company and the former Trustee, shall be vested with all the rights, powers and duties of the Trustee under this Agreement, and the retiring Trustee shall be released and discharged from all further liability with respect to the Trust. The retiring Trustee shall transfer, assign and deliver to its successor all of the property then held by it under the Agreement, except such reasonable compensation and expenses in connection with the settlement of accounts and the delivery of the assets to the successor Trustee. After settlement of the retiring Trustee's final accounting, the retiring Trustee shall also transfer to the successor Trustee true copies of its records as relate to the Trust Account, as may be requested by the successor Trustee. The successor Trustee shall not be liable or responsible for anything done or omitted in the administration of the Trust Account pursuant to this Agreement prior to the date it shall have become Trustee, nor to audit or otherwise inquire into or take any action concerning the acts of any retiring Trustee.
- 7.3 Final Periodic Report. Within sixty (60) days after the transfer of the assets of the Trust Account to the successor Trustee, unless a different period is mutually agreed to, the Trustee shall file with the Company a final periodic report, covering the period since the close of the last periodic report.

- 7.4 Deemed Acceptance. In the absence of any exception thereto filed in writing with the Trustee within ninety (90) days after the date of filing with the Company, any periodic report filed with the Company shall constitute a final periodic report by and discharge of the Trustee from all claims and liabilities with respect to the acts and transactions as shown in such report, and shall be binding and conclusive upon all persons.

ARTICLE VIII AMENDMENT AND TERMINATION

- 8.1 Amendment. This Agreement may be modified at any time by writing signed by the Parties.
- 8.2 Termination. The Agreement may be terminated at anytime by the Company with the express written consent of the Executive Director of the California Coastal Commission, consistent with the requirements of coastal development permit E-00-014. Should the Company decide to terminate this Agreement, it shall provide written notice of intent to terminate, together with evidence of the Executive Director of the California Coastal Commission's consent, to the Trustee no less than thirty (30) days prior to the desired termination date, provided, however, that this Agreement shall continue thereafter for such period as may be necessary for the complete divestiture of all cash, securities and other instruments held hereunder by the Trustee, but solely to the extent necessary to effect such complete divestiture. Upon such termination, all assets remaining in the Trust Account after payment of all expenses properly chargeable thereto shall be paid or distributed in accordance with written directions of the Company. Unless sooner terminated in accordance with other provisions hereof, any Trust created hereunder shall terminate December 31, 2022.
- 8.3 Final Periodic Report. Within sixty (60) days after the termination of the Trust Account, unless a different period is mutually agreed to by the Parties, the Trustee shall file with the Company a final periodic report, covering the period since the close of the last periodic report.
- 8.4 Deemed Acceptance. In the absence of any exception thereto filed in writing with the Trustee within ninety (90) days after the date of filing with the Company, any periodic report filed with the Company shall constitute a final periodic report by and discharge of the Trustee from all claims and liabilities with respect to the acts and transactions as shown in such report, and shall be binding and conclusive upon all persons.
- 8.5 Notification to the California Coastal Commission. The Trustee shall within three (3) business days of its sending or receiving amendments, termination notices and/or periodic reports under this Agreement, give copies thereof to the Executive Director of the California Coastal Commission. Such copies shall be deemed to have been duly given if delivered or mailed first class, certified mail, postage prepaid, addressed as follows:

California Coastal Commission
Attn: Executive Director
45 Fremont Street, Suite 2000
San Francisco, CA 94105-2219
Tel: (415) 904-5200
Fax: (415) 904-5400

ARTICLE IX LIMITATION ON LIABILITY

- 9.1 Liability of Trustee. In performing any duties under this Agreement, Trustee shall not be liable for any damages, losses, or expenses, except for gross negligence or willful misconduct on the

part of the Trustee. Trustee shall not incur any liability for: (a) any act or failure to act made or omitted in good faith, or (b) any action taken or omitted in reliance upon any instrument, including any written statement or affidavit provided for in this Agreement that the Trustee shall in good faith believe to be genuine, nor will the Trustee be liable or responsible for forgeries, fraud, impersonations or determining and verifying the scope of any representative authority, or any person acting or purporting to act on behalf of any party to this Agreement.

9.2 Indemnification by Company. Except to the extent attributable to Trustee's liability as set forth in Section 9.1 herein, Company further agrees to pay on demand, and to indemnify and hold Trustee harmless from and against, all costs, damages, judgments, attorneys fees, expenses, obligations and liabilities of any kind or nature which, in good faith, Trustee may incur or sustain in connection with or arising out of the Agreement, and Trustee is hereby given a lien upon all the rights, titles and interests of the Company in the Trust Account, to protect Trustee's rights and to indemnify and reimburse Trustee under this Agreement.

9.3 Force Majeure. The Trustee shall not be liable for any delay or failure to act as may be required hereunder when such delay or failure is due to fire, earthquake, any act of God, interruption or suspension of any communication or wire facilities or services, war, emergency conditions or other circumstances beyond its control, provided it exercises such diligence as the circumstances may reasonably require.

9.4 Scope. The Trustee shall have no duties or obligations hereunder except those specifically set forth herein, and such duties and obligations shall be determined solely by the express provisions of this Agreement.

9.5 Controversies.

9.5.1 Upon receipt of conflicting demands or notices relating to this Agreement, Trustee may, at its election, without liability to Company, do either or both of the following:

9.5.1.1 Withhold and stop all further proceedings in, and performance of, this Agreement, until such conflict is removed to Trustee's satisfaction;

9.5.1.2 File a suit in interpleader and obtain an order from the court requiring the parties to litigate their several claims and rights among themselves, in which case, Trustee shall be fully released and discharged from any obligation to perform any further duties imposed upon it with respect to this Agreement, and the parties shall pay Trustee all costs, expenses and reasonable attorney fees expended or incurred by it, the amount thereof to be fixed and a judgment thereof to be rendered by the court in such suit.

9.5.2 Any dispute arising out of or relating to this Agreement, including a breach of this Agreement, will be decided by reference under California Code of Civil Procedure Section 638 and related sections. A referee, either an active attorney or retired judge, will be selected according to the procedures of the American Arbitration Association and then appointed by the court in which the action regarding the dispute or controversy originated. The dispute will be submitted to the referee for determination in place of a trial before a judge and jury.

9.6 Legal Counsel. The Trustee may consult with, and obtain advice from, legal counsel of its own selection as to the construction of any of the provisions of this Agreement or the Trustee's obligations and duties, and shall incur no liability in acting in good faith in accordance with the reasonable advice and opinion of such counsel.

ARTICLE X
MISCELLANEOUS

- 10.1 Governing Law. This Agreement shall be governed, construed, regulated and administered under the laws of the State of California.
- 10.2 Invalid Provisions. It is not the intention of the Parties to violate any statute, regulation, ruling, judicial decision, or other legal provision applicable to this Agreement or the performance thereof. If any term of this Agreement, or any act or omission in the performance thereof, is or becomes violative of any such provision, such term, act or omission shall be of no force or effect and any such term shall be severed from this Agreement. Any such invalid term, act or omission shall not affect the validity of any other term of this Agreement that is otherwise valid, nor the validity of any otherwise valid act or omission in the performance thereof, unless such invalidity prevents accomplishment of the objectives and purposes of this Agreement. In the event any such term, act or omission is determined to be illegal or otherwise invalid, the necessary steps to remedy such illegality or invalidity shall be taken immediately by the Parties.
- 10.3 Counterparts. This Agreement may be executed in several counterparts, each of which shall be deemed an original, and said counterparts shall constitute but one and the same instrument, which may be sufficiently evidenced by any one counterpart.
- 10.4 Successors and Assigns. This Agreement shall inure to the benefit of, and be binding upon, the Parties hereto and their successors and assigns, except as is expressly provided to the contrary herein.

IN WITNESS WHEREOF, the Parties hereto have caused this Agreement to be executed by their respective duly authorized officers on the dates set forth below.

COMPANY
Southern California Edison Company

Date: _____

By _____

Title: _____

TRUSTEE
City National Bank, national association

Date: _____

By _____

Title: _____

TRUST ACCOUNT #: _____

CALIFORNIA COASTAL COMMISSION

45 FREMONT, SUITE 2000
SAN FRANCISCO, CA 94105-2219
VOICE AND TDD (415) 904-5200
FAX (415) 904-5400



Tu14a

| | |
|------------------------|----------------|
| Filed: | 6/11/15 |
| 180 th Day: | 12/8/15 |
| Staff: | J. Street - SF |
| Staff Report: | 9/25/15 |
| Hearing Date: | 10/6/15 |
| Commission Vote: | 11 – 0 |

ADOPTED FINDINGS: REGULAR PERMIT

| | |
|-----------------------------|--|
| Application No.: | 9-15-0228 |
| Applicant: | Southern California Edison Company |
| Location: | San Onofre Nuclear Generating Station, San Diego County. |
| Project Description: | Construct and operate an Independent Spent Fuel Storage Installation (ISFSI) to store spent nuclear fuel from SONGS Units 2 and 3. |
| Commission Action: | Approval with conditions. |

SUMMARY OF STAFF RECOMMENDATION

Southern California Edison Company (SCE) proposes to construct and operate a temporary facility to store spent nuclear fuel produced at the San Onofre Nuclear Generating Station (SONGS), on Camp Pendleton, in northern San Diego County (**Exhibit 1**). The facility, known as an Independent Spent Fuel Storage Installation (ISFSI), would consist mainly of a partially-below grade concrete and fill berm surrounding an array of 75 fuel storage modules, which would contain and protect stainless steel casks filled with spent fuel. The ISFSI would be located within the SONGS North Industrial Area (NIA), the former site of the decommissioned Unit 1 power plant, adjacent to and seaward of an existing ISFSI facility permitted in 2001 (**Exhibit 2**).

SONGS Units 2 and 3 were shut down in 2012, and some 2668 spent fuel assemblies remain in wet storage pools in the Units 2 and 3 fuel handling buildings. This fuel is highly radioactive and

requires secure storage for thousands of years to prevent harm to humans and the environment. Because the existing ISFSI does not have the capacity to hold the remaining spent fuel, a new ISFSI is being proposed in order to provide for the interim storage of the spent fuel until such time as it can be accepted at a federal permanent repository or other off-site interim storage facility. Removing the fuel from the existing wet storage pools would also facilitate the full decommissioning of SONGS Units 2 and 3 and the restoration of the site. The ISFSI is proposed to be installed beginning in 2016, fully loaded by 2019, and operated until 2049, when SCE assumes that the federal Department of Energy will have taken custody of all of the SONGS spent fuel. The facility would then be decommissioned, and the site restored, by 2051.

At present, there are no feasible off-site alternatives to the proposed project. No permanent fuel repository or other interim storage facility exists, and there are no near-term prospects for such a facility. SCE evaluated several on-site locations and ISFSI designs, and found the proposed project to be preferable in terms of site suitability and geologic stability, security, and cost, among other considerations. However, additional potentially superior on-site locations will become available for consideration upon completion of Units 2 and 3 decommissioning in 2032.

Within SCE's proposed 35-year timeframe, the siting and design of the ISFSI would be sufficient to assure stability and structural integrity against geologic hazards, including seismic ground shaking, slope failure, tsunamis and flooding, and coastal erosion, without requiring shoreline protection. Operation of the ISFSI would not involve the discharge of contaminants into coastal waters, and the implementation of construction BMPs designed to control runoff and prevent sediment and debris from entering the storm drain system would protect water quality and marine resources. Because of its location within the previously-developed SONGS site, the ISFSI would not interfere with coastal access and recreation within the proposed project life and would not significantly degrade visual resources so long as the other SONGS facilities remain in place.

Crucially, however, it remains uncertain whether it will be possible for SCE to remove the ISFSI as planned, in 2051. In the event that no permanent repository or other offsite interim storage facility emerges, if the shipment of SONGS spent fuel to an off-site location is otherwise delayed, or if the steel fuel storage casks proposed for use in the ISFSI (which is certified by the Nuclear Regulatory Commission for a 20-year period of use) degraded to the point of becoming unsafe to transport, the proposed ISFSI could be required beyond 2051, possibly for many decades. The ISFSI would eventually be exposed to coastal flooding and erosion hazards beyond its design capacity, or else would require protection by replacing or expanding the existing SONGS shoreline armoring. In either situation, retention of the ISFSI beyond 2051 would have the potential to adversely affect marine and visual resources and coastal access.

In order to address these uncertainties, and assure that the ISFSI facility remains safe from geologic hazards and avoids adverse impacts to coastal resources over the actual life of the project, the Commission adopts **Special Condition 2**, which authorizes the proposed development for a period of twenty years and requires SCE to return for a CDP Amendment to retain, remove or relocate the ISFSI facility, supported by: (i) an alternatives analysis, including locations within the decommissioned Units 2 and 3 area; (ii) assessment of coastal hazards and managed retreat; (iii) information on the physical condition of the fuel storage casks and a

maintenance and monitoring program; and (iv) proposed measures to avoid/minimize visual resource impacts. The Commission also adopts **Special Condition 7**, which requires SCE to submit, as soon as technologically feasible and no later than October 6, 2022, a maintenance and inspection program designed to ensure that the fuel storage casks will remain in a physical condition sufficient to allow both on-site transfer and off-site transport, for the term of the project as authorized under **Special Condition 2**. The Commission also adopts **Special Condition 3**, which requires SCE to agree to not enlarge or replace the existing NIA seawall for purposes of protecting the proposed project from coastal hazards. Additionally, the Commission attaches **Special Conditions 1, 4, 5, and 6** which require evidence of the Applicant's legal ability to undertake the development as conditioned by the Commission, assumption of risk, liability for attorney's fees, and restrictions on future development.

The Commission finds that, as conditioned, the project would be consistent with the hazards, marine resources, water quality, and view protection policies of the Coastal Act, and therefore the Commission **APPROVES** coastal development permit application 9-15-0228, as conditioned.

TABLE OF CONTENTS

| | |
|--|----|
| I. MOTION AND RESOLUTION | 5 |
| II. STANDARD CONDITIONS | 5 |
| III. SPECIAL CONDITIONS | 6 |
| IV. FINDINGS AND DECLARATIONS | 8 |
| A. PROJECT DESCRIPTION AND BACKGROUND | 8 |
| B. OTHER AGENCY APPROVALS | 14 |
| C. OTHER PROJECT RELATED ISSUES | 16 |
| D. GEOLOGIC HAZARDS | 22 |
| E. MARINE RESOURCES AND WATER QUALITY | 40 |
| F. COASTAL ACCESS AND RECREATION | 42 |
| G. VISUAL RESOURCES | 45 |
| H. ATTORNEYS' FEES AND COSTS | 46 |
| I. RESPONSE TO PUBLIC COMMENTS ON STAFF RECOMMENDATION | 46 |
| J. CALIFORNIA ENVIRONMENTAL QUALITY ACT | 51 |

APPENDICES

Appendix A – Substantive File Documents

Appendix B – Ground Shaking as a Measure of Earthquake Strength

EXHIBITS

Exhibit 1 – Project Vicinity

Exhibit 2 – SONGS Site and On-site Location Alternatives

Exhibit 3 – Project Plans

Exhibit 4 – ISFSI Components

Exhibit 5 – Structures to Be Removed

Exhibit 6 – ISFSI Seismic Design Spectra

Exhibit 7 – Flood Risk in Year 2117

Exhibit 8 – Views of Existing Seawall

Exhibit 9 – Site Views and Visual Simulations

I. MOTION AND RESOLUTION

Motion:

*I move that the Commission **approve** Coastal Development Permit 9-15-0228 subject to conditions set forth in the staff recommendation specified below.*

Staff recommends a **YES** vote on the foregoing motion. Passage of this motion will result in approval of the permit as conditioned and adoption of the following resolution and findings. The motion passes only by affirmative vote of a majority of Commissioners present.

Resolution:

The Commission hereby approves the Coastal Development Permit for the proposed project and adopts the findings set forth below on grounds that the development as conditioned will be in conformity with the policies of Chapter 3 of the Coastal Act. Approval of the permit complies with the California Environmental Quality Act because either 1) feasible mitigation measures and/or alternatives have been incorporated to substantially lessen any significant adverse effects of the development on the environment, or 2) there are no further feasible mitigation measures or alternatives that would substantially lessen any significant adverse impacts of the development on the environment.

II. STANDARD CONDITIONS

This permit is granted subject to the following standard conditions:

1. **Notice of Receipt and Acknowledgment.** The permit is not valid and development shall not commence until a copy of the permit, signed by the applicant or authorized agent, acknowledging receipt of the permit and acceptance of the terms and conditions, is returned to the Commission office.
2. **Expiration.** If development has not commenced, the permit will expire two years from the date on which the Commission voted on the application. Development shall be pursued in a diligent manner and completed in a reasonable period of time. Application for extension of the permit must be made prior to the expiration date.
3. **Interpretation.** Any questions of intent of interpretation of any condition will be resolved by the Executive Director or the Commission.
4. **Assignment.** The permit may be assigned to any qualified person, provided assignee files with the Commission an affidavit accepting all terms and conditions of the permit.
5. **Terms and Conditions Run with the Land.** These terms and conditions shall be perpetual, and it is the intention of the Commission and applicant to bind all future owners and possessors of the subject property to the terms and conditions.

III. SPECIAL CONDITIONS

This permit is granted subject to the following special conditions:

1. **Evidence of Landowner Approval.** PRIOR TO ISSUANCE OF THE COASTAL DEVELOPMENT PERMIT, the applicant shall submit to the Executive Director for review and approval evidence of their legal ability to undertake the development as conditioned by the Commission.
2. **Duration of Approval.** This coastal development permit authorizes the approved project for a period of twenty years from the date of approval (i.e., until October 6, 2035). No later than six months prior to the end of this authorization period, the Permittee shall apply for an amendment to this coastal development permit to retain, remove or relocate the ISFSI facility. This application shall be supported by:
 - a. An evaluation of current and future coastal hazards based on the best available information;
 - b. An analysis examining the merits and feasibility of off-site and on-site alternatives, including potential locations that are landward and/or at a higher elevation within areas made available by the decommissioning of SONGS Units 2 and 3;
 - c. A plan for managed retreat, if retention of the ISFSI facility beyond 2051 is contemplated and coastal hazards may affect the site within the timeframe of the amended project;
 - d. Evidence that the fuel storage casks will remain in a physical condition sufficient to allow off-site transport, and a description of a maintenance and inspection program designed to ensure that the casks remain transportable for the full life of the amended project.
 - e. An evaluation of the effects on visual resources of retaining the project, an analysis of available project alternatives and their implications for coastal visual resources, and proposed mitigation measures to minimize adverse impacts to coastal views.

Provided the application is received no later than six months prior to the end of the twenty-year period of development authorization, the date of development authorization shall be automatically extended until the time the Commission acts on the application. Failure to obtain an amendment to this coastal development permit by the specified deadline shall constitute a violation of the terms and conditions of this permit.

3. **No Future Shoreline Protective Device(s) to Protect the Proposed Development.**
 - A. The existing shoreline protective devices (rock revetment, concrete retaining wall, and steel sheet-pile seawall) located seaward of the North Industrial Area shall not be extended, expanded, enlarged or replaced for purposes of protecting the development approved by this coastal development permit. As used in this condition, replaced is defined to include either an alteration of 50% or more of a shoreline protective device or an alteration of less than 50% or more of a shoreline protective device wherein the

alteration would result in a combined alteration of 50% or more of the structure from its condition on October 6, 2015.

PRIOR TO ISSUANCE OF THE COASTAL DEVELOPMENT PERMIT, the Applicant shall submit evidence of the condition of each of the shoreline protective devices adjoining the North Industrial Area.

- B. No new shoreline protective device(s) shall ever be constructed to protect the development approved pursuant to Coastal Development Permit #9-15-0228, including the ISFSI facility, associated ancillary structures and any future improvements, in the event that the development is threatened with damage or destruction from erosion, landslides, waves, storm conditions, flooding, sea level rise or other natural coastal hazards in the future. By acceptance of this permit, the applicant hereby waives, on behalf of itself and all successors and assigns, any rights that may exist under Public Resources Code Section 30235 to augment, enlarge and/or replace any of the existing shoreline protective devices adjoining the NIA in order to protect the development approved by this coastal development permit.
4. **Assumption of Risk, Waiver of Liability and Indemnity.** By acceptance of this permit, the Permittee acknowledges and agrees:
- a. That the site may be subject to hazards from coastal erosion, storm conditions, wave uprush, and tsunami runup;
 - b. To assume the risks to the Permittee and the property that is the subject of this permit of injury and damage from such hazards in connection with this permitted development;
 - c. To unconditionally waive any claim of damage or liability against the Commission, its officers, agents, and employees for injury or damage from such hazards; and,
 - d. To indemnify and hold harmless the Commission, its officers, agents, and employees with respect to the Commission's approval of the project against any and all liability, claims, demands, damages, costs (including costs and fees incurred in defense of such claims), expenses, and amounts paid in settlement arising from any injury or damage due to such hazards.
5. **Restriction on Future Development.** This permit is only for the development described in the project description set forth in this staff report. Pursuant to Title 14 California Code of Regulations (CCR) Section 13253(b)(6), the exemptions otherwise provided in Public Resources Code (PRC) Section 30610(b) shall not apply to the development governed by this permit. Accordingly, any future improvements to this structure shall require an amendment to this permit from Commission, including but not limited to an increase in storage capacity of spent fuel. In addition, a permit amendment shall be required for any repair or maintenance of the authorized development identified as requiring a permit in PRC Section 30610(d) and Title 14 CCR Sections 13252(a)-(b).
6. **Liability for Costs and Attorneys Fees:** SCE shall reimburse the Coastal Commission in full for all Coastal Commission costs and attorneys fees -- including (1) those charged by

the Office of the Attorney General, and (2) any court costs and attorneys fees that the Coastal Commission may be required by a court to pay – that the Coastal Commission incurs in connection with the defense of any action brought by a party other than SCE against the Coastal Commission, its officers, employees, agents, successors and assigns challenging the approval or issuance of this permit, the interpretation and/or enforcement of permit conditions, or any other matter related to this permit. The Coastal Commission retains complete authority to conduct and direct the defense of any such action against the Coastal Commission.

7. Inspection and Maintenance Program.

- A. As soon as technologically feasible, and no later than October 6, 2022, the Permittee shall provide for Commission review and approval an inspection and maintenance program designed to ensure that the fuel storage casks will remain in a physical condition sufficient to allow both on-site transfer and off-site transport, for the term of the project as authorized under Special Condition 2 (i.e., until October 6, 2035). The program shall include a description of: (1) the cask inspection, monitoring and maintenance techniques that will be implemented, including prospective non-destructive examination techniques and remote surface inspection tools; (2) what data will be collected and how often the results of the inspection and maintenance program will be reported to the Commission; (3) all available evidence related to the physical condition of the casks and their susceptibility to degradation processes such as stress corrosion cracking, and (4) remediation measures that will be implemented, including the submission of a coastal development permit amendment, if the results of the cask inspection and maintenance do not ensure that the fuel storage casks will remain in a physical condition sufficient to allow on-site transfer and off-site transport for the term of the project as authorized under Special Condition 2.
- B. If the Commission determines that the inspection and maintenance program required by Subsection A is not sufficient to assure cask transportability over the term of the project authorized under Special Condition 2, the Applicant shall submit an amendment to this coastal development permit proposing measures to assure cask transportability.
- C. The Permittee shall implement the inspection and maintenance program approved by the Commission. If the Permittee wishes to propose changes to the program approved by the Commission, it shall submit the proposed changes to the Executive Director. No changes to the approved program shall occur without an amendment to this coastal development permit unless the Executive Director determines no amendment is legally required.

IV. FINDINGS AND DECLARATIONS

A. PROJECT DESCRIPTION AND BACKGROUND

Project Purpose

The primary purpose of the project is to move spent nuclear fuel from its current location in a wet storage facility at Units 2 and 3 of the San Onofre Nuclear Generating Station (SONGS) to a

dry storage system, known as an Independent Spent Fuel Storage Installation (ISFSI). An existing ISFSI at SONGS contains approximately 51 fuel storage modules filled with spent fuel from SONGS Units 1, 2 and 3, with space for 38 more. SCE proposes to construct a new ISFSI, with a capacity of 75 fuel storage modules (**Exhibit 3**), because the existing facility soon will reach full capacity while hundreds of spent fuel assemblies remain in the Units 2 and 3 pools. Only fuel and material generated at the SONGS is proposed to be stored at the ISFSI. Moving the spent fuel out of wet storage would facilitate dismantling the nuclear units at SONGS Units 2 and 3 and would allow their eventual decommissioning.

SCE proposes to store the material at the ISFSI until it can be moved to an off-site permanent repository to be established by the federal government. The ISFSI is proposed to remain in place through the year 2051. SCE plans to begin relocating SONGS spent fuel to the DOE as early as 2030, and to continue this process until 2049, when the last remaining spent fuel storage casks would be removed from the site (SCE 2014b). Based on the federal Department of Energy's (DOE) statutory obligation to accept commercial spent fuel (see below) and SCE's planned schedule for shipping the spent fuel to a federal off-site repository, the final two years of the proposed project term would be devoted to the decommissioning and removal of the ISFSI and site restoration. However, as discussed in more detail below, no such federal permanent repository currently exists, alternative interim off-site storage options (e.g., state- or privately-operated ISFSIs or repositories) are not currently available, and it is uncertain when or if such off-site facilities will become available. Thus, there is a possibility that the ISFSI would remain at SONGS beyond 2051.

The spent fuel that would be stored in the ISFSI is considered high-level radioactive waste and must be stored securely for tens of thousands of years. As the fuel is used in a nuclear reactor, its level of radioactivity increases significantly due to radioisotopes formed during the nuclear fission process. When the fuel is removed from the reactor, it is initially stored in a "wet storage" pool adjacent to the power plant. The water in the pool and the materials used in the pool's construction provide the shielding necessary to prevent human and environmental exposure to the high level of radioactivity present when the fuel is first removed from the reactor. The fuel must remain in the pool for several years until that initial level of radioactivity, and the heat that it produces, is reduced. It can then be relocated to another facility, if one is available. At SONGS, all fuel has been removed from the nuclear reactors and placed in the spent fuel pools. The spent fuel currently stored in the SONGS pools has been there for varying amounts of time; some of the fuel has been cooling for decades, such that much of its capacity to generate heat and radiation through radioactive decay has dissipated, while the youngest fuel assemblies in the pools have been cooling for only two to three years since the permanent shutdown of the Units 2 and 3 reactors. The SONGS spent fuel pools also contain a large number of "high burn-up" fuel assemblies, which produce greater amounts of radiation and heat and require more time to cool than regular fuel assemblies. In all cases, the inventory of spent fuel at SONGS requires secure storage, whether on-site or elsewhere, for many thousands of years.

Site Characteristics & Background

SONGS occupies an 84 acre site on the northern San Diego County coast, within the U.S. Marine Corps Base, Camp Pendleton, and approximately 2.5 miles south of the city of San

Clemente (**Exhibit 1**). SONGS is bounded on the north and northeast by Old Pacific Coast Highway and Interstate 5 (I-5), on the northwest by a surface parking lot for SCE employees, and on the west and south by San Onofre State Beach and the Pacific Ocean. The SONGS site comprises just over one mile of shoreline. The northern and southern portions of the site, consisting mostly of parking lots and auxiliary structures and facilities, respectively, are located on top of coastal bluffs of up to 120 feet above mean lower low water (MLLW). The generating units and other core facilities are located along the central portion of the site on a set of artificially-graded terraces, ranging in elevation from 13 to 80 feet MLLW, cut into the bluff at the time of construction. Shoreline protection devices, including a rip-rap revetment, a concrete bulkhead supporting a public access walkway, and a seawall, extend for approximately 2000 feet along the shoreline in front of the Units 1, 2 and 3 areas. **Exhibit 2** provides an overview of the SONGS site and its major features.

The plant is collectively owned by SCE (78.2% interest), San Diego Gas and Electric Company (20%) and the City of Riverside (1.8%). As a previous owner, the City of Anaheim is also a co-participant on the ISFSI project. The plant operates subject to a long-term easement granted by the U.S. Department of the Navy (Navy), executed in 1964 and effective through 2024.

SONGS previously consisted of three nuclear power reactors operated by SCE. The 430 MW generator at Unit 1 began operations in 1968, was shut down in 1992, and has since been decommissioned and dismantled. CDP #E-00-001, approved by the Commission on February 15, 2000, authorized the demolition of the structures comprising Unit 1 and the construction of an ISFSI comprising 19 fuel storage modules, located within the Unit 1 area (now referred to as the North Industrial Area) (**Exhibit 2**).

SONGS Units 2 and 3 were constructed beginning in 1974 (under CDP #183-73), and operated as twin 1127-MW commercial nuclear power plants beginning in 1983 and 1984, respectively. In 2000, in order to create additional storage capacity needed as the existing spent fuel pools begin to fill, SCE applied for and was granted authorization (CDP #E-00-014) for the construction of a much larger ISFSI facility (of up to 104 fuel storage modules) to store Units 2 and 3 spent fuel. The new ISFSI was co-located with and integrated into the previously-approved Unit 1 ISFSI. At present, the existing ISFSI contains 51 loaded and 12 empty fuel storage modules, with space remaining for an additional 26 modules. The location of the existing ISFSI within the North Industrial Area (NIA) is shown in **Exhibits 2 and 3**. Power generation at Units 2 and 3 ceased in 2012. Following an extended shutdown period, SCE announced plans to decommission Units 2 and 3 on June 7, 2013. Since then, SCE has taken a number of actions in preparation for decommissioning, including the installation of new electrical systems needed to supply the plant with power now that electricity generation at SONGS has ceased (CDP Waiver # 9-14-1550-W) and back-up diesel generators (CDP Waivers # 9-14-1550-W and 9-15-0265-W). Most recently, SCE has received Commission approval for projects to install a new spent fuel pool cooling system to replace the existing ocean water once-through cooling system (CDP 9-15-0162), and to replace the large seawater intake pumps serving Units 2 and 3 with smaller pumps better suited to the plant's reduced water needs (CDP Waiver #9-15-0417-W).

Project Description

SCE proposes to construct a new ISFSI incorporating 75 fuel storage modules within the NIA. The ISFSI, including its concrete approach aprons, would occupy approximately 40,000 square

feet and would be located immediately seaward of the existing ISFSI, approximately 100 feet inland of the seawall adjoining Unit 1 (**Exhibit 3**). In addition, the proposed project includes the construction of a new security building within the NIA to the east of the ISFSI, a new perimeter security fence, and associated lighting and security equipment. The total project area, including the ISFSI, ancillary structures, and security perimeter, is approximately 100,000 square feet.

There are several types of ISFSI designs, with most being a variation of different types of storage casks bolted to a thick concrete pad within a secured area. The storage casks are generally multi-layer containers made of concrete, steel and other metals, designed to contain most of the radiation emanating from the spent fuel assemblies. Depending on the ISFSI design, storage casks may be stored horizontally or vertically within a concrete superstructure or outer shell. To date, the NRC has licensed 75 ISFSIs at nuclear power plants around the country. Many power plants have constructed ISFSIs to provide additional storage in their wet storage pools for ongoing power plant operations. At SONGS, there is no additional spent fuel being produced, but SCE is proposing the ISFSI in part to allow the emptying of the existing spent fuel pools and to facilitate decommissioning of the power plant complex.

The ISFSI design at SONGS would differ from most other ISFSIs in that the storage casks would be stored partially below grade, encompassed by a berm composed of concrete and fill. The ISFSI system, known as a HI-STORM UMAX, is expected by its manufacturer (Holtec International) to provide better performance during seismic events, provide better security, and reduce radiation doses at the site boundary in comparison to competing designs (Holtec 2014a). The HI-STORM UMAX “ventilated vertical module” (VVM) is a vertical underground storage system designed to accommodate multi-purpose container (MPC) models produced by Holtec. The MPCs proposed for use at SONGS are Holtec MPC-37 canisters, composed of 5/8-inch thick austenitic stainless steel. Each MPC-37 contains an internal grid or “basket” allowing for the storage of up to 37 individual spent fuel assemblies. A 9.5-inch thick canister lid would be welded to the canister shell after loading.

As proposed, the SONGS facility would consist of 75 VVMs set in a surrounding berm measuring approximately 160 ft wide by 260 ft long by 24.5 ft in vertical height, including a 3-foot thick concrete foundation pad. Although the HI-STORM UMAX system has been designed to be 24.5 ft in vertical height, the proposed ISFSI would be installed 12.25 ft below the existing grade. In order to fully enclose the structure, as intended for the underground system, the portion of the structure above the NIA grade (approximately 12.25 feet) will be encased in a berm sloped from the top of the structure to the grade elevation at an approximate forty-five degree angle. As a result, no vertical wall of the concrete structure will be exposed. The top of the ISFSI pad would be at an elevation of approximately 32 feet MLLW. In addition to the array of VVMs, the ISFSI structure would include a reinforced concrete ramp and approach apron for use during the loading, unloading, and maintenance of the storage modules at the top of the ISFSI pad. Plan-view and cross-sectional diagrams of the proposed ISFSI are shown in **Exhibit 3**.

Within the HI-STORM UMAX, each individual VVM would operate independently from any other, and would allow for the storage of one MPC in a vertical configuration inside a cylindrical cavity entirely below the top of grade of the facility. The MPC storage cavity is defined by a so-called Cavity Enclosure container (CEC) comprised of a stainless steel Container Shell welded to a stainless steel Base Plate. Internal parts within the CEC include MPC bearing surfaces, upper

and lower guides to aid in the insertion of the MPC into the CEC and limit lateral movement of the MPCs during an earthquake, and a metal Divider Shell, which separates the space between the MPC and the wall of the CEC to allow for the inflow and outflow of air around the MPC. The CEC is capped with a 24,000-pound Closure Lid made of steel and concrete, which provides radiation shielding at the top of the ISFSI. The Closure Lid also includes inlet and outlet vents which connect to the ventilation space within the CEC and allow for the air cooling of the MPCs. Diagrams of the HI-STORM UMAX storage system and components are provided in **Exhibit 4**.

The ISFSI “berm”, or surrounding support structure, would consist of a foundation pad and top pad (“ISFSI Pad”) made of 3-foot thick reinforced concrete, and subgrade fill. The interstitial spaces between and surrounding the fuel storage modules would be composed of self-consolidating concrete with a minimum compressive strength of 3000 psi, while the subgrade of the outer perimeter of the berm would be composed of the material excavated from below the NIA grade during site preparation. The subgrade, foundation pad, and top pad and Closure Lid would completely surround the CECs and provide radiation shielding for the long-term storage of the MPCs.

Construction

The proposed project is anticipated to be constructed in a single phase, with field work commencing in January 2016. Construction activities, including site preparation and removal of several existing structures, grading, excavation and material placement, ISFSI construction, and the construction of the new security building, fencing, and lighting, are expected to continue for approximately one year. Most of the existing structures to be removed are temporary facilities storing non-radioactive remnants from Unit 1 (**Exhibit 5**). Because the proposed ISFSI would be installed partially below the existing NIA grade, project construction will require the excavation of approximately 14,800 cubic yards of material. This material would be stored on-site following SONGS best management practices and is proposed to be used in the peripheral berm surrounding the ISFSI. Project construction would also include utility extensions to existing water, sewer, electric, and telephone lines to accommodate operational activities at the proposed security building.

Project construction will require heavy equipment, only some of which is currently located on the SONGS site. Off-site construction vehicles (such as delivery trucks) would access the site via Old Pacific Coast Highway and Interstate 5. In general, construction activities would be limited to daylight hours, with the possible exception of operations requiring the continuous placement of concrete, which could last for 12 to 16 hours and result in a limited amount of nighttime operations.

Fuel Loading and Transfer of Casks from Spent Fuel Pools to the ISFSI

To transfer the spent fuel from wet to dry storage, the MPCs would be brought to the wet storage pools, located in the Units 2 and 3 Fuel Handling Buildings approximately 1,200 feet east of the project site. The MPCs would be placed in a licensed transfer cask, lowered into the pools, loaded with spent fuel assemblies, and then removed from the pools. Water would be drained from the MPCs and replaced with helium, and they would be welded shut. Subsequently, the transfer casks containing the MPCs would be loaded onto a transfer vehicle that would use existing roads within the SONGS Protected Area to move the MPCs to the project site. The transfer vehicle would access the top of the ISFSI pad using the built-in access ramp and

approach pad (*see Exhibit 3*), and the MPCs would be loaded into the fuel storage modules and capped. Approximately six days are required to complete the transfer of one MPC, though more than one MPC can be processed for loading at any given time. SCE expects to begin the transfer of spent fuel to the new ISFSI facility beginning in 2017, and to complete the effort by June 2019.

Maintenance & Monitoring

The NRC requires licensees to implement an Aging Management Plan (AMP) to provide for the continued safe dry cask storage of spent fuel in order to renew the initial 20-year license for the HI-STORM UMAX ISFSI. SCE has indicated that it will develop its aging management program shortly after the fuel is transferred to the proposed ISFSI, in advance of NRC requirements. In a 9/14/2015 document submitted to Commission staff (SCE 2015f), SCE described this program as follows:

SCE's program will focus on engineered controls (i.e., conservative design, material selection and fabrication controls), operational controls (e.g., inspection and monitoring) and developing mitigation plans to address material degradation and/or mitigate its consequences. Site monitoring of environmental parameters such as temperature and humidity will be used to help determine the risk of corrosion to the canister and predict the time of onset of degradation. Inspections will include visual observation, collection of surface deposits and temperature, and more extensive non-destructive examination (NDE) techniques. Industry efforts are well underway to develop NDE methods, deployment methods, qualification processes and acceptance criteria. It is not unusual for such efforts to evolve over time and with greater collective experience. With the commitment that SCE will not wait until it is required by the NRC to implement an AMP, SCE expects to be an early, if not the first, user of such techniques.

One of the challenges of inspections is getting to the entire surface of the loaded canisters which have a radiation environment that limits access. Remote surface inspection tools are currently being developed and are expected to be available for use at SONGS shortly after the fuel is transferred to the expanded ISFSI. In addition to developing these remote inspection tools, SCE will place an empty canister in the same environment as the loaded systems. This type-test specimen (i.e., coupon) can be thoroughly inspected and monitored in ways that a loaded canister cannot due to the presence of a spent fuel assembly. SCE has selected a canister to test, which will be located in the vicinity of the proposed ISFSI pad and will begin its initial exposure by the fourth quarter of 2015.

SCE's AMP will include a combination of the inspections described above to monitor the condition of the ISFSI components throughout their service life. This will provide assurance that the ISFSI components are performing as designed and allow for the spent fuel to be safely removed when the DOE is ready to transfer the fuel to an interim storage facility or permanent repository.

In summary, SCE's intended aging management program would include (a) the monitoring of environmental conditions, such as temperature and humidity, that could influence the risk of corrosion and degradation of the stainless steel MPCs; (b) visual observation, surface measurements, and other inspection techniques to provide information on the physical condition

of the MPCs; and (c) use of an empty cask (“coupon”) as a surrogate for filled casks to allow for more thorough inspection and evaluation. However, the “non-destructive examination techniques”, “remote surface inspection tools” and “NDE methods, employment methods, qualification processes and acceptance criteria” referenced by SCE are “in development”, and their utility for the maintenance and monitoring of the spent fuel casks has not been demonstrated. Nor is it clear when these techniques, tools and standards would become available for use at SONGS.

Off-site Transport & ISFSI Decommissioning

Transportation of commercial spent nuclear fuel is regulated by the US Department of Transportation (49 CFR Part 172) and the NRC (10 CFR Part 71). The SONGS operating license issued by the NRC (10 CFR Part 50) allows for the off-site shipment of spent fuel, with no additional licensing action, so long as the transportation cask to be used has a current NRC Certificate of Compliance (CoC). Holtec has recently applied (August 7, 2015) to the NRC for a CoC for a new spent fuel transport cask (HI STAR 190) which would be designed and licensed to ship the MPC-37 storage casks that would be used in the proposed ISFSI (SCE 2015e). SCE anticipates that the HI STAR 190 transportation casks will have received NRC approval prior to the first planned shipments in 2030. When another facility becomes available for spent fuel storage (e.g., a federal repository, federal interim storage site, or a private storage site) the MPCs to be stored in the proposed ISFSI would be removed from the fuel storage modules and placed in transport casks, which would then be loaded onto transport vehicles (railcar or truck).

The timing of spent fuel shipments to an off-site storage site depends in part on the NRC requirements related to fuel composition, cooling time, the type of cladding used to shield the fuel assemblies, and the capabilities and design of the storage and transportation casks that would be used. Based on these factors, SCE anticipates that all of the Units 2 and 3 fuel assemblies currently stored in the spent fuel pools and awaiting transfer to the proposed ISFSI would be available for transportation between 2025 and 2030 (SCE 2015e). The actual removal of this fuel from the SONGS site would additionally depend on the availability of a permanent or interim storage site, and in the case of a federal repository, the DOE’s need to coordinate spent fuel shipments from other nuclear power plants. Under the schedule contemplated in SCE’s final SONGS Irradiated Fuel Management Plan (IFMP) and Decommissioning Cost Estimate (DCE) submitted to the NRC, offsite shipment of spent fuel would begin in 2030 and be completed by 2049 (SCE 2014a, 2014b).

The decommissioning of SONGS Units 2 and 3, comprising several distinct stages, is scheduled to continue through 2032. Major above-grade structures are slated to be removed by 2028, and sub-surface structures would be removed by 2031 (SCE 2014a). Due to the potential for effects on coastal resources, the deconstruction and removal activities associated with decommissioning will require Commission review under one or more separate CDP applications. Site clean-up, removal of the retaining walls, shore protection, berm and guard house and final disposition of other facilities will be addressed in these later permits.

B. OTHER AGENCY APPROVALS

U.S. Nuclear Regulatory Commission

The construction and operation of new facilities at SONGS are subject to the approval and oversight of the federal Nuclear Regulatory Commission (NRC) pursuant to NRC regulations.

The NRC regulates ISFSIs pursuant to 10 CFR Part 72. Part 72 provides for two types of licenses for ISFSIs:

- (1) General license. The wet storage of spent fuel generated at a nuclear power plant is authorized under the plant's existing license issued pursuant to 10 CFR Part 50 (or Part 52 for newer plants). A plant may extend this general license to cover an ISFSI facility, without the need for a license amendment, by satisfying the requirements in Subpart K to 10 CFR Part 72, which include a variety of siting, safety and security requirements.
- (2) Specific license. In order to construct and operate an ISFSI outside the licensed 10 CFR Part 50 area of a nuclear power plant, an operator (or other entity) must apply for and be granted a specific license from the NRC pursuant to 10 CFR Part 72. Such applications are subject to NRC review and approval and public hearing requirements.

The proposed ISFSI would be installed under SCE's 10 CFR Part 50 general operating license, and thus does not require additional NRC approval, though it is subject to NRC oversight to assure compliance with Part 72, Subpart K and other applicable regulations. The SONGS Part 50 license requires specific performance standards and operating conditions at the facility, including design specifications, testing requirements, security measures, and other measures. When the NRC acknowledged the cessation of power operations at SONGS, the Part 50 license was modified to allow for the possession of nuclear fuel by SCE and prohibit further power operations. NRC regulations provide for a 60-year decommissioning period once power operations have ceased. No further action is required by SCE unless the license cannot be terminated within 60 years. SCE will request NRC approval to reduce the licensed area to that of the ISFSI and its security footprint on or about 2031, as Units 2 and 3 decommissioning nears its conclusion. The SONGS Part 50 general operating license can only be terminated after meeting all the conditions specified in 10 CFR 50.82 for license termination, including the decontamination and demolition of the ISFSI.

Federal Pre-emption

The NRC has exclusive jurisdiction over radiological aspects of the proposed project. The state is preempted from imposing upon operators of nuclear facilities any regulatory requirements concerning radiation hazards and nuclear safety. The state may, however, impose requirements related to other issues. The U.S. Supreme Court, in *Pacific Gas and Electric Company v. State Energy Commission*, 461 U.S. 190, 103 S.Ct. 1713 (1983), held that the federal government has preempted the entire field of "radiological safety aspects involved in the construction and operation of a nuclear plant, but that the states retain their traditional responsibility in the field of regulating electrical utilities for determining questions of need, reliability, costs, and other related state concerns." The Coastal Commission findings herein address only those state concerns related to conformity to applicable policies of the Coastal Act, and do not evaluate or condition the proposed project with respect to nuclear safety or radiological issues.

U. S. Department of the Navy

SCE operates the SONGS site under the terms of a 60-year grant of easement from the U.S. Department of the Navy (Navy), executed on May 12, 1964 and effective through May 12, 2024. The easement was authorized by an act of Congress (Public Law 88-82, July 30, 1963). SCE has requested Navy authorization to renew the grant of easement to allow for plant

decommissioning, required site restoration, and the transfer of all SONGS spent fuel to DOE custody.

Pursuant to Coastal Act section 30601.5, where the Applicant is not the owner of a fee interest in the property on which a proposed development is to be located, but can demonstrate a legal right, interest, or other entitlement to use the property for the proposed development, the commission shall not require the holder or owner of the fee interest to join the applicant as co-applicant. Prior to issuance of the CDP, however, the Applicant must demonstrate their ability to comply with all conditions of approval. Accordingly, the Commission is imposing **Special Condition 1**, which requires SCE to submit, for the Executive Director's review and approval, evidence of their legal ability to comply with all conditions of approval.

C. OTHER PROJECT-RELATED ISSUES

Lack of a Permanent Storage Facility

The need for onsite storage of spent nuclear fuel at power plants around the country is a consequence of the United States not yet establishing a permanent and safe repository for spent fuel and other nuclear materials. In 1977, the federal government announced it would take on the responsibility for spent fuel from all nuclear power plants in the U.S. In 1982, the Nuclear Waste Policy Act required the Department of Energy to accept spent fuel for permanent disposal by 1998. In 1987, after studies of several potential sites, the Act was amended to make a site at Yucca Mountain, Nevada, the only site undergoing further consideration. Spent fuel was to be shipped to the Yucca Mountain facility from power plants around the country in priority order – generally, the older the fuel, the earlier it would be accepted.

Since that time, the U.S. Department of Energy (DOE), the U.S. Environmental Protection Agency (EPA), and the NRC have conducted numerous studies at Yucca Mountain and have constructed parts of the facility. It has not yet opened, however, due to several significant technological issues and court challenges. The facility was scheduled to start accepting materials in 2010; however, in July 2004, a decision by the District of Columbia Circuit Court (*Nuclear Energy Institute, Inc. v. Environmental Protection Agency*, D.C. App. 2004, No.01-1258) found that the EPA had improperly set the facility's design standard well below the safety level required by Congress.¹ In 2008, the DOE applied to the NRC for license to dispose of spent fuel at Yucca Mountain. However, the application received strong opposition from the State of Nevada and several local governments, as well as several threats of litigation. Following the 2008 presidential election, the Obama administration decided not to pursue the license application, and in 2010, the DOE filed a motion with the NRC seeking permission to withdraw its application for the Yucca Mountain repository. Although the motion was denied, the NRC process was subsequently suspended due to a lack of congressional funding. Although the

¹ In 2002, Congress determined that the facility must meet an "individual risk standard" for exposure to radioactive elements "based on and consistent with" the recommendations of the National Academy of Sciences. The Academy determined that the facility required designs ensuring exposures would not be exceeded for tens to hundreds of thousands of years. The EPA, however, set the exposure standard at 10,000 years. The court determined the EPA's selection of the 10,000 year standard was not "based upon and consistent with" the recommendations of the National Academy of Sciences, as had been required by Congress.

federal government has continued to study options for permanent or interim repositories, no federal facility for the disposal of spent fuel currently exists, and there are no near term prospects for the licensing and development of such a repository. As a result, it remains uncertain when, or if, the DOE will be in a position to accept SONGS spent fuel.

Commission staff is aware of two active proposals to develop private interim storage facilities that would, if built, accept commercial spent fuel. Waste Control Specialists (WCS) has announced its intention to apply for a 10 CFR Part 72 site-specific license for an ISFSI at the site of its existing low-level waste storage facility in Andrews County, Texas. WCS believes it could begin accepting spent fuel as early as December 2020 (SCE 2015c). More recently, Holtec and Eddy Lea Energy have announced plans to develop an underground consolidated interim storage facility in southeastern New Mexico. The facility is envisioned to consist of a greatly enlarged version of the HI-STORM UMAX system proposed for use at SONGS. While these private storage facilities hold promise for expanding the range of long-term storage options in the absence of a permanent federal repository, both proposals are likely to face significant opposition and have yet to undergo NRC licensing, and it is unclear when, or if, either would become available, or if they would be able to accept all of the SONGS spent fuel.

Project Alternatives

As part of its proposal, and in response to Commission staff queries, SCE evaluated several alternatives to the proposed project. These included a “no action” alternative, shipping the material offsite, siting the ISFSI at other locations on the SONGS site, and consideration of several design and configuration alternatives for the facility (SCE 2015a, b, c). In addition, Commission staff has evaluated the implications of several different project timeframes.

As detailed below, many of the potential alternatives were determined by the SCE to be infeasible. “Feasible” is defined in Coastal Act section 30108 as capable of being accomplished in a successful manner within a reasonable period of time, taking into account economic, environmental, social and technological factors. SCE has indicated that a key project objective is to offload the spent fuel pools by mid-2019, and that a multi-year delay in meeting the project objective would significantly disrupt its schedule for decommissioning SONGS Units 2 and 3 and introduce significant new costs in comparison to the proposed project.

No Action

In the absence of the proposed project, the SONGS 2 and 3 spent fuel would remain in the existing spent fuel pools until it could be transferred to an off-site permanent repository or interim storage facility. While the NRC considers wet storage pools to provide adequate safety for the stored materials, as a general matter, dry cask storage is thought to provide an increased margin of safety. In part, this is because ISFSIs are a passive storage system, and unlike fuel pools, do not depend on active cooling systems or require continual maintenance (though they do require regular inspections). The ISFSIs additionally encapsulate the spent fuel into hardened structures, which are less likely than the wet storage pools to be affected by forces such as seismic activity, terrorist attack, or other phenomena. For example, the SONGS ISFSI has been designed to withstand significantly greater ground shaking intensities (1.5 g in two orthogonal directions, net 2.12 g) than the existing spent fuel pools (0.67 g in each direction). SCE has also indicated that keeping the spent fuel in the existing pools would interfere with the planned

decommissioning of Units 2 and 3, and would require SCE to maintain more infrastructure and active systems than the dry storage option. For these reasons, SCE does not consider continued storage of spent fuel in the pools as the preferred alternative.

Off-site Locations

Of the offsite storage alternatives considered by SCE, all were either unavailable or otherwise found to be infeasible. Alternatives considered included:

- Shipping the material to a reprocessing facility: There are several reprocessing facilities in other countries, but none in the U.S. This option was not considered feasible due to several significant political, legal, and logistical uncertainties.
- Shipping the material to a private storage facility: While there is one proposed private facility currently licensed by the NRC (at Skull Valley, Utah), the developer has been unable to obtain required non-nuclear permits from other agencies and the facility was never constructed. At present, there are no further plans to construct and operate the Skull Valley ISFSI. There are two active proposals to develop interim consolidated dry spent fuel storage facilities in New Mexico and Texas, respectively (see above). However, these facilities are not licensed and have not been constructed, and it is uncertain if or when these facilities might become available. There are no other private storage facilities available in the U.S. Therefore, this alternative is unavailable.
- Shipping the material to another nuclear power plant that had sufficient storage space: SCE found that other nuclear power plants either do not have adequate storage or have not included in their storage licenses the possibility of accepting spent fuel from other power plants. While in concept it may be possible for a plant to amend its license to accept fuel generated off-site, actually doing so would depend on another reactor operator being willing to take possession of SONGS spent fuel. Any such proposal would be controversial, as it would involve the shipment of spent fuel from one location to another, and in the unlikely event that another licensee were willing to accept the fuel, the NRC license amendment process would likely take a number of years, preventing the project from being accomplished within a reasonable timeframe. Thus, this alternative was deemed infeasible.
- Shipping the material to an off-site ISFSI to be developed by SCE: In theory, SCE could apply for a specific license to develop its own ISFSI away from the SONGS licensed area. In order to construct an ISFSI at an off-site location, SCE would need to identify suitable available land under its ownership, acquire new land, or obtain landowner approval for a project on land it did not own.

One potential location evaluated by SCE and Commission staff is the SONGS “Mesa”, a SCE-operated, non-nuclear auxiliary facility located within Camp Pendleton immediately north and inland of SONGS proper. While the Mesa has the advantages of being a previously-developed site also under SCE control, it is, like SONGS, located on an easement granted by the Navy, which is planned to be terminated in 2017 (SCE 2014a). Camp Pendleton representatives have informed Commission staff that the Marine Corps has other development plans for the off-site Mesa location once the site has been restored, and that the authorization of new SONGS-related projects here was highly unlikely.

More generally, at any off-site location, SCE would need to evaluate the site suitability, including geological characteristics, against NRC criteria, a process which could take several years with no guarantee of a favorable outcome. For example, an ISFSI located outside the SONGS Part 50 licensed area could not be authorized under the general license provisions of 10 CFR Part 72 and a new, site-specific license would be required. As discussed above, the process of acquiring a new site-specific license is expected to take many years and would exceed the timeline for completion of the proposed project.

SCE has stated that it will continue to monitor the availability of offsite alternatives – in particular the emerging proposals for private consolidated storage facilities -- and will evaluate the feasibility of moving the SONGS spent fuel if other options become available.

On-site Locations within SONGS Part 50 Licensed Area

SCE evaluated possible on-site storage locations and haul paths as a part of the initial project design process (SCE 2015a, b, c). Taking into account the estimated area of the ISFSI footprint (including safety and security requirements), SCE selected five locations for further evaluation: the NIA, the Reservoir, the K Buildings, the MUD Area, and the South Yard (**Exhibit 2**). SCE then ranked these alternative sites based on multiple criteria. The highest-weighted criteria were as follows:

- Suitability of site for long-term storage
- Ease/duration of licensing & permitting
- Costs and potential for DOE reimbursement
- Exposure to known or potential geologic hazards
- Avoidance of natural or man-made events that could affect safety
- Site grade & foundation properties (e.g., bearing capacity, seismic response, etc.)
- Potential for environmental resource impacts (e.g., sensitive habitats)

The NIA site proposed in this application was ranked highest among the five on-site alternatives examined in SCE's analysis. In addition to having adequate space to accommodate the proposed ISFSI, the NIA possesses several key advantages: (1) It has been previously graded and developed (with an existing ISFSI), minimizing needed site preparation, and would not result in new impacts to land resources; (2) it lies in close proximity (within approx. 1200 feet) to the existing spent fuel pools along a stable, secure and proven haul path; (3) it is underlain by relatively stable San Mateo formation sandstone; (4) it could make use of existing security arrangements; and (5) as stated above, was available for use in the near term. Of particular importance for the Commission's analysis is the fact that the NIA has superior foundation conditions; each of the other four selected sites is partially or entirely underlain by poorly consolidated marine terrace deposits, which are considered to be more susceptible to erosion, slope failure, and seismic shaking than the San Mateo Formation. The Reservoir and South Yard sites in particular are located on top of high, erosion-prone bluffs and nearer to sensitive habitats and scenic areas. Thus, the NIA was judged by the Applicant to be the superior location of the 5 alternative sites examined within the SONGS licensed area.

Nonetheless, it cannot be ignored that the proposed ISFSI location within the NIA lies just over 100 feet from the shoreline, at some of the lowest grade elevations (approx. 13 to 20 feet MLLW) present at the SONGS site. As discussed in greater detail in the Geologic Hazards findings (Subsection D), the site could potentially be exposed to several coastal hazards

depending on how long the facility were to remain in place. During its review of SCE's alternatives analysis and in view of the fact that the applicant seeks authorization for temporary, interim storage, Commission staff noted that several areas currently occupied by Units 2 and 3 and related structures may share some of the advantages of the NIA (e.g., foundational stability sufficient to support two nuclear reactors) while also being both located farther inland (300 – 900 feet) and at a higher grade elevation (>30 feet MLLW) than the proposed ISFSI location. Though currently occupied by existing structures, these areas are expected to become available over the next 15 years as the decommissioning and dismantlement of Units 2 and 3 proceeds (SCE 2014b). SCE has expressed its willingness to reevaluate alternative locations as they become available, and, if warranted, relocate the spent fuel to a new ISFSI facility at a later date.

Design & Technological Alternatives

In addition to considering alternative locations, SCE evaluated several possible ISFSI configuration alternatives within the NIA. According to SCE, the currently proposed configuration (**Exhibit 3**) was selected because it would maximize the distance between the facility and the shoreline and avoid the need to fill or modify the existing NIA drainage sump, while still providing adequate storage capacity (75 modules). Other configurations, while feasible, would lessen the distance between the facility and the shoreline and/or require more extensive site preparation and modifications to existing structures.

Similarly, SCE considered several different ISFSI storage systems and cask types. While it would be feasible to use one of the other ISFSI designs and storage casks which are currently licensed by the NRC and in use at other U.S. facilities – such as the Areva NUHOMS horizontal storage system currently employed at the existing SONGS ISFSI – SCE did not find any clear environmental or practical benefit to selecting an alternate system. SCE has indicated that, in comparison to other options, the proposed HI-STORM UMAX system offers significant advantages in terms of increased security, greater protection against coastal airborne salinity, reduced visual impacts, improved ventilation, ease of cask handling, and increased stability during a seismic event (Holtec 2014b; SCE 2015a).

Opponents of SCE's proposed ISFSI system have argued that the thin-walled stainless steel storage casks that would be used are at risk of degradation, especially stress corrosion cracking, over time, and are not suitable for long-term storage in a coastal environment. These critics additionally state that thick-walled cask varieties commonly used in Europe, such as the CASTOR series (manufactured by GNS, a German company), would be superior in terms of safety, aging management, and future transportability. However, these thick-walled casks are not generally licensed for use at U.S. sites by the NRC.²

Length of Development Authorization

Though SCE seeks temporary development authorization until 2051, there is no assurance that SCE will be able to transfer the spent fuel to DOE custody and decommission the proposed facility as planned by 2051, complicating the analysis of the project's exposure to geologic hazards and its potential to adversely affect coastal resources. The uncertain duration of the ISFSI's presence at the proposed location also has implications for SCE's alternatives analysis,

² CASTOR models V/21 and X/33 are currently being used at the Surry Power Station in Virginia under a site-specific license (SCE 2015b).

as summarized above. A number of the project alternatives were rejected by SCE not because they were necessarily inferior in terms of safety, geologic hazards or environmental effects, but because they would introduce delays (and additional costs) into SCE's plans for transferring the spent fuel from the pools to the ISFSI. However, under a scenario in which there is no near-term prospect for transporting the spent fuel off-site to a permanent federal repository, considerations related to expedience, scheduling, and cost must be weighed against other factors, including the long-term vulnerability of the site to coastal hazards.

Over the next several decades, new information is likely to emerge that will clarify the current uncertainties: progress (or a lack thereof) on the development of a permanent federal repository and/or off-site interim storage facilities will influence SCE's schedule for spent fuel transfer, and the continued need for and expected lifespan of the ISFSI; the decommissioning of SONGS Units 2 and 3 will open up new on-site locations which may prove to be less vulnerable to geologic hazards over the long-term; new scientific observations and modeling (e.g., regional sea level rise, hazards risks) will help refine projections of the ISFSI site's vulnerability to coastal hazards; and new information, based on the actual experience at multiple nuclear power plants, will be available on the suitability of thin-walled casks for storage and transport beyond the NRC's initial 20-year license. Given the (albeit uncertain) transport of the spent fuel from these interim facilities to a more permanent repository, it is appropriate for the Commission to require a re-evaluation of the project and the available alternatives at a later date, but prior to the end of the 35-year project life proposed by SCE.

The Commission staff considered two potential CDP timeframes for the re-evaluation of the proposed project, including after seven years (at the time of the expiration of CDP #E-00-014 covering the existing ISFSI), and 20 years (after the anticipated completion of Units 2 and 3 decommissioning). As discussed above, staff also considered the implications of assuming that the ISFSI would remain at the proposed location in perpetuity. After seven years, in 2022, the proposed ISFSI is expected to be fully loaded, and all fuel removed from the existing pools. However, Units 2 and 3 would not have been decommissioned or deconstructed and the potential to relocate the ISFSI to other locations within the Part 50 licensed area would not yet be available. Further, there is a reasonable likelihood that the status of both the permanent federal repository and proposed private interim storage facilities would remain unresolved.

The Commission finds that in this case, a 20-year period of development authorization, with a requirement for the Applicant to propose a CDP Amendment to retain, remove or relocate the ISFSI at least six months prior to the end of this term, is justified by a number of considerations. First, by 2035, SONGS Units 2 and 3 will have been decommissioned, and additional on-site locations for the potential relocation of the ISFSI will be available for consideration. Second, 2035 occurs after the first planned shipments of SONGS spent fuel to the DOE, and at that point it will be apparent whether SCE's assumptions about the possibility and timing of the transport to DOE and the decommissioning of the ISFSI by 2051 are justified. It will also be apparent whether the current proposals for private interim storage facilities are viable alternatives. Third, 2035 is near enough in the future that it will precede the time at which the existing site will be threatened by coastal hazards, even accounting for the uncertainties associated with these hazards. Fourth, a 20-year period of authorization aligns closely with the period for which the NRC has certified the safety and structural integrity of the proposed ISFSI system, providing

assurance that the MPCs will still be transportable, and thus the ISFSI still removable, within that timeframe. Finally, it is expected that within 20 years, SCE will have developed the aging management strategies, and the tools and techniques needed for monitoring and inspection of the storage casks, which are necessary for ensuring the long-term transportability of the casks and eventual removal of the ISFSI from the site, which are not available at present.

Therefore, the Commission adopts **Special Condition 2**, which authorizes the project for a duration of twenty years from the date of approval (i.e., until October 6, 2035). At least six months prior to that date, SCE must apply for a new or amended CDP to retain, remove or relocate the ISFSI. Such application must be supported by, among other things, a re-evaluation of the available project alternatives.

D. GEOLOGIC HAZARDS

Coastal Act Section 30253 states, in relevant part:

New development shall:

- (a) Minimize risks to life and property in areas of high geologic, flood, and fire hazard.*
- (b) Assure stability and structural integrity, and neither create nor contribute significantly to erosion, geologic instability, or destruction of the site or surrounding area or in any way require the construction of protective devices that would substantially alter natural landforms along bluffs and cliffs ...*

The proposed ISFSI site is located within the SONGS North Industrial Area (NIA, formerly the site of SONGS Unit 1) on a heavily-modified coastal bluff, as close as 115 feet to the Pacific Ocean. The site is potentially subject to several geologic and coastal hazards, including seismic activity, slope failure, coastal flooding and tsunamis, and coastal erosion, each of which is evaluated below. During the staff review of the prior ISFSI project (CDP #E-00-014), the Commission's Staff Geologist conducted an extensive evaluation of geologic hazards at the SONGS site, drawing on the information available at the time (through early 2001). This section summarizes his conclusions (contained in the staff report to CDP #E-00-014) as a starting point, but also evaluates new information, data, and analysis tools related to geologic hazards that have emerged in the last fifteen years.

As described above in subsection B, the Commission is proscribed from applying Section 30253 – or any section of the Coastal Act – to issues related to nuclear and radiological safety. Nevertheless, the proposed development must minimize hazards and assure geologic stability and structural integrity in order to conform to the California Coastal Act. The analysis and findings that follow relate to the susceptibility of the proposed development to geologic hazards pursuant to the Coastal Act, but does not attempt to address the consequences of these hazards in terms of nuclear safety. Such consequences are under the jurisdiction of the federal NRC.

Geologic Setting

The SONGS site lies in the Peninsular Ranges geomorphic province of southern California. Bedrock at the proposed ISFSI is the San Mateo Formation, a dense, well-lithified sandstone of Pliocene to Pleistocene age, which is thought to extend to a depth of approximately 900 feet below grade at the site. In the natural state, this bedrock unit is overlain by a series of marine

and non-marine terrace deposits, approximately 50 feet thick, of late Pleistocene age. During the construction of Unit 1, encompassing the current NIA, the terrace deposits and the upper 10 – 20 feet of the San Mateo Formation were removed, and the finished grade of the area is set well below the top of the coastal bluffs at an elevation of approximately 19 feet MLLW. The excavated material was placed on the beach in front of SONGS as sand nourishment, initially increasing the width of the beach, but much of the material has since been removed by longshore drift. A narrow beach still exists seaward of the NIA seawall.

Seismic Hazards

Like most of coastal California, the SONGS site lies in an area subject to earthquakes. SONGS is approximately 8 km from the Newport-Inglewood-Rose Canyon fault system, 38 km from the Elsinore Fault, 73 km from the San Jacinto Fault, and 93 km from the San Andreas Fault, all of which are considered “active” (evidence of movement in the past 11,700 years) by the California Geological Survey (Jennings and Bryant 2010). Several relatively nearby offshore faults, including the Coronado Bank Fault Zone, the San Diego Trough Fault Zone, the Thirty-Mile Bank Fault, and the Oceanside Thrust also may have been active during Quaternary time. Several smaller faults exist in closer proximity to SONGS, but are considered to be inactive. The Cristianitos fault, a low-angle normal fault, lies south and east of the site, intersecting the seac cliff approximately 1 mile south of SONGS. The Cristianitos fault separates two zones of distinct bedrock (San Mateo Formation to the north, Miocene Monterey Formation to the south), but is overlain by undisturbed terrace deposits, indicating that this fault has not been active in the last ~120,000 years (Shlemon, 1987), and probably not within the last 1.6 million years (Jennings and Bryant 2010). Four minor, inactive faults have also been mapped in the San Onofre Hills to the east of the site (USNRC 1981). In general, seismicity in the vicinity of SONGS has historically been relatively quiet compared to much of the rest of southern California, probably because of the relatively great distance from the San Andreas Fault, which accommodates most of the plate motion in the area, and the relatively low slip rates of the nearer faults (Peterson et al., 1996). A magnitude (M_L) 5.4 earthquake, associated with an unusually large swarm of aftershocks, occurred near the offshore San Diego Trough Fault Zone in 1986, but no other moderate or large ($M > 5.0$) earthquake has occurred within 50 km in historic time.³

Seismic hazards (excluding tsunami hazards) at the site include ground shaking, surface rupture, liquefaction, and slope instability. Each of these issues is addressed in these findings.

Ground Shaking⁴

Geologists’ understanding of the ground shaking risk at SONGS has evolved along with ongoing research into the tectonic setting of the Southern California borderland. Studies

³ M_L refers to locally-measured Richter scale magnitude. See **Appendix B** for a discussion of the various measures of earthquake magnitude and ground shaking used by geologists.

⁴ Seismic hazards are often discussed in terms of the strength or intensity of ground shaking rather than earthquake magnitude. Measures of ground-shaking account for the attenuation of seismic waves due to distance from a rupture and amplification or damping due to substrate types (e.g., soft sediments vs. hard rock) and thus provide a better estimate of the amount of damage that may occur at a given site. Ground shaking is often expressed as the *acceleration* experienced by an object during an earthquake. The *spectral acceleration* occurs at different oscillation frequencies, which can be plotted to form a ground shaking *response spectrum*. The *peak ground acceleration* (PGA) is a measure of is the maximum force (expressed as a % of the acceleration of gravity, g) experienced by a small mass located at the surface of the ground during an earthquake. PGA is often used in seismic design as a hazard index for short, stiff structures. **Appendix B** provides additional discussion of ground-shaking measurement.

undertaken at the time of the licensing of SONGS Units 2 and 3 identified an earthquake on the Newport-Inglewood-Rose Canyon fault system, centered on the portion of the fault nearest SONGS, to be the seismic event with the greatest potential for ground shaking at the SONGS site (NRC 1981). Based on the estimated magnitudes of the few historical earthquakes thought to have occurred on or near this fault system, and on an assessment of fault parameters (e.g., long-term rate of slip, etc.), the NRC adopted a magnitude (M_S) 7.0 event, occurring 8 km from the SONGS site, as the “design basis earthquake”. Modeling of ground shaking associated with this event yielded response spectra with a peak ground acceleration (PGA) of 0.31 g. After comparison with empirical models, and in order to build in conservatism for inaccuracies in the model, the NRC approved the calculated spectra multiplied by a factor of about 2, resulting in a design basis PGA of 0.67 g.

The approach taken by the NRC during licensing review was deterministic in nature: A design basis earthquake was established, and that earthquake was used to calculate expected ground acceleration. In 1995, SCE and a team of consultants undertook a probabilistic study of seismic hazards at SONGS (SCE Geotech Group 1995). The results represent the annual frequency of exceedance of various ground motions at SONGS, shown as a family of seismic hazard curves and ground motion response spectra. Under this analysis, the “safe shutdown earthquake” (synonymous with the design basis earthquake discussed above), with a PGA of 0.67 g, had an annual probability of occurrence of 0.00014 (0.7% in 50 years), or a recurrence interval of 7,143 years.

In addition, a number of studies have provided evidence that, in addition to the strike-slip faulting recognized at the time of the SONGS licensing review, thrust faults exist in the area offshore of the SONGS site which might interact with the Newport-Inglewood-Rose Canyon fault system in a complex way during an earthquake (e.g., Rivero et al. 2000; Kuhn et al. 2000; Shlemon 2000; Rivero and Shaw 2011). Notably, the 1986 Oceanside earthquake (M_L) 5.4 was centered on one of these low-angle faults, and showed a thrust fault mechanism. Rivero et al. (2000) and Rivero and Shaw (2011) have hypothesized that blind thrust faults related to the Newport-Inglewood-Rose Canyon fault system may be capable of an earthquake ranging in magnitude from M_W 7.1 to 7.6, larger than that of the design basis earthquake considered during SONGS licensing. However, other studies dispute the existence of blind thrust faults offshore of Orange and San Diego counties, and suggest that the observational data (seismic reflection profiling, earthquake clustering patterns, etc.) used by Rivero et al. to infer thrust faulting can be interpreted within a framework of step-overs and trend changes along known north-to-northwest oriented strike-slip fault systems (Ryan et al. 2012). New and reprocessed on- and offshore seismic reflection profiling data collected by SCE and Scripps Institute of Oceanography have been interpreted as supporting the step-over and trend change model (Malloney et al., *in press*), suggesting that the previously posited blind thrust faults do not exist. SCE has also sponsored a recent study of marine terrace uplift in coastal San Diego and southern Orange counties over the late Quaternary, which appears to have found no evidence of the deformation and differential uplift which could be expected to result from any recent activity on blind thrust faults in the vicinity of SONGS (SCE 2013).

In 2010, as an update to the older studies, SCE commissioned a new study (*Probabilistic Seismic Hazard Analysis Report*, GeoPentech, 2010) to assess the seismic hazard presented by both the previously-recognized strike-slip faulting and postulated offshore blind thrust faults (e.g.,

Oceanside and Thirty-Mile Bank thrust faults) near SONGS. Probabilistic peak ground accelerations and spectral accelerations for the SONGS site are shown below:

| | 10% in 50 yr (475-yr return period) (GeoPentech 2010) | 2% in 50 yr (2475-yr return period) (GeoPentech 2010) |
|-------------------|--|--|
| PGA | 0.227 g | 0.477 g |
| 0.2 sec SA | 0.530 g | 1.111 g |
| 1.0 sec SA | 0.261 g | 0.501 g |

The GeoPentech analysis suggests that the inclusion of an offshore blind thrust fault earthquake source does not greatly increase the ground shaking hazard at the SONGS site, and that the PGA of 0.67 g assigned to the design basis earthquake at the time of Units 2 and 3 licensing remains conservative.

Independent evaluations of earthquake ground shaking hazards in the vicinity of SONGS are provided by the California Geological Survey (CGS) and U.S. Geological Survey (USGS). The CGS Earthquake Shaking Potential Map for California (Branum et al., 2008) portrays the San Onofre area as a region of relatively low ground shaking potential, with the Big Sur coast being the only other part of coastal California having a comparably low shaking potential according to this assessment. Comparable, quantitative assessments are provided by the USGS Seismic-Hazard Map for the Coterminous United States, 2014 (Peterson et al. 2015) and online analysis tools developed by both CGS and USGS. Probabilistic peak ground accelerations and spectral accelerations for the San Onofre area, assuming firm bedrock conditions, are shown below:

| | 10% in 50 yr (475-yr return period) (USGS) ⁵ | 10% in 50 yr (475-yr return period) (CGS) ⁶ | 2% in 50 yr (2475-yr return period) (USGS) ³ | 2% in 50 yr (2475-yr return period) (CGS) ⁴ |
|-------------------|--|---|--|---|
| PGA | 0.20 – 0.25 g | 0.245 g | 0.40 – 0.50 g | 0.505 g |
| 0.2 sec SA | 0.50 – 0.60 g | 0.564 g | 1.0 – 1.2 g | 1.113 g |
| 1.0 sec SA | 0.15 – 0.20 g | 0.200 g | 0.30 – 0.40 g | 0.377 g |

These estimates of ground shaking potential at the SONGS site are quite similar to those from SCE's probabilistic study (GeoPentech 2010).

It is important to note that these assessments of ground shaking risk were based on the current understanding of the likelihood of earthquakes of varying intensities on nearby faults at the time they were released, and that as geologists' understanding of the network of faults underlying coastal California continues to evolve, estimates of ground-shaking risk at a specific site, such as SONGS, may change. A recent example of this iterative process is provided by the USGS *Uniform California Earthquake Rupture Forecast*, Version 3 (UCERF3) report (Field et al. 2014), which provided new estimates of the magnitude, location, and time-averaged frequency of potentially damaging earthquakes in California based on research since the previous report (UCERF2) in 2007. On a statewide basis, the estimated likelihood of a M 8.0 or greater earthquake in the next 30 years has increased from about 4.7% in UCERF2 to about 7.0% in UCERF3, in part due to

⁵ U. S. Geological Survey, Seismic Hazards Science Center, Custom Hazard Maps tool, <http://geohazards.usgs.gov/hazards/apps/cmmaps/>, and Peterson et al. (2015).

⁶ California Geological Survey, Probabilistic Seismic Hazards Ground Motion Interpolator (2008), http://www.quake.ca.gov/gmaps/PSHA/psa_interpolator.html.

new research highlighting the potential for multi-fault ruptures during a single event. The implications of the revised earthquake forecast for ground shaking hazards at SONGS are not clear, though it is notable that the 30-year likelihood of a large ($>M$ 6.7) earthquake on the offshore Newport-Inglewood-Rose Canyon fault system has been revised downward slightly since the 2007 forecast.

ISFSI Seismic Design

The proposed ISFSI has been designed to withstand ground shaking of much greater magnitude than contemplated in either the Units 2 and 3 licensing review or the more recent probabilistic analyses summarized above. The “Most Severe Earthquake” (MSE) variant of the spent fuel storage system,⁷ for which the NRC approved an amendment to HI-STORM UMAX Certificate of Compliance (CoC) on September 8, 2015, has been designed to withstand a net horizontal zero-period acceleration (ZPA) of 2.12 g and vertical ZPA of 1.0 g (for a very high-rigidity structure, such as the proposed ISFSI, $ZPA \approx PGA$). **Exhibit 6** shows the horizontal (X+Y) and vertical seismic spectra for which the proposed project is designed, together with spectra corresponding to the seismic design for SONGS as a whole, derived from the design basis earthquake described above (Holtec 2015). The spectra labeled “SONGS” are derived from the NRC-approved “free-field” spectra and take into account the interaction of the proposed structure with ground motions, which tends to amplify shaking. The design spectra for the ISFSI were generated following NRC Regulatory Guide 1.60, “Design response spectra for seismic design of nuclear power plants.” Comparison of the ISFSI design spectra with the calculated spectra corresponding to the SONGS design basis earthquake shows a large factor of safety. The ISFSI design spectra exceed those of the design basis earthquake at all frequencies. It is accordingly reasonable to conclude that even an earthquake larger and/or closer to the site than the SONGS design basis earthquake, will not produce ground shaking exceeding the design of the proposed project.

Accordingly, the Commission finds that the proposed project, as conditioned, assures stability and structural integrity relating to seismic hazards, consistent with section 30253 of the Coastal Act.

Surface Rupture

No active faults were found at the SONGS site during geologic studies related to licensing and construction of Units 2 and 3 (Fugro 1977; Shlemon 1977, 1979). Though several sets of shears in the San Mateo Formation were uncovered during the excavation for Units 2 and 3, they did not offset the overlying terrace deposits, indicating that they had not been active for at least 120,000 years and do not represent recent faulting at the site. Hence, the risk of surface rupture at the SONGS site is very low.

The largest fault near the SONGS site is the Cristianitos fault, a low-angle normal fault passing less than one mile south of the site. Based on several observations, several studies have proposed recent right-lateral strike-slip movement on the onshore Cristianitos normal fault, as well as a re-

⁷ The MSE version of the HI-STORM UMAX incorporates three physical design changes to augment the structural integrity of the system: (a) Addition of a hold-down system to the closure lid to prevent its uplift during the seismic event; (b) Use of plain concrete (min. compressive strength 3000 psi) in the interstitial space between storage modules instead of soil fill; (c) Strengthening of the MPC guides to increase their load bearing capacity. (NRC 2015)

activated extension of this fault offshore of northern San Diego County (Fisher and Mills 1991). However, others have shown that the Cristianitos fault near San Onofre beach is overlain by undisturbed terrace deposits, indicating that there has been no movement on it for at least 120,000 years (e.g., Shlemon 1987). The Cristianitos fault is not considered an active fault by the California Geological Survey (Jennings and Bryant 2010).

Accordingly, the Commission finds that the proposed project, as conditioned, assures stability and structural integrity with respect to surface rupture, consistent with Section 30253 of the Coastal Act.

Liquefaction

Like all existing SONGS structures, the proposed ISFSI would be underlain by the dense, well-consolidated sands of the San Mateo Formation, which are considered to be at low risk of seismically-induced liquefaction. The overlying terrace deposits were removed during the construction of Units 1, 2 and 3. Although the water table is shallow at the site (approximately +5 feet MLLW) (SCE 2015b), cyclic triaxial tests, field density tests, and very high blow counts during standard penetrometer tests show that liquefaction should not occur during a design basis earthquake (PGA of 0.67 g) (SCE 1998; GEI 2015). Minimum factors-of-safety against liquefaction in the plant area have been calculated at 1.5 to 2.0 (SCE 1998). An independent assessment of liquefaction hazards in the area has identified the SONGS site as an area at low risk of liquefaction (CGS 2002).

A number of studies in northern San Diego County have identified stratigraphic features, including sand dikes, lenses, fissures and disturbed bedding, which have been interpreted as the results of liquefaction occurring in recent geologic history (e.g., Kuhn et al. 1996; Kuhn et al. 2000; Shlemon 2000; Kuhn 2005). For example, Kuhn (2005) noted that a number of these paleo-liquefaction features disturbed late Holocene Native American middens and burial sites within the past 1,000 to 3,000 years, and suggested that they “were likely caused by M ~ 7+ tectonic events inferentially generated by the nearby offshore Newport-Inglewood-Rose Canyon fault system.”

Although these features are suggestive, the Commission does not consider them indicative of a serious liquefaction hazard at the proposed project site. Liquefaction in sandstones as dense as those encountered at the SONGS site have not previously been documented in even very large earthquakes; it is far more common for unconsolidated sands or artificial fills to fail by liquefaction. While it is possible that an earthquake much larger than the design basis earthquake might be capable of causing liquefaction of the San Mateo formation sands, no estimates have been provided by any of the cited studies as to the required ground shaking needed to induce such cyclic stresses. In light of the high factor of safety evident in the site-specific studies, and without credible data to the contrary, the Commission finds that the applicant has adequately addressed the liquefaction hazard at the site.

Accordingly, the Commission finds that the proposed project, as conditioned, assures stability and structural integrity with respect to liquefaction, consistent with Section 30253 of the Coastal Act.

Slope Stability

The proposed ISFSI site is located approximately 55 feet southeast of a cut slope rising to 77 feet above the NIA grade, and approximately 300 feet southwest of a somewhat lower cut slope (**Exhibits 3, 9**). Both slopes are largely covered in gunnite. During studies for the SONGS Unit 1 ISFSI facility (CDP #E-00-001), SCE analyzed the stability of these slopes along four cross-sections during seismic shaking corresponding to the design basis earthquake (ground-shaking intensity of 0.67 g, described above), concluding that only minor sloughing of near slope surface material would occur and that minimum factors of safety ranged from 1.7 to greater than 3 (SCE 1995). An additional evaluation concluded that, if a massive failure on the nearer northwest slope were to occur, the maximum distance the soil would be likely to travel would be 120 feet from the toe of the bluff (Hadidi 2000). More recent re-analyses of slope stability and slope toe run-out at the site yielded factors of safety of about 1.5 and projected slope toe run-out distances between 91 feet and 107 feet (Pham 2007; Hinkle 2011; Ninyo and Moore 2015).

The design of the ISFSI is such that the storage modules will be built partially below grade and encased in a concrete and fill berm, with only the tops of the modules (the steel and concrete closure lids) exposed at the top of the ISFSI Pad, at an elevation of approximately 32 feet MLLW (about 12.5 feet above the NIA grade (**Exhibit 3**). Although portions of the ISFSI would be within the potential run-out zone during a large slope failure, but due to the design of the facility, would not be vulnerable to damage. The portion of the ISFSI nearest the northwest slope, the “the “Approach Slab”, though only 54 feet from the bluff toe, is a flat expanse of concrete at the top of the ISFSI berm that could be covered by soil during a slope failure without affecting the structural integrity of the facility. The closure lids of the nearest row of storage modules would be 98 feet from the bluff toe (**Exhibit 3**), and thus within the larger of the projected run-out zones (107 ft; Ninyo and Moore 2015). However, the Ninyo and Moore (2015) analysis did not account for the relief of the ISFSI berm, which rises to a height of approximately 12.5 above the NIA grade, with a 45 degree slope at its margins. A more recent analysis provided by SCE, which accounts for the presence of the ISFSI berm, indicates that the maximum soil run-out could advance up the ISFSI berm to point approximately 70 feet from the bluff toe, well short of the nearest storage modules (Pham 2015).

In summary, the relatively high factors of safety calculated for the cut slopes adjacent to the project site suggest that the slopes are likely to remain stable during a large earthquake. Moreover, in the event that a major slope failure does occur, soil run-out would not reach the fuel storage modules or otherwise compromise the stability and structural integrity of the proposed ISFSI.

Previous studies have identified several coalescing large active landslides affecting the coastal bluffs south of SONGS (e.g., Kuhn 2000, Kuhn and McArthur 2000). These slides are seated within the Monterey Formation, which is known to contain weak layers making it vulnerable to landsliding. In contrast, the project site, and the SONGS as a whole, is underlain by well-consolidated San Mateo Formation sandstone to a depth of at least 900 feet, and there is very little risk that a landslide similar to those occurring to the south could involve the SONGS site itself. Information provided by SCE to the Commission during the review of the previous ISFSI project (CDP #E-00-014) demonstrated that the SONGS site has experienced very little

settlement or differential vertical movement since it was constructed, ruling out the existence of a slow-moving, deep-seated landslide beneath the site.

Based on this information, the Commission finds that the proposed project, as conditioned, assures stability and structural integrity with respect to the stability of the slopes adjacent to and underlying the proposed project, consistent with Section 30253 of the Coastal Act.

Bearing Capacity

The proposed ISFSI facility is a massive structure (approximately 584,000 cubic feet in volume), consisting of a concrete foundation pad, a concrete and fill subgrade, a concrete surface pad, and 75 steel and concrete fuel storage modules, each receiving a stainless steel MPC (containing the spent fuel assemblies) and weighing approximately 190,000 pounds. When fully loaded, the UMAX system would weigh approximately 87 million pounds. For perspective, this figure can be compared with the weight of the terrace deposits and upper portions of the San Mateo Formation formerly overlying the site. Since these deposits were approximately 70 feet thick, with a unit weight of approximately 102 – 117 pounds per cubic foot, the deposits formerly overlying the 25,000 square foot area of the UMAX system would have weighed approximately 179 to 205 million pounds. Thus, even after the construction of the project, the weight applied to the San Mateo Formation would be less than 50% of the weight of the overlying rock prior to the development of SONGS.

More relevant to the question of the ability of the site materials to support the ISFSI is a calculation of the bearing capacity of the San Mateo Formation relative to general or local shear failure. SCE has provided a technical analysis showing the static ultimate bearing capacity for the proposed ISFSI (SCE 2015g). When calculating the allowable static bearing capacity, a standard safety-factor equal to 3 is built into the capacity value for a static loading combination.

The calculated allowable static bearing capacity for substrates underlying the ISFSI (San Mateo Formation plus overlying sand/gravel fill layer) is approximately 43,500 pounds per square foot. When considering the calculated weight of the ISFSI and the effective area, the foundation will only be loaded to approximately 3,900 pounds per square foot (additional factor of safety > 11). SCE also provided a dynamic analysis of the proposed ISFSI demonstrating the capacity of the pad design under seismic loading. This analysis uses 1.5 g horizontal and 1.0 g vertical ground acceleration in order to demonstrate the adequacy of the foundation and to show that the concrete pads will not fail during an earthquake with the specified ground accelerations. When calculating the allowable seismic loading combination bearing capacity, a standard safety-factor equal to 2 is built into the capacity value for a seismic loading combination. The calculated seismic allowable bearing capacity is shown to be approximately 65,150 pounds per square foot while the seismic bearing pressure as a result of the ISFSI is shown to be 12,800 pounds per square foot (additional factor of safety > 5). In both the static and dynamic cases, a sufficient factor of safety exists to conclude that the ISFSI will not exceed the bearing capacity of the site, and that the concrete pad will not fail during an earthquake with the specified ground accelerations.

Accordingly, the Commission finds that the proposed project, as conditioned, assures stability and structural integrity, with respect to materials at the site have sufficient bearing capacity, consistent with section 30253 of the Coastal Act.

Coastal Hazards

Tsunamis

Several previous studies have estimated the potential run-up and inundation that would occur on the SONGS site during a tsunami event. The Safety Evaluation Report prepared by the NRC at the time of licensing hearing of Units 2 and 3 examined both local- and distant-sourced tsunamis (NRC 1981). SCE's model of the local-source tsunami (resulting from a 7.5 earthquake occurring along the Newport-Inglewood-Rose Canyon fault system, 8 km offshore, with vertical ground motion of 7.1 feet) projected a wave height of 7.6 feet. Superimposing this tsunami on a 7-foot high tide (the 10% exceedance Spring high tide for the site) and a one-foot storm surge, resulted in a maximum "still" water level of 15.6 feet MLLW (SONGS 2&3 FSAR). In its review, the NRC generally agreed with this model, arriving at a maximum still water level of 15.83 feet MLLW. In these calculations, the presence of the seawall was ignored. In its application to the Commission for the 2001 ISFSI (CDP #E-00-014), SCE provided additional modeling addressing the wave runup that could be expected if tsunami struck the site in conjunction with both high tide and storm surge (SCE Geotech Group 1995). Under these conditions, and discounting the presence of the Unit 1 seawall, it was projected that maximum wave runup would reach an elevation of 18.8 feet MLLW. Notably, these analyses considered only tsunamis generated by earthquakes, but did not address the potential for tsunamis generated by submarine landslides, which are known to have occurred along the Southern California coast in the past (Legg and Kamerling 2003).

More recently, a new site-specific analysis was conducted as part of SCE's 2013 *Calculations for a Probable Maximum Tsunami* report (Kirby 2013), which considered both local- and distant-sourced events as well as local tsunamis generated by submarine landslides. Models of far field tsunami sources associated with large subduction-zone earthquakes (M 9.0 – 9.5) from around the Pacific Rim (e.g., Aleutians, Kuril Islands, Japan Islands, Chile) yielded tsunami wave run-up elevations ranging from 8.5 to 22 feet MLLW, with the largest tsunamis produced by earthquakes in the eastern Aleutian Islands.⁸ Models of locally-sourced tsunamis, including those resulting from a M 7.5 earthquake along a theorized offshore blind thrust fault and from submarine landslides offshore of San Diego County, yielded maximum run-up elevations ranging from 10 to 21.5 feet MLLW. A recent, independent evaluation of potential tsunami inundation at the SONGS site is provided by the *Tsunami Inundation Map for Emergency Planning* (San Onofre Bluff quadrangle), prepared by the State of California in 2009. The purpose of this series of maps was to identify a "credible upper bound" of potential inundation at any location along the coast, based on a combination of potential tsunami source events, including both local and fair field sources. At SONGS, the map shows the entire NIA area to be within the potential tsunami inundation zone and suggests a credible upper bound to potential inundation of 20 to 23 feet MLLW.

Given that the grade elevation within the NIA is approximately 19-20 feet above MLLW, it is possible that the base of the ISFSI structure could be inundated or subject to wave runup during a

⁸ For comparison, actual tsunami run-up heights observed along the Southern California coast following large historical earthquakes on the Pacific Rim, including the M9.5 1960 Chilean earthquake, M9.2 1964 Alaskan earthquake, and M8.8 2010 Chilean earthquake, ranged from 4.9 to 12.5 feet above MLLW. (California Geologic Survey, *Historic Tsunamis in California*, http://www.conservation.ca.gov/cgs/geologic_hazards/Tsunami/Pages/About_Tsunamis.aspx#historic)

large tsunami event at some point during the life of the project. In the near term, the top of the ISFSI pad, at +32 feet MLLW, would likely remain above the inundation elevation under the scenarios discussed above. However, the entire structure could be subject to wave run-up in the most extreme scenario, if a large tsunami were to coincide with both high tide and major winter storm and high wave conditions (see below). Rising sea level will further exacerbate this situation (e.g., see **Exhibit 7**).

Information provided by SCE indicates that temporary inundation has been factored into the design of the ISFSI and its components, including the MPCs, such that overtopping of the facility by a large tsunami would not adversely affect its stability and structural integrity. Specifically, the storage module components, including the Cavity Enclosure Containers (CEC), Closure Lids, and MPCs, have been designed to withstand water submergence to a depth of 125 feet and missile impacts exceeding those that could be expected from tsunami-carried debris (Holtec 2014a, b). Additionally, the weld-sealed MPCs have been designed to prevent water intrusion in the event that flood water entered the ventilation space between the MPC and CEC.

In summary, the Commission concludes that although the project could be subject to tsunami flooding within the next 35 years, particularly if projected levels of sea level rise occur, the proposed ISFSI has been designed to resist temporary inundation, wave run-up and water contact. Therefore, the proposed development, as conditioned, will minimize flooding hazards consistent with Section 30235 of the Coastal Act.

Coastal Flooding & Sea Level Rise

With a grade elevation of approximately 19-20 feet MLLW, and a top elevation of 32 feet MLLW, the proposed ISFSI would not, at present, be vulnerable to inundation under normal high tide (MHHW \approx +5.8 feet MLLW) and/or storm conditions. As a part of its CDP application, SCE prepared an analysis of future flood conditions over the proposed life of the development (SCE 2015a, d, h), using the sea level rise projections (National Research Council 2012) recommended in the Commission's 2015 Sea-level Rise Policy Guidance (CCC 2015). The analysis examined changes in water level and wave run-up conditions resulting from several sea level rise scenarios at different points in the future. SCE used an additive approach to examining changes in runup, assuming that the future high still water level would be the current mean high tide plus some amount of sea level rise, and that the future runup would be the current runup plus future sea level rise plus some forcing and surge. The analysis indicates that sea level can be expected to rise 0.4 to 2.0 feet by 2051, depending on which scenario is used. Under the high sea level rise scenario, and assuming an additional foot of sea level height associated with wind and storm surge and/or oceanographic forcing (such as due to an El Niño event), SCE estimated that the still-water level in 2051 at mean high tide could reach 7.8 feet MLLW. A more extreme high tide of +6.9 feet MLLW, combined with 1 foot of storm surge, 2 feet of sea level rise and maximum wave run-up, could result in temporary flooding up to 25.0 feet MLLW (SCE 2015h).⁹ Commission staff notes that a maximum high tide at SONGS (>7.2 feet MLLW), 1 foot of storm surge *and* temporary high sea level associated with a large El Niño event (+0.4 to 1 ft) (Flick 1998; CCC 2015) could add an additional 0.5 to 1.5 feet to this projected flooding.

⁹ However, run up does not change linearly with changes in water level, so these estimates of how run-up will change with changes in water levels likely underestimate potential run-up.

In summary, it appears possible that, in the absence of expanded or enlarged shoreline protection, the ISFSI site could be subject to occasional coastal flooding. However, as discussed above in relation to tsunami hazards, the proposed ISFSI has been designed to resist temporary inundation, wave run-up and water contact. Therefore, the proposed development, as conditioned, will minimize flooding hazards consistent with Section 30235 of the Coastal Act.

Coastal Erosion & Bluff Retreat

In their natural state, coastal bluffs at the SONGS are composed of highly-erodible terrace deposits underlain by the more resistant San Mateo Formation sandstone. During the construction of Unit 1 in the 1960s, the bluff was essentially removed. Over 70 vertical feet of terrace deposits and upper layers of the San Mateo Formation were removed, and the plant foundations were set in San Mateo Formation bedrock. The result of the excavation is that the new “bluff face” and upper edge is situated landward of the NIA. At this time SCE also installed a shoreline protection system, consisting of a rock revetment and a concrete encased, steel sheet-pile seawall rising to an elevation of approximately 28 feet MLLW, in front of Unit 1 at the time of construction. As a result, there has been little or no measurable shoreline retreat at the project site over the past 50 years.

The natural rate of bluff retreat in the San Onofre area is somewhat difficult to assess, due both to its episodic nature and to the varying mechanisms of retreat along the coast. Active bluff retreat is occurring south of the project site at San Onofre State Beach, where the bluffs consist of Monterey Formation bedrock overlain by terrace deposits and where runoff has been artificially concentrated in drainage channels associated with Interstate 5. Substantial subaerial erosion of the terrace deposits and Monterey formation has occurred in this area, taking the form of headward erosion of gullies, slumping of the bluff faces, and deep-seated landslides. However, as discussed above, these landslides are seated in the Monterey Formation (known to be susceptible to sliding) south of the Cristianitos Fault, and have not occurred in the dense San Mateo Formation sandstones underlying the SONGS site. The mechanisms of seacliff retreat in the San Mateo Formation at the SONGS site are less clear, but the shape of the seacliff suggests dominantly marine processes, such as undercutting, block collapse, and slumping of poorly consolidated upper bluff terrace materials. Distinct gullying of the terrace deposits is also evident in the unaltered seacliffs to the north and south of the SONGS seawall (**Exhibit 2**).

Studies undertaken by the U.S. Army Corps of Engineers in the 1950s concluded that no measureable retreat of the bluff line occurred near the SONGS site between 1889 and 1954 (USACE 1960). More recently, the U.S. Geological Survey has evaluated coastal bluffs to the north and south of SONGS, and estimated that long-term bluff retreat rates range from 6 - 20 inches per year at the base of unprotected slopes within the San Mateo Formation (Hapke and Reed 2007; Hapke et al. 2007). Due to the presence of shoreline protection at the project site, no site-specific estimates of bluff retreat rates are available, but it is likely that the USGS upper estimate of 20 inches per year provides a conservative basis for evaluating the project’s vulnerability to undercutting by coastal erosion in the absence of shoreline protection.

At its nearest, the proposed ISFSI pad would be located approximately 100 feet from the seawall adjoining the NIA (**Exhibit 3**), which, based on shoreline cross-sections provided by SCE, is

assumed to correspond to the toe of the remnant bluff underlying the project site. The nearest UMAX storage module would be approximately 125 feet from the seawall. Discounting the presence of the existing shoreline armoring, a maximum average bluff retreat rate of 20 inches per year over the proposed 35-year life of the project would equate to a total bluff retreat of 58 feet, or about half of the distance between the existing seawall and the proposed ISFSI facility. Even recognizing that shoreline erosion processes are highly episodic, and that the actual magnitude of bluff retreat from year to year can deviate greatly from the long-term average, the proposed setback of approximately 100 feet would appear to be adequate to assure stability of the project site through the proposed project duration, without requiring new or expanded shoreline protection.

NIA Seawall Adjoining Proposed Development

Past bluff erosion at the project site has been greatly retarded over natural rates by the existing shoreline armoring in front of the NIA, consisting of a steel sheet pile and gunnite seawall, a concrete public access walkway and retaining wall, and a rock revetment (**Exhibit 8**).

The NIA seawall was built in 1966 to protect SONGS Unit 1 from tsunami hazards. The wall extends approximately 650 feet on the seaward side of the NIA between the northwestern bluff and the junction with the Units 2 and 3 seawall. The seawall is composed of $\frac{3}{8}$ -inch thick steel sheet piling covered on both faces by a $2\frac{1}{2}$ -inch layer of gunnite secured by wire mesh. The sheet piling is embedded to a depth of approximately 22 feet below the NIA grade (to an elevation of approx. -10 feet MLLW), and extends to a height of approximately 28 feet MLLW. The toe of the seawall was initially protected by a 12-foot wide rock revetment (1-4 ton rocks), but in 1982 a 15-foot wide public access walkway and reinforced concrete retaining wall were built over the original revetment, and a new, 20-foot wide revetment was placed at the base of the retaining wall to protect the walkway and seawall from undercutting.

Information provided by SCE indicates that the embedded portion of the seawall suffers from areas of localized corrosion, including several through-going holes, and that the structure has outlived its project design life (SCE 2015b). In 1986, when the corrosion was first discovered, SCE installed a corrosion monitoring system to ensure that the seawall sheet piling was structurally adequate, but this monitoring was discontinued in 2007 with the final decommissioning of Unit 1. SCE has acknowledged that as of 1996, the seawall is “no longer credited in the design for tsunami protection of the site” (SCE 2015b). In contrast, SCE has indicated that the condition of the rock revetment has not changed since its emplacement, and argues that the seawall is protected from scour by the revetment (extending down to +3 feet MLLW) and retaining wall (extending to +7 feet MLLW).

The uncertain level of degradation to the seawall sheet piling, together with its relatively shallow depth of emplacement, lack of foundation elements, and the lack of an engineered key to the rock revetment, suggests that maintenance and repairs may be necessary for the continued function of the shoreline protection structures, and that they cannot be counted upon to prevent erosion and flooding at the site in future decades.

Reasonably Foreseeable Long-term Hazards

As discussed previously, there remains a significant degree of doubt as to when, or if, a permanent, off-site repository for the SONGS spent nuclear fuel will become available. It is

similarly uncertain whether an off-site interim storage facility will be developed which could eventually accept SONGS spent fuel after the proposed project term of 2051. The proposed life of the ISFSI project is based on the assumption that the DOE will begin accepting spent fuel, on a nation-wide basis, beginning in 2024, with the first transport of SONGS 2 and 3 fuel beginning in 2030 (SCE 2014a, 2014b). If the DOE is unable to fulfill this commitment, or if the shipment of spent fuel to an off-site location is otherwise delayed, storage in the proposed ISFSI could be required beyond 2049, and the ISFSI would not be decommissioned and removed by 2051, as proposed. In the worst case, no federal repository or other storage alternative would be developed, and the proposed ISFSI would remain on the SONGS site in perpetuity.

In this scenario, or any other in which the ISFSI remained in its proposed location for many decades, there would come a time when the facility would be exposed to geologic hazards, and when the proposed project configuration and design could no longer assure stability and structural integrity without requiring shoreline protection, and would thus no longer fulfill the requirements of Coastal Act Section 30253.

For purposes of illustration, it is useful to consider potential future coastal hazards in relation to the project after 100 years, in the early 22nd century. SCE's flood risk analysis suggests that after 100 years, in the year 2117, sea level could have risen between 1.8 and 7 feet; at future mean higher high tide, the still water elevation could be up to 12.8 feet above modern MLLW, approaching the lowest elevations within the NIA (about 13 ft MLLW in the drainage sump area and near the seawall). Factoring in additional water height attributable to storm surge, oceanographic forcing, and wave run-up could result in flooding to elevations above 30 feet MLLW. The combined results of high tide, storm surge, and a large tsunami would be expected to flood the entire NIA area, as illustrated in **Exhibit 7**.¹⁰ If, as expected, sea level continues to rise in response to global warming, higher water levels would expose the project site to ever more frequent flooding, and eventually permanent inundation.¹¹ Even if the proposed ISFSI could be shown to be designed to withstand frequent flooding, inundation and exposure to ocean waves, a location within the surf zone would place major practical constraints on SCE's ability to load and unload fuel-filled MPCs, monitor and maintain the ISFSI components, and eventually decommission and remove the facility without adverse impacts to marine resources.

Similarly, in the absence of shoreline protection, the natural processes of coastal erosion and bluff retreat would eventually undermine the proposed project site and compromise the stability and structural integrity of the ISFSI. A crude calculation using a maximum estimated bluff retreat rate of 20 inches per year (Hapke et al. 2007, for unprotected slopes in San Mateo Formation bedrock) indicates that erosion could begin to undermine the ISFSI structure by approximately 2077. However, several factors, including the fact that the upper layers of the

¹⁰ **Exhibit 7** illustrates a scenario of complete flooding within the NIA in the year 2100, based on the water level contributions sea level rise (National Research Council 2012 high scenario), mean higher high tide conditions, 1 foot of storm surge and/or oceanographic forcing, and an additional tsunami wave run-up of 22 feet. A maximum flood scenario would factor in storm waves in addition to the tsunami and a larger term for surge and oceanographic forcing.

¹¹ For example, one recent modeling study projected between 7 – 17 feet of sea level rise (base year 2000) by the year 2300 under a moderate greenhouse gas emissions scenario (Schaeffer et al. 2012); another, examining a high emissions (“business-as-usual”) scenario, projected between 7.4 and 38 feet of sea level rise by the year 2500 (Jevrejeva et al. 2012). The broad ranges in these projections reflect the high degree of uncertainty inherent to long-term modeling, but nonetheless demonstrate the potential for extreme sea level rise within the next several centuries.

subsurface within the NIA consist of fill, which may be more easily eroded than native bedrock, that the rate of erosion would be expected to increase with rising sea level, and the inherently unpredictable and episodic nature of bluff retreat, could put the ISFSI at risk much sooner.

The Commission cannot conclude that the proposed ISFSI location would assure stability and structural integrity and minimize risks to life and property from coastal hazards, and shoreline erosion in particular, without requiring new or expanded shoreline protection. Thus, in order to find the project consistent with the policies of Coastal Act Section 30253(a) and (b), it must be able to assure the following:

- (1) Shoreline protection devices would not be extended, nor new devices constructed;
- (2) The ISFSI would no longer be present when the project site became threatened by long-term coastal hazards.

Given that there is presently no certainty that the spent fuel to be stored in the ISFSI will have been removed to a federal repository (or other off-site facility) by 2051 or any other specific future date, assurance of (2) above would need to be supported by three additional assurances:

- (a) The fuel could be transferred to a new, on-site ISFSI at lower risk from long-term geologic hazards than the proposed NIA facility; or
- (b) Based on the best evidence available at the time, the proposed ISFSI location within the NIA would not be threatened by geologic hazards within the timeframe of a revised/updated schedule for off-site transfer of the fuel; and
- (c) The MPCs stored within the ISFSI fuel modules would remain in a physical condition adequate to allow safe off-site transport (i.e., to a DOE facility) or on-site relocation (i.e., to a new ISFSI), and thus allow the proposed ISFSI to be removed.

No New or Extended Shoreline Protection

The existing shoreline protection system (rock revetment, sheet-pile seawall) seaward of the NIA was installed in 1966 to protect Unit 1, and was later expanded (to include the public access walkway and retaining wall) and effectively joined with the newer structures protecting Units 2 and 3. During this time, the SONGS shoreline protective devices have adversely affected shoreline sand supply and contributed to the erosion of the beach by (a) directly encroaching on beach area; and (b) retarding the natural retreat of the bluff, which both prevents new beach area from being created and eliminates the delivery of sand to the beach and local littoral cell through bluff erosion.

In the absence of a permanent federal repository for spent nuclear fuel, or the development of some other federal, state or private off-site interim storage facility, the SONGS spent fuel could remain in the proposed ISFSI for many years beyond the intended date of removal. The long-term potential therefore exists that the proposed ISFSI site could be undermined by shoreline retreat and/or subjected to flooding as a result of sea level rise, storm waves or a tsunami event and the proposed new development could potentially require an expanded or replaced shoreline protective device.

Coastal Act section 30253 prohibits the approval of new development if hazards would affect the proposed development and necessitate construction of a new, expanded or replaced shoreline

protective device to protect it. Because this policy requires that new development avoid the need for a new, expanded or replaced shoreline protective device, the Commission finds that the proposed development is consistent with the Coastal Act only if it is conditioned to provide that such shoreline protection will not be constructed. Therefore, in order to find the proposed development consistent with Section 30253 of the Coastal Act, the Commission imposes **Special Condition 3**. This condition requires that SCE agree to not extend, enlarge or replace the existing shoreline protective devices, or to construct new shoreline protection, for purposes of protecting the proposed ISFSI facility and ancillary structures (e.g., security building, fencing, etc.) from future coastal hazards.

Future On-site Alternatives and Managed Retreat

As discussed in a previous section, the decommissioning of SONGS Units 2 and 3 is planned to occur over the next 15 – 20 years, and would result in the removal of most major structures currently occupying the site. Thus, beginning in the early 2030s, there will be a number of additional locations within the area covered by the SONGS Part 50 site license where an ISFSI could conceivably be built, which were not available at the time SCE initially conducted its alternatives analysis. A number of these locations are at higher elevations (+30 – 80 feet MLLW) and greater distances from the shoreline (up to 900 feet) than the proposed ISFSI site in the NIA, and may prove to be safe from coastal hazards over a longer period of time. If the proposed ISFSI must remain on-site beyond 2051 for a long or indefinite period of time, it may prove necessary to relocate the ISFSI to another site better able to minimize hazards and assure the stability of the facility over the long-term.

In order to guard against the possibility that the proposed ISFSI would remain in place beyond 2051 and become exposed to geologic hazards in the future, the Commission adopts **Special Condition 2**, which authorizes the proposed development for a period of twenty years from the date of approval (i.e., until October 6, 2035). Special Condition 2 also requires that, at least six months prior to the end of this term, SCE apply for a CDP Amendment to retain, remove or relocate the proposed ISFSI facility. The CDP Amendment application shall be supported by (a) an evaluation of current and future coastal hazards based on the best available information; (b) an alternatives analysis examining the merits and feasibility of both off-site and on-site alternatives, including potential locations within areas made available by the decommissioning of SONGS Units 2 and 3; and (c) a plan for managed retreat, if retention of the ISFSI facility beyond 2051 is contemplated and coastal hazards may affect the site within the timeframe of the amended project.

Cask Transportability and Removal of the ISFSI

Ultimately, SCE's ability to avoid long term coastal hazards and the need for shoreline protection, and thus assure consistency with Coastal Act Section 30253, depends on its ability to eventually remove the ISFSI from the proposed site. In turn, the removal of the ISFSI depends on the fuel storage casks (MPCs) remaining in a condition adequate to allow safe removal from the storage modules and transfer to a new location. This is true regardless of the timing and circumstances of the ISFSI removal, whether in 2051, with the fuel being transferred to a permanent repository, in 2035, in conjunction with relocation to a new on-site ISFSI, or at some future date as a part of a plan of managed retreat to avoid coastal hazards.

The storage cask that would be used in the proposed ISFSI, the Holtec model MPC-37, is constructed from corrosion-resistant stainless steel, with a design life of 60 years (Holtec 2014a, b). With implementation of a monitoring and maintenance program, as well as an Aging Management Plan to be developed as a condition of license renewal for the HI-STORM UMAX system beyond the initial 20-yr term, SCE expects the service life of the ISFSI and casks to be at least 100 years (SCE 2015b). SCE does not anticipate that major repairs to the ISFSI or components would be needed within either the 60-year design life or 100-year service life of the system, but has stated that corrective actions and contingency plans will be developed in the future as a part of the Aging Management Plan (*see* Subsection A, above).

While the designs of the ISFSI and fuel storage casks appear to be robust, there are several uncertainties. The first is that the stainless steel MPCs will be in continual contact with moist, salt-laden marine air, and as a result could, over time, experience a type of degradation known as stress corrosion cracking. The initiation and growth of stress corrosion cracking in stainless steel fuel storage casks are not fully understood and remain a topic of active research, but these processes are likely to be accelerated in a coastal environment such as at SONGS (e.g., Kain 1990; Bryan and Enos 2014; EPRI 2014). Commission staff is not aware of any documented instances of stress corrosion cracking in fuel storage casks at other nuclear power plants. However, the NRC has collected evidence of stress corrosion cracking in other welded stainless steel components at several coastal nuclear power plants (Dunn 2014). The components in question had been in service for 16 to 33 years (average 25 years), and estimated crack growth rates ranged from 0.11 to 0.91 mm/yr. Elsewhere, the NRC has estimated that at least 30 years would be required for the initiation of stress corrosion cracking in steel fuel storage casks (NRC 2014).

Additional long-term uncertainties remain due to lack of completion of SCE's proposed MPC monitoring and maintenance program. Based on information provided to staff, SCE would implement the following measures: (a) the monitoring of environmental conditions, such as temperature and humidity, that could influence the risk of corrosion and degradation of the stainless steel MPCs; (b) visual observation, surface measurements, and other inspection techniques to provide information on the physical condition of the MPCs; and (c) use of an empty cask ("coupon") as a surrogate for filled casks to allow for more thorough inspection and evaluation (SCE 2015f). However, SCE has also indicated that the "non-destructive examination techniques" and "remote surface inspection tools" that would be used to inspect the storage casks have not yet been developed or tested for effectiveness, and it is unclear when they would be available for use at SONGS. It must also be noted that the only existing requirements for the development of a monitoring and inspection program are associated with the Aging Management Plan required for *renewal* of the 20-year NRC license for the ISFSI system. Though SCE has indicated that it would seek to begin the monitoring and inspection of the ISFSI components well before the end of the initial license, it is possible that no detailed inspection of the casks would occur within the first 20 years of their emplacement.

As a part of its licensing processes, the NRC has reviewed the design of the HI-STORM UMAX (version MSE) system and the supporting documentation and analyses supplied by Holtec, the manufacturer (e.g., Holtec FSAR, CoC amendment application). In the Preliminary Safety

Evaluation Report (SER) supporting the September 8, 2015, final approval of an amendment to the UMAX system's Certificate of Compliance, the NRC determined the following:

F3.3 The applicant has met the specific requirements of 10 CFR 72.236(g) and (h) as they apply to the structural design for spent fuel storage cask approval. The cask system structural design acceptably provides for

- *Storage of the spent fuel for **a certified term of 20 years.***

F3.4 The applicant has met the requirements of 10 CFR 72.236 with regard to the inclusion of the following provisions in the structural design:

- *Adequate structural protection against environmental conditions and natural phenomena.*

...

- *Structural design that is compatible with retrievability of spent nuclear fuel (SNF).*

*The staff concludes that the structural properties of the structures, systems and components of the CoC No. 1040, Amendment No. 1 are in compliance with 10 CFR Part 72, and that the applicable design and acceptance criteria have been satisfied. **The evaluation of the structural properties provides reasonable assurance that the HI-STORM UMAX Canister Storage System Amendment No. 1 will allow safe storage of SNF for a licensed (certified) life of 20 years.** This finding is reached on the basis of a review that considered the regulation itself, appropriate regulatory guides, applicable codes and standards, and accepted engineering practices. [Emphasis added]*

As described previously, the Commission is preempted from imposing regulatory requirements concerning radiation hazards and safety. However, in order to find the project consistent with the geologic hazards policies of the Coastal Act and in recognition that the project itself proposes interim temporary storage for eventual transport to a federal or other off-site repository, the Commission must have reasonable assurance that the SONGS spent fuel will continue to be transportable, and the ISFSI itself removable, as long as the facility occupies its proposed location. The 20-year NRC licensing and certification of the structural adequacy of the proposed ISFSI system provides such assurance within this limited timeframe, and is roughly consistent with the limited available evidence on when stress corrosion cracking may begin to affect certain stainless steel components in marine environments. Thus, in order to minimize the possibility that the proposed ISFSI would become unremovable, and thus subject to long-term geologic hazards necessitating the use of shoreline protection devices, the Commission adopts **Special Condition 2**, which authorizes the proposed development for a period of twenty years from the date of approval (i.e., until October 6, 2035), and requires that SCE apply for a CDP Amendment to retain, remove or relocate the ISFSI facility prior to the end of this term. Among other things, Special Condition 2 requires that the CDP Amendment application be supported by evidence that the fuel storage casks will remain in a physical condition sufficient to allow off-site transport, and a description of a maintenance and inspection program designed to ensure that the casks remain transportable for the full life of the amended project. The Commission also adopts **Special Condition 7**, which requires that, as soon as technologically feasible and no later than October 6, 2022, SCE provide, for Commission review and approval, a maintenance and inspection program designed to ensure that the ISFSI system and fuel storage casks will remain

in a physical condition sufficient to allow both on-site transfer and off-site transport, for the term of the project authorized under **Special Condition 2**. The program shall include descriptions of the cask inspection, monitoring and maintenance techniques that will be implemented (including prospective non-destructive examination and remote surface inspection tools), a data collection and reporting regime, all available evidence related to the physical condition of the casks and their susceptibility to degradation processes such as stress corrosion cracking, and remediation measures that would be implemented if the results of the cask inspection and maintenance do not ensure that the fuel storage casks will remain in a physical condition sufficient to allow on-site transfer and off-site transport for the term of the project as authorized under **Special Condition 2**. If the Commission determines that the maintenance and inspection program is not sufficient to assure cask transportability over the term of the project authorized under **Special Condition 2**, the Applicant shall submit an amendment to the coastal development permit proposing measures to assure cask transportability.

Assumption of Risk & Restriction on Development

Although the proposed project has been evaluated, designed and conditioned in a manner to minimize the risk of geologic hazards, the underlying uncertainties of any geotechnical evaluation and the fact that the risks associated with inherently hazardous oceanfront property can never be completely eliminated support a finding that no guarantees can be made regarding the safety of the proposed development with respect to coastal hazards. Geologic hazards are episodic, and areas that may seem stable now may not be so in the future. Accordingly, the Commission is adopting **Special Condition 4**, which requires the Permittee to assume the risks of extraordinary erosion and geologic hazards of the property and waive any claim of liability on the part of the Commission. Given that the applicants have chosen to implement the project despite these risks, the applicants must assume the risks. In this way, the applicants are notified that the Commission is not liable for damage as a result of approving the permit for development. The condition also requires the applicants to indemnify the Commission in the event that third parties bring an action against the Commission as a result of the failure of the development to withstand hazards.

The Commission further finds that Section 30610(b) of the Coastal Act exempts certain additions to existing structures from coastal development permit requirements. Depending on its nature, extent, and location, such an addition or accessory structure at this location could contribute to geologic hazards at the site. Accordingly, Section 30610(b) requires the Commission to specify by regulation those classes of development which involve a risk of adverse environmental effects and require that a permit be obtained for such improvements. Pursuant to Section 30610(b) of the Coastal Act, the Commission adopted Section 13253 of Title 14 of the California Code of Regulations (CCR). Section 13253(b)(6) specifically authorizes the Commission to require a permit for additions to existing structures that could involve a risk of adverse environmental effect by indicating in the development permit issued for the original structure that any future improvements would require a development permit. Since certain additions or improvements to the approved structure could involve a risk of creating geologic hazards at the site, pursuant to Section 13253 (b)(6) of Title 14 of the CCR, the Commission attaches **Special Condition 5**, which requires that all future development on the subject parcel that might otherwise be exempt from coastal permit requirements requires an amendment or coastal development permit. This

condition will allow future development to be reviewed by the Commission to ensure that future improvements will not be sited or designed in a manner that would result in a geologic hazard.

Conclusion

Based on the proposed project design and construction, and with the special conditions described above, the Commission finds that the proposed project, as conditioned, is consistent with Coastal Act Section 30253(a) and (b).

E. MARINE RESOURCES & WATER QUALITY

Section 30230 of the Coastal Act states:

Marine resources shall be maintained, enhanced, and where feasible, restored. Special protection shall be given to areas and species of special biological or economic significance. Uses of the marine environment shall be carried out in a manner that will sustain the biological productivity of coastal waters and that will maintain healthy populations of all species of marine organisms adequate for long-term commercial, recreational, scientific, and educational purposes.

Section 30231 of the Coastal Act states:

The biological productivity and the quality of coastal waters, streams, wetlands, estuaries, and lakes appropriate to maintain optimum populations of marine organisms and for the protection of human health shall be maintained and, where feasible, restored through, among other means, minimizing adverse effects of waste water discharges and entrainment, controlling runoff, preventing depletion of ground water supplies and substantial interference with surface water flow, encouraging waste water reclamation, maintaining natural vegetation buffer areas that protect riparian habitats, and minimizing alteration of natural streams.

Section 30232 of the Coastal Act states:

Protection against the spillage of crude oil, gas, petroleum products or hazardous substances shall be provided in relation to any development or transportation of such materials. Effective containment and cleanup facilities and procedures shall be provided for accidental spills that do occur.

The ISFSI would be built approximately 100 feet from the shoreline and would involve construction, excavation and grading activities within the NIA, a previously graded, paved and developed area of the SONGS site. The SONGS site is currently subject to NPDES permits issued by the San Diego Regional Water Quality Control Board (RWQCB); the NIA area is governed by the Unit 2 NPDES permit. The permit includes conditions related to allowable volumes and types of non-radiological discharges from the various facilities on the site and other measures meant to prevent adverse impacts to coastal waters. To the extent that it could lead to new discharges, construction of the ISFSI would be subject to additional review and possible permitting by the RWQCB for conformity to requirements for construction stormwater discharges.

Construction-related Discharges

Normal operation of the proposed ISFSI would not result in the discharge of pollutants to coastal waters or otherwise affect marine resources. However, grading and ground disturbance during construction could mobilize sediments which, if washed into the ocean, could adversely affect coastal water quality and marine organisms. Similarly, accidental leaks or spills from construction vehicles and heavy equipment could introduce pollutants into coastal waters.

The proposed construction and grading activities during the installation of the ISFSI would comply with existing water quality, storm water management, and spill prevention plans and their associated best management practices (BMPs). Because these activities – excavation, pouring of concrete, earth movement, use of heavy equipment, etc. – are similar to activities already occurring at SONGS, the existing plans and BMPs provide appropriate controls to avoid and minimize potential water quality impacts. The facility's Storm Water Management Plan (SWMP) includes procedures regard dust control, sediment management and debris cleanup that apply to the types of equipment to be used and activities to be conducted during construction, and use of these procedures will minimize storm water runoff and prevent soil and sediment from entering the ocean. The approximately 14,800 cubic yards of soil that would be excavated from within the NIA would be repurposed as fill material within the ISFSI berm.

The risk of spills of oil or fuel from construction equipment would be minimized by implementation of the existing SONGS Spill Prevention, Control and Countermeasures (SPCC) Plan, which describes the procedures and equipment availability needed to prevent and control spills of hazardous materials on site. SCE will stage all project-related construction machinery and heavy equipment in paved, developed areas inside the SONGS perimeter where the necessary spill prevention controls are already in place, and will refuel vehicles within already authorized areas.

Potential for Reasonably Foreseeable Impacts

As discussed in greater detail in previous sections, there remain a number of significant uncertainties related to SCE's ability to decommission and remove the ISFSI facility by 2051, as proposed. In the absence of a permanent federal repository for spent nuclear fuel, or the development of some other federal, state or private off-site interim storage facility, the SONGS spent fuel could remain in the proposed ISFSI for many years beyond the intended date of removal. There is therefore the potential that the proposed ISFSI site will be undermined by shoreline retreat and/or subjected to flooding as a result of sea level rise, storm waves or a tsunami event. Despite the facility's robust design, these geologic forces would eventually result in a loss of stability and structural integrity, and cause the discharge of debris into the coastal ocean to the detriment of water quality and marine organisms.

In order to avoid this outcome, the Commission imposes **Special Condition 2**, which authorizes the approved project for twenty years from the date of approval (i.e., until October 6, 2035), and requires SCE, before this date, to submit an application for a CDP amendment to retain, remove or relocate the ISFSI. This application shall be supported by (a) an evaluation of current and future coastal hazards based on the best available information; (b) an analysis examining the merits and feasibility of off-site and on-site alternatives, including potential locations within areas made available by the decommissioning of SONGS Units 2 and 3; (c) a plan for managed retreat, if retention of the ISFSI facility beyond 2051 is contemplated and coastal hazards may

affect the site within the timeframe of the amended project; and (d) evidence that the fuel storage casks will remain in a physical condition sufficient to allow off-site transport, and a description of a maintenance and inspection program designed to ensure that the casks remain transportable for the full life of the amended project. In addition, the Commission imposes **Special Condition 7**, which requires that as soon as technologically feasible, and no later than October 6, 2022, SCE provide, for Commission review and approval, a maintenance and inspection program designed to ensure that the fuel storage casks will remain in a physical condition sufficient to allow both on-site transfer and off-site transport, for the term of the project as authorized under **Special Condition 2**. If the Commission determines that the maintenance and inspection program is not sufficient to assure cask transportability over the term of the project authorized under **Special Condition 2**, the Applicant shall submit an amendment to this coastal development permit proposing measures to assure cask transportability.

These requirements will afford the Commission the opportunity to re-evaluate the likelihood of SCE's proposed timeline for the removal of the ISFSI before the site becomes vulnerable to coastal hazards and when potential alternative locations on and off-site may be available (including by the decommissioning of SONGS Units 2 and 3), and if necessary impose conditions necessary to mitigate and avoid adverse impacts to marine resources.

Conclusion

With the special conditions described above, the Commission finds that the proposed project is consistent with Coastal Act Sections 30230, 30231, and 30232.

F. COASTAL ACCESS AND RECREATION

Section 30210 of the Coastal Act states:

In carrying out the requirement of Section 4 of Article X of the California Constitution, maximum access, which shall be conspicuously posted, and recreational opportunities shall be provided for all the people consistent with public safety needs and the need to protect public rights, rights of private property owners, and natural resource areas from overuse.

Section 30211 of the Coastal Act states:

Development shall not interfere with the public's right of access to the sea where acquired through use or legislative authorization, including, but not limited to, the use of dry sand and rocky coastal beaches to the first line of terrestrial vegetation.

Section 30220 of the Coastal Act states:

Coastal areas suited for water-oriented recreational activities that cannot readily be provided at inland water areas shall be protected for such uses.

Section 30212(a) of the Coastal Act states:

Public access from the nearest public roadway to the shoreline and along the coast shall be provided in new development projects except where: (1) It is inconsistent with public safety, military security needs, or the protection of fragile coastal resources, (2) Adequate access exists nearby, or, (3) Agriculture would be adversely affected. Dedicated accessways shall not be required to be opened to public use until a public agency or private association agrees to accept responsibility for maintenance and liability of the accessway.

Coastal Act policies generally require that developments such as the proposed ISFSI, located adjacent to the shoreline in an area with ongoing public use, not interfere with that use and provide access to the shoreline. The proposed ISFSI would be located within the existing SONGS restricted area, to which public access is prohibited under NRC security requirements. Thus, the project would not directly interfere with existing public access. Adequate public access and recreational opportunities are already available in close proximity to the SONGS site, including at public beaches to the north, south and directly in front of the plant, and along the existing pedestrian pathway below the SONGS seawall. However, the project could potentially result in a number of indirect adverse effects on coastal access and recreation through construction-related traffic and noise, and through impacts to shoreline sand supply should the retention and/or extension of the existing shoreline protective devices become necessary to protect the project from future coastal hazards.

Construction Traffic and Noise

During project construction, trucks and workers travelling to and from the project site could increase traffic congestion along Old Pacific Coast Highway, a coastal access route inland of the plant. However, the expected traffic volumes are small, would be concentrated during off-peak hours, and would be limited to the approximately one-year period of construction. Construction would not occur during weekends and holidays, with the possible exception of operations such as excavation, pouring concrete or other activities that require continuous work. As a result, increased traffic associated with project construction would not significantly interfere with access to the coast along public roads.

Construction activities also will generate noise, which if loud enough could discourage public shoreline access and recreational activities and adversely affect other sensitive receptors (i.e., sensitive wildlife species). The closest sensitive receptors to the project site would be recreational users and wildlife on the shoreline (including the pedestrian walkway) immediately seaward of the NIA and the Unit 1 seawall, approximately 100 – 150 feet from the project site. Noise impact analyses conducted by SCE indicate that in the worst case, with multiple construction vehicles and heavy equipment operating simultaneously, the maximum noise level at 50 feet would reach 90 dBA (L_{max}) (SCE 2015a). At the pedestrian walkway, factoring in the shielding provided by the seawall, the maximum noise levels are estimated to be 60 – 65 dBA, which would not be significantly greater than ambient noise levels at this location. Other sensitive receptors (more distant recreational and habitat areas) would not be significantly affected by construction-related noise.

Public Beach Access and Recreation

The existing shoreline protection system (rock revetment, access walkway and retaining wall, and sheet-pile seawall) at SONGS extends approximately 2000 feet between the bluffs northwest of the NIA to beyond the Units 2 and 3 K Buildings (**Exhibits 2, 8**). The segment of this structure seaward of the NIA was installed in 1966 to protect SONGS Unit 1, and was later effectively joined with the structures protecting Units 2 and 3. Landward of the mean high tide line, public access to the SONGS site is prohibited in conformance with NRC requirements, except for passage between sections of San Onofre State Beach north and south of SONGS along the designated public access walkway (*see Exhibit 8*).

The NIA shoreline protective devices have adversely affected the beach area and shoreline sand supply by (a) directly encroaching on beach area; and (b) retarding the natural retreat of the bluff, which both prevents new beach area from being created and eliminates the delivery of sand to the beach and local littoral cell through bluff erosion.¹² The direct and indirect loss of public beach below the mean high tide line as a result of these processes necessarily reduces public access and recreational opportunities. This loss of coastal access may occur on the beach area in front of the shoreline protective device or at beaches on either side, depending on local patterns of littoral sand transport. San Onofre lies near the boundary between two local littoral cells (Patsch and Griggs 2006), suggesting that under different conditions, sand may be transported either the north or the south of the SONGS site.

As discussed previously, there are a number of significant uncertainties related to SCE's ability to decommission and remove the ISFSI facility by 2051, as planned. In the absence of a permanent federal repository for spent nuclear fuel, or the development of some other federal, state or private off-site interim storage facility, the SONGS spent fuel could remain in the proposed ISFSI for many years beyond the intended date of removal. Under this scenario, the ISFSI will eventually become threatened by coastal hazards, such as erosion or coastal flooding. As stated above, Section 30253 of the Coastal Act prohibits the approval of new development if hazards would affect the proposed development and necessitate construction of a new or expanded shoreline protective device to protect it. Further, any enlargement or replacement of the existing NIA seawall undertaken in order to protect the proposed ISFSI from coastal hazards has the potential to prolong or increase the adverse effects of the NIA seawall on shoreline sand supply and beach access and recreation in the vicinity of San Onofre.

In order to avoid this outcome, the Commission attaches **Special Condition 2**, which authorizes the approved project for twenty years from the date of approval (i.e., until October 6, 2035), and requires SCE, before this date, to submit an application for CDP amendment to retain, remove or relocate the ISFSI, supported by (a) an evaluation of current and future coastal hazards based on the best available information; (b) an analysis examining the merits and feasibility of off-site and on-site alternatives, including potential locations within areas made available by the decommissioning of SONGS Units 2 and 3; (c) a plan for managed retreat, if retention of the ISFSI facility beyond 2051 is contemplated and coastal hazards may affect the site within the timeframe of the amended project; and (d) evidence that the fuel storage casks will remain in a physical condition sufficient to allow off-site transport, and a description of a maintenance and

¹² This latter effect is likely to have been ameliorated by the placement on the beach of several hundred-thousand cubic yards of sand-sized material excavated from the bluff during plant construction.

inspection program designed to ensure that the casks remain transportable for the full life of the amended project. Additionally, **Special Condition 7** requires that as soon as technologically feasible, and no later than October 6, 2022, SCE provide, for Commission review and approval, an inspection and maintenance program designed to ensure that the ISFSI system and fuel storage casks will remain in a physical condition sufficient to allow both on-site transfer and off-site transport, for the term of the project as authorized under **Special Condition 2**. If the Commission determines that the maintenance and inspection program is not sufficient to assure cask transportability over the term of the project authorized under **Special Condition 2**, the Applicant shall submit an amendment to this coastal development permit proposing measures to assure cask transportability. The Commission also adopts **Special Condition 3**, which requires that SCE agree to not extend, enlarge or replace the existing shoreline protective devices, or to construct new shoreline protection, for purposes of protecting the proposed ISFSI facility and ancillary structures (e.g., security building, fencing, etc.) from future coastal hazards.

With the implementation of the special conditions described above, the Commission finds that the proposed project is consistent with the public access and recreation policies of the Coastal Act.

G. VISUAL RESOURCES

Section 30251 of the Coastal Act states:

The scenic and visual qualities of coastal areas shall be considered and protected as a resource of public importance. Permitted development shall be sited and designed to protect views to and along the ocean and scenic coastal areas, to minimize the alteration of natural land forms, to be visually compatible with the character of surrounding areas, and, where feasible, to restore and enhance visual quality in visually degraded areas. New development in highly scenic areas such as those designated in the prepared by the Department of Parks and Recreation and by local government shall be subordinate to the character of its setting.

The SONGS site is situated adjacent to the Pacific Ocean and in close proximity to several scenic areas, including San Onofre State Beach and Camp Pendleton, which were identified in the *California Coastline Preservation and Recreation Plan* (Baker1971). Existing structures at SONGS are partially visible from public roads (Interstate 5, Old Pacific Coast Highway) inland of the site, and from nearby beach and shoreline vantage points. However, the proposed location of the new ISFSI, within the NIA, is one of the least visible portions of the site. Due to the relatively low grade elevation of the NIA (+19 feet MLLW) and the partially below-ground configuration of the proposed ISFSI, the top of the ISFSI pad would rise to only +32 feet MLLW, and thus would be situated below the lines of sight of drivers on the public roads inland of the site. Views of the NIA from shoreline vantage points to the north (such as San Onofre State Beach) are blocked by the 96-foot high bluff immediately northwest of the NIA, while SONGS Units 2 and 3 structures obscure views of the site from the beaches and bluffs to the south. The existing NIA seawall, which rises 14 feet above the public access walkway seaward of SONGS, would block views of the ISFSI site from the walkway and the beach. To the extent that the proposed ISFSI would be visible from public vantage points, it would be visually

compatible with the heavily developed, industrial character of the SONGS site. Existing and simulated post-project views of the site are provided in **Exhibit 9**.

Although a substantial amount of excavation (approx. 14,800 cubic yards) will be necessary in order to install the concrete foundation pad and the other subgrade portions of the ISFSI, the coastal bluff remnant on which the NIA is situated was heavily graded (more than 70 vertical feet of bluff material removed) during the construction of SONGS Unit 1, and the present project would not result in significant further alteration of natural landforms.

However, during the process of plant decommissioning it is anticipated that most, if not all, of the structures comprising SONGS will be dismantled and removed, leaving the ISFSI as one of the few remaining major structures on site (SCE 2014a). If the planned work proceeds according to SCE's plans, decommissioning and site restoration will be substantially complete by 2032. On a restored site, the proposed ISFSI will be much more obtrusive and visually incompatible. In the best case, if SCE's assumptions about the removal of the spent fuel to an off-site repository prove true, the adverse visual effects of the ISFSI would persist through 2051. In the event that no permanent repository becomes available, or if the off-site transport of fuel is otherwise delayed, the adverse visual effects of the ISFSI could persist for much longer. In order to minimize impacts to scenic resources, assure that the proposed development would be visually compatible with the character of the surrounding area and allow for the restoration and enhancement of visual quality in a visually degraded area to the maximum extent feasible, the Commission adopts **Special Condition 2**, which will authorize the project for a duration of twenty years from the date of approval (i.e., until October 6, 2035). At least six months prior to that date, SCE is required to submit an application for a new or amended CDP supported by an evaluation of the effects on visual resources of retaining the project, an analysis of available project alternatives and their implications for coastal visual resources, and proposed mitigation measures to minimize adverse impacts to coastal views.

As conditioned, the Commission finds that the proposed project is consistent with Section 30251 of the Coastal Act.

H. ATTORNEYS' FEES AND COSTS

Coastal Act section 30620(c)(1) authorizes the Commission to require applicants to reimburse the Commission for expenses incurred in processing CDP applications. *See also* 14 C.C.R. § 13055(e). Thus, the Commission is authorized to require reimbursement for expenses incurred in defending its action on the pending CDP application. Therefore, consistent with Section 30620(c), the Commission imposes **Special Condition 6**, requiring reimbursement of any costs and attorneys' fees the Commission incurs "in connection with the defense of any action brought by a party other than the Applicant/Permittee ... challenging the approval or issuance of this permit."

I. RESPONSE TO PUBLIC COMMENTS ON STAFF RECOMMENDATION

Public comments received on the staff recommendation and included in the October 5, 2015 staff report addendum provided disparate perspectives on the proposed project and staff recommendation. A number of commenters expressed support for the staff recommendation. Southern California Edison (SCE), the applicant, offered several comments and multiple

clarifications and technical corrections, but also supported the staff recommendation. Numerous other commenters opposed the project and urged the Commission to deny SCE's coastal development permit (CDP) application. The U. S. Marine Corps did not comment on the project itself, but argued that the Commission lacks jurisdiction to require or issue a CDP for development at the San Onofre Nuclear Generating Station (SONGS) site. The Commission provides the following summary and responses to the arguments made by commenters opposing the staff recommendation:

Comments Related to Geologic Hazards

Several commenters, including Ray Lutz, Dorah Shuey, Patricia Borchmann, and Jane Swanson, expressed concern that the proposed ISFSI could be undermined by shoreline erosion, fail during an earthquake, or be flooded during a tsunami or as a result of future sea level rise. Mr. Lutz and Ms. Swanson also noted that the groundwater table at the project site would be near the bottom of the ISFSI structure, and expressed concern that the ISFSI could be adversely affected by contact with groundwater during its period of emplacement.

As discussed at length in the September 25, 2015 staff report, Commission staff evaluated the vulnerability of the proposed project to geologic hazards, including earthquakes, erosion, and coastal flooding, and concluded that the proposed project, with the adoption of **Special Condition 2**, would minimize hazards to life and property and assure stability and structural integrity consistent with Section 30253 of the Coastal Act. No changes to the staff recommendation were made in response to comments regarding these hazards.

Commission staff also evaluated the hydrogeology of the project site and reviewed monitoring well data provided by SCE (SCE 2015b). At the two monitoring wells within the proposed ISFSI footprint, the water table elevation varies by approximately 0.7 feet above and below a mean elevation of about +5.4 feet MLLW, indicating that, at present, natural variability in the water table is not likely to bring groundwater into contact with the base of the concrete ISFSI foundation pad (at +7.5 feet MLLW). Increases in the water table elevation related to sea level rise could potentially lead to intermittent groundwater contact with the base of the ISFSI toward the end of the proposed 35-year life of the project. However, the design of the ISFSI is such that there are multiple barriers, including the 3-foot thick foundation pad and the steel cavity enclosure container (CEC), between the groundwater and the fuel storage casks, and limited contact with groundwater would not undermine the structural integrity of the ISFSI during the proposed project life. Furthermore, as a part of **Special Condition 2**, SCE would be required to evaluate current and future coastal hazards, including the effects of groundwater intrusion, as part of its CDP amendment application should it wish to retain the ISFSI in its proposed location beyond 2035.

Comments Related to Site Alternatives

Comments submitted by Michael Aguirre, Ray Lutz and several others argued that SCE has not adequately explored alternative project locations off of the SONGS site. Mr. Lutz's comments included an extensive discussion of the benefits of siting the project away from the coast, and present a conceptual analysis of a hypothetical ISFSI site in the Mojave Desert. In their comments, Ms. Gilmore and Ms. Lynch stated that the potential future alternative (discussed in

the staff report) of relocating the ISFSI within the SONGS site would require a major expense and would greatly increase the current estimate of decommissioning costs.

As discussed previously, Commission staff has reviewed SCE's analysis of off-site alternatives and the Commission agrees with the conclusion that such alternatives are either unavailable or infeasible. No off-site federal permanent repository or private interim storage facility currently exists, and there is no prospect of such a facility becoming available in the near term. Nor is there another inland nuclear power plant with an existing ISFSI that is willing to or licensed to accept spent fuel from another site. Finally, there is no other site under SCE's control that is licensed for the siting of an ISFSI or at which an ISFSI could be developed in a reasonable period of time.

The staff recommendation was based on findings that the proposed project, as conditioned, would be consistent with Coastal Act policies related to geological hazards, the protection of marine and visual resources, and public access and recreation, excluding matters of radiological safety, and does not evaluate the potential cost of any future relocation of the ISFSI within the SONGS site. **Special Condition 2** requires that SCE evaluate the merits and feasibility (including costs) of such alternatives as part of a CDP amendment application to retain, remove or relocate the ISFSI prior to the end of a 20-year term of approval.

Comments Related to ISFSI and Cask Safety & Radiological Issues

Comments submitted by Donna Gilmore, Laura Lynch, Gary Headrick, Donald Mosier, Dorah Shuey, Patricia Borchmann, Jane Swanson, Michael Aguirre, Rita Conn, Marv Lewis, Rick Morgal and many others offered numerous arguments for why the proposed Holtec HI-STORM UMAX ISFSI and storage casks are inadequate or inappropriate for storing spent fuel at the proposed site. The main contentions of these comments are summarized below:

- (a) *The proposed underground system is unproven and experimental.*
- (b) *The 60-year design life and 100-year service life for the UMAX system claimed by SCE and Holtec are unsubstantiated; the Holtec warranty for the system is only ten years.*
- (c) *The proposed fuel storage casks are unsafe; stress corrosion cracking can be expected to occur in the stainless steel casks within 20 years.*
- (d) *Storage casks used in the existing ISFSI have been loaded since 2003, so SCE will need to have an aging management plan much sooner than 20 years from now.*
- (e) *The UMAX system configuration planned for SONGS has not been approved by the NRC; the NRC has only licensed a fully underground system using 1/2-inch thick fuel storage casks, not the partially-underground system and 5/8-inch casks proposed by SCE.*
- (f) *The proposed aging management program is inadequate, and the proposed casks cannot be repaired if damaged.*
- (g) *The NRC does not consider or require aging management in their initial 20-year license approvals.*
- (h) *High burn-up fuel to be stored in the proposed ISFSI could require up to 45 years of cooling prior to transport to permanent storage.*
- (i) *The Commission should not rely on vendor promises of future solutions for inspecting the casks in order to approve this project; there is already sufficient evidence that the*

proposed casks may not be transportable and maintainable to reject their use; the Commission should demand SCE use a proven system that can be inspected, maintained, monitored and transported, and that doesn't crack.

- (j) Thick-walled casks are available, and currently used in the U.S., that would provide superior performance in terms of safety and future transportability; the need to acquire a site-specific license to use such casks at SONGS is not sufficient grounds for rejection; the Commission should require SCE to use thick-walled casks as a special condition for approval.*
- (k) Numerous past discharges of radioactive materials have occurred at SONGS; locating the ISFSI at the proposed site would make the area unsafe for public access.*
- (l) SCE is considering loading Areva storage casks from the existing ISFSI into the new UMAX system.*

Without assessing the validity of these concerns, the Commission notes that the consequences of any failure, malfunction, or defects in the proposed ISFSI system are primarily a matter of radiological safety, which is under the exclusive jurisdiction of the federal Nuclear Regulatory Commission (NRC). The state is preempted from imposing upon operators of nuclear facilities any regulatory requirements concerning radiation hazards and nuclear safety. Thus, the findings contained in the staff recommendation addressed only those state concerns related to conformity to applicable policies of the Coastal Act, and do not evaluate or condition the proposed project with respect to nuclear safety or radiological issues.

Staff's analysis indicates that the avoidance of long-term coastal erosion and flooding hazards at the project site (without resorting to shoreline armoring) is dependent on the ability to remove the ISFSI before it becomes vulnerable. At present, the integrity of the proposed ISFSI system is certified by the NRC for 20 years, providing assurance that the casks will be transportable, and the ISFSI system removable, within this timeframe. Commission staff believes that the 20-year duration of approval recommended in **Special Condition 2** is necessary to assure that potential future geologic hazards (and the need for shoreline protection) are avoided, is consistent with the 20-year certification of the HI-STORM UMAX system granted by the NRC, and does not impose any additional regulatory requirements concerning radiation hazards and nuclear safety.

SCE has informed Commission staff that SONGS fuel transported within a HI-STAR 190 transportation cask will require less than 15 years of cooling time starting from reactor shutdown in 2012, with even the most recently offloaded spent fuel ready for transport by 2027 (SCE 10/5/2015). Furthermore, fuel transport schedules contained in SCE's Irradiated Fuel Management Plan and Decommissioning Cost Estimate, both formal regulatory documents submitted to the NRC, indicate that all SONGS spent fuel can be transported offsite by 2049, 37 years after the 2012 reactor shutdown.

Commission staff is not aware of any plan to transfer older fuel storage casks from the existing ISFSI to the new system. This activity was not proposed in SCE's CDP application and would not be authorized by the proposed CDP.

U. S. Marine Corps Comments

On October 1, 2015, Commission staff received a letter from the United States Navy and Marine Corps asserting that the Commission lacks jurisdiction to require or issue a CDP for development occurring on the SONGS site. The basis for the Navy and Marine Corps position is that under the Federal Coastal Zone Management Act (CZMA), land, “the use of which is by law subject solely to the discretion of ... the Federal Government, its officers or agents” is excluded from the definition of the coastal zone. (16 U.S.C. § 1453(1)).

The U.S. Supreme Court, however, has addressed this issue and determined that the CZMA does not pre-empt application of the California Coastal Act to private activities on federal land. It held that “[b]ecause Congress specifically disclaimed any intention to pre-empt pre-existing state authority in the CZMA, we conclude that even if all federal lands are excluded from the CZMA definition of ‘coastal zone,’ the CZMA does not automatically pre-empt all state regulation of activities on federal lands.” *California Coastal Commission v. Granite Rock Co.* (1987) 480 U.S. 572, 593. Thus, under *Granite Rock*, the Commission retains the authority under the Coastal Act to require coastal development permits for non-federal activities taking place on federal land, such as Southern California Edison’s proposed project pending before the Commission.

The U.S. Navy and Marine Corps support their argument that the Commission does not have coastal development permit jurisdiction on federal land by reference to an unpublished U.S. District Court decision, *Manchester Pacific Gateway v. California Coastal Commission* (2008 WL 5642245 (S.D. Cal.)). First, to the extent that the *Manchester* case is inconsistent with the Supreme Court holding in *Granite Rock*, the Supreme Court’s decision in *Granite Rock* controls. Second, the *Manchester* case is factually distinguishable from the situation presented by the pending proposal from SCE. The *Manchester* case involved a Congressionally authorized public-private venture that resulted in the Navy obtaining new office space at no cost to the federal government. *Id.* at 1. The court acknowledged that the purpose of that project, as mandated by Congress, was to “provide for the use of private parties to accomplish the federal objective to construct Navy administrative facilities.” *Id.* at 5. The project was authorized through legislation that spelled out the general parameters of the project and specifically authorized the project to be jointly developed by the Navy and the private developer. *Id.* at 6. Thus, the project was both a Navy and a private project.

The pending application from SCE does not involve a joint public-private venture. Thus, the facts are not analogous to those presented in the *Manchester* case. Thus, both under *Granite Rock* and due to factual distinctions between these facts and those raised in the *Manchester* case, the CZMA does not pre-empt the California Coastal Act here, and the Commission does have the jurisdiction to require a coastal development permit for the proposed development.

Finally, the Commission notes that the October 1, 2015 letter includes a statement, without elaboration, that the SONGS site is under exclusive federal jurisdiction where State law generally does not apply and the Commission only has jurisdiction over the SONGS site through the consistency provisions of the Coastal Zone Management Act. While the Commission does not disagree that it has jurisdiction over the SONGS site through the consistency provisions of the Federal Coastal Zone Management Act, the Commission finds that the singular statement in the October 1, 2015 letter neither establishes that the SONGS site is under exclusive federal

jurisdiction where state law generally does not apply nor provides sufficient documentation, analysis or other supporting evidence.

J. CALIFORNIA ENVIRONMENTAL QUALITY ACT

Section 13096 of the Commission's administrative regulations requires Commission approval of coastal development permit applications to be supported by a finding showing the application, as modified by any conditions of approval, to be consistent with any applicable requirements of the California Environmental Quality Act ("CEQA"). Section 21080.5(d)(2)(A) of CEQA prohibits approval of a proposed development if there are feasible alternatives or feasible mitigation measures available that would substantially lessen any significant impacts that the activity may have on the environment. The project as conditioned herein incorporates measures necessary to avoid any significant environmental effects under the Coastal Act, and there are no less environmentally damaging feasible alternatives or mitigation measures. Therefore, the proposed project is consistent with CEQA.

The Coastal Commission's review and analysis of CDP applications has been certified by the Secretary of Resources as being the functional equivalent of environmental review under CEQA. As a responsible agency, the Commission conducted its analysis of the potential impacts of the proposed development that the Commission is authorized by the Coastal Act to review. The Commission has reviewed the relevant coastal resource issues associated with the proposed project and has identified appropriate and necessary conditions to assure protection of coastal resources consistent with the requirements of the Coastal Act. The staff report discusses the relevant coastal resource issues with the proposed development. All public comments received to date have been addressed in the staff report, including staff's oral presentation and the findings adopted by the Commission. The Commission incorporates its findings on Coastal Act consistency at this point as if set forth in full. As conditioned, there are no additional feasible alternatives or feasible mitigation measures available, beyond those required, which would substantially lessen any significant adverse environmental effect that approval of the proposed project, as modified, would have on the environment. Therefore, the Commission finds that the proposed project can be found to be consistent with the Coastal Act and CEQA Section 21080.5(d)(2)(A).

Appendix A – Substantive File Documents

- Baker, R.M. (1971). *California Coastline Preservation and Recreation Plan*. California Department of Parks and Recreation, August 1971, 123 p.
- Branum, D., S. Harmsen, E. Kalkan, M. Petersen and C. Wills (2008). *Earthquake Shaking Potential for California*, Map Sheet 48 (Revised), California Geological Survey, Sacramento, California, 2008.
- Bryan, C.R., and D.G. Enos (2014). “Understanding the Environment on the Surface of Spent Nuclear Fuel Interim Storage Containers”, Probabilistic Safety Assessment and Management PSAM 12 (conference), Honolulu, Hawaii, June 2014.
- California Coastal Commission (2015). *California Coastal Commission Sea Level Rise Policy Guidance: Interpretive Guidelines for Addressing Sea Level Rise in Local Coastal Programs and Coastal Development Permits*. Adopted August 12, 2015.
- California Coastal Commission, *Coastal Development Permit #E-00-014*, issued to Southern California Edison for construction of an ISFSI, consisting of up to 104 steel-reinforced concrete fuel storage modules, to provide temporary dry storage for SONGS 2&3 spent fuel, July 11, 2001.
- California Coastal Commission, *Coastal Development Permit #E-05-001*, issued to Pacific Gas and Electric for construction of an ISFSI to store used nuclear fuel from the Humboldt Bay Power Plant, September 5, 2005.
- California Coastal Commission, *Coastal Development Permit #9-15-0162*, issued to Southern California Edison for installation of an independent cooling system known to replace the existing once-through cooling system at SONGS Units 2 and 3, August 13, 2015.
- California Coastal Commission, *Coastal Development Permit De Minimis Waiver #9-14-1550-W*, issued to Southern California Edison for the removal of existing switchyard controls and installation of a new 12kV power source and back-up diesel generators at SONGS, September 10, 2014.
- California Coastal Commission, *Coastal Development Permit De Minimis Waiver #9-15-0265-W*, issued to Southern California Edison for the on-site relocation of a back-up diesel generator at SONGS, April 17, 2015.
- California Coastal Commission, *Coastal Development Permit De Minimis Waiver #9-15-0417-W*, issued to Southern California Edison for the replacement of the SONGS Units 2 and 3 cooling water pumps with smaller dilution pumps, and retrofitting of plant HVAC system, May 14, 2015.
- California Emergency Management Agency, California Geological Survey, and University of Southern California (2009). *Tsunami Inundation Map for Emergency Planning, San Onofre Bluff Quadrangle*, June 1, 2009.
- California Geological Survey (2002). *Seismic Hazard Zone Report for the San Clemente 7.5-Minute Quadrangle, Orange County, California*. Seismic Hazard Zone Report 062, California Department of Conservation.
- Dunn, D.S. (2014). “Chloride-Induced Stress Corrosion Cracking Tests and Example Aging Management Program”, Presentation for U.S. Nuclear Regulatory Commission, at “Public Meeting with Nuclear Energy Institute on Chloride Induced Stress Corrosion Cracking Regulatory Issue Resolution Protocol, August 5, 2014.
<http://pbadupws.nrc.gov/docs/ML1425/ML14258A082.pdf>
- Electric Power Research Institute (EPRI) (2014). Flaw Growth and Flaw Tolerance Assessment for Dry Cask Storage Canisters, EPRI Technical Report #3002002785, October 2014.
- Field, E.H., Biasi, G.P., Bird, P., Dawson, T.E., Felzer, K.R., Jackson, D.D., Johnson, K.M., Jordan, T.H., Madden, C., Michael, A.J., Milner, K.R., Page, M.T., Parsons, T., Powers, P.M., Shaw, B.E.,

- Thatcher, W.R., Weldon, R.J., II, and Zeng, Y. (2013) Uniform California earthquake rupture forecast, version 3 (UCERF3)—The time-independent model: U.S. Geological Survey Open-File Report 2013–1165, 97 p., California Geological Survey Special Report 228, and Southern California Earthquake Center Publication 1792, <http://pubs.usgs.gov/of/2013/1165/>.
- Fisher, P. J., and G. I. Mills, 1991, The offshore Newport–Inglewood Rose Canyon fault zone, California: Structure, segmentation and tectonics, in P. L. Abbott and W. J. Elliott, eds., *Environmental perils San Diego region: San Diego, California*, San Diego Association of Geologists, p. 17–36.
- Flick, R.E. (1998). Comparison of California tides, storm surges, and mean sea level during the El Niño winters of 1982–1983 and 1997–1998. *Shore & Beach* 66(3): 7-11.
- Fugro, Inc. (1977). Geologic investigation of offsets in Target Canyon, Camp Pendleton. Report No. 77-206-03, prepared for Southern California Edison, 19 pp.
- GEI Consultants (2015). *Rev 2 - Geotechnical Data Report, San Onofre Nuclear Generating Station (SONGS) ISFSI, San Clemente, California*, prepared for Southern California Edison, April 2015.
- GeoPentech (2010). *San Onofre Nuclear Generating Station Seismic Hazard Assessment Program 2010 Probabilistic Seismic Hazard Analysis Report*, prepared for Southern California Edison, Dec 2010.
- Hadidi, H. (2000). Calculation No. C-296-01-03, ISFSI Pad Slope Stability Evaluation. Southern California Edison, March 30, 2000.
- Hapke, C.J. and D. Reid (2007). *National Assessment of Shoreline Change, Part 4: Historical Coastal Cliff Retreat along the California Coast*. U.S. Geological Survey Open-File Report 2007-1133.
- Hapke, C.J., D. Reid and B. Richmond (2007). Rates and trends of coastal change in California and the regional behavior of the beach and cliff system. *Journal of Coastal Research* 25: 603-615.
- Hinkle, R.D. (2011). Third Party Review - Slope Evaluation, Independent Spent Fuel Storage Installation (ISFSI), San Onofre Nuclear Generating Station. Prepared for Southern California Edison, May 27, 2011.
- Holtec International (2014a). *Final Safety Analysis Report on the HI-STORM FW MPC Storage System (Non-Proprietary Rev. 2)*. Holtec Report No. HI-2114830, February 18, 2014.
- Holtec International (2014b). *Environmental Report on the HI-STORM UMAX MPC Based Storage System (Docket No. 72-1040)*. Holtec Report No. HI-2146232, December 17, 2014.
- Holtec International (2015). “SONGS Design Spectra 2015-09-22”, unpublished report provided to Commission staff by SCE on September 22, 2015.
- Jennings, C.W., and W.A. Bryant (2010). *Fault activity map of California*. California Geological Survey, Sacramento, California, 2010.
- Jevrejeva S, JC Moore, A Grinsted (2012). Sea level projections to AD2500 with a new generation of climate change scenarios. *Global and Planetary Change* 80-81: 14-20.
[doi:10.1016/j.gloplacha.2011.09.006](https://doi.org/10.1016/j.gloplacha.2011.09.006).
- Kain, R.M. (1990). Marine atmospheric stress corrosion cracking of austenitic stainless steels. *Materials Performance* 29(12): 60.
- Kirby, J.T. (2013). *SONGS Calculations for Probable Maximum Tsunami*, prepared for Southern California Edison Company.
- Kuhn, G.G. (2000) Sea cliff, canyon, and coastal terrace erosion between 1887 and 2000: San Onofre State Beach, Camp Pendleton Marine Corps Base, San Diego County, California, in Legg, M. R., Kuhn, G. G., and Shlemon, R. J., eds., *Neotectonics and coastal instability: Orange and northern San*

- Diego Counties, California: Long Beach, California, AAPG-Pacific Section and SPE-Western Section, p. 31-87.
- Kuhn, G.G. (2005). "Paleoseismic features as indicators of earthquake hazards in North Coastal, San Diego County, California, USA." *Engineering Geology*, 10.1016/j.enggeo.2005.04.006, 115-150.
- Kuhn, G. G., Legg, M. R., Johnson, A., Shlemon, R. J., and Frost, E. G. (1996). Paleoliquefaction evidence for large pre-historic earthquake(s) in north-coastal San Diego County, California, *in* Munasinghe, T., and Rosenberg, P., eds., *Geology and natural resources of coastal San Diego county, California*, San Diego Association of Geologists Field Trip Guidebook, p. 16-24.
- Kuhn, G. G., Legg, M. R., and Shlemon, R. J. (2000) Neotectonics in the north coastal area, San Diego County, California, *in* Legg, M. R., Kuhn, G. G., and Shlemon, R. J., eds., *Neotectonics and coastal instability: Orange and northern San Diego Counties, California: Long Beach, California, AAPG-Pacific Section and SPE-Western Section*, p. 88-104.
- Legg, M. R. and Kamerling, M.J. (2003). Large-scale basement-involved landslides, California continental borderland. *Pure Appl. Geophys.*, 160, 2033-2051.
- Malloney, J., N. Driscoll, G. Kent, S. Duke, T. Freeman, and J. Bormann (in press). Segmentation and step-overs along strike-slip fault systems in the inner California Borderlands: Implications for fault architecture and basin formation. *Applied Geology in California*.
- National Research Council (2012). *Sea-Level Rise for the Coasts of California, Oregon, and Washington: Past, Present, and Future*. The National Academies Press, Washington, D.C., 202 p.
- Ninyo and Moore (2015). SONGS Slope Calculations (Project No. 107925001), April 16, 2015.
- Patsch, K., and Griggs, G. (2006). *Littoral cells, sand budgets and beaches: Understanding California's shoreline*. Prepared for the California Department of Boating and Waterways and California Coastal Sediment Management WorkGroup, October 2006, 40 p.
- Petersen, M.D., Byrant, W.A., Cramer, C.H., Cao, T., Reichle, M.S., Frankel, A.D., Leinkaemper, J.J., McCrory, P.A., and Schwarta, D.P. (1996). *Probabilistic seismic hazard assessment for the state of California*, California Division of Mines and Geology, Sacramento, California, 1996.
- Petersen, M.D., M.P. Moschetti, P.M. Powers, C.S. Mueller, K.M. Haller, A.D. Frankel, Y. Zeng, S. Rezaeian, S.C. Harmsen, O.S. Boyd, E.H. Field, R. Chen, N. Luco, R.L. Wheeler, R. A. Williams, A.H. Olsen and K.S. Rukstales (2015). *Seismic-hazard maps for the conterminous United States, 2014*. U.S. Geological Survey Scientific Investigations Map 3325, <http://dx.doi.org/10.3133/sim3325>.
- Pham, L.Q. (2007). Calculation No. C-296-01.03, ISFSI Pad Slope Stability Evaluation. Southern California Edison, August 3, 2007.
- Pham, L.Q. (2015). Calculation No. C-296-01.03, ISFSI Pad Slope Stability Evaluation (Revised). Southern California Edison, September 14, 2015.
- Rivero, C. and J.H. Shaw (2011). Active folding and blind thrust faulting induces by basin inversion processes, inner California borderlands. In: Shaw, J.H., and J. Suppe, eds., *Thrust Fault Related Folding*, AAPG Memoir Vol. 94, pp. 187-214.
- Rivero, C., J.H. Shaw and K. Mueller (2000). Oceanside and Thirtymile Bank blind thrusts: Implications for earthquake hazards in coastal southern California. *Geology* 28(10): 891-894.
- Ryan, H.F., J.E. Conrad, C.K. Paull and M. McGann (2012) Slip rate on the San Diego Trough fault zone, inner California borderland, and the 1986 Oceanside earthquake swarm revisited. *Bulletin of the Seismological Society of America* 102(6): 2300-2312.

- San Diego Regional Water Quality Control Board, *National Pollutant Discharge Elimination System (NPDES) Permit and Waste Discharge Requirements, San Onofre Nuclear Generating Station, Unit 2* (NPDES No. CA0108073; Order No. R9-2005-0005).
- San Diego Regional Water Quality Control Board, *National Pollutant Discharge Elimination System (NPDES) Permit and Waste Discharge Requirements, San Onofre Nuclear Generating Station, Unit 3* (NPDES No. CA0108181; Order No. R9-2005-0006).
- Schaeffer M, W Hare, S Rahmstorf, M Vermeer (2012). Long-term sea-level rise implied by 1.5°C and 2°C warming levels. *Nature Climate Change* 2: 867-870. doi:10.1038/nclimate1584.
- Shlemon, R.J. (1977). Geomorphic analysis of Fault "E" Camp Pendleton, California: Roy J. Shlemon and Associates, Inc., unpublished geologic report for Southern California Edison Company, 20 p.
- Shlemon, R.J. (1979). Age of "Dana Point," "Vaciadero," and "Carr" Faults Capistrano Embayment coastal area, Orange County, California: Roy J. Shlemon and Associates, Inc. unpublished geologic report for Southern California Edison Company, 19 p.
- Shlemon, R.J. (1987). The Cristianitos fault and Quaternary geology, San Onofre State Beach, California. *Geological Society of America Centennial Field Guide*, Cordilleran Section: Boulder, CO, Geological Society of America, p. 171-174.
- Shlemon, R.J. (2000). State-of-the-art to standard-of-practice: Active faults, paleoliquefaction and tsunamis in the Carlsbad area, San Diego County, California: Geological Society of America Abstracts with Programs, v. 32, no. 7, p. A-121.
- Southern California Edison, *SONGS Units 1, 2 and 3 Spill Prevention, Control and Countermeasures (SPCC) Plan*, Revision 11 (SO123-XV-16).
- Southern California Edison, *SONGS Units 1, 2 and 3 Storm Water Management Plan (SWMP)*, Revision 9 (SO123-XV-32).
- Southern California Edison Geotechnical Group (1995). Final Report: Geotechnical Investigation of Alternate Independent Spent Fuel Storage Installation (ISFSI), November 1995.
- Southern California Edison (1998). *Final Safety Analysis Report, San Onofre Nuclear Generating Station, Units 2 and 3*. U.S. Nuclear Regulatory Commission Docket Nos. 50-361, 50-362, version 13.
- Southern California Edison (2013). Marine Terrace Report: Palos Verdes Peninsula, California to Punta Banda, Baja California (Rev. 0). Prepared for Southern California Edison SONGS Seismic Research Project, September 2013.
- Southern California Edison (2014a). *San Onofre Nuclear Generating Station Units 2 and 3 Site Specific Decommissioning Cost Estimate*. U.S. Nuclear Regulatory Commission Docket Nos. 50-361, 50-362, September 23, 2014, 90 pp.
- Southern California Edison (2014b). *San Onofre Nuclear Generating Station Units 2 and 3 Irradiated Fuel Management Plan*. U.S. Nuclear Regulatory Commission Docket Nos. 50-361, 50-362, September 23, 2014, 12 pp.
- Southern California Edison (2014c). *San Onofre Nuclear Generating Station Units 2 and 3 Post-Shutdown Decommissioning Activities Report*, U.S. Nuclear Regulatory Commission Docket Nos. 50-361, 50-362, September 23, 2014, 34 pp.
- Southern California Edison (2015a) "SONGS ISFSI Expansion Project Coastal Development Permit Application Package", February 20, 2015.
- Southern California Edison (2015b) "SCE Responses to 3/19/2015 CCC Questions Re: ISFSI Expansion", submitted to the Coastal Commission, May 12, 2015.

- Southern California Edison (2015c) “SONGS Spent Fuel Storage: Offsite and Onsite Location Alternatives”, Attachment 6a to “SCE Responses to 3/19/2015 CCC Questions Re: ISFSI Expansion”, submitted to the Coastal Commission, May 12, 2015.
- Southern California Edison (2015d) “Coastal Development Permit Application #9-15-0228 (SONGS ISFSI Expansion), Changes to Noise, Sea Level Rise and Tsunami Calculations”, submitted to Coastal Commission staff, May 13, 2015.
- Southern California Edison (2015e). “Transportation of SONGS Spent Fuel”, transmitted by e-mail from Kim Anthony (SCE) to J. Street (CCC), September 10, 2015.
- Southern California Edison (2015f). “SCE Responses to CCC Request for Additional Information (RAI) Dated 9/1/2015”, transmitted by e-mail from K. Anthony (SCE) to J. Street (CCC), September 14, 2015.
- Southern California Edison (2015g). “Response to CCC 9-15-2015 Request for Additional Information re ISFSI Bearing Capacity” (including attached calculations from Holtec), transmitted by e-mail from L. Anabtawi (SCE) to J. Street (CCC), September 17, 2015.
- Southern California Edison (2015h). “Projected Sea Level Rise Given the Project’s Design Service Life”, transmitted by e-mail from L. Anabtawi (SCE) to J. Street (CCC), September 17, 2015.
- U.S. Army Corps of Engineers (1960). Beach erosion control report on cooperative study of San Diego County, California. U.S. Army Corps of Engineers W004-193-ENG-5196.
- U.S. Nuclear Regulatory Commission (1981). *Safety evaluation report related to the operation of San Onofre Nuclear Generating Station, Units 2 and 3, Docket numbers 50-361 and 50-362, Southern California Edison Company, et al.*, U.S. Nuclear Regulatory Commission, Office of Nuclear Reactor Regulation, Washington, D.C., 1981.
- U.S. Nuclear Regulatory Commission (2014). “Summary of August 5, 2014, Public Meeting with Nuclear Energy Institute on Chloride Induced Stress Corrosion Cracking Regulatory Issue Resolution Protocol”, September 9, 2014. <http://pbadupws.nrc.gov/docs/ML1425/ML14258A081.pdf>
- U.S. Nuclear Regulatory Commission (2015). *Preliminary Safety Evaluation Report (Docket No. 72-1040), HI-STORM UMAX Canister Storage System Amendment No. 1*, March 4, 2015.

Appendix B – Ground Shaking as a Measure of Earthquake Strength

By Dr. Mark Johnsson, Coastal Commission Staff Geologist

Many different measures have been used over the years to assess earthquake magnitude. The familiar Richter, or local, magnitude (M_L) is based on the ground shaking observed on a particular type of seismograph that is most sensitive to short period (0.8 second) seismic waves. These waves die out with distance, and so this measure is inappropriate when applied over long distances ($> \sim 500$ km) to measure distant earthquakes. Moreover, for large earthquakes, the Richter magnitude “saturates,” and fails to accurately reflect differences between large earthquakes of different magnitudes. The surface wave magnitude (M_S) was developed to measure shaking of long period (20 second) waves, and is more suited to larger earthquakes. This scale, like its counterpart the body wave magnitude (M_B) also saturates in large earthquakes and, like the Richter magnitude, is based solely on ground shaking, not the amount of energy released by an earthquake. Currently, most seismologists prefer the moment magnitude (M_W) for measuring large earthquakes. This measure is based on the strength of the rocks, the area of fault rupture, and the amount of slip during an earthquake, and is a better measure of the amount of energy released by an earthquake.

An earthquake of a given magnitude will produce different levels of ground shaking at different locations, depending on the distance of the location from the earthquake hypocenter, the nature of the soil or rock between the location and the earthquake, and soil and rock conditions at the site. The level of shaking is expressed by a term called “intensity,” and is quantified by the Modified Mercalli Index, whereby intensities ranging from I (not felt) through XII (near total destruction) are assigned based on the level of damage sustained by structures. Better quantification of the level of shaking also is possible; and the standard measure is peak ground acceleration (PGA), usually expressed as a fraction of the acceleration due to gravity (9.81 m/s^2 , or 1.0 g). Peak ground acceleration is typically measured in horizontal and vertical directions. It can be expressed deterministically (“a given earthquake can be expected to produce a peak horizontal ground accelerations at the site of X g”), or probabilistically (“given the seismic environment at the site, there is a 10% chance that a peak ground acceleration of X g will be exceeded in 50 years”). The current trend is to express seismic risk in probabilistic terms. The State of California has defined ground accelerations with a 10% chance of exceedance in 50 years as corresponding to the “maximum probable earthquake” for the site. Ground shaking with a 10% chance of exceedance in 100 years is defined as the “maximum credible earthquake.” Peak ground accelerations depend not only on the intensity of the causative earthquake and the distance of the site from the hypocenter of the earthquake, but also on site characteristics. Most important is the depth and firmness of the soil and/or bedrock underlying the site. All of these parameters are evaluated in producing a seismic shaking hazard assessment of a site.

In evaluating the response of structures to ground shaking, the frequency (cycles per second) of that shaking is important—higher frequency shaking is more damaging to smaller, more rigid structures, whereas lower frequency shaking is more damaging to larger, or more flexible structures. The proposed ISFSI facility fits into the latter category. Different ground acceleration values apply to seismic waves with different frequencies. The inverse of the frequency of a seismic wave is its period. Thus, an earthquake with a peak ground acceleration of 0.7 g may have a peak “spectral acceleration” (SA) of 1.1 g for waves of 0.3 second period, but only 0.5 g for waves with periods of 1 second. A typical earthquake produces seismic waves with many different periods, and a plot of spectral accelerations for an earthquake shows the ground accelerations for waves of all periods. In addition, the duration of shaking appears to be important in determining the amount of damage caused by ground shaking. The duration of shaking correlates reasonably well with earthquake magnitude, but there are no currently accepted means of estimating the expected duration of ground shaking from a given earthquake.



FIGURE 1

SONGS ISFSI Expansion Project
Regional Project Location

Exhibit 1
Application No. 9-15-0228
Southern California Edison
Project Vicinity
Page 1 of 1

L S A



0 1000 2000
FEET

SOURCE: Bing Maps

I:\HLT1401\G\Location.cdr (12/1/14)



FIGURE 3

Exhibit 2
Appl. No. 9-15-0228
SONGS Site &
Alternative
On-site Locations
Page 1 of 2



LSA



LEGEND

Project Site

SONGS Site

Potential Post-Decommissioning Alternative ISFSI Locations

FIGURE 2

Exhibit 2
Appl. No. 9-15-0228
SONGS Site &
Alternative
On-site Locations
Page 2 of 2

SONGS ISFSI Expansion Project
Site Boundaries



Existing View



Proposed Project View

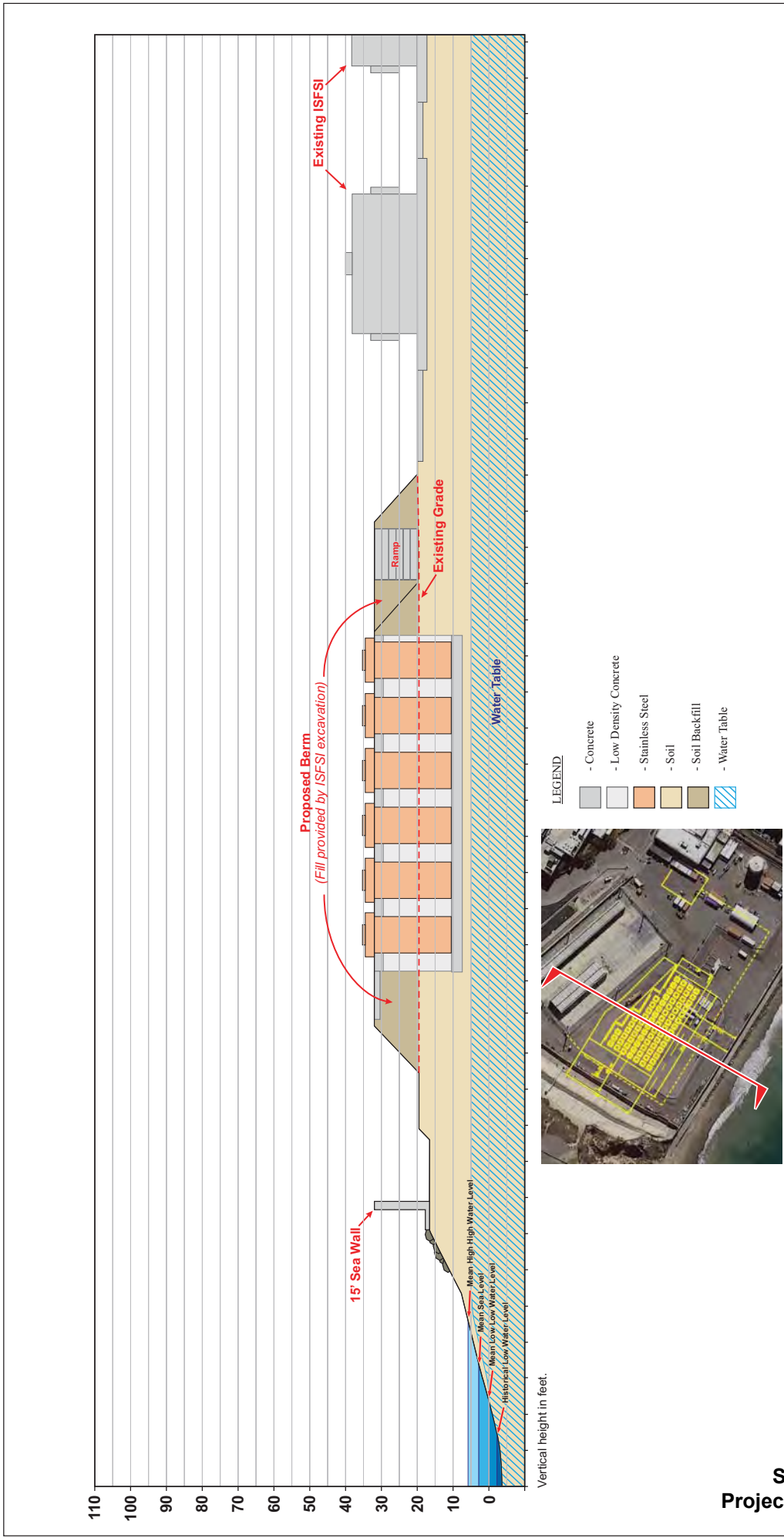
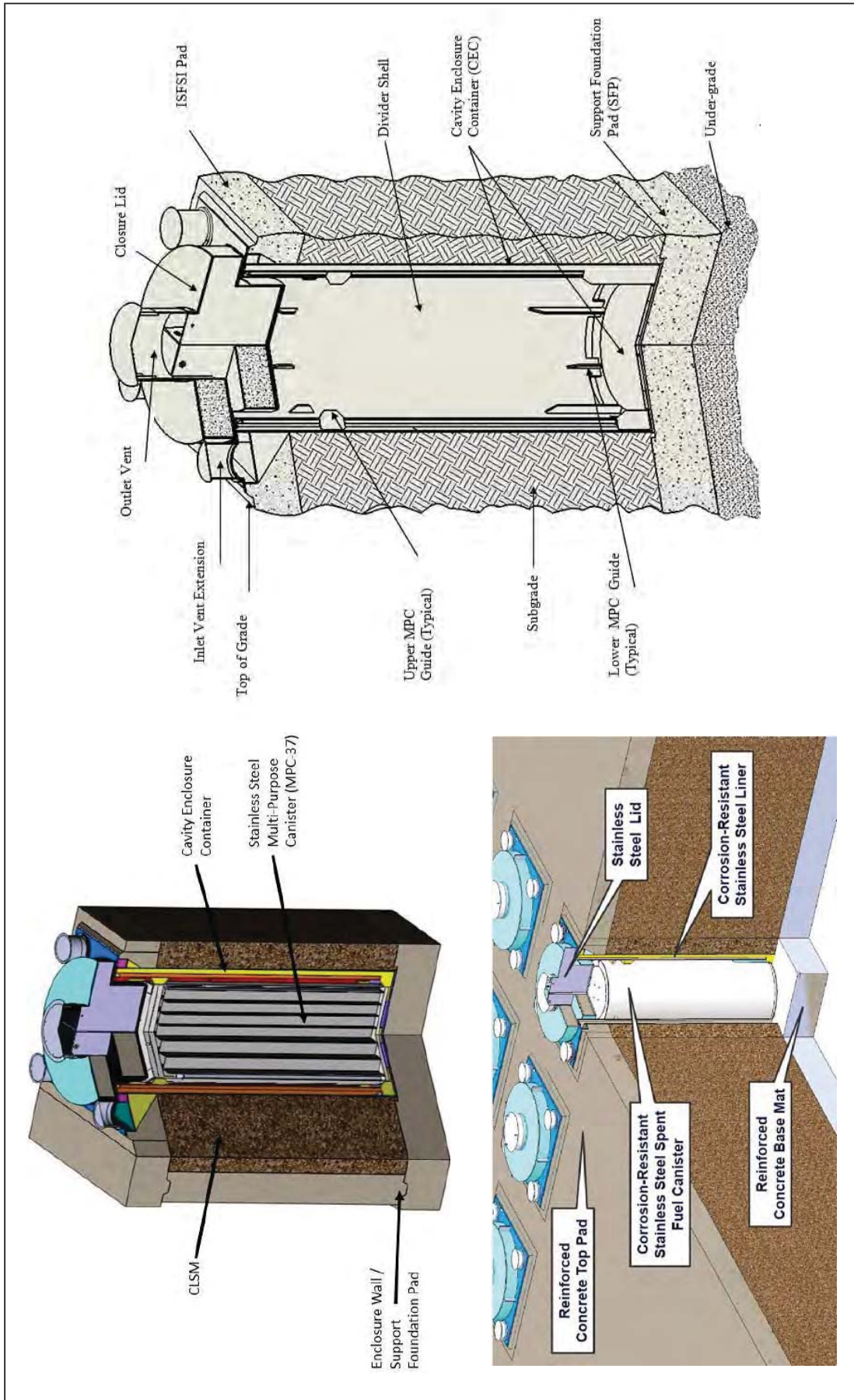


FIGURE A2



LSA

FIGURE 7



Figure 1. Cross section illustration of the concrete pads and storage modules. The space between the cylindrical storage modules is filled with concrete.

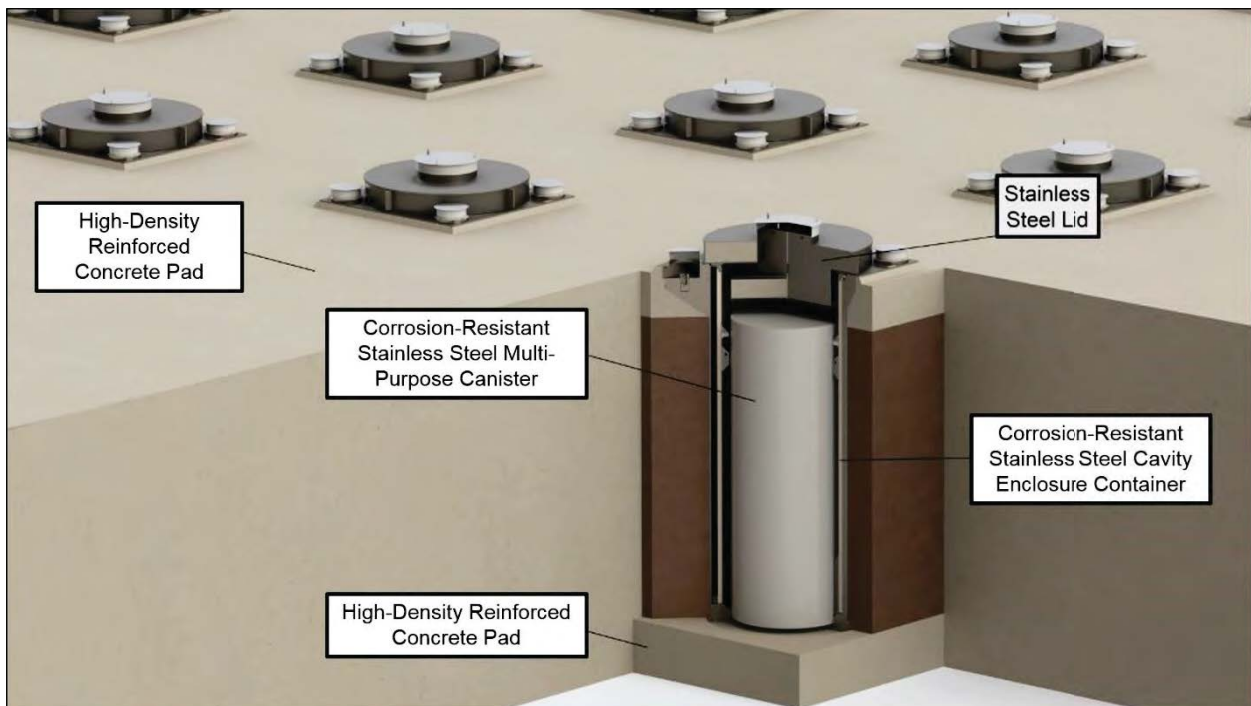


Figure 2. Illustration of a multi-purpose canister in a storage module supported by the concrete pad and surrounded by flowable grouting material.



FIGURE 9

LSA



0 75 150
FEET

SOURCE: Google Earth

I:\HLT1401\G\Buildings Demolished.cdr (2/10/15)

LEGEND



Structures to be Removed



If necessary, pumps within the NIA sump area would be relocated, not removed

SONGS ISFSI Expansion Project

Structures to be Removed

Exhibit 5
Application No. 9-15-0228
NIA Structures to be Removed
Page 1 of 1

HOLTEC INTERNATIONAL

Figure 3: Comparison of 5% Damped UMAX MSE and SONGS DBE HOR Response Spectra

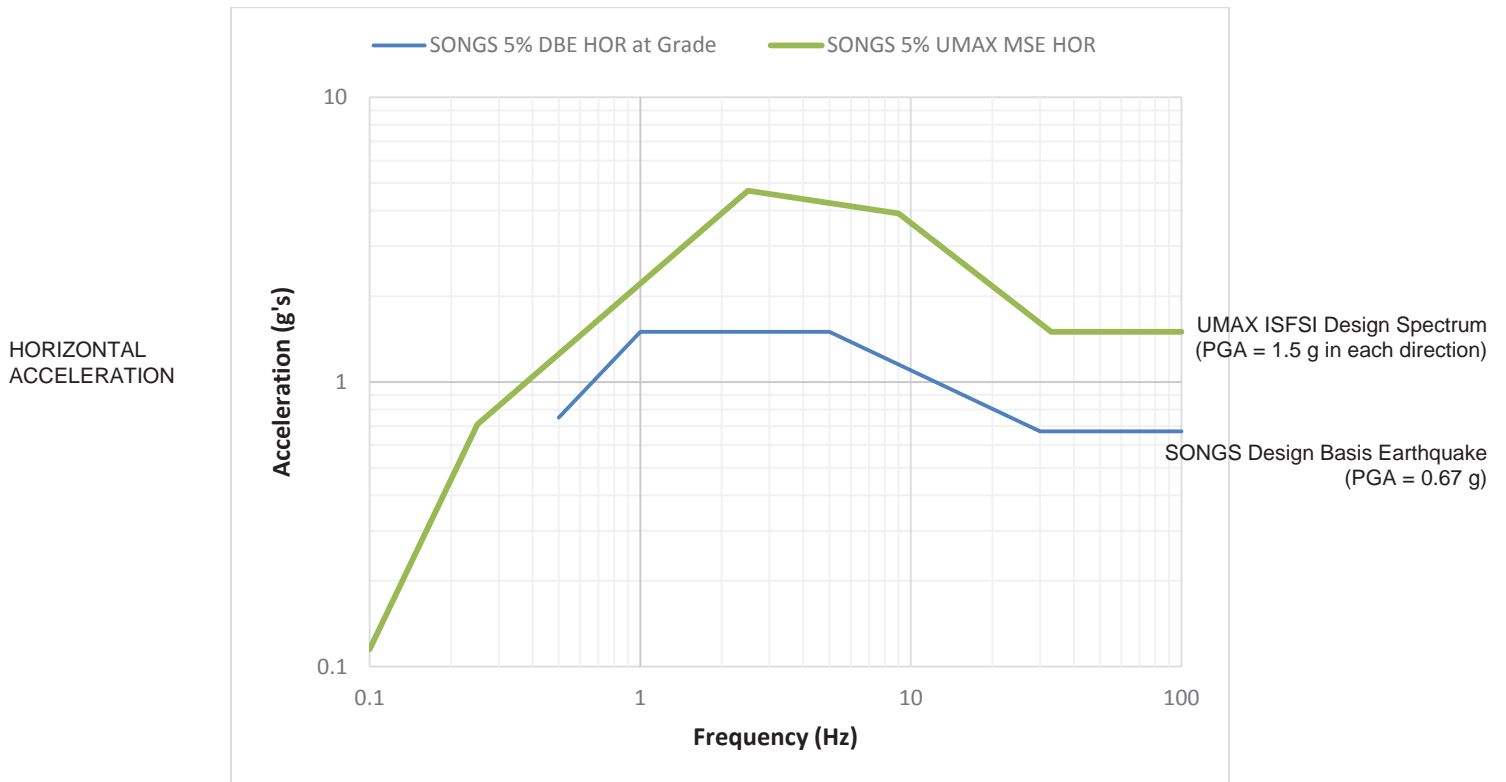


Figure 4: Comparison of 5% Damped UMAX MSE and SONGS DBE VT Response Spectra

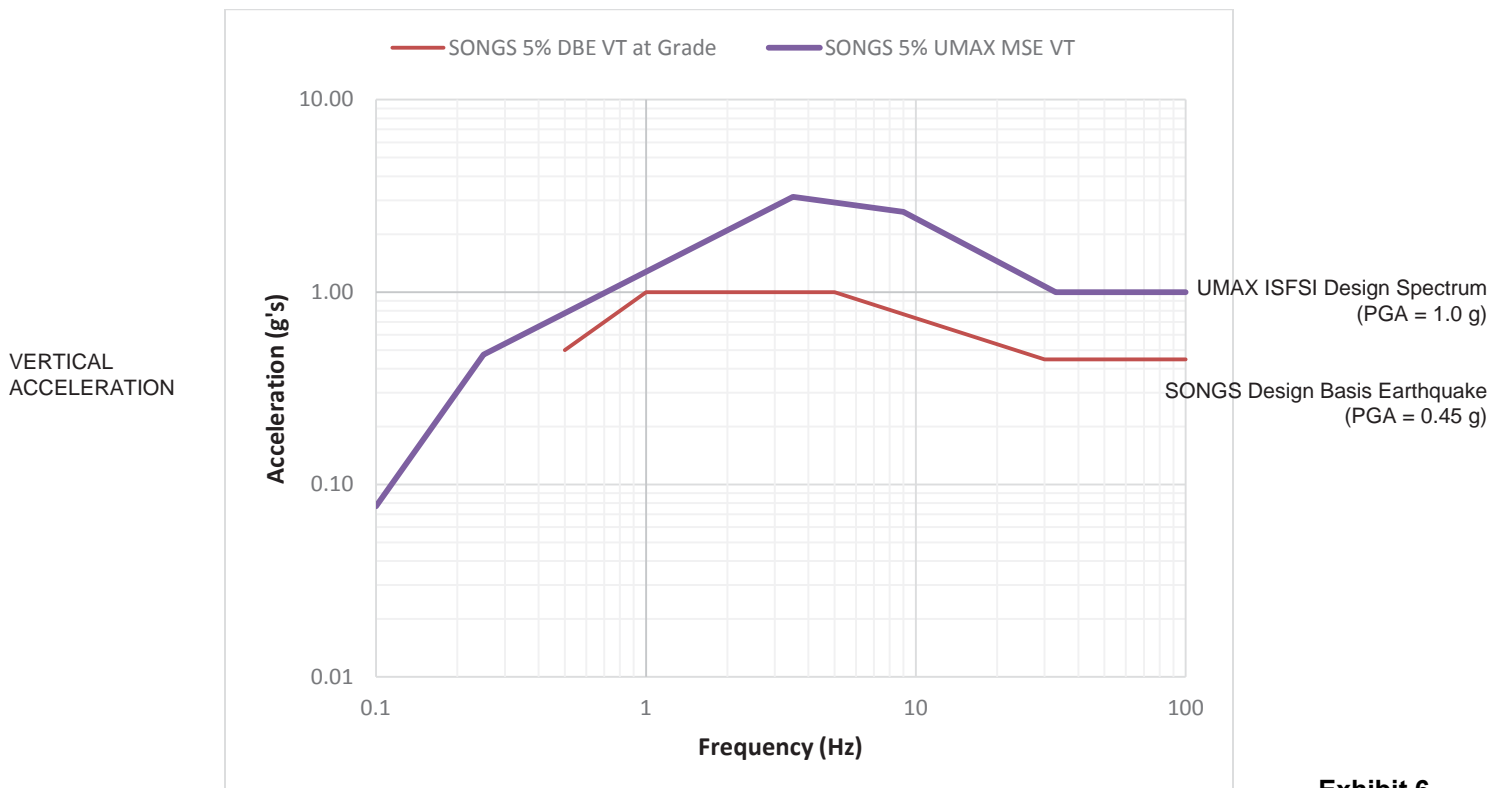


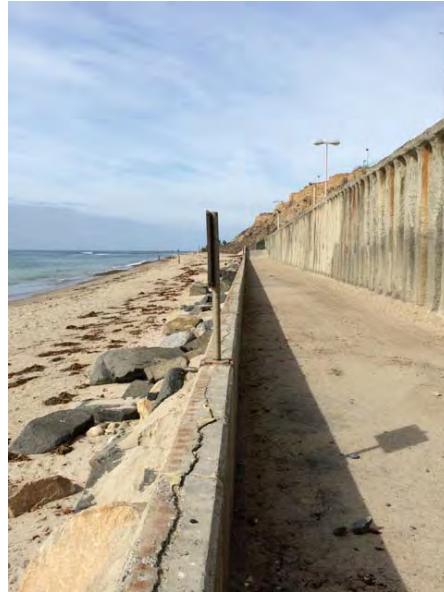


FIGURE 11
(Revised)

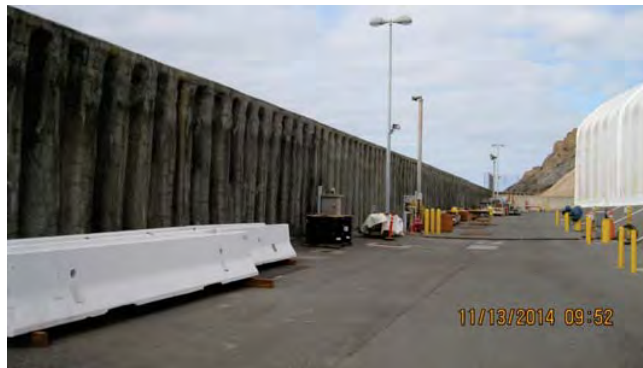
Exhibit 7
Application No. 9-15-0228
Southern California Edison
Flood Risk in Year 2117
Page 1 of 1

SONGS ISFSI Expansion Project
Sea Level Rise Flood Risk without Sea Wall

SOURCE: Bing Maps (c. 2014); UCSD (2015); Pacific Institute (2014) * Using the 0.7 feet/year maximum provided by the California Coastal Commission and assuming that the rate is held true for 85 years
E:\HLT1401\GIS\FloodRisk_NoWall_Lidar.mxd (5/4/2015)



Views of seawall from public access way on San Onofre State Beach looking inward towards the SONGS site.



View of seawall from SONGS site looking outwards towards San Onofre State Beach.

LSA

FIGURE 10

SONGS ISFSI Expansion Project
Existing Seawall

SOURCE: LSA and <http://www.californiacoastline.org>
I:\HLT1401\G\Existing Seawall.cdr (1/6/15)

Exhibit 8
Application No. 9-15-0228
Southern California Edison
Views of Existing NIA Seawall
Page 1 of 1



Existing View



Proposed Project View

View from Beach Northwest of the NIA



Existing View



Proposed Project View

View from Parking Area Near Old Pacific Coast Highway
(Looking Southeast toward NIA)



Existing View



Proposed Project View

View To Southwest Toward NIA From SONGS AWS Building



Existing View



Proposed Project View

View from NIA Toward Northwestern Bluff

CALIFORNIA COASTAL COMMISSION

45 FREMONT, SUITE 2000
SAN FRANCISCO, CA 94105-2219
VOICE (415) 904-5200
FAX (415) 904-5400
TDD (415) 597-5885



Tu14a

October 5, 2015

To: Coastal Commissioners and Interested Parties

From: Alison Dettmer, Deputy Director
Joseph Street, Environmental Scientist

Subject: **Addendum to 9-15-0228 – Southern California Edison SONGS
ISFSI Project**

This addendum provides correspondence on the above-referenced staff report, *ex parte* communications, proposed revisions to the staff report, and staff's response to comments. The proposed modifications to the staff report do not change staff's recommendation that the Commission **approve** CDP # 9-15-0228, as conditioned.

Correspondence Received

- Four e-mails from Donna Gilmore, San Onofre Safety, to Joseph Street, Coastal Commission, dated September 1, 2015
- Letter from Donna Gilmore, San Onofre Safety, to Joseph Street, Coastal Commission, September 17, 2015
- E-mail from Donna Gilmore, San Onofre Safety, to Joseph Street, Coastal Commission, September 21, 2015
- Letter from Ted Quinn, Technology Resources, to California Coastal Commission, September 27, 2015
- Letter from Jerome Kern, Oceanside City Council, to Joseph Street, Coastal Commission, September 29, 2015
- Letter from David Lochbaum, Union of Concerned Scientists, to Joseph Street, Coastal Commission, September 30, 2015
- E-mail from Lyn Harris Hicks, Coalition for Responsible and Ethical Environmental Decisions (CREED), to Joseph Street, Coastal Commission, October 1, 2015
- E-mail from Jane Swanson, San Luis Obispo Mothers for Peace, to Joseph Street and Tom Luster, Coastal Commission, October 1, 2015
- Letter (via e-mail) from Patricia Borchmann to California Coastal Commission, October 1, 2015

- E-mail from Donna Gilmore, San Onofre Safety.org, to Joseph Street, Coastal Commission, October 1, 2015
- E-mail from Dorah Shuey to Joseph Street, Coastal Commission, October 1, 2015
- E-mail from Ray Lutz, Citizens Oversight, to California Coastal Commission, October 1, 2015
- E-mail from Laura Lynch to California Coastal Commission, October 2, 2015
- Letter from David Victor, Tim Brown and Daniel Stetson, SONGS Community Engagement Panel, to Joseph Street, Coastal Commission, October 2, 2015
- E-mail from Linda Anabtawi, Southern California Edison, to Joseph Street, Coastal Commission, October 2, 2015
- Letter from Captain W. L. Whitmire, U. S. Marine Corps – Camp Pendleton, to Joseph Street, Coastal Commission, October 2, 2015
- E-mail from Charles Langley to Joseph Street, Coastal Commission, October 2, 2015
- E-mail from Donna Gilmore, San Onofre Safety, to Joseph Street, Coastal Commission, October 2, 2015
- E-mail from Dr. Donald Mosier, Del Mar City Council, to Joseph Street, Coastal Commission, October 2, 2015
- Letter from Garry Brown, Orange County CoastKeeper, to Joseph Street, Coastal Commission, October 2, 2015
- E-mail from Gary Headrick, San Clemente Green, to California Coastal Commission, October 2, 2015
- Letter from Glenn Pascall, Sierra Club Task Force on San Onofre, to California Coastal Commission, October 2, 2015
- Letter from Rita Conn, Let Laguna Vote, to Dr. Charles Lester, Coastal Commission, October 2, 2015
- Letter from Jack Monger, Industrial Environmental Association, to Joseph Street and Coastal Commission, October 3, 2015
- Letter from Donna Gilmore, San Onofre Safety, to California Coastal Commission, October 4, 2015
- E-mail from Laura Lynch to Joseph Street, Coastal Commission, October 4, 2015
- Six e-mails, with attachments, from Michael Aguirre, Aguirre & Severson, to Joseph Street, Coastal Commission, October 5, 2015
- E-mail from Marv Lewis to Joseph Street, Coastal Commission, October 5, 2015

Revisions to the Staff Report

Recommended revisions to the staff report include changes to **Special Conditions 1** and **3**, the inclusion of a revised and clarified sea level rise analysis examining flooding in 2051 (35-year timeframe) rather than 2047 (30-year timeframe), as well as a number of minor clarifications and corrections. Additions to the staff report are shown below in underline and deletions in ~~strikethrough~~.

The proposed revisions below as well as the below responses to public comments are recommended findings and will be incorporated into the relevant portions of the staff report as adopted findings.

Page 6, Special Condition 1:

- “1. **Evidence of Landowner Approval.** PRIOR TO ISSUANCE OF THE COASTAL DEVELOPMENT PERMIT, the applicant shall submit to the Executive Director for review and approval evidence of their legal ability to undertake the development as conditioned by the Commission. ~~Such evidence shall include documentation demonstrating that the U.S. Department of the Navy has renewed or extended its existing easement for use of the Part 50 licensed area for a term encompassing the authorized development (i.e., through October 6, 2035).~~”

Reason for Proposed Revision: There are a variety of ways an Applicant who does not own a fee interest in the property being developed can satisfy their obligation, prior to permit issuance, to demonstrate their ability to comply with the conditions of approval. Since the Applicant, prior to permit issuance, can demonstrate their authority to comply with the conditions of approval in a manner other than that specified, the sentence limiting the manner of compliance to one method is proposed for deletion.

Page 7, Special Condition 3:

- ~~“C. All development and redevelopment of the property by the Permittee shall be sited and designed to ensure geologic stability without reliance on any of the existing shoreline protective devices adjoining the North Industrial Area. As used in this condition, redevelopment is defined to include: (1) additions, or; (2) expansions, or; (3) demolition, renovation or replacement that would result in 50% or more of a structure, structural wall or structural foundation, or; (4) demolition, renovation or replacement of less than 50% of a structure where the renovation or addition would result in a combined alteration of 50% or more of the structure from its condition on October 6, 2015.”~~

Reason for Proposed Revision: Staff is recommending that clause C of **Special Condition 3** be deleted because it is duplicative of the restrictions on future shoreline protection development contained in clauses A and B, and therefore unnecessary.

Page 9, paragraph 4, lines 1-3:

“The plant is collectively owned by SCE (75.0576.8%), San Diego Gas and Electric Company (20%), and the City of Anaheim (3.16%) and the City of Riverside (1.79%). As a previous owner, the City of Riverside is also a co-participant on the ISFSI project. The plant operates subject to a long-term easement ...”

Page 10, paragraph 3, lines 2-3:

“The ISFSI, including its concrete approach aprons, would occupy approximately ~~32,000~~ 40,000 square feet ...”

Page 11, paragraph 2, lines 1-2:

“...the SONGS facility would consist of 75 VVMs set in a surrounding berm measuring approximately ~~111~~160 ft wide by ~~211~~260 ft long...”

Page 11, paragraph 3, lines 4-5:

“...Cavity Enclosure Container (CEC), comprised of a ~~low carbon~~ stainless steel Container Shell welded to a stainless steel Base Plate.”

Page 11, footnote 1:

⁴¹ “A small HI-STORM UMAX system with six storage modules was previously installed at the Humboldt Bay Power Plant (see CDP #E-05-001).”

Page 12, paragraph 4, lines 3-7:

“The MPCs would be placed in a licensed transfer cask, lowered into the pools, loaded with spent fuel assemblies, and then removed from the pools. Water would be drained from the MPCs; ~~the air inside of them would be~~ and replaced with helium, and they would be welded shut. Subsequently, ~~the MPCs would be placed in a licensed~~ transfer casks containing the MPCs would be ~~and~~ loaded onto a transfer vehicle that would use existing roads ...”

Page 15, paragraph 3, lines 3-6:

“SCE has requested Navy authorization to renew the grant of easement ~~until 2051, at which time SCE expects to have completed~~ to allow for plant decommissioning, ~~and~~ required site restoration, and the transferred of all SONGS spent fuel to DOE custody.”

Page 17, paragraph 4, lines 9-11:

“...the SONGS ISFSI has been designed to withstand significantly greater ground shaking intensities (1.5 g in two orthogonal directions, net 2.12 g) than the existing spent fuel pools (0.67 g in each direction).”

Page 19, paragraph 3, lines 2-3:

“...at some of the lowest grade elevations (approx. ~~14~~13 to 20 feet MLLW)...”

Page 19, paragraph 3, lines 5-7:

“During its review of SCE’s alternatives analysis and in view of the fact that the ~~proposed~~ project applicant seeks authorization for temporary, interim storage ...”

Page 26, paragraph 1, lines 10-11:

“The spectra labeled “SONGS” ~~is~~are derived from the NRC-approved “free field” spectra and takes into account ...”

Page 26, paragraph 1, lines 15-16:

“The ISFSI design spectra exceed ~~that~~ those of the design basis earthquake ...”

Page 30, paragraph 1, lines 6-8:

“Superimposing this tsunami on a 7-foot high tide (the 10% exceedance Spring high tide for the site) and a one-foot storm surge, resulted in a maximum “still” water level of 15.6 feet MLLW (SONGS 2&3 FSAR).”

Page 31, paragraph 4, lines 3-5:

“As a part of its CDP application, SCE prepared an analysis of future flood conditions over the life of the development (SCE 2015a, d, h), using the sea level rise projections ...”

Page 31, fourth paragraph, lines 11-16:

“The analysis indicates that sea level can be expected to rise ~~0.30.4~~ to 1.82.0 feet by ~~2047~~2051 ~~(30-year time horizon)~~, depending on which scenario is used. Under the high sea level rise scenario, and assuming an additional foot of sea level height associate with wind and storm surge and/or oceanographic forcing (such as due to an El Niño event), SCE estimated that in 2051 the still-water level at mean high tide could reach 7.68 feet MLLW. A more extreme high tide of +6.9 feet MLLW, combined with 1 foot of storm surge, 2 feet of sea level rise and maximum wave run-up, could result in temporary flooding up to 25.0 feet MLLW (SCE 2015h).¹⁰ Commission staff notes that a maximum high tide at SONGS (>7.2 feet MLLW) (SONGS 2&3 FSAR), 1 foot of storm surge and temporary high sea level associated with a large El Nino event (+0.4 to 1 ft) (Flick 1998; CCC 2015) could add an additional 0.5 to 1.5 feet to this projected flooding elevation.

Page 31, paragraph 4, continuing to page 32:

~~“For several reasons, Commission staff believes that SCE’s analysis underestimates the potential for future flooding at the project site. First, short-term fluctuations in water level (assumed by SCE to amount to +1 foot) may include both surge and the underlying effects of oceanographic forcing. Temporary increases in sea level associated with storm surge in Southern California may reach +1 foot, while short-term sea level increases in sea level associated with the large 1982-83 El Nino event ranged from 0.4 to 1 foot (Flick 1998; CCC 2015). Thus, a more conservative estimate of the contribution to sea level from short-term phenomena would be approximately +2 feet. Second, SCE examined flooding only under mean tidal conditions of 5.8 feet MLLW. High tides equal or exceed 7.0 feet MLLW about 10% of the time and high tide levels equal or exceed 7.2 feet about 1.5% of the time, based~~

~~on the distribution of five years of tide data¹⁰. Using these higher tide levels, present day extreme high still water level could reach 9.2 to 9.3 feet MLLW (SONGS 2&3 FSAR), and current wave runup could exceed 24 feet MLLW. Using the same additive method that SCE used to modify runup for future sea level rise, wave runup in 2051, with 2.0 feet of sea level rise, could exceed 27 feet MLLW. However, run up does not change linearly with changes in water level, so these estimates of how run-up will change with changes in water levels likely underestimate potential run-up.”~~

Page 31, *new* footnote 10:

¹⁰ However, run up does not change linearly with changes in water level, so these estimates of how run-up will change with changes in water levels likely underestimate potential run-up.”

Page 32, footnote 10:

¹⁰ Based on distribution of Table 2.4-11: Distribution of Spring High Tides at San Diego During Five Years, from the San Onofre 2&3 Final Safety Analysis Report (FSAR) Section 2.4, (Revision 24), adjusted by the amplitude ratio of 0.92.”

Page 33, *second* paragraph, lines 5-8:

“a maximum average bluff retreat rate of 20 inches per year over the proposed 35-year life of the project would equate to a total bluff retreat of 29 58 feet, or about one-third-half of the distance between the existing seawall and the proposed ISFSI facility.”

Page 35, *second* paragraph, lines 3-6:

“A crude calculation using a maximum estimated bluff retreat rate of 0.8 feet/20 inches per year (Hapke et al. 2007, for unprotected slopes in San Mateo Formation bedrock) indicates that erosion could begin to undermine the ISFSI structure by approximately 2130 2077.”

Page 37, *fourth* paragraph, lines 4-10:

“The initiation and growth of stress corrosion cracking in stainless steel fuel storage casks are not fully understood and remain a topic of active research, but these processes are likely to be accelerated in a coastal environment such as at SONGS (e.g., Kain 1990; Bryan and Enos 2014; EPRI 2014). Commission staff is not aware of any documented instances of stress corrosion cracking in fuel storage casks at other nuclear power plants. However, the NRC has collected evidence of stress corrosion cracking in other welded stainless steel components at several coastal nuclear power plants (NRC Dunn 2014).”

Page 37, *fourth* paragraph, lines 12-14:

“Elsewhere, the NRC has estimated that at least 30 years would be required for the initiation of stress corrosion cracking in steel fuel storage casks (NRC 2014).”

Page 38, *second* paragraph, lines 3-4:

“In the Preliminary Safety Evaluation Report (SER) supporting the September ~~X~~8, 2015, final approval of an amendment ...”

Page 39, paragraph 2, lines 6-7:

“Accordingly, the Commission is adopting **Special Condition 4**, which requires the ~~landowners~~Permittee to assume the risks...”

Page 43, paragraph 3, lines 4-5:

“Construction would not occur during weekends and holidays, with the possible exception of operations such as excavation, pouring concrete or other activities that require continuous work.”

Appendix A, Substantive File Documents

“Bryan, C.R., and D.G. Enos (2014). “Understanding the Environment on the Surface of Spent Nuclear Fuel Interim Storage Containers”, Probabilistic Safety Assessment and Management PSAM 12 (conference), Honolulu, Hawaii, June 2014.”

“Dunn, D.S. (2014). “Chloride-Induced Stress Corrosion Cracking Tests and Example Aging Management Program”, Presentation for U.S. Nuclear Regulatory Commission, at Public Meeting with Nuclear Energy Institute on Chloride Induced Stress Corrosion Cracking Regulatory Issue Resolution Protocol, August 5, 2014. <http://pbadupws.nrc.gov/docs/ML1425/ML14258A082.pdf>”

“Electric Power Research Institute (EPRI) (2014). Flaw Growth and Flaw Tolerance Assessment for Dry Cask Storage Canisters, EPRI Technical Report #3002002785, October 2014.”

“Kain, R.M. (1990). Marine atmospheric stress corrosion cracking of austenitic stainless steels. *Materials Performance* 29(12): 60.”

“Southern California Edison (2015h). “Projected Sea Level Rise Given the Project’s Design Service Life”, transmitted by e-mail from L. Anabtawi (SCE) to J. Street (CCC), September 17, 2015.”

“U.S. Nuclear Regulatory Commission (2014). “Summary of August 5, 2014, Public Meeting with Nuclear Energy Institute on Chloride Induced Stress Corrosion Cracking Regulatory Issue Resolution Protocol”, September 9, 2014. <http://pbadupws.nrc.gov/docs/ML1425/ML14258A081.pdf>”

Exhibit 4, page 2, caption to Figure 1:

“The space between the cylindrical storage modules is filled with a ~~flowable grout material~~concrete.”

Exhibit 5, page 1, addition to legend, with indicative coloring:

“If necessary, pumps within the NIA sump area would be relocated, not removed”

Exhibit 6, Figure 3 (Horizontal Acceleration), curve label:

“UMAX ISFSI Design Spectrum (PGA = ~~2.42~~ g 1.5 g in each direction”

Exhibit 6, Figure 4 (Vertical Acceleration), curve labels:

“UMAX ISFSI Design Spectrum (PGA = ~~2.42~~ g 1.0 g)”

“SONGS Design Basis Earthquake (PGA = ~~0.67~~ g 0.45 g)”

Staff Response to Comments

The below responses to public comments are recommended findings and would be incorporated into the relevant portions of the staff report as adopted findings.

In the attached correspondence, the commenters provide disparate perspectives on the proposed project and staff recommendation. A number of commenters, including Garry Bown (Orange County CoastKeeper), Jerome Kern (Oceanside City Council), David Lochbaum (Union of Concerned Scientists), Jack Monger (Industrial Environmental Association), Glenn Pascall (Sierra Club), Ted Quinn (Techonology Resources) and David Victor, Tim Brown and Daniel Stetson (SONGS Community Engagement Panel) express support for the staff recommendation. Southern California Edison (SCE), the applicant, offers several comments and multiple clarifications and technical corrections, but also supports the staff recommendation. A number of other commenters, including Michael Aguirre (Aguirre & Severson), Patricia Borchmann, Rita Conn (Let Laguna Vote), Donna Gilmore (San Onofre Safety), Gary Headrick (San Clemente Green), Charles Langley (Public Watchdogs), Marv Lewis, Ray Lutz (Citizens Oversight), Laura Lynch, Donald Mosier (Del Mar City Council), Dorah Shuey and Jane Swanson (San Luis Obispo Mothers for Peace) oppose the project and urge the Commission to deny SCE’s coastal development permit (CDP) application. The U. S. Marine Corps does not comment on the project itself, but argues that the Commission lacks jurisdiction to require or issue a CDP for development at the San Onofre Nuclear Generating Station (SONGS) site. Commission staff provides the following summary and response to the arguments made by commenters opposing the staff recommendation and hereby amends its proposed Commission findings to include these responses:

Comments Related to Geologic Hazards

Several commenters, including Ray Lutz, Dorah Shuey, Patricia Borchmann, and Jane Swanson, express concern that the proposed ISFSI could be undermined by shoreline erosion, fail during an earthquake, or be flooded during a tsunami or as a result of future sea level rise. Mr. Lutz and Ms. Swanson also noted that the groundwater table at the project site would be near the bottom of the ISFSI structure, and expressed concern that the ISFSI could be adversely affected by contact with groundwater during its period of emplacement.

As discussed at length in the September 25, 2015 staff report, Commission staff evaluated the vulnerability of the proposed project to geologic hazards, including earthquakes, erosion, and coastal flooding, and concluded that the proposed project, with the adoption of **Special Condition 2**, would minimize hazards to life and property and assure stability and structural integrity consistent with Section 30253 of the Coastal Act. No changes to the staff recommendation are proposed in response to comments regarding these hazards.

Commission staff also evaluated the hydrogeology of the project site and reviewed monitoring well data provided by SCE (SCE 2015b). At the two monitoring wells within the proposed ISFSI footprint, the water table elevation varies by approximately 0.7 feet above and below a mean elevation of about +5.4 feet MLLW, indicating that, at present, natural variability in the water table is not likely to bring groundwater into contact with the base of the concrete ISFSI foundation pad (at +7.5 feet MLLW). Increases in the water table elevation related to sea level rise could potentially lead to intermittent groundwater contact with the base of the ISFSI toward the end of the proposed 35-year life of the project. However, the design of the ISFSI is such that there are multiple barriers, including the 3-foot thick foundation pad and the steel cavity enclosure container (CEC), between the groundwater and the fuel storage casks, and limited contact with groundwater would not undermine the structural integrity of the ISFSI during the proposed project life. Furthermore, as a part of **Special Condition 2**, SCE would be required to evaluate current and future coastal hazards, including the effects of groundwater intrusion, as part of its CDP amendment application should it wish to retain the ISFSI in its proposed location beyond 2035.

Comments Related to Site Alternatives

Comments submitted by Michael Aguirre and Ray Lutz argue that SCE has not adequately explored alternative project locations off of the SONGS site. Mr. Lutz's comments include an extensive discussion of the benefits of siting the project away from the coast, and present a conceptual analysis of a hypothetical ISFSI site in the Mojave desert. In their comments, Ms. Gilmore and Ms. Lynch stated that the potential future alternative (discussed in the staff report) of relocating the ISFSI within the SONGS site would require a major expense and would greatly increase the current estimate of decommissioning costs.

As discussed in greater detail in the staff report, Commission staff has reviewed SCE's analysis of off-site alternatives and agrees with the conclusion that such alternatives are either unavailable or infeasible. No off-site federal permanent repository or private interim storage facility currently exists, and there is no prospect of such a facility becoming available in the near term. Nor is there another inland nuclear power plant with an existing ISFSI that is willing to or licensed to accept spent fuel from another site. Finally, there is no other site under SCE's control that is licensed for the siting of an ISFSI or at which an ISFSI could be developed in a reasonable period of time.

The staff recommendation is based on findings that the proposed project, as conditioned, would be consistent with Coastal Act policies related to geological hazards, the protection of marine and visual resources, and public access and recreation, excluding matters of radiological safety, and does not evaluate the potential cost of any future relocation of the ISFSI within the SONGS site. **Special Condition 2** requires that SCE evaluate the merits and feasibility (including costs)

of such alternatives as part of a CDP amendment application to retain, remove or relocate the ISFSI prior to the end of a 20-year term of approval.

Comments Related to ISFSI and Cask Safety & Radiological Issues

Comments submitted by Donna Gilmore, Laura Lynch, Gary Headrick, Donald Mosier, Dorah Shuey, Patricia Borchmann, Jane Swanson, Michael Aguirre, Rita Conn and Marv Lewis offer numerous arguments for why the proposed Holtec HI-STORM UMAX ISFSI and storage casks are inadequate or inappropriate for storing spent fuel at the proposed site. The main contentions of these comments are summarized below:

- (a) *The proposed underground system is unproven and experimental.*
- (b) *The 60-year design life and 100-year service life for the UMAX system claimed by SCE and Holtec are unsubstantiated; the Holtec warranty for the system is only ten years.*
- (c) *The proposed fuel storage casks are unsafe; stress corrosion cracking can be expected to occur in the stainless steel casks within 20 years.*
- (d) *Storage casks used in the existing ISFSI have been loaded since 2003, so SCE will need to have an aging management plan much sooner than 20 years from now.*
- (e) *The UMAX system configuration planned for SONGS has not been approved by the NRC; the NRC has only licensed a fully underground system using ½-inch thick fuel storage casks, not the partially-underground system and 5/8-inch casks proposed by SCE.*
- (f) *The proposed aging management program is inadequate, and the proposed casks cannot be repaired if damaged.*
- (g) *The NRC does not consider or require aging management in their initial 20-year license approvals.*
- (h) *High burn-up fuel to be stored in the proposed ISFSI could require up to 45 years of cooling prior to transport to permanent storage.*
- (i) *The Commission should not rely on vendor promises of future solutions for inspecting the casks in order to approve this project; there is already sufficient evidence that the proposed casks may not be transportable and maintainable to reject their use; the Commission should demand SCE use a proven system that can be inspected, maintained, monitored and transported, and that doesn't crack.*
- (j) *Thick-walled casks are available, and currently used in the U.S., that would provide superior performance in terms of safety and future transportability; the need to acquire a site-specific license to use such casks at SONGS is not sufficient grounds for rejection; the Commission should require SCE to use thick-walled casks as a special condition for approval.*
- (k) *Numerous past discharges of radioactive materials have occurred at SONGS; locating the ISFSI at the proposed site would make the area unsafe for public access.*
- (l) *SCE is considering loading Areva storage casks from the existing ISFSI into the new UMAX system.*

Without assessing the validity of these concerns, the Commission staff notes that the consequences of any failure, malfunction, or defects in the proposed ISFSI system are primarily a matter of radiological safety, which is under the exclusive jurisdiction of the federal Nuclear Regulatory Commission (NRC). The state is preempted from imposing upon operators of nuclear

facilities any regulatory requirements concerning radiation hazards and nuclear safety. Thus, the findings contained in the staff recommendation address only those state concerns related to conformity to applicable policies of the Coastal Act, and do not evaluate or condition the proposed project with respect to nuclear safety or radiological issues.

Staff's analysis indicates that the avoidance of long-term coastal erosion and flooding hazards at the project site (without resorting to shoreline armoring) is dependent on the ability to remove the ISFSI before it becomes vulnerable. At present, the integrity of the proposed ISFSI system is certified by the NRC for 20 years, providing assurance that the casks will be transportable, and the ISFSI system removable, within this timeframe. Commission staff believes that the 20-year duration of approval recommended in **Special Condition 2** is necessary to assure that potential future geologic hazards (and the need for shoreline protection) are avoided, is consistent with the 20-year certification of the HI-STORM UMAX system granted by the NRC, and does not impose any additional regulatory requirements concerning radiation hazards and nuclear safety.

SCE has informed Commission staff that SONGS fuel transported within a HI-STAR 190 transportation cask will require less than 15 years of cooling time starting from reactor shutdown in 2012, with even the most recently offloaded spent fuel ready for transport by 2027 (SCE 10/5/2015). Furthermore, fuel transport schedules contained in SCE's Irradiated Fuel Management Plan and Decommissioning Cost Estimate, both formal regulatory documents submitted to the NRC, indicate that all SONGS spent fuel can be transported offsite by 2049, 37 years after the 2012 reactor shutdown.

Commission staff is not aware of any plan to transfer older fuel storage casks from the existing ISFSI to the new system. This activity was not proposed in SCE's CDP application and would not be authorized by the proposed CDP.

U. S. Marine Corps Comments:

On October 1, 2015, Commission staff received a letter from the United States Navy and Marine Corps asserting that the Commission lacks jurisdiction to require or issue a CDP for development occurring on the SONGS site. The basis for the Navy and Marine Corps position is that under the Federal Coastal Zone Management Act (CZMA), land, "the use of which is by law subject solely to the discretion of ... the Federal Government, its officers or agents" is excluded from the definition of the coastal zone. (16 U.S.C. § 1453(1)).

The U.S. Supreme Court, however, has addressed this issue and determined that the CZMA does not pre-empt application of the California Coastal Act to private activities on federal land. It held that "[b]ecause Congress specifically disclaimed any intention to pre-empt pre-existing state authority in the CZMA, we conclude that even if all federal lands are excluded from the CZMA definition of 'coastal zone,' the CZMA does not automatically pre-empt all state regulation of activities on federal lands." *California Coastal Commission v. Granite Rock Co.* (1987) 480 U.S. 572, 593. Thus, under *Granite Rock*, the Commission retains the authority under the Coastal Act to require coastal development permits for non-federal activities taking place on federal land, such as Southern California Edison's proposed project pending before the Commission.

The U.S. Navy and Marine Corps support their argument that the Commission does not have coastal development permit jurisdiction on federal land by reference to an unpublished U.S. District Court decision, *Manchester Pacific Gateway v. California Coastal Commission* (2008 WL 5642245 (S.D. Cal.)). First, to the extent that the *Manchester* case is inconsistent with the Supreme Court holding in *Granite Rock*, the Supreme Court's decision in *Granite Rock* controls. Second, the *Manchester* case is factually distinguishable from the situation presented by the pending proposal from SCE. The *Manchester* case involved a Congressionally authorized public-private venture that resulted in the Navy obtaining new office space at no cost to the federal government. *Id.* at 1. The court acknowledged that the purpose of that project, as mandated by Congress, was to "provide for the use of private parties to accomplish the federal objective to construct Navy administrative facilities." *Id.* at 5. The project was authorized through legislation that spelled out the general parameters of the project and specifically authorized the project to be jointly developed by the Navy and the private developer. *Id.* at 6. Thus, the project was both a Navy and a private project.

The pending application from SCE does not involve a joint public-private venture. Thus, the facts are not analogous to those presented in the *Manchester* case. Thus, both under *Granite Rock* and due to factual distinctions between these facts and those raised in the *Manchester* case, the CZMA does not pre-empt the California Coastal Act here, and the Commission does have the jurisdiction to require a coastal development permit for the proposed development.

Finally, the Commission notes that the October 1, 2015 letter includes a statement, without elaboration, that the SONGS site is under exclusive federal jurisdiction where State law generally does not apply and the Commission only has jurisdiction over the SONGS site through the consistency provisions of the Coastal Zone Management Act. While the Commission does not disagree that it has jurisdiction over the SONGS site through the consistency provisions of the Federal Coastal Zone Management Act, the Commission finds that the singular statement in the October 1, 2015 letter neither establishes that the SONGS site is under exclusive federal jurisdiction where state law generally does not apply nor provides sufficient documentation, analysis or other supporting evidence.

**COASTAL HAZARD ANALYSIS AT
SAN ONOFRE NUCLEAR GENERATING STATION**

Part 2: Geological Hazards



for

SOUTHERN CALIFORNIA EDISON
P.O. Box 128, MS D3D
5000 Pacific Coast Highway
San Clemente, CA 92672

Coastal Environments, Inc.
2166 Avenida de la Playa, Suite E
La Jolla, CA 92037

CE Reference No. 22-03
31 March 2022

TABLE OF CONTENTS

| | |
|---|------------|
| EXECUTIVE SUMMARY | iii |
| 1.0 INTRODUCTION..... | 1 |
| 2.0 SEISMIC HAZARDS | 3 |
| 2.1 BACKGROUND – REGIONAL TECTONIC DEFORMATION | 3 |
| 2.2 GROUND SHAKING HAZARDS | 12 |
| 2.2.1 Seismogenic Faults..... | 12 |
| 2.2.2 Probabilistic Seismic Hazard Assessment..... | 13 |
| 2.2.3 Methods of the GeoPentech 2010 PSHA | 15 |
| 2.2.4 Seismic Sources..... | 16 |
| 2.2.5 Seismic Risk..... | 18 |
| 2.2.6 Coastal Fault System..... | 20 |
| 2.2.7 Hypothetical M_w 7.6 Scenario Earthquake..... | 23 |
| 2.3 GROUND FAILURE HAZARDS | 27 |
| 2.3.1 Surface Rupture..... | 27 |
| 2.3.2 Liquefaction | 27 |
| 2.3.3 Slope Stability | 28 |
| 2.3.4 Bearing Capacity | 31 |
| 3.0 REFERENCES..... | 32 |

LIST OF APPENDICES

| | |
|---|-----|
| Appendix A. SONGS ISFSI Slope Stability | A-1 |
| Appendix B. ISFSI Foundation Design..... | B-1 |

LIST OF FIGURES

| | |
|--|----|
| Figure 2-1. Map of complex geologic structure of Pacific-North America tectonic plate boundary..... | 4 |
| Figure 2-2. Potential seismic source map with updated UCERF3 faults in orange, and upper tips of detachments, black with hashes in dip direction | 8 |
| Figure 2-3. Southwest California historic earthquakes, 1850-2008 are Seismicity cross-sections with 15-mile wide buffers | 9 |
| Figure 2-4. SONGS with 1981-2019 magnitude $M > 2$ relocated earthquake positions..... | 10 |
| Figure 2-5. Earthquake swath profiles across the Inner Borderland offshore San Onofre | 11 |
| Figure 2-6. Thickness of late Quaternary sediments in the Inner Borderland between Dana Point and La Jolla | 17 |
| Figure 2-7. Comparison of hazard curves 2010 PSHA and 1995 PSHA | 19 |
| Figure 2-8. Map and photograph of paleoliquefaction sites exposed in a cut slope along Encinas Creek, Carlsbad | 22 |
| Figure 2-9. Photograph of paleo-earthquake fault rupture with liquefaction sand deposits covering 40,000-yr soil and fault scarp | 22 |

| | | |
|--------------|---|----|
| Figure 2-10. | Map of simplified fault rupture model for M_w 7.6 earthquake along the Coastal Fault System..... | 25 |
| Figure 2-11. | High-resolution 24-channel seismic profile of Newport-Inglewood fault uplift that blocks Quaternary paleochannels offshore Oceanside..... | 26 |
| Figure 2-12. | Plan view of West UMAX and NUHOMS ISFSIs | 30 |

EXECUTIVE SUMMARY

The coast of southern California lies within the active tectonic plate boundary between the oceanic Pacific plate and the continental North America plate. The San Andreas fault system represents the major strike-slip transform fault along this boundary, but tectonic deformation and complex fault zones cover a broad area across the Continental Borderland and Peninsular Ranges relevant to the San Onofre Nuclear Generating Station (SONGS). Geological hazards analyzed for the SONGS NUHOMS Independent Spent Fuel Storage Installation (ISFSI) include seismic hazards associated with earthquakes, ground failure, surface rupture, liquefaction, slope stability, and bearing capacity.

Background Studies

Decades of geological research sponsored by Southern California Edison (SCE) in the SONGS area have provided a good understanding of the active deformation of this complex region to assist in safe design and construction of facilities at SONGS, including the NUHOMS ISFSI. These investigations recognized the right-lateral Newport-Inglewood-Rose Canyon (NIRC) strike-slip fault zones as critical features that control the earthquake hazard at SONGS. The Design Basis Earthquake DBE for SONGS was set at 0.67g (gravitational acceleration). This estimate was based on a 7.0 magnitude earthquake.

The Oceanside blind thrust low-angle fault system (OBT) shows deformation characteristic of strain reversal, proceeding from prior extension to present-day contraction with blind thrust faulting. Seismic hazard assessments based on the strike-slip faulting of the NIRC were adjusted to include the potential for large blind thrust earthquakes, similar to events observed elsewhere in California (GeoPentech, 2010).

SCE in conjunction with scientists at the Southern California Earthquake Center (SCEC) worked together to develop a more comprehensive earthquake hazard model with the numerous active faults mapped in the past 10-15 years. The Unified California Earthquake Rupture Forecast, version 2 (UCERF2), was the basis for the report provided by GeoPentech (2010). The research continued as SCE held several workshops from 2011 to 2013 and SCEC updated the comprehensive model to UCERF3 to specifically address the multi-fault rupture earthquakes.

Probabilistic seismic hazard assessments (PSHAs), based on the early models, predicted substantially more moderate (M5.5-6.5) earthquakes than were recorded in the seismicity records. Increasing the maximum magnitudes in the model afforded by multi-fault rupture scenarios produced better agreement with the historical earthquake records. With fewer moderate, but relatively frequent earthquakes in the model, the expected peak ground acceleration (PGA) values dropped from 0.31g for the NIRC to about 0.23g at the 475-yr return period (10% exceedance in 50 years). Consequently, the 1.5g design value remains conservative for shaking hazard at the ISFSI.

Recent Work

In the past decade, additional large complex earthquakes struck, including the 2014 MW7.2 El Mayor-Cucapah (Baja California) and MW7.8 Kaikōura (New Zealand) earthquakes that involved combinations of strike-slip and low-angle faults (detachments and subduction thrusts) that produced extreme levels of deformation and strong ground motions. The complex fault rupture pattern of the Kaikōura earthquake resembles the complex faulting in the Coastal Fault System, dominated by the strike-slip NIRC and including the San Mateo, San Onofre, and Carlsbad faults all underlain by the OBT and Thirtymile Bank Detachment.

In 2022, Coastal Environments analyzed a large hypothetical 7.6 magnitude earthquake model at SCE's request to evaluate the worst-case seismic hazards at SONGS. The hypothetical modeled earthquake exceeds previous maximum magnitude events (M7.0-7.3) considered for SONGS design and could produce greater damage, including tsunami inundation. However, the large magnitude events are extremely rare, with return periods estimated at about 10,000 years. This exceeds the 7,143 year recurrence of the Design Basis Earthquake (DBE) for SONGS Units 2 and 3, having a peak ground acceleration of 0.67g. For the design of the NUHOMS ISFSI in 2001, a much higher 1.5g peak ground acceleration (considerably higher than the NRC-approved SONGS DBE criteria) was selected to ensure that seismic design basis did not underestimate the seismic risk at the site. Consequently, the existing 1.5g peak ground acceleration established for the ISFSI design remains conservative for the seismic hazards identified for the SONGS site, even in light of new modeling that accounts for recent earthquake information.

With respect to liquefaction hazards, the SONGS ISFSIs are built on dense, well-consolidated sands of the San Mateo Formation, which extend about 900 feet below the ISFSI site (SCE, 1995; GEI, 2015), and are considered to be at low risk of seismically-induced liquefaction. Ground water measurements at the ISFSI site were at elevation 5.03 ft. MLLW in 2020, or about 14.72 feet below the NUHOMS concrete support pad. Even under the extreme hypothetical H++ sea level scenario (+2.80 ft MSLR by 2050), groundwater under the ISFSI site is still projected to remain about 11.92 feet below the NUHOMS ISFSI support pad and will not affect the previous Coastal Commission findings that subgrade under the support pad is stable with respect to bearing capacity and liquefaction.

With respect to slope instability, the slopes north of the NUHOMS ISFSI are about 105 feet away from the ISFSI's spent fuel canisters. Hinkle (2007) found that when conservatively assuming a slope failure during a design seismic or a tsunami event, the anticipated slope run-out distance of the adjacent slope is about 91 ft. Therefore, any slope failures from the north bluff would not result in run-out that comes closer than about 15 feet away from the ISFSI. Accordingly, the previous findings by the Coastal Commission related to stability of the slopes adjacent to the NUHOMS ISFSI and potential effects on the project remain valid.

As part of this analysis, Coastal Environments has reviewed the 2001 and 2015 SONGS ISFSI Coastal Development Permit (CDP) and staff report materials and found that the Coastal Commission's conclusions in those reports remain correct.

COASTAL HAZARD ANALYSIS AT SAN ONOFRE NUCLEAR GENERATING STATION

Part 2: Geological Hazards

1.0 INTRODUCTION

The objective of this study is to update the seismic hazard analysis for the San Onofre Nuclear Generating Station (SONGS) and to evaluate the most recent current available geologic, seismic, and ground motion information in the vicinity of SONGS to determine their impacts on the NUHOMS Independent Spent Fuel Storage Installation (ISFSI). We have reviewed newly published reports, papers, and data regarding geological, geophysical, and seismic hazards along the coast of southern California.

SONGS is located on an elevated coastal plain in San Diego County, California, about 18 km south of Dana Point and 24 km north of Oceanside. The site is adjacent to the north end of San Onofre State Beach at the northwest corner of Marine Corps Base Camp Pendleton (MCBCP). The ISFSI is located in the North Industrial Area (NIA) where the decommissioned SONGS Unit 1 was located before its deconstruction in 1999. The ISFSI is constructed on a pad cut into the former Pleistocene marine terrace deposits and underlying Pliocene San Mateo Formation of marine sandstone and conglomerate beds. The ISFSI is planned to store spent nuclear fuel until 2050, by which time the U.S. Department of Energy (DOE) is expected to take custody of the spent fuel for permanent storage at as yet an undetermined location.

In this report, we review the advancements in understanding of active faulting that determine earthquake potential at San Onofre. Changes in seismic hazard estimates over the past two decades are discussed, and new information presented and compared with previous studies. According to the California Coastal Commission staff report (CCC, 2001), *“Within Southern California Edison’s proposed 35-year timeframe, the siting and design of the ISFSI would be sufficient to assure stability and structural integrity against geologic hazards ..., without requiring shoreline protection.”*

Geological hazards at the ISFSI include earthquake hazards, slope movement or failures (landslides) along the coastal bluffs and inland natural and cut slopes, coastal erosion, sea level rise, and coastal flooding from storm surge or tsunami. Seismic hazards are discussed in Chapter 2. These hazards include earthquake fault rupture, strong ground motion (shaking), and secondary ground failures – liquefaction, landslide, and tectonic fractures such as tectonic uplift or subsidence.

Regional tectonic deformation is described in Section 2.1. An important observation is that the Pacific plate has always been moving away from the North America plate in California, resulting in a highly complex network of faults and extensional rifts along the continental margin, both on land and offshore. In addition, the San Andreas fault system and the California Continental Borderland also include numerous strike-slip and extensional “normal” faults.

Section 2.2 discusses ground shaking hazards. Ground shaking is dependent on earthquake magnitude, distance from the fault rupture and its direction of propagation, and soil conditions. Secondary ground failures, including liquefaction of susceptible materials, or slope failures could be induced in areas of strong shaking. Evaluating these hazards probabilistically depends on characterizing the processes that produce these risks, including seismogenic faults and their sources.

In Sections 2.2.5 and 2.2.6, we discuss seismic risk and the Coastal Fault System in the vicinity of San Onofre. New research has increased the likelihood estimation of large ($M > 7$) magnitude earthquakes and determined these to be, on average, 10,000-year events. Simultaneously, this work has shown that moderate quakes ($M 5-7$) are less frequent to occur than previously thought.

Section 2.3 concerns seismic ground failure, summarizing surface rupture and liquefaction risks, and slope stability and bearing capacity relevant to the SONGS ISFSI. We determine that large, but low probability multi-fault earthquakes may produce subsurface fractures, but that the rigid ISFSI construction will reduce impacts from such effects. We also show that horizontal and vertical shaking is within the original design parameters of the ISFSI. Additionally, the nearest slopes are sufficiently distant to pose no direct hazard, and that the underlying bearing capacity is more than sufficient to support the ISFSI as designed.

Chapter 3 presents an extensive list of references cited in this study, including pertinent papers published from 2015-2021.

2.0 SEISMIC HAZARDS

SONGS is located along the coast of southern California between Dana Point and Oceanside on the northwest end of MCBCP. Seismic hazards that may affect the ISFSI at SONGS include earthquake fault rupture, strong ground motion (shaking), and secondary ground failures – liquefaction, landslide, and non-tectonic fractures. In addition, tsunami induced by tectonic or landslide deformation offshore in the adjacent California Continental Borderland or from tectonic or volcanic activity around the Pacific “Ring-of-Fire” may be destructive to coastal structures. Tsunami hazards are discussed further in Part III Tsunami Hazards.

2.1 BACKGROUND – REGIONAL TECTONIC DEFORMATION

Earthquakes are the result of tectonic deformation, which can create major geographic features including mountain ranges or ocean basins. In southern California, tectonic deformation is controlled by the Pacific-North America transform fault plate boundary and faults of the San Andreas fault system (Atwater, 1970; Lonsdale, 1991; Atwater and Stock, 1998). The crust along the western edge of North America has been sliced by many faults that were active during different time periods of the plate boundary evolution. The former trench at the Patton Escarpment was the major subduction shear zone where the ancient Farallon oceanic plate was thrust beneath the North American continent. Broad-scale overview of these features and relative plate motions is illustrated in Figure 2-1.

About 30 million years ago, the East Pacific Rise seafloor spreading center reached the edge of North America. This seafloor spreading ridge was segmented in a zig-zag configuration with extensional rifts separated by oceanic transform faults. The resulting strike-slip transform fault interaction with the North American continent grew outward with the Mendocino transform fault triple junction moving to the north past San Francisco and the Rivero extensional rift triple junction moving south past Baja California. Some blocks of ancient Farallon oceanic crust were captured as microplates (Nicholson *et al.*, 1994) along with the western edge of North America continental crust to join the Pacific Plate on its northwest trek towards Alaska.

An important observation is that the Pacific Plate has always been moving away from the North American continental margin in California. The resulting complex network of faults includes strike-slip and extensional rift zones created along the continental margin above the former subduction mega-thrust as the San Andreas transform fault system evolved. The California Continental Borderland formed as a major rift area that includes numerous strike-slip faults in addition to the extensional “normal” faults.

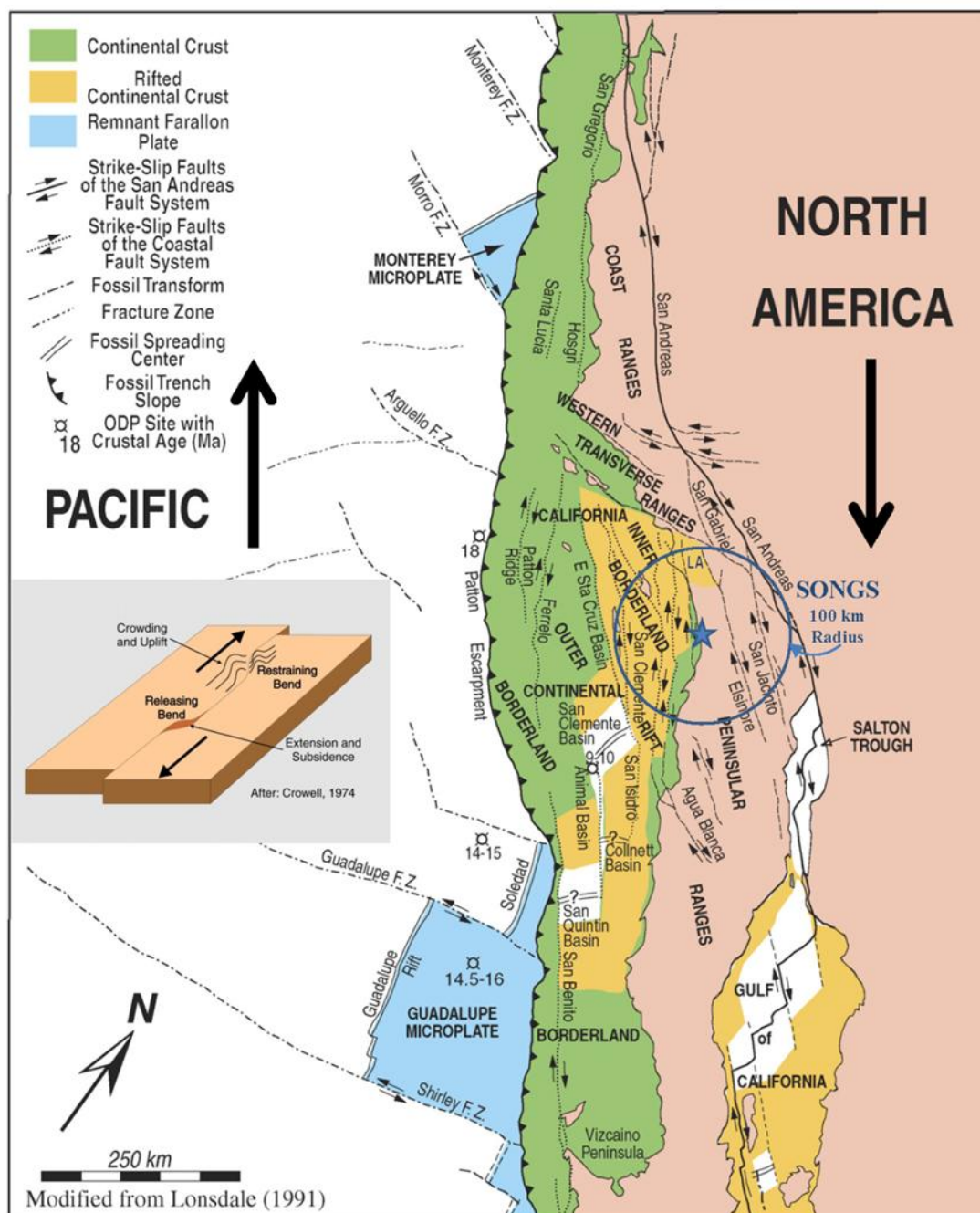


Figure 2-1. Map of complex geologic structure of Pacific-North America tectonic plate boundary (green and yellow areas are offshore). San Onofre near middle of broad shear zone accommodating Pacific-North America relative plate motion.

The San Andreas and other major northwest-trending faults along the plate boundary are right-lateral strike-slip faults that accommodate the northwest translation of the Pacific oceanic plate relative to the North America continental plate. Complications in the geometry and rheology (mechanical properties) of the crust along the plate boundary produce zones of oblique-deformation where combinations of horizontal strike-slip and vertical displacements occur on faults with varying orientations. Fault surfaces with strike or dip directions that deviate from the predominant northwest-trending vertical strike-slip fault surfaces produce oblique-deformation. In particular, a major westward bend of the San Andreas fault zone in southern California creates a restraining fault geometry where crustal material converges and produces vertical deformation (Crowell, 1974).

Uplift of the Transverse Ranges and down-welling of crustal material into the mantle produce crustal thickening to accommodate the horizontal shortening. The strike-slip faults of the region have numerous restraining bends, where convergence produces crustal uplift (transpression), and releasing bends or stepovers, where divergence, produces crustal subsidence (transtension, Figure 2-1).

The complex deformation is evident offshore where the former subduction zone was replaced by a Miocene oblique-rift – the Inner Borderland located between the fault zone west of San Clemente Island and the coast (Moore, 1969; Legg, 1991; Crouch and Suppe, 1993; Bohannon and Geist, 1998). The collision of the Inner Borderland with the Western Transverse Ranges enhances the oblique-slip with transpression offshore southern California (Sorlien *et al.*, 2016) whereas transtension persists offshore northwest Baja California (Legg, 1985; 1991; Legg *et al.*, 1991). Within the continent to the east, the Salton Trough and Gulf of California maintain a system of right-lateral transform faults that link nascent and growing seafloor spreading centers (Lonsdale, 1991) to accommodate the northwest translation of the Baja California and Borderland microplates along with the Pacific oceanic crust.

Other important active right-slip faults, with northwest trends parallel to the Pacific-North America relative plate motion, include the San Jacinto and Elsinore faults onshore, and the San Clemente and San Diego Trough faults offshore illustrated in Figure 2-2. The GeoPentech's (2010) report's Figure 3-7 has been modified to include a subsequent update (#3) of the Unified California Earthquake Risk Forecast (UCERF3, 2013)¹. Although SONGS is located near the center of the broad Pacific-North America transform plate boundary, it lies on the edge of a relatively stable crustal block consisting of the Peninsular Range granitic crust with the nearest Type A² fault located 22 miles northeast across the Santa Margarita and Elsinore Mountains.

The faults along the San Andreas transform fault system are numerous and sustain widely-varying geometry and slip character. Although most of the active strike-slip faults are vertical, the dip-slip and oblique-slip faults have dips that span the full range from vertical to nearly horizontal, including nearly flat-lying detachments associated with Miocene rifting,

¹ UCERF updates are numbered.

² Type A, B, and C faults are USGS and California Geological Survey definitions. A=very active and well-defined, slip rate >5 m/yr; B=active and well-defined but slower or unknown slip rate; C=faults that are known or thought to exist, but have poor data to define their traces or activity, which includes many offshore faults.

roughly 10-20 million years ago (Ma). Consequently, the character of deformation and earthquake potential affecting the SONGS site is complicated. The distribution of historic earthquake sequences provides a direct indication of where active faulting exists (Figure 2-3). Faults located within 60 miles of the site are considered in this seismic hazard assessment.

Additional faults have been identified and mapped since the 2010 analysis, including steep strike-slip and reverse faults (Figure 2-3, orange), as well as the low-angle detachments that may be reactivated as blind thrust faults (gray with hachures). Historic earthquakes show that the fault activity is clustered along major faults, but also includes widespread events located between mapped faults. In areas of convergence, including the Transverse Ranges, blind thrust faults produce broad aftershock distributions where no surface faults are mapped, as for example during the 1994 $M_w6.7$ Northridge earthquake (Teng and Aki, 1996). Relocation of seismicity using advanced methods (waveform cross-correlation) and 3D seismic velocity models provides a more accurate representation of active faulting below the surface (Figure 2-4).

Decades of careful research have compiled reasonably accurate descriptions of the hazard potential in the San Onofre region (e.g., GeoPentech, 2010). Hazard estimates are updated as results from new research unearth additional details of the complex tectonic environment.

Black lines (Figure 2-4) show locations of a portion of the exploration industry seismic profiles available through the U.S. Geological Survey USGS NAMSS database (Treizenberg *et al.*, 2016). The 1933 $M_w6.3$ Long Beach earthquake ruptured the mapped Newport-Inglewood-Rose Canyon (NIRC) fault zone (Hauksson and Gross, 1991). In contrast, the offshore 1986 $M_s5.8$ Oceanside earthquake involved a complex zone of subseafloor faults that included a low-angle detachment “blind thrust” (Hauksson and Jones, 1988; Astiz and Shearer, 2000). Cross-sections of earthquake hypocenters (3D locations) in Figure 2-5 show the complex vertical distribution of the earthquakes (Legg, 2021).

Relocation of the hypocenters (Latitude, Longitude, Depth coordinates) for events recorded since 1981 used advanced waveform cross-correlation techniques (Hauksson *et al.*, 2012) and 3D seismic velocity models (Hauksson, 2000) to provide more accurate images of earthquake distributions in the southern California crust (Figures 2-4 and 2-5). The solid dots show the most accurate relocations and red symbols have the best depth estimates. These 3D earthquake locations show that both vertical (predominately strike-slip) and moderate-to-low angle faults (possible blind thrusts) are seismically-active offshore southern California. It also appears that some earthquakes occur very deep in the crust and possibly within the upper mantle (below MOHO³).

This report reviews the advancements in understanding the active faulting that determines the earthquake potential affecting the SONGS site. Changes in seismic hazard estimates over the two decades since the 2001 study, are discussed, and new information is provided to compare with the previous investigations. In particular, recent large, complex, multi-fault, earthquake ruptures provide important evidence for the severity of earthquake hazards in California and elsewhere around the world. Deformation observed in excavations along the North San Diego County coastal zone is consistent with large prehistoric earthquakes in the San Onofre region

³ Mohorovičić discontinuity (MOHO) is the boundary between the crust and the mantle in the earth.

(Kuhn, 2005). The Southern California Earthquake Center (SCEC) has led much of the research for such events in California and works closely with SCE and consultants responsible for evaluating these hazards and designing damage mitigation strategies.

The updated UCERF3 was published after the GeoPentech (2010) report, and SCEC, working with the USGS and National Science Foundation, continue to update the Community Fault Model (CFM) used for comprehensive assessment of earthquake hazards in California. Another update of the SCEC CFM and USGS Quaternary Fault Model used for the National Seismic Hazard Mapping Program is also planned (S. Marshall, 2022, Personal Communication).

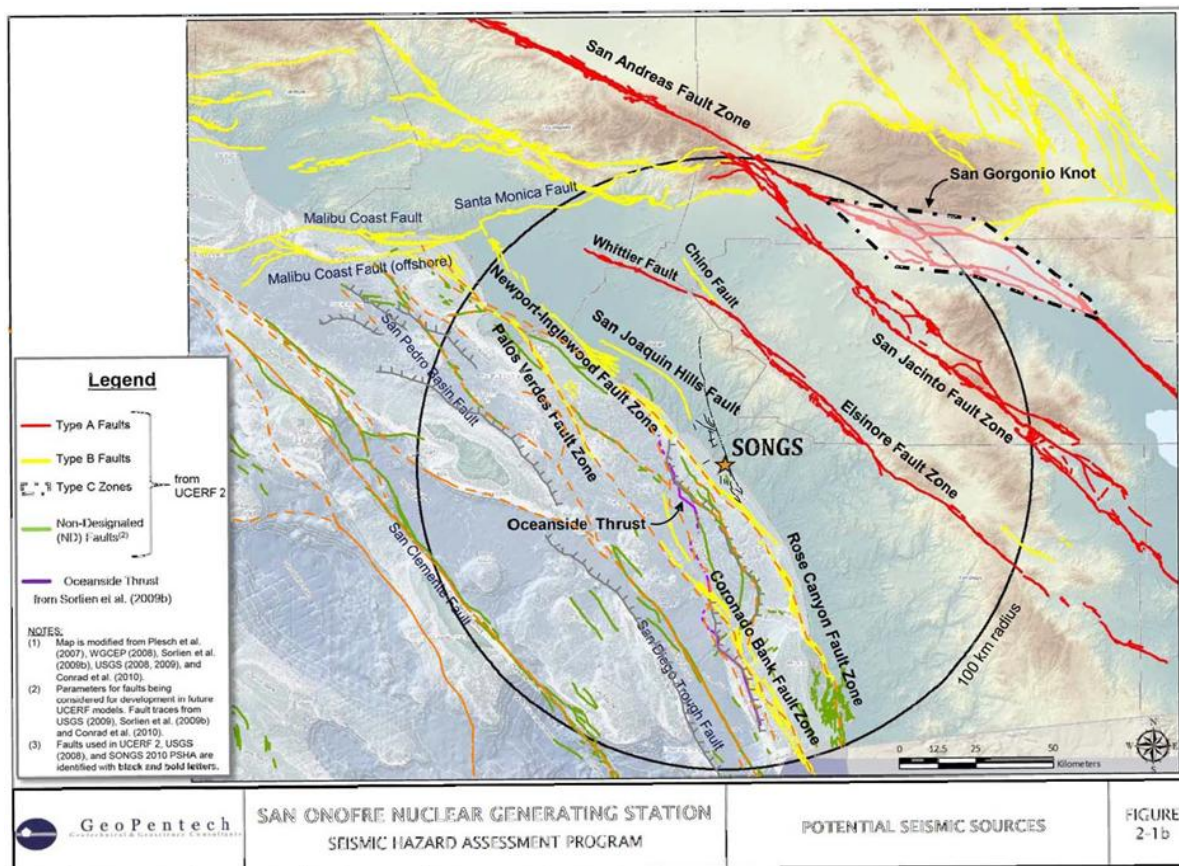


Figure 2-2. Potential seismic source map (GeoPentech, 2010) with updated UCERF3 faults in orange, and upper tips of detachments (Sorlien *et al.*, 2015), black with hashes in dip direction.

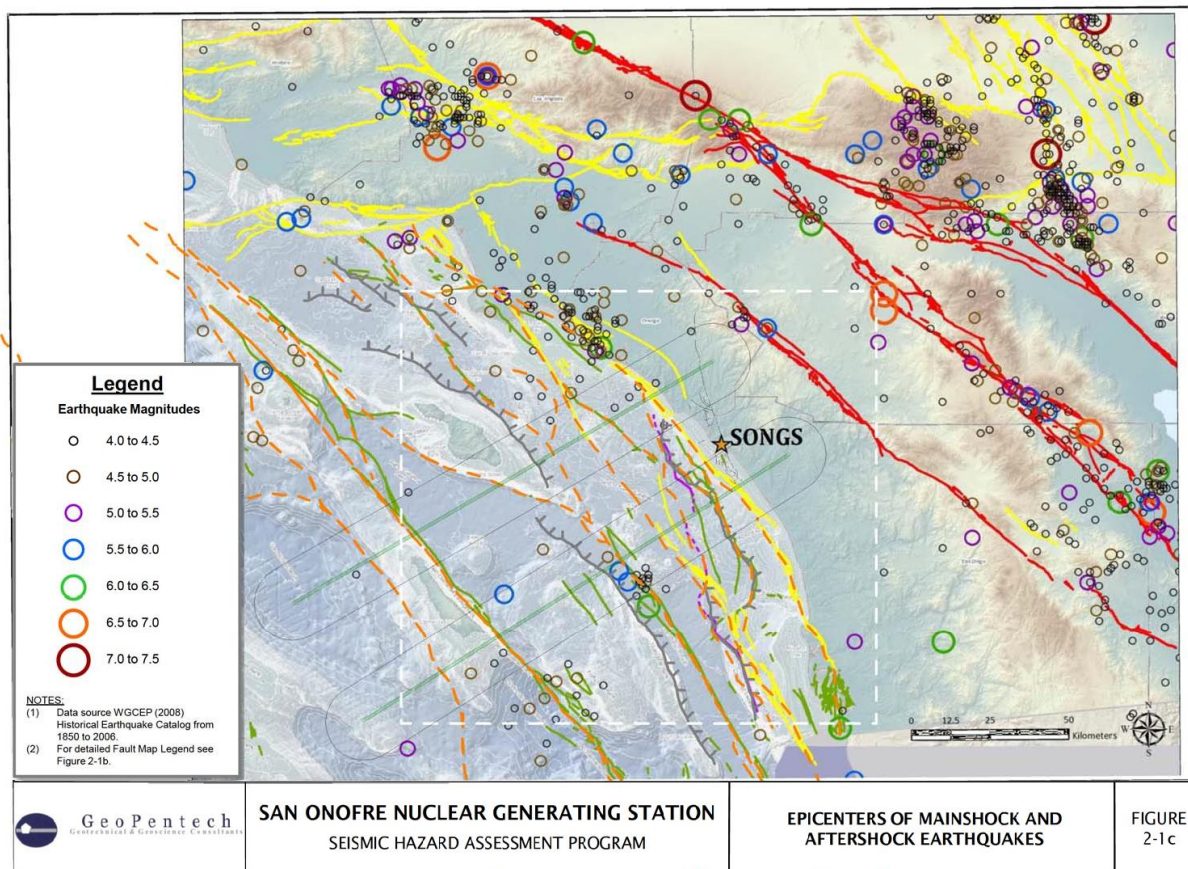


Figure 2-3. Southwest California historic earthquakes, 1850-2008 (GeoPentech, 2010) are Seismicity cross-sections (green lines) with 15-mile wide buffers (Legg, 2020).

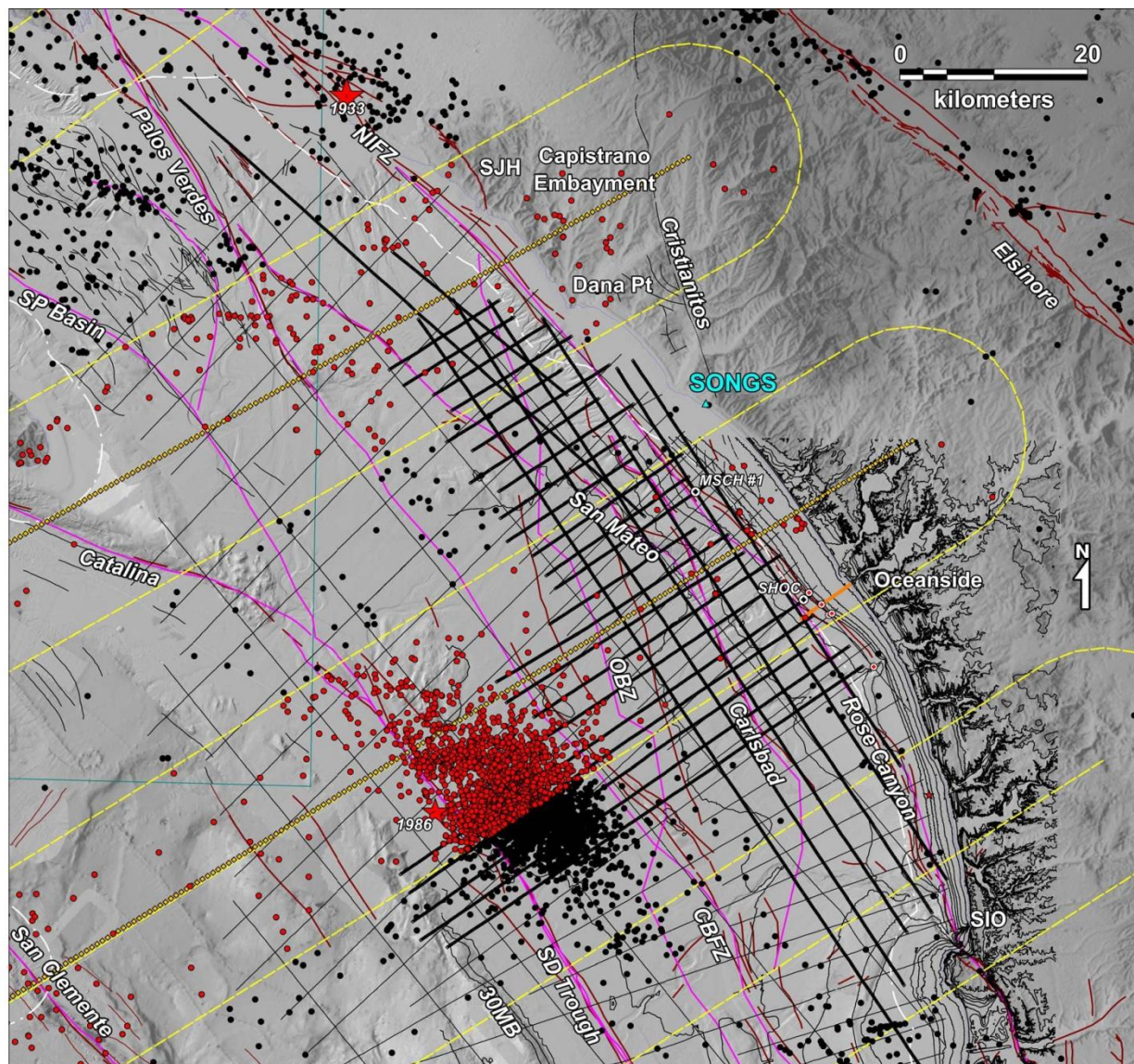


Figure 2-4. SONGS with 1981-2019 magnitude $M > 2$ relocated earthquake positions. Earthquake data from Hauksson *et al.* (2012), red dots in cross-sections.

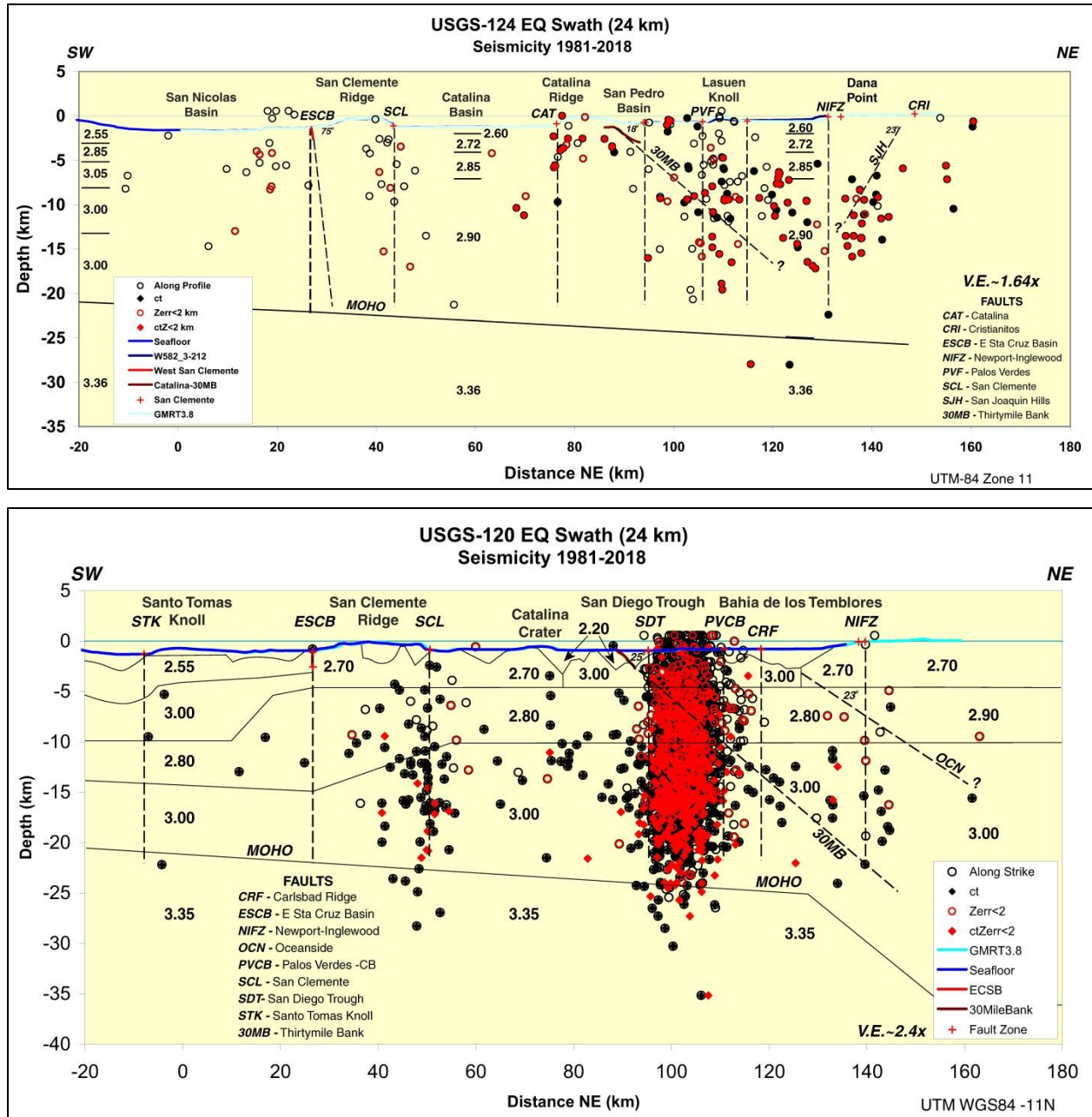


Figure 2-5. Earthquake swath profiles across the Inner Borderland offshore San Onofre. Data from Hauksson *et al.* (2012), upper, and 2019 update, lower.

2.2 GROUND SHAKING HAZARDS

Fault rupture and slip in the brittle upper crust produce seismic waves that propagate through the earth and along the surface to great distances from the source fault(s). Strong ground shaking may damage buildings and other structures and produce ground failure, including surface fault rupture with offset of the ground and structures across the active fault zone. Secondary ground failures including liquefaction of susceptible materials below the ground surface or failure of slopes may be induced in areas of strong shaking. For seismic hazard assessment, identification of faults in the region that may produce potentially damaging earthquakes (*seismogenic* faults) must be identified, mapped, and characterized for estimation of earthquake effects (Figure 2-2).

Ground shaking hazard is dependent upon the *magnitude* of the earthquake; *distance* of the site from the fault rupture; *direction* of propagation for the fault rupture (*directivity*); and, for the seismic waves, *geologic conditions* along the seismic wave path, *local soil conditions* for wave amplification, and possible *resonant basin effects* (Kramer, 1996). Mathematical formulations called *attenuation relationships or ground motion prediction equations* (GMPE), based on empirical data from historic earthquakes, are used to estimate the expected shaking levels for earthquake scenarios using the modeled fault surfaces, measured distance from the fault to the site, and amplification factors for the site-specific soil conditions.

Seismic waves propagate at a wide range of frequencies, from short-period compressional waves (*P-waves*) to moderate and long-period shear waves (*S-waves*), which propagate through the crust (*body waves*). Long period surface waves propagate along the earth surface and attenuate at slower rates than body waves. Shear waves and surface waves produce strong horizontal accelerations that cause damage to structures built to withstand mainly vertical gravity forces but may lack strength to withstand these horizontal forces.

Buildings and other structures respond differently to earthquakes according to the natural resonant frequency of the structure and the type of waves. P-waves travel fastest and arrive first, followed by shear waves and long-period surface waves, which tend to produce greater shaking amplitudes. Attenuation relationships account for all types of waves but are based upon the maximum amplitudes recorded during earthquakes at each observation site. Digital recordings of the seismic waves from earthquakes are processed to create response spectra – charts of amplitude versus wave frequency, which can provide important information for structural engineering design and damage assessment. The Probabilistic Seismic Hazard Assessment (PSHA) considers several response spectral periods (inverse of frequency) that are relevant to the structures of concern. For critical structures, a fully dynamic earthquake rupture and seismic wave propagation model can be used to produce realistic earthquake strong-motion time-histories (*seismograms*) to evaluate structural response to earthquakes.

2.2.1 Seismogenic Faults

Numerous faults have been mapped in the SONGS coastal and offshore region that are aligned with the northwest trend of the coast and the Pacific-North America transform plate boundary (Clarke *et al.*, 1987; Fischer and Mills, 1991; Plesch *et al.*, 2007; Maloney *et al.*, 2016; Sorlien *et al.*, 2016; Sahakian *et al.*, 2017; Conrad *et al.*, 2019). The most prominent coastal fault

zone is the NIRC mapped from Santa Monica to San Diego Bay and continues south along the northern Baja California coast as far as the Agua Blanca fault at Punta Banda, offshore Ensenada (Legg, 1985; Legg *et al.*, 1991; Ryan *et al.*, 2009). The Palos Verdes, Coronado Bank (CBFZ), San Diego Trough and San Clemente fault zones are other prominent faults within 60 miles offshore from San Onofre. Few Quaternary faults are located onshore in the coastal region between Dana Point and Oceanside. The prominent N18°W-trending Cristianitos fault crosses the shoreline about one mile southeast of San Onofre (Ehlig, 1979; Shlemon, 1987). The Elsinore fault is located about 25 miles east of San Onofre and represents one of the more significant active faults in southern California (Kennedy, 1977; Jennings, 1994). It was considered in the seismic hazard assessments for construction of the power plant (GeoPentech, 2010) and ISFSI.

Immediately offshore of SONGS is the South Coast Offshore section of the Newport-Inglewood fault zone, which links with the Rose Canyon fault zone forming a major *Coastal Fault System* (Legg, 1985; Legg, 1991; Grant and Rockwell, 2002; Legg *et al.*, 2018) that reaches from the Los Angeles Basin to Bahía Todos Santos in northern Baja California. A *fault system* is a collection of faults and fault zones that interact to accommodate tectonic plate motion. For example, the San Andreas Fault System comprises all of the major faults and fault zones along the Pacific-North America transform plate boundary in California (Wallace, 1990). The San Mateo, Carlsbad, and San Onofre fault zones (Conrad *et al.*, 2019) appear connected with the NIRC in the Coastal Fault System forming a complex zone of tectonic deformation that includes horizontal strike-slip and oblique reverse-slip on non-vertical faults. Seismic reflection profiles provide the major data used to map this submerged fault zone, but few deep penetration exploration industry profiles (Figure 2-4, reprocessed data, thick black lines) exist within the California State Lands boundary (Maloney *et al.*, 2016). Consequently, the deep structure of this fault zone is poorly known near the coast just offshore of the ISFSI.

Accurately located hypocenters of seismicity shown in Figures 2-4 and 2-5 recorded by the Southern California Seismograph Network (SCSN), show the complicated spatial distribution of seismicity associated with the complex array of shallow fault traces mapped in the area. Major clusters of seismicity span 3-6 mile wide swaths between mapped faults as seen in the area of the 1986 M_{5.8} Offshore Oceanside earthquake sequence (Hauksson and Jones, 1988; Astiz and Shearer, 2001; Legg *et al.*, 2015). A somewhat narrower northwest alignment of epicenters exists along the Newport-Inglewood fault zone where the 1933 M_{6.2} Long Beach earthquake initiated (Hauksson and Gross, 1991).

2.2.2 Probabilistic Seismic Hazard Assessment

A Seismic Hazard Assessment (SHA) considers all earthquake sources within about a 60-mile radius that may produce surface fault rupture, strong shaking, secondary ground failures including liquefaction and slope failure, and tsunami generation in coastal areas. Two analysis techniques are used in an SHA: (1) deterministic analysis, which models specific earthquake scenarios to estimate the maximum effects of large earthquakes at a site, and (2) a Probabilistic Seismic Hazard Assessment (PSHA), which is used to account for uncertainty in the levels of hazard that may be produced from many different potential earthquakes on numerous faults with different frequencies of earthquake production. In complex areas of tectonic deformation, along broad tectonic plate boundaries as exist in southern California, fault zones or systems with

multiple fault segments and zones must be considered carefully. GeoPentech (2010) produced a thorough SHA at the SONGS facility based on the Unified California Earthquake Rupture Forecast, Version 2 (UCERF2, WGCEP, 2008). This analysis was “state-of-the-art” and used fault and recurrence models available at that time.

Subsequent investigations provided new or updated data based on reprocessing and interpretation of existing exploration industry Multichannel Seismic Reflection Profiling (MCS) data, acquisition of new high-resolution, moderate-to-shallow penetration (upper kilometer) MCS data, and digital single-channel seismic data (Sorlien *et al.*, 2015; Maloney *et al.*, 2016; Sahakian *et al.*, 2017; Conrad *et al.*, 2019; Holmes *et al.*, 2021). Completion of the third version of the Unified California Earthquake Prediction Model (UCERF3, 2013) included three deformation models to reduce uncertainties in the time-independent source model. The three models were based on kinematically-consistent inversions of geodetic and geologic data, which helped provide some constraints on slip rates for faults lacking geologic data.

Alternate models, including multi-fault ruptures, were considered in the inversion. Continuous acquisition of digital seismograms for southern California regional earthquakes expanded the historical event database with more accurate locations and magnitudes. Relocation of the hypocenters (Latitude, Longitude, Depth coordinates) for events recorded since 1981 used advanced waveform cross-correlation techniques (Hauksson *et al.*, 2012) and 3D seismic velocity models (Hauksson, 2000) to provide more accurate images of earthquake distributions in the southern California crust (Figures 2-4 and 2-5). Interpretations made in 2010 require reviews and updates to incorporate the greater knowledge obtained in the past decade necessary for more accurate evaluation of the seismic hazard at the site.

The *Strike-slip Seismic Source Characterization Model* for the NIRC fault zone (section 2.1, GeoPentech, 2010) is based on the wrench tectonics mode of deformation (Wilcox *et al.*, 1973; Sylvester, 1984; 1988). As stated by GeoPentech: “*This theory is compatible with the presence of shorter, shallower dipping, normal and thrust subsidiary faults in a system dominated by high--angle, through-going primary strike-slip fault.*” The wrench tectonics model has been used successfully to predict or interpret structure at depth for petroleum exploration. However, proper application of the theory requires careful consideration of boundary and initial conditions in the model. Existing geologic structure resulting from a prolonged (20-100+ million years) tectonic evolution of the Pacific and North America plate boundaries that involved subduction and oblique -rifting before creating the current transform plate boundary dominated by the onshore San Andreas strike-slip fault.

Active faults within the San Andreas fault system include the full range of tectonic deformation styles-low-angle thrusts (blind or surface breaching), moderate to low-angle normal faults (Basin-and-Range, Continental Borderland), and both parallel and oblique strike-slip faults (San Andreas, San Jacinto, Elsinore, San Clemente, San Diego Trough, Newport-Inglewood). Initially considered the South Coast Offshore fault zone (Barrows, 1974; Ehlig, 1977), 50 years of investigation led to recognition of the Coastal Fault System as a combination of high-angle strike--slip, oblique-reverse, and low-angle detachment faults (Clarke *et al.*, 1987; Fischer and Mills, 1991; Rivero *et al.*, 2000; Ryan *et al.*, 2009; Rivero and Shaw, 2011; Sorlien *et al.*, 2016; Maloney *et al.*, 2016; Sahakian *et al.*, 2017; Conrad *et al.*, 2019).

Seismicity demonstrates the activity of numerous faults within this complex zone of deformation (Figures 2-3 and 2-4, Legg, 1980; Legg, 1987; Nicholson and Crouch, 1989; Legg and Kennedy, 1991; Grant and Shearer, 2004; Legg, 2021). Fault interaction within this fault system may produce large, complex, multi-fault, multi-segment, earthquakes (Legg *et al.*, 2018). Both horizontal strike-slip and vertical dip-slip components result to accommodate the northwest translation of the Pacific Plate with its Borderland and Baja California captured microplates (Figure 2-1) along the continental margin.

2.2.3 Methods of the GeoPentech 2010 PSHA

Ground shaking hazard is dependent upon the magnitude of the earthquake, distance of the site from the fault rupture, direction of propagation for rupture and seismic waves, geologic conditions along the seismic wave path (ray path), local soil conditions for wave amplification, and possible resonant basin effects (Kramer, 1996). Mathematical equations called *attenuation relationships*, based on empirical data from historic earthquakes, are used to estimate the expected shaking levels for earthquake scenarios using the modeled fault surfaces, distance from the fault to the site, and amplification factors for the site-specific soil conditions. A new generation of Ground Motion Prediction Equations (GMPE), (Abrahamson and Silva, 2008; Boore and Atkinson, 2008) were used for the 2010 investigation. Development of improved GMPE has continued based on additional data from recent California and global earthquakes.

Seismic waves propagate at a wide range of frequencies, from short-period compressional waves (P-waves) to moderate and long-period shear waves (S-waves) and surface waves. Buildings and other structures respond differently to earthquakes according to the natural resonant frequency of the structure and the type of waves. P-waves travel fastest and arrive first, followed by shear waves and long-period surface waves, which tend to produce greater shaking amplitudes. Attenuation relationships account for all types of waves but are based upon the maximum amplitudes recorded during earthquakes at each observation site.

Digital recordings of the seismic waves from earthquakes are processed to create response spectra – charts of amplitude versus wave frequency, which can provide important information for structural engineering design and damage assessment. The PSHA considers several response spectral periods (inverse of frequency), which are relevant to the structures of concern. For a rigid structure like the ISFSI, peak ground acceleration (PGA) is an appropriate measure for the earthquake forces. Horizontal ground motions are typically considered as most buildings can withstand vertical forces (gravity) but must be constructed to resist the strong lateral motions produced by earthquakes.

GeoPentech (2010) defined two “end member” fault model cases for estimating the seismic hazard at SONGS. The “strike-slip” end member consisted of the various segments of the NIRC fault zone; the second “blind thrust” end member consisted of the various models for the OBT and related faults – “wedge/thrust” model of Rivero *et al.* (2000); Rivero, (2004), and Rivero and Shaw (2011). Based on lack of evidence confirming the Pleistocene or younger activity on the OBT as a major through-going thrust fault, GeoPentech (2010) applied relatively low weight in the PSHA for this end member source model. Interaction between the OBT and strike-slip faults was not directly modeled, reasoning that the PSHA with the two models would average out these effects and provide an assessment of the seismic hazard potential (*risk*).

2.2.4 Seismic Sources

Past evaluations of the seismic hazard at sites throughout California including SONGS have relied on the Alquist-Priolo Act (AP) definition of active faults based on evidence for Holocene, less than 11,700 year-old fault rupture (surface faulting). The AP definition applies to surface fault rupture hazards. Fault rupture that produces tectonic earthquakes initiates deep, (typically 3-12 miles; Figure 2-5) within the Earth's brittle crust. Therefore, recent large earthquake that occurred on faults were unknown or not recognized as active.

Most earthquake ruptures fail to reach the ground surface. Moderate to large earthquakes ($M > 5$) on "blind" faults cause substantial damage without producing surface rupture, as for example, did the 17 October 1989 $M_w 6.9$ Loma Prieta (Plafker and Galloway, 1989), and 17 January 1994 $M_w 6.6$ Northridge (Teng and Aki, 1996) earthquakes. Furthermore, there have been several large ($M7+$) earthquakes striking southern California in the past few decades on faults that were either unmapped, or unrecognized as active ("Holocene"), or capable of producing large earthquakes. In particular, the 28 June 1992 $M_w 7.5$ Landers (SCEC, 1992), 10 October 1999 $M_w 7.1$ Hector Mine (Rymer *et al.*, 2002), 4 April 2010 $M_w 7.5$ El Mayor-Cucapah system (Fletcher *et al.*, 2014), and July 2019 $M_w 6.6$ and $M_w 7.4$ Ridgecrest (SCSN, 2019) earthquakes provided abundant data to educate the earthquake science community about large, complex, multi-fault earthquake ruptures on previously unidentified or poorly known faults. The faults located offshore SONGS fit in that category where better models of such fault interactions are needed to provide more accurate earthquake hazard assessments.

Earthquake history and recent seismicity data from SCSN and other seismograph networks in California and beyond provide important data to identify active faulting below ground and offshore. Advances in digital technology and computer algorithms to locate earthquake hypocenters, the latitude, longitude, and depth, more accurately are now able to delineate many buried or offshore fault zones (Figure 2-5; Hauksson *et al.*, 2012). Every significant earthquake in California and elsewhere brought new understanding and revision of seismic hazard estimates. Furthermore, improvements in data acquisition and processing for mapping offshore geologic structure and stratigraphy include multichannel seismic profiling systems, other geophysical methods, and Global Positioning System (GPS) for navigation.

Seismic stratigraphy as a method for more accurate sub-seafloor mapping and stratigraphic interpretation of geologic history provide better estimates of timing prehistoric activity and slip rates on faults. However, the weak link remains the lack of deep penetration boreholes or wells offshore to constrain the age of the seafloor stratigraphic sequences. Fortunately, there are two exploration wells located offshore near San Onofre (MSCH#1 and SHOC, Figure 2-4). Sorlien *et al.* (2016) traced prominent seismic reflection horizons from the abundant seismic profiles and well data from San Pedro Bay to San Diego to provide a coarse stratigraphic correlation for timing deformation and fault activity. The USGS (Normark *et al.*, 2009; Conrad *et al.*, 2019) used shallow piston cores in the area to determine the Holocene and Quaternary horizons in high-resolution seismic profiles. Stratigraphic thickness maps offshore southern California (Sorlien *et al.*, 2016) show late Quaternary uplift (post-600 ka) along the San Mateo-Carlsbad fault zone (Figure 2-6).

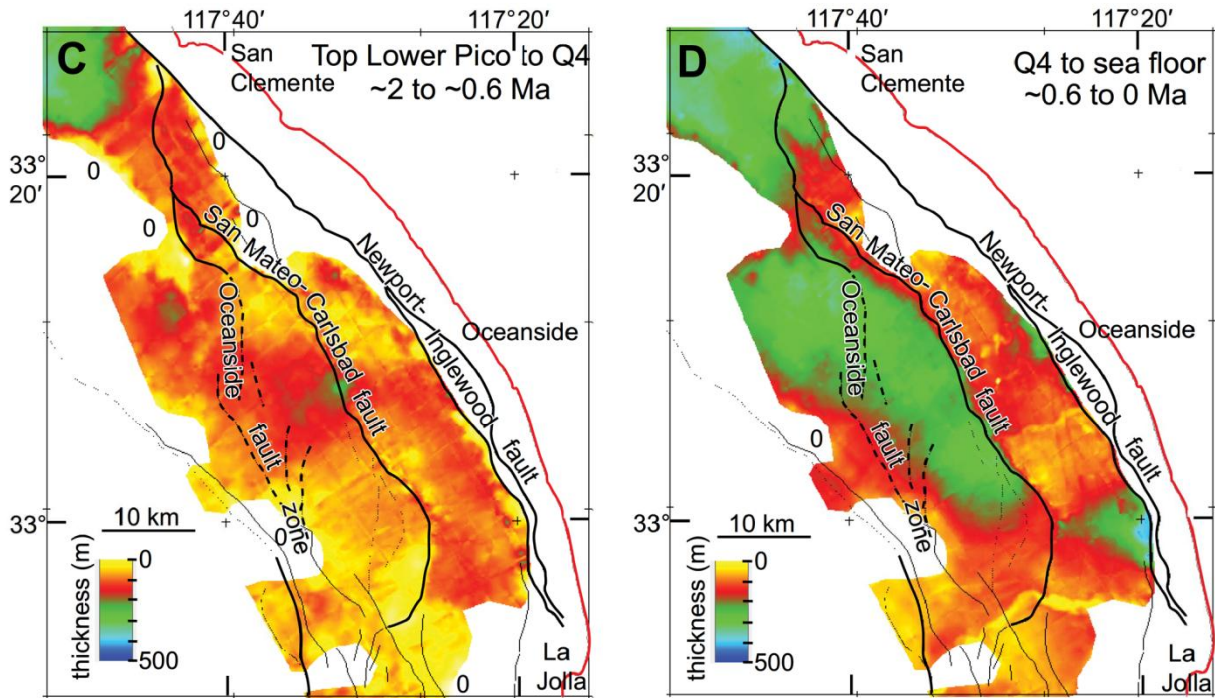


Figure 2-6. Thickness of late Quaternary sediments in the Inner Borderland between Dana Point and La Jolla (Sorlien *et al.*, 2016). Thick sediments (green) west of San Mateo-Carlsbad fault show uplift occurred during late Quaternary.

2.2.5 Seismic Risk

SCE has worked with the SCEC and other earth scientists to update the seismic hazard model for SONGS (GeoPentech, 2010). Research accomplished in the past decade since the 2010 GeoPentech report includes substantial interaction with SCEC scientists at meetings and workshops held to review ongoing research regarding the regional geology and earthquake hazards. In 2011, a workshop was held for the update of the Unified California Earthquake Risk Forecast (UCERF), which has been updated to version 3 (UCERF3, 2013). The main improvement in the model is to include the potential for multi-fault ruptures that produce large ($M > 7$) earthquakes. This change reduces the probability (frequency) of moderate earthquakes ($M 5-7$), which is more consistent with the historical record of California seismicity. The previous model suggested more frequent moderate magnitude events than have been observed in the historic record since about 1875.

The multi-fault rupture concept was adopted in the 2010 GeoPentech report by considering alternative fault configurations and rupture scenarios for the primary faults that affect the SONGS location. In particular, different configurations of the NIRC fault zone, as well as deep slip on the OBT, were considered in the PSHA. The models used were restricted to the vertical strike-slip faulting of the NIRC separately from the low-angle thrust faulting of the OBT. The NIRC-OBT combination dominated the PGA hazard for longer return periods ($>600-700$ years). The Elsinore, San Jacinto and San Andreas Class A faults (well-defined with slip rates >5 mm/yr) dominate the short return period hazard.

According to the California Coastal Commission staff report for the SONGS Holtec ISFSI CDP (CCC, 2015), strong-motion hazard for the 10% chance of exceedance during a 50-year interval risk level, 475-year return period that is used for building codes, the expected horizontal PGA is 0.227g, or about one-quarter gravitational acceleration. For the 100-year return period, the expected PGA drops to 0.11g. The Design Basis Earthquake (DBE) for a M7.0 event at 5 miles from SONGS was computed to be 0.31g. The design value with safety factor was set at 0.67g, which has an estimated return interval of $\sim 7,100$ years⁴. The SONGS ISFSIs are designed to withstand 1.5g in each horizontal direction (2.12g vector sum), and 1.0g vertical.

The Annual Frequency of Exceedance risk of strong ground motion levels was reduced in the 2010 PSHA compared to the 1995 PSHA (Figure 2-7). Increasing the maximum magnitudes by including multi-fault ruptures reduces the frequency of moderate earthquakes ($M 5-7$), which define the short term hazard. Note that shaking level (weighted spectral acceleration) for the longest return period of 10,000 years, was only slightly reduced. This return period is important for the nuclear hazard issues, but for the short period of concern to the California Coastal Commission requirements (15-30 years or until 2050), expected shaking levels were reduced to about 0.2g (from 0.3g or 33% decrease at the 100-year return period). The NIRC was assigned a weight of 88% compared to the 12% used for the OBT and represented the significant earthquake source.

⁴ The California Geological Survey (CGS) and U.S. Geological Survey (USGS) have carried out independent evaluations of earthquake ground shaking hazards. The CGS Earthquake Shaking Potential Map for California portrays the San Onofre areas as region of relatively low ground shaking potential (Branum et al., 2008). With a PGA of 0.67 the recurrence interval is 7,143 years (GeoPentech, 2010).

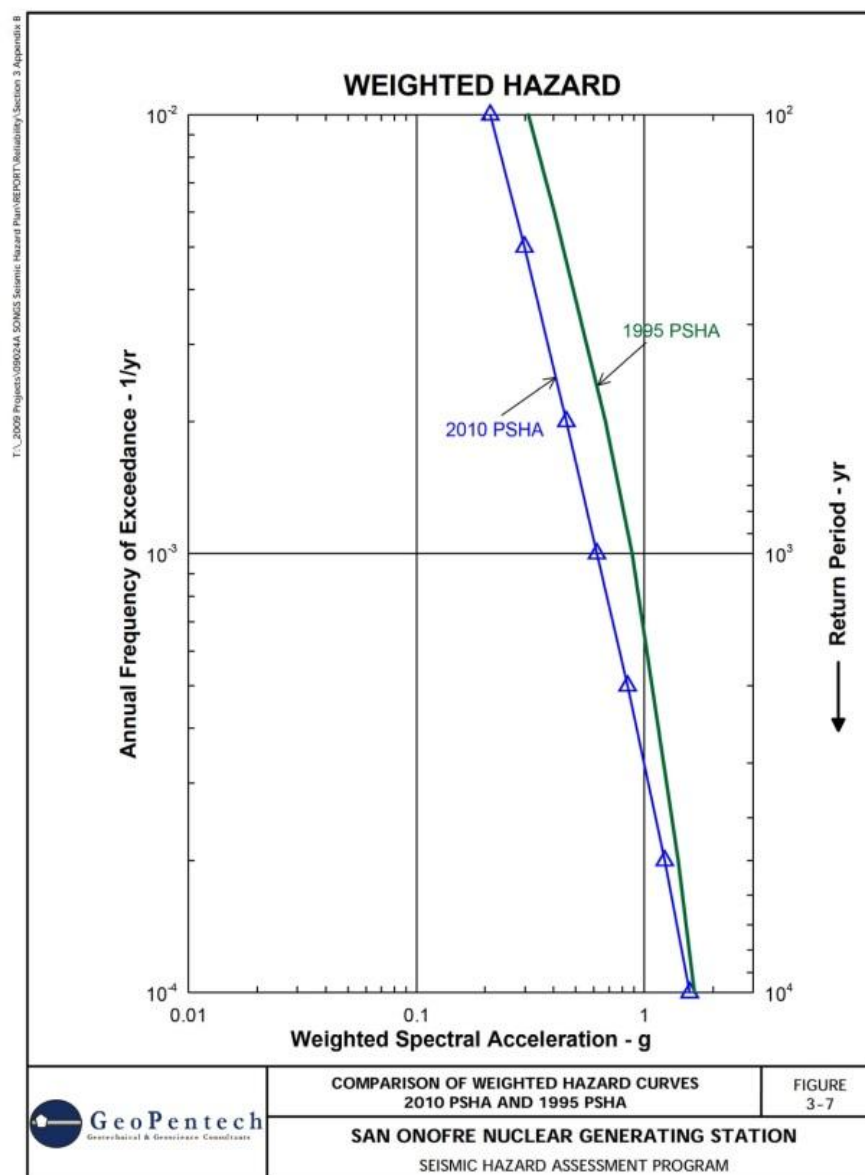


Figure 2-7. Comparison of hazard curves 2010 PSHA and 1995 PSHA. From GeoPentech (2010, Figure 3-7).

2.2.6 Coastal Fault System

The recent investigations of the Coastal Fault System supported by SCE (Maloney et al. 2016; Sahakian et al, 2017, Holmes et al, 2021) and the USGS (Conrad et al. 2019) provided a more accurate mapping of the shallow crustal faulting beyond the California State Lands boundary. The reprocessed deep-penetration exploration industry MCS survey data (Maloney et al. 2016) were used to evaluate a broad blind thrust fault model (Rivero and Shaw, 2011; Rivero et al., 2000) and compare with strike-slip or wrench fault models for tectonic deformation along the Coastal Fault System. The strike-slip model for the Newport-Inglewood-Rose Canyon fault zone was used for previous earthquake hazard evaluations at SONGS (GeoPentech, 2010). The deep seismic imaging of the fault zones showed the significance of fault bends and stepovers that produce significant vertical deformation in addition to the dominant strike-slip. Better imaging and understanding of the faulting on the continental slope was obtained and was sufficient to demonstrate zones of oblique faulting with components of reverse-slip at restraining fault geometries (left bends or stepovers) and normal slip at releasing fault geometries (right bends or stepovers). The characteristic downward convergent fault geometry known as “flower structure” (Wilcox et al. 1973) was recognized.

Sorlien et al (2016) mapped the Inner Continental Borderland from San Pedro Bay to San Diego using exploration industry MCS profiles available through the USGS National Archive of Marine Seismic Surveys (NAMSS) and recognized several major fault bends and stepovers with oblique-slip including those offshore La Jolla, Carlsbad, and San Onofre. An important observation of these studies is the recognition of the change from an extensional (transtension) to a convergent (transpressional) faulting style that occurred near the Miocene-Pliocene time period (about 6 Million years ago). This change in tectonic style, related to changes in the Pacific-North America plate boundary relative motion (Lonsdale, 1991) correlates with the eastward jump of the plate boundary to form the Gulf of California system of strike-slip transform faults and extensional spreading centers.

The result of this fundamental change in the plate boundary system caused former releasing bends and pull-apart basins within the Inner Continental Borderland (and Los Angeles Basin) to become transpressional “pop-up” structures, inverting the former structural basins (Legg et al. 2007). Maloney et al. (2016) concluded that activity on the OBT modeled by Rivero and Shaw (2011) ceased in Pliocene time and suggested the strike-slip model for the NIRC fault zone was appropriate for evaluating large earthquake potential at San Onofre. Sahakian et al. (2017) provided updated mapping and evaluated the potential for large, complex, multi-segment fault ruptures involving the NIRC including oblique-slip at bends and stepovers. Use of Coulomb failure criteria to infer probability of rupture propagation jumping to adjacent segments provided models for estimating maximum magnitudes and likelihood of occurrence. What appears to have been overlooked by these strike-slip models and the blind fault models is the fact that a system of major low-angle detachments, i.e., the Thirtymile Bank and Coronado Bank – Oceanside faults (Sorlien et al. 2016) underlie these steep-dipping faults of the Coastal Fault System.

The San Onofre coast is located at the hinge between uplift and subsidence induced by large-scale transpression across this region south of the San Andreas Bend Region. The Coastal Fault System, comprised of the NIRC strike-slip fault zone along the continental shelf and the San Mateo-Carlsbad oblique-reverse faults located along the base of the continental slope, may

present a severe earthquake hazard. The existence of the OBT and deeper Thirtymile Bank detachment as low-angle slip surfaces may facilitate linkage between the high-angle strike-slip faults to produce large, complex, multi-fault earthquake ruptures (Legg *et al.*, 2018). For example, the 2019 M_w 7.8 Kaikōura, New Zealand earthquake (Hamling *et al.*, 2017) produced substantial surface rupture on at least 12 shallow faults underlain by a major blind thrust fault associated with oblique subduction beneath the north end of the South Island. In addition to the severe ground shaking and deformation, a tsunami (up to 3m at Kaikōura) was observed along the coasts adjacent to the vertical fault displacements.

Deformation recognized and mapped in the coastal zone near SONGS (Carlsbad; Kuhn, 2005), appears consistent with large prehistoric coastal earthquakes. Observed deformation and related features include paleo-liquefaction sand blows, injection dikes, and lateral spread surfaces, severe and widespread ground fracturing, secondary faulting, and tsunami deposits (Figures 2-8 and 2-9). The liquefaction involved Pleistocene, and dense Eocene sands, which were injected through overlying late Quaternary soils and Holocene Indigenous habitation sites. Liquefaction of dense sands requires extreme shaking from a large, nearby fault source. The complexity of faulting along the Coastal Fault System (NIRC and related faults) combined with the existence of at least two (Oceanside and Thirtymile Bank) detachment/blind thrust/oblique-reverse surfaces beneath the entire coastal zone from (at least) Huntington Beach to San Diego represents the prime suspect for producing such large coastal earthquakes. Historic seismicity confirms fault activity in the area.

In addition to surficial deformation, coastal uplift including the San Joaquin Hills and late Pleistocene marine terraces document late Quaternary and possibly Holocene activity (Grant *et al.*, 2002). Recent work on coastal marine terrace uplift shows that subsidence may also occur (Castillo *et al.*, 2019). Offshore research with seismic reflection imaging recognized progressive tilting of Pleistocene and older surfaces that suggest overall subsidence of the Inner Borderland (Sorlien *et al.*, 2009; Sorlien *et al.*, 2016). Progressive tilting at the hinge of a mega-fold (syncline) along the coast may explain the apparent lack of Holocene marine terrace near SONGS (Rockwell, 2018 personal communication).

Based on the repetitive lateral spread surfaces⁵ within marine terrace deposits located above the wave-cut platform Marine Isotope Stage 5e (MIS-5e, 125 ka), the recurrence interval for such large earthquakes is about 10,000 years.

⁵ Liquefied sand layer that enables more competent material above to slide laterally down gentle slopes.

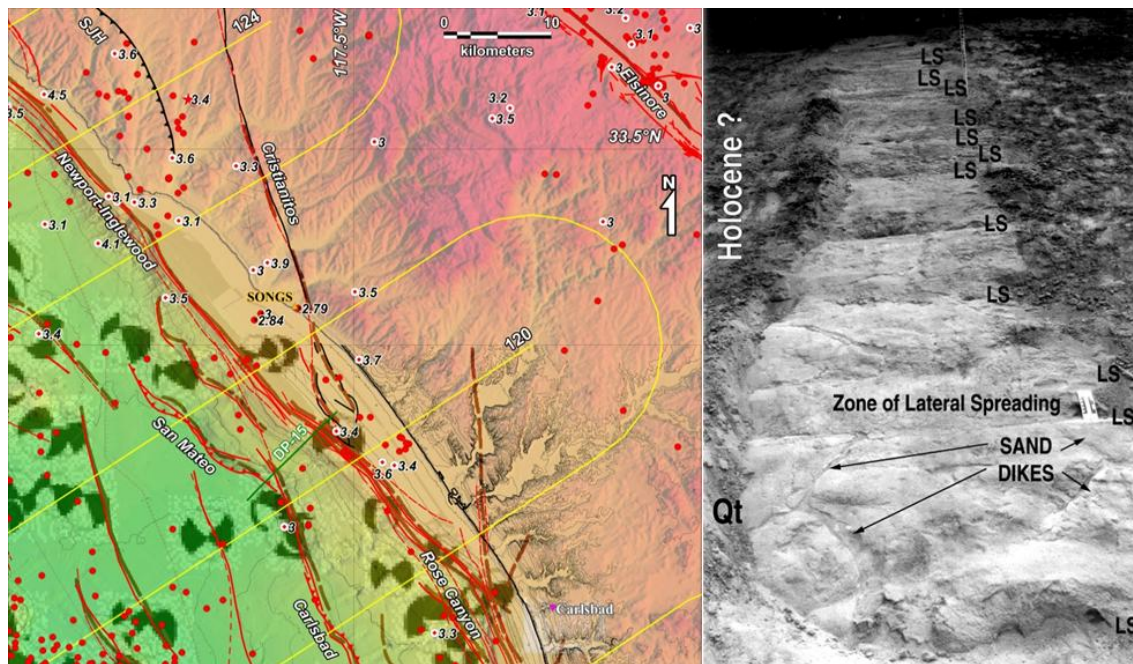


Figure 2-8. Map (left) and photograph (right) of paleoliquefaction sites exposed in a cut slope along Encinas Creek, Carlsbad. Repeated lateral spreads (LS) record at least 12 large prehistoric earthquakes. (Kuhn, 2005).

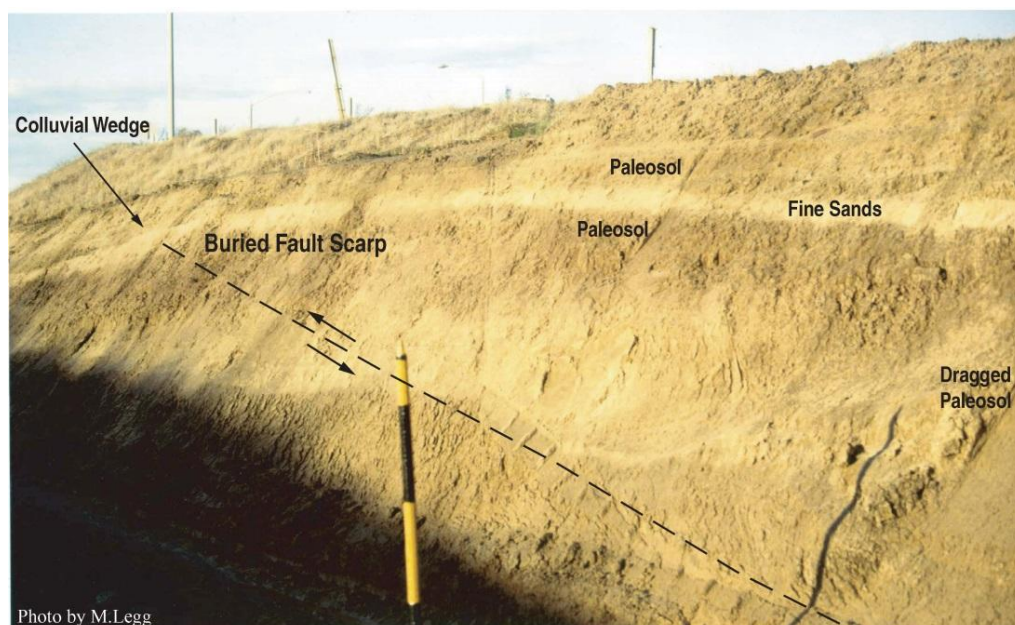


Figure 2-9. Photograph of paleo-earthquake fault rupture with liquefaction sand deposits covering 40,000-yr soil and fault scarp (Kuhn, 2005; Legg *et al.*, 2018). Fault continues above paleosol an unknown distance into vegetated slope area.

2.2.7 Hypothetical M_w 7.6 Scenario Earthquake

In this section, we provide estimates for seismic hazards anticipated (and observed) from extreme ($M_w > 7$) events to compare with the design criteria provided for the ISFSI and SONGS facilities. The complex pattern of faulting observed following the 14 November 2016, M_w 7.8 Kaikōura earthquake in New Zealand (Hamling *et al.*, 2017), resembles updated mapping of the Coastal Fault System described in previous sections. Shaking with PGA exceeding 1.0g horizontal and vertical directions was recorded in Kaikōura (Jibson *et al.*, 2018). A similar event may strike the southern California coast (Legg *et al.*, 2018) reaching from Los Angeles to San Diego (Figure 2-10).

Here we describe a similar model for a M_w 7.6 Coastal Fault System event that extends from Huntington Beach to La Jolla, excluding the strike-slip segments of the Newport-Inglewood fault zone, which ruptured in 1933, and the San Diego segments of the Rose Canyon fault, which ruptured in 1862 (Legg and Agnew, 1979; Singleton *et al.*, 2019). Nine fault segments defined include the South Coast section of the Newport-Inglewood fault zone (NIFZ), the Oceanside segment of the Rose Canyon fault zone, the San Mateo-Carlsbad fault zone, and the San Onofre Trend (SOT).

A continuation of the South Coast zone toward the southeast reaches the coast near the Agua Hedionda lagoon, which is bent to the southeast. Abundant paleo-liquefaction and surface fracturing from large prehistoric earthquakes have been mapped in that area (Kuhn, 2005). Details of the nine-segment fault rupture model, and two subset models (San Mateo-San Onofre-Carlsbad and NIRC fault sections) are described in the Local Tsunami hazards section. Subsidence at the north along the coast (blue shading) could be replaced by including reverse-slip on the San Joaquin Hills blind thrust (Grant *et al.*, 2002). Tsunami deposits found at Batiquitos Lagoon reached 22-30 ft above sea level (Kuhn, 2005).

Updated mapping of the NIRC fault zone (Sahakian *et al.*, 2017) recognized most of the fault segments originally defined by Fischer and Mills (1991) but missed nearshore faulting that lie inside the California State Lands three-mile limit. The new seismic profiles acquired by Scripps Institution of Oceanography were unable to cross into this area.

Exploration industry profiles available from the USGS NAMSS database (Treizenberg *et al.*, 2016) show a South Coast fault branch that trends toward the coast inside the continental shelf break offshore Oceanside (Figures 2-4 and 2-11). High-resolution seismic profiles show a tectonic dam produced by uplift along this fault segment (Figure 2-11). This creates a nearshore sedimentary basin where sediments from the coastal river deltas are channeled to the north to eventually empty into the deep basin along the San Mateo and San Onofre submarine canyons/slope gullies (Darigo and Osborne, 1986).

Multi-fault earthquake scenarios were evaluated by Sahakian *et al.*, (2017) using elastic dislocation modeling and Coulomb stress change to determine which stepovers between faults may fail when an adjacent fault slips. They concluded that the stepover near La Jolla was unfavorable for rupture continuation, but “*rupture along the full fault zone is possible.*” The large $M > 7$ earthquakes considered for the Coastal Fault System would be severe, but rare events with the long recurrence periods necessary to rebuild the tectonic strain (6-16 ft) at the slow 1-2

mm/yr slip rate. More frequent moderate earthquakes (M6-7) located close to the site define the seismic hazard response spectral values (GeoPentech, 2010).

The nine-segment earthquake source model representing the prominent offshore fault sections between Dana Point and La Jolla was used to evaluate the local tsunami potential at the SONGS ISFSI (CE, 2022-Section 7.5, Tsunami Hazards Analysis). The deformation model resembles that derived from the $M_w7.8$ Kaikoura earthquake with combined strike-slip and oblique reverse-slip on various segments. The largest local earthquake scenario consists of all nine segments with $M_w7.62$ (CE, 2022 in Table 7-5, source Local-sc1). Two other composite source models included the four segments of the Newport-Inglewood and Oceanside (Rose Canyon) strike-slip fault, with oblique-slip on the north and south segments of the South Coast Offshore fault (Table 7-5, source Local-sc3, $M_w7.41$), and the San Mateo-San Onofre-Carlsbad oblique-reverse fault, with strike-slip on the San Onofre segment (Table 7-5, source Local-sc2 $M_w7.44$).

Calculations of the expected PGA for the site were made for the nine-segment earthquake source model used in the Tsunami Hazards Analysis (Section 7.5). The closest horizontal distance of the site from the surface projection of the fault was measured as seven kilometers. Two different attenuation relations (ground motion prediction equations, GMPE) were used including the Joyner and Boore (1993; JB93) and Boore and Atkinson (2008; BA08) models. A site condition 'B' was used for the JB93 equation and a $V_{s30} = 760$ m/s equivalent to the B/C boundary site condition for the BA08 equation. Non-linear amplifications, which would take into account soft soils, were not considered because the SONGS site is based on a San Mateo bedrock formation that is the foundation of the site. The computed median PGA is 0.65g for the JB93 equation and 0.77g for the BA08 equation. These values are similar to the DBE with safety factor used for the power plant (0.67g). and well below the 1.50g used for the ISFSI design.

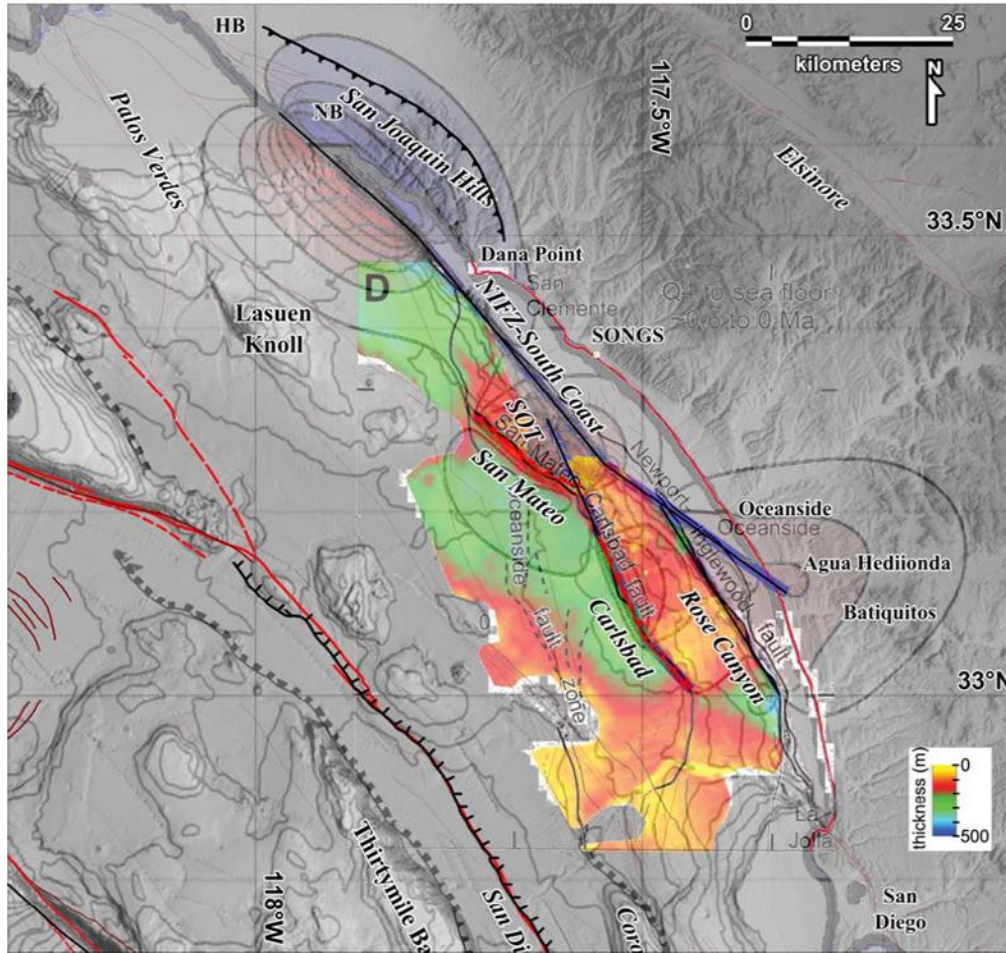


Figure 2-10. Map of simplified fault rupture model (thick lines with red-blue uplift contours) for MW7.6 earthquake along the Coastal Fault System. Sediment thickness overlay (Figure 2-6) of late Quaternary uplift along San Mateo-Carlsbad fault.

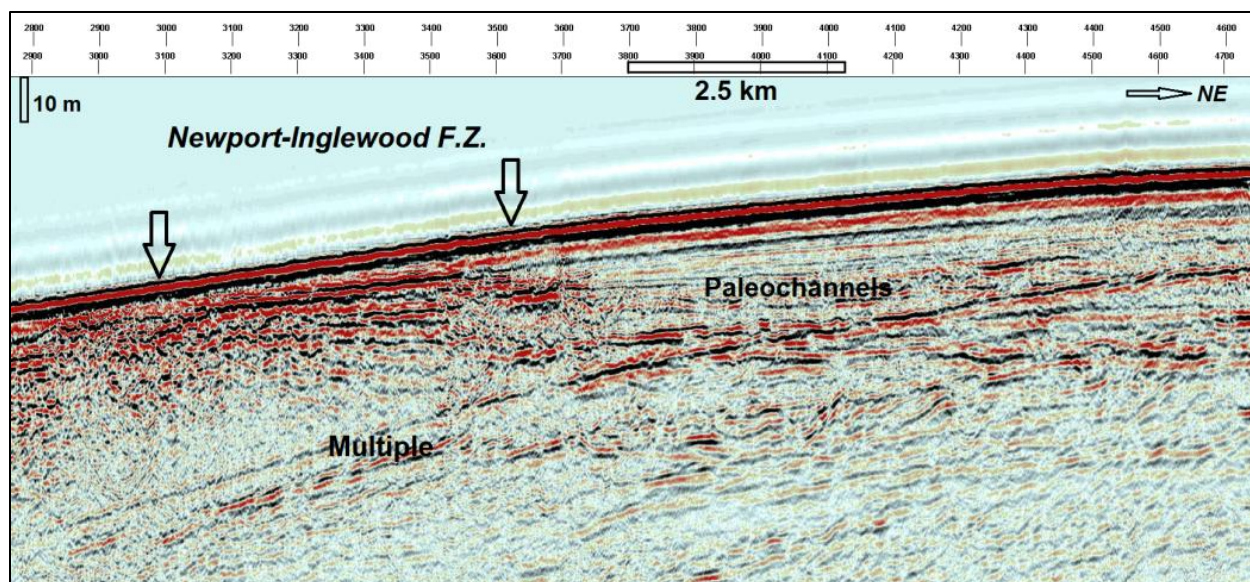


Figure 2-11. High-resolution 24-channel seismic profile of Newport-Inglewood fault uplift that blocks Quaternary paleochannels offshore Oceanside.

2.3 GROUND FAILURE HAZARDS

2.3.1 Surface Rupture

The Cristianitos fault is located about 0.75 miles west of SONGS (Figure 2-8). The fault is exposed in the coastal bluff to the south of SONGS where no evidence of rupture above the Eemian Interglacial 125 ka year old (OIS5e) marine terrace platform is observed (Shlemon, 1987). Although originally considered a low-angle normal fault (Ehlig, 1979), the roughly linear trace of the fault across the eastern boundary of the Capistrano Embayment suggests strike-slip character. Reverse drag inferred to represent listric (concave, flattening with depth) faulting may be due to the southwest curvature of the fault trace at the coastal bluff. Furthermore, reverse drag character observed in folded hanging wall sediments above the normal separation fault may be produced by structural inversion of the hanging wall basin due to a tectonic strain change from extension to contraction, or from transtension to transpression for strike-slip systems. Transtension during the Miocene microplate capture of the Western Transverse Ranges rifted the crustal block away from the continental margin by the northwest-translation of the Pacific oceanic plate. Subsequent changes in the relative plate motion vector and inland jump of the plate boundary to the Gulf of California produced a transpressional (oblique-convergence) regime within the southern California region west of the San Andreas fault and Salton Sea (Legg, 1991; Crouch and Suppe, 1993; Nicholson *et al.*, 1994).

SONGS is located within the Capistrano Embayment above the hanging wall of the west-dipping Cristianitos fault. The Cristianitos fault and fractures identified in the Tertiary (San Mateo Formation) bedrock foundation at Units 2 and 3 are considered inactive, by surface fault rupture standards (Alquist-Priolo). Notwithstanding, there are several small earthquakes (M3-4) recorded within the Capistrano Embayment, and some are located close to SONGS (Figures 2-5 and 2-8). Activity on the San Joaquin Hills (SJH) blind thrust (Mueller *et al.* 1998) may be responsible for some of these events, but uplift due to structural inversion above the Cristianitos fault is also feasible. Uplift or folding of the San Mateo Formation within the Capistrano Embayment during large ($M > 7$) multi-fault earthquake ruptures may produce subsurface fractures on more brittle layers such as those observed in the coastal bluff near the fault. Grant *et al.* (2002) presented evidence for a large coastal earthquake that produced uplift along the coast and in Newport Bay since A.D. 1635. The SJH was not modeled for the tsunami analysis because it lies onshore. The potential for shallow deformation at SONGS due to blind faulting in the Capistrano Embayment is uncertain at this time. The secondary fractures that could result from such events would not adversely affect the SONGS ISFSI, given its reinforced concrete slab support foundation and rigid construction.

2.3.2 Liquefaction

The NUHOMS ISFSI is underlain by the dense, well-consolidated sands of the San Mateo Formation, which are considered to be at low risk of seismically-induced liquefaction.

Strong shaking of water-saturated, cohesionless, surficial sediments may induce liquefaction or liquefaction of the material. Pressure from the overlying intact material forces the liquefied material upward through cracks to form “sand blows” or sand volcanoes. Layers of liquefiable material buried beneath more cohesive soils including clays and hard-pan may create

cracks in the more cohesive material, and the entire soil sequence may slide laterally on very gentle slopes (lateral spread; Figure 2-8). In the North San Diego County area, there are numerous features that record prehistoric (and possibly historic) episodes of earthquake-induced liquefaction (Kuhn, 2005; Legg et al., 2018). Pre-WWII aerial photographs (1941) of the coastal area taken before the widespread development show features that resemble sand blows identified in the New Madrid, Missouri, area where a series of large earthquakes shook the Midwest in the winter of 1811-1812. (Obermeier, 1996). Although engineering geologists typically consider that only youthful cohesionless deposits are susceptible to liquefaction, that is, deposits older than 15,000 years are considered too dense to liquefy, there is abundant evidence of liquefaction events involving Pleistocene (MIS-5e terrace sands >125,000 years; Figure 2-8) and dense Eocene sands (Santiago Formation, 40-46 Million years; Kuhn, 2005) were found in the Carlsbad area. However, no liquefaction evidence of sands or silts within the Miocene San Mateo Formation have been identified through the scientific literature review for this report. Identification of fractures in the San Mateo Formation during excavation for Units 2 and 3 suggest brittle behavior, and slight cementation was observed, indicating that liquefaction of the soil beneath the ISFSI is unlikely.

While Quaternary deformation in the Capistrano Embayment remains poorly understood, it appears to be minor compared to the offshore deformation. Lack of offset above the wave-cut platform suggests little or no shallow fault deformation since about 125,000 years ago. However, at least 12 lateral spread events are documented (Kuhn, 2005) along Encinas Creek slopes (Figure 2-8, bottom left) within the overlying late Pleistocene soils (<125,000 years ago). These indications were previously considered in the 2015 CCC Staff Report for the UMAX ISFSI, which found that “although these features are suggestive, the Commission does not consider them indicative of a serious liquefaction hazard at the proposed project site.”

Although the water table is shallow at the site (approximately +5 feet MLLW), cyclic triaxial tests, field density tests, and very high blow counts during standard penetrometer tests have shown that liquefaction is not expected to occur during a design basis earthquake (GEI 2015). Minimum factors-of-safety against liquefaction in the plant area have been calculated at 1.5 to 2.0.

In light of the high factor of safety evident in the site-specific studies, and in the absence of any recent scientific research to suggest anything to the contrary, the previous conclusion of the CCC Staff remains valid “that the stability of the site with respect to liquefaction can be assured, to the greatest extent feasible, consistent with section 30253 of the Coastal Act.”

2.3.3 Slope Stability

This section summarizes studies estimating slope displacement that could result from ground shaking or common slope failure (SCE, 1995; Hinkle 2011; Nino and Moore, 2015) impacting the SONGS ISFSI. Figure 2-12 shows the locations of the two ISFSI facilities, referred to as “NUHOMS” for the eastern site housing Unit 1 material, and “Holtec-UMAX” for the western site containing material from Unit 2. The NUHOMS ISFSI for Unit 1 material was approved by the California Commission in February 2000. Ascending slopes are located at the north and east of the ISFSI sites.

The north and east slopes are about 105 ft and 200 ft away from the ISFSI, respectively. In the geotechnical investigation performed by SCE (1995), it was found that only minor sloughing of the surficial slope materials is likely to occur during the DBE-level ground shaking. Hinkle (2007) found that when conservatively assuming a slope failure during a design seismic or a tsunami event, the anticipated slope run-out distance of the adjacent slope is about 91 ft (Appendix A). When assuming a 20° to 25° angle of repose (from horizontal) for soils formed by the failed slope, a slope run-out distance of 50-70 ft is estimated. Therefore, any slope failures from the north bluff will be more than about 20 ft away from the ISFSI (Figure 2-12), and a much large distance away for east bluff failures.



**Figure 2-12. Plan view of Holtec (west, lower) and NUHOMS (east, upper) ISFSIs.
Minimum distance between the north and east bluffs is 105 ft.**

2.3.4 Bearing Capacity

SCE constructed SONGS Units 1, 2, and 3 in accordance with the seismic standards established by the Nuclear Regulatory Commission (NRC). The NRC performed a comprehensive evaluation of the soil properties and stability of the site foundation prior to issuing the operating licenses for these units, in part, for the purposes of assuring stability and structural integrity, and assuring that the units do not create or contribute to erosion or geologic instability of the surrounding area.

The static bearing pressure of the NUHOMS ISFSI is computed as 2,020 lb/ft². The allowable static bearing capacity of the soil was determined to be 15,630 lb/ft² (Appendix B). This is more than 7 times the required static bearing capacity.

The seismic soil pressure of the NUHOMS ISFSI, which considers the 1.5g horizontal and 1.0g vertical design ground stress, is computed as 6,670 lb/ft². The allowable bearing value can be increased by 50% for loads of short duration, including wind and seismic forces. Therefore, the allowable dynamic soil bearing capacity is approximately 23,400 lb/ft². This is more than three times the required dynamic bearing capacity. Appendix C presents the ISFSI Foundation Design calculations.

3.0 REFERENCES

- Astiz, L. and Shearer, P.M., 2000. Earthquake locations in the inner Continental Borderland offshore southern California. *Seismological Society of America Bulletin*, v. 90, p. 425-449.
- Atwater, T., 1970. Implications of plate tectonics for the Cenozoic evolution of western North America. *Geological Society of America Bulletin*, v.81, 3515-3536.
- Atwater, T., and J. Stock, 1998. Pacific-North American plate tectonics of the Neogene southwestern United States: An update. *International Geology Review*, 40,375-402.
- Barrows, A.G., 1974. A review of the geology and earthquake history of the Newport-Inglewood Structural Zone, southern California. California Division of Mines and Geology, Special Report 114, 115 pp.
- Bohannon, R.G., and Geist, E., 1998. Upper crustal structure and Neogene tectonic development of the California Continental Borderland. *Geological Society of America Bulletin*, 110, 779-800.
- Boore, D.M., and Atkinson, G.M., 2008, Ground-Motion prediction equations for the average horizontal component of PGA, PGV, and 5%-damped PSA at spectral periods between 0.01 s and 10.0 s: *Earthquake Spectra*, v. 24, n. 1, p. 99-138, Earthquake Engineering Research Institute.
- Borrero, J.C., M.R. Legg, and C.E. Synolakis, 2004. Tsunami sources in the southern California bight. *Geophysical Research Letters*, v. 31, p. L13211.
- Branum, D. S., Harmsen, E. K., M. Petersen and C Wills, 2008. Earthquake Shaking Potential for California, Map Sheet 48 (revised), California Geological Survey, Sacramento, California.
- California Coastal Commission (CCC), 2015. Construct and operate an Independent Spent Fuel Storage Installation (ISFSI) to store spent nuclear fuel from SONGS Units 2 and 3. Staff Report: Regular Permit, Application #9-15-022, Approval with conditions, 47 pp., 2 Appendices, 9 Exhibits.
- Clarke, S.H., Greene, H.G., Kennedy, M.P., and Vedder, J. G., 1987. Geologic map of the inner-southern California continental margin. California Division of Mines and Geology, California Continental Margin Geologic Map Series, Area 1 of 7, sheet 1 of 4, scale 1:250,000.
- Clements, T., and Emery, K.O., 1947. Seismic activity and topography of the sea floor off southern California. *Bulletin of the Seismological Society of America*, v. 37, p. 309-313.
- Coastal Environments, Inc. (CE), 2022. Tsunami Hazards Analysis at San Onofre Nuclear Generating Station, Report prepared for Southern California Edison, CE Reference No. 22-04, 82 pp.

- Conrad, J.E., Brothers, D.S., Maier, K.L., Ryan, H.F., Dartnell, P., and Sliter, R.W., 2019. Right-lateral fault motion along the slope-basin transition, Gulf of Santa Catalina, Southern California. In Marsaglia, K.M., Schwalbach, J.R., and Behl, R.J., *From the Mountains to the Abyss: The California Borderland as an Archive of Southern California Geologic Evolution*. SEPM Special Publication No. 110, p. 256-272. Doi: 10.2110/sepm.sp.110.07.
- Crouch, J.K., and Suppe, J., 1993. Late Cenozoic tectonic evolution of the Los Angeles basin and inner California borderland: A model for core complex-like crustal extension. *Geological Society of America Bulletin*, 105, 1415-1434.
- Crowell, J.C., 1974. Origin of late Cenozoic basins in southern California. In Dickinson, W. R., ed., *Tectonics and Sedimentation*. Society of Economic Paleontologists and Mineralogists Special Publication 22, 190-204.
- Dartnell, P., Driscoll, N.W., Brothers, D., Conrad, J.E., Kluesner, J., Kent, G., and Andrews, B., 2015. Colored shaded-relief bathymetry, acoustic backscatter, and selected perspective views of the inner continental borderland, Southern California, U.S. Geological Survey Scientific Investigations Map 3324, 3 sheets <https://dx.doi.org/10.3133/sim3324>.
- Ehlig, P.L., 1979. The late Cenozoic evolution of the Capistrano Embayment. In D. L. Fife, ed., *Geologic guide of San Onofre nuclear generating station and adjacent regions of southern California: Pacific Sections*. AAPG-SEPM-Society of Exploration Geophysicists, Guide Book 46, p. A38-A46.
- Emery, K.O., 1960. *The Sea Off Southern California, A Modern Habitat of Petroleum*. John Wiley & Sons, Inc., New York, New York, 366 p.
- Fischer, P.J., and Mills, G.I., 1991. The offshore Newport-Inglewood-Rose Canyon Fault zone, California: Structure, segmentation and tectonics. In Abbott, P. L., and Elliott, W. J., eds., *Environmental Perils San Diego Region*. San Diego Association of Geologists, p. 17-36.
- Fletcher, J.M., Teran, O.J., Rockwell, T.K., Oskin, M.E., Hudnut, K.W., Spelz, R.M., Lacan, P., Dorsey, M.T., Ostermeijer, G., Mitchell, T.M., Akciz, S.O, Hernandez-Flores, A.P., Hinojosa-Corona, A., Pena-Villa, I., and Lynch, D.K., 2020. An analysis of the factors that control fault zone architecture and the importance of fault orientation relative to regional stress. *Geological Society of America Bulletin*, September/October v. 132, no. 9/10, p. 2084-2104.
- GeoPentech, 2010. San Onofre Nuclear Generating Station Seismic Hazard Assessment Program 2010 Probabilistic Seismic Hazard Analysis Report. Prepared for Southern California Edison, December 2010.
- Grant, L.B., and Rockwell, T.K., 2002. A northward-propagating earthquake sequence in coastal California? *Seismological Research Letters*, v. 73, n. 4, p. 461-469.

- Grant, L.B., Ballenger, L.J., and Runnerstrom, E.E., 2002. Coastal uplift of the San Joaquin Hills, southern Los Angeles Basin, California, by a large earthquake since 1635 A.D. *Bulletin of the Seismological Society of America*, v. 92, p. 590-599.
- Grant, L.B., and Shearer, P.M., 2004. Activity of the offshore Newport- Inglewood Rose Canyon Fault Zone, coastal southern California, from relocated microseismicity. *Bulletin of the Seismological Society of America*, v. 94, no. 2, p. 747- 752.
- Hammling, I.J., Hreinsdóttir, Clark, K., and 23 others, 2017. Complex multifault rupture during the 2016 M_w 7.8 Kaikōura earthquake, New Zealand. *Science*, doi:10.1126/science.aaam7194.
- Hauksson, E., and Jones, L.M., 1988. The July 1986 Oceanside ($M_L=5.3$) earthquake sequence in the continental borderland, southern California. *Seismological Society of America Bulletin*, v. 78, p. 1885-1906.
- Hauksson, E., and S. Gross, 1991. Source parameters of the 1933 Long Beach earthquake. *Bull. Seis. Soc. Am.*, 81, 81-98.
- Hauksson, E., 2000. Crustal structure and seismicity distribution adjacent to the Pacific and North America plate boundary I southern California. *Journal of Geophysical Research*, v. 105, no. B6, p. 13,875-13,903.
- Hauksson, E., W. Yang, and P.M. Shearer, 2012. Waveform relocated earthquake catalog for southern California (1981 to June 2011). *Bull. Seis. Soc. Am* (short note), 102(5), 2239–2244, doi: 10.1785/0120120010.
- Hinkle, D., 2011. Third-Party Review – Slope Evaluation, Independent Spent Fuel Storage Installation (ISFSI), San Onofre Nuclear Generating Station: dated 17 May, 2011.
- Holmes, J.J., Perea, H., Driscoll, N.W., and Kent, G.M., 2021. Revealing geometry and fault interaction on a complex structural system based on 3D-Cable data: The San Mateo and San Onofre trends, offshore Southern California. *Frontiers in Earth Science*, 9:653366 doi:10.3389/feart.2021.653366.
- Holtec International, 2015. 2001 CDP Permit Structural Calculations: dated 19 February 2015.
- Hutton, K., J. Woessner, and E. Hauksson, 2010. Earthquake monitoring in southern California for seventy-seven years (1932-2008). *Bull. Seis. Soc. Am.*, 100, 423-446.
- Jennings, C.W., 1994. Fault activity map of California and adjacent areas. California Division of Mines and Geology, Map No. 6, scale 1:750,000.
- Joyner, W.B., and Boore, D.M., 1993, Methods for regression analysis of strong-motion data: *Bull. Seismol. Soc. Am.*, v. 83, p. 469-487.

- Kennedy, M.P., 1977. Recency and character of faulting along the Elsinore fault zone in southern Riverside County, California. California Division of Mines & Geology Special Report 131, 12 p. Map scale 1:24,000.
- Kramer, S.L., 1996. *Geotechnical Earthquake Engineering*. Prentice Hall, Upper Saddle River, New Jersey, 653 p.
- Langenheim, V.E., P.F. Halvorson, E.L. Castellanos, and R.C. Jachens, 1993. Aeromagnetic Map of the Southern California Borderland East of the Patton Escarpment, U.S. Geol. Survey. Open-File Rept. 93-250, scale 1:500,000.
- Legg, M.R., 1980. Seismicity and tectonics of the inner continental borderland of southern California and northern Baja California, Mexico [unpublished M.S. thesis]: University of California, Santa Diego, San Diego, California, 60 p.
- Legg, M.R., 1985. *Geologic Structure and tectonics of the inner continental borderland offshore northern Baja California, Mexico*. [Ph.D. dissertation] University of California, Santa Barbara, Santa Barbara, California, 410 p.
- Legg, M.R., 1987. Earthquake epicenters and selected fault plane solutions of the inner-southern California continental margin. Map No. 1B in Greene, H.G., and M.P. Kennedy, eds., *Geologic Map Series of the California Continental Margin*, Calif. Div. Mines & Geology, Area 1 of 7 (NOS 1206N-16), Scale 1:250,000 (also 3B).
- Legg, M.R., 1991. Developments in understanding the tectonic evolution of the California Continental Borderland. In Osborne, R. H. ed., *From Shoreline to Abyss*, SEPM Shepard Commemorative Volume, 46, 291-312.
- Legg, M.R., 2021. Develop Geological Model of Offshore Southern California (Borderland) for the Community Rheology Model: Southern California Earthquake Center (SCEC5) Project Report #20117.
- Legg, M.R., Wong-Ortega, V., and Suarez-Vidal, F., 1991. Geologic structure and tectonics of the inner continental borderland of northern Baja California. In Dauphin, P., and G. Ness, editors, *The Gulf and Peninsular province of the Californias*: American Association of Petroleum Geologists *Memoir #47*, p. 145-177.
- Legg, M.R., and Goldfinger, Chris, 2002. Earthquake potential of major faults offshore southern California: Collaborative research with Oregon State University and Legg Geophysical, Final Technical Report, U.S. Geological Survey Grant No. 01HQGR0017, 24 p.
- Legg, M.R., J.C. Borrero, and C.E. Synolakis, 2004. Tsunami hazards associated with the Catalina fault in southern California. *Earthquake Spectra*, vol. 20, p. 917 -950.
- Legg, M.R., C. Goldfinger, M.J. Kamerling, J.D. Chaytor, and D.E. Einstein, 2007. Morphology, structure and evolution of California Continental Borderland restraining bends. In Cunningham, W.D. & Mann, P. (eds), *Tectonics of strike-slip restraining & releasing*

- bends in continental and oceanic settings*, Geological Society of London Special Publications, v. 290, p. 143-168.
- Legg, M.R., M.D. Kohler, N. Shintaku, and D.S. Weeraratne, 2015. High-resolution mapping of two large-scale transpressional fault zones in the California Continental Borderland: Santa Cruz-Catalina Ridge and Ferrelo. *Journal of Geophysical Research: Earth Surface*, vol. 120, doi:10.1002/2014JF003322.
- Legg, M., C. Sorlien, C. Nicholson, M. Kamerling, and G. Kuhn, 2018. Potential for large complex multi-fault earthquakes offshore southern California. *Proceedings Eleventh U.S. National Conference on Earthquake Engineering*, Los Angeles, CA.
- Maloney, J.M., Driscoll, N.W., Kent, G.M., Duke, S., Freeman, T., and Bormann, J.M., 2016. Segmentation and stepovers along strike-slip fault systems in the Inner California Borderlands: Implications for fault architecture and basin formation. In Anderson R., and Ferriz, H., eds., *Applied Geology in California*, Association of Environmental and Engineering Geologists, Special Publication Number 26, Chapter 36, p. 655-677, Star Publishing Company, Redwood, California.
- Mueller, K.J., Grant, L.B., and Gath, E., 1998. Late Quaternary growth of the San Joaquin Hills anticline a – new source of blind thrust earthquakes in the Los Angeles basin [abstract]. Seismological Society of America 1998 Annual Meeting, *Seismological Research Letters*, v. 69, no.2, P. 161-162.
- National Archive of Marine Seismic Surveys (NAMSS), 2006.
<http://walrus.wr.usgs.gov/NAMSS/>
- Nicholson, C., and J.K. Crouch, 1989. Neotectonic structures along the central and southern California margin: Predominantly a thrust regime? *Seis. Res. Letters*, 60, 23-24.
- Ninyo & Moore, 2015. SONGS ISFI Slope Calculations: Report submitted to Southern California Edison, dated 16 April 2015.
- Pacheco, J., and Nabelek, J., 1988. Source mechanisms of three moderate California earthquakes of July 1986. *Seismological Society of America Bulletin*, v. 78, p. 1907-1929.
- Plesch, A., Shaw, J.H., Benson, C., Bryant, W.A., Carena, S., Cooke, M., Dolan, J., Fuis, G., Gath, E., Grant, L., Hauksson, E., Jordan, T., Kamerling, M., Legg, M., Lindvall, S., Magistrale, H., Nicholson, C., Niemi, N., Oskin, M., Perry, S., Planansky, G., Rockwell, T., Shearer, P., Sorlien, C., Suss, M.P., Suppe, J., Treiman, J., and Yeats, R., 2007. Community Fault Model (CFM) for southern California. *Bulletin Seismological Society of America*, v. 97, p. 1793-1802, DOI: 10.1785/0120050211.
- Rivero, C., Shaw, J.H., and Mueller, K., 2000. Oceanside and Thirtymile Bank blind thrusts: Implications for earthquake hazards in coastal southern California. *Geology*, v. 28, p. 891-894.

- Rivero, C., and Shaw, J. H., 2011. Active folding and blind-thrust faulting induced by basin inversion processes, Inner California Borderlands. In McClay, K., Shaw, J., and Suppe, J., eds., *Thrust fault-related folding*, AAPG Memoir 94, p. 187-214.
- Ryan, H.F., Legg, M.R., Conrad, J.E., and Sliter, R.W., 2009. Recent faulting in the Gulf of Santa Catalina; San Diego to Dana Point; Earth science in the urban ocean; the Southern California continental borderland. In Lee, H.J., and Normark, W.R., eds., *Earth Science in the Urban Ocean—The Southern California Continental Borderland*. Geological Society of America Special Paper v. 454, p. 291-315, doi:[10.1130/2009.2454\(4.2\)](https://doi.org/10.1130/2009.2454(4.2))
- Ryan, H.F., J.E. Conrad, C.K. Paull, and M. McGann, 2012. Slip rate on the San Diego Trough fault zone, Inner California Borderland, and the 1986 Oceanside earthquake swarm revisited. *Seis. Soc. Am. Bull.*, 102, 2300-2312.
- Sahakian, V., Bormann, J., Driscoll, N., Harding, A., Kent, G., and Wesnousky, S., 2017. Seismic constraints on the architecture of the Newport-Inglewood/Rose Canyon fault: Implications for the length and magnitude of future earthquake ruptures. *Journal of Geophysical Research Solid Earth*, v. 122, p. 2085-2105. Doi: 10.102/2016JB013467.
- Shepard, F.P., and Emery, K.O., 1941. Submarine topography off the southern California coast: Canyons and tectonic. *Geological Society of America, Special Paper 31*, 171 p.
- Shlemon, R.J., 1987. *The Cristianitos fault and Quaternary geology, San Onofre State Beach, California. Geological Society of America Centennial Field Guide – Cordillera Section*, p. 171-174.
- Sorlien, C.C., J.T. Bennett, M.-H. Cormier, B.A. Campbell, C. Nicholson, and R. L. Bauer, 2016. Late-Miocene-Quaternary fault evolution and interaction in the southern California Inner Continental Borderland. *Geosphere*, v. 11, p. 1111-1132, doi:10.1130/GES01118.1.
- Southern California Edison Company, 1995. Final Report, Geotechnical Investigation of Yee, Torrey, 2001. Calculation of Ultimate Bearing Capacity, Exhibit 14, E-00-014, dated February 15.
- Sylvester, A.G., 1984. Wrench Fault Tectonics: Selected papers reprinted from the AAPG Bulletin and other geological journals, *AAPG Reprint Series No. 28*, 374 pp.
- Thompson, M., and Francis, R.D., 2019. Tectonic evolution of the Palos Verdes fault-Lasuen Knoll segment, offshore southern California. In Marsaglia, K.M., Schwalbach, J.R., and Behl, R.J., eds., *From the Mountains to the Abyss: The California Borderland as an archive of Southern California Geologic Evolution*. SEPM Special Publication No. 110, p. 241-255. Doi: 10.2110/sepm.sp.110.17.
- Yee, Torrey, 2001, Calculation of Ultimate Bearing Capacity, Exhibit 14, E-00-014, dated February 15.

U.S. Geological Survey and California Geological Survey. Quaternary fault and fold database for the United States, accessed February 2, 2020, at: <https://www.usgs.gov/natural-hazards/earthquake-hazards/faults>.

Vedder, J.G., Beyer, L.A., Junger, Arne, Moore, G.W., Roberts, A.E., Taylor, J.C., and Wagner, H.C., 1974. *Preliminary report on the geology of the Continental Borderland of southern California*. U.S. Geological Survey, Miscellaneous Field Studies Map MF-624, Scale 1:500,000.

Wallace, R.E., 1990. *The San Andreas Fault System, California*. U.S. Geological Survey Professional Paper 1515, 283 pp.

Wilcox, R.E., Harding, T.P., and Seeley, D.R., 1973. Basic wrench tectonics. *American Association of Petroleum Geologists Bulletin*, 57, 74-96.

APPENDIX A

SONGS ISFSI

SLOPE STABILITY

Dale Hinkle P.E., PLLC

P.O. Box 1016
Bonner, MT 59823
(406)244-0498
e-mail: hinklepe@gmail.com

CA RGE# 402
CARCE# 23023
MT PE#14041

Federal I.D.
45-2139130

May 27, 2011

Mr. Zaid Ahmad
Southern California Edison Company
300 North Lone Hill
San Dimas, CA 91773

Dear Mr. Ahmad:

Re: Third Party Review – Slope Evaluation
Independent Spent Fuel Storage Installation (ISFSI)
San Onofre Nuclear Generating Station

At your request, I have performed a third party review of the two reports describing the uphill slope stability (seismic case) for the above-referenced facility. The two reports are listed in the Appendix. They consist of a November, 1995 report issued by the SCE Geotechnical Group and an August 3, 2007 report/notice of calculation change by SCE Site Engineer, L. Pham. The difference in the studies is that the original 1995 study did not consider the 15-foot wide slope bench above the storage site. The 2007 study concluded that the maximum slope failure could reach 91 feet out from the existing toe of the ½:1 (horizontal to vertical) cut slope instead of 120 feet as mentioned in the 1995 report.

Observations

1. My review of the studies found their sources of data and assumptions were very similar. Both used Woodward-Clyde soil slope conditions and strengths. They are simply differences in judgment of the persons.
2. The sections analyzed (A-A' through D-D') were not shown on a plan by either report. I assume that the section modeled is on the north side of the facility where they show a 105 foot setback. This would be approximately 150 feet west of the north guard tower. It is interesting that Woodward-Clyde Sections A and B both showed the 15-foot bench and it was used in original stability calculations but was not used in the toe run-out calculations.
3. The failed slope profile was arbitrarily assumed in 1995 to be one-half the height of the original slope. The 2007 study used the same assumption. Both studies assumed a 15° lower failed slope angle. These assumptions are very arbitrary and very conservative.

2

The 1995 report indicated in Section 4.3 four profiles (A-A' through D-D') which were considered to be representative of the most critical slope geometry and closeness to the cask storage sides. These cross sections are missing in the report.

The angle of repose of the combined terrace soil would be in the 20° to 30° range. If we modeled the failure using a worst-case 20° to 25° slope, the toe run-out would be 50 to 70 feet. The value calculated is 91 feet and the available space is 105 feet. The setback of 105 feet is exceedingly conservative.

Conclusions

Based on my review of the two above-mentioned reports and my independent calculations of the setback using STABL7, and using the same assumptions as the 2007 report, I found a slope run-out of 92 feet which is almost identical to the original findings.

The arbitrary assumption that the failed slope would be half as high as the original is very conservative. The angle of repose for the soils formed by failed terrace would give a slope of at least 20° to 25° (not 15°) and would yield a toe run out of 50 to 70 feet.

Using the 15-foot wide mid-slope bench is the correct procedure and the 91 foot slope run-out is very conservative.

We appreciate the opportunity to be of service to you on this project. If you have any questions, please call our office.

Sincerely,



R. D. Hinkle
RGE #402

Attachments

APPENDIX B

ISFSI FOUNDATION DESIGN

CALCULATION TITLE PAGE

ECN NO./
PRELIM. CCN NO.

PAGE ____ OF ____

Calc. No. C-296-01.04 ECP No. & Rev. 061000254-2, REV. 0

Subject ISFSI FOUNDATION DESIGN Sheet 1 of

System Number/Primary Station System Designator 2208/XDC SONGS Unit 1, 2&3 Q-Class II

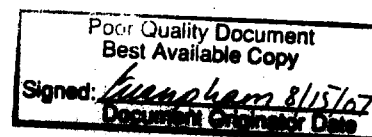
Tech. Spec./LCS Affecting? ☒ NO ☐ YES, Section No. Equipment Tag No. S1232208AHSM001

Site Programs/Procedure Impact? ☒ NO ☐ YES, AR No.

| | | | |
|--|---|---|--|
| 10CFR50.59/72.48 REVIEW | CONTROLLED COMPUTER PROGRAM / DATABASE | | |
| IS THIS CALCULATION REVISION BEING ISSUED SOLELY TO INCORPORATE CCNs/ECNs? <input checked="" type="checkbox"/> NO <input type="checkbox"/> YES AR No. <u>010901113</u> | <input type="checkbox"/> PROGRAM <input type="checkbox"/> DATABASE <u>N/A</u> ACCORDING TO SO123-XXIV-5.1 | PROGRAM / DATABASE NAME(S) <input type="checkbox"/> ALSO, LISTED BELOW <u>N/A</u> | VERSION / RELEASE NO.(S) <u>N/A</u> |

| RECORDS OF ISSUES | | | | |
|-------------------|---|-----------------------------|---|---|
| REV. DISC. | DESCRIPTION | TOTAL SHTS. LAST SHT. | PREPARED BY: (Print name/sign/date) Initial PQS Block - Requires PQS T3EN64 | APPROVED BY: (Signature/date) Initial PQS Block - Requires PQS T3EN64 |
| 3 | Revised sheets: Cross index, 5, 10 & 12. | 37 | ORIG. L.PHAM PQS VER. BY: <u>4</u> <u>Luanpham 5/17/07</u> | FLS <u>[Signature]</u> PQS VER. BY: <u>8/10/07</u> |
| CIVIL | Replaced sheets: 8, 9, 10 Added sheets: 34 thru 37 | 37 | IRE T. YEE PQS VER. BY: <u>38</u> <u>Sorey Yee 8/3/07</u> | Other |
| | | | ORIG. PQS VER. BY: ____ | FLS PQS VER. BY: ____ |
| | | | IRE PQS VER. BY: ____ | Other |
| | | | ORIG. PQS VER. BY: ____ | FLS PQS VER. BY: ____ |
| | | | IRE PQS VER. BY: ____ | Other |
| | | | ORIG. PQS VER. BY: ____ | FLS PQS VER. BY: ____ |
| | | | IRE PQS VER. BY: ____ | Other |

Space for RPE Stamp, identify use of an alternate calc., and notes as applicable.



SITE FILE COPY

This calc. was prepared for the identified ECP. ECP completion and turnover acceptance to be verified by receipt of ECP Turnover/Closure form directing conversion. Upon receipt, this calc. represents the as-built condition. ECP Turnover/Closure form date ____ by ____.

CALCULATION CROSS-INDEX

| | | |
|-------------------------------|------------------------------|---------------------|
| Calculation No. C-296 - 01.04 | ICCN NO./PRELIM. CCN NO. | PAGE _____ OF _____ |
| Sheet No. 2 of _____ | CCN CONVERSION: CCN NO. CCN- | |

| Calc. rev. number and responsible FLS initials and date | INPUTS | | OUTPUTS | | Does the output interface calc/document require change? | Identify output interface calc/document CCN, DCN, TCN/Rev., FIDCN, or tracking number. |
|---|---------------------|----------|---------------------|----------|---|--|
| | Calc / Document No. | Rev. No. | Calc / Document No. | Rev. No. | YES / NO | |
| 0 By 64-01 | 501-207-1-C11 | 5 | 28010 | 0 | No | |
| | C-296-1.01 | 0 | | | | |
| | C-296-01.02 | 0 | | | | |
| | 501-207-1-M135 | 0 | | | | |
| 1 8/15/02 | | | 28002 | 0 | No | |
| 2 8/15/02 | 501-207-1-D173 | 0 | | | No | |
| | S-02-C-001 | 0 | | | | |
| 3 8/16/02 | 5023-207-16-D109 | 0 | 28002 | 1 | YES | ECN A46647 |

EC&FS DEPARTMENT
CALCULATION SHEET

| | |
|-----------------|-------------------|
| ICCN NO./ C-1 | PAGE ____ OF ____ |
| PRELIM. CCN NO. | CCN CONVERSION: |
| CCN NO. CCN - | |

Project or DCP/FCN SONGS 1 Calc No. C-296-01.04

Subject ISFSI Foundation Design Sheet 3 of ____

| REV | ORIGINATOR | DATE | IRE | DATE | REV | ORIGINATOR | DATE | IRE | DATE | REV INDICATOR |
|-----|-------------------------|---------|---------|---------|-----|------------|------|-----|------|------------------|
| 0 | H. Hadidi ^{HH} | 3/12/01 | J. Wang | 5/3/01 | | | | | | |
| 3 | | | T. Yee | 7/31/07 | | | | | | |

| <u>TABLE OF CONTENTS</u> | <u>SHEET</u> |
|--|--------------|
| 1. Introduction / Purpose | 4 |
| 2. Results / Conclusions | 4 |
| 3. Assumptions | 4 |
| 4. Design Inputs | 5 |
| 5. Methodology | 5 |
| 6. References | 6 |
| 7. Nomenclature | 6 |
| 8. Calculations | 7 |
| • ISFSI FOUNDATION FOR SINGLE ROW OF MODULES | 7 |
| • SLAB ON GRADE FOR DRY CASK TRANSPORTATION | 11 |
| • CONCRETE PAD TARGET HARDNESS | 27 |
| • PAD INSPECTION | 33 |
| • ISFSI FOUNDATION FOR BACK TO BACK MODULES | 34 |

EC&FS DEPARTMENT CALCULATION SHEET

| | |
|----------------------------------|-------------------|
| ICCN NO./ C-1 | PAGE ____ OF ____ |
| PRELIM. CCN NO. | |
| CCN CONVERSION: CCN NO. CCN - | |

Project or DCP/FCN SONGS 1 Calc No. C-296-01.04

Subject ISFSI Foundation Design Sheet 4 of ____

| REV | ORIGINATOR | DATE | IRE | DATE | REV | ORIGINATOR | DATE | IRE | DATE | REV INDICATOR |
|-----|------------|---------|--------|---------|-----|------------|------|-----|------|---------------|
| 0 | H. Hadidi | 5/11/01 | J Wang | 7/1/01 | | | | | | |
| 2 | T. YEE | 3/4/03 | DC | 3/24/03 | | | | | | |

1. Introduction / Purpose

The purpose of this calculation is to design the reinforced concrete pad for the storage modules of Independent Spent Fuel Storage Installation (ISFSI). There are multiple storage modules placed on the concrete pad and they are connected together to form a single structure.

The purpose of this calculation is also to design the slab-on-grade adjacent to the ISFSI pad. The design of a concrete vault that would provide access to an existing man-hole (that will be completely covered by the pad) is included in this calculation for information only. Current design does not include this vault since access to the manhole is not required.

The Pad's Target Hardness is calculated for gask drops. Baseline inspections of the pad are included in this calc.

2. Results / Conclusions

Design loads are based on seismic accelerations of 1.5g horizontal and 1.0g vertical.

ISFSI concrete pad : 3'-0 thick

Moment (Capacity) = 322 foot kips > Moment (Design Load) = 260 ft kips

Allowable Soil Bearing = 23.5 ksf > Soil Bearing (Design) = 10.11 ksf

Slab-on-grade :

1'-0 thick

Jack load (Capacity) = 106.7 kips > Jack load (Design) = 105.6 kips

Punching shear (Capacity) = 334 kips > Jack load (Design) = 105.6 kips

Capacities based on S. F. of 1.6 and base plate size of 29"x29".

Existing manhole

top plate :

1-3/4" thick steel plate

Moment (Capacity) = 41.3 ft kips > Moment (Design Load) = 36.34 ft kips

Existing manhole:

Bearing capacity = 6,807 kips > Bearing load = 595 kips

~~3. Assumptions - Stated in calculation.~~

Pad Target Hardness: $S = 83,697 < 400,000$

Concrete cracks are classified as "hairline", except for one crack which is a "fine crack." All cracks are acceptable.

3. Assumptions - Stated in calculation.

EC&FS DEPARTMENT CALCULATION SHEET

| | |
|-----------------|----------------------------------|
| ICCN NO./ C-1 | PAGE ____ OF ____ |
| PRELIM. CCN NO. | CCN CONVERSION: CCN NO. CCN - |

Project or DCP/FCN SONGS 1 Calc No. C-296-01.04

Subject ISFSI Foundation Design Sheet 5 of ____

| REV | ORIGINATOR | DATE | IRE | DATE | REV | ORIGINATOR | DATE | IRE | DATE | |
|-----|-------------------------|---------|---------|---------|-----|------------|------|-----|------|-----------------------|
| 0 | H. Hadidi ^{HK} | 5/11/01 | J. Wang | 5/11/01 | | | | | | REV INDICATOR ↓ |
| 3 | L. PHAM | 5/06/07 | T. Yee | 8/3/07 | | | | | | |

4. Design Inputs

Module weight = 400 + 70 = 470 kips with back wall (Ref. 6.1, Table H1 and page H9). Used 471 kips in this calculation which is conservative.

Concrete compressive strength = 4000 psi; Fy = 60 ksi for A615, Grade 60

Seismic load: DBE 1.5g horizontal and 1.0g vertical (Reference TN West design spectra included in C-296-1.01, Rev. 0). SONGS requirements are actually based on a 0.67g seismic event. ~~The higher seismic accelerations were conservatively used to be consistent with the TN West design.~~ DUE TO THE MODULES SLIDING, THE HORIZONTAL ACCELERATION WILL BE 1.0g WHEN ASSUMING THE COEFFICIENT OF FRICTION HAS AN UPPER LIMIT OF 0.7. BY CONSIDERING SLIDING, THE VERTICAL ACCELERATION WILL ALSO BE LIMITED TO 0.44g. THEREFORE, THE TOTAL VERTICAL FORCE OF (DL + 0.44g) 0.7 = 1.0g FOR HORIZONTAL DIRECTION

5. Methodology

The multiple storage modules are placed in a single row without any separation between them. The modules are not anchored to the concrete pad.

Soil pressure is calculated by using a two-component horizontal seismic load of ^{1.0g}1.5g and a vertical component of 1.0 g, and combining them by SRSS method. The reinforcing design is based on the moment calculated for a 10 feet cantilever one-way slab, loaded with the resultant of maximum soil pressure. Reinforced concrete design is in accordance with ACI 349.

The structural design and stability of the storage module are given in Ref. 6.4.

The concrete vault walls are designed to resist the loads before and after the construction of the ISFSI pad. The walls are considered to be cantilever before pad construction and simply supported after the pad construction. The bottom slab of the vault is designed to resist the soil pressures due to the dead and live loads. The steel plate covering the vault is designed for 3' of soil on top of the plate plus a truck wheel load of 16 kips.

The slab-on-grade is designed for both the transporter truck wheel loads and the jack loads corresponding to the loading of the spent fuel cask into the modules.

EC&FS DEPARTMENT CALCULATION SHEET

| | |
|-----------------------------------|-------------------|
| ICCN NO. / C-1 PRELIM. CCN NO. | PAGE ____ OF ____ |
| CCN CONVERSION: CCN NO. CCN - | |

Project or DCP/FCN SONGS 1 Calc No. C-296-01.04

Subject ISFSI Foundation Design Sheet 6 of ____

| REV | ORIGINATOR | DATE | IRE | DATE | REV | ORIGINATOR | DATE | IRE | DATE | |
|-----|-------------------------|---------|----------------------|---------|-----|----------------------|--------|----------------------|---------|------------------|
| 0 | H. Hadidi ^{HH} | 5/11/01 | J. Wang | 5/31/01 | 2 | T. YEE ^{SY} | 3/4/03 | q.e. ^{q.e.} | 3/24/03 | REV INDICATOR |
| 1 | T. YEE ^{SY} | 4/3/02 | q.e. ^{q.e.} | 4/5/02 | | | | | | |

6. References (See Sheets 27 & 32 for additional references)

- 6.1 SO1-207-1-C11, Rev. 5, DSC/AHSM/0S197 Cask Component Weights, Mass Properties, and Lift Weight Calculation and Evaluation by TN West.
- 6.2 SCE Calculation C-296-1.01, Rev. 0, Seismic Response of ISFSI Pad.
- 6.3 ACI Manual Of Concrete Practice-Code Requirements for Nuclear Safety Related Concrete Structures (ACI-349).
- 6.4 SO1-207-1-M135, Rev. ²0, Safety Analysis Report for the Standardized Advanced NUHOMS Horizontal Modular Storage System for Irradiated Nuclear Fuel, by TN West.
- 6.5 SONGS 2&3 Preliminary Safety Analysis Report, Appendix 2B, Seismic and Foundation Studies for Proposed Units 2 and 3, San Onofre Nuclear Generating Station - Dames and Moore.
- 6.6 Designing Floor Slabs on Grade Design Manual, Second Edition.
- 6.7 SCE Calculation C-296-01.02, Rev. 0, ISFSI Pad Other Events Hazard Evaluation.
- 6.8 S01-207-1-M19, Rev. 2.
- 6.9 Bowles, J. E., "Foundation Analysis and Design," Third Edition.
- 6.10 Gaylord and Gaylord, "Structural Engineering Handbook," Second Edition.
- 6.11 SONGS 2&3 UFSAR, Appendix 3.7C, Soil-Structure Interaction Parameters, Woodward-McNeill.

7. Nomenclature

ISFSI - Independent Spent Fuel Storage Installation
 AHSM - Advanced Horizontal Storage Module
 TNW - TransNuclear West
 SRSS- Square Root of the Summation of Squares
 g - Acceleration of Gravity
 q - Soil pressure

CALCULATION SHEET

FORM NO. CEN NO.

CCN CONVERSION:
CCN NO. CCN -

Project or DCP/FCN

Calc No.

C-296-01.04

Subject ISFSI FOUNDATION DESIGN

Sheet 7 of

| REV | ORIGINATOR | DATE | REV | ORIGINATOR | DATE |
|-----|---------------|---------|-----|------------|---------|
| 0 | HASSAN HADIDA | 3/12/01 | 1 | Wang | 5/31/01 |

REV
INDICATOR

8.0 CALCULATIONS

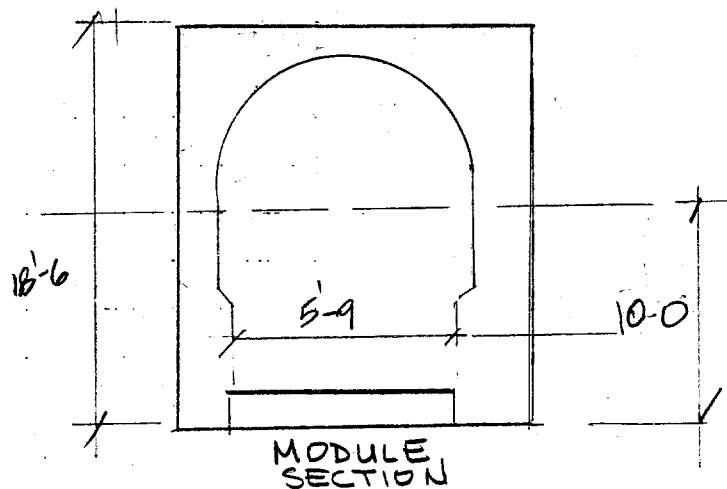
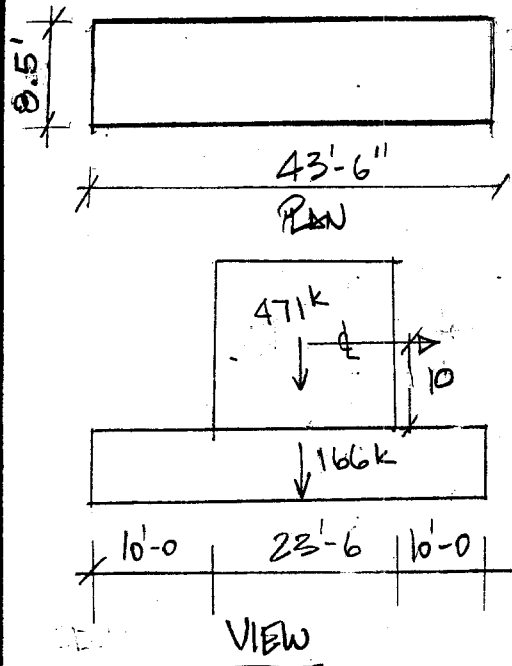
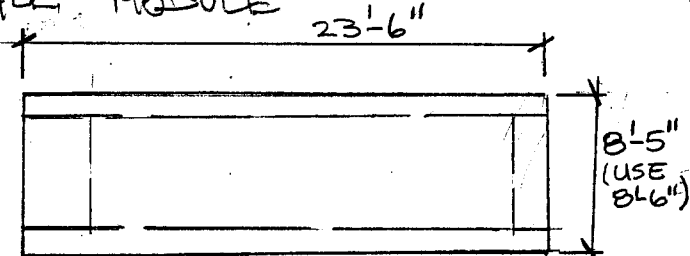
ISFSI FOUNDATION DESIGN:

MODULE WEIGHT = 400k

FOR REFERENCE SOI-207-1-C11, TABLE 41

PAD SIZE FOR A SINGLE MODULE

USE 43.5' x 8.5' x 3.0'
(REF. 6.1)



REAR SHIELDING WALL WT:

$$18.5 \times 3 \times 8.5 = 71k$$

TOTAL MODULE WT. = 400 + 71 = 471k
(INCLUDING REAR SHIELD WALL)

$$\text{WEIGHT OF PDN} = 43.5 \times 3 \times 8.5 \times 1.5 = 166k$$

$$\therefore \sum W = 471 + 166 = 637k \text{ MODULE + PAD}$$

E&TS DEPARTMENT CALCULATION SHEET

| | |
|-----------------------------|-------------------|
| ECN NO./ PRELIM. CCN NO. | PAGE ____ OF ____ |
|-----------------------------|-------------------|

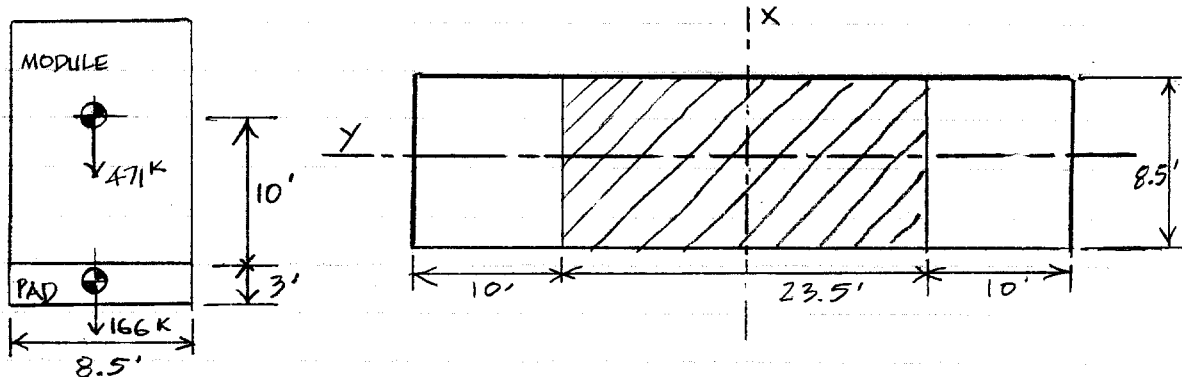
Project or ECP 061000254-2 Calc No. C-296-01.04

CCN CONVERSION:
CCN NO. CCN -

Subject ISFSI FOUNDATION DESIGN Sheet 8 of

| REV | ORIGINATOR | DATE | IRE | DATE | REV | ORIGINATOR | DATE | IRE | DATE | REV INDICATOR |
|-----|------------|------|--------|--------|-----|------------|------|-----|------|---------------|
| 3 | L. Pham | | T. Yee | 8/3/07 | | | | | | ↓ |
| | | | | | | | | | | |

CHECK SOIL PRESSURE DUE TO SEISMIC & DEAD WEIGHT OF MODULES



DEADLOAD SOIL PRESURE: $q_{DL} = \frac{V}{A} = \frac{471 + 166}{8.5 \times 43.5} = 1.72 \text{ KSF}$

SEISMIC ACCELERATIONS:

SINCE THE MODULES ARE NOT ATTACHED TO THE PAD, THE HORIZONTAL ACCELERATION OF $1g$ IS USED IN DESIGN OF THE PAD

VERTICAL SEISMIC ACCEL. OF $0.44g$ IS USED WITH $m=0.7$ TO GET $1g$ HORIZONTAL.

IT SHOULD BE NOTED THAT THE HORIZONTAL SEISMIC ACCELERATION OF $1.5g$ HAS BEEN SHOWN TO DEVELOP @ THE C.G OF THE MODULE PER C-296-01.01 HOWEVER, THIS EXCESSIVE ACCELERATION IS DUE TO THE FACT THAT THE MODULES WERE MODELED AS RIGIDLY CONNECTED TO THE PAD. IN THE ANALYSIS,

IN ALLOWING SLIDING THE HORIZ. ACCELERATION IS $1.0g$ WHEN THE VERTICAL ACCELERATION IS $0.44g$ (SONGS DBE). THE VERT. ACCELERATION OF $1.0g$ WILL BE USED IN DESIGN.

SEISMIC SOIL PRESSURE ABOUT X-X:

$$OTM_x = 1.0g \times 471 \times 13 + 1.5g \times 166 \times 1.5 = 6497 \text{ K-FT}$$

$$e_x = \frac{OTM}{V} = \frac{6497}{637} = 10.2' > \frac{L}{6} = \frac{43.5}{6} = 7.25'$$

$$q_x = \frac{2V}{3B\left(\frac{L}{2} - e\right)} = \frac{2 \times 637}{3(8.5)\left(\frac{43.5}{2} - 10.2\right)} = 4.326 \text{ KSF}$$

SEISMIC SOIL PRESSURE ABOUT Y-Y

SINCE THE MODULES ARE TIED TOGETHER, THE SOIL PRESSURE WILL BE BASED ON 10 MODULES. ACTUALLY, 19 MODULES ARE PLANNED FOR SONGS 1

E&TS DEPARTMENT CALCULATION SHEET

ECN NO./
PRELIM. CCN NO.

PAGE ____ OF ____

Project or ECP 061000254-2 Calc No. C-296-01.04

CCN CONVERSION:
CCN NO. CCN -

Subject ISFSI FOUNDATION DESIGN Sheet 9 of

| REV | ORIGINATOR | DATE | IRE | DATE | REV | ORIGINATOR | DATE | IRE | DATE | REV INDICATOR |
|-----|------------|------|--------|--------|-----|------------|------|-----|------|---------------|
| 3 | L. Pham | | T. Yee | 8/3/07 | | | | | | ↓ |
| | | | | | | | | | | |

$$OTM_y = 10 [1.0 \times 471 \times 13 + 1.5 \times 166 \times 1.5] = 64945 \text{ K-FT}$$

$$e_y = \frac{64965}{10 \times 637} = 10.2' < \frac{L}{6} = \frac{10 \times 8.5}{6} = 14.17'$$

$$q_y = \frac{MC}{I} = \frac{64965 \times (85/2)(12)}{43.5(85)^3} = 1.24 \text{ KSF}$$

TOTAL SOIL PRESSURE:

$$q_{TOT} = q_{DL} + [q_x^2 + q_y^2 + q_z^2]^{1/2} = 1.72 + [4.33^2 + 1.24^2 + 1.72^2]^{1/2}$$

$$= 1.72 + 4.82 = 6.54 \text{ KSF} < 15.63 \times 1.5 = 23.5 \text{ KSF}$$

ALLOWABLE SOIL BEARING OF 3FT EMBEDMENT AND 50% INCREASE FOR SEISMIC LOAD (REF. 6.5). THIS IS CONSERVATIVE IN COMPARISON TO FIGURE 13 OF REF. 6.11 WHICH ALLOWS A NET ALLOWABLE BEARING CAPACITY OF $25 + \frac{1}{2}(b-3)$, WHERE B = FOOTING WIDTH.

CONCRETE DESIGN (ACI 349)

ASSUME 10' OF PAD FROM MODULE TO THE EDGE OF CANTILEVER.

$$M_u = \frac{qL^2}{2} = \frac{(6.54 - 0.45)(10)^2}{2} = 304.5 \text{ K-FT/FT}$$

$$K_u = \frac{M_u}{bd^2} = \frac{304.5 \times 12}{12 \times 32^2} = 0.297 \text{ KSI}$$

$$\rho = \frac{0.85 \cdot f'_c}{f_y} \left[1 - \sqrt{1 - \frac{2K_u}{\phi \cdot 0.85 f'_c}} \right] = \frac{0.85 \times 4}{60} \left[1 - \sqrt{1 - \frac{2(0.297)}{0.9 \times 0.85 \times 4}} \right]$$

$$\rho = 0.0058 < 0.018 \text{ MAX}, A_s = \rho bd = 0.0058(12)(32) = 2.226 \text{ IN}^2 > 0.0033 \text{ MIN}$$

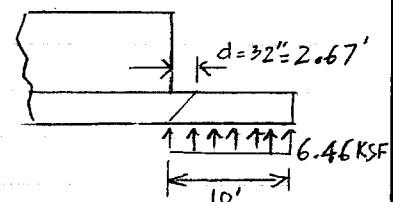
$$\text{USE } \#11 @ 8", A_s = 1.56 \times 12/8 = 2.34 \text{ IN}^2 > 2.226 \text{ IN}^2 \text{ REQ.}$$

$$V_u = (6.54 - 0.45)(10 - 2.67) = 44.64 \text{ K/FT}$$

$$\phi V_c = \phi 2\sqrt{f'_c} bd = 0.75 \times 2 \times \sqrt{4000} \times 12 \times 32 = 36.43 \text{ K/FT}$$

$$\phi V_s = V_u - \phi V_c = 44.64 - 36.43 = 8.2 \text{ K/FT}$$

$$V_s = 8.2 / 0.75 = 10.95 \text{ K/FT}$$



E&TS DEPARTMENT
CALCULATION SHEET

ECN NO./
PRELIM. CCN NO.

PAGE ____ OF ____

Project or ECP 061000254-2 Calc No. C-296-01.04

CCN CONVERSION:
CCN NO. CCN -

Subject ISFSI FOUNDATION DESIGN Sheet 10 of

| REV | ORIGINATOR | DATE | IRE | DATE | REV | ORIGINATOR | DATE | IRE | DATE | REV INDICATOR ↓ |
|---|------------|------|--------|--------|-----|------------|------|-----|------|-----------------------|
| 3 | L. Pham | | T. Yee | 8/3/07 | | | | | | |
| <p>TRY # 4 @ 12" ON CENTER $A_v = 0.2 \text{ IN}^2 > 50 \frac{b_s}{f_y} = \frac{50(12)(12)}{60,000} = 0.12 \text{ IN}^2 \text{ (OK)}$</p> <p>$V_s = \frac{A_s f_y d}{s} = \frac{0.2(60)(32)}{12}$</p> <p>$V_s = 32 \text{ K/FT} > 10.95 \text{ K/FT (OK)}$</p> <p>$\frac{36.43}{6.54 - 0.45} = 5.98 \text{ FT} \therefore \text{ @ } 5.98 \text{ FT FROM EDGE OF PAD}$</p> <p>$V_u = 36.43 \text{ K/FT} = \phi V_c$ THUS, PROVIDE # 4 STIRRUP @ 12 IN SPACING FROM 4' TO 10' FROM EDGE OF PAD.</p> <p>TEMPERATURE & SHRINKAGE REINFORCING STEEL IN LONGITUDINAL DIR.</p> <p>$A_s = 0.0018 \times 12 \times 36 = 0.78 \text{ IN}^2/\text{FT}$</p> <p>USE # 7 @ 12" TOP & BOTTOM $A_s = 1.2 \text{ IN}^2/\text{FT} > 0.78 \text{ IN}^2/\text{FT}$</p> <p>FOR EAST WEST DIRECTION, USE # 9 @ 12" O.C FOR TOP REINFORCING STEEL.</p> <p>(SEE SHEET 34 FOR BACK TO BACK MODULE FOUNDATION DESIGN).</p> | | | | | | | | | | |

EC&FS DEPARTMENT
CALCULATION SHEET

| | |
|-----------------|-------------------|
| ICCN NO./ | PAGE ____ OF ____ |
| PRELIM. CCN NO. | |
| CCN CONVERSION: | |
| CCN NO. | CCN - |

Project or DCP/FCN _____ Calc No. C-296-01.04

Subject SFS FOUNDATION DESIGN

Sheet 11 of ____

| REV | ORIGINATOR | DATE | IRE | DATE | REV | ORIGINATOR | DATE | IRE | DATE | REV INDICATOR |
|-----|---------------|---------|---------|--------|-----|------------|------|-----|------|---------------|
| 0 | HASSAN HADIDI | 3/12/01 | J. Wang | 5/1/01 | | | | | | |
| | | | | | | | | | | |

DESIGN OF SLAB ON GRADE FOR DRY ASK
TRANSPORTATION [REF. G.6]

MAX. TIRE PRESSURE = 120 PSI [REF. G.8]

MAX. LOAD PER TIRE = 8250# [" "]

TIRE AREA = $\frac{8250}{120} = 68.75 \text{ sq in}$

FLEXURAL STRENGTH OF
CONCRETE

$$MR = 9\sqrt{f'_c} = 569 \text{ PSI}$$

SLAB STRESS PER 1000# OF AXLE LOAD

$$s = \frac{569}{2(\text{WHEEL FACTOR})} \times \frac{1}{46^k} = 6.2$$

WHERE 46 IS AXLE LOAD IN KIPS CALCULATED AS FOLLOWS:

$$264,000\# / 4 = 66,000\# / \text{AXLE}$$

DUAL WHEEL SPACING $\approx 32"$ \Rightarrow EQUIVALENT LOAD FACTOR = 0.7 [REF. G.6, FIG 18]

$$66^k \times 0.7 = 46^k$$

REF. G.6, FIG 16 $\Rightarrow t = 11.2"$ USING SLAB STRESS OF 6.2 CALCULATED

ABOVE. USE $t = 12"$.

EC&FS DEPARTMENT CALCULATION SHEET

CCN NO.
PRELIM. CCN NO.

PAGE OF

CCN CONVERSION:
CCN NO. CCN -

Project or DCP/FCN

Calc No. C-296-01.04

Sheet 12 of

Subject SPS FOUNDATION DESIGN

| REV | ORIGINATOR | DATE | IRE | DATE | REV | ORIGINATOR | DATE | IRE | DATE | REV INDICATOR |
|-----|---------------------|---------|---------|---------|-----|------------|------|-----|------|---------------|
| 0 | HH HASSAN HADIDI | 3/12/01 | J. Wang | 5/31/01 | | | | | | |

CHECK OF AREA REQUIRE FOR THE JACK LOAD

$$t^2 = P_u \times A \times \log_{10} \left[\frac{Bt^3}{C} \right] \rightarrow \text{from DESIGNING FLOOR SLABS ON GRADE}$$

P_u = the factored column load in

prands
 $A = 0.03 \text{ ft}^2$

$B = 915,000 \times \sqrt{f'_c}$

$C = K \times b^4$

t = slab thickness

b = base plate dimension, inches

$P_u = 264,000$

ASSUMED LOAD FACTOR
 $= 66,000 \times 1.6 = 105,600 \#$

4 (jacks)

$$A = .03 : \sqrt{4000} = .000474$$

$$B = 915,000 \times 63.24 = 57,869,681$$

$$C = 200 \times b^4$$

$$t = 12$$

K subgrade modulus

Conservative value
 $= 200 \text{ pci}$

$$144 = 105,000 \times .000474 \times$$

$$C = \frac{Bt^3}{10 [t^2 / P_u A]} = 200 \times b^4 = \frac{57,869,681 \times 12^3}{10^{(144 / 105,600 \times .000474)}} = 782$$

$$b^4 = 639.378$$

$$b = 28.27"$$

Area requires for jack load = $29 \times 29 = 841 \text{ in}^2$

$$P_u = \frac{(12)^2}{106,619} \log_{10} \left[\frac{57,869,681 \times 12^3}{200 \times 29^4} \right] = 105,600 \#$$

FOR $P_u = 105,600 \#$

E&TS DEPARTMENT CALCULATION SHEET

| | |
|------------------------------|-------------------|
| ICCN NO./ PRELIM. CCN NO. | PAGE ____ OF ____ |
|------------------------------|-------------------|

| |
|----------------------------------|
| CCN CONVERSION: CCN NO. CCN - |
|----------------------------------|

Project or DCP/FCN _____ Calc No. C-296-01.04

Subject ISFSI FOUNDATION DESIGN

Sheet 13 of ____

| REV | ORIGINATOR | DATE | IRE | DATE | REV | ORIGINATOR | DATE | IRE | DATE | REV | INDICATOR |
|-----|-----------------------------|---------|---------|---------|-----|------------|------|-----|------|-----|-----------|
| 0 | HASSAN HADIDI ^{HH} | 3/12/01 | J. Wang | 5/21/01 | | | | | | | |
| | | | | | | | | | | | |

8.0 CALCULATIONS (CONTINUED)

$$\begin{aligned}
 \text{PUNCHING SHEAR CAP} &= 4 \sqrt{f'_c} b_o d \\
 &= 4 \sqrt{4000} (4 \times (29" + 8.75")) (8.75") \\
 &= 334,252^\# > 105,600^\# \quad \text{O.K.}
 \end{aligned}$$

$b_o = 4(b+d)$
 $d = 12" - 3.25" = 8.75"$

SLAB DESIGN SUMMARY :

$t = 12"$, #4 @ 12" TOP & BOTTOM , EACH WAY

29"x29" BASE PLATE FOR THE JACK LOAD

CALCULATION SHEET

 ICCN NO. /
 PRELIM. CCN NO.

PAGE ____ OF ____

 CCN CONVERSION:
 CCN NO. CCN -

 Project or DCP/FCN _____ Calc No. C-296-01.04

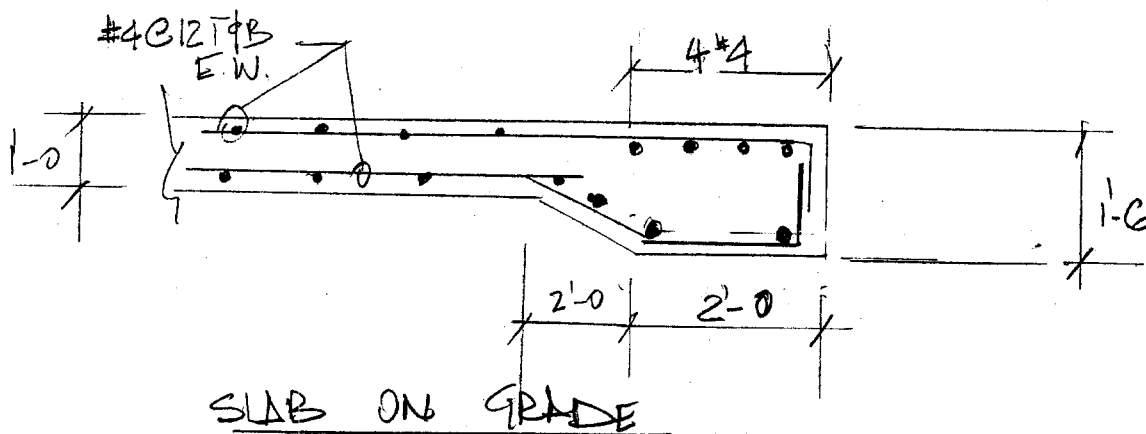
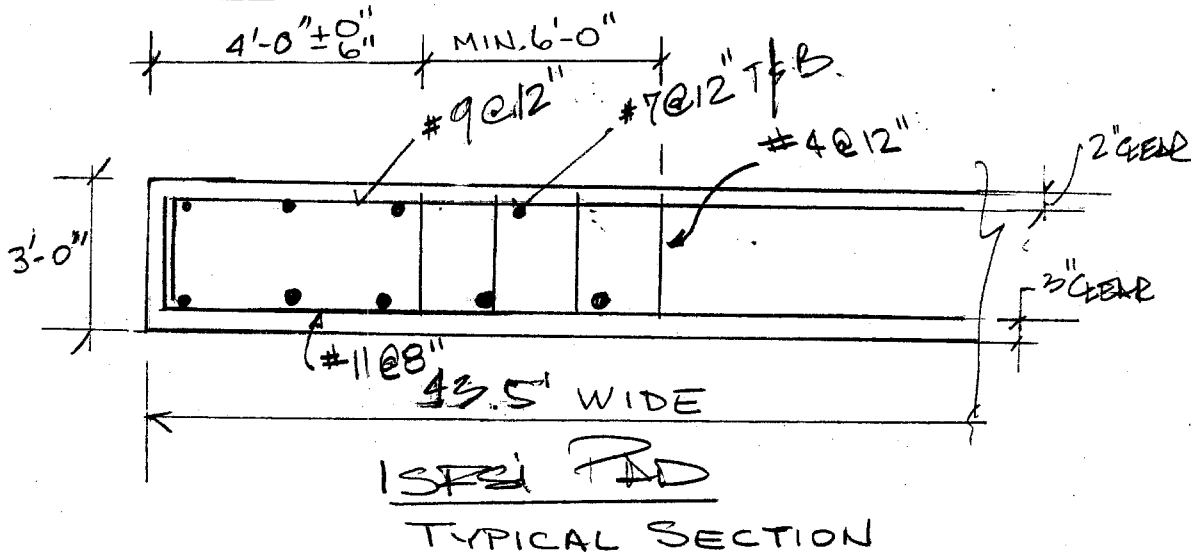
 Subject ISFS FOUNDATION DESIGN

 Sheet 14 of ____

| REV | ORIGINATOR | DATE | IRE | DATE | REV | ORIGINATOR | DATE | IRE | DATE |
|-----|---------------|---------|-----------|---------|-----|------------|------|-----|------|
| 0 | HASSAN HANADI | 3/12/01 | J. Wang | 5/31/01 | | | | | |
| 1 | T. Yee S. Yee | 4/03/02 | q.e. q.e. | 4/1/02 | | | | | |

 REV
 INDICATOR

DWG 28002



E&TS DEPARTMENT CALCULATION SHEET

| | | |
|-----------------|-------------------|--|
| ICCN NO./ | PAGE ____ OF ____ | |
| PRELIM. CCN NO. | | |
| CCN CONVERSION: | | |
| CCN NO. | CCN - | |

Project or DCP/FCN SONGS 1 Calc No. C-296-01.04

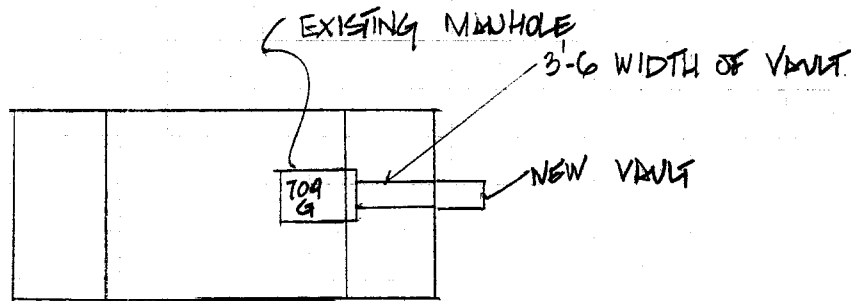
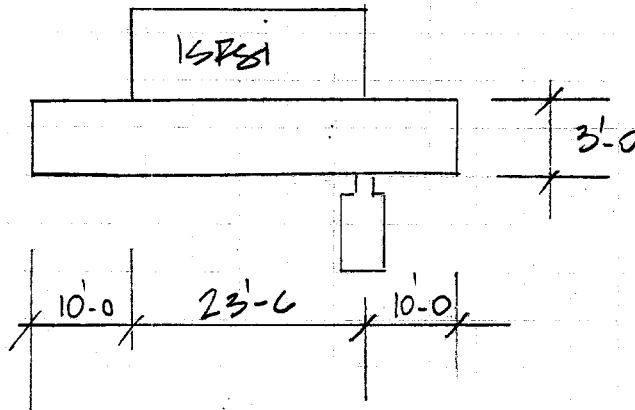
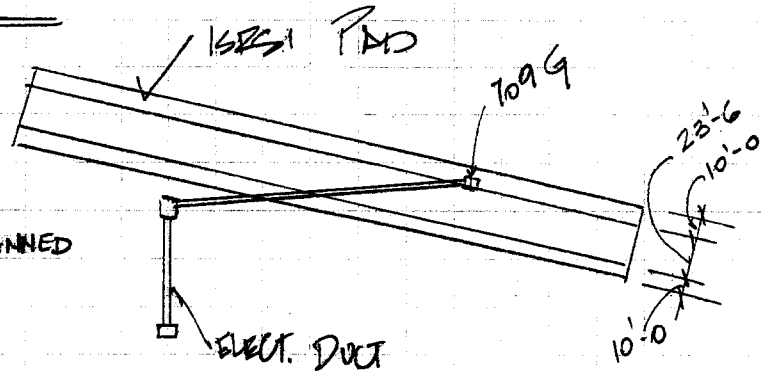
Subject FOUNDATION DESIGN KPSI Sheet 15 of 15

| REV | ORIGINATOR | DATE | TRE | DATE | REV | ORIGINATOR | DATE | TRE | DATE | REV INDICATOR |
|-----|---------------|---------|----------|--------|-----|------------|------|-----|------|---------------|
| 0 | HASSAN HADIDI | 3/12/01 | J. Dwyer | 5/1/01 | | | | | | |

FOUNDATION DESIGN

VAULT DESIGN

VAULT DESIGN IS PROVIDED FOR INFORMATION ONLY. ACCESS TO EXISTING MANHOLE IS NOT PLANNED IN THE CURRENT DESIGN.



AN EXISTING MANHOLE 709 G IS LOCATED UNDER KPSI PAD. FOR INSPECTION OF EXISTING MANHOLE BUILD A VAULT CONNECTING 709 G MANHOLE TO THE MANHOLE WHICH WILL BE LOCATED OUTSIDE THE KPSI PAD. THE SIDE WALLS OF THE VAULT WILL HAVE SAME HEIGHT AS WALLS OF THE EXISTING MANHOLE.

E&TS DEPARTMENT
CALCULATION SHEET

| | |
|----------------------------------|-------------------|
| CCN NO./ PRELIM. CCN NO. | PAGE ____ OF ____ |
| CCN CONVERSION: CCN NO. CCN - | |

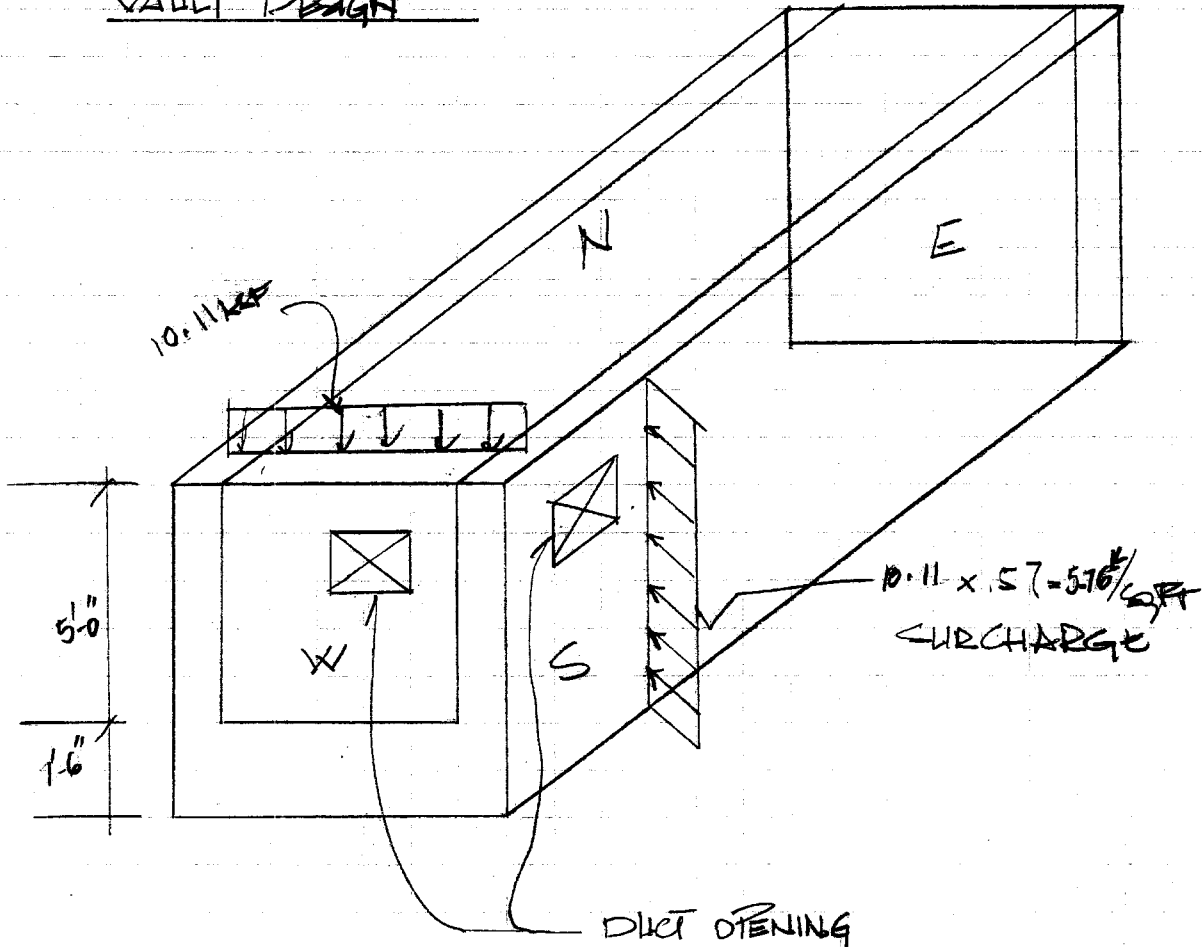
Project or DCP/FCN SONGS 1 Calc No. C-296-01.04

Subject FOUNDATION DESIGN ICSI

Sheet 16 of ____

| REV | ORIGINATOR | DATE | TRE | DATE | REV | ORIGINATOR | DATE | TRE | DATE | REV INDICATOR |
|-----|---------------|---------|---------|---------|-----|------------|------|-----|------|---------------|
| 0 | HASSAN HABIBI | 3/12/01 | J. Jang | 5/21/01 | | | | | | |

FOUNDATION DESIGN ICSI
VAULT DESIGN



E&TS DEPARTMENT CALCULATION SHEET

| | |
|-----------------|-------------------|
| ICCN NO./ | PAGE ____ OF ____ |
| PRELIM. CCN NO. | |

| |
|----------------------------------|
| CCN CONVERSION: CCN NO. CCN - |
|----------------------------------|

Project or DCP/FCN _____ Calc No. C-296-01.04

Subject ISFSI FOUNDATION DESIGN

Sheet 17 of ____

| REV | ORIGINATOR | DATE | IRE | DATE | REV | ORIGINATOR | DATE | IRE | DATE | REV INDICATOR |
|-----|-----------------------------|---------|---------|--------|-----|------------|------|-----|------|---------------|
| 0 | HASSAN HADIDI ^{HH} | 3/12/01 | J. Wang | 5/1/01 | | | | | | |
| | | | | | | | | | | |

8.0 CALCULATIONS (CONTINUED)

WALL DESIGN: CONSIDER TWO LOADING CONDITIONS 1) BEFORE PAD AND MODULES ARE CONSTRUCTED 2) AFTER PAD AND MODULES ARE CONSTRUCTED.

1) BEFORE PAD CONSTRUCTION, CANTILEVER WALL, TENSION REBAR OUTSIDE

FACE, MAX. MOMENT AT THE BASE OF THE WALL:

D + L LOADS:

$$M_1 = \frac{1}{6} (K_a \gamma) h^3 \quad \text{DUE TO SOIL}$$

$$M_1 = \frac{1}{6} (0.57 \times 0.126) (5)^3 = 1.50 \text{ K-FT/FT}$$

$$M_2 = \frac{w \ell^2}{2} = \overset{\substack{\text{PAD WT} \\ \swarrow \\ K_a}}{(0.45 \times 0.57)} (5)^2 / 2 = 3.21 \text{ K-FT/FT}$$

ADD THIS TO ACCOUNT FOR THE SURCHARGE LOADING DUE TO PAD

WEIGHT BEFORE THE CONNECTION BETWEEN PAD AND WALL IS 100%

EFFECTIVE.

$M_3 =$ MOMENT DUE TO SURCHARGE FROM THE WHEEL LOADS (REF. 6.9, PAGE 415)

E&TS DEPARTMENT CALCULATION SHEET

ICCN NO./

PRELIM. CCN NO.

PAGE ____ OF ____

CCN CONVERSION:

CCN NO. CCN -

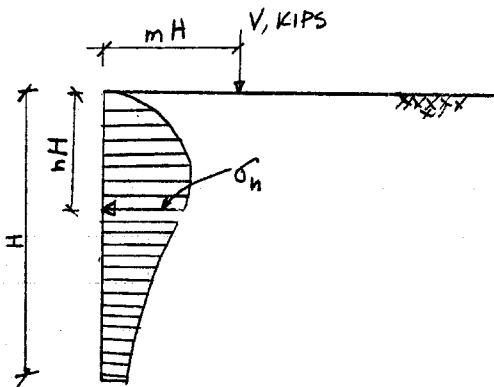
 Project or DCP/FCN _____ Calc No. C-296-01.04

 Subject ISFSI FOUNDATION DESIGN

 Sheet 18 of ____

| REV | ORIGINATOR | DATE | IRE | DATE | REV | ORIGINATOR | DATE | IRE | DATE | REV INDICATOR |
|-----|---------------|--------|--------|---------|-----|------------|------|-----|------|---------------|
| 0 | HASSAN HADIDI | 5/7/01 | Jubong | 5/21/01 | | | | | | |

B.O CALCULATIONS (CONTINUED)



$$m > 0.4 \quad \sigma_h = \frac{1.77V}{H^2} \frac{m^2 n^2}{(m^2 + n^2)^3}$$

$$m \leq 0.4 \quad \sigma_h = \frac{0.28V}{H^2} \frac{n^2}{(0.16 + n^2)^3}$$

FOR A GIVEN V , $m = 0.4 \Rightarrow$ maximum σ_h

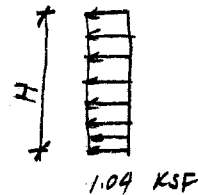
USE $\sigma_h = \frac{0.28V}{H^2} \frac{n^2}{(0.16 + n^2)^3}$

$V = 16^k$ (WHEEL LOAD)

$H = 5'$

| n | σ_h (KSF) |
|------|------------------|
| 0 | 0 |
| 0.1 | 0.36 |
| 0.2 | 0.90 |
| 0.25 | 1.02 |
| 0.26 | 1.02 |
| 0.27 | 1.03 |
| 0.28 | 1.04 ← MAXIMUM |
| 0.29 | 1.04 |
| 0.3 | 1.03 |
| 0.35 | 0.97 |
| 0.4 | 0.88 |
| 0.5 | 0.65 |
| 0.6 | 0.46 |
| 0.7 | 0.32 |
| 0.8 | 0.22 |
| 0.9 | 0.16 |
| 1.0 | 0.11 |

CONSERVATIVE USE $\sigma_h = 1.04$ KSF UNIFORMLY OVER FULL HEIGHT.



$$M_3 = 1.04 (5') (5'/2)$$

$$M_3 = 13 \text{ K-FT/FT}$$

E&TS DEPARTMENT CALCULATION SHEET

| | |
|------------------------------|-------------------|
| ICCN NO./ PRELIM. CCN NO. | PAGE ____ OF ____ |
|------------------------------|-------------------|

| |
|----------------------------------|
| CCN CONVERSION: CCN NO. CCN - |
|----------------------------------|

Project or DCP/FCN _____ Calc No. C-296-01.04

Subject ISFSI FOUNDATION DESIGN

Sheet 19 of ____

| REV | ORIGINATOR | DATE | IRE | DATE | REV | ORIGINATOR | DATE | IRE | DATE | REV | INDICATOR |
|-----|---------------|--------|---------|---------|-----|------------|------|-----|------|-----|-----------|
| 0 | HASSAN HADIDI | 5/7/01 | J. Dany | 5/21/01 | | | | | | | ↓ |

8.0 CALCULATIONS (CONTINUED)

LOAD FACTOR DUE TO
EARTH PRESSURE

← L.L.
← D.L.

$$M_u = 1.7 M_1 + 1.4 M_2 + 1.7 M_3$$

$$M_u = 1.7(1.50) + 1.4(3.21) + 1.7(13) = 29.1 \text{ K-FT/FT}$$

2) AFTER PAD AND MODULE ADDED:

SEISMIC LOAD CASE:

$$M = \frac{w h^2}{8} + \frac{1}{2} \left[\frac{1}{6} (K_a \delta) h^3 \right] \quad \text{MAXIMUM @ WALL MIDHEIGHT}$$

$$M = \frac{(0.57 \times 10.11)(5)^2}{8} + \frac{1}{2} \left[\frac{1}{6} (0.57 \times 0.126)(5)^3 \right] = 18.8 \text{ K-FT/FT}$$

∴ DESIGN WALLS FOR
29.1 K-FT/FT

E&TS DEPARTMENT
CALCULATION SHEET

| | |
|-----------------|-------------------|
| ICCN NO./ | PAGE ____ OF ____ |
| PRELIM. CCN NO. | |
| CCN CONVERSION: | |
| CCN NO. | CCN - |

Project or DCP/FCN _____ Calc No. C-296-01.04

Subject ISFSI FOUNDATION DESIGN

Sheet 20 of ____

| REV | ORIGINATOR | DATE | IRE | DATE | REV | ORIGINATOR | DATE | IRE | DATE | REV INDICATOR |
|-----|---------------|---------|---------|--------|-----|------------|------|-----|------|---------------|
| 0 | HASSAN HADIDI | 3/12/01 | J. Wang | 5/2/01 | | | | | | |

8.0 CALCULATIONS (CONTINUED)

$$P_s = \frac{0.85 f'_c}{f_y} \left[1 - \sqrt{1 - \frac{2 K_u}{\phi (0.85) (f'_c)}} \right]$$

$$K_u = \frac{M \times 12000}{b d^2} = \frac{29.1 \times 12000}{12 \times 15^2} = 129.3$$

$$P_s = \frac{0.85 \times 4}{60} \left[1 - \sqrt{1 - \frac{2 \times 129.3}{0.9 \times 0.85 \times 4000}} \right] = 0.0024$$

USE $P_{min} = 0.0033$ FOR VERTICAL REBARS $\approx \frac{4}{3} P_s = 0.0032$ O.K.

$$A_s = 0.0033 \times 12 \times 15 = 0.59 \text{ IN}^2/\text{FT}$$

USE #8 @ 12" USE SAME REINFORCING FOR INSIDE AND OUTSIDE FACES

$$0.79 \text{ IN}^2/\text{FT} > 0.59 \text{ IN}^2/\text{FT} \text{ O.K.}$$

$$\phi M_n = 0.9 \times 0.79 \times 60 \left[15 - \frac{1}{2} \frac{0.79 \times 60}{0.85 \times 4 \times 12} \right] / 12 = 51.3 \text{ K-FT/FT} > 29.1 \text{ K-FT/FT}$$

O.K.

HORIZONTAL REINF: $0.0025 \times 12 \times 15 / 2 = 0.23 \text{ IN}^2/\text{FT/FACE}$

$\leftarrow P_{min}$

USE #6 @ 12" EACH FACE = $0.44 \text{ IN}^2/\text{FT/FACE} > 0.23$ O.K.

∴ VERTICAL #8 @ 12" EACH FACE

HORIZONTAL #6 @ 12" EACH FACE

E&TS DEPARTMENT
CALCULATION SHEET

ICCN NO./
PRELIM. CCN NO. PAGE ____ OF ____

CCN CONVERSION:
CCN NO. CCN -

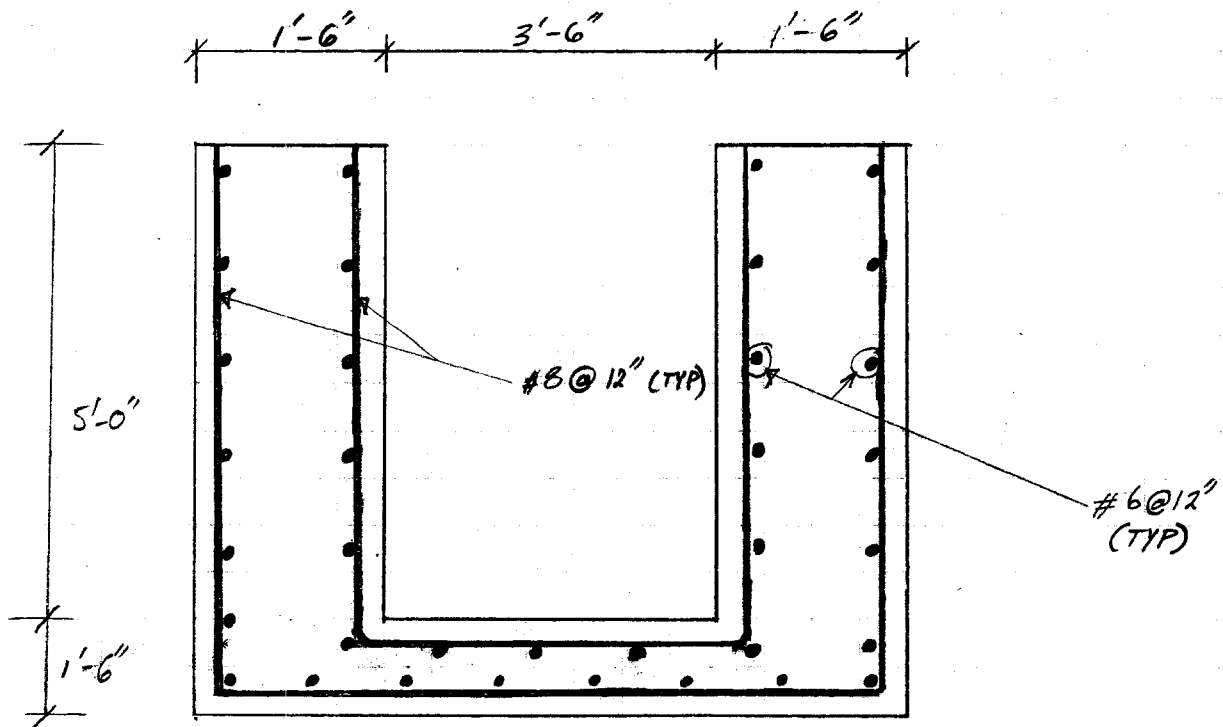
Project or DCP/FCN _____ Calc No. C-296-01.04

Subject 1 SPS1 FOUNDATION DESIGN

Sheet 21 of ____

| REV | ORIGINATOR | DATE | IRE | DATE | REV | ORIGINATOR | DATE | IRE | DATE | REV INDICATOR |
|-----|---------------|---------|---------|--------|-----|------------|------|-----|------|---------------|
| 0 | HASSAN HADIDI | 3/12/01 | J. Wong | 5/2/01 | | | | | | |

8.0 CALCULATIONS (CONTINUED)



EC&FS DEPARTMENT CALCULATION SHEET

| | |
|----------------------------------|-------------------|
| ICCN NO./ PRELIM. CCN NO. | PAGE ____ OF ____ |
| CCN CONVERSION: CCN NO. CCN - | |

Project or DCP/FCN _____ Calc No. C-296-01.04

Subject ISFSI FOUNDATION DESIGN

Sheet 71 of ____

| REV | ORIGINATOR | DATE | IRE | DATE | REV | ORIGINATOR | DATE | IRE | DATE | REV INDICATOR |
|-----|--------------|----------|---------|--------|-----|------------|------|-----|------|---------------|
| 0 | HASSAN HADID | 12/26/00 | J. Wong | 5/2/01 | | | | | | |
| | | | | | | | | | | |

CHECK BOTTOM SLAB

TOP SLAB D.L. $150 \times (3.5 + 1.5 + 1.5) \times 1.4 \times 3 \times 1 = 4,045 \text{ LB/FT}$
 BOTTOM SLAB D.L. $150 \times (3.5 + 1.5 + 1.5) \times 1.4 \times 1.5 \times 1 = 2,048 \text{ LB/FT}$
 SIDE WALLS D.L. $150 \times 5 \times 1.5 \times 2 \times 1.4 \times 1 = 3,150 \text{ LB/FT}$
 LIVE LOAD $100 \times 3.5 \times 1 \times 1.7 = 595 \text{ LB/FT}$
 D.L. FROM PAD $\frac{[(471^k + 166^k) / (43.5' \times 8.5')] \times 1.4 \times (3.5' + 1.5' + 1.5')}{25,565 \text{ LB/FT}} = 15,677 \text{ LB/FT}$
 ↑ ↑
 MODULE WT WT OF PAD

BOTTOM SOIL PRESSURE = $(25,565 \text{ LB/FT}) / (3.5' + 1.5' + 1.5') = 3,933 \text{ PSF}$

$V_u = 3,933 \text{ PSF} \times 3.5' / 2 = 6,883 \text{ \# / FT}$

$\phi V_c = 0.85 \times 2 \sqrt{4,000} \times 12" \times 15" = 19,353 \text{ \# / FT} > 6,883 \text{ \# / FT} \text{ O.K.}$

$M_u = 3,933 (3.5')^2 / 8 = 6.02 \text{ K-FT / FT}$

$K_u = M_u / b d^2 = 6.02 \times 12000 / [(12)(15)^2] = 26.8$

$\rho = \frac{0.85 f'_c}{f_y} \left[1 - \sqrt{1 - \frac{2 K_u}{\phi (0.85) f'_c}} \right] = \frac{0.85 \times 4}{60} \left[1 - \sqrt{1 - \frac{2 \times 26.8}{19 \times 0.85 \times 4000}} \right]$

$\rho = 0.00050 < \rho_{min}$

$\rho_{min} = 200 / f_y = 200 / 60,000 = 0.0033 \text{ USE } \rho = \rho_{min} = 0.0033$

EC&FS DEPARTMENT
CALCULATION SHEET

| | |
|----------------------------------|-------------------|
| ICCN NO./ PRELIM. CCN NO. | PAGE ____ OF ____ |
| CCN CONVERSION: CCN NO. CCN - | |

Project or DCP/FCN _____ Calc No. C-296-01.04

Subject ISFSI FOUNDATION DESIGN Sheet 27 of ____

| REV | ORIGINATOR | DATE | IRE | DATE | REV | ORIGINATOR | DATE | IRE | DATE | REV INDICATOR |
|-----|--------------|----------|---------|---------|-----|------------|------|-----|------|---------------|
| 0 | HASSAN HADID | 12/26/00 | J. Wang | 5/21/01 | | | | | | ↓ |
| | | | | | | | | | | |

USE #8 @ 12" TO MATCH THE WALL REINFORCING

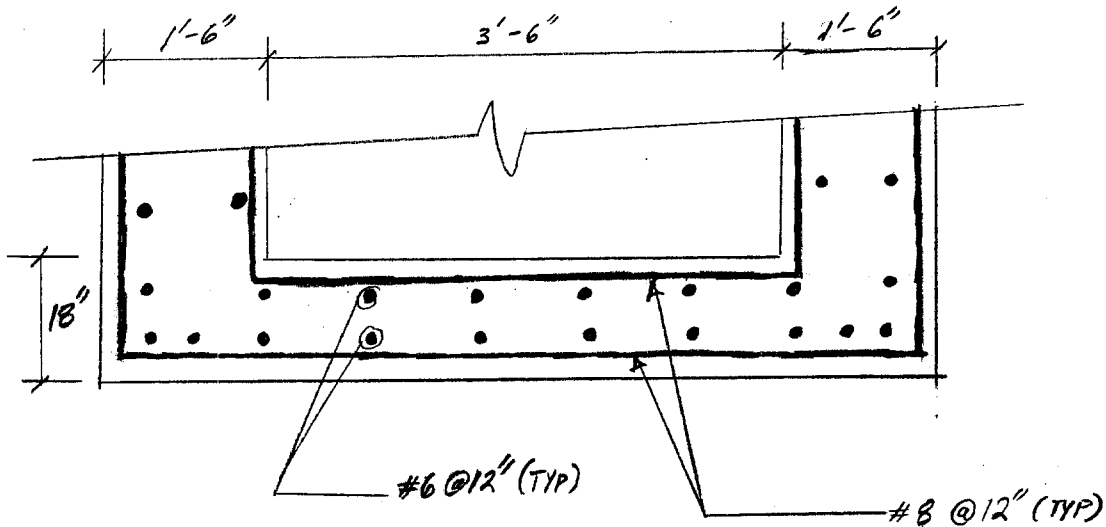
$$\rho = \frac{0.79 \text{ IN}^2}{(12'')(15'')} = 0.0044 > 0.0033 \text{ O.K.}$$

$$\phi M_n = 0.9 \times 0.79 \times 60 \left[15 - \frac{1}{2} \frac{0.79 \times 60}{0.85 \times 4 \times 12} \right] / 12 = 51.3 \text{ K-FT/FT} > 6.02 \text{ K-FT/FT O.K.}$$

USE #6 @ 12" LONGITUDINAL REINFORCING (SAME AS WALL HORIZONTAL REINFORCING)

$$\rho = \frac{0.44 \text{ IN}^2 \times 2^{\leftarrow \text{TOP \& BOTTOM}}}{12'' \times 18''} = 0.0041 > 0.0018 \text{ MIN. SHRINKAGE REINF O.K.}$$

* ON GROSS CONC. AREA



E&TS DEPARTMENT CALCULATION SHEET

| | |
|----------------------------------|-------------------|
| ICCN NO./ PRELIM. CCN NO. | PAGE ____ OF ____ |
| CCN CONVERSION: CCN NO. CCN - | |

Project or DCP/FCN _____ Calc No. C-296-1.04

Subject ISFSI FOUNDATION DESIGN

Sheet 24 of ____

| REV | ORIGINATOR | DATE | IRE | DATE | REV | ORIGINATOR | DATE | IRE | DATE | REV INDICATOR |
|-----|----------------------------|---------|---------|---------|-----|------------|------|-----|------|---------------|
| 0 | HASSAN HADID ^{HH} | 3/12/01 | J. Wang | 5/21/01 | | | | | | ↓ |

BIO CALCULATIONS (CONTINUED)

DESIGN THE STEEL PLATE TO COVER THE EXISTING MANHOLE: (DWG. 28010).

DESIGN LOAD: H2O TRUCK LOAD OF 32^K PER AXLE, 16^K EACH

SET OF WHEELS, 6' APART. ADD THE DEAD LOAD DUE TO 3' OF SOIL

COVERING THE STEEL PLATE.

$$M = \frac{16^k (6')}{4} (1.3) + \frac{(3' \times 0.126 \times 3') (6')^2}{8}$$

[↑] δ_{SOIL} [↑] HALF OF DISTANCE BETWEEN WHEELS
[↑] IMPACT FACTOR (REF. 6.10 PAGE 18-17)

$$= 31.2 \text{ K-FT} + 5.1 \text{ K-FT} = 36.3 \text{ K-FT}$$

$$\text{PLATE THICKNESS} = t = \sqrt{\frac{(36.3 \text{ K-FT})(12)}{(0.75 \times 36 \text{ KSI}) (3' \times 12'') / 6}}$$

$f_b = 0.75 f_y$ [↑] HALF OF DISTANCE BETWEEN WHEELS

$$t = 1.64'' \quad \text{USE } 1\frac{3}{4}'' \text{ PLATE}$$

$$\text{MOMENT CAPACITY} = f_b S = (0.75 \times 36 \text{ KSI}) (36'' \times 1.75^2 / 6) / 12 = 41.3 \text{ K-FT}$$

$> 36.3 \text{ K-FT}$
 O.K.

$$\Delta = \frac{16^k (1.3) (72)^3}{48 \times 29,000 \times 16.1} + \frac{5 [(3' \times 0.126 \times 3') / 12] (72)^4}{384 \times 29,000 \times 16.1} = 0.35'' + 0.07'' = 0.42''$$

[↑] IMPACT LOAD FACTOR [↑] δ_{SOIL} [↑] HALF OF DIST. BETWEEN WHEELS
 $I = \frac{1}{12} (36'') (1.75)^3 = 16.1 \text{ IN}^4$
[↑] HALF OF DISTANCE BETWEEN WHEELS

O.K.

E&TS DEPARTMENT
CALCULATION SHEET

| | |
|----------------------------------|-------------------|
| ICCN NO./ PRELIM. CCN NO. | PAGE ____ OF ____ |
| CCN CONVERSION: CCN NO. CCN - | |

Project or DCP/FCN _____ Calc No. C-296-1.04

Subject 15FS/ FOUNDATION DESIGN

Sheet 25 of ____

| REV | ORIGINATOR | DATE | IRE | DATE | REV | ORIGINATOR | DATE | IRE | DATE | REV INDICATOR |
|-----|---------------|---------|---------|---------|-----|------------|------|-----|------|---------------|
| 0 | HASSAN HADIDI | 3/12/01 | J. Wang | 5/21/01 | | | | | | |

8.0 CALCULATIONS (CONTINUED)

DESIGN THE STEEL PLATE TO COVER THE VAULT :

$$M = \frac{16K(3.5')}{4} (1.3) + \frac{(3' \times 0.126 \times 3')(3.5')^2}{8}$$

$$= 18.2 \text{ K-FT} + 1.7 \text{ K-FT} = 19.9 \text{ K-FT}$$

$$\text{PLATE THICKNESS} = t = \sqrt{\frac{(19.9 \text{ K-FT})(12)}{(0.75 \times 36 \text{ KSI})(3' \times 12'')/6}}$$

$$t = 1.21 \quad \text{USE } 1\frac{1}{4}" \text{ PLATE}$$

$$\text{MOMENT CAPACITY} = f_b S = (1.75 \times 36 \text{ KSI})(36 \times 1.25^2/6)/12 = 21.1 \text{ K-FT}$$

$$> 19.9 \text{ K-FT}$$

O.K.

$$\Delta = \frac{16K(1.3)(42)^3}{48 \times 29,000 \times 5.9} + \frac{5[(3' \times 0.126 \times 3')/12](42)^4}{384 \times 29,000 \times 5.9}$$

$$I = \frac{1}{12} (36'')(1.25')^3 = 5.9$$

$$\Delta = 0.19" + 0.02" = 0.21" \quad \text{O.K.}$$

E&TS DEPARTMENT CALCULATION SHEET

ICCN NO./
PRELIM. CCN NO.

PAGE ____ OF ____

CCN CONVERSION:
CCN NO. CCN -

Project or DCP/FCN _____ Calc No. C-296-01-04

Subject ISFSI FOUNDATION DESIGN

Sheet 26 of 28

| REV | ORIGINATOR | DATE | IRE | DATE | REV | ORIGINATOR | DATE | IRE | DATE | REV INDICATOR |
|-----|---------------|---------|---------|---------|-----|------------|------|-----|------|---------------|
| 0 | HASSAN HADIDI | 5/11/01 | J. Wang | 5/21/01 | | | | | | |

8.0 CALCULATIONS (CONTINUED)

CHECK EXISTING MANHOLE FOR THE PAD PLUS SEISMIC LOADS:

SINCE CONCRETE HAS A HIGHER STIFFNESS THAN THE SURROUNDING SOILS,
THE PAD AND MODULE SEISMIC LOADS WILL BE MOSTLY RESISTED BY THE
MANHOLE WALLS IN BEARING.

CHECK THE BEARING STRESS ON THE EXISTING MANHOLE WALLS:

$$\text{TOTAL BEARING LOAD} = (10.11 \text{ KSF})(7.67' \times 7.67') = 595^{\text{K}}$$

$$\phi P_n = 0.7 P_n = 0.7 \times 0.85 f'_c \times A_c = 0.595 f'_c A_c$$

$$A_c = (4 \times 82" - 42)(10") = 2860 \text{ IN}^2$$

↑ 3'-6" OF MANHOLE
WALL TO BE REMOVED

$$\phi P_n = 0.595 \times 4 \times 2860 = 6807^{\text{K}} > P_u = 595^{\text{K}} \quad \text{O.K.}$$

↑ ASSUME $f'_c = 4000 \text{ PSI}$

EC&FS DEPARTMENT
CALCULATION SHEET

ICCN NO./
PRELIM. CCN NO. PAGE ____ OF ____

CCN CONVERSION:
CCN NO. CCN -

Project or DCP/FCN SONGS 1 Calc No. C-296-01.04

Subject ISFSI Foundation Design Sheet 27 of ____

| REV | ORIGINATOR | DATE | IRE | DATE | REV | ORIGINATOR | DATE | IRE | DATE | REV INDICATOR |
|-----|------------|--------|-----------|---------|-----|------------|------|-----|------|---------------|
| 2 | T. Yee | 3/4/03 | g e g m e | 3/24/03 | | | | | | |
| | | | | | | | | | | |

CHECK CONCRETE PAD TARGET HARDNESS

Per Section 12.4.4.2 of TN SAR (Ref. 6A), the concrete pad properties must meet the concrete parameters specified in EPRI Report NP-4830, "The Effects of Target Hardness on the Structural Design of Concrete Storage Pads for Spent Fuel Casks," October 1986.

In order to meet this requirement, the target hardness will be calculated and must be less than 400,000. TN West drop analysis used a max. acceleration of 75g which corresponds to a target hardness of 400,000 (EPRI Report, Fig. 2B).

The target hardness equations are given the EPRI Report (Equations 4 and 5) as:

$$S = 2rAkMu\sigma_u / (W^3(1 - e^{-\beta r} \cos \beta r)) \quad \text{End Drop}$$

$$S = 2AE_sMu\sigma_u / (W^3\beta) \quad \text{Edge Drop}$$

NOTE: Edge Drop is the same as Side Drop for TN analysis.

EC&FS DEPARTMENT
CALCULATION SHEET

ICCN NO./
PRELIM. CCN NO.

PAGE ____ OF ____

CCN CONVERSION:
CCN NO. CCN -

Project or DCP/FCN SONGS 1 Calc No. C-296-01.04

Subject ISFSI Foundation Design Sheet 28 of ____

| REV | ORIGINATOR | DATE | IRE | DATE | REV | ORIGINATOR | DATE | IRE | DATE | REV ↓ INDICATOR |
|-----|------------|--------|-----|---------|-----|------------|------|-----|------|-----------------------|
| 2 | T. Yee | 3/4/03 | gc | 3/24/03 | | | | | | |
| | | | | | | | | | | |

CHECK CONCRETE PAD TARGET HARDNESS (CONT.)

where:

S = target hardness number (non dimensional)

M_u = ultimate moment capacity of the slab (lb-in)

W = weight of Cask (lb.)

σ_u = ultimate strength of concrete (psi)

A = cask footprint area (in²)

E_s = elastic modulus of soil

E_c = elastic modulus of concrete

ν_s = Poisson's ratio of soil

ν_c = Poisson's ratio of concrete = .17 (EPRI Report)

r = cask radius

End Drop

$$\beta = (E_s / 4D_c)^{1/4}$$

$$D_c = E_c h^3 / (12(1 - \nu_c^2))$$

$$k = \pi E_s / (1 - \nu_s^2)$$

EC&FS DEPARTMENT
CALCULATION SHEET

ICCN NO./
PRELIM. CCN NO.

PAGE ____ OF ____

CCN CONVERSION:
CCN NO. CCN -

Project or DCP/FCN SONGS 1 Calc No. C-296-01.04

Subject ISFSI Foundation Design

Sheet 29 of ____

| REV | ORIGINATOR | DATE | IRE | DATE | REV | ORIGINATOR | DATE | IRE | DATE | REV INDICATOR |
|-----|------------|--------|-----|---------|-----|------------|------|-----|------|---------------|
| 2 | T. Yee | 3/4/03 | gcm | 3/24/03 | | | | | | |
| | | | | | | | | | | |

CHECK CONCRETE PAD TARGET HARDNESS (CONT.)

h = concrete pad thickness

Edge Drop

$$\beta = (E_s / 4E_c I_c)^{1/4}$$

$$I_c = \frac{1}{12} L h^3$$

$$L = \text{length of cask} = 203 \text{ in. (Ref. SOI-207-1-D173)}$$

Target Hardness - End Drop:

$$r \approx \frac{80}{2} = 40" \text{ (Ref. SOI-207-1-D173)}$$

$$A = \pi r^2 = \pi (40)^2$$

$$= 5026 \text{ in}^2$$

$$E_s = 13000 \text{ ksi} \quad (\text{Ref. SONGS 2\&3 FSAR, Sect. 2.5.4.10A})$$

$$= 90,278 \text{ psi}$$

$$\nu_s = .35$$

$$k = \pi E_s / (1 - \nu_s^2) = \pi (90278) / (1 - .35^2)$$

$$= 323,210$$

$$M_u = \frac{M_{CAP}}{.9} = \frac{322}{.9} = 358 \text{ k-ft} = 4.293 \times 10^6 \text{ lb-in}$$

$$\sigma_u = 4000 \text{ psi}$$

$$W = 200,000 \text{ lb. (Ref. SOI-207-1-C11)}$$

EC&FS DEPARTMENT
CALCULATION SHEET

ICCN NO./
PRELIM. CCN NO.

PAGE ____ OF ____

CCN CONVERSION:
CCN NO. CCN -

Project or DCP/FCN SONGS 1 Calc No. C-296-01.04

Subject ISFSI Foundation Design Sheet 30 of ____

| REV | ORIGINATOR | DATE | IRE | DATE | REV | ORIGINATOR | DATE | IRE | DATE | REV INDICATOR |
|-----|------------|--------|--------|---------|-----|------------|------|-----|------|---------------|
| 2 | T. Yee Sy | 3/4/03 | 92 gnu | 3/24/03 | | | | | | |
| | | | | | | | | | | |

CHECK CONCRETE PAD TARGET HARDNESS (CONT.)

$$D_c = E_c h^3 / (12 (1 - \nu_c^2))$$

$$= \frac{3.6 \times 10^6 (36)^3}{12 (1 - .17^2)}$$

$$= 1.44 \times 10^{10}$$

$$E_c = 57000 \sqrt{f'_c}$$

$$= 57000 \sqrt{4000}$$

$$= 3.6 \times 10^6 \text{ psi}$$

$$\beta = \left(\frac{E_s}{4 D_c} \right)^{\frac{1}{4}} = \left[\frac{90278}{4 (1.44 \times 10^{10})} \right]^{\frac{1}{4}}$$

$$= .0354$$

$$S = \frac{2(40)(5026)(323210)(4.293 \times 10^6)(4000)}{200000^3 (1 - e^{-.0354(40)} \cos .0354(40))}$$

$$= 368,305 < 400,000 \quad \text{OK}$$

(End Drop)

Target Hardness - Edge Drop (Side Drop):

$$A = DL = 10 \times 203$$

$$= 2030 \text{ in}^2$$

$$I_c = \frac{1}{12} L h^3 = \frac{1}{12} (203)(36)^3$$

$$= 789,264 \text{ in}^4$$

$$\beta = \left(\frac{E_s}{4 E_c I_c} \right)^{\frac{1}{4}} = \left(\frac{90278}{4 (3.6 \times 10^6) (789264)} \right)^{\frac{1}{4}}$$

$$= .0094$$

EC&FS DEPARTMENT
CALCULATION SHEET

ICCN NO./
PRELIM. CCN NO. PAGE ____ OF ____

Project or DCP/FCN SONGS 1 Calc No. C-296-01.04

CCN CONVERSION:
CCN NO. CCN -

Subject ISFSI Foundation Design Sheet 31 of

| REV | ORIGINATOR | DATE | IRE | DATE | REV | ORIGINATOR | DATE | IRE | DATE | REV INDICATOR |
|-----|------------|--------|-----|---------|-----|------------|------|-----|------|---------------|
| 2 | T. Yee Sy | 3/4/03 | JE | 3/27/03 | | | | | | |
| | | | | | | | | | | |

CHECK CONCRETE PAD TARGET HARDNESS (CONT.)

$$S = \frac{2(2030)(90278)(4.293 \times 10^6)(4000)}{200000^3 (1.0094)}$$

$$= 83,697 < 400,000 \quad \underline{\text{OK.}}$$

(Edge Drop or Side Drop)

∴ The concrete pad and soil at SONGS have target hardnesses of less than 400,000. Therefore, the TN West cask drop analysis is valid for SONGS.

Although the end drop case was evaluated on ISFSI pad, the scenario is not credible because the transfer cask cannot fall on its end from the transfer trailer. Also, there is sufficient margin to account for actual concrete strength for the edge drop case (Target Hardness is proportional to concrete strength)

E&TS DEPARTMENT
CALCULATION SHEET

| | |
|----------------------------------|-------------------|
| ICCN NO./ PRELIM. CCN NO. | PAGE ____ OF ____ |
| CCN CONVERSION: CCN NO. CCN - | |

Project or DCP/FCN SONGS 1 Calc No. C-296-01.04

Subject ISFSI Foundation Design Sheet 32 of

| REV | ORIGINATOR | DATE | IRE | DATE | REV | ORIGINATOR | DATE | IRE | DATE | REV INDICATOR |
|-----|------------------|--------|-----------------|---------|-----|------------|------|-----|------|------------------|
| 2 | T. Yee <i>SY</i> | 3/4/03 | <i>J. Appel</i> | 3/24/02 | | | | | | ↓ |
| | | | | | | | | | | |

Pad Inspection

The concrete pad was inspected for cracks and the results of the inspection are noted on the following sheet which indicates the approximate crack widths and the locations of the cracks.

The concrete pad was inspected on 7/24/2002 before the Large Component Removal (LCR) crane was placed on the pad. At that time only Cracks A, B and C were noted because they were about 0.1 mm or larger.

A subsequent inspection was performed on 12/3/2002 after the LCR crane was demobilized to see if the condition of the concrete pad had changed significantly. More cracks were observed and the transverse pattern of the cracks is indicative of cracks caused by concrete shrinkage. The cracks were less than 0.4 mm wide and thus classified as "hairline" with the exception of Crack C. Some portions of Crack C were about 0.5 mm wide which is classified as "fine," but there were no other signs of distress. All the cracks are acceptable per the acceptance criteria for concrete cracks that are given in Calc. No. S-02-C-001.

Some edge spalls were also observed and the movement of the crane's crawler tracks over the pad caused these cracks. No rebar was exposed and these spalls were repaired to ensure proper concrete cover over the rebars.

Conclusion:

The concrete condition of the pad is acceptable for the storage modules and the noted results of the inspection will be the baseline for future inspections.

EC&FS DEPARTMENT CALCULATION SHEET

ICCN NO./
PRELIM. CCN NO. PAGE ____ OF ____

CCN CONVERSION:
CCN NO. CCN -

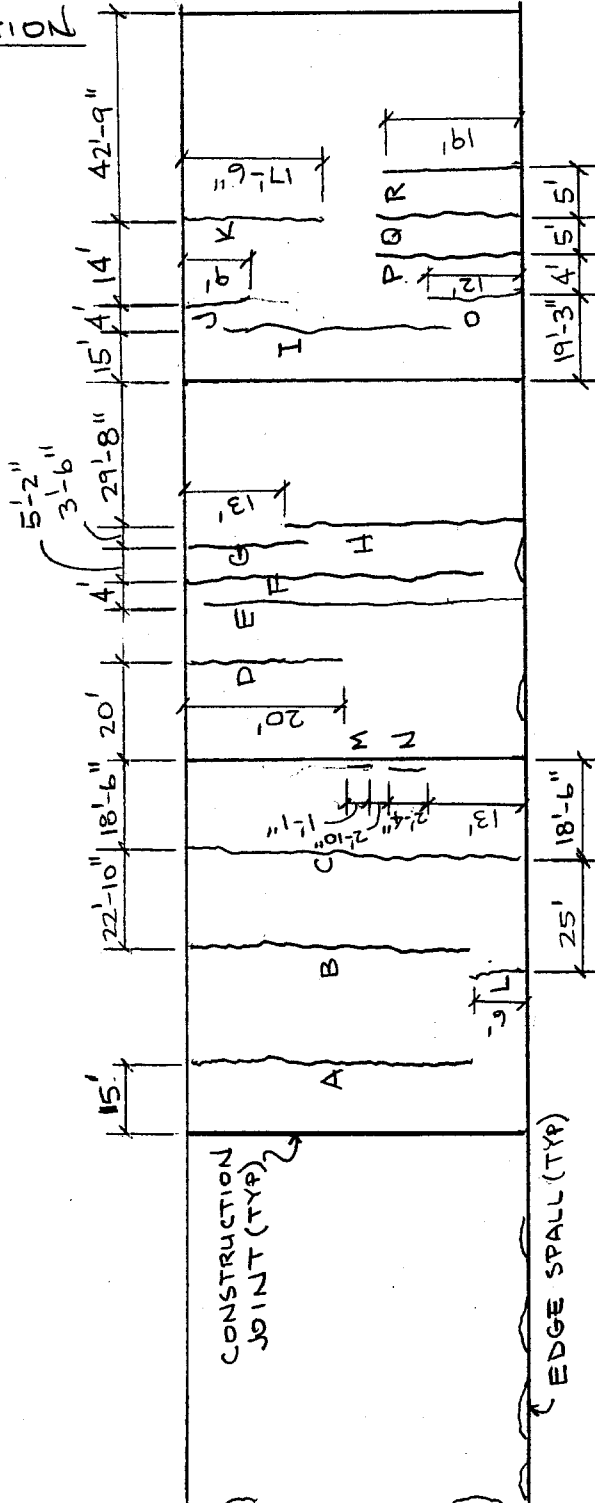
Project or DCP/FCN SONGS 1 Calc No. C-296-01.04

Subject ISFSI FOUNDATION DESIGN Sheet 33 of 37 ②

| REV | ORIGINATOR | DATE | IRE | DATE | REV | ORIGINATOR | DATE | IRE | DATE | REV INDICATOR |
|-----|------------------|---------|--------------|---------|-----|------------|------|-----|------|---------------|
| 2 | T. Yee <i>SY</i> | 3/4/03 | JE <i>am</i> | 3/24/02 | | | | | | |
| 3 | Luan Pham | 5/16/07 | T. Yee | 8/3/07 | | | | | | |

PAD INSPECTION

CRACKS OBSERVED ON
7/24/02 & 12/3/02



PLAN

| CRACKS | WIDTH (7/24/02) | WIDTH (12/3/02) |
|----------------|-----------------|-----------------|
| A | <.1mm | <.1mm |
| B | .2mm | .3mm |
| C | .3mm | .4 to .5mm |
| D | — | <.2mm |
| E | — | <.1mm |
| F | — | .4mm |
| G | — | <.1mm |
| H | — | <.2mm |
| I | — | <.2mm |
| J | <.1mm | <.1mm |
| K | .2mm | .2mm |
| L | .2mm | .2mm |
| M (Edge Crack) | .1mm | .2mm |
| N (Edge Crack) | .2mm | .2mm |
| O | <.1mm | <.1mm |
| P | <.1mm | <.1mm |
| Q | <.1mm | <.1mm |
| R | <.1mm | <.1mm |

E&TS DEPARTMENT CALCULATION SHEET

ECN NO. / ~~A48347~~ 45/16/07
PRELIM. CCN NO.

PAGE ____ OF ____

Project or ECP 061000254-2 Calc No. C-296-01.04

CCN CONVERSION:
CCN NO. CCN -

Subject ISFSI FOUNDATION DESIGN

Sheet 34 of ____

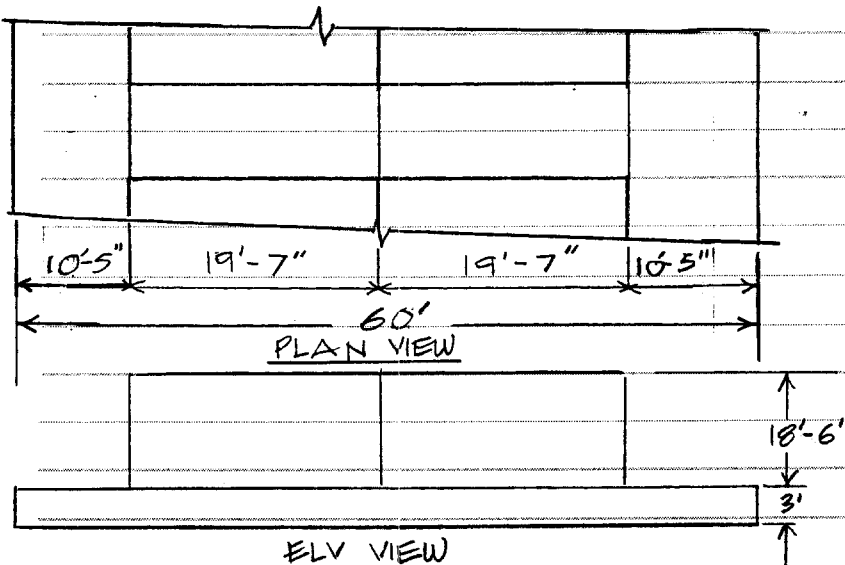
| REV | ORIGINATOR | DATE | IRE | DATE | REV | ORIGINATOR | DATE | IRE | DATE | REV INDICATOR |
|-----|------------|-----------|--------|--------|-----|------------|------|-----|------|---------------|
| 3 | L. Pham | 2/26/2007 | T. Yee | 8/3/07 | | | | | | ↓ |
| | | | | | | | | | | |

ISFSI FOUNDATION FOR BACK TO BACK MODULES

DIMENSIONS: 293' L x 60' W x 3' D [REF: 28002, ECN A46647]

BACK TO BACK MODULES DIMENSIONS:

39'-2" L x 8'-5" W x 18'-6" H [REF: 501-207-1, M135]

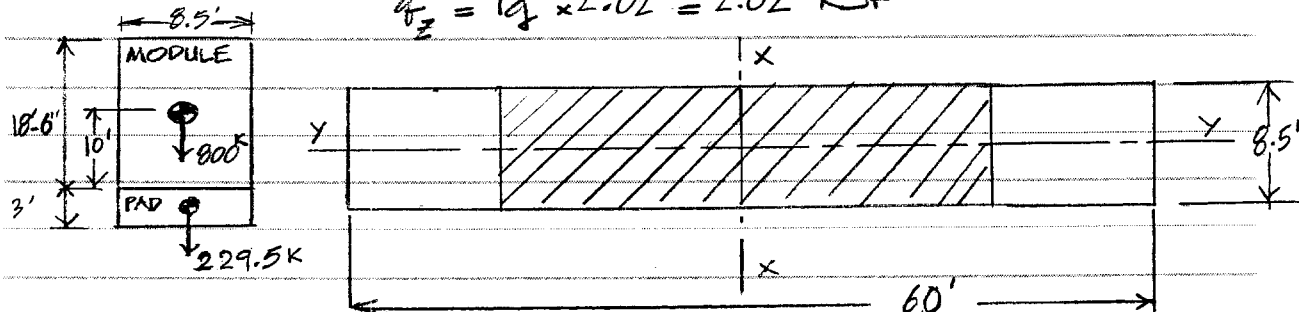


- MODULES WEIGHT: $400 \times 2 = 800$ KIPS
(NO REAR SHIELD WALL FOR BACK TO BACK MODULES).
- FOUNDATION WEIGHT $60 \times 3 \times 8.5 \times 0.15 = 229.5$ KIPS. [8.5' STRIP]
- TOTAL WEIGHT $800 + 229.5 = 1029.5$, SAY 1030 KIPS

CHECK SOIL PRESSURE:

SOIL PRESSURE DUE TO DEAD LOAD: $q_{PL} = \frac{V}{A} = \frac{1030}{8.5 \times 60} = 2.02$ KSF

SEISMIC VERTICAL: $q_z = 1q \times 2.02 = 2.02$ KSF



E&TS DEPARTMENT
CALCULATION SHEET

ECN NO. / ~~A48347~~ 45/16/07
PRELIM. CCN NO.

PAGE ____ OF ____

Project or ECP 061000254-2 Calc No. C-296-01.04

CCN CONVERSION:
CCN NO. CCN -

Subject ISFSI FOUNDATION DESIGN

Sheet 35 of ____

| REV | ORIGINATOR | DATE | IRE | DATE | REV | ORIGINATOR | DATE | IRE | DATE | REV INDICATOR |
|-----|------------|-----------|--------|--------|-----|------------|------|-----|------|---------------|
| 3 | L. Pham | 2/26/2007 | T. Yee | 8/3/07 | | | | | | ↓ |
| | | | | | | | | | | |

SEISMIC SOIL PRESSURE ABOUT X-X:

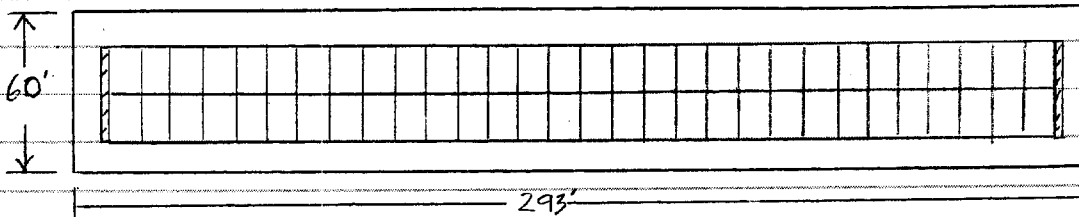
USE ACCELERATION OF 1.0g FOR BOTH LATERAL & LONGITUDINAL DR.

$$OTM_x = 1.0g(800 \times 13) + 1.5g(230 \times 1.5) = 10918 \text{ K-FT}$$

$$e_x = \frac{OTM_x}{V} = \frac{10918}{1030} = 10.6 \text{ FT} > \frac{L}{6} = \frac{60}{6} = 10 \text{ FT}$$

$$q_x = \frac{2V}{3B\left(\frac{L}{2} - e\right)} = \frac{2 \times 1030}{3(8.5)\left(\frac{60}{2} - 10.6\right)} = 4.164 \text{ KSF}$$

SEISMIC SOIL PRESSURE ABOUT Y-Y



FOUNDATION WEIGHT: $60' \times 293' \times 3 \times 0.15 = 7911 \text{ K}$

MODULES' WEIGHT: $31 \times 800 = 24800 \text{ K}$

END SHIELD WALLS: $(39.17 \times 18.5 \times 3 \times 0.15) \times 2 = 652 \text{ K}$

$$TOT = 33363 \text{ K}$$

$$OTM_y = 1.0g \cdot (24800 + 652)(13) + 1.5g(7911 \times 1.5) = 330,876 + 17800 = 348,676 \text{ FT-K}$$

$$e_y = \frac{M}{V} = \frac{348,676}{33,363} = 10.45 < \frac{L}{6} = \frac{293}{6} = 48.83 \text{ FT}$$

$$q_y = \frac{MC}{I} \quad \text{WHERE } C = \frac{293}{2}, I = \frac{60(293)^3}{12} = 1.26 \times 10^8 \text{ FT}^4$$

$$q_y = 0.41 \text{ KSF}$$

$$q_{TOT} = q_n [q_x^2 + q_y^2 + q_z^2]^{\frac{1}{2}} = 2.02 + [4.164^2 + 0.41^2 + 2.02^2]^{\frac{1}{2}} = 6.67 \text{ KSI}$$

E&TS DEPARTMENT
CALCULATION SHEET

ECN NO. / ~~A48347~~ 5/16/07
PRELIM. CCN NO.

PAGE ____ OF ____

Project or ECP 061000254-2 Calc No. C-296-01.04

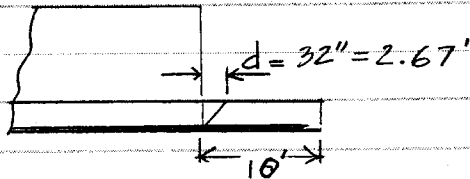
CCN CONVERSION:
CCN NO. CCN -

Subject ISFSI FOUNDATION DESIGN

Sheet 36 of ____

| REV | ORIGINATOR | DATE | IRE | DATE | REV | ORIGINATOR | DATE | IRE | DATE | REV INDICATOR |
|-----|------------|-----------|--------|--------|-----|------------|------|-----|------|---------------|
| 3 | L. Pham | 2/26/2007 | T. Yee | 8/3/07 | | | | | | ↓ |
| | | | | | | | | | | |

CONCRETE DESIGN:



$$M_u = \frac{qL^2}{2} = \frac{(6.67 - 0.45)(10)^2}{2} = 311 \text{ K-FT}$$

$$K_u = \frac{M_u}{bd^2} = \frac{311 \times 12}{12 \times 32^2} = 0.304 \text{ KSI}$$

$$\rho = \frac{0.85 \times f'_c}{f_y} \left[1 - \sqrt{1 - \frac{2K_u}{0.85f'_c}} \right] > 0.0033 \text{ MIN}$$

$$\rho = \frac{0.85 \times 4}{60} \left[1 - \sqrt{1 - \frac{2(0.304)}{0.85 \times 4}} \right] = 0.00594 < 0.018 \text{ MAX}$$

$$A_s = \rho bd = 0.00594(12)(32) = 2.28 \text{ IN}^2/\text{FT} \text{ REQUIRED}$$

$$\text{PROVIDE \#11 @ 8" } \therefore A_s = 1.56 \text{ IN}^2 \left(\frac{12}{8} \right) = 2.34 \text{ IN}^2$$

$$V_u = (6.67 - 0.45)(10 - 2.67) = 45.6 \text{ K/FT}$$

$$\phi V_c = \phi 2 \sqrt{f'_c} \cdot bd = 0.75 \times 2 \sqrt{4000} (12)(32) = 36.43 \text{ K/FT}$$

$$\phi V_s = V_u - \phi V_c = 45.6 - 36.43 = 9.17 \text{ K/FT}$$

$$V_s = \frac{9.17}{0.75} = 12.23 \text{ K/FT}$$

$$\text{TRY \#4 @ 12 IN ON CENTER } A_v = 0.2 \text{ IN}^2 > 50 \frac{b_s}{f_y} = \frac{50(12)(12)}{60000} = 0.12 \text{ IN}^2 \text{ (OK)}$$

$$V_s = \frac{A_v f_y d}{s} = \frac{0.2(60)(32)}{12} = 32 \text{ K}_f > 12.23 \text{ K/FT (OK)}$$

36.43 = 5.86' \therefore AT 5.86' FROM EDGE OF PAD $V_u = 36.43 \text{ K/FT} = \phi V_c$
(6.67 - 0.45) THUS, PROVIDE #4 STIRRUP @ 12 IN SPACING FROM
4' TO 10' FROM EDGE OF PAD

E&TS DEPARTMENT
CALCULATION SHEET

ECN NO. / ~~A48347~~ ^{45116/07}
PRELIM. CCN NO.

PAGE ____ OF ____

Project or ECP 061000254-2 Calc No. C-296-01.04

CCN CONVERSION:
CCN NO. CCN -

Subject ISFSI FOUNDATION DESIGN

Sheet 37 of 37

| REV | ORIGINATOR | DATE | IRE | DATE | REV | ORIGINATOR | DATE | IRE | DATE | REV INDICATOR |
|-----|------------|-----------|--------|--------|-----|------------|------|-----|------|---------------|
| 3 | L. Pham | 2/26/2007 | T. Yee | 8/3/07 | | | | | | ↓ |
| | | | | | | | | | | |

TEMPERATURE & SHRINKAGE STEEL IN LONGITUDINAL DIRECTION:

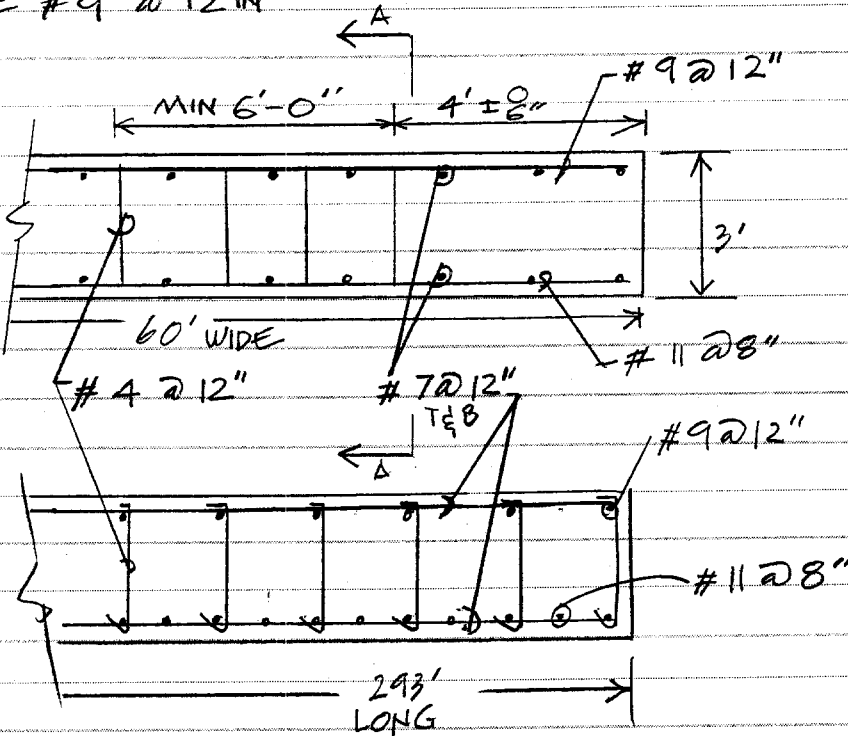
$$A_s = 0.0018 \times 36 \times 12 = 0.78 \text{ IN}^2/\text{FT}$$

USE #7 @ 12" @ TOP & BOTTOM

$$A_{s \text{ PROV}} = 2(0.6) = 1.2 \text{ IN}^2/\text{FT} > 0.78 (\text{OK})$$

TOP LAYER REINFORCEMENT STEEL (HOR DIRECTION)

USE #9 @ 12 IN



SEE A-A

COASTAL HAZARD ANALYSIS AT SAN ONOFRE NUCLEAR GENERATING STATION

Part 3: Tsunami Hazards



for

**SOUTHERN CALIFORNIA EDISON
P.O. Box 128, MS D3D
5000 Pacific Coast Highway
San Clemente, CA 92672**

**Coastal Environments, Inc.
2166 Avenida de la Playa, Suite E
La Jolla, CA 92037**

**CE Reference No. 22-04
31 March 2022**

TABLE OF CONTENTS

| | |
|--|-----------|
| EXECUTIVE SUMMARY | v |
| 1.0 INTRODUCTION..... | 1 |
| 2.0 PREVIOUS WORK..... | 1 |
| 2.1 HOUSTON AND GARCIA (1974) | 2 |
| 2.2 INUNDATION COMPUTATIONS | 5 |
| 2.3 USLU (2008) | 6 |
| 2.4 THE SHI ET AL. (2016) SONGS REPORT | 7 |
| 3.0 NUMERICAL MODELING PROGRAM..... | 8 |
| 4.0 TSUNAMI HAZARD TERMINOLOGY | 9 |
| 5.0 SEISMIC SOURCE DEFINITIONS..... | 10 |
| 6.0 NUMERICAL MODEL | 11 |
| 6.1 NUMERICAL MODELING BOUNDARY CONDITIONS..... | 11 |
| 6.2 NUMERICAL MODELING INITIAL CONDITIONS | 11 |
| 7.0 INPUT DATA..... | 13 |
| 7.1 EXTREME WATER LEVEL..... | 13 |
| 7.2 NUMERICAL GRIDS..... | 13 |
| 7.3 NOAA TSUNAMI UNIT SOURCES DATABASE | 14 |
| 7.4 FAR-FIELD SEISMIC SOURCES | 15 |
| 7.4.1 Unit source sensitivity study | 15 |
| 7.4.2 Source specification | 15 |
| 7.5 NEAR-FIELD SEISMIC SOURCES..... | 17 |
| 8.0 COMPUTATIONS | 33 |
| 8.1 RESULTS FOR FAR-FIELD SEISMIC TSUNAMI CASES | 33 |
| 8.1.1 Eastern Aleutians..... | 33 |
| 8.1.2 Kuril Islands | 35 |
| 8.2 RESULTS FOR LOCAL SEISMIC TSUNAMI CASES..... | 37 |
| 8.2.1 Source Local-sc1 | 37 |
| 8.2.2 Source Local-sc2 | 37 |
| 8.2.3 Source Local-sc3 | 38 |
| 9.0 RESULTS SUMMARY | 61 |
| 10.0 ABBREVIATIONS | 62 |
| 11.0 REFERENCES..... | 63 |

LIST OF APPENDICES

| | | |
|-------------|--|-----|
| Appendix A. | NOAA/PMEL Unit Source Parameters | A-1 |
|-------------|--|-----|

LIST OF TABLES

| | | |
|------------|---|-----|
| Table 2-1. | 100-and 500-year tsunami runup* heights at San Onofre as computed by Houston and Garcia (1974) | 4 |
| Table 2-2. | 100-and 500-year tsunami runup* heights at San Onofre as computed by Houston (1980) | 5 |
| Table 2-3. | Maximum wave runup at San Onofre for earthquake- and landslide-generated tsunamis in southern California computed by Borrero et al. (2004) | 5 |
| Table 2-4. | Wave height return periods for a numerical wave gauge offshore of San Diego, values from Uslu (2008)..... | 7 |
| Table 7-1. | Bathymetry/topography numerical grids used for the hydrodynamic simulations | 19 |
| Table 7-2. | Subduction zone 4-letter labeling used for the NOAA tsunami unit sources by Arcas (2015)..... | 19 |
| Table 7-3. | Source specification for the far-field seismic scenarios modeled in this report | 20 |
| Table 7-4. | Near-field fault parameters for the elastic dislocation model tsunami source | 21 |
| Table 7-5. | Near-field composite seismic sources..... | 21 |
| Table 9-1. | Table of maximum and minimum amplitudes occurring at the node offshore the SONGS site, and the maximum tsunami elevation and flow depth values inside the NUHOMS polygon for all simulated tsunami events | 61 |
| Table A-1. | Earthquake parameters for the Aleutian-Alaska-Cascadia Subduction Zone NOAA/PMEL unit sources | A-2 |
| Table A-2. | Earthquake parameters for the Kamchatka-Kuril-Japan-Izu-Mariana-Yap Subduction Zone NOAA/PMEL unit sources..... | A-5 |

LIST OF FIGURES

| | | |
|-------------|---|----|
| Figure 4-1. | Tsunami hazard terminology used to describe the computational results in this report | 9 |
| Figure 7-1. | The Pacific Ocean bathymetry grid (grid <i>P</i>) of 4 arc-min spatial resolution used with MOST for the far-field tsunami simulations | 22 |
| Figure 7-2. | Nested grids of increasing resolution used for the numerical computations | 23 |
| Figure 7-3. | NOAA/PMEL's unit sources and labeling along the Japan subduction zone | 24 |
| Figure 7-4. | Tsunami hazard sensitivity for the study site to the location of the unit sources..... | 25 |

| | | |
|--------------|--|----|
| Figure 7-5. | Definition of the five Eastern Aleutian (far-field) seismic sources using NOAA/PMEL's unit sources | 26 |
| Figure 7-6. | Vertical seismic displacement for the Eastern Aleutian (far-field) seismic sources..... | 27 |
| Figure 7-7. | Definition of the two Kuril (far-field) seismic sources using NOAA/PMEL's unit sources | 28 |
| Figure 7-8. | Vertical co-seismic displacement for the two Kuril (far-field) seismic sources..... | 28 |
| Figure 7-9. | Map showing seafloor deformation produced by local tsunami source 1 with all nine fault segments, with bathymetry and relocated seismicity | 29 |
| Figure 7-10. | Map comparing rupture model for the 2016 Kaikoura, New Zealand earthquake with the Coastal Fault System located between Los Angeles and San Diego | 30 |
| Figure 7-11. | Maps showing the simple rectangular fault models for the local tsunami cases | 31 |
| Figure 7-12. | Vertical co-seismic displacement for the three composite near-field sources..... | 32 |
| Figure 8-1. | Maps showing the maximum tsunami amplitudes (in part of the spatial extent) of grid P from the numerical simulation of all five Eastern Aleutian sources..... | 39 |
| Figure 8-2. | Maps showing the maximum tsunami amplitudes inside the domains of grids AA, A, and B during the numerical simulation of the Eastern Aleutian source EA-sc1 | 40 |
| Figure 8-3. | Numerical simulation results for the Eastern Aleutian seismic source EA-sc1..... | 41 |
| Figure 8-4. | Maps showing the maximum tsunami amplitudes inside the domains of grids AA, A, and B during the numerical simulation of the Eastern Aleutian source EA-sc2 | 42 |
| Figure 8-5. | Numerical simulation results for the Eastern Aleutian seismic source EA-sc2..... | 43 |
| Figure 8-6. | Maps showing the maximum tsunami amplitudes inside the domains of grids AA, A, and B during the numerical simulation of the Eastern Aleutian source EA-sc3 | 44 |
| Figure 8-7. | Numerical simulation results for the Eastern Aleutian seismic source EA-sc3..... | 45 |
| Figure 8-8. | Maps showing the maximum tsunami amplitudes inside the domains of grids AA, A, and B during the numerical simulation of the Eastern Aleutian source EA-sc4 | 46 |
| Figure 8-9. | Numerical simulation results for the Eastern Aleutian seismic source EA-sc4..... | 47 |
| Figure 8-10. | Maps showing the maximum tsunami amplitudes inside the domains of grids AA, A, and B during the numerical simulation of the Eastern Aleutian source EA-sc5 | 48 |
| Figure 8-11. | Numerical simulation results for the Eastern Aleutian seismic source EA-sc5..... | 49 |

| | | |
|--------------|---|----|
| Figure 8-12. | Maps showing the maximum tsunami amplitudes (in part of the spatial extent) of grid <i>P</i> from the numerical simulation of all two Kuril sources | 50 |
| Figure 8-13. | Maps showing the maximum tsunami amplitudes inside the domains of grids AA, A, and B during the numerical simulation of the Kuril source KU-sc1 | 51 |
| Figure 8-14. | Numerical simulation results for the Kuril seismic source KU-sc1 | 52 |
| Figure 8-15. | Maps showing the maximum tsunami amplitudes inside the domains of grids AA, A, and B during the numerical simulation of the Kuril source KU-sc2 | 53 |
| Figure 8-16. | Numerical simulation results for the Kuril seismic source KU-sc2 | 54 |
| Figure 8-17. | Maps showing the maximum tsunami amplitudes inside the domains of grids A and B during the numerical simulation of the near-field source Local-sc1 | 55 |
| Figure 8-18. | Numerical simulation results for the near-field seismic source Local-sc1 | 56 |
| Figure 8-19. | Maps showing the maximum tsunami amplitudes inside the domains of grids A and B during the numerical simulation of the near-field source Local-sc2 | 57 |
| Figure 8-20. | Numerical simulation results for the near-field seismic source Local-sc2 | 58 |
| Figure 8-21. | Maps showing the maximum tsunami amplitudes inside the domains of grids A and B during the numerical simulation of the near-field source Local-sc3 | 59 |
| Figure 8-22. | Numerical simulation results for the near-field seismic source Local-sc3 | 60 |

EXECUTIVE SUMMARY

The objective of this report is to assess tsunami hazards at the San Onofre Nuclear Generating Station (SONGS). Numerous cases are discussed in this study with the objective of determining the worst-case scenario. This study considered 10 extreme tsunami cases, seven generated in the far-field and three from near-field and local areas. The numerical results are summarized in Section 9 and Table 9-1. Full inundation simulations at high resolution were performed for the seven far-field and three local worst-case seismic sources. The simulations produced runup results that allow the evaluation of potential flooding at the site.

The analysis presented herein conservatively assumes that the SONGS seawall is not present, exposing the NIA at ground elevation of about 6.1 m (20 ft) MLLW. The numerical modeling initial conditions considered an extreme water level (EWL), which accounts for, among other things, the H++ scenario, as well as astronomical tides, storm surge, limited wave setup caused by breaking waves, and mean sea level rise in response to climate change. Based on that updated modeling, the EWL estimated for 2050 is 3.17 m (10.4 ft) MLLW.

The far-field tsunami cases were initially assessed by comparing the time series of amplitudes from the National Oceanic and Atmospheric Administration's Pacific Marine Environmental Laboratory (NOAA/PMEL) unit-source database at a location offshore of San Onofre. This far-field source sensitivity study shows which subduction zones produce the highest wave amplitudes near the site. Figure 7-4 suggests that the unit sources from the Alaska-Aleutians subduction zone produce the highest tsunami amplitudes offshore SONGS for M9.5 earthquake scenarios, since the high-amplitude source area in the eastern Aleutian region is the longest across all Pacific subduction zones. We have thus focused our attention on the eastern Aleutians to define the worst-case tsunami scenario and analyze five cases for the eastern Aleutian source area. Two sources from the Kuril Islands were also examined since Shi et al. (2016) showed that sources from the Kurils produced significant tsunami wave amplitudes at San Onofre. The largest tsunami amplitudes offshore and the main tsunami impact at the SONGS NUHOMS Independent Spent Fuel Storage Installation (ISFSI) originates in the eastern Aleutians from source EA-sc3. This produces a tsunami elevation of 9.1 m (MLLW), and flow depth of 2.8 m around the NUHOMS ISFSI, respectively. A description of all far-field sources considered in this study is given in Section 7.4.2. The results for far-field seismic tsunami simulations are discussed in Section 8.1.

Near-field seismic tsunami generation can mainly occur in the Coastal Fault System (CFS), as detailed in Part II of this report. The CFS stretches from Santa Monica to northern Baja California, Mexico. The northern section from Santa Monica to San Diego is well mapped, but the southern part to Punta Banda, Mexico where the Agua Blanca fault passes offshore, with similar faulting, is poorly mapped (e.g., Legg, 1985). A nine-segment model representing the prominent offshore fault sections between Dana Point and La Jolla was used to evaluate the local tsunami potential at the SONGS ISFSI (Table 7-4). The largest local earthquake scenario consists of all nine segments (Table 7-5, source Local-sc1.). Two other composite source models used the four segments of the Newport-Inglewood and Oceanside (Rose Canyon) strike-slip fault, with oblique-slip on the north and south segments of the South Coast Offshore fault (Table 7-5, source Local-sc3), and the San Mateo-San Onofre-Carlsbad oblique-reverse fault, with

strike-slip on the San Onofre segment (Table 7-5, source Local-sc2). From the three highest-case local seismic sources considered, source Local-sc1 produces the highest tsunami at the NUHOMS ISFSI, with maximum elevation of 7.2 m (MLLW), and maximum flow depth of 1.2 m.

Geopentech (2010) provides an extensive discussion of potential sub-marine landslide tsunami sources in southern California. Two potentially large sources were analyzed based on screening carried out in Geopentech (2010). These included a slide from the Thirtymile Bank formation landward into the San Diego Trough, and from the Fortymile Bank formation into North San Clemente Basin. Geopentech (2010) simulations of tsunami runup at the SONGS seawall was significantly higher for these two sources than for other potential offshore landslide locations considered, which produced height three to 10 times smaller. Shi et al. (2016) likewise considered the Thirtymile Bank and Fortymile Bank sources and estimated high water elevations at the San Onofre cliffs adjacent to SONGS. The results were 6.6 m (MLLW) for Thirtymile Bank, and 5.7 m (MLLW) for Fortymile Bank, also smaller than the present analysis. Both of these elevations imply insignificant flooding at the surface grade elevation of the NUHOMS ISFSI.

Based on a review of these earthquake and landslide scenarios, the worst-case hypothetical tsunami would be if a magnitude 9.53 earthquake occurred in the eastern Aleutians and the tsunami source was distributed along the entire subduction zone. For that event, the maximum potential water elevation at the SONGS site would be 9.08 m (29.8 ft) MLLW, with flow depth (i.e., water depth above ground surface) of 2.77 m (9.1 ft) around the NUHOMS ISFSI. The extreme case water level of 9.08 m (29.8 ft) MLLW would be 0.49 m (1.6 ft) greater than the 8.59 m (28.2 ft) MLLW elevation for the top of the existing NIA seawall, but would be below the top of the NUHOMS ISFSI concrete module height of 9.91 m (32.5 ft) MLLW.

The flow depth elevation analyzed in the new extreme hypothetical scenario of 9.08 m (29.8 ft) MLLW is lower than the top elevation of the NUHOMS ISFSI of 9.91 m (32.5 ft) MLLW by about 0.82 m (2.7 ft), and much lower than the NUHOMS ISFSI water submergence design depth of 15.24 m (50 ft). Moreover, although the NIA seawall was conservatively assumed not present for the updated tsunami propagation model, the continued presence of the NIA seawall at elevation 8.59 m (28.2 ft) MLLW reduces or eliminates the exposure of the NUHOMS ISFSI to most of the worst-case projected tsunami hazards from near and far-field sources. Further, as acknowledged in the Coastal Commission's 2001 Adopted Findings, inundation has been factored into the ISFSI design, and it would not adversely affect the stability of the site.

As part of this analysis, Coastal Environments has reviewed the 2001 and 2015 SONGS ISFSI Coastal Development Permit (CDP) and staff report materials and found that the Coastal Commission's conclusions in those reports remain correct.

COASTAL HAZARD ANALYSIS AT SAN ONOFRE NUCLEAR GENERATING STATION

Part 3: Tsunami Hazards

1.0 INTRODUCTION

This is a report to assess the hazards at the San Onofre Nuclear Generating Station (SONGS) located in California, from earthquake-generated tsunamis. The analysis was done through deterministic worst-case scenarios, both for far-field and near-field tsunamis. Maximum magnitude far-field earthquake scenarios along the Pacific subduction zones were designed based on recent studies. The far-field tsunami impact on SONGS was initially assessed by comparing the time series of pre-computed tsunami amplitudes from the NOAA/PMEL unit-source database, in a location offshore of the SONGS site. Near-field tsunami earthquake sources were re-evaluated from existing studies, and new worst-case scenarios were introduced. In all cases, the scenarios exceeded earlier estimates. Full inundation simulations at high resolution were performed for seven far-field and three local worst-case seismic sources. The simulations produced runup results, which allow the evaluation of potential flooding at the site.

2.0 PREVIOUS WORK

In performing any hazard assessment, the first step is to examine the available historic record in catalogs or scientific publications. California is believed to have a long history of tsunamis, although few had been historically documented before 1992.

The first comprehensive calculation of tsunami hazards for California is the work of Houston and Garcia (1974) and of Houston (1980). Both reports focused on the hazard in southern California from far-field events. McCulloch (1985) focused on the hazards in the Los Angeles region primarily from far-field events, but also considered several local events. Following the 1992 magnitude 7.1 Cape Mendocino earthquake, which triggered an about 1 m tsunami, McCarthy et al. (1993) analyzed the historic records of tsunamis in California and assessed very qualitatively the hazard over the entire State.

Synolakis et al. (1998) reviewed pre-1997 studies and observed that the earlier runup estimates did not include inundation calculations. When performed with the newer generation of inundation models available then, runup estimates were up to 100% higher than what the earlier calculations suggested, depending on the nearshore topography. Borrero et al. (2001) studied nearshore tectonic, landslide and slump sources in East Santa Barbara Channel and produced runup estimates ranging from 2 m to 13 m in Santa Barbara County.

Eisner et al. (2001) argued that California presents nontrivial challenges for assessing tsunami hazards, including a short historic record and the possibility of nearshore events with less than 20 min propagation times to the target coastlines. More specifically, whereas in Japan and in Greece over 1,000-year historic records exist, in California there are no known tsunami records before the 19th century, except the 1700 Cascadia tsunami. Several tsunamis have been reported since 1800, but in most cases the information is not sufficient for reasonable inferences

of the inundation. Quantitative measurements of inundation exist for the 1964 Alaskan tsunami and for most post-2010 transpacific tsunamis that have been recorded in tide gages, but none appear to exist for SONGS.

Legg et al. (2004) examined tsunami hazards associated with the Catalina fault. Several earthquake scenarios with moment magnitudes ranging between 7.0 and 7.6 were used as initial conditions for tsunami simulations, and up to 4 m runup was predicted along the southern California coastline. Barberopoulou et al. (2011) assessed tsunami hazards in San Diego Bay, California, using what was then recently identified offshore tsunami sources and recently available high resolution bathymetric/topographic data.

As a preamble, and following Synolakis et al. (2001), it is important to define the terms runup and inundation, which are sometimes misused (also see Section 4.0). Wave runup is the rush of water up a structure or a beach; it is also called the uprush. The maximum runup is the vertical height above still water (or the initial position of the shoreline) that the rush of water reaches to, as it climbs onshore. The term inundation height is a term sometimes used interchangeably with runup, but other times it refers to either the maximum flow depth or runup along a particular transect. The term tsunami elevation is the local height the tsunami flood reaches with respect to the datum, defined by the initial position of the shoreline.

Often in the field, it is hard to identify tsunami elevations at more than one location, although of course they can be computed everywhere. Specific knowledge of the maximum wave runup on a given beach is essential both in shore protection and in the design of coastal structures. In earlier pre-1990s studies the term tsunami height offshore was used interchangeably with the maximum runup height. References to offshore tsunami heights are generally not useful in inundation predictions as the tsunami height varies substantially with depth, particularly in the extreme nearshore region.

Inundation refers to the horizontal distance the wave penetrates inland. Depending on land use, either runup or inundation are relevant, and most often both. An inundation map includes a line corresponding to the maximum penetration of the tsunami wave triggered by the event under study.

Here, the most extensive historic studies for tsunami hazards in southern California are briefly summarized.

2.1 HOUSTON AND GARCIA (1974)

The earliest comprehensive attempt of quantifying the tsunami hazard in California is by Houston and Garcia (1974). They performed a Probabilistic Tsunami Hazard Assessment (PTHA) study to establish the 100- and 500-year tsunami runup elevations on the west coast of the US by far-field earthquake sources. Due to the limited historical data of tsunami activity on the west coast (at the time of the report), the authors identified tsunamigenic earthquakes only emanating from the Alaska-Aleutian and South America subduction zones.

The tsunamigenic potential of the Cascadia subduction zone was not known at that time, which would have considerably changed the outcome of their study. They only considered two

subduction zones to generate tsunamis which they propagated through the Pacific Ocean using a linear shallow-water numerical code and coarse bathymetric grid (20 arc-min). The coarse grid tsunami propagation calculations were stopped at 500 m depth.

Then, a non-linear model and finer grid resolution (2 miles cell size) was used to propagate tsunamis from the deep ocean over the continental slope and shelf to a vertical-wall coast. (Back then, neither the analysis or the computational power existed to perform inundation computations and predict the wave runup, see Synolakis (2003) for a discussion of the evolution of tsunami inundation computations). The nearshore grids extended to one and a half wavelengths of a 30-min period wave from the shore, so that at least three typical tsunami waves could propagate to the shore before being reflected from the boundary.

As written above, inland inundation computations were not performed, and the term “runup” in Houston and Garcia (1974) actually corresponds to the tsunami elevation at the initial position of the shoreline. Titov and Synolakis (1998) showed that models which do not perform runup/inundation calculations, a.k.a. *threshold models*, have significant discrepancies compared to models which compute inundation. Yet, threshold models were standard before the development of more advanced hydrodynamic models and the availability of more computational power. Even today (Spring 2022), some engineering studies are still performed by threshold models simply because the design firms or their consultants are either not aware or have no access to inundation models (Synolakis and Kânoğlu, 2015).

Houston and Garcia (1974) discretized the Alaska-Aleutian subduction zone (AASZ) into 12 segments, and the South America subduction zone (SASZ) into three. The finer discretization of the AASZ was due to the realization that the US West Coast tsunami hazard is more sensitive to the location of AASZ earthquakes rather than the location of earthquakes generated in the SASZ.

The initial conditions for the propagation computations were approximated by ellipses of uplift, with the ellipse major axis parallel to the trench and the spatial size held constant and independent of what they referred to as tsunami intensity. This was standard back then, as there was no understanding of the dipolar nature of the seafloor motion associated with earthquakes. In each of the segments of AASZ and SASZ, Houston and Garcia (1974) generated tsunamis of “intensities” from 2 to 5 in increments of 0.5 (105 sources in total), where the intensity (i) is given by (Soloviev, 1970):

$$i = \log_2(\bar{2}H_{avg}) \quad (2-1)$$

where H_{avg} is the average runup over a coast segment considered as appropriate. The probability $n(i)$ of a certain tsunami intensity i being generated during any given year is given by the following expression:

$$n(i) = p_1 e^{p_2 i} \quad (2-2)$$

where p_1 and p_2 are empirical parameters which were estimated as $p_1 = 0.074$, $p_2 = -0.63$ and $p_1 = 0.113$, $p_2 = -0.71$ for SASZ and AASZ respectively, with these parameters being uniformly applicable along each trench.

Post the 1992 Nicaraguan tsunami, the concept of the tsunami intensity as derived from historic reports has been debunked, because it was observed that runup can vary substantially over adjacent beaches, begging the question of how to define an appropriate segment in real coastlines with substantial cross shore variations. As Ambraseys and Synolakis (2010) pointed out, “The only justification for ever using an intensity scale is to quantify information in a single index from various historic sources, for the purposes of comparison of effects of different earthquakes in the same locale. Hydrodynamic computational models provide detailed geographic distributions of inundation heights, overland flow depths and flow velocities, allowing for a comprehensive determination of risk.”

Each of the 105 sources of variable location and tsunami intensity produced 2-hr time series along the US west coast. The time-series were extended to 24 hr. by adding a sinusoidal signal with amplitude 40% that of the maximum amplitude of the modeled time-series. Astronomical tidal variation at each coastal cell was calculated from available data for the year 1964, during which modal factors are near their average values of the 18.6-year cycle. The tidal signal was calculated with a 15 min time interval. The 24-hr tsunami time-series was then linearly superimposed to the tidal signal, varying the starting time (shifting the starting time by 15 min at each iteration). The maximum amplitude of the combined tsunami and tidal signal was assigned a probability equal to the probability of the tsunami with intensity i occurring and the probability of the waves arriving at that particular 15 min period of the yearly tidal cycle.

Maximum elevations at the shoreline and their corresponding probabilities of occurrence were re-organized in descending order for each coastal location. The probabilities were summed (from smaller to larger) until the desired probability P was reached, which corresponds to the return period $T=1/P$. Table 2-1 shows the resulting 100- and 500-year tsunami runup heights at San Onofre.

Table 2-1. 100-and 500-year tsunami runup* heights at San Onofre as computed by Houston and Garcia (1974). Values in the report are in *ft* and were converted to *m*.

| 100-year “runup”* (m) | 500-year “runup”* (m) |
|-----------------------|-----------------------|
| 1.74 | 3.38 |

*see how runup is defined in Houston and Garcia (1974).

Houston (1980) later updated the 100- and 500-year tsunami wave heights, for the southern California coastal stretch from Point Conception to Ensenada, Mexico. He used a different numerical model for nearshore computations, which allowed for variable spatial size. He modeled only large earthquake sources (initial wavelengths greater than 100 miles) to justify the use of a linear non-dispersive shallow water model for the trans-Pacific wave propagation. Table 2-2 shows the resulting 100- and 500-year tsunami runup heights at San Onofre.

Table 2-2. 100-and 500-year tsunami runup* heights at San Onofre as computed by Houston (1980). Values in the report (for gage 152, plate 76 in the report) are in *ft* and were converted to *m*.

| 100-year "Runup"* (m) | 500-year "Runup"* (m) |
|-----------------------|-----------------------|
| 1.18 | 1.43 |

*see how runup is defined in Houston (1980).

2.2 INUNDATION COMPUTATIONS

The breakthrough in terms of tsunami hazard assessment came in the 1990s with advancement in numerical models and the capability of computing onland inundation and runup (see Synolakis and Bernard 2006 for details in the development of hydrodynamic codes). Based on excellent comparisons between numerical and field runup data for the 1993 Hokkaido-Nansei-Oki tsunami in Japan (Titov and Synolakis, 1997), as well as comparisons of model predictions with laboratory measurements by Titov and Synolakis (1995, 1998), the contemporary state-of-the-art methodology for estimating tsunami risk from near- and far-field for California was set.

Following the 1998 Papua New Guinea tsunami (Synolakis et al., 2002a), the tsunami hazard potential of submarine landslides was re-discovered. In light of those new findings and with more detailed information about the local tectonic setting and bathymetry off southern California, Borrero et al. (2001), Borrero (2002) and Borrero et al. (2004) examined the tsunamigenic potential of local earthquakes and landslides in southern California; the wave runup values at San Onofre for the earthquake and landslide scenarios considered by Borrero et al. (2004) are shown in Table 2-3. The local sources database was incorporated in preparing the first- and second-generation tsunami inundation maps used for evacuation planning for California (Eisner et al., 2001; Barberopoulou et al., 2009, 2011).

Table 2-3. Maximum wave runup at San Onofre for earthquake- and landslide-generated tsunamis in southern California computed by Borrero et al. (2004) - runup data is inferred from Figure 2 of Borrero et al. (2004).

| Source Name | M_w | Maximum Runup (m) |
|-----------------------------|-------|-------------------|
| <i>Earthquake Scenarios</i> | | |
| Santa Catalina | 7.6 | 1.0 |
| Lasuen Knoll | 7.1 | 1.0 |
| San Mateo Thrust | 7.0 | 4.2 |
| <i>Landslide Scenarios</i> | | |
| Palos Verdes Slide 1 | -- | 0.3 |
| Palos Verdes Slide 2 | -- | 0.3 |

In the first decade of the 21st century, tsunamis generated around the world allowed for validation of computational models (Synolakis et al., 2008). Major advances in numerical codes and computational power and the availability of higher resolution bathymetric and topographic data allowed for full inundation computations for design earthquake scenarios with unprecedented accuracy. Also, geological studies re-evaluated the tsunamigenic potential of subduction zones by identifying tsunami evidence in the field and linking them to historical

tsunami records. Through these studies, new tsunami events with long return periods were added to the tsunami catalogs.

The most important finding concerning the tsunami hazard of California is the 1700 trans-Pacific tsunami that originated from the Cascadia Subduction Zone (CSZ) (Atwater et al., 2016). Even though it had been identified as an event in the Japanese tsunami records, with ~3 m maximum tsunami height (Satake et al., 1996), its source was not local, and it remained unidentified until the work of Atwater (1987) and Satake et al. (1996).

2.3 USLU (2008)

Uslu (2008), in his PhD thesis entitled, “Deterministic And Probabilistic Tsunami Studies In California From Near-Field And Far-Field Sources,” used all potential tsunami sources known until then, applying high-resolution bathymetric/topographic data and a validated numerical code with full inundation computation capabilities.

In the deterministic part of his work, Uslu (2008) modeled tsunami scenarios for San Francisco Bay, Crescent City and Humboldt Bay to re-evaluate tsunami hazard for each location. For the far-field sources (sources located at distance greater than 1800 km travelling at depths >1 km, he took advantage of the FACTS (Facility for the Analysis and Comparison of Tsunami Simulations) tsunami sources database of NOAA/PMEL and designed new, composite scenarios of tsunami sources. Based on source directivity and on evidence of past tsunami events in California, he only included the Alaska-Aleutian, Kurils-Japan and South American subduction zones in the analysis. The only historical events included were the Chile 1960 and Alaska 1964 earthquakes. The rest of his far-field sources were plausible scenarios with moment and slip magnitudes ranging from M_w 8.7-9.4 and 5-25 m, respectively.

In the near-field, he put together a list of potential tsunamigenic earthquake sources in California and Cascadia that had been published until then. For Cascadia, six different scenarios were included with earthquake moment magnitudes ranging between M_w 8.44-9.02. The rest of the local earthquake sources were on faults in central and southern California and San Francisco Bay with M_w ranging 6.6-7.66. The latter are threats only for near-field coastal locales. Finally, he considered three landslide sources, two in southern California (Goleta and Palos Verdes, Borrero et al., 2001) and one in San Francisco Bay (Farallon Islands). The landslide sources were implemented using static dipole-shaped initial conditions, per Borrero (2001) and Synolakis et al. (2002a).

For the probabilistic part of his work, Uslu (2008) generated tsunami sources in the Kuril, West and East Aleutian, Central and South American subduction zones. Each subduction zone was discretized in a number of segments along its (along-strike) length, and 20 earthquake scenarios (of magnitudes ranging between M_w 7.65-9.3) were fit in each segment, resulting in hundreds of runs for each subduction zone. All the earthquake scenarios were implemented as combinations of FACTS sources, for which the amplitudes across the Pacific Ocean had been precomputed. For each run, the maximum wave height was evaluated just offshore seven locations across California, with local depth varying between 31-448 m. The nearest locations to SONGS in Uslu (2008) are in Los Angeles and San Diego.

In computing the return period of certain offshore wave heights, Uslu (2008) employed both time-dependent and time-independent probabilistic hazard assessment methodologies (Table 2-4). In the time-independent seismic hazard assessment methodology, the memory-less Poisson distribution was employed, where subduction zones have no memory of past seismicity.

Table 2-4. Wave height return periods for a numerical wave gauge offshore of San Diego (at coordinates: 242.68°E 32.713°N and local depth 83 m), values from Uslu (2008).

| Wave Height (m) | 0.50 | 1.00 | 1.50 |
|---------------------------------------|-------------|-------------|-------------|
| Time-independent return period (yrs.) | 67 | 218 | 335 |
| Time-dependent return period (yrs.) | 52 | 189 | 360 |

Uslu (2008) went further with his analysis and resolved the nearshore hydrodynamics of each scenario at three harbors, Crescent City, San Francisco and Los Angeles, using the MOST model (see Section 6.0 for model description). The aforementioned probabilistic analysis was also performed for the three harbors. It was found that the tsunami risk in California decreases from north to south. The northern California coastline is more susceptible to tsunamis originating from the Alaska-Aleutians subduction zones, whereas southern California is exposed to tsunamis originating from the central and south American subduction zones as well as from Alaska-Aleutians. Landslide scenarios were not considered in Uslu's probabilistic analysis.

Barberopoulou et al. (2011) considered far-field and near-field sources, including landslides from the Coronado Canyon and Thirtymile Bank to reassess the tsunami hazard in San Diego bay. None of their earthquake or slide scenarios exceeded 4 m wave runup, although they noted that the Strand - the spit fronting San Diego Bay - would experience overland flooding. The Coronado Canyon slide as examined directed large waves further south of the harbor mouth.

2.4 THE SHI ET AL. (2016) SONGS REPORT

Shi et al. (2016) did another analysis of tsunami hazards at SONGS including far-field and near-field earthquake tsunamis and landslides tsunamis, as provided by Geopentech (2010). They did not include the historical analysis provided by these studies in the report.

In terms of far-field sources, Shi et al. (2016) considered sources in the Eastern and Western Aleutians, in the Kurils and in Chile. They did not perform a sensitivity analysis to examine how other possible source combinations around the Pacific might result in higher amplification at the site - such analysis is standard, at least since Uslu (2008). For due diligence, one would have to consider sources around the Pacific rim, refer to the consequences of not doing so in Synolakis and Kânoğlu (2015). It shows the wave height just offshore at Fukushima, Japan from unit sources around the Pacific, and indicates that the wave height from other sources is comparable to that from the one source they considered in Chile. While sources in Alaska may have the highest impact, one cannot possibly expect *a priori* and without analysis that all the other subduction zones in the world may have less impact on the site, than Alaska. Such analysis is performed in this report in Section 7.4.1 (Figure 7-4).

3.0 NUMERICAL MODELING PROGRAM

Program Name: Method of Splitting Tsunamis (MOST).

Program Revision: v4, last revised by NOAA/PMEL on 1/10/2012.

Computer Type and Description: Apple Mac Mini (2018) personal computer, 3 GHz Intel Core i5 processor, 8 GB memory.

Computer Program Validated: Yes.

Model Validation References: Titov and Synolakis (1995, 1997, 1998).

4.0 TSUNAMI HAZARD TERMINOLOGY

The following terminology is used to describe the computational results in this report (see Figure 4-1):

- Runup (or runup elevation): the elevation above the still water level at the furthest inland location reached by the waves.
- Inundation distance: the horizontal distance between the shoreline (corresponding to the still water level) and the furthest inland point reached by the waves.
- Tsunami elevation: the vertical difference between the wave amplitude (over land) and the still water level.
- Flow depth: the vertical difference between the wave amplitude (over land) and the ground.

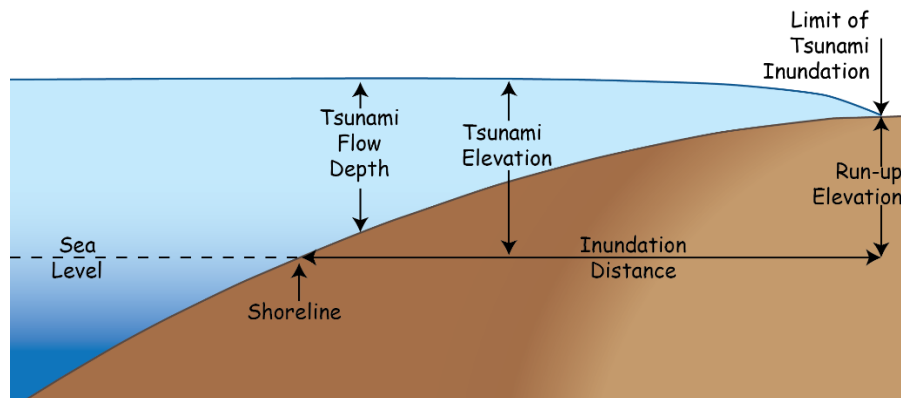


Figure 4-1. Tsunami hazard terminology used to describe the computational results in this report (Source: http://ds.iris.edu/aed2/c/alaska/popups/tsunamis/tsu_1.html).

5.0 SEISMIC SOURCE DEFINITIONS

This section lists a number of parameters used to define the seismic source. The seismic moment M_0 is a measure of the energy released by an earthquake. The seismic moment is defined as:

$$M_0 = \mu L W \Delta u, \quad (5-1)$$

where μ is the elastic modulus of elasticity, L is the fault rupture length, W is the fault rupture width, and Δu is the slip magnitude (i.e., the distance covered by the relative motion between the two fault planes during the seismic rupture). In the cases of composite sources (seismic sources composed of individual sub faults), the seismic moment of the composite source ($M_{0,comp}$) is the sum of the seismic moments of the N individual sub faults ($M_{0,i}$):

$$M_{0,comp} = \sum_i^N M_{0,i} \quad (5-2)$$

The moment magnitude M_w is a measure of the magnitude of an earthquake based on the seismic moment. The moment magnitude is expressed as (Hanks and Kanamori, 1979):

$$M_w = (2/3) \log_{10} (M_0) - 10.7, \quad (5-3)$$

where the seismic moment M_0 is expressed in *dyne cm* (10^{-7} N m).

6.0 NUMERICAL MODEL

The results from the numerical simulations presented in this report were produced using the MOST (Method Of Splitting Tsunamis) model (Titov and Synolakis, 1995, 1998). MOST has been extensively validated and used for tsunami hazard assessments in the United States and is currently maintained and in operational use at NOAA/PMEL. Variants of MOST have been in continuous use for tsunami hazard assessments in California, since the mid 1990's (Titov et al., 2016).

MOST solves the 2+1 Nonlinear Shallow Water equations (Titov and Synolakis, 1995, 1998):

$$h_t + (uh)_x + (vh)_y = 0, \quad (6-1)$$

$$u_t + uu_x + vu_y + gh_x = gd_x, \quad (6-2)$$

$$v_t + uv_x + vv_y + gh_y = gd_y, \quad (6-3)$$

where $h = \eta(x, y, t) + d(x, y, t)$, $\eta(x, y, t)$ =wave amplitude; $d = (x, y, t)$ =undisturbed water depth; $u(x, y, t)$ and $v(x, y, t)$ are the depth-averaged velocities along-longitude (x) and along-latitude (y), respectively. The governing equations are solved in characteristic form through an explicit finite difference scheme using the method of fractional steps of Janenko (1971).

6.1 NUMERICAL MODELING BOUNDARY CONDITIONS

Section 7.2 describes the nested numerical grids. Briefly, numerical computations were stopped at 5 m depth in grids P, AA and A, at which depth waves are reflected back (solid wall boundary condition). Runup and inundation computations were only performed in grids B and C, for which a moving boundary condition was used as described in Titov and Synolakis (1995). For runup/inundation computations, a bottom friction term is included in the momentum equations using a Manning's roughness coefficient of $n = 0.03 \text{ s/m}^{1/3}$ which corresponds to a weedy earth channel surface material.

The hydrodynamic information (free surface elevation η and the two depth-averaged velocity components u , v along the longitude and latitude, respectively) were passed from the domain of the coarser-resolution grids to the boundaries of the finer-resolution numerical grids. An absorbing boundary condition was applied at the open (sea) boundaries of the numerical grids.

6.2 NUMERICAL MODELING INITIAL CONDITIONS

The initial conditions of the hydrodynamic simulations presented in this report are defined by the co-seismic seafloor deformation. Fault ruptures due to earthquakes deform the surface of the earth in all three Cartesian components. The surface deformation due to finite rectangular faults is computed through the analytical equations of Okada (1985) in an elastic half-space, implemented through the Matlab code of Beauducel (2011). The inputs for the Okada (1985) analytical equations are the fault rupture location (longitude, latitude), depth of the

rupture, the fault rupture dimensions (length L and width W), the slip magnitude (Δu), and the dip, rake and strike angles (see Aki and Richards, 1980, for definitions). The Matlab code output is the surface displacement in all three Cartesian components.

The vertical component of the seafloor deformation was directly translated to the free surface of the sea (Derakhti et al., 2019). This simplification is allowed since the seafloor rise speed due to the fault rupture is much faster compared to the speed of wave propagation. Numerical simulations were thus initiated using the vertical free surface deformation computed using the Okada (1985) analytic equations, with zero initial velocities.

In the cases of composite sources (seismic sources composed of individual subfaults), the vertical co-seismic deformation of the composite source was computed by adding the vertical deformation resulting from the rupture of the individual subfaults, i.e., the analytic equations of Okada (1985) were applied for each individual subfault rupture.

7.0 INPUT DATA

7.1 EXTREME WATER LEVEL

Water surface elevation is dependent on astronomical tides, storm surge, limited wave setup caused by breaking waves, and mean sea level rise (MSLR) in response to climate change. The 1% annual probability of exceedance extreme water level due to tides, storm surge and wave setup at La Jolla, CA, was estimated by the NOAA in 2018 (<https://tidesandcurrents.noaa.gov/est/stickdiagram.shtml?stnid=9410230>) as $h_{EWL,NOAA} = 2.37$ m, MLLW (1.54 m, MSL). The sea level rise projection estimate by OPC (Ocean Protection Council) from 2000 to 2050 is $h_{MSLR} = 0.85$ m (2.8 ft) (OPC, 2018). Since the NOAA estimate was published in 2018, we adjusted the projection of OPC to reflect the changes from 2018 to 2050 by $h_{MSLR,cor} = -0.045$ m. The extreme water level (h_{EWL}) estimate for 2050, considering tides, storm surge, wave setup, MSLR is the sum of the NOAA extreme water level estimate in 2018 and the adjusted OPC estimate:

$$h_{EWL} = h_{EWL,NOAA} + h_{MSLR} + h_{MSLR,cor} = 3.18 \text{ m, with respect to MLLW.} \quad (7-1)$$

7.2 NUMERICAL GRIDS

During shoaling, as the waves propagate unto shallower water the cell size of the numerical grid needs to be reduced to accurately resolve the steepening wave profiles (increasing non-linearity), and the decrease of the wavelength. In MOST, wave shoaling is accounted for by using nested grids of increasing spatial resolution.

For the far-field simulations, a bathymetry grid of 4 arc-min (~7421 m at equator; grid cell size varies along latitudes) resolution named grid P was used which is available with the ComMIT model (COMmunity Model Interface for Tsunami, Titov et al., 2011). The bathymetry grid (Figure 7-1) is based on the Smith and Sandwell (1994) 2 arc-min data. For the far-field simulations, also a 30 arc-sec (~779 m) bathymetry/topography grid named grid AA was used that covers the Channel Islands, Santa Monica Bay and San Pedro Bay (Figure 7-2a). The bathymetry/topography information was downloaded from the 2021 global dataset of the General Bathymetric Chart of the Oceans (GEBCO, 2021). The 15 arc-sec original dataset was sub-sampled to 30 arc-sec for the purposes of this study.

Another three nested grids were used with both far- and near-field sources, namely grids A, B and C. The coarsest grid (grid A) which covers the largest area has 6 arc-sec (~156 m) resolution, whereas the intermediate (grid B) and finest grids (grid C) have 1 arc-sec (~26 m) and 1/6 arc-sec (~4 m) spatial resolutions, respectively (Figure 7-2b-d). Grid A was built based on the 3 arc-sec NOAA/NGDC Coastal Relief Model for Southern California (NGDC, 2003), sub-sampled to 6 arc-sec. Grid B was built based on the San Diego 1/3 arc-sec NOAA/NGDC Tsunami Inundation Digital Elevation Model (NGDC, 2010), sub-sampled to 1 arc-sec.

Grid C is composed by two datasets, a 0.5 m resolution topobathymetry grid provided by the Coastal Environments firm (CE), and the 1/3 arc-sec San Diego NOAA/NGDC Tsunami Inundation Digital Elevation Model - the area covered by the 0.5 m resolution topobathymetry grids is denoted with the red polygon in Figure 7-2d. The bathymetry data of the 0.5 m resolution

topobathymetry grid is the result of merging two multibeam surveys carried out by Coastal Environment in 2016 with topobathymetry data downloaded from the NOAA website (<https://www.fisheries.noaa.gov/inport/item/55359>), prepared by the USGS Coastal National Elevation Database. The inland data of the CE grid derive from the 2016 Lidar¹ data that was combined with the 2008 Lidar data. The 2008 Lidar data were used to add the grade elevation of SONGS structures behind the existing seawall. The two (CE and NOAA/NGDC) high-resolution topobathymetry grids were combined to create grid C with a 1/6 arc-sec resolution.

In summary, five nested grids were used for the far-field numerical simulations (grids P, AA, A, B and C) and three nested grids were used for the near-field numerical simulations (grid A, B and C). The grid sizes, spatial extents and resolutions are summarized in Table 7-1. All the DEMs used for the numerical simulations were referenced to the design Extreme Water Level vertical datum (see Section 7.1) and the World Geodetic System of 1984 (WGS 84) horizontal datum, in spherical coordinates.

7.3 NOAA TSUNAMI UNIT SOURCES DATABASE

NOAA/PMELAs part of its real-time tsunami forecasting system, the NOAA/PMEL has discretized the circum-Pacific subduction-zones into sub-faults of size 100x50km (along-strike length x along-dip width). The sub-faults are prescribed a strike angle that follows the plate boundaries defined by Bird (2003). The dip angle and the down-dip extend of unit sources are based on the best knowledge of local fault geometry (e.g., Kirby, 2006). While the pre-defined fault geometry of the unit sources, i.e., dip and strike angles, is assumed to be accurately represented, it has also been shown by Titov et al. (1999) that these parameters do not have a big effect in the far-field tsunami amplitudes.

As an example, Figure 7-3 shows the sub-faults and the NOAA labeling for the Japan subduction zone. The numbers represent the source column number which runs along the subduction zone and the letters in front of the numbers represent the source row name in the down-dip direction. The rows go from shallowest to deepest in the following order: B, A, Z, Y, X, W, V. Source rows C and D represent normal faulting sources which were not considered in this report. Finally, the sources are assigned a four-lettered code, depending on which subduction zone they are part of (see Table 7-2).

For the purposes of tsunami modeling, rake angle is fixed at 90°, thus representing pure thrust rupture. The surface deformation from the rupture of each sub-fault has been computed using the analytical equations of Okada (1985) for 1m slip magnitude, thus calling the sub-fault *unit* sources. The tsunami amplitudes and velocities across the Pacific basin were computed using MOST on a 4 arc-min grid and have been stored in an on-line database at 16 arc-min resolution.

Since surface deformation and deep-water propagation are linear functions of slip magnitude, the tsunami amplitudes across the Pacific Ocean can be readily obtained for any

¹ Light Detection and Ranging (Lidar), is a remote sensing method that uses light in the form of a pulsed laser to measure ranges (variable distances) to the Earth.

combination of unit-sources and slip magnitudes. Therefore, the variation of slip magnitude during seismic rupture can be accounted for by creating more complex faulting scenarios (Titov et al., 2011). This linear property of deep water tsunami propagation is the basis of NOAA's tsunami source inversion procedure during real time tsunami forecasts, which is described in more detail by Percival et al. (2009).

7.4 FAR-FIELD SEISMIC SOURCES

7.4.1 Unit source sensitivity study

SONGS is located along the coast of southern California and therefore only tsunami sources around the Pacific Ocean are considered. To identify which subduction zones around the Pacific direct more energy towards the study area, we performed a sensitivity analysis by utilizing the NOAA/PMEL unit sources database. The tsunami amplitude time series for each unit source are available at discrete nodes with 16arc-min spacing. We selected the closest node directly offshore from the SONGS site (see inset of Figure 7-4) and compared the maximum (positive) amplitude from each unit source. Figure 7-4 shows the maximum amplitude from all the row B (shallowest) unit sources considered here.

All unit sources have the same dimensions (100 x 50 km) and the same slip magnitude (1 m), and consequently have the same moment magnitude (assuming earth's rigidity μ is constant everywhere). Therefore, in this type of sensitivity test, earthquake magnitude is not per se important. Maximum amplitude varies between sources due to differences in location, fault geometry (dip angle), the distance from source to site, and the oceanic bathymetry/topography that refracts/reflects the waves and dictates where the tsunami energy is beamed towards (directivity). Consequently, it cannot be immediately concluded, without taking earthquake magnitudes into consideration, where the worst-case tsunami source for the study area is located.

From Figure 7-4 it is evident that the unit sources from the Alaska-Aleutians subduction zone produce the highest amplitudes offshore the SONGS site. The Alaska-Aleutians unit sources produce progressively higher maximum amplitudes near the site as we move from the Western to the Eastern Aleutians. The high-amplitude patch across the Eastern Aleutian sources is also the longest across all Pacific subduction zones. Attention thus focused on Eastern Aleutians in search of the worst-case tsunami scenario. Sources from the Kurils were also examined, since the Shi et al. (2016) report showed that sources from the Kurils produced significant wave amplitudes at the SONGS site. In the following section, we describe all the far-field sources considered in this study.

7.4.2 Source specification

The subduction zones located around the Pacific Rim produce great earthquakes along the subduction megathrust ($M > 8$). The large vertical displacements of the seafloor generate tsunamis that propagate across the entire Pacific Ocean Basin, which may continue to oscillate back-and-forth for days (e.g., 22 May 1960 Chile ($M_w 9.5$) earthquake, 27 March 1964 Alaska ($M_w 9.2$) earthquake, and the 11 March 2011 Tohoku, Japan, ($M_w 9.0$) earthquake). In addition, explosive volcanism produced by subduction processes in the volcanic arc may produce basin-wide tsunamis as recently observed from the 15 January 2022 Tonga ($M_s 5.8$) explosive subsea

eruption. Assessments of tsunami hazards to southern California ports (Los Angeles and San Diego) determined that the Eastern Aleutians-Alaska region produced the greatest inundation hazards from Pacific Rim earthquake sources of M_w 9.0 (Uslu, 2008; Barberopoulou et al., 2011; Thio et al., 2010; Kirby et al., 2013). Other significant distant sources include Chile and Kuril-Kamchatka regions where the shape of the subduction zone focuses the tsunami energy toward California. Here, we model five variations of the Eastern Aleutian-Alaska subduction source and two variations of the Kuril-Kamchatka subduction source to evaluate the range of inundation that may be expected for extreme M_w 9.5 events.

The NOAA 100-km by 50-km unit sources were used to create the models. The magnitude, rupture area and slip magnitude of all the far-field sources modeled in this report are outlined in Table 7-3. The unit sources corresponding to each source are also provided using NOAA/PMEL's labels - the full list of parameters of all NOAA/PMEL unit sources used to define the far-field sources are provided in Tables A-1 and A-2 of Appendix A. The slip distribution across the unit sources for the Eastern Aleutians and Kurils far-field composite sources are depicted in Figures 7-5 and 7-6, respectively. The vertical co-seismic displacement fields used as initial conditions for the hydrodynamics simulations are shown in Figures 7-7 and 7-8 for the Eastern Aleutians and Kurils far-field sources, respectively.

Eastern Aleutians – Alaska subduction source regions include up to six rows of source patches in the down-dip direction and as many as 15 columns of patches parallel to the trench. The extra width in this region results from the shallow dip of the subduction which was demonstrated in the 1964 M_w 9.2 Prince William Sound earthquake (Johnson et al., 1996). Source models were designed to address the issues of focusing tsunami energy by source geometry and tapered slip distributions, and distribution of high-slip areas that may increase runup and inundation at the SONGS location.

The magnitude of the design event was kept at the 9.5 level. A two-row by 15 column model with uniform 33.25-m slip for a 1500-km length by 100-km width rupture (source EA-sc3 in Table 7-3) was similar to the model used by Shi et al. (2016). For 800-km length ruptures with six rows (300-km width), both a uniform slip model (source EA-sc2 in Table 7-3) and two tapered models with the 20-m high-slip patches were created: one with the slip patch located deeper in the central part of the subduction zone (source EA-sc1 in Table 7-3), and the second with the patch near the trench (source EA-sc4 in Table 7-3). The fifth model used a 1000-km length with the six rows for 300-km width, and larger (30-40 m) slip patch closer to the trench (source EA-sc5 in Table 7-3).

The Kurils - Kamchatka models included one 1200-km by 100-km (two rows) uniform slip (41.57 m) version (source KU-sc1 in Table 7-3) and a second slip patch version with maximum slip of 50-60 meters near the northeast end of the subduction zone (source KU-sc2 in Table 7-3). The latter model was designed to focus energy toward California by putting the high-slip patches closer to Alaska and North America.

7.5 NEAR-FIELD SEISMIC SOURCES

Previous estimates of earthquake and tsunami hazards for the SONGS site considered large strike-slip earthquakes along the Newport-Inglewood (South Coast Offshore Zone of Deformation as described before 1981 NRC hearings) and the Rose Canyon fault continuation to the south. The strike-slip character at the time was considered unlikely to produce a significant tsunami. The Oceanside blind thrust (OBT) fault (Rivero et al., 2000; Rivero and Shaw, 2011) was proposed to represent a severe earthquake and tsunami hazard because this low-angle fault surface dips eastward and lies directly beneath the site at about 7-8 km depth. Maloney et al. (2016) concluded that the OBT is inactive based on lack of Quaternary deformation observed in offshore seismic reflection profiles.

What was not recognized then is that the OBT and the larger Thirtymile Bank detachment fault system provide slip surfaces that enable interaction between the shallow steep strike-slip faults of the Coastal Fault System. The Thirtymile Bank detachment continues on a shallow dip to the east beneath the OBT/detachment and the coast, possibly connected to the ancient (Mesozoic) subduction megathrust. It is uncertain whether the detachments are offset or terminated by the steep Newport-Inglewood and other strike-slip faults of the Inner Borderland. However, accurately located seismicity data (Hauksson et al., 2012, Figure 7-9) and earthquake focal mechanisms provide evidence for activity on both vertical strike-slip and moderate to shallow-dipping detachments that may act as blind thrusts or oblique-reverse faults. Fault interaction between the steep strike-slip and oblique-slip faults with the low-angle detachments may produce large, complex, multi-fault earthquakes (Legg et al., 2018) similar to those observed recently in New Zealand (M_w 7.8 Kaikoura, Hamling et al., 2017) and northern Baja California (M_w 7.2 El Mayor-Cucapah, Fletcher et al., 2014).

The major local earthquake tsunami source for the San Onofre area is the nearby Coastal Fault System which includes the Newport-Inglewood-Rose Canyon strike-slip fault zone along the continental shelf edge, and the San Mateo, San Onofre, and Carlsbad oblique reverse-slip faults that lie beneath the continental slope to the west (Figure 7-10). The Newport-Inglewood–Rose Canyon (NIRC) fault zone lies about 7 km offshore from the ISFSI. Although considered to be a strike-slip fault zone, branch and secondary faults adjacent to the NIRC include the San Mateo-Carlsbad, San Onofre, and Oceanside fault zones which exhibit seafloor uplift (Figure 7-10). The combined fault zones form a Coastal Fault System that stretches from Santa Monica to San Diego and beyond with similar poorly mapped faults offshore northern Baja California as far south as Punta Banda where the Agua Blanca fault passes offshore (Legg, 1985, others). A simple nine-segment model representing the prominent fault sections offshore between Dana Point and La Jolla is used to evaluate the local tsunami potential to the ISFSI (Table 7-4).

Elastic dislocation models (Okada, 1985) were used to determine the seafloor uplift for simple rectangular fault segments (Figure 7-11) with different strike, dip, rake and slip for each segment determined from seismic reflection profile observations (Sorlien et al., 2006) and seafloor morphology. The models are very simple compared to actual slip distributions modeled from historic earthquakes but are sufficient to provide reasonable estimates of the static seafloor deformation for tsunami source and propagation models. Similar models were used for tsunami inundation modeling offshore California (Synolakis et al., 2002b; Legg et al., 2004; Borrero et al., 2004).

The largest earthquake source (Local-sc1, Table 7-5) used all nine segments with parameters given in Table 7-4. Two other composite source models used the four segments of the Newport-Inglewood and Oceanside (Rose Canyon) strike-slip fault, with oblique-slip on the north and south segments of the South Coast Offshore fault (source Local-sc3, Table 7-5), and the San Mateo-San Onofre-Carlsbad oblique-reverse fault, with strike-slip on the San Onofre segment (source Local-sc2, Table 7-5).

The slip values used were based on observations from the M_w 7.8 Kaikoura earthquake, which had up to 25-m of strike-slip and 9-m of reverse-slip near a major left-step (restraining bend) between the Jordan thrust and Kekerengu faults (Hamling et al., 2017). We put the maximum slip on the South San Mateo fault with oblique-reverse rake (Table 7-4). Larger slip with oblique-reverse rake was also placed on the South Carlsbad segment where the strike bends more to the southeast (restraining bend). The resulting magnitudes are: M_w 7.62 for the 9-segment model, M_w 7.44 for the 4-segment South Coast Offshore model, and M_w 7.41 for the 5-segment San Mateo-San Onofre-Carlsbad model. The seafloor uplift for the three composite sources, computed using the Okada (1985) analytical equations, ranges from a maximum of 4 m for the scenarios with the San Mateo segments, and over 2.5 m for the oblique-slip on the Newport-Inglewood-Rose Canyon-Oceanside model (Figure 7-12). The large uplift occurs on the northern fault segment offshore from the San Joaquin Hills and does not include potential uplift on the San Joaquin Hills blind thrust, which would mostly occur on land.

Offshore landslides along the steep escarpments that bound the major basins of the Inner Borderland have been considered as potential tsunami sources. Some of these were modeled including the San Pedro Basin debris slide (Borrero et al., 2004) and large basement-involved landslides (Legg and Kamerling, 2003; Shi et al., 2016). The frequency of large submarine slides capable of producing significant tsunamis appears to be very low, 7,500 years or greater. Continued acquisition of high-resolution multi-beam bathymetry provides better data to enable more accurate identification of slope failures around the Borderland (Brothers et al., 2019). The landslide areas mapped near San Onofre from older surveys (Clarke et al., 1987) are now recognized as the complex seafloor deformation along the San Mateo-San Onofre-Carlsbad fault zone at the base of the continental slope. Therefore, we have not attempted additional modeling of submarine landslides at this time.

Table 7-1. Bathymetry/topography numerical grids used for the hydrodynamic simulations.

| Grid name | Data source | Longitude range (°E) | Latitude range (°N) | Grid cell size (arc-sec) | Grid cell size* (m) | Grid size ($N_{LON} \times N_{LAT}$) |
|-----------|--------------|----------------------|---------------------|--------------------------|---------------------|--|
| P | NOAA/PMEL | 120.0167-292.0167 | -73.9598-62.0001 | 240 | ~7421 | 2581*2879 |
| AA | GEBCO (2021) | 237.00-243.39 | 32.0-34.0 | 30 | 778.8 | 768*360 |
| A | NOAA/NGDC | 240.7-243.0 | 32.3-34.2 | 6 | 155.8 | 1381*1141 |
| B | NOAA/NGDC | 242.2517-242.5483 | 33.2617-33.4783 | 1 | 26.0 | 1069*781 |
| C | NOAA/NGDC-CE | 242.4253-242.4597 | 33.3503-33.3747 | 1/6 | 4.3 | 745*529 |

*Cell size in meters computed at equator for grid P and latitude 33°N for grids AA, A, B and C.

Table 7-2. Subduction zone 4-letter labeling used for the NOAA tsunami unit sources (Arcas, 2015).

| Subduction Zone | NOAA/PMEL 4-letter code |
|---------------------------------------|-------------------------|
| Aleutian-Alaska-Cascadia | acsz |
| Central and South America | cssz |
| Eastern Philippines | epsz |
| Kamchatka-Bering | kbsz |
| Kamchatka-Kuril-Japan-Izu-Mariana-Yap | kisz |
| Manus-Oceanic Convergent Boundary | mosz |
| New Guinea | ngsz |
| New Zealand-Kermadec-Tonga | ntsz |
| New Britain-Solomons-Vanuatu | nvsz |
| New Zealand-Puysegur | nzzs |
| Ryukyu-Kyushu-Nankai | rnsz |

Table 7-3. Source specification for the far-field seismic scenarios modeled in this report.

| Source Name | Subduction zone* | Location | M_w ** | Length (km) | Width (km) | Slip (m) | Fault model specification*** |
|-------------|------------------|----------|----------|-------------|------------|----------|--|
| EA-sc1 | acsz | Alaska | 9.36 | varies | varies | varies | 4m*(b31, b38) + 8m*(b32-b33, b36-b37, a31, a38, z31, z38, y31) + 8.67m*(y38, x31, w31-w36) + 10m*(b34-b35, a32, a37, z32, z37, y32, y37) + 15m*(a33-a36, z33, z36, y33, y36, x32, x37) + 20m*(z34-z35, y34-y35, x33-x36) |
| EA-sc2 | acsz | Alaska | 9.52 | varies | varies | 20 | b30-b38, a30-a37, z30-z37, y30-y37, x30-x37, w30-w36 |
| EA-sc3 | acsz | Alaska | 9.53 | 1500 | 100 | 33.25 | b25-b39, a25-a39 |
| EA-sc4 | acsz | Alaska | 9.32 | varies | varies | varies | 2m*(w31-w33, w36) + 4m*(z31, z38, y31, y38, x31, w34-w35) + 6m*(a31, a38) + 8.67m*(b31, b38, y32, y37, x32-x33, x36-x37) + 10m*(b32, b37, a32, a37, z32, z37, x34-x45) + 15m*(a33, a36, z33, z36, y33-y36) + 20m*(b33-b36, a34-a35, z34-z35) |
| EA-sc5 | acsz | Alaska | 9.53 | varies | varies | varies | 8m*(w30-w31) + 10m*(b30, z30, y30, y38, x30-x31, x37, w32-w36) + 15m*(b39, a30, z31, z38, y31-y32, y37, x32-x36) + 20m*(b31-b38, a31, a38-a39, z32, z37, y33-y36) + 30m*(a32, a37, z33-z36) + 40m*(a33-a36) |
| KU-sc1 | kisz | Kurils | 9.53 | 1200 | 100 | 41.57 | b4-b15, a4-a15 |
| KU-sc2 | kisz | Kurils | 9.53 | 1200 | 100 | varies | 30m*(b4, b13-b15, a14-a15) + 40m*(b5, b9-b12, a4, a10-a13) + 50m*(b6-b8, a5, a8-a9) + 60m*(a6-a7) |

*Refer to Table 7-2 for description of subduction zones.

** M_w computed using modulus of elasticity $\mu = 45$ GPa.

***Refer to Appendix A for unit source earthquake parameters.

Table 7-4. Near-field fault parameters for the elastic dislocation model tsunami source.

| Segment (#) | Segment Description | Length (km) | Width (km) | Strike (°) | Dip (°) | Slip (m) | Rake (°) | Top (km) | M_0^* (Nm/10 ¹⁹) | M_w^* |
|-------------|--------------------------|--------------|------------|------------|---------|----------|----------|------------|--------------------------------|-------------|
| | S. Coast Offshore | 84.5 | 12 | | | | | 0.5 | 12.49 | 7.36 |
| 1 | S. Coast Offshore N | 22.32 | 12 | 138.1 | 90 | 2 | 180 | 0.5 | 1.61 | 6.77 |
| 2 | S. Coast Offshore m | 35.34 | 12 | 129.3 | 80 | 4 | 165 | 0.5 | 5.09 | 7.10 |
| 3 | S. Coast Offshore S | 26.84 | 12 | 144.7 | 80 | 6 | 105 | 0.5 | 5.80 | 7.14 |
| | San Mateo Reverse | 15.70 | 14 | | | | | 1.0 | 3.53 | 7.00 |
| 4 | San Mateo Reverse N | 10.40 | 14 | 319.0 | 60 | 4 | 115 | 1.0 | 1.75 | 6.79 |
| 5 | San Mateo Reverse S | 5.30 | 14 | 339.0 | 60 | 8 | 105 | 1.0 | 1.78 | 6.80 |
| | San Onofre Trend | 15.33 | 5 | | | | | 1.0 | 0.46 | 6.41 |
| 6 | San Onofre Trend | 15.33 | 5 | 294.2 | 90 | 2 | 180 | 1.0 | 0.46 | 6.41 |
| | Carlsbad Reverse | 21.49 | 50 | | | | | 1.0 | 10.46 | 7.31 |
| 7 | Carlsbad Reverse N0 | 13.37 | 50 | 294.2 | 30 | 4 | 105 | 1.0 | 8.02 | 7.24 |
| 8 | Carlsbad Reverse N1 | 8.12 | 50 | 133.2 | 30 | 2 | 165 | 1.0 | 2.44 | 6.89 |
| | Oceanside | 26.63 | 12 | | | | | 0.5 | 3.83 | 7.02 |
| 9 | Oceanside | 26.63 | 12 | 302.4 | 90 | 4 | 165 | 0.5 | 3.83 | 7.02 |

* M_0 and M_w computed using modulus of elasticity $\mu = 30$ GPa.

Table 7-5. Near-field composite seismic sources.

| Source (#) | Segments* (#) | M_0^{**} (Nm/10 ¹⁹) | M_w^{**} |
|------------|---------------|-----------------------------------|------------|
| Local-sc1 | 1-9 | 30.77 | 7.62 |
| Local-sc2 | 4-8 | 14.45 | 7.41 |
| Local-sc3 | 1-3, 9 | 16.33 | 7.44 |

*Refer to Table 7-4 for description of segments.

** M_0 and M_w computed using modulus of elasticity $\mu = 30$ GPa.

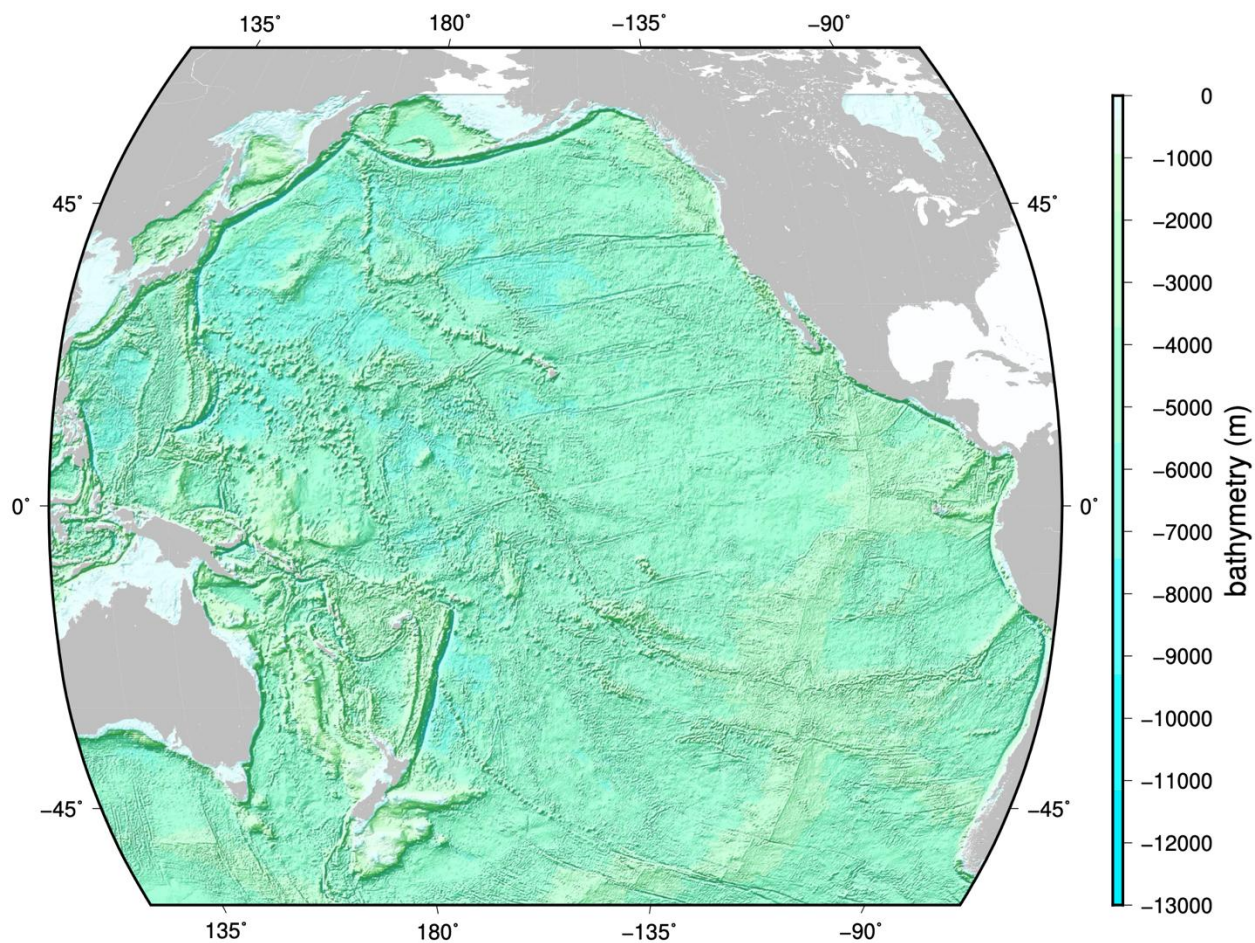


Figure 7-1. The Pacific Ocean bathymetry grid (grid *P*) of 4 arc-min spatial resolution used with MOST for the far-field tsunami simulations.

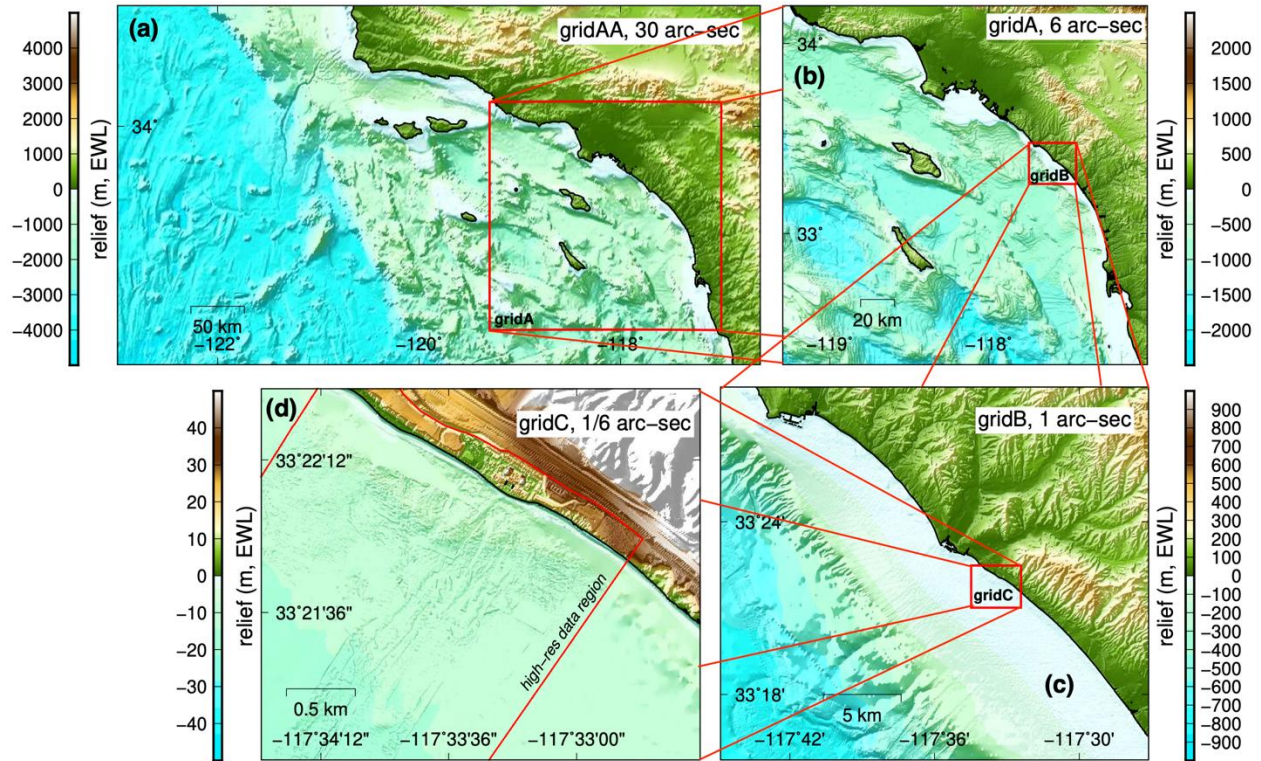


Figure 7-2. Nested grids of increasing resolution (grid AA: 30 arc-sec; grid A: 6 arc-sec; grid B: 1 arc-sec; grid C: 1/6 arc-sec) used for the numerical computations.

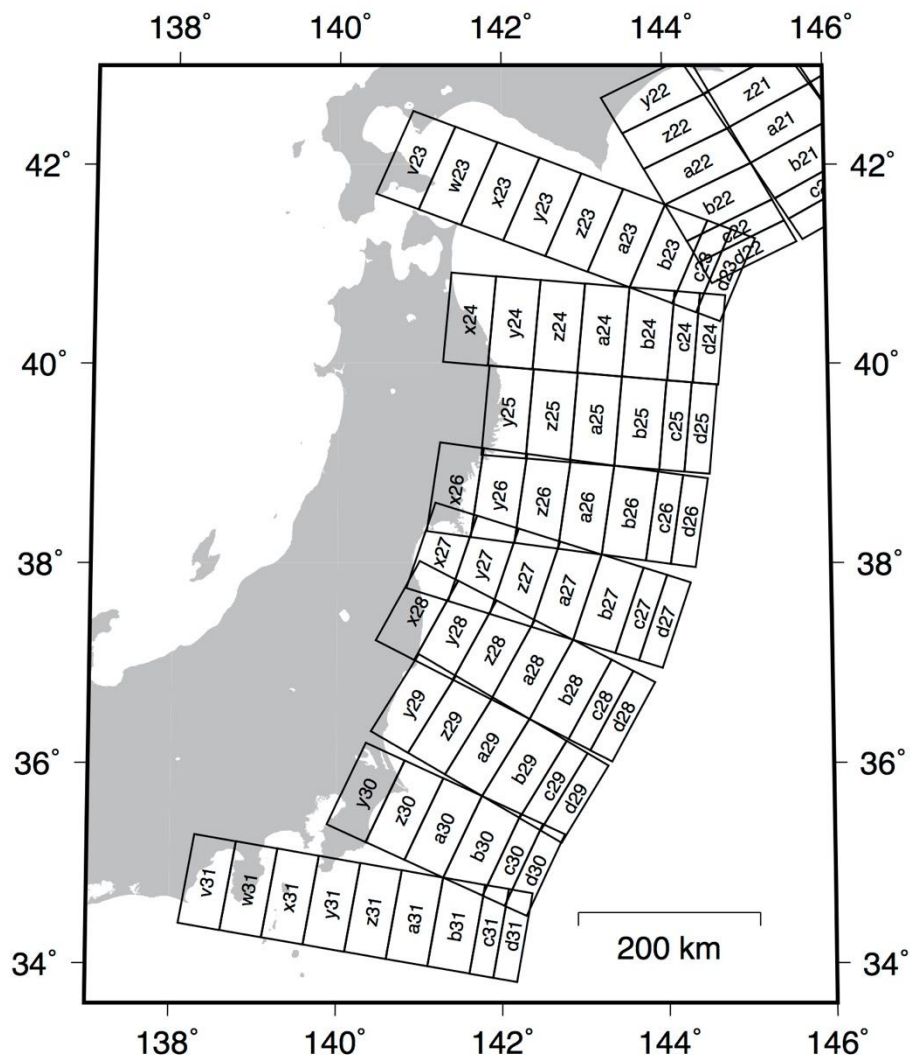


Figure 7-3. NOAA/PMEL's unit sources and labeling along the Japan subduction zone (kisz).

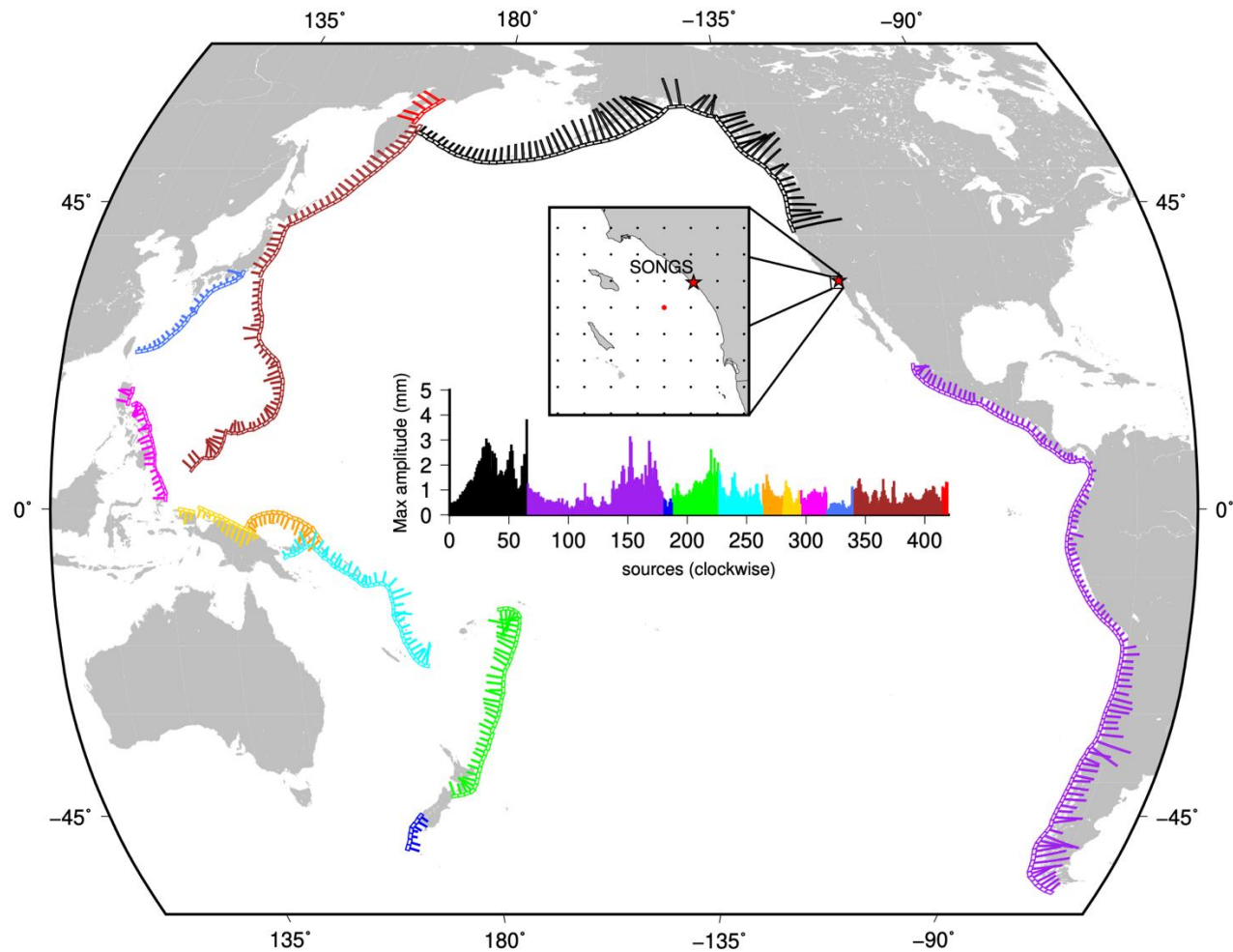


Figure 7-4. Tsunami hazard sensitivity for the study site to the location of the unit sources (only shallowest (row B) unit sources shown here). The length of the bars shows the relative maximum amplitude offshore SONGS from each unit source. The inset bar figure shows the maximum amplitude values, moving clockwise around the Pacific Ocean, starting from W. Aleutians and ending at N. Kamchatka. The inset map figure shows the NOAA/PMEL unit source output grid nodes with 16 arc-min spacing (black dots) and the grid node selected to extract the unit source maximum amplitudes (red dot) relative to the location of SONGS (red star).

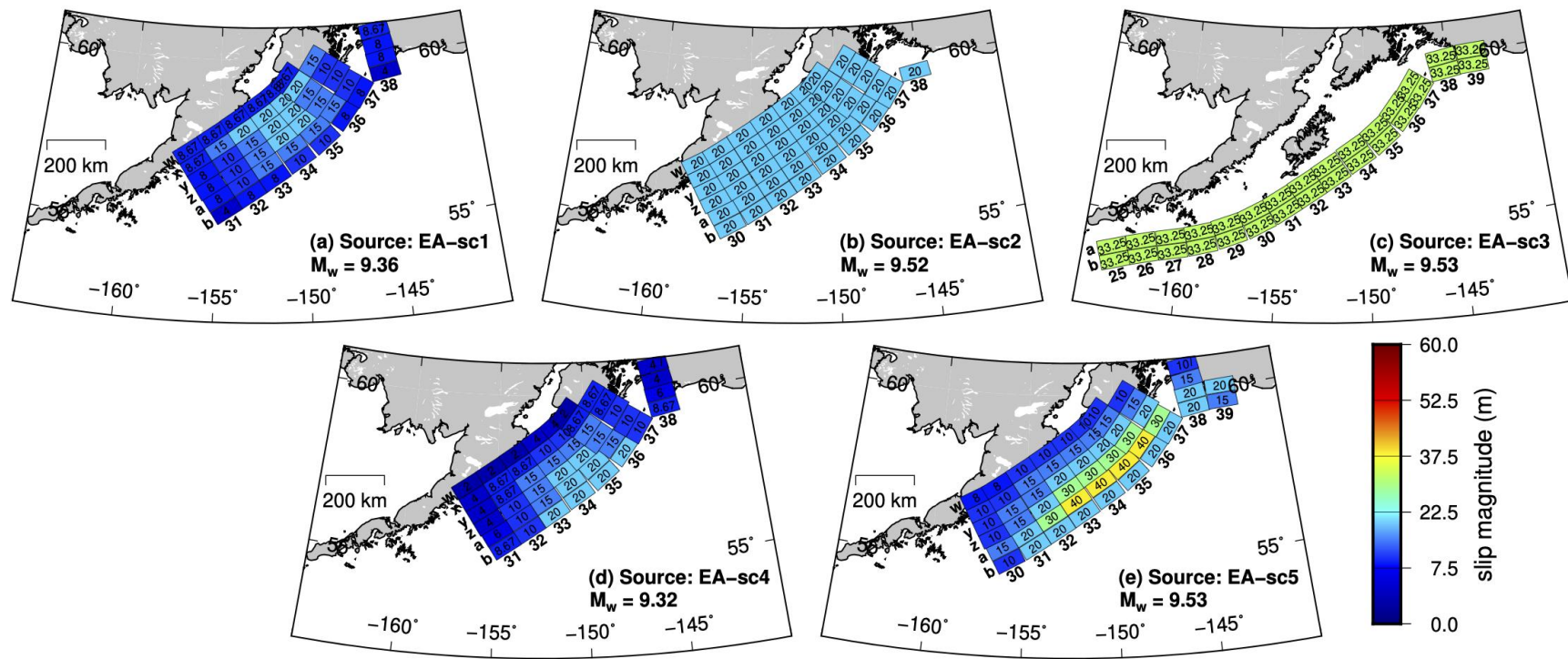


Figure 7-5. Definition of the five Eastern Aleutian (far-field) seismic sources using NOAA/PMEL's unit sources - see Table 7-3 for sources description and Appendix A for the earthquake parameters of the unit sources.

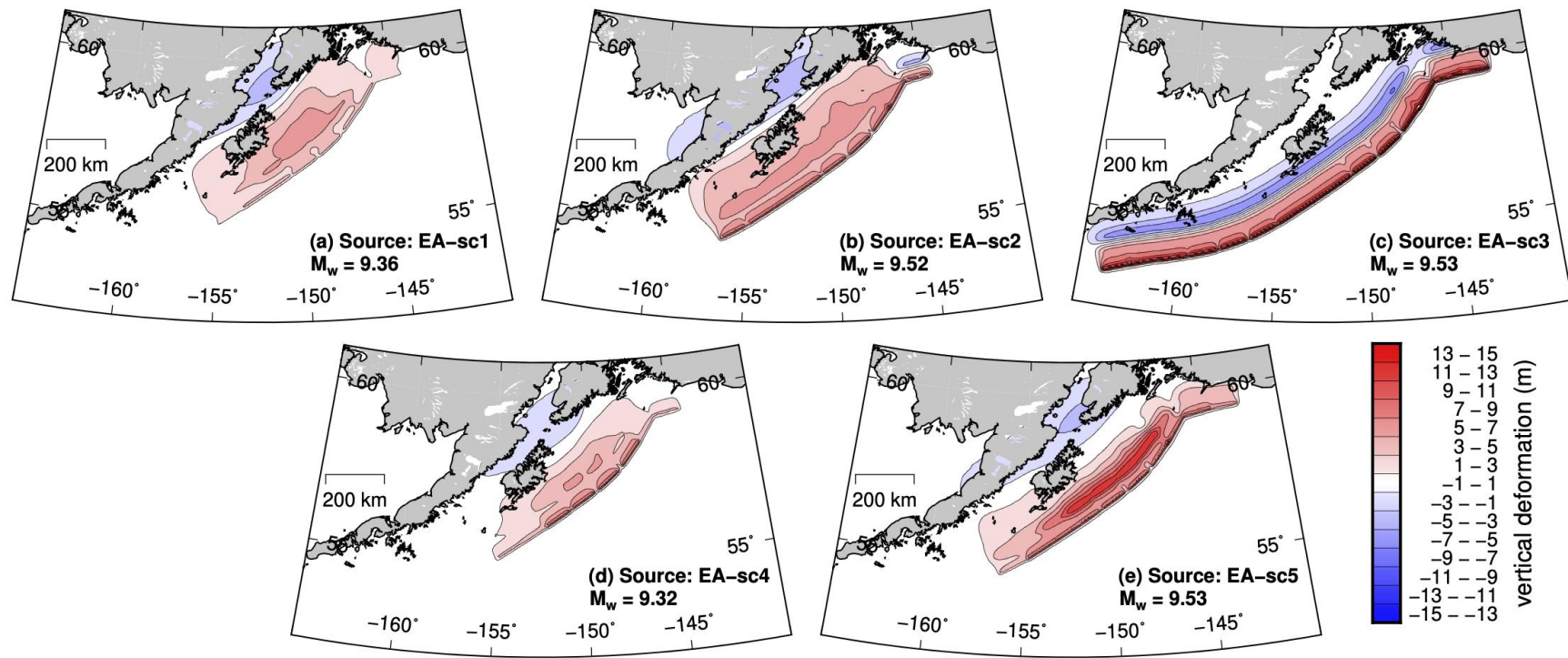


Figure 7-6. Vertical co-seismic displacement for the five Eastern Aleutian (far-field) seismic sources. Contours of vertical deformation drawn every 2 m starting from ± 1 m. Blue and red colors show negative (subsidence) and positive (uplift) vertical deformation, respectively.

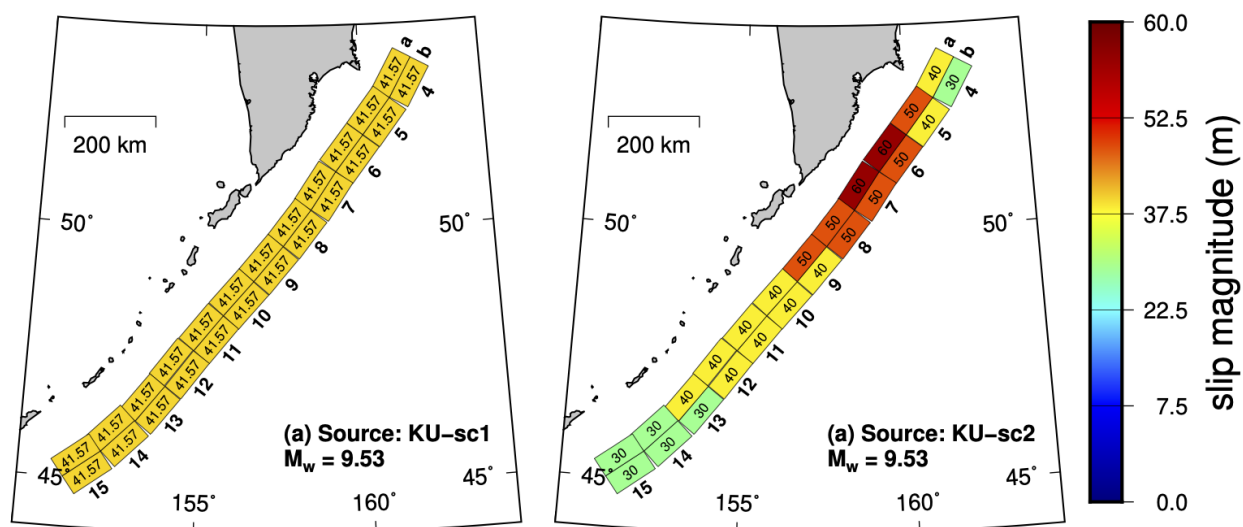


Figure 7-7. Definition of the two Kuril (far-field) seismic sources using NOAA/PMEL's unit sources - see Table 6-3 for source descriptions and Appendix A for the earthquake parameters of the unit sources.

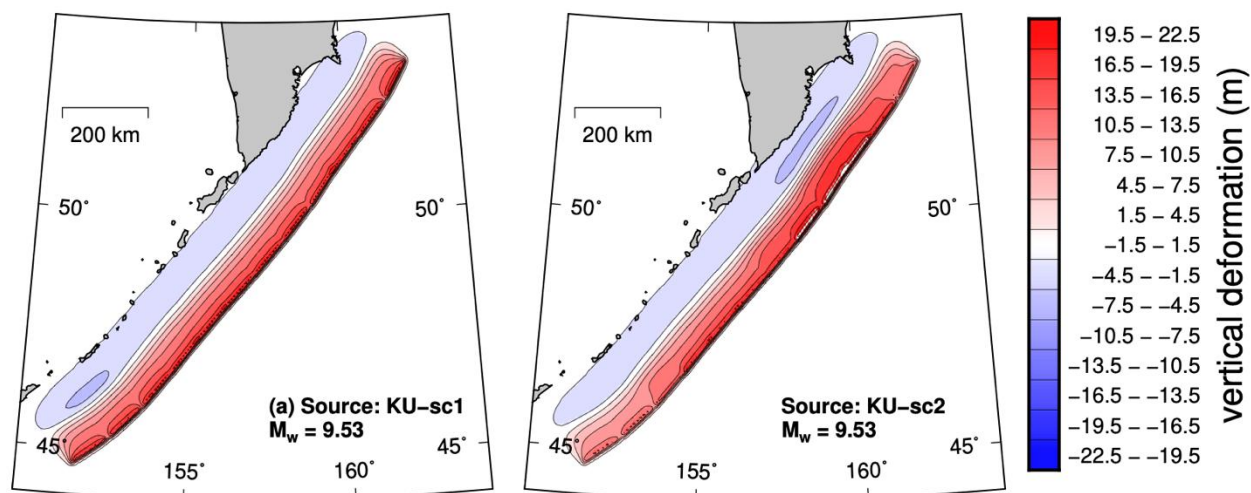


Figure 7-8. Vertical co-seismic displacement for the two Kuril (far-field) seismic sources. Contours of vertical deformation drawn every 3 m starting from ± 1.5 m. Blue and red colors show negative (subsidence) and positive (uplift) vertical deformation, respectively.

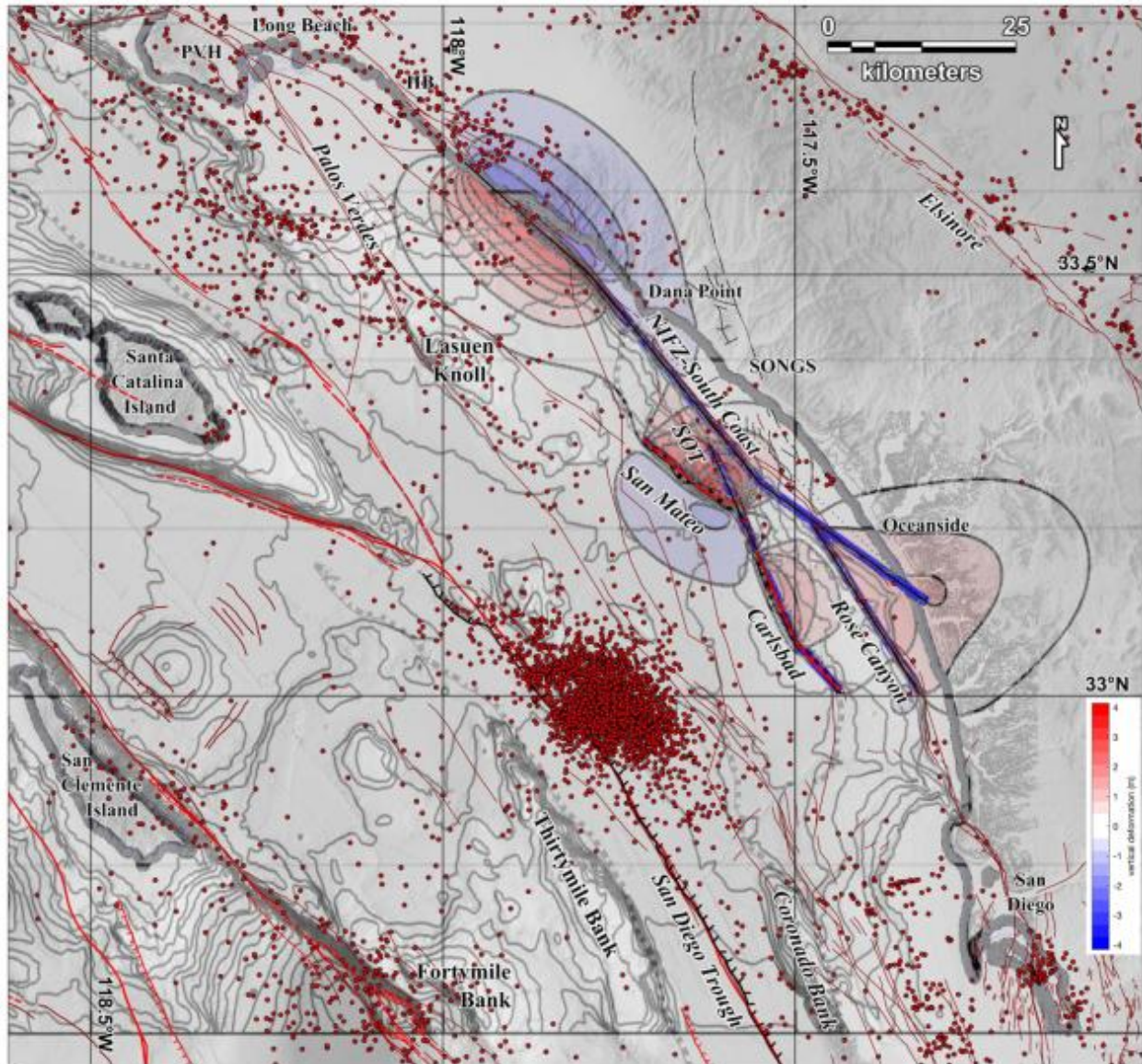


Figure 7-9. Map showing seafloor deformation produced by local tsunami source 1 with all nine fault segments, with bathymetry and relocated seismicity ($M > 2$, 1981-2019; Hauksson et al., 2012, 2019 update). Modeled uplift matches bathymetry in most areas, except north of Dana Point where the San Joaquin Hills blind thrust (Grant et al., 2002) is absent from this model.

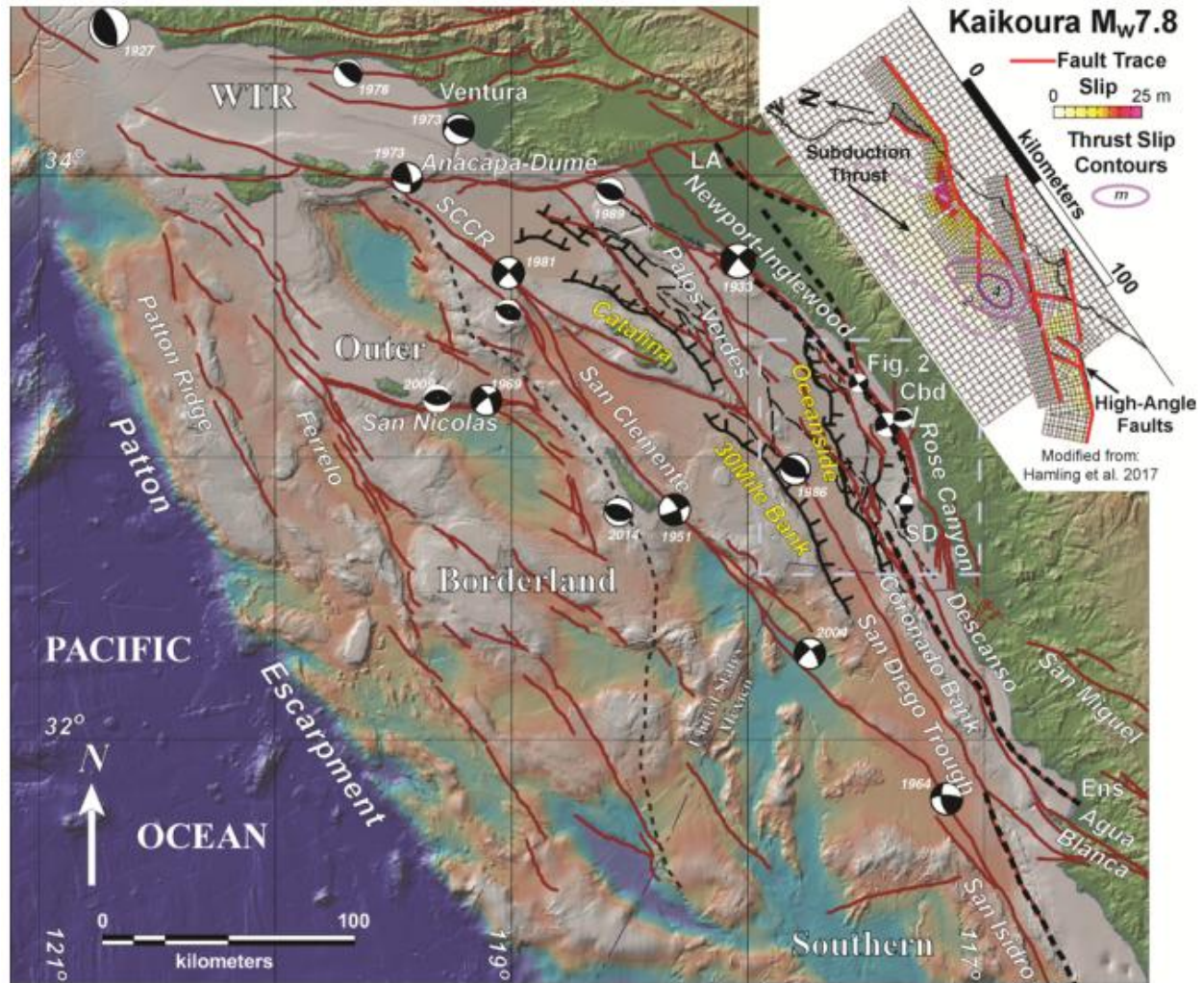


Figure 7-10. Map comparing rupture model for the 2016 Kaikoura, New Zealand earthquake with the Coastal Fault System located between Los Angeles (LA) and San Diego (SD) (Source: Legg et al. (2018)).

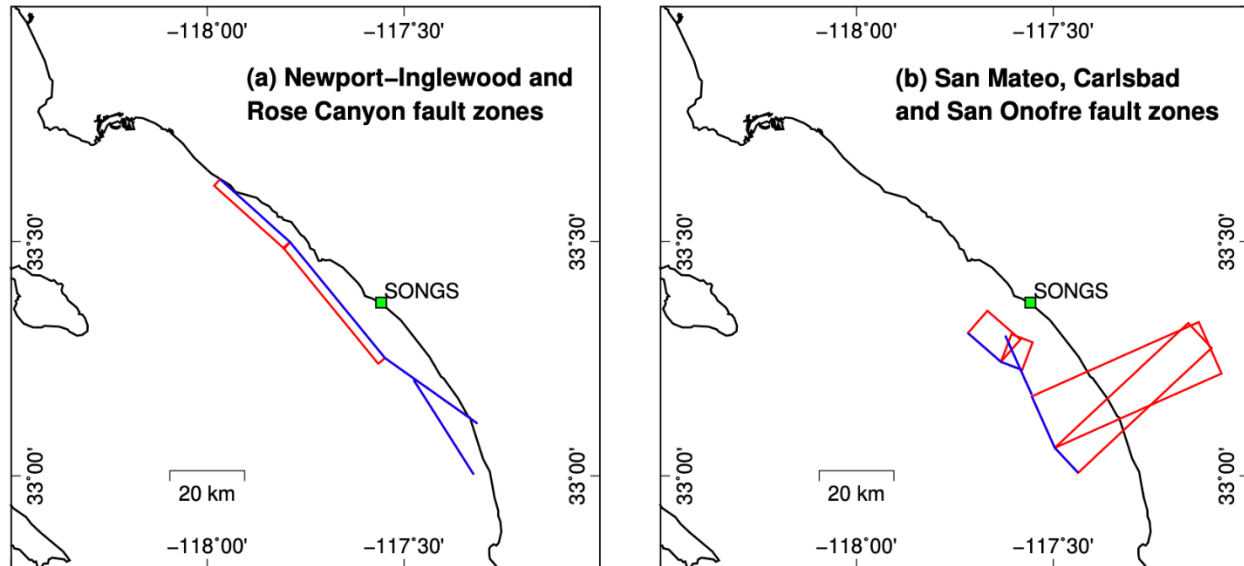


Figure 7-11. Maps showing the simple rectangular fault models for the local tsunami cases. (a) Four-segments with strike-slip and oblique-slip used for the Newport-Inglewood and Rose Canyon fault zones. (b) Two-segments each with oblique-slip used for the San Mateo and Carlsbad faults, and one-segment strike-slip model for the San Onofre Trend. Blue lines are upper tip of fault segments, red outlines deep fault extent.

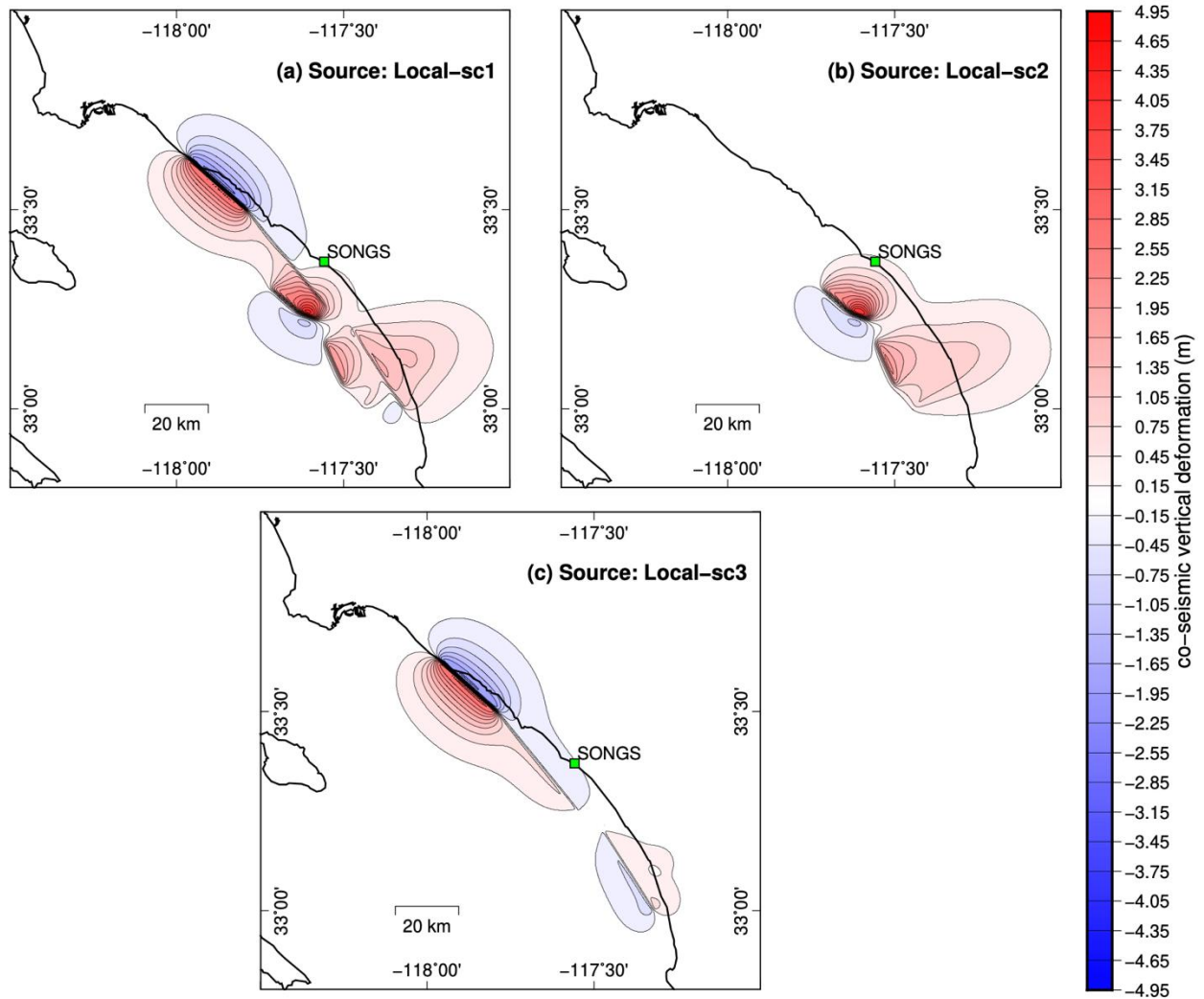


Figure 7-12. Vertical co-seismic displacement for the three composite near-field sources - see Table 6-5. Contours of vertical deformation drawn every 0.3 m starting from ± 0.15 m. Blue and red colors show negative (subsidence) and positive (uplift) vertical deformation, respectively.

8.0 COMPUTATIONS

8.1 RESULTS FOR FAR-FIELD SEISMIC TSUNAMI CASES

8.1.1 Eastern Aleutians

The distribution of maximum wave amplitudes across the Pacific Ocean for all five Eastern Aleutians sources is shown in Figure 8-1. The plots show how seismic sources from the Eastern Aleutians have an efficient directivity towards the West Coast of the United States. Sources EA-sc3 and EA-sc5 (subplots *c* and *e* in Figure 8-1, respectively), both assigned $M_w9.5$, beam the most tsunami energy towards southern California and the SONGS site compared to the other Eastern Aleutian sources considered in this report. Source EA-sc2 (subplot *b* in Figure 8-1), also with $M_w9.5$ but being assigned a smaller maximum slip magnitude, does not produce maximum wave amplitudes in southern California as high as the other two $M_w9.5$ Eastern Aleutian sources. Sources EA-sc1 and EA-sc4 (subplots *a* and *d* in Figure 8-1, respectively), which were assigned smaller magnitudes ($M_w9.4$ and $M_w9.3$, respectively), produce the smallest maximum wave amplitudes across the Pacific Ocean.

Source EA-sc1

Maximum wave amplitudes produced during the numerical simulations inside the domains of grids AA, A and B for source EA-sc1 are shown in Figure 8-2. Maximum wave amplitude in grid AA is more pronounced along the NW coastline section of the grid (i.e., the west-facing coastline stretch near Lompoc), the section between Oxnard and Carpinteria, the section between Long Beach and Huntington Beach, and San Diego. SE of the SONGS site, computed maximum wave amplitude is somewhat higher compared to just offshore SONGS. This local amplification just SE of SONGS is the result of complex reflection patterns at the shoreline, with the Channel Islands also playing a significant role in the distribution of maximum amplitudes along the mainland coastline. The observations made for the maximum amplitudes computed across grids AA, A and B for source EA-sc1 are common between all Eastern Aleutian sources.

The results for the finest-resolution grid (grid C) are shown in Figure 8-3. The maximum tsunami amplitude in the numerical domain ranges between 1.5 and 2.0 m (inferred from the color bar of Figure 8-3a). Time series of wave amplitude extracted from a numerical tide gauge located just offshore SONGS at a depth of 5.57 m (EWL) show the maximum and minimum amplitudes of 1.88 and -2.73 m (EWL) occurring ~6 and ~7.8 hr. after the seismic rupture, respectively (Figure 8-3e). Wave runup along the coastline stretch of the grid is relatively uniform. The simulation (which assumes that the seawall is not present) yields a maximum runup of 2.0 m (EWL), and the waves would not produce runup/inundation at the SONGS site (Figure 8-3c).

Source EA-sc2

Maximum wave amplitudes for source EA-sc2 produced during the numerical simulations inside the domains of grids AA, A and B are shown in Figure 8-4. The same

maximum wave amplitude patterns are observed as for source EA-sc1, but with higher amplitudes. The local wave amplification just SE of the SONGS site appearing in the grid B domain is also more pronounced.

The results for the finest-resolution grid (grid C) are shown in Figure 8-5. The maximum tsunami amplitude in the numerical domain ranges between 2.5 and 4.5 m (inferred from the color bar of Figure 8-5a). Time series of wave amplitude extracted from a numerical tide gauge located just offshore SONGS at a depth of 5.57 m (EWL) show the maximum and minimum amplitudes of 3.34 and -5.30 m (EWL) occurring ~6 and ~7.8 hr. after the seismic rupture, respectively (Figure 8-5e). Wave runup along the coastline stretch of the grid is relatively uniform. The simulation (which assumes that the seawall is not present) yields a maximum runup of 4.1 m (EWL) at the eastern grid boundary and 3.4 m (EWL) at the SONGS site (at longitudes between -117.5594 and -117.5574°W). The waves would produce runup/inundation at the SONGS site (Figure 8-5c-d). Maximum tsunami elevation and maximum flow depth around the NUHOMS ISFSI would be 3.4 m (EWL) and 0.6 m, respectively.

Source EA-sc3

Maximum wave amplitudes produced during the numerical simulations inside the domains of grids AA, A and B for source EA-sc3 are shown in Figure 8-6. The same maximum wave amplitude patterns are observed as for sources EA-sc1 and EA-sc2, but with even higher amplitudes. The local wave amplification just SE of SONGS appearing in the grid B domain is the most pronounced across all Eastern Aleutian source simulations.

The results for the finest-resolution grid (grid C) are shown in Figure 8-7. The maximum tsunami amplitude in the numerical domain ranges between 4.0 and 5.5 m (inferred from the color bar of Figure 8-7a). Time series of wave amplitude extracted from a numerical tide gauge located just offshore SONGS at a depth of 5.57 m (EWL) show the maximum and minimum amplitudes of 5.03 and -5.09 m (EWL) occurring ~7 and ~6.9 hr. after the seismic rupture, respectively (Figure 8-7e). The third crest is the highest, but with almost equal amplitude to the first rise. These wave amplitudes are the highest across all sources considered in this study. The simulation (which assumes that the seawall is not present) yields a maximum runup of 7.0 m (EWL) at a steep topographic node and 5.9 m (EWL) at the SONGS site (at longitudes between -117.5594 and -117.5574°W). The maximum runup produced for source EA-sc3 is also the highest across all seismic sources considered in this study. The waves would produce runup/inundation at the SONGS site (Figure 8-7c-d). Maximum tsunami elevation and maximum flow depth around the NUHOMS ISFSI would be 5.9 m (EWL) and 2.8 m, respectively.

Source EA-sc4

Maximum wave amplitudes produced during the numerical simulations inside the domains of grids AA, A and B for source EA-sc4 are shown in Figure 8-8. The same maximum wave amplitude patterns are observed as with the other Eastern Aleutian simulations. EA-sc4 is one of the two Eastern Aleutian sources assigned a smaller magnitude of M_w 9.3 (the other being source EA-sc1). Compared to EA-sc1, maximum amplitudes for EA-sc4 are higher because of the 20 m-slip patches in the source being assigned to the shallower unit sources (Figure 7-5).

The results for the finest-resolution grid (grid C) are shown in Figure 8-9. The maximum tsunami amplitude in the numerical domain ranges between 1.5 and 3.0 m (inferred from the color bar of Figure 8-9a). Time series of wave amplitude extracted from a numerical tide gauge located just offshore SONGS at a depth of 5.57 m (EWL) show the maximum and minimum amplitudes of 2.22 and -2.99 m (EWL) occurring ~7 and ~7.7 hr. after the seismic rupture, respectively (Figure 8-9e). The third crest is the highest, but with almost equal amplitude to the first rise. Wave runup along the coastline stretch of the grid is relatively uniform. The simulation (which assumes that the seawall is not present) yields a maximum runup of 2.73 m (EWL) near the eastern grid boundary and 2.46 m (EWL) at SONGS (at longitudes between -117.5594 and -117.5574°W). The waves would not produce runup/inundation at the SONGS site (Figure 8-9c).

Source EA-sc5

Maximum wave amplitudes produced during the numerical simulations inside the domains of grids AA, A and B for source EA-sc5 are shown in Figure 8-10. The same maximum wave amplitude patterns and similar amplitudes are observed as for source EA-sc3, with both sources being assigned equal magnitude ($M_w 9.5$), but different source characteristics (see Table 7-3). The local wave amplification just SE of the SONGS site appearing in the grid B domain is pronounced as with source EA-sc3.

The results for the finest-resolution grid (grid C) are shown in Figure 8-11. The maximum tsunami amplitude in the numerical domain ranges between 4.0 and 5.0 m (inferred from the color bar of Figure 8-11a). Time series of wave amplitude extracted from a numerical tide gauge located just offshore SONGS at a depth of 5.57 m (EWL) show the maximum and minimum amplitudes of 4.73 and -5.44 m (EWL) occurring ~6 and ~7.9 hr. after the seismic rupture, respectively (Figure 8-11e). The first rise is the highest, but with almost equal amplitude to the third rise. Wave runup along the coastline stretch of the grid is relatively uniform. The simulation (which assumes that the seawall is not present) yields a maximum runup of 5.75 m (EWL) at a steep topographic point and 5.51 m (EWL) at the SONGS site (at longitudes between -117.5594 and -117.5574°W). The waves would produce runup/inundation at the SONGS site (Figure 8-11c-d). Maximum tsunami elevation and maximum flow depth around the NUHOMS ISFSI would be 5.5 m (EWL) and 2.7 m, respectively.

8.1.2 Kuril Islands

The distribution of maximum wave amplitudes across the Pacific Ocean for the two Kuril sources is shown in Figure 8-12. Both the two Kuril sources considered were assigned magnitude $M_w 9.5$, equal to three worst-case scenarios for the Eastern Aleutian seismic sources. However, the maximum slip magnitude assigned to the Kuril sources is higher compared to the Eastern Aleutian sources.

Figure 8-12 shows that the maximum wave amplitudes from the Kuril sources are not directed towards southern California, but to the west of the islands of Hawaii. Kuril source KU-sc2 (subplot *b* in Figure 8-12), which was assigned a variable slip distribution with higher maximum slip values, produces somewhat higher maximum amplitudes in southern California compared to the uniform slip scenario KU-sc1 (subplot *a* in Figure 8-12), but the amplitudes in

southern California are deficient compared to the Eastern Aleutian worst-cases scenarios. Based on Figure 8-12, tsunami impact at SONGS from the two Kuril sources is not expected to be higher compared to the Eastern Aleutian worst-case scenarios. The high-resolution results for the Kuril far-field source are presented below.

Source KU-sc1

Maximum wave amplitudes produced during the numerical simulations inside the domains of grids AA, A and B for source KU-sc1 are shown in Figure 8-13. The same maximum wave amplitude general patterns are observed as for the Eastern Aleutian sources.

The results for the finest-resolution grid (grid C) are shown in Figure 8-14. The maximum tsunami amplitude in the numerical domain ranges between 1.5 and 3.0 m (inferred from the color bar of Figure 8-14a). Time series of wave amplitude extracted from a numerical tide gauge located just offshore SONGS at a depth of 5.57 m (EWL) show the maximum and minimum amplitudes of 2.01 and -2.73 m (EWL) occurring ~11.7 and ~11.0 hr. after the seismic rupture, respectively (Figure 8-14e). The maximum amplitude near the SONGS site is produced by the sixth wave. Wave runup along the coastline stretch of grid C increases from west to east. The simulation (which assumes that the seawall is not present) yields a maximum runup of 2.9 m (EWL) at the eastern grid boundary and 2.2 m (EWL) at the SONGS site (at longitudes between -117.5594 and -117.5574°W), and the waves would not produce runup/inundation at the SONGS site (Figure 8-14c-d).

Source KU-sc2

Maximum wave amplitudes produced during the numerical simulations inside the domains of grids AA, A and B for source KU-sc2 are shown in Figure 8-15. The same maximum wave amplitude general patterns are observed as for Kuril source KU-sc1, but with somewhat higher maximum amplitudes due to the higher maximum slip values assigned to source KU-sc2 compared to the uniform slip source KU-sc1 - both sources were assigned the same magnitude ($M_w 9.5$).

The results for the finest-resolution grid (grid C) are shown in Figure 8-16. The maximum tsunami amplitude in the numerical domain ranges between 2.0 and 3.5 m (inferred from the color bar of Figure 8-16a). Time series of wave amplitude extracted from a numerical tide gauge located just offshore SONGS at a depth of 5.57 m (EWL) show the maximum and minimum amplitudes of 2.62 and -2.99 m (EWL) occurring ~11.7 and ~11.1 hr. after the seismic rupture, respectively (Figure 8-16e). The maximum amplitude near the SONGS site is produced by the sixth wave, as is the case with source KU-sc1. Wave runup along the coastline stretch of grid C increases from west to east. The simulation (which assumes that the seawall is not present) yields a maximum runup of 3.4 m (EWL) at the eastern grid boundary and 2.8 m (EWL) at the SONGS site (at longitudes between -117.5594 and -117.5574°W). The waves would produce runup/inundation at the SONGS site (Figure 8-16d), but the inundation does not reach the NUHOMS ISFSI.

8.2 RESULTS FOR LOCAL SEISMIC TSUNAMI CASES

8.2.1 Source Local-sc1

Maximum wave amplitudes produced during the numerical simulations inside the domains of grids A and B for near-field source Local-sc1 are shown in Figure 8-17. Source Local-sc1 is a combination of all nine fault rupture segments listed in Table 7-4. Maximum amplitudes are observed along the coastal stretch between Long Beach and Oceanside. Wave energy is also beamed towards the SE coast of San Clemente Island. Figure 8-17*b* shows highly localized maximum wave amplitude patterns due to the complex characteristics of the fault rupture, the proximity of the source to the coastline, but also due to reflections off the coastline.

The results for the finest-resolution grid (grid C) are shown in Figure 8-18. The maximum tsunami amplitude in the numerical domain ranges between 2.0 and 5.0 m (inferred from the color bar of Figure 8-18*a*). Time series of wave amplitude extracted from a numerical tide gauge located just offshore SONGS at a depth of 5.57 m (EWL) show the maximum and minimum amplitudes of 4.16 and -3.85 m (EWL) occurring ~8 and ~13 min after the seismic rupture, respectively (Figure 8-18*e*). The maximum amplitude near the SONGS site is produced by the first wave. Wave runup along the coastline stretch of grid C ranges between 3.5 to 5.6 m (EWL). The simulation (which assumes that the seawall is not present) yields a maximum runup of 4.8 m (EWL) at the SONGS site (at longitudes between -117.5594 and -117.5574°W). The waves would produce runup/inundation at the SONGS site (Figure 8-18*c-d*). Maximum tsunami elevation and maximum flow depth around the NUHOMS ISFSI would be 4.0 m (EWL) and 1.2 m, respectively.

8.2.2 Source Local-sc2

Maximum wave amplitudes produced during the numerical simulations inside the domains of grids A and B for near-field source Local-sc2 are shown in Figure 8-19. Source Local-sc2 is a combination of the San Mateo, San Onofre and Carlsbad segments listed in Table 7-4. Maximum amplitudes are thus more pronounced along the coastal stretch between San Clemente and Oceanside compared to the coastal stretch between San Clemente and Long Beach that is more impacted in source Local-sc1. Similar to source Local-sc1, wave energy is also beamed towards the SE coast of San Clemente Island. Figure 8-19*b* also shows highly localized maximum wave amplitude patterns as with source Local-sc1.

The results for the finest-resolution grid (grid C) are shown in Figure 8-20. The maximum tsunami amplitude in the numerical domain ranges between 1.5 and 4.0 m (inferred from the color bar of Figure 8-20*a*). Time series of wave amplitude extracted from a numerical tide gauge located just offshore SONGS at a depth of 5.57 m (EWL) show the maximum and minimum amplitudes of 2.92 and -3.98 m (EWL) occurring ~9 and ~13 min after the seismic rupture, respectively (Figure 8-20*e*). The maximum amplitude near the SONGS site is produced by the first wave. Wave runup along the coastline stretch of grid C ranges between 2.9 to 4.8 m (EWL). The simulation (which assumes that the seawall is not present) yields a maximum runup of 3.8 m (EWL) at the SONGS site (at longitudes between -117.5594 and -117.5574°W). The waves would produce runup/inundation at the SONGS site (Figure 8-20*c-d*). Maximum tsunami

elevation and maximum flow depth around the NUHOMS ISFSI would be 3.4 m (EWL) and 0.4 m, respectively.

8.2.3 Source Local-sc3

The maximum wave amplitudes produced during the numerical simulations inside the domains of grids A and B for near-field source Local-sc3 are shown in Figure 8-21. Source Local-sc3 is a combination of the South Coast and Oceanside segments listed in Table 7-4. Maximum amplitudes are thus subdued along the coastal stretch between San Clemente and Oceanside compared to sources Local-sc1 and Local-sc2. Contrary to sources Local-sc1 and Local-sc2, more wave energy is beamed towards Catalina Island than toward San Clemente Island.

The results for the finest-resolution grid (grid C) are shown in Figure 8-22. The maximum tsunami amplitude in the numerical domain ranges between 0.5 and 2.5 m (inferred from the color bar of Figure 8-22a). Time series of wave amplitude extracted from a numerical tide gauge located just offshore SONGS at a depth of 5.57 m (EWL) show the maximum and minimum amplitudes of 1.38 and -1.65 m (EWL) occurring ~97 and ~26 min after the seismic rupture, respectively (Figure 8-22e). Wave runup along the coastline stretch of grid C ranges between 1.7 to 3.2 m (EWL). The simulation yields a maximum runup of 2.6 m (EWL) at the SONGS site (at longitudes between -117.5594 and -117.5574°W). The waves would not produce runup/inundation at the SONGS site (Figure 8-22c-d).

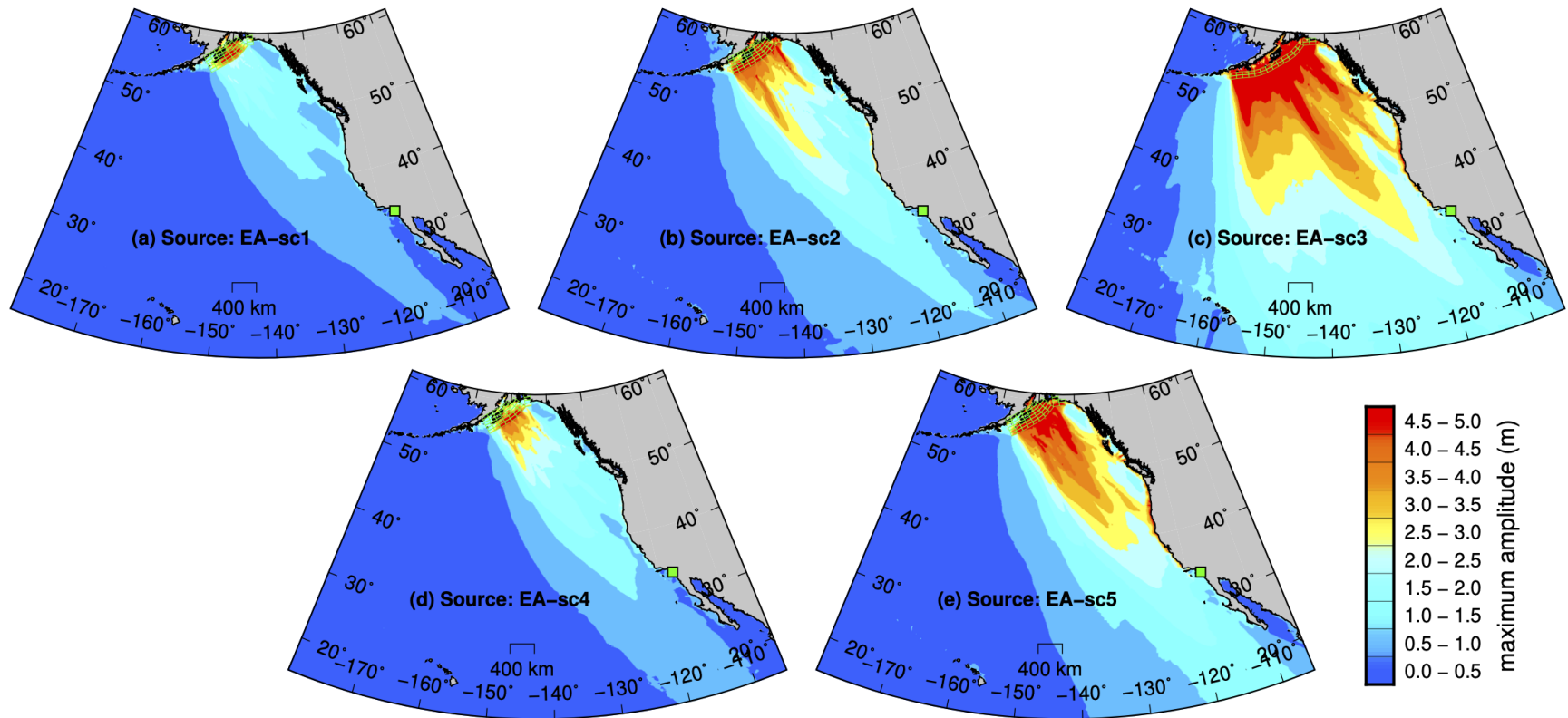


Figure 8-1. Maps showing the maximum tsunami amplitudes (in part of the spatial extent) of grid *P* from the numerical simulation of all five Eastern Aleutian sources - see Table 7-3 for information on the sources.

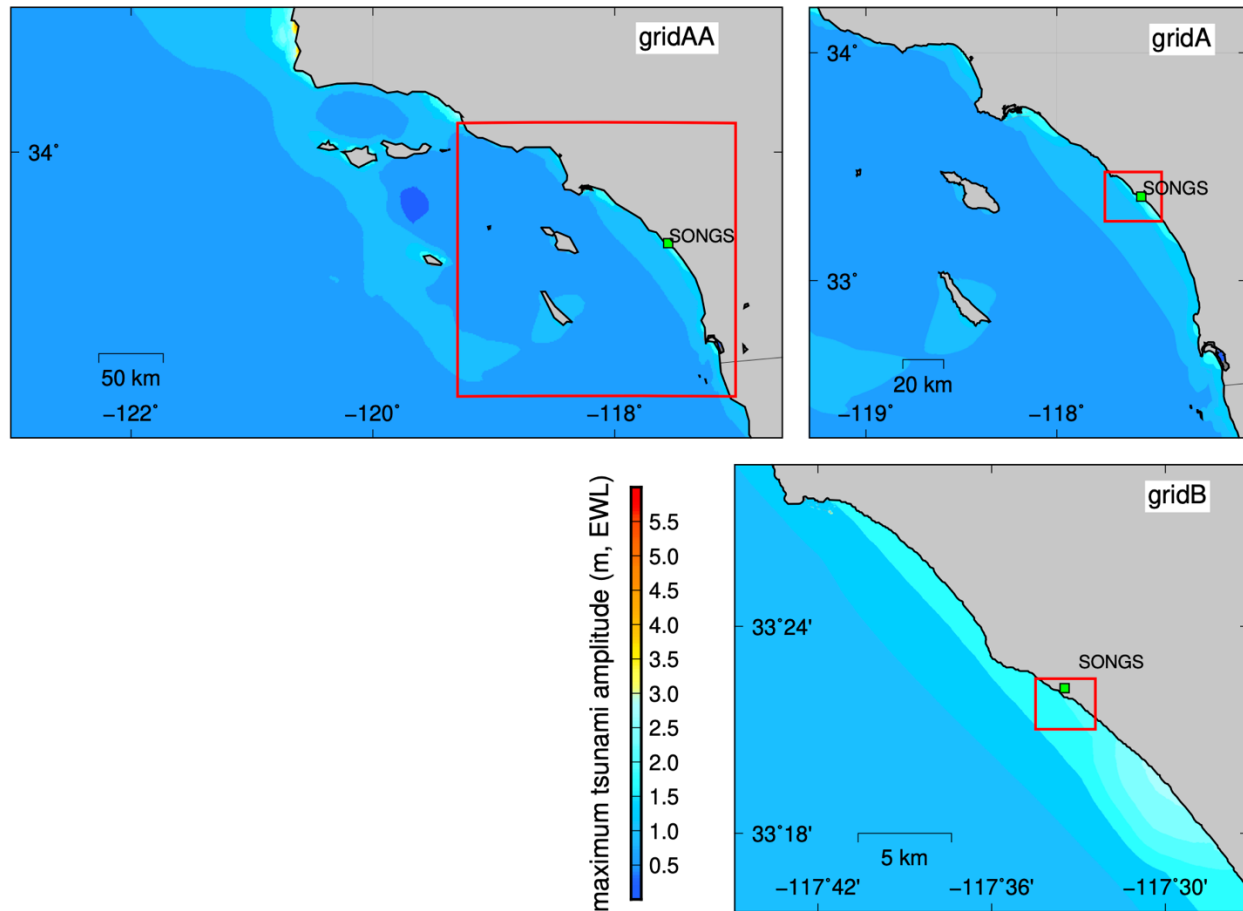


Figure 8-2. Maps showing the maximum tsunami amplitudes inside the domains of grids AA, A, and B during the numerical simulation of the Eastern Aleutian source EA-sc1 - see Table 7-3 for information on the sources.

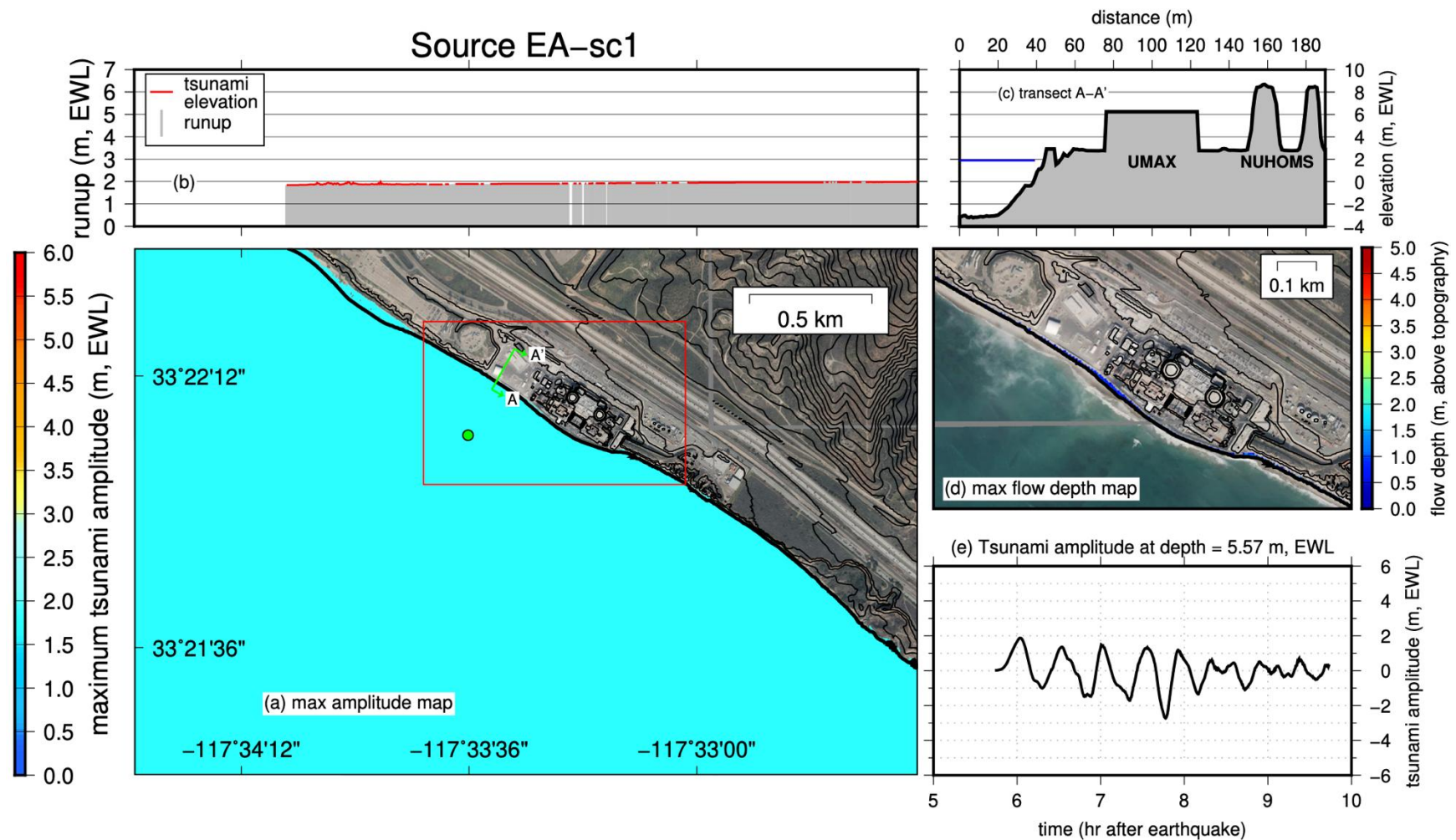


Figure 8-3. Numerical simulation results for the Eastern Aleutians seismic source EA-sc1. (a) Maximum tsunami amplitude across the domain of grid C. (b) Maximum runup and tsunami elevation distribution across the coastline in grid C. (c) Transect of maximum tsunami elevation across the SONGS site - see (a) for position of transect. (d) Maximum flow depth distribution across the SONGS site. (e) Time series of free surface elevation just offshore the SONGS site - time series extracted from the location shown with the green dot in (a).

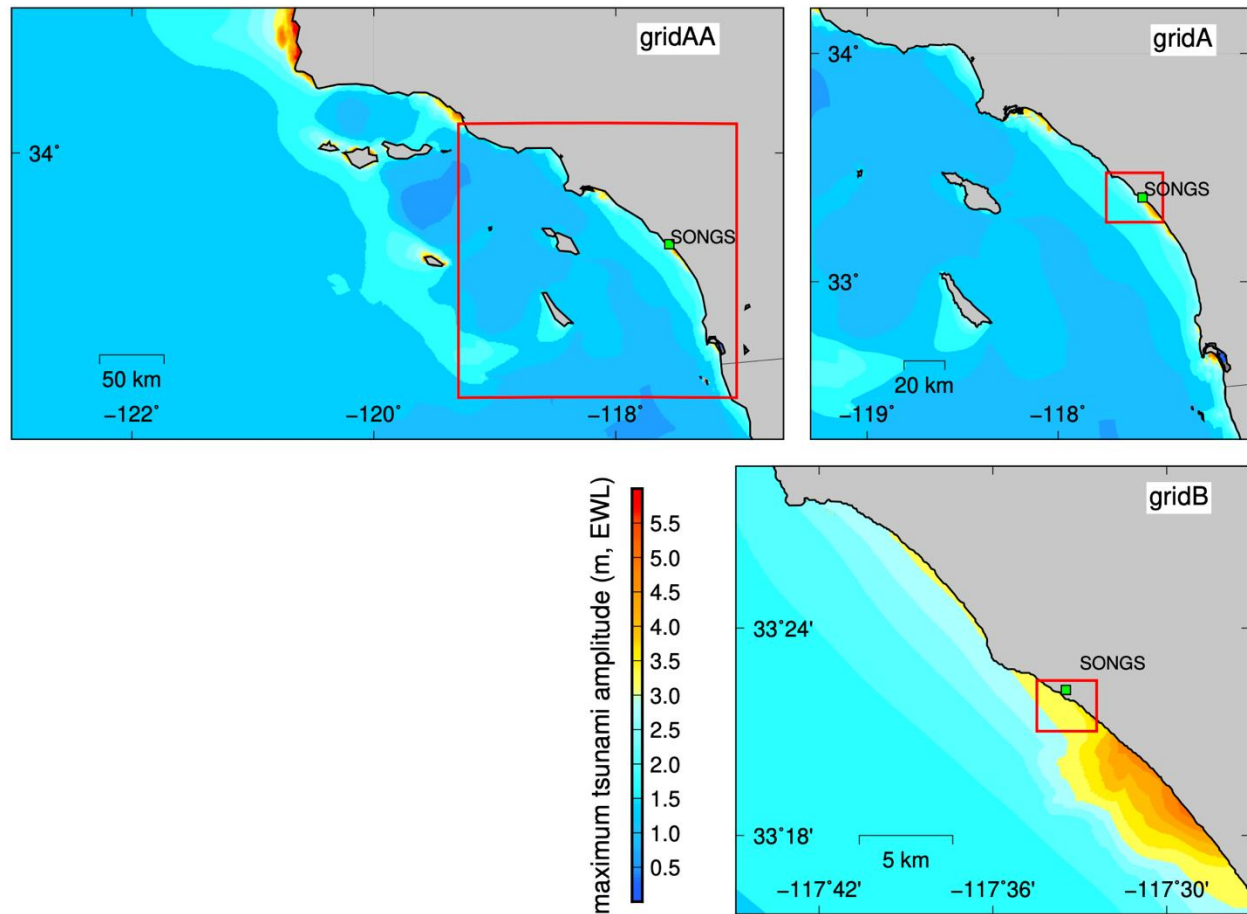


Figure 8-4. Maps showing the maximum tsunami amplitudes inside the domains of grids AA, A, and B during the numerical simulation of the Eastern Aleutian source EA-sc2 - see Table 7-3 for information on the sources.

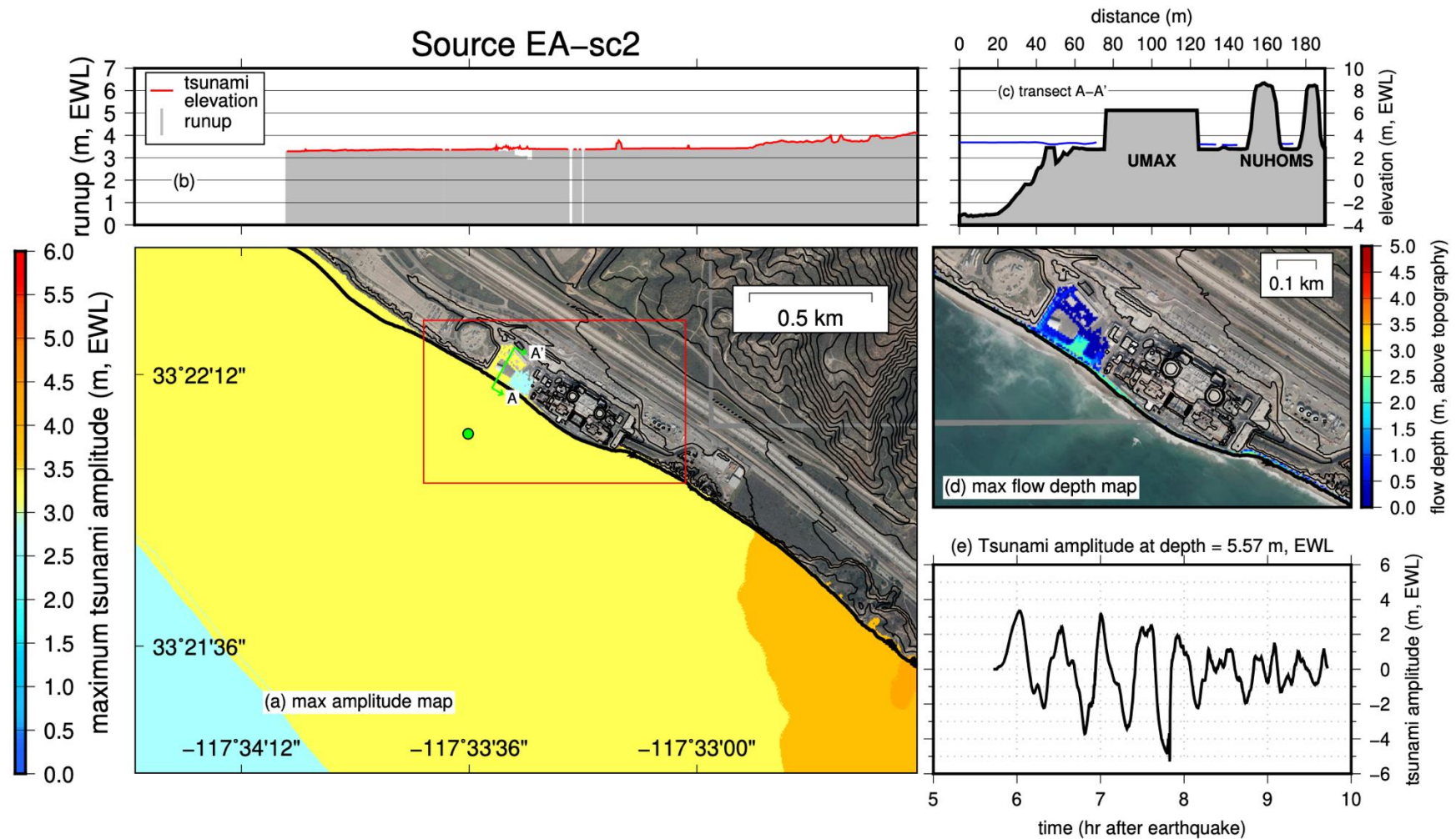


Figure 8-5. Numerical simulation results for the Eastern Aleutians seismic source EA-sc2. (a) Maximum tsunami amplitude across the domain of grid C. (b) Maximum runup and tsunami elevation distribution across the coastline in grid C. (c) Transect of maximum tsunami elevation across the SONGS site - see (a) for position of transect. (d) Maximum flow depth distribution across the SONGS site. (e) Time series of free surface elevation just offshore the SONGS site - time series extracted from the location shown with the green dot in (a).

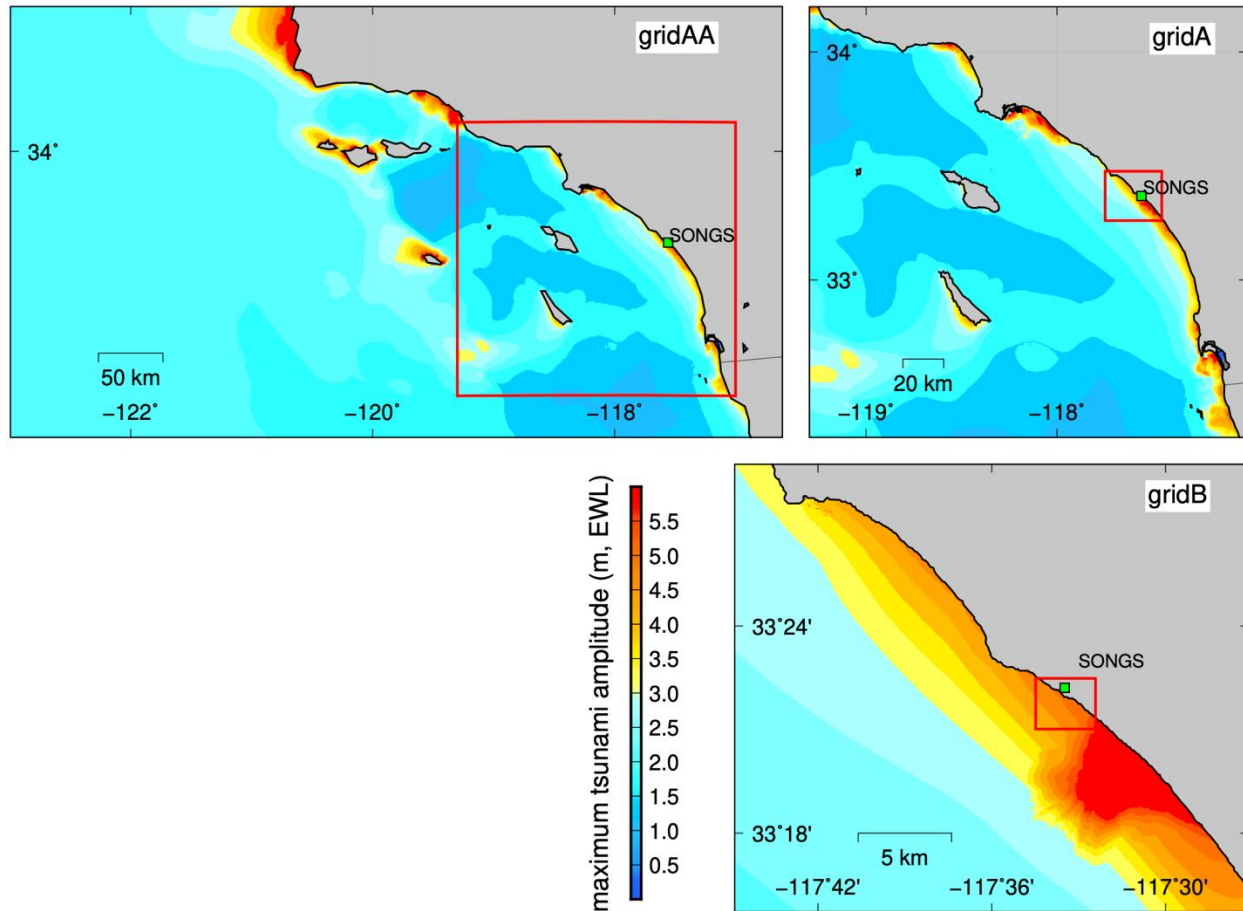


Figure 8-6. Maps showing the maximum tsunami amplitudes inside the domains of grids AA, A, and B during the numerical simulation of the Eastern Aleutian source EA-sc3 - see Table 7-3 for information on the sources.

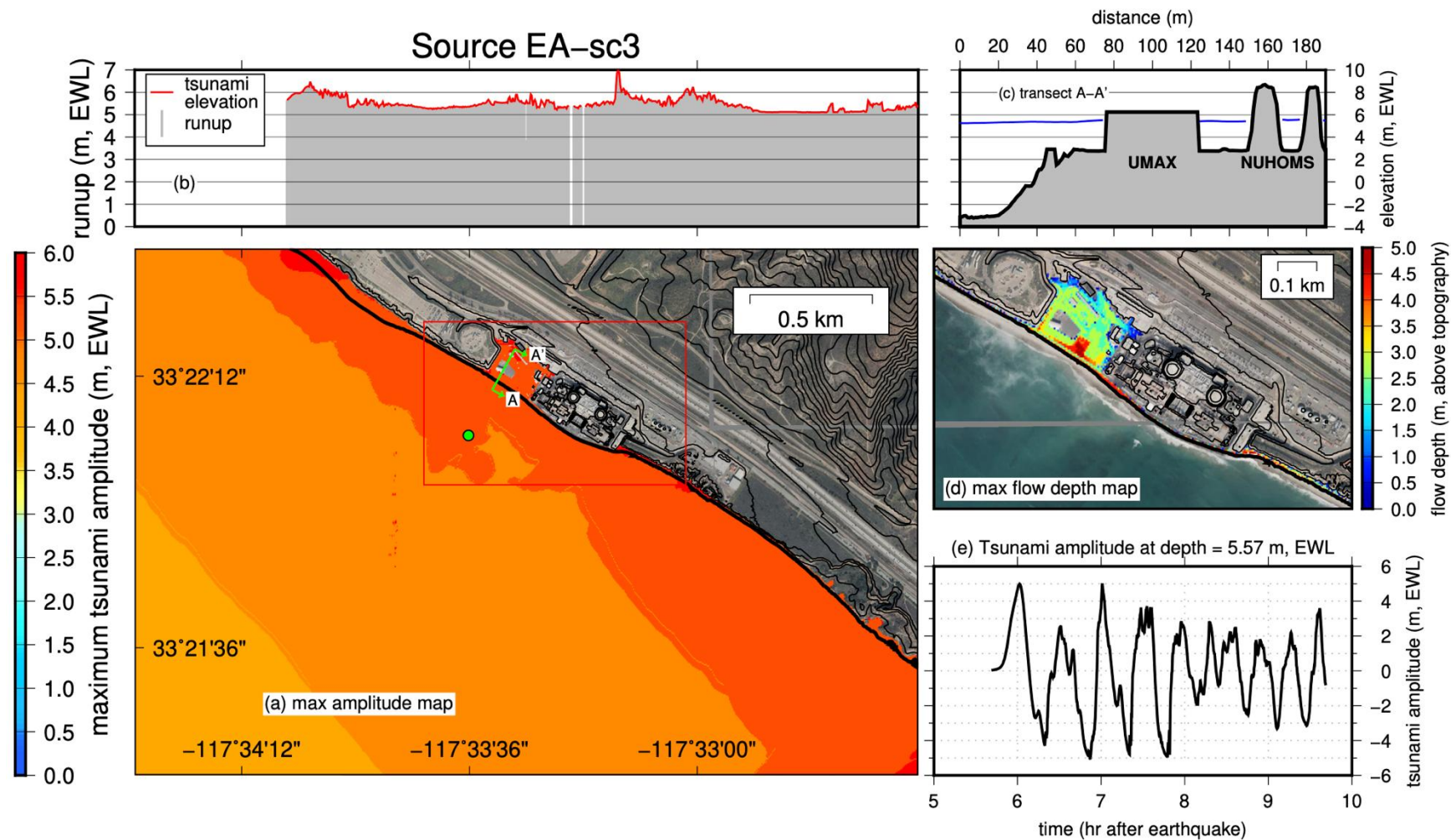


Figure 8-7. Numerical simulation results for the Eastern Aleutians seismic source EA-sc3. (a) Maximum tsunami amplitude across the domain of grid C. (b) Maximum runup and tsunami elevation distribution across the coastline in grid C. (c) Transect of maximum tsunami elevation across the SONGS site - see (a) for position of transect. (d) Maximum flow depth distribution across the SONGS site. (e) Time series of free surface elevation just offshore the SONGS site - time series extracted from the location shown with the green dot in (a).

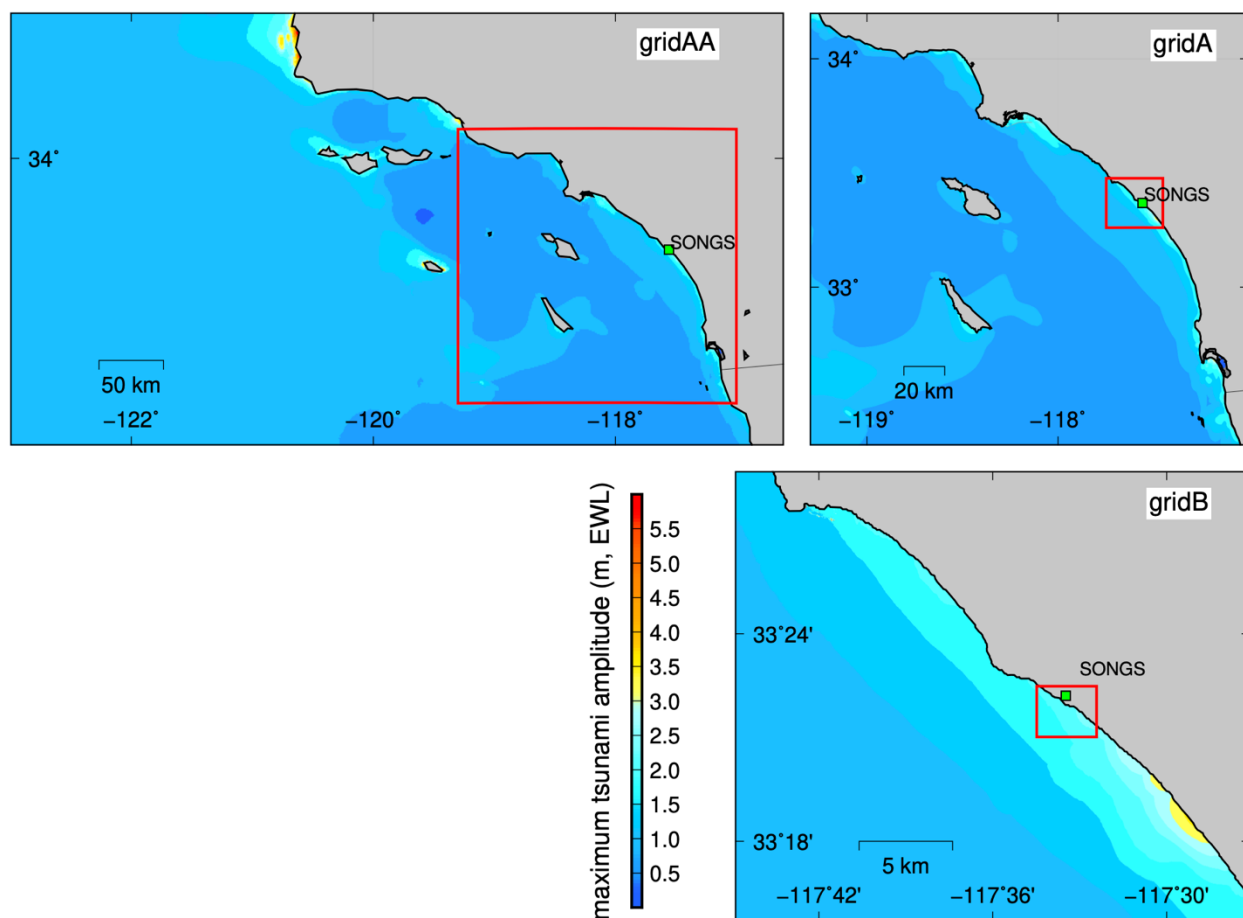


Figure 8-8. Maps showing the maximum tsunami amplitudes inside the domains of grids AA, A, and B during the numerical simulation of the Eastern Aleutian source EA-sc4 - see Table 7-3 for information on the sources.

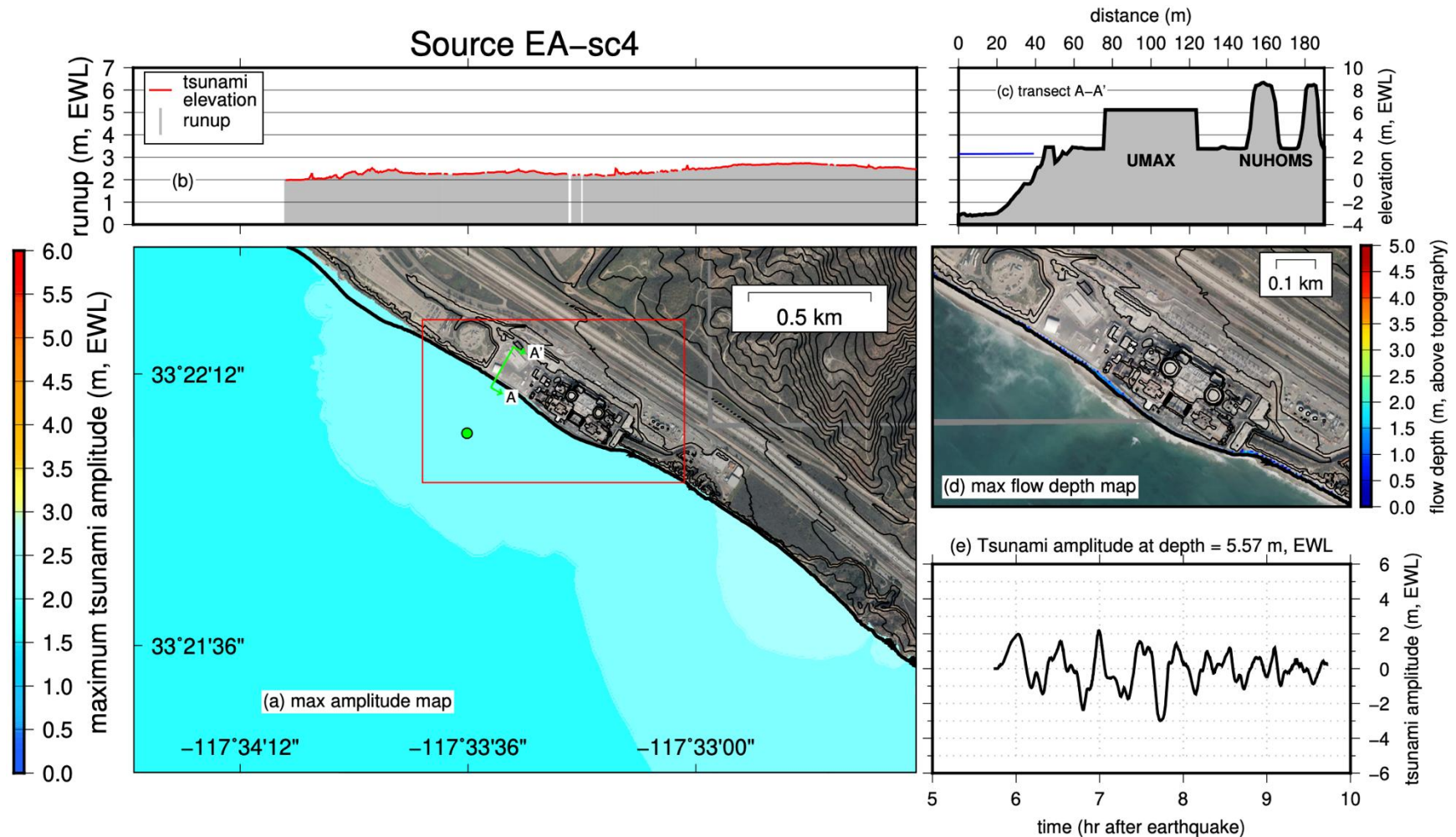


Figure 8-9. Numerical simulation results for the Eastern Aleutians seismic source EA-sc4. (a) Maximum tsunami amplitude across the domain of grid C. (b) Maximum runup and tsunami elevation distribution across the coastline in grid C. (c) Transect of maximum tsunami elevation across the SONGS site - see (a) for position of transect. (d) Maximum flow depth distribution across the SONGS site. (e) Time series of free surface elevation just offshore the SONGS site - time series extracted from the location shown with the green dot in (a).

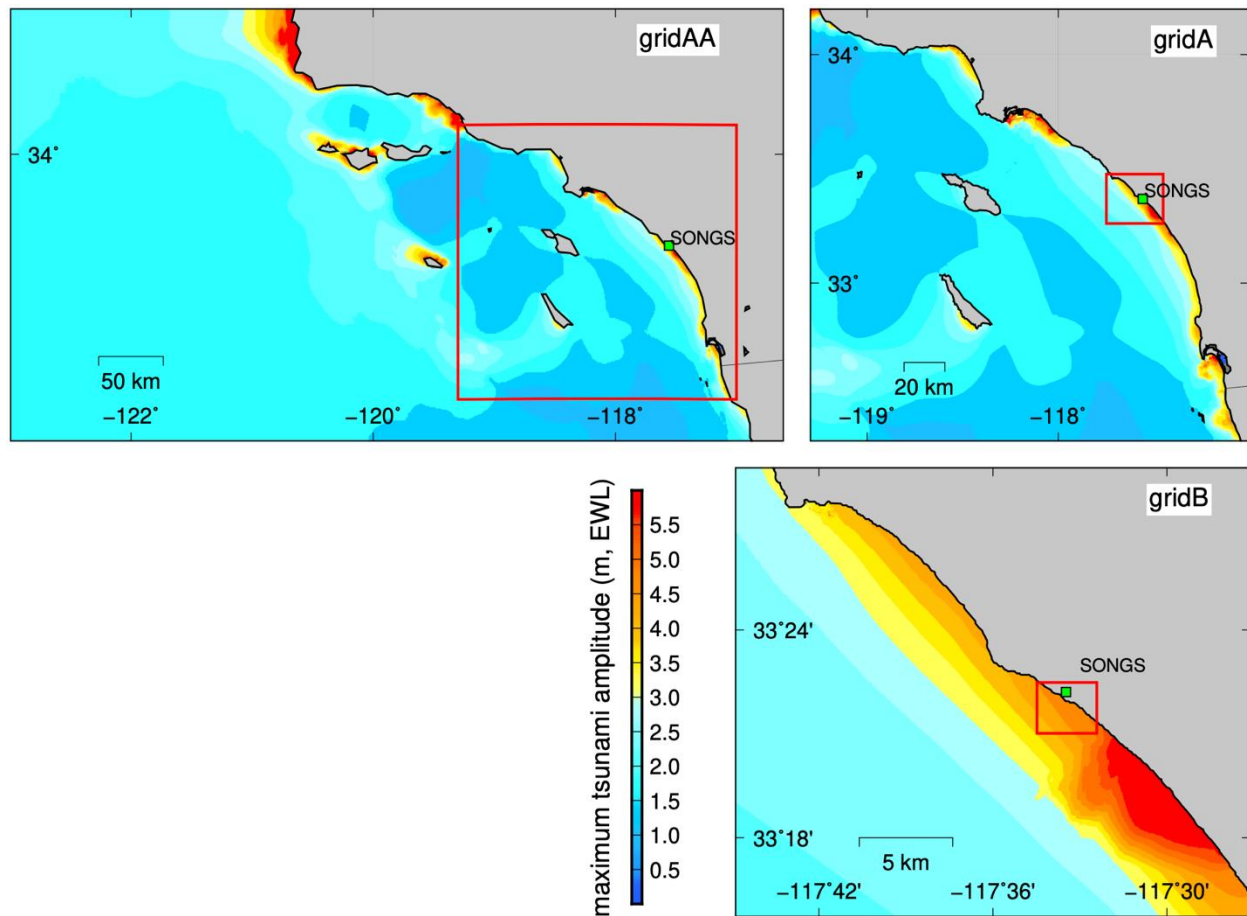


Figure 8-10. Maps showing the maximum tsunami amplitudes inside the domains of grids AA, A, and B during the numerical simulation of the Eastern Aleutian source EA-sc5 - see Table 7-3 for information on the sources.

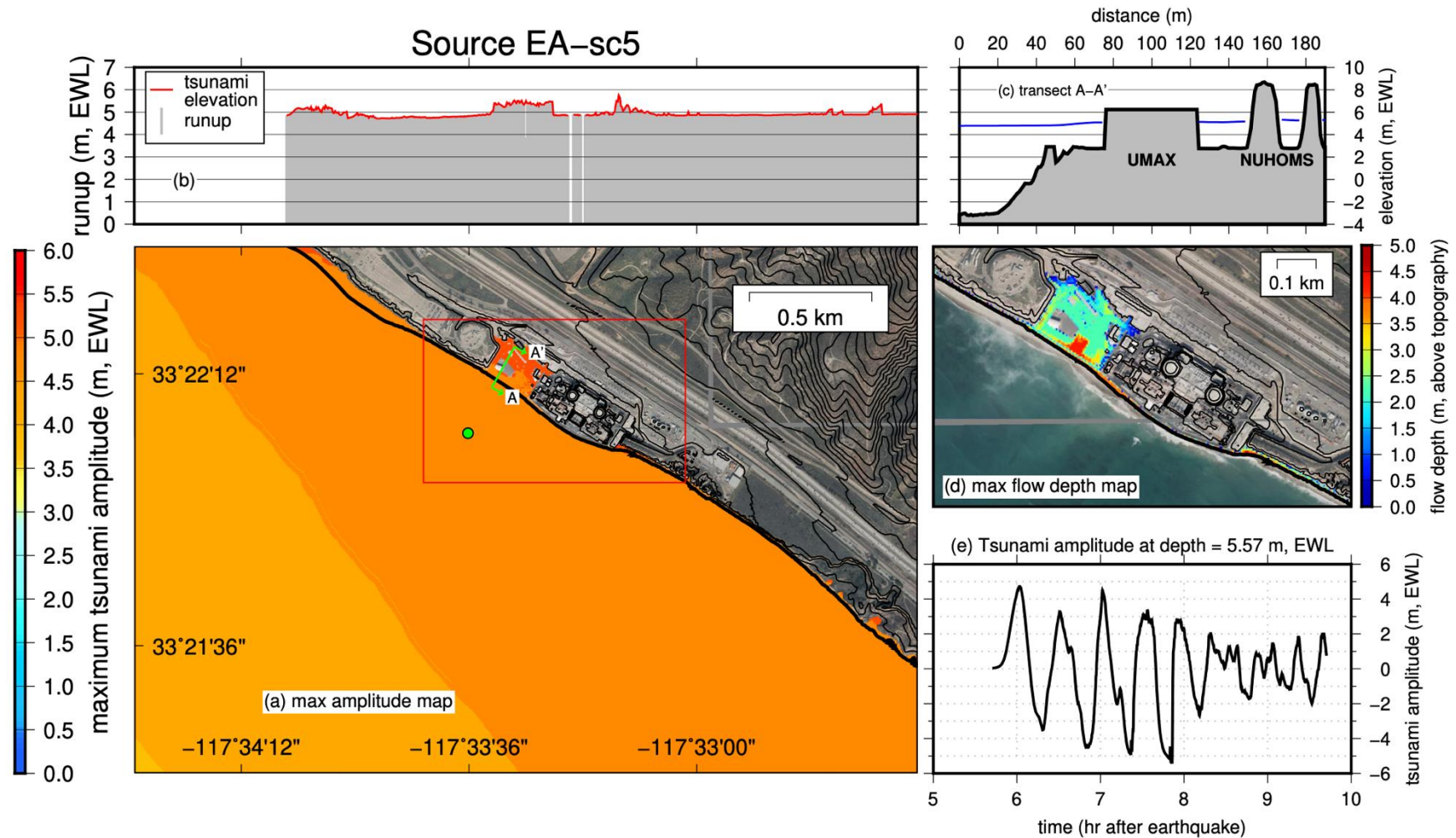


Figure 8-11. Numerical simulation results for the Eastern Aleutians seismic source EA-sc5. (a) Maximum tsunami amplitude across the domain of grid C. (b) Maximum runup and tsunami elevation distribution across the coastline in grid C. (c) Transect of maximum tsunami elevation across the SONGS site - see (a) for position of transect. (d) Maximum flow depth distribution across the SONGS site. (e) Time series of free surface elevation just offshore the SONGS site - time series extracted from the location shown with the green dot in (a).

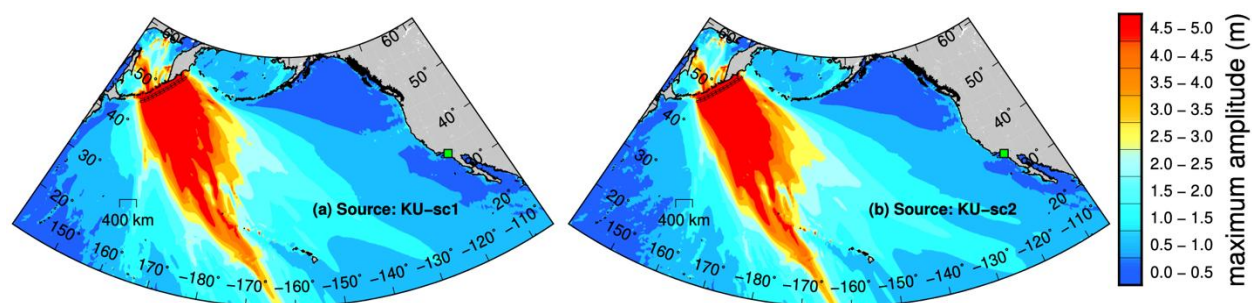


Figure 8-12. Maps showing the maximum tsunami amplitudes (in part of the spatial extent) of grid *P* from the numerical simulation of all two Kurils sources – see Table 7-3 for information on the sources.

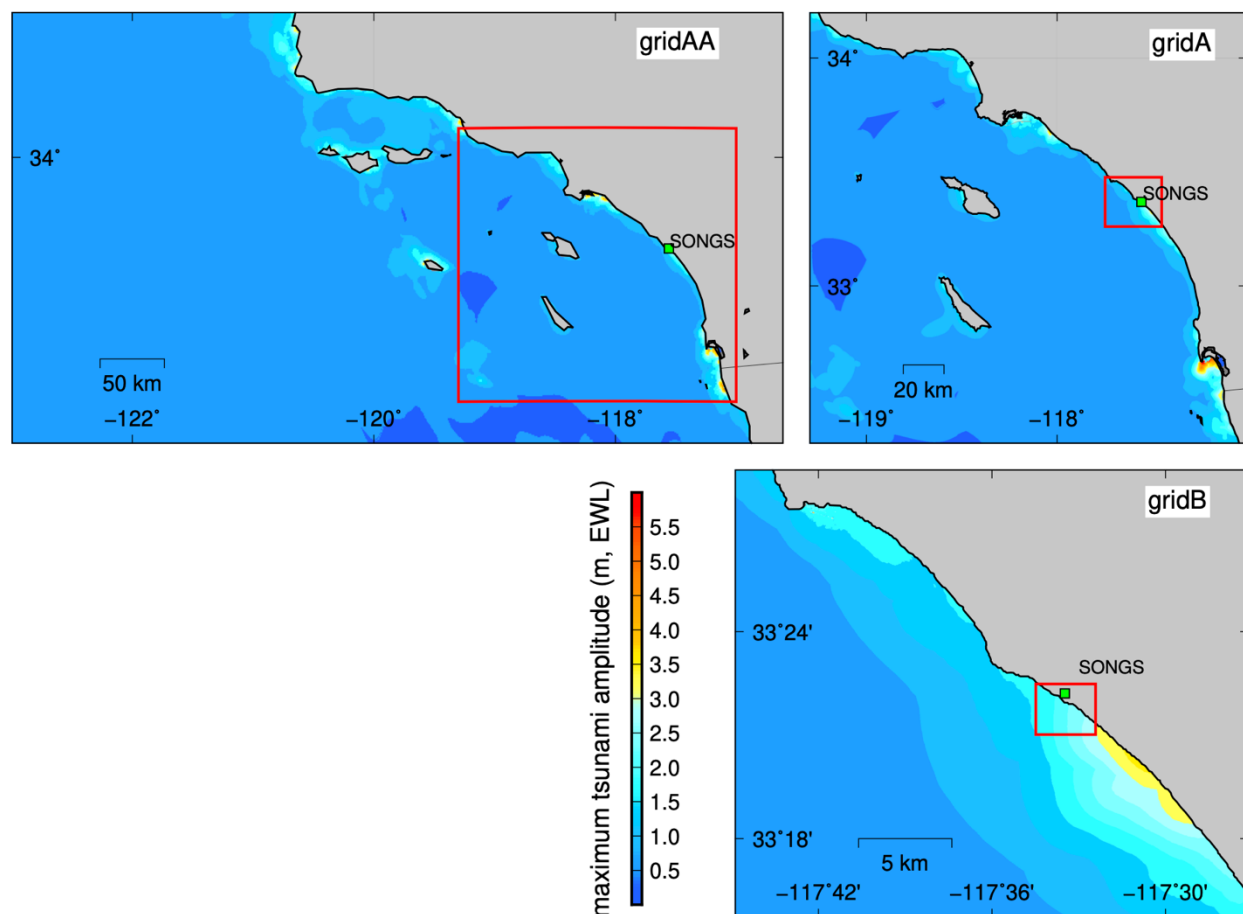


Figure 8-13. Maps showing the maximum tsunami amplitudes inside the domains of grids AA, A, and B during the numerical simulation of the Kurils source KU-sc1 - see Table 7-3 for information on the sources.

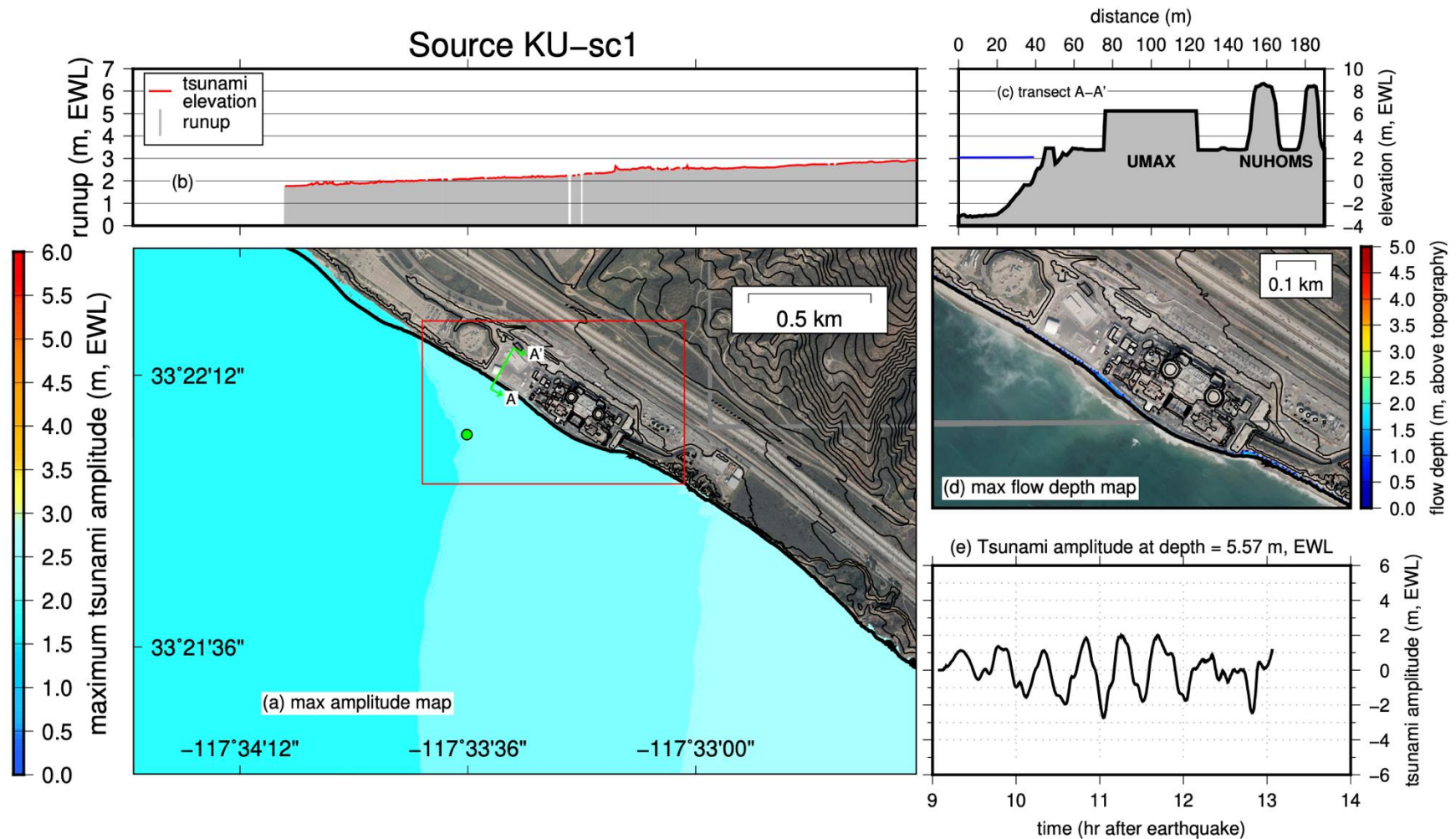


Figure 8-14. Numerical simulation results for the Kurils seismic source KU-sc1. (a) Maximum tsunami amplitude across the domain of grid C. (b) Maximum runup and tsunami elevation distribution across the coastline in grid C. (c) Transect of maximum tsunami elevation across the SONGS site - see (a) for position of transect. (d) Maximum flow depth distribution across the SONGS site. (e) Time series of free surface elevation just offshore the SONGS site - time series extracted from the location shown with the green dot in (a).

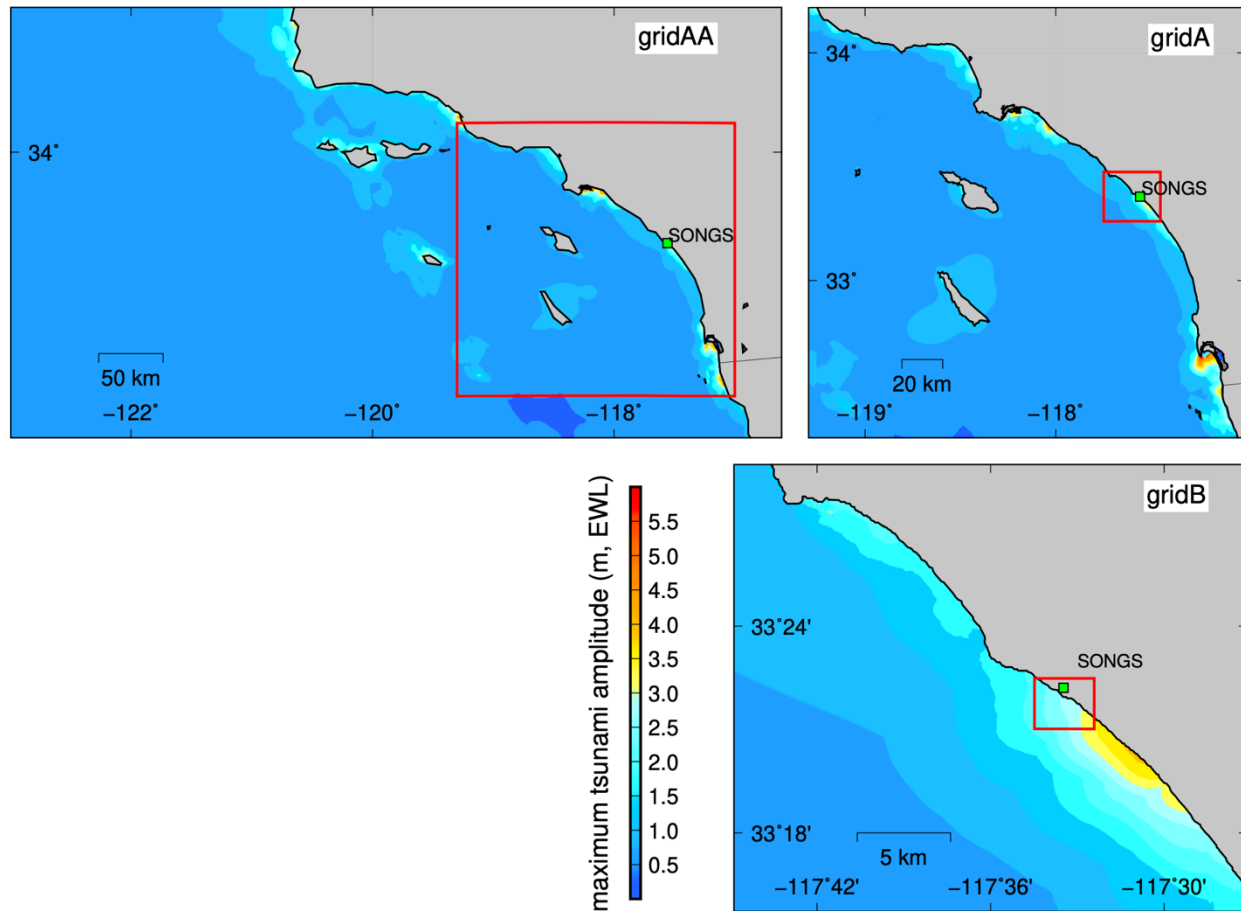


Figure 8-15. Maps showing the maximum tsunami amplitudes inside the domains of grids AA, A, and B during the numerical simulation of the Kurils source KU-sc2 - see Table 7-3 for information on the sources.

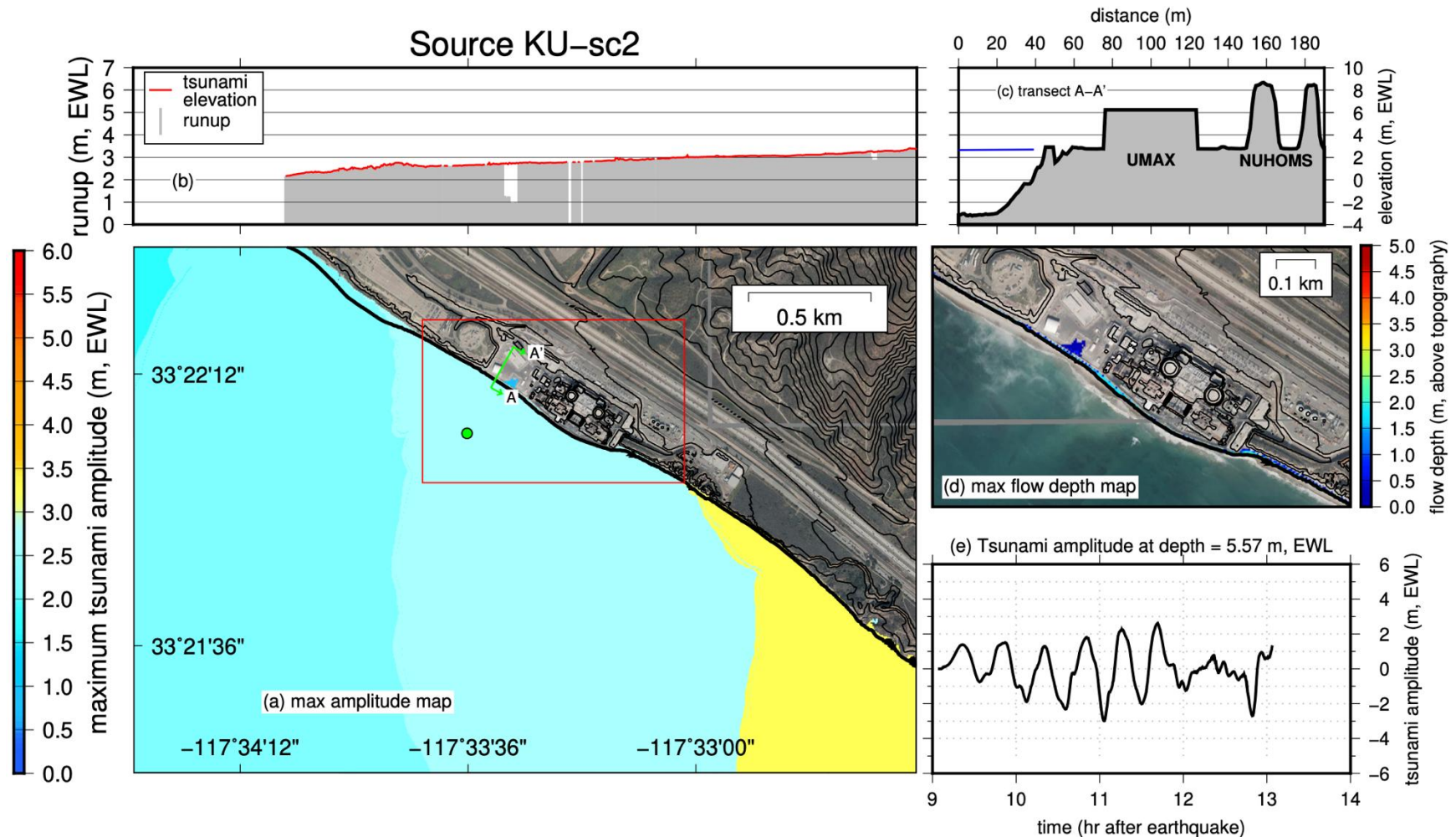


Figure 8-16. Numerical simulation results for the Kurils seismic source KU-sc2. (a) Maximum tsunami amplitude across the domain of grid C. (b) Maximum runup and tsunami elevation distribution across the coastline in grid C. (c) Transect of maximum tsunami elevation across the SONGS site - see (a) for position of transect. (d) Maximum flow depth distribution across the SONGS site. (e) Time series of free surface elevation just offshore the SONGS site - time series extracted from the location shown with the green dot in (a).

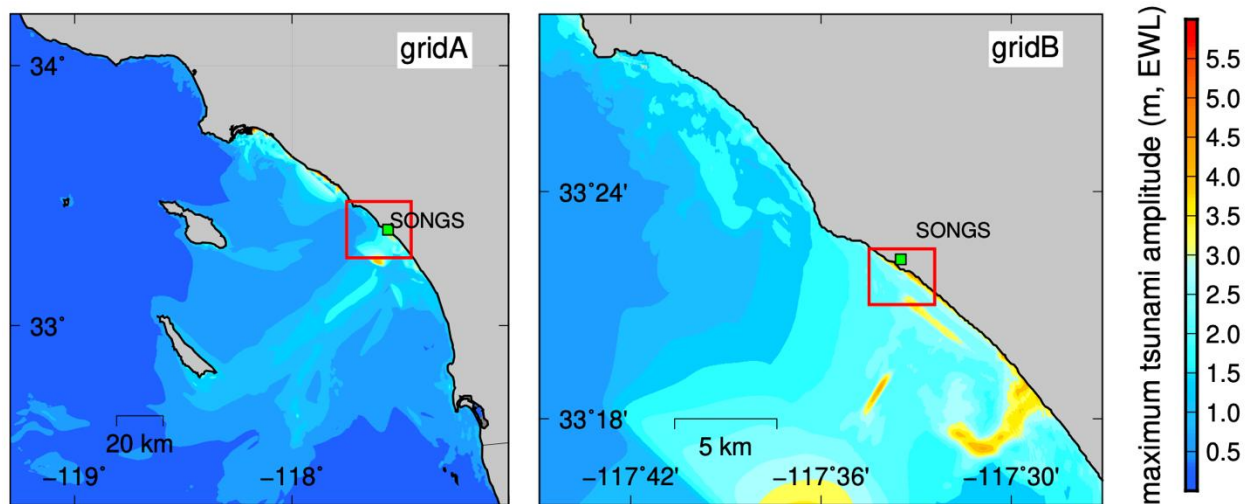


Figure 8-17. Maps showing the maximum tsunami amplitudes inside the domains of grids A and B during the numerical simulation of the near-field source Local-sc1 - see Table 7-5 for information on the sources.

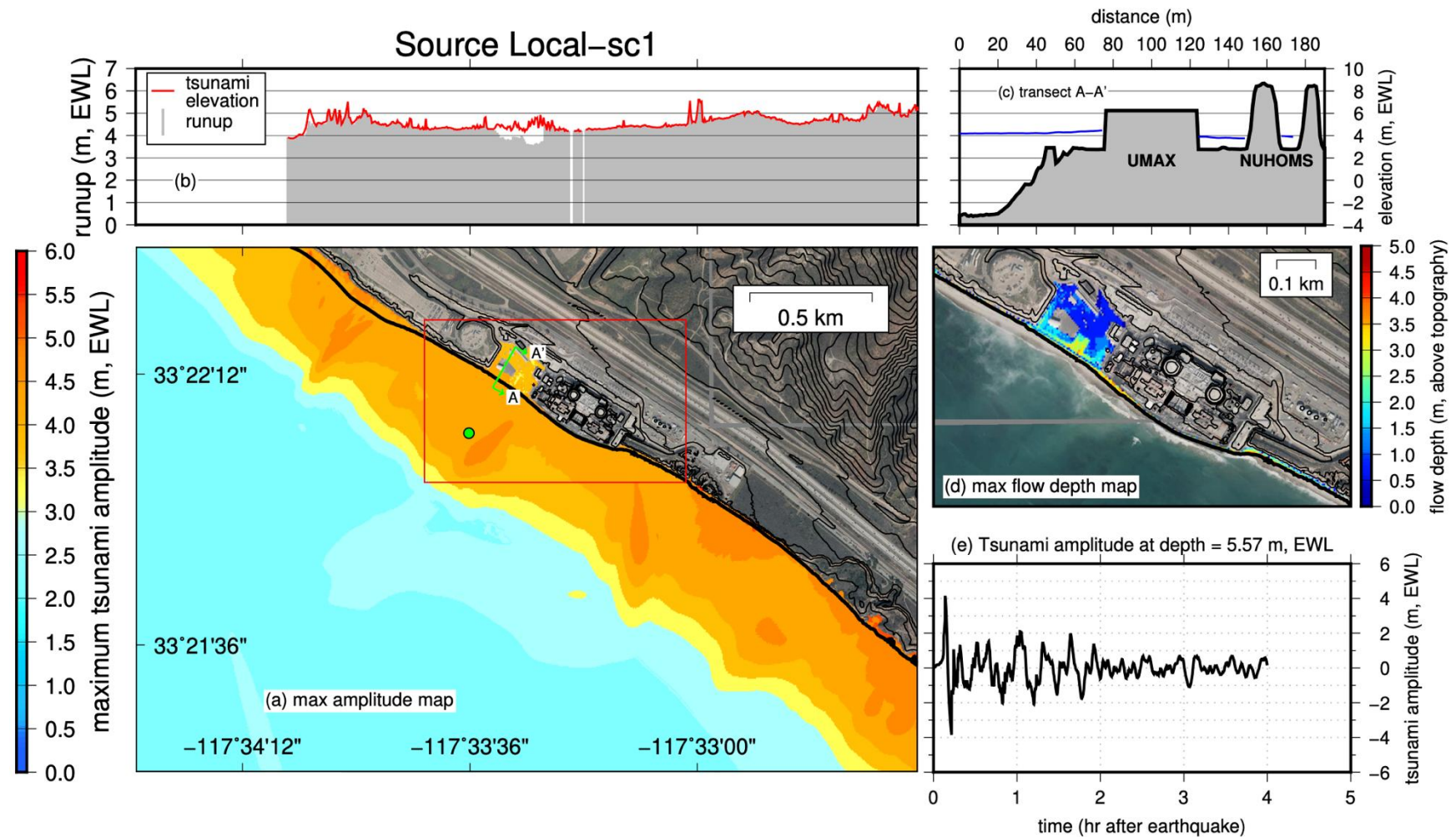


Figure 8-18. Numerical simulation results for the near-field seismic source Local-sc1. (a) Maximum tsunami amplitude across the domain of grid C. (b) Maximum runup and tsunami elevation distribution across the coastline in grid C. (c) Transect of maximum tsunami elevation across the SONGS site - see (a) for position of transect. (d) Maximum flow depth distribution across the SONGS site. (e) Time series of free surface elevation just offshore the SONGS site - time series extracted from the location shown with the green dot in (a).

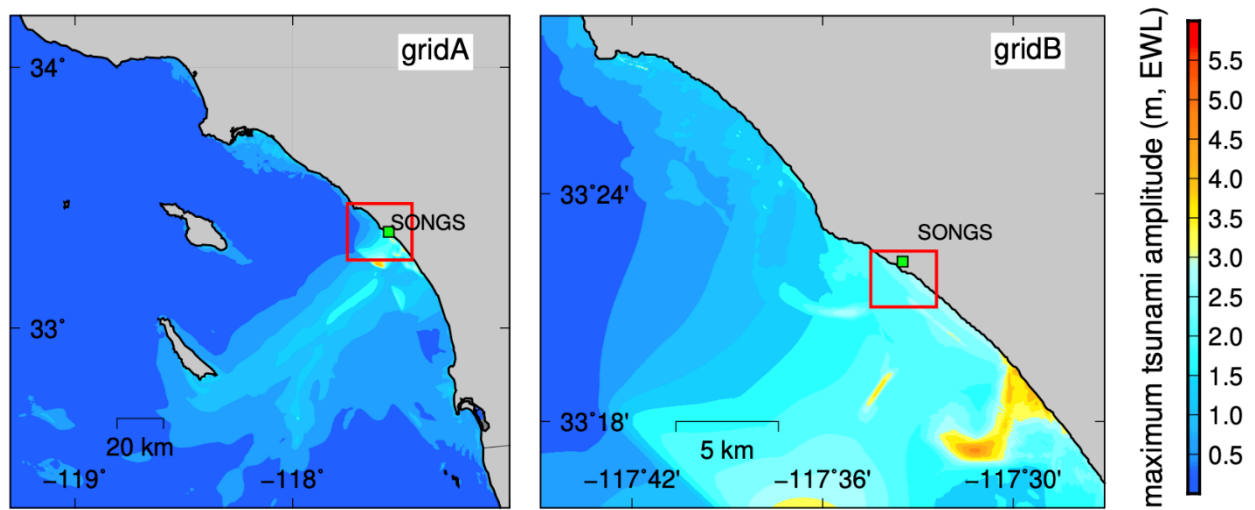


Figure 8-19. Maps showing the maximum tsunami amplitudes inside the domains of grids A and B during the numerical simulation of the near-field source Local-sc2 - see Table 7-5 for information on the sources.

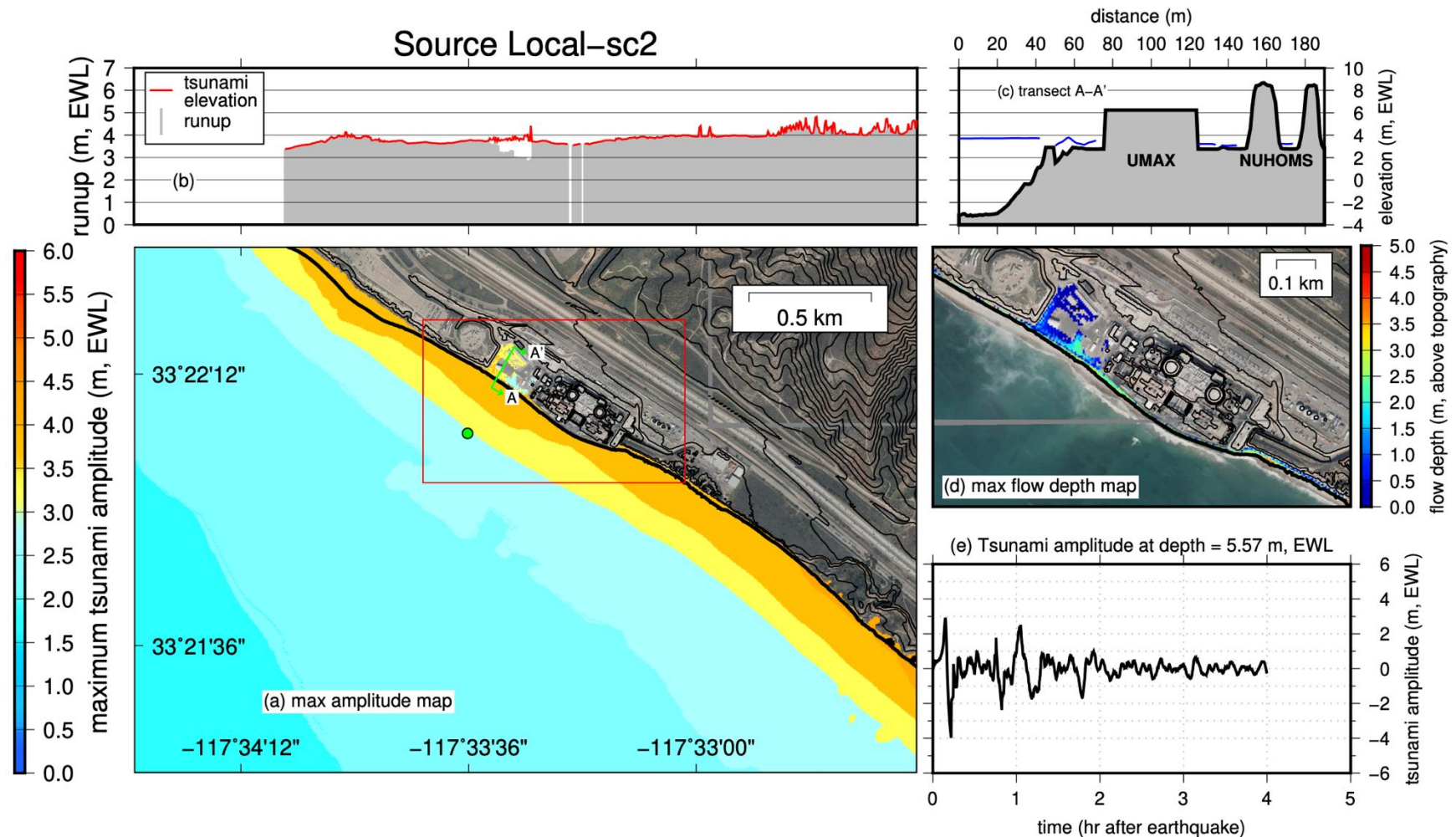


Figure 8-20. Numerical simulation results for the near-field seismic source Local-sc2. (a) Maximum tsunami amplitude across the domain of grid C. (b) Maximum runup and tsunami elevation distribution across the coastline in grid C. (c) Transect of maximum tsunami elevation across the SONGS site - see (a) for position of transect. (d) Maximum flow depth distribution across the SONGS site. (e) Time series of free surface elevation just offshore the SONGS site - time series extracted from the location shown with the green dot in (a).

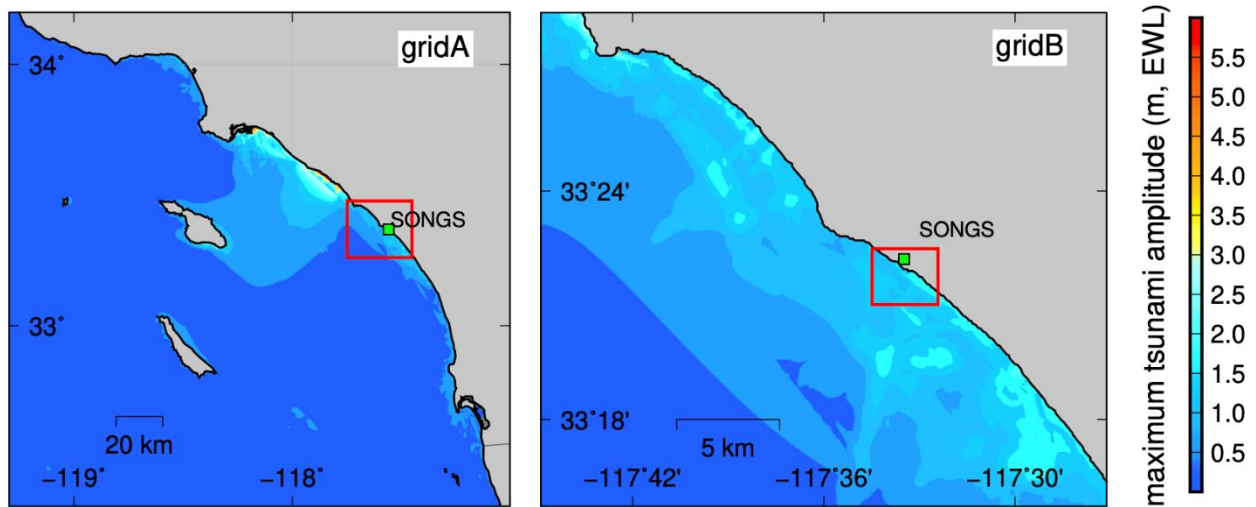


Figure 8-21. Maps showing the maximum tsunami amplitudes inside the domains of grids A and B during the numerical simulation of the near-field source Local-sc3 - see Table 7-5 for information on the sources.

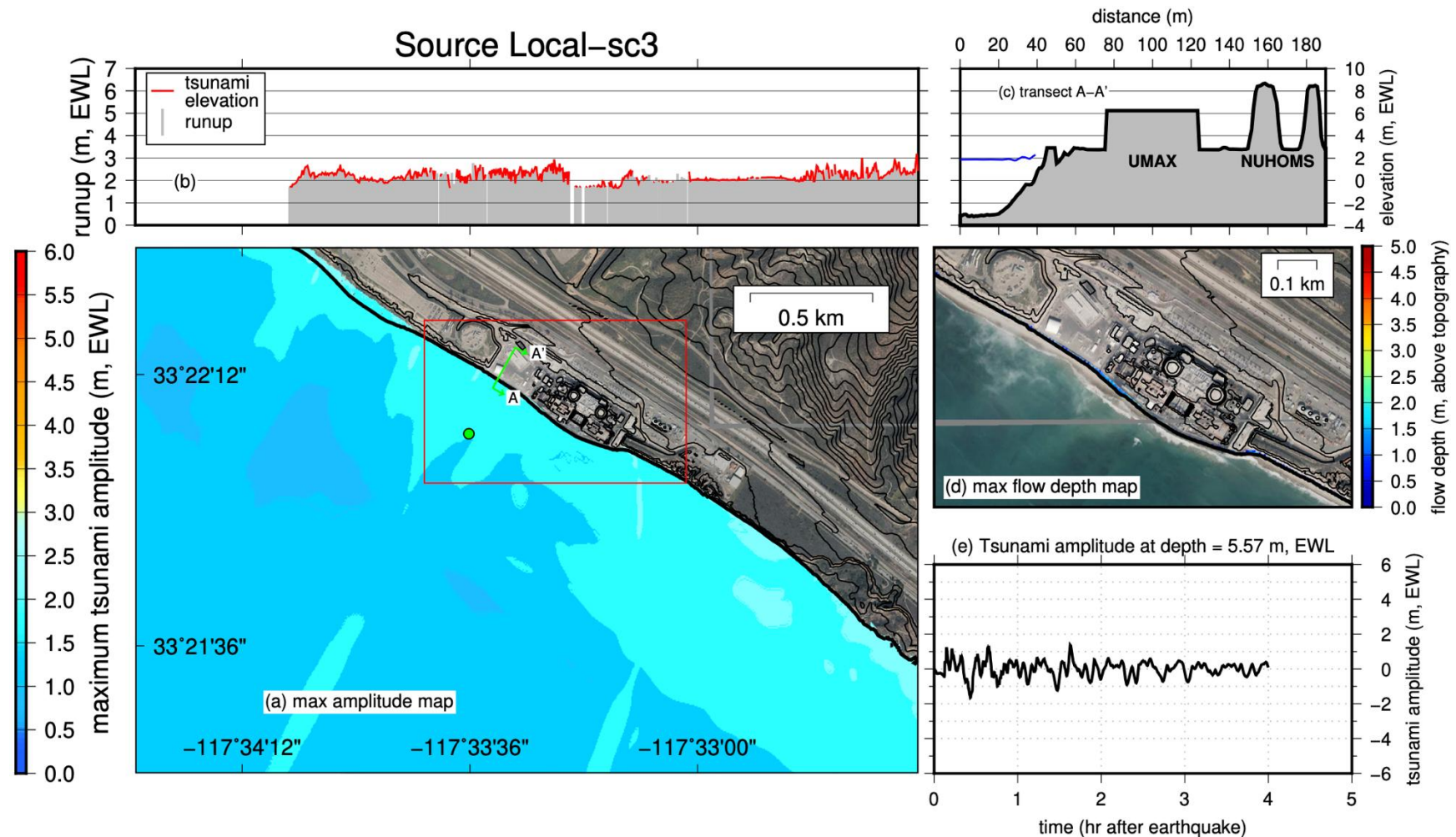


Figure 8-22. Numerical simulation results for the near-field seismic source Local-sc3. (a) Maximum tsunami amplitude across the domain of grid C. (b) Maximum runup and tsunami elevation distribution across the coastline in grid C. (c) Transect of maximum tsunami elevation across the SONGS site - see (a) for position of transect. (d) Maximum flow depth distribution across the SONGS site. (e) Time series of free surface elevation just offshore the SONGS site - time series extracted from the location shown with the green dot in (a).

9.0 RESULTS SUMMARY

The numerical results are summarized in Table 9-1. The largest tsunami amplitudes offshore, and the largest tsunami impact around the NUHOMS ISFSI from the sources studied resulted from the simulation of the Eastern Aleutian source EA-sc3, which is similar to the Eastern Aleutian source modeled by Shi et al. (2016). Source EA-sc3 produces maximum tsunami elevation and maximum flow depth values of ~9.1 m (MLLW) and ~2.8 m (above ground), respectively, around the NUHOMS ISFSI, which is ~3.7 m above ground.

From the three worst-case local seismic sources considered, the simulation of source Local-sc1 produces the highest offshore wave amplitudes (7.3 m, MLLW) and tsunami impact around the NUHOMS ISFSI, with maximum tsunami elevation of ~7.2 m (MLLW) and maximum flow depth of ~1.2 m (above ground).

Table 9-1. Table of maximum and minimum amplitudes occurring at the node offshore the SONGS site (with coordinates $-117.56004^{\circ}\text{W}$, 33.36782°N), and the maximum tsunami elevation (TE) and flow depth (FD) values inside the NUHOMS polygon for all simulated tsunami events. Maximum (absolute) values are provided in boldface.

| Source Name | Wave Amplitudes Offshore at 5.6 m (EWL) Depth | | | Values Inside NUHOMS Polygon | | |
|-------------|---|--------------|---------------|------------------------------|------------------|------------|
| | Min (m, EWL) | Max (m, EWL) | Max (m, MLLW) | Max TE (m, EWL) | Max TE (m, MLLW) | Max FD (m) |
| EA-sc1 | -2.7 | 1.9 | 5.1 | N/A | N/A | N/A |
| EA-sc2 | -5.3 | 3.3 | 6.5 | 3.4 | 6.5 | 0.6 |
| EA-sc3 | -5.1 | 5.0 | 8.2 | 5.9 | 9.1 | 2.8 |
| EA-sc4 | -3.0 | 2.2 | 5.4 | N/A | N/A | N/A |
| EA-sc5 | -5.4 | 4.7 | 7.9 | 5.5 | 8.7 | 2.7 |
| KU-sc1 | -2.7 | 2.0 | 5.2 | N/A | N/A | N/A |
| KU-sc2 | -3.0 | 2.6 | 5.8 | N/A | N/A | N/A |
| Local-sc1 | -3.9 | 4.2 | 7.3 | 4.0 | 7.2 | 1.2 |
| Local-sc2 | -4.0 | 2.9 | 6.1 | 3.4 | 6.6 | 0.4 |
| Local-sc3 | -1.7 | 1.4 | 4.6 | N/A | N/A | N/A |

We note that we cannot directly compare our results with Shi et al. (2016), because it is unclear if they performed inundation computations. The maximum value given in their table (Table 5) is 6.66 m (MLLW) for the Eastern Aleutians far-field seismic source.

10.0 ABBREVIATIONS

| | |
|--------|--|
| CE | Coastal Environments, Inc. |
| CRM | NOAA/NGDC Coastal Relief Model |
| DEM | Digital Elevation Model |
| EWL | Extreme Water Level (extreme tidal, surge and wave setup level+ sea level rise projection) |
| GEBCO | General Bathymetric Chart of the Oceans |
| ISFSI | Independent Spent Fuel Storage Installation |
| MHW | Mean High Water datum |
| MLLW | Mean Low Lower Water datum |
| MSL | Mean Sea Level datum |
| MSLR | Mean Sea Level Rise |
| NCEI | National Centers for Environmental Information of NOAA |
| NCTR | NOAA Center for Tsunami Research |
| NGDC | National Geophysical Data Center of NOAA |
| NIRC | Newport-Inglewood-Rose Canyon |
| NOAA | National Oceanographic and Atmospheric Administration |
| NRC | Nuclear Regulatory Commission |
| NUHOMS | Eastern ISFSI at SONGS |
| OPC | Ocean Protection Council |
| PMEL | Pacific Marine Environmental Laboratory of NOAA |
| PTHA | Probabilistic Tsunami Hazard Assessment |
| SONGS | San Onofre Nuclear Generating Station |

11.0 REFERENCES

- Aki, K. and P.G. Richards, 1980. *Quantitative seismology: Theory and methods* (volume 842). Freeman, San Francisco, CA.
- Ambraseys, N. and C. Synolakis, 2010. Tsunami catalogs for the eastern Mediterranean, revisited. *Journal of Earthquake Engineering*, 14(3), pp. 309-330.
- Arcas, D., 2015. A tsunami forecast model for Santa Monica, California. *NOAA OAR Special Report Tsunami Forecast Series PMEL-140*, 22. doi: 10.7289/V5D50JX8.
URL <https://doi.org/10.7289/V5D50JX8>.
- Atwater, B.F., 1987. Evidence for great Holocene earthquakes along the outer coast of Washington state. *Science*, 236 (4804), pp. 942-944.
- Atwater, B.F., S. Musumi-Rokkaku, K. Satake, Y. Tsuji, K. Ueda, and D.K. Yamaguchi, 2016. *The orphan tsunami of 1700: Japanese clues to a parent earthquake in North America*. University of Washington Press.
- Barberopoulou, A., J.C. Borrero, B. Uslu, N. Kalligeris, J.D. Goltz, R.I. Wilson, and C.E. Synolakis, 2009. New maps of California to improve tsunami preparedness. *Eos, Transactions American Geophysical Union*, 90(16), pp. 137–138.
URL http://www.tsunamiresearchcenter.com/wp-content/uploads/2010/10/2009EOS_TsunamiMaps.pdf.
- Barberopoulou, A., M.R. Legg, B. Uslu, and C.E. Synolakis, 2011. Reassessing the tsunami risk in major ports and harbors of California: San Diego. *Natural Hazards*, 58(1), pp. 479-496.
- Beauducel, F., 2011. *Okada: Surface deformation due to a finite rectangular source*. MATLAB Central File Exchange. Last updated on 2011-03-06.
URL <https://www.mathworks.com/matlabcentral/fileexchange/25982-okada-surface-deformation-due-to-a-finite-rectangular-source>.
- Bird, P., 2003. An updated digital model of plate boundaries. *Geochemistry, Geophysics, Geosystems*, 4(3).
- Borrero, J.C., 2002. *Tsunami hazards in southern California*. PhD thesis.
- Borrero, J.C., J.F. Dolan, and C.E. Synolakis, 2001. Tsunamis within the eastern Santa Barbara channel. *Geophysical Research Letters*, 28(4), pp. 643-646.
- Borrero, J.C., M.R. Legg, and C.E. Synolakis, 2004. Tsunami sources in the southern California Bight. *Geophysical Research Letters*, 31(13), L13211.

- Brothers, D.S., K.L. Maier, J.W. Kluesner, J.E. Conrad, and J.D. Chaytor, 2019. The Santa Cruz basin submarine landslide complex, southern California: Repeated failure of uplifted basin sediment. *Journal of Sedimentary Research*, 17 (1), pp. 117-134.
- Clarke, S.H., H.G. Greene, M.P. Kennedy, and J.G. Vedder, 1987. Geologic map of the inner-southern California continental margin. *California Continental Margin Geologic Map Series*, Area 1 of 7, sheet 1 of 4, scale 1:250,000, California Division of Mines and Geology.
- Derakhti, M., R.A. Dalrymple, E.A. Okal, and C.E. Synolakis, 2019. Temporal and topographic source effects on tsunami generation. *Journal of Geophysical Research: Oceans*, 124(7), pages 5270-5288.
- Eisner, R.K., J.C. Borrero, and C.E. Synolakis, 2001. *Inundation maps for the State of California*. NOAA/Pacific Marine Environmental Laboratory.
http://www.tsunamiresearchcenter.com/wp-content/uploads/2010/11/2001ITS_CalinundationMaps.pdf.
- Fletcher, J.M., O.J. Teran, T.K. Rockwell, M.E. Oskin, K.W. Hudnut, K.J. Mueller, R.M. Spelz, S.O. Akciz, E. Masana, G. Faneros, et al., 2014. Assembly of a large earthquake from a complex fault system: Surface rupture kinematics of the 4 April 2010 El Mayor-Cucapah (Mexico) mw 7.2 earthquake. *Geosphere*, 10(4), pages 797-827.
- GEBCO, 2021. Gebco 2021 grid. URL <https://doi.org/10.5285/c6612cbe-50b3-0cff-e053-6c86abc09f8f>.
- Geopentech, 2010. *Probabilistic tsunami hazard analysis report, draft*. Prepared for Southern California Edison, May 16.
- Grant, L.B., L.J. Ballenger, and E.E. Runnerstrom, 2002. Coastal uplift of the San Joaquin hills, southern Los Angeles basin, California, by a large earthquake since AD 1635. *Bulletin of the Seismological Society of America*, 92(2), pp. 590-599.
- Hamling, I.J., S. Hreinsdóttir, K. Clark, J. Elliott, C. Liang, E. Fielding, N. Litchfield, P. Villamor, L. Wallace, T.J. Wright, et al., 2017. Complex multifault rupture during the 2016 m w 7.8 Kaikoura earthquake, New Zealand. *Science*, 356(6334).
- Hanks, T.C. and H. Kanamori, 1979. A moment magnitude scale. *Journal of Geophysical Research: Solid Earth*, 84(B5), pages 2348-2350.
- Hauksson, E., W. Yang, and P.M. Shearer, 2012. Waveform relocated earthquake catalog for southern California (1981 to June 2011). *Bulletin of the Seismological Society of America*, 102(5), pages 2239-2244.
- Houston, J.R., 1980. *Type 19 flood insurance study: Tsunami predictions for southern California* (volume 80). U.S. Army Corps of Engineers Waterways Experiment Station.

- Houston, J.R. and A.W. Garcia, 1974. *Type 16 flood insurance study: Tsunami predictions for Pacific coastal communities* (volume 74). U.S. Army Corps of Engineers Waterways Experiment Station.
- Janenko, N.N., 1971. *The method of fractional steps* (volume 160). Springer.
- Johnson, J.M., K. Satake, S.R. Holdahl, and J. Sauber, 1996. The 1964 Prince William sound earthquake: Joint inversion of tsunami and geodetic data. *Journal of Geophysical Research: Solid Earth*, 101(B1), pages 523-532.
- Kirby, S., E.L. Geist, W.H.K. Lee, D. Scholl, and R. Blakely, 2006. *Tsunami source characterization for western Pacific subduction zones: A preliminary report*. Tsunami sources workshop.
- Kirby, S., D. Scholl, R.E. von Huene, and R. Wells, 2013. *Alaska earthquake source for the SAFRR tsunami scenario: Chapter B in the SAFRR (Science Application for Risk Reduction) tsunami scenario*. Technical report, US Geological Survey.
- Legg, M.R., 1985. *Geologic structure and tectonics of the inner continental borderland offshore Northern Baja California, Mexico (Wrench Faults, San Diego, Ensenada)*. PhD thesis, University of California, Santa Barbara.
- Legg, M.R., V. Wong-Ortega, and F. Suarez-Vidal, 1991. Geologic structure and tectonics of the inner continental borderland of northern Baja California. In Dauphin, P., and G. Ness, editors, *The Gulf and Peninsular Province of the Californias. American Association of Petroleum Geologists Memoir #47*, pages 145-177.
- Legg, M.R. and M.J. Kamerling, 2003. Large-scale basement-involved landslides, California Continental Borderland. In *Landslide Tsunamis: Recent Findings and Research Directions*, pages 2033–2051. Springer.
- Legg, M.R., J.C. Borrero, and C.E. Synolakis, 2004. Tsunami hazards associated with the Catalina fault in southern California. *Earthquake Spectra*, 20(3), pages 917-950.
- Legg, M., C. Sorlien, C. Nicholson, M. Kamerling, and G. Kuhn, 2018. Potential for large complex multi-fault earthquakes offshore southern California. In *Proceedings of the 11th National Conference in Earthquake Engineering, Earthquake Engineering Research Institute, Los Angeles, CA*.
- Maloney, J.M., N. Driscoll, G. Kent, S. Duke, T. Freeman, J. Bormann, R. Anderson, and H. Ferriz, 2016. Segmentation and step-overs along strike-slip fault systems in the inner California borderlands: Implications for fault architecture and basin formation. *Applied Geology in California, Environmental Engineering Geologists*, 26, pages 655-677.
- McCarthy, R.J., E.N. Bernard, and M.R. Legg, 1993. The Cape Mendocino earthquake: A local tsunami wakeup call? In *Coastal Zone '93*, pages 2812-2828. ASCE.

- McCulloch, D.S., 1985. Evaluating tsunami potential. *USGS Prof. Paper*, 1360, pages 374-413.
- NOAA/NGDC, 2003. *U.S. Coastal Relief Model* (volume 6, southern California). NOAA/National Centers for Environmental Information. doi: 10.7289/V500001J.
<https://doi.org/10.7289/V500001J>.
- NOAA/NGDC, 2010. *One-third arc-second NAVD 88 coastal digital elevation model, San Diego, CA*. NOAA/National Centers for Environmental Information.
<https://www.ncei.noaa.gov/metadata/geoportal/rest/metadata/item/gov.noaa.ngdc.mgg.dem:3542/html#>.
- Okada, Y., 1985. Surface deformation due to shear and tensile faults in a half-space. *Bulletin of the Seismological Society of America*, 75(4), pages 1135-1154.
- Ocean Protection Council, 2018. State of California sea level rise guidance, 2018 update. *California Natural Resources Agency Ocean Protection Council*. 84 pages.
- Percival, D.B., D. Arcas, D.W. Denbo, M.C. Eble, E. Gica, H.O. Mofjeld, M.C. Spillane, L. Tang, and V.V. Titov, 2009. Extracting tsunami source parameters via inversion of dart buoy data. NOAA technical memorandum. *OAR PMEL-144*, p. 22.
- Rivero, C. and J.H. Shaw, 2011. *Active Folding and Blind Thrust Faulting Induced by Basin Inversion Processes, Inner California Borderlands*.
- Rivero, C., J.H. Shaw, and K. Mueller, 2000. Oceanside and Thirty-Mile Bank blind thrusts: Implications for earthquake hazards in coastal southern California. *Geology*, 28(10), pages 891-894.
- Satake, K., K. Shimazaki, Y. Tsuji, and K. Ueda, 1996. Time and size of a giant earthquake in Cascadia inferred from Japanese tsunami records of January 1700. *Nature*, 379(6562), pages 246-249.
- Shi, F., J.T. Kirby, and L. Young, 2016. *SONGS Calculations for Probable Maximum Tsunami*. Technical report, CH2M Hill, Calculation No. 458144-CALC-004.
- Smith, W.H.F. and D.T. Sandwell, 1994. Bathymetric prediction from dense satellite altimetry and sparse shipboard bathymetry. *Journal of Geophysical Research: Solid Earth*, 99(B11), pages 21803-21824.
- Soloviev, S.L., 1970. Recurrence of tsunamis in the pacific. *Tsunamis in the Pacific Ocean*.
- Sorlien, C.C., J. T. Bennett, M.-H. Cormier, B. A. Campbell, C. Nicholson, and R. L. Bauer, 2016. Late-Miocene-Quaternary fault evolution and interaction in the southern California Inner Continental Borderland. *Geosphere*, 11, pages 1111-1132.

- Synolakis, C.E., D. McCarthy, V.V. Titov, and J. Borrero, 1998. Evaluating the tsunami risk in California. In *California and the World Ocean '97: Ocean Resources, An Agenda for the Future*, pages 1225-1236. ASCE.
- Synolakis, C.E., J.-P. Bardet, J.C. Borrero, H.L. Davies, E.A. Okal, E.A. Silver, S. Sweet, and D.R. Tappin, 2002a. The slump origin of the 1998 Papua New Guinea tsunami. *Proceedings of the Royal Society of London, Series A: Mathematical, Physical and Engineering Sciences*, 458(2020), pages 763-789.
- Synolakis, C.E., J. Borrero, and R. Eisner, 2002b. Developing inundation maps for southern California. In *Solutions to Coastal Disasters '02*, pages 848-862.
- Synolakis, C.E., 2003. Tsunami and seiche. *Earthquake Engineering Handbook*, 9:1-9.
- Synolakis, C.E. and E.N. Bernard, 2006. Tsunami science before and beyond Boxing Day 2004. *Philosophical Transactions of the Royal Society A: Mathematical, Physical and Engineering Sciences*, 364(1845), pages 2231-2265.
- Synolakis, C.E., E.N. Bernard, V.V. Titov, U. Kânoğlu, and F.I. Gonzalez, 2008. Validation and verification of tsunami numerical models. In *Tsunami Science Four Years After the 2004 Indian Ocean Tsunami*, pages 2197-2228. Springer.
- Synolakis, C.E. and U. Kânoğlu, 2015. The Fukushima accident was preventable. *Philosophical Transactions of the Royal Society A: Mathematical, Physical and Engineering Sciences*, 373(2053), 20140379.
- Thio, H.K., P. Somerville, and J. Polet, 2010. *Probabilistic tsunami hazard in California*. Pacific Earthquake Engineering Research Center, Peer Report 2010/108. University of California, Berkeley. http://peer.berkeley.edu/publications/peer_reports.html.
- Titov, V.V. and C.E. Synolakis, 1995. Modeling of breaking and nonbreaking long-wave evolution and runup using vcs-2. *Journal of Waterway, Port, Coastal, and Ocean Engineering*, 121(6), pages 308-316.
- Titov, V.V. and C.E. Synolakis, 1997. Extreme inundation flows during the Hokkaido-nansei-oki tsunami. *Geophysical Research Letters*, 24(11), pages 1315-1318.
- Titov, V.V. and C.E. Synolakis, 1998. Numerical modeling of tidal wave runup. *Journal of Waterway, Port, Coastal, and Ocean Engineering*, 124(4), pages 157-171.
- Titov, V.V., H.O. Mofjeld, F.I. Gonzalez, and J.C. Newman, 1999. *Offshore forecasting of Alaska-Aleutian subduction zone tsunamis in Hawaii*. NOAA Technical Memorandum, ERL PMEL-114, PMEL, Seattle, WA, 2.

- Titov, V.V., C.W. Moore, D.J.M. Greenslade, C. Pattiaratchi, R. Badal, C.E. Synolakis, and U. K^anořglu, 2011. A new tool for inundation modeling: Community modeling interface for tsunamis (commit). *Pure and Applied Geophysics*, 168(11), pages 2121-2131.
- Titov, V., U. K^anořglu, and C. Synolakis, 2016. Development of most for real-time tsunami forecasting. *Journal of Waterway, Port, Coastal, and Ocean Engineering*, 142(6), 03116004.
- Uslu, B., 2008. *Deterministic and probabilistic tsunami studies in California from near and far field sources*. PhD thesis, University of Southern California.

APPENDIX A

NOAA/PMEL UNIT SOURCE PARAMETERS

NOAA/PMEL UNIT SOURCE PARAMETERS

This section lists the earthquake parameters of the NOAA/PMEL unit sources used to define the far-field sources as listed by Arcas (2015). Table A-1 lists the earthquake parameters of the NOAA/PMEL unit sources used with the Eastern Aleutians far-field sources, and Table A-2 lists the unit sources used with the Kuril far-field sources. All unit sources used have a rake angle of 90° , rupture length $L = 100$ km and rupture width $W = 50$ km. Longitude/Latitude correspond to the coordinates of the center of the down-dip edge of the unit sources. The Depth parameter corresponds to the depth of the up-dip edge of the unit sources.

Table A-1. Earthquake parameters for the Aleutian-Alaska-Cascadia Subduction Zone (acsz) NOAA/PMEL unit sources (Arcas, 2015).

| Unit Source Name | Longitude (°E) | Latitude (°N) | Strike (°) | Dip (°) | Depth (km) |
|---------------------|-------------------|------------------|---------------|------------|---------------|
| acsz-a25 | 196.434 | 54.076 | 250.0 | 15.0 | 17.94 |
| acsz-b25 | 196.693 | 53.6543 | 250.0 | 15.0 | 5.0 |
| acsz-a26 | 197.897 | 54.36 | 253.0 | 15.0 | 17.94 |
| acsz-b26 | 198.12 | 53.93 | 253.0 | 15.0 | 5.0 |
| acsz-a27 | 199.434 | 54.596 | 256.0 | 15.0 | 17.94 |
| acsz-b27 | 199.62 | 54.16 | 256.0 | 15.0 | 5.0 |
| acsz-a28 | 200.882 | 54.83 | 253.0 | 15.0 | 17.94 |
| acsz-b28 | 201.108 | 54.4 | 253.0 | 15.0 | 5.0 |
| acsz-a29 | 202.261 | 55.133 | 247.0 | 15.0 | 17.94 |
| acsz-b29 | 202.565 | 54.72 | 247.0 | 15.0 | 5.0 |
| acsz-a30 | 203.604 | 55.509 | 240.0 | 15.0 | 17.94 |
| acsz-b30 | 203.997 | 55.12 | 240.0 | 15.0 | 5.0 |
| acsz-w30 | 201.9901 | 56.9855 | 239.5195 | 15.0 | 69.12 |
| acsz-x30 | 202.3851 | 56.6094 | 239.8491 | 15.0 | 56.24 |
| acsz-y30 | 202.7724 | 56.232 | 240.1722 | 15.0 | 43.82 |
| acsz-z30 | 203.1521 | 55.8534 | 240.4869 | 15.0 | 30.88 |
| acsz-a31 | 204.895 | 55.97 | 236.0 | 15.0 | 17.94 |
| acsz-b31 | 205.34 | 55.598 | 236.0 | 15.0 | 5.0 |
| acsz-w31 | 203.0825 | 57.374 | 234.544 | 15.0 | 69.12 |
| acsz-x31 | 203.5408 | 57.0182 | 234.9266 | 15.0 | 56.24 |
| acsz-y31 | 203.9904 | 56.6607 | 235.3043 | 15.0 | 43.82 |
| acsz-z31 | 204.4315 | 56.3016 | 235.669 | 15.0 | 30.88 |
| acsz-a32 | 206.208 | 56.473 | 236.0 | 15.0 | 17.94 |

| | | | | | |
|----------|----------|----------|----------|------|-------|
| acsz-b32 | 206.658 | 56.1 | 236.0 | 15.0 | 5.0 |
| acsz-w32 | 204.4129 | 57.8908 | 234.324 | 15.0 | 69.12 |
| acsz-x32 | 204.8802 | 57.5358 | 234.716 | 15.0 | 56.24 |
| acsz-y32 | 205.3385 | 57.1792 | 235.1002 | 15.0 | 43.82 |
| acsz-z32 | 205.788 | 56.821 | 235.4756 | 15.0 | 30.88 |
| acsz-a33 | 207.537 | 56.975 | 236.0 | 15.0 | 17.94 |
| acsz-b33 | 207.993 | 56.603 | 236.0 | 15.0 | 5.0 |
| acsz-w33 | 205.7126 | 58.3917 | 234.2356 | 15.0 | 69.12 |
| acsz-x33 | 206.1873 | 58.0371 | 234.6375 | 15.0 | 56.24 |
| acsz-y33 | 206.6527 | 57.6808 | 235.0298 | 15.0 | 43.82 |
| acsz-z33 | 207.1091 | 57.3227 | 235.4119 | 15.0 | 30.88 |
| acsz-a34 | 208.9371 | 57.51237 | 236.0 | 15.0 | 17.94 |
| acsz-b34 | 209.4 | 57.14 | 236.0 | 15.0 | 5.0 |
| acsz-w34 | 206.9772 | 58.8804 | 233.4678 | 15.0 | 69.12 |
| acsz-x34 | 207.4677 | 58.5291 | 233.8837 | 15.0 | 56.24 |
| acsz-y34 | 207.9485 | 58.176 | 234.2919 | 15.0 | 43.82 |
| acsz-z34 | 208.4198 | 57.8213 | 234.6891 | 15.0 | 30.88 |
| acsz-a35 | 210.2597 | 58.04408 | 230.0 | 15.0 | 17.94 |
| acsz-b35 | 210.8 | 57.7 | 230.0 | 15.0 | 5.0 |
| acsz-w35 | 208.0204 | 59.3199 | 228.8144 | 15.0 | 69.12 |
| acsz-x35 | 208.5715 | 58.9906 | 229.2854 | 15.0 | 56.24 |
| acsz-y35 | 209.1122 | 58.659 | 229.7465 | 15.0 | 43.82 |
| acsz-z35 | 209.6425 | 58.3252 | 230.1971 | 15.0 | 30.88 |
| acsz-a36 | 211.3249 | 58.65653 | 218.0 | 15.0 | 17.94 |
| acsz-b36 | 212.0 | 58.38 | 218.0 | 15.0 | 5.0 |
| acsz-w36 | 208.5003 | 59.5894 | 215.592 | 15.0 | 69.12 |
| acsz-x36 | 209.1909 | 59.3342 | 216.1822 | 15.0 | 56.24 |
| acsz-y36 | 209.8711 | 59.0753 | 216.7637 | 15.0 | 43.82 |
| acsz-z36 | 210.5412 | 58.8129 | 217.3327 | 15.0 | 30.88 |
| acsz-a37 | 212.2505 | 59.272 | 213.71 | 15.0 | 17.94 |
| acsz-b37 | 212.9519 | 59.0312 | 213.71 | 15.0 | 5.0 |
| acsz-x37 | 210.1726 | 60.0644 | 213.0379 | 15.0 | 56.24 |
| acsz-y37 | 210.8955 | 59.8251 | 213.6592 | 15.0 | 43.82 |
| acsz-z37 | 211.6079 | 59.582 | 214.2669 | 15.0 | 30.88 |
| acsz-a38 | 214.6555 | 60.1351 | 260.08 | 15.0 | 17.94 |

| | | | | | |
|----------|----------|---------|----------|------|-------|
| acsz-b38 | 214.8088 | 59.6927 | 260.08 | 15.0 | 5.0 |
| acsz-y38 | 214.3737 | 60.9838 | 259.0313 | 15.0 | 43.82 |
| acsz-z38 | 214.5362 | 60.5429 | 259.0313 | 15.0 | 30.88 |
| acsz-a39 | 216.5607 | 60.248 | 267.04 | 15.0 | 17.94 |
| acsz-b39 | 216.6068 | 59.7994 | 267.04 | 15.0 | 5.0 |

Table A-2. Earthquake parameters for the Kamchatka-Kuril-Japan-Izu-Mariana-Yap Subduction Zone (kisz) NOAA/PMEL unit sources (Arcas, 2015).

| Unit Source | Longitude | Latitude | Strike | Dip | Depth |
|-------------|-----------|----------|--------|------|-------|
| Name | (°E) | (°N) | (°) | (°) | (km) |
| kisz-a4 | 160.7926 | 53.1087 | 210.0 | 29.0 | 26.13 |
| kisz-b4 | 161.3568 | 52.9123 | 210.0 | 25.0 | 5.0 |
| kisz-a5 | 160.0211 | 52.41125 | 218.0 | 29.0 | 26.13 |
| kisz-b5 | 160.5258 | 52.1694 | 218.0 | 25.0 | 5.0 |
| kisz-a6 | 159.1272 | 51.70338 | 218.0 | 29.0 | 26.13 |
| kisz-b6 | 159.6241 | 51.4615 | 218.0 | 25.0 | 5.0 |
| kisz-a7 | 158.2625 | 50.95486 | 214.0 | 29.0 | 26.13 |
| kisz-b7 | 158.7771 | 50.73519 | 214.0 | 25.0 | 5.0 |
| kisz-a8 | 157.4712 | 50.24591 | 218.0 | 31.0 | 27.7 |
| kisz-b8 | 157.9433 | 50.00888 | 218.0 | 27.0 | 5.0 |
| kisz-a9 | 156.6114 | 49.55835 | 220.0 | 31.0 | 27.7 |
| kisz-b9 | 157.0638 | 49.31087 | 220.0 | 27.0 | 5.0 |
| kisz-a10 | 155.7294 | 48.8804 | 221.0 | 31.0 | 27.7 |
| kisz-b10 | 156.169 | 48.62782 | 221.0 | 27.0 | 5.0 |
| kisz-a11 | 154.8489 | 48.18207 | 219.0 | 31.0 | 27.7 |
| kisz-b11 | 155.2955 | 47.93978 | 219.0 | 27.0 | 5.0 |
| kisz-a12 | 153.9994 | 47.47286 | 217.0 | 31.0 | 27.7 |
| kisz-b12 | 154.4701 | 47.23201 | 217.0 | 27.0 | 5.0 |
| kisz-a13 | 153.2239 | 46.75639 | 218.0 | 31.0 | 27.7 |
| kisz-b13 | 153.6648 | 46.51936 | 218.0 | 27.0 | 5.0 |
| kisz-a14 | 152.3657 | 46.15145 | 225.0 | 23.0 | 24.54 |
| kisz-b14 | 152.7855 | 45.8591 | 225.0 | 23.0 | 5.0 |
| kisz-a15 | 151.4663 | 45.59629 | 233.0 | 25.0 | 23.73 |
| kisz-b15 | 151.8144 | 45.27119 | 233.0 | 22.0 | 5.0 |

COASTAL HAZARD ANALYSIS AT SAN ONOFRE NUCLEAR GENERATING STATION

Part 1: Coastal Hazards



for

**SOUTHERN CALIFORNIA EDISON
P.O. Box 128, MS D3D
5000 Pacific Coast Highway
San Clemente, CA 92672**

**Coastal Environments, Inc.
2166 Avenida de la Playa, Suite E
La Jolla, CA 92037**

**CE Reference No. 22-02
31 March 2022**

TABLE OF CONTENTS

| | |
|--|------------|
| EXECUTIVE SUMMARY | vii |
| 1.0 INTRODUCTION..... | 1 |
| 1.1 SONGS UNITS 1, 2, AND 3 DESCRIPTION | 2 |
| 1.2 HISTORICAL CONTEXT | 3 |
| 1.3 GEOLOGIC SETTING AND CLIFF COMPOSITION | 4 |
| 1.4 HISTORICAL CLIFF RETREAT..... | 4 |
| 2.0 MEAN SEA LEVEL RISE IMPACT ASSESSMENT | 11 |
| 2.1 SONGS SEA LEVEL INFORMATION..... | 11 |
| 2.2 MEAN SEA LEVEL RISE GUIDANCE..... | 12 |
| 2.2.1 California OPC (2018) MSLR Projections | 12 |
| 2.2.2 IPCC (2021) MSLR Projections | 14 |
| 2.3 SONGS SEA LEVEL EXTREMES | 17 |
| 3.0 BEACH AND CLIFF RETREAT MODEL | 25 |
| 3.1 MODEL SCENARIO | 26 |
| 3.2 MODEL INPUTS AND PARAMETERS | 27 |
| 3.3 MODEL RESULTS | 28 |
| 4.0 SONGS REVETMENT | 36 |
| 4.1 DESCRIPTION OF THE SONGS REVETMENT | 36 |
| 4.1.1 Revetment and Walkway Maintenance 2018-2019 | 36 |
| 4.2 SITE VISIT..... | 36 |
| 4.2.1 Rock Measurement Discussion | 37 |
| 4.2.2 Revetment Laser Scanner Survey | 37 |
| 4.3 RIPRAP ROCK UNIT WEIGHT | 38 |
| 4.4 DESIGN WATER LEVEL..... | 38 |
| 4.5 DESIGN WAVE ESTIMATION..... | 39 |
| 4.6 SONGS REVETMENT STABILITY ESTIMATION | 39 |
| 4.7 ASSESSMENT OF SAN ONOFRE BEACH | 40 |
| 4.8 EVALUATION CRITERIA | 41 |
| 4.9 REVETMENT STABILITY FROM FEBRUARY 2020 TO FEBRUARY 2021 | 41 |
| 4.10 MAINTENANCE AND ADAPTIVE CAPACITY | 42 |
| 4.11 GROUNDWATER..... | 43 |
| 5.0 RUN-UP AND OVERTOPPING ANALYSIS | 76 |
| 5.1 RANDOM WAVE METHOD | 76 |
| 5.2 OVERTOPPING..... | 77 |
| 5.3 RESULTS | 78 |
| 5.4 PROBABILITY ANALYSIS | 78 |
| 5.5 SUMMARY | 79 |
| 6.0 SUMMARY AND CONCLUSIONS | 86 |
| 7.0 REFERENCES..... | 88 |

LIST OF APPENDICES

| | | |
|-------------|--|-----|
| Appendix A. | Modeled Beach and Cliff Profile Changes by 2050 due to MSLR | A-1 |
| Appendix B. | Digital Elevation Models (DEM) from 2020 and 2021 Revetment Surveys..... | B-1 |
| Appendix C. | Cross Section Elevations of SONGS Revetment..... | C-1 |
| Appendix D. | Aerial Photographs North and South SONGS, 2003-2020..... | D-1 |

LIST OF FIGURES

| | | |
|-------------|---|----|
| Figure 1-1. | Location of SONGS | 5 |
| Figure 1-2. | Location of Cristianitos Fault with respect to SONGS, at the south end of the fault line | 6 |
| Figure 1-3. | Unit 1 (left dome), and Units 2 and 3 (right domes), prior to dismantlement of Unit 1..... | 7 |
| Figure 1-4. | Locations of the Independent Spent Fuel Storage Installations (ISFSIs) at the North Industrial Area (NIA) where Unit 1 was previously located..... | 7 |
| Figure 1-5. | Maps of the study area showing 1889 topography, 1934 topography and cliff edge, and 2009 topography and cliff edge lines..... | 8 |
| Figure 1-6. | Long-term cliff retreat rates and spatial distribution for Oceanside littoral cell..... | 9 |
| Figure 1-7. | Geological description of cliffs north of SONGS and south of SONGS | 10 |
| Figure 2-1. | Annual and monthly average water level relative to NAVD88 at La Jolla, 1925-2021, and annual global MSL reconstruction..... | 21 |
| Figure 2-2. | La Jolla average MSL data, 1925-2021, annual, monthly. Same for 2000-2021. Both with OPC (2018) La Jolla MSLR projections, 2000-2050 | 22 |
| Figure 2-3. | La Jolla average MSL data, 1925-2021, annual, monthly, with IPCC (2021) LA MSLR projections, 2004.5-2050..... | 23 |
| Figure 2-4. | Monthly maximum sea level at La Jolla relative to NAVD88 datum, 1925-2021. Maximum observed 7.62 ft height on 25 November 2015 during 2015-16 El Niño | 24 |
| Figure 3-1. | Model profile adjustments and erosion from MSLR | 29 |
| Figure 3-2. | Map showing model transects and contours displayed over aerial photograph and the 2009 bare earth digital elevation model..... | 30 |
| Figure 3-3. | Modeled beach retreat on all 27 modeled profiles at SONGS for each scenario | 32 |
| Figure 3-4. | Modeled cliff retreat for profiles south of SONGS, intersecting SONGS, and north of SONGS for each scenario..... | 33 |
| Figure 3-5. | Modeled H++ extreme-scenario cliff retreat for Scenarios A and B at transect 227 located north of SONGS..... | 34 |
| Figure 3-6. | Modeled extreme-scenario cliff retreat for Scenarios A and B at transect 217 located south of SONGS..... | 35 |
| Figure 4-1. | Photo of SONGS revetment, 20 August 2018 | 44 |
| Figure 4-2. | Photo of southern end of SONGS revetment..... | 45 |

| | | |
|--------------|---|----|
| Figure 4-3. | Photo of riprap revetment toward south, 20 March 2018 before placement of additional rock. Photo on 17 December 2019 after placement of rock in gaps and settled areas..... | 46 |
| Figure 4-4. | Photo of south end of riprap and access walkway on 15 October 2019 before repairs. Photo on 17 December 2019 after repairs | 47 |
| Figure 4-5. | Measurement of long axis (length) of riprap rock | 48 |
| Figure 4-6. | Histograms of rock length, width, and height..... | 49 |
| Figure 4-7. | Cumulative distributions of rock length, width, and height..... | 50 |
| Figure 4-8. | Photo of Trimble SX10 scanning total station used by Coastal Environments for SONGS topographic surveys | 51 |
| Figure 4-9. | Location of 21 transects along the revetment, spaced 100 ft apart..... | 52 |
| Figure 4-10. | Elevation model of SONGS revetment from laser scanner, Transects 1-7..... | 53 |
| Figure 4-11. | Elevation model of SONGS revetment from laser scanner, Transects 8-15..... | 54 |
| Figure 4-12. | Elevation model of SONGS revetment from laser scanner, Transects 16-21..... | 55 |
| Figure 4-13. | Typical revetment cross sections showing slope “ β ”..... | 56 |
| Figure 4-14. | Elevation of the top of revetment for the 21 transects | 58 |
| Figure 4-15. | Weight distribution of existing SONGS revetment rocks..... | 61 |
| Figure 4-16. | Design wave heights for various return periods at San Onofre | 62 |
| Figure 4-17. | Measured wave spectral density for various storms | 63 |
| Figure 4-18. | Historical beach width adjacent to Unit 1, 1928-2000 | 67 |
| Figure 4-19. | Beach width fronting SONGS, 1991-1993 and 2016-2020..... | 68 |
| Figure 4-20. | Wave height and wave period at SONGS, 1 January 2020 to 28 February 2021..... | 70 |
| Figure 4-21. | Wave height and wave period at SONGS, 6-11 November 2020..... | 71 |
| Figure 4-22. | Wave height and wave period at SONGS, 1 January to 28 February 2021 | 72 |
| Figure 4-23. | Wave height and wave period at SONGS, 25-29 January 2021 | 73 |
| Figure 4-24. | Photos of north portion of SONGS revetment covered by beach sand, spring 2020, but covered with cobble, winter 2021 | 74 |
| Figure 4-25. | Groundwater elevations in 2020, and for OPC (2018) 0.5% and H++ MSLR projections by 2050..... | 75 |
| Figure 5-1. | Wave run-up on a slope | 80 |
| Figure 5-2. | Exposed area in the walkway wall..... | 83 |
| Figure 5-3. | Probability of 10-, 25-, 50-, and 100-year waves return period to occur in the next 100 years | 84 |
| Figure 5-4. | Joint Probability distribution between significant wave height and tide level..... | 85 |

LIST OF TABLES

| | | |
|------------|---|----|
| Table 2-1. | OPC (2018) MSLR Projections, La Jolla | 19 |
| Table 2-2. | IPCC (2021) Mid-Range MSLR Projections, Los Angeles..... | 19 |
| Table 2-3. | IPCC (2021) Low-High Range MSLR Projections, Los Angeles | 19 |
| Table 2-4. | Highest Maximum Observed Total Water Levels, La Jolla | 20 |
| Table 2-5. | NOAA La Jolla Extreme Water Level Statistics | 20 |
| Table 3-1. | Beach and cliff retreat 2010-2050..... | 31 |
| Table 4-1. | Riprap and walkway wall heights and revetment slope β | 57 |

| | | |
|------------|---|----|
| Table 4-2. | Length, width, height, and estimated weight of the measured rocks | 59 |
| Table 4-3. | Mean and standard deviation for rock parameters | 60 |
| Table 4-4. | Design wave characteristics at San Onofre | 64 |
| Table 4-5. | Largest 20 waves at San Onofre ranked in descending order (1976-1994) | 65 |
| Table 4-6. | Rock weights (W50) needed for revetment stability, 2020 and 2050 | 66 |
| Table 4-7. | Mean beach widths (ft) at San Onofre, 1990-1993 vs 2017-2020 | 69 |
| Table 5-1. | Run-up and overtopping summary for 0.5 % (1:200) scenario | 81 |
| Table 5-2. | Run-up and overtopping summary for OPC (2018) H++ scenario | 82 |

APPENDIX FIGURES

| | | |
|--------------|--|------|
| Figure A-1. | Observed 2010 and modeled 2050 Profile 210 | A-2 |
| Figure A-2. | Observed 2010 and modeled 2050 Profile 211 | A-3 |
| Figure A-3. | Observed 2010 and modeled 2050 Profile 212 | A-4 |
| Figure A-4. | Observed 2010 and modeled 2050 Profile 213 | A-5 |
| Figure A-5. | Observed 2010 and modeled 2050 Profile 214 | A-6 |
| Figure A-6. | Observed 2010 and modeled 2050 Profile 215 | A-7 |
| Figure A-7. | Observed 2010 and modeled 2050 Profile 216 | A-8 |
| Figure A-8. | Observed 2010 and modeled 2050 Profile 217 | A-9 |
| Figure A-9. | Observed 2010 and modeled 2050 Profile 218 | A-10 |
| Figure A-10. | Observed 2010 and modeled 2050 Profile 219 | A-11 |
| Figure A-11. | Observed 2010 and modeled 2050 Profile 220 | A-12 |
| Figure A-12. | Observed 2010 and modeled 2050 Profile 221 | A-13 |
| Figure A-13. | Observed 2010 and modeled 2050 Profile 222 | A-14 |
| Figure A-14. | Observed 2010 and modeled 2050 Profile 223 | A-15 |
| Figure A-15. | Observed 2010 and modeled 2050 Profile 224 | A-16 |
| Figure A-16. | Observed 2010 and modeled 2050 Profile 225 | A-17 |
| Figure A-17. | Observed 2010 and modeled 2050 Profile 226 | A-18 |
| Figure A-18. | Observed 2010 and modeled 2050 Profile 227 | A-19 |
| Figure A-19. | Observed 2010 and modeled 2050 Profile 228 | A-20 |
| Figure A-20. | Observed 2010 and modeled 2050 Profile 229 | A-21 |
| Figure A-21. | Observed 2010 and modeled 2050 Profile 230 | A-22 |
| Figure A-22. | Observed 2010 and modeled 2050 Profile 231 | A-23 |
| Figure A-23. | Observed 2010 and modeled 2050 Profile 232 | A-24 |
| Figure A-24. | Observed 2010 and modeled 2050 Profile 233 | A-25 |
| Figure A-25. | Observed 2010 and modeled 2050 Profile 234 | A-26 |
| Figure A-26. | Observed 2010 and modeled 2050 Profile 235 | A-27 |
| Figure A-27. | Observed 2010 and modeled 2050 Profile 236 | A-28 |

| | | |
|--------------|--|------|
| Figure B-1. | Location of 21 transects along the revetment, spaced 100 ft apart..... | B-2 |
| Figure B-2. | DEM comparison between 2021 and 2020 showing Transect 1..... | B-3 |
| Figure B-3. | DEM comparison between 2021 and 2020 showing Transect 2..... | B-4 |
| Figure B-4. | DEM comparison between 2021 and 2020 showing Transect 3..... | B-5 |
| Figure B-5. | DEM comparison between 2021 and 2020 showing Transect 4..... | B-6 |
| Figure B-6. | DEM comparison between 2021 and 2020 showing Transect 5..... | B-7 |
| Figure B-7. | DEM comparison between 2021 and 2020 showing Transect 6..... | B-8 |
| Figure B-8. | DEM comparison between 2021 and 2020 showing Transect 7..... | B-9 |
| Figure B-9. | DEM comparison between 2021 and 2020 showing Transect 8..... | B-10 |
| Figure B-10. | DEM comparison between 2021 and 2020 showing Transect 9..... | B-11 |
| Figure B-11. | DEM comparison between 2021 and 2020 showing Transect 10..... | B-12 |
| Figure B-12. | DEM comparison between 2021 and 2020 showing Transect 11..... | B-13 |
| Figure B-13. | DEM comparison between 2021 and 2020 showing Transect 12..... | B-14 |
| Figure B-14. | DEM comparison between 2021 and 2020 showing Transect 13..... | B-15 |
| Figure B-15. | DEM comparison between 2021 and 2020 showing Transect 14..... | B-16 |
| Figure B-16. | DEM comparison between 2021 and 2020 showing Transect 15..... | B-17 |
| Figure B-17. | DEM comparison between 2021 and 2020 showing Transect 16..... | B-18 |
| Figure B-18. | DEM comparison between 2021 and 2020 showing Transect 17..... | B-19 |
| Figure B-19. | DEM comparison between 2021 and 2020 showing Transect 18..... | B-20 |
| Figure B-20. | DEM comparison between 2021 and 2020 showing Transect 19..... | B-21 |
| Figure B-21. | DEM comparison between 2021 and 2020 showing Transect 20..... | B-22 |
| Figure B-22. | DEM comparison between 2021 and 2020 showing Transect 21..... | B-23 |
| | | |
| Figure C-1. | Cross sections of SONGS revetment along transects 1-3..... | C-2 |
| Figure C-2. | Cross sections of SONGS revetment along transects 4-6..... | C-3 |
| Figure C-3. | Cross sections of SONGS revetment along transects 7-9..... | C-4 |
| Figure C-4. | Cross sections of SONGS revetment along transects 10-12..... | C-5 |
| Figure C-5. | Cross sections of SONGS revetment along transects 13-15..... | C-6 |
| Figure C-6. | Cross sections of SONGS revetment along transects 16-18..... | C-7 |
| Figure C-7. | Cross sections of SONGS revetment along transects 19-21..... | C-8 |

LIST OF PHOTOGRAPHS

| | | |
|------------|--|-----|
| Photo D-1. | Photograph showing revetment covered by sand and fronted by a wide beach at the northern end of SONGS (10 March 2003)..... | D-2 |
| Photo D-2. | Photograph showing waves from north swell attacking SONGS revetment at the southern end of SONGS (10 March 2003)..... | D-2 |
| Photo D-3. | Photograph showing waves attacking the revetment and the presence of a sand beach at the northern end of SONGS (26 November 2003)..... | D-3 |
| Photo D-4. | Photograph showing waves attacking SONGS revetment at the southern end of SONGS (26 November 2003)..... | D-3 |
| Photo D-5. | Photograph showing revetment covered by sand and fronted by a wide beach at the northern end of SONGS (2 August 2006) | D-4 |
| Photo D-6. | Photograph showing waves from north swell attacking SONGS revetment at the southern end of SONGS (2 August 2006)..... | D-4 |

| | | |
|-------------|--|------|
| Photo D-7. | Photograph showing revetment covered by sand and fronted by a wide beach at the northern end of SONGS (31 January 2006)..... | D-5 |
| Photo D-8. | Photograph showing waves from north swell attacking SONGS revetment and refracting towards south at the southern end of SONGS (31 January 2006) | D-5 |
| Photo D-9. | Photograph showing revetment covered by sand and fronted by a wide beach at the northern end of SONGS (31 January 2008)..... | D-6 |
| Photo D-10. | Photograph showing waves attacking SONGS revetment at the southern end of SONGS (31 January 2008) | D-6 |
| Photo D-11. | Photograph showing revetment covered by sand and fronted by a wide beach at the northern end of SONGS (12 November 2013) | D-7 |
| Photo D-12. | Photograph showing waves attacking SONGS revetment and refracting towards south at the southern end of SONGS (12 November 2013)..... | D-7 |
| Photo D-13. | Photograph showing revetment exposed and fronted by a wide beach at the northern end of SONGS (27 April 2014)..... | D-8 |
| Photo D-14. | Photograph showing waves attacking SONGS revetment and refracting towards south at the southern end of SONGS (27 April 2014) | D-8 |
| Photo D-15. | Photograph showing revetment exposed and fronted by a sand beach at the northern end of SONGS (19 February 2018)..... | D-9 |
| Photo D-16. | Photograph showing waves from north swell attacking SONGS revetment and refracting towards south at the southern end of SONGS (19 February 2018) | D-9 |
| Photo D-17. | Photograph showing revetment exposed and fronted by a wide beach at the northern end of SONGS (24 August 2018)..... | D-10 |
| Photo D-18. | Photograph showing waves from north swell attacking SONGS revetment and refracting towards south at the southern end of SONGS (24 August 2018) | D-10 |
| Photo D-19. | Photograph showing revetment exposed and fronted by a wide beach at the northern end of SONGS (15 October 2020) | D-11 |
| Photo D-20. | Photograph showing waves attacking SONGS revetment and refracting towards south at the southern end of SONGS (15 October 2020)..... | D-11 |

EXECUTIVE SUMMARY

The objective of this study is to discuss coastal hazards at San Onofre Nuclear Generating Station (SONGS) in order to evaluate impacts of sea level rise, waves, and wave run-up on the beach, nearshore zone, and SONGS facilities, specifically the SONGS NUHOMS Independent Spent Fuel Storage Installation (ISFSI). The present report describes the possible future effects of sea level rise on the ongoing and long-term influences of waves on the beach, cliffs, protective structures, and wave run-up and overtopping under extreme conditions.

Projections of future Mean Sea Level Rise (MSLR) are evolving rapidly and continuously as the understanding of key climate change processes improves. MSLR projections through 2050 that could impact SONGS are presented in Chapter 2. Discussion and summaries of the currently applicable MSLR guidance, unchanged since OPC (2018), and the newly issued IPCC (2021, 2022) findings are presented in Sections 2.2.1 and 2.2.2, respectively. Maximum high-water level applicable to SONGS is discussed in Section 2.3. Overall, the new IPCC (2021, 2022) projections are lower than existing guidance.

The Young *et al.* (2014) beach and cliff erosion model presented in Chapter 3 is used to compute coastal retreat from MSLR to 2050. The model is tested by simulating historical cliff retreat at Marine Corps Base Camp Pendleton from 1934 to 1998 reported by Hapke and Reid (2007) and using the associated historical MSLR rate and sand budgets from Inman and Masters (1991). Minimum, mean, and maximum modeled retreat rates were generally similar to the observations, suggesting the model is valid for use at San Onofre.

An assessment of the SONGS revetment is given in Chapter 4, including a review of routine maintenance and repair in 2018 and 2019. Section 4.2 gauges the current revetment condition, describes its characteristics, including dimension and weight distributions, from a 2021 inspection. Sections 4.3-4.6 discuss factors influencing revetment stability. Threats in the future remain wave storms exacerbated by MSLR. During winter 2020-2021, the revetment was subject to large waves higher than the previously estimated wave height for the 100-year-return period. Despite these conditions, damage to the revetment and walkway was minimal. This study concludes that with routine maintenance, the revetment can continue to function as intended until at least 2050.

Impacts of groundwater on the ISFSI based on quarterly measurements of the groundwater from nine coastal wells located near the ISFSI are also presented in Chapter 4. The OPC (2018) “medium high-risk aversion” 1:200 (0.5%) and extreme H++ MSLR scenarios for groundwater elevation by 2050 are discussed.

Revetment wave run-up and overtopping analysis is presented in Chapter 5. This work considers the same projection scenarios as in Chapter 4, in combination with ranges of extreme wave return periods, and future high-water elevations. Study conclusions are stated in Chapter 6.

As part of this analysis, Coastal Environments has reviewed the 2001 and 2015 SONGS ISFSI Coastal Development Permit (CDP) and staff report materials and found that the Coastal Commission’s conclusions in those reports remain correct.

COASTAL HAZARD ANALYSIS AT SAN ONOFRE NUCLEAR GENERATING STATION

Part 1: Coastal Hazards

1.0 INTRODUCTION

Southern California Edison (SCE) is undertaking the decommissioning and dismantlement of the San Onofre Nuclear Generating Station (SONGS) (Figure 1-1). Ultimately, the site will be returned to the U.S. Marine Corps Base, Camp Pendleton (MCBCP), under the authority of the Department of the Navy. The present study seeks to determine future coastal hazards impacts at SONGS with respect to climate change, focused on mean sea level rise (MSLR) and waves.

This report discusses the results of our efforts to project future beach, cliff, and nearshore evolution, as well as impact on protected structures, and to assess the probability of flooding at the site with and without the existing seawalls up to 2050.

Following this introduction, the report is organized as follows: Chapter 2 discusses MSLR projections from 2000-2050. The long-term beach and cliff retreat coastal analysis model is described in Chapter 3. Results for revetment stability and beach erosion and accretion due to waves, as well as estimated extreme wave statistics and water surface levels, are discussed in Chapter 4. Estimation of wave run-up and overtopping due to MSLR are presented in Chapter 5. A summary of the study with its conclusions is presented in Chapter 6, followed by a list of references in Chapter 7. Lastly, there are four appendices, A-D.

The best approach to determining future cliff and beach changes is to apply existing peer-reviewed coastal retreat and shoreline fluctuation models, and wave shoaling, run-up, and overtopping methods, with the latest available MSLR guidance.

Power generation at SONGS involved three units, called Units 1, 2, and 3 (Figure 1-3). Construction of SONGS Unit 1 took place from 1964-1966. Unit 1 began operation in 1968. SONGS Units 2 and 3 were built on a prominent natural point of land south of Unit 1, from 1974-1984. Temporary adjacent sheet-pile laydown pads existed for the construction on the beach adjacent to Unit 1 and Units 2 and 3 for each period, respectively. Sand from cliff excavations was placed in each laydown pad. The Units 2 and 3 pads extended about 300 ft across the beach from the seawall. The sand used for both pads dispersed naturally along the beach after each pad was removed, and moved both northward and southward (Flick *et al.*, 2010).

Shoreline change modeling covers about 0.6 mi to the north and south of SONGS, encompassing about 4 mi of coastline from San Mateo Creek in the north to the Cristianitos Fault in the south (Figure 1-2). This coastline consists of an uplifted marine terrace backed by coastal slopes. Erosion of the terrace by marine and subaerial processes has resulted in coastal cliffs and

gullies dissecting the terrace. The sea cliffs extend along the seaward edge of the terrace and are typically 80-125 ft high.

Waves and sand supply from offshore areas, rivers, and cliffs are the major factors controlling the cyclic erosion and accretion of the beach. Waves, rainfall, and drainage from inland areas are primarily responsible for cliff erosion and landslides. The coast is oriented northwest-southeast and is exposed to waves generated by local winds and distant storms in both hemispheres (Flick, 1994). During the winter, swells from the North Pacific and Gulf of Alaska are most energetic, whereas during the summer, swell from the South Pacific dominates (Shepard, 1950). Waves reaching the southern California coast undergo a complex transformation, and wave shadowing from the Channel Islands creates strong alongshore variations in wave height (Pawka, 1983).

Wave erosion of the cliff base and talus occurs when the total water level, defined as the sum of tides and the vertical height of wave run-up (Shih *et al.*, 1994; Kirk *et al.*, 2000; Ruggiero *et al.*, 2001), exceeds the beach elevation at the cliff base. Total water levels are tidally modulated, and tidal fluctuations are more than 6-7 ft during spring tides. However, even large swells arriving during relatively low tides may not reach the cliff base.

Unit 1 was permanently shut down on 30 November 1992. Deconstruction of SONGS Unit 1 began in 1999, and all of the above-ground major structures associated with it below 20 ft MLLW¹ (Mean Lower Low Water, 1941-1960 Epoch), have been demolished and removed. The Unit 1 conduits have been plugged and the intake and discharge risers have also been removed. The Unit 1 site is currently being used as an Independent Spent Fuel Storage Installation (ISFSI) for storing spent nuclear fuel. Units 2 and 3 began commercial operation in 1983 and 1984, and were shut down on 9 January and 31 January 2012, respectively. Small volumes of water intake by the Units 2 and 3 conduits for waste water dilution continues, but heat production no longer occurs. A brief description of Units 1, 2, and 3 may be found in Section 1.1. Sections 1.2 through 1.4 describe changes in the grading of the study area associated with SONGS construction from 1964-1984, the geological composition of the cliffs, and the historical cliff retreat.

1.1 SONGS UNITS 1, 2, AND 3 DESCRIPTION

SONGS Unit 1 was constructed on 12 acres of land facing San Onofre State Beach. The area where Unit 1 was located is now known as the North Industrial Area (NIA). The construction of Unit 1 began with cliff excavation and site grading in March 1964. Unit 1 was positioned along a low straight cliff area next to somewhat higher cliffs, immediately to the northwest and southeast. The cliffs were excavated and some of the sand from the cliffs was placed on the beach to fill a temporary sheet-pile laydown pad seaward of the site that was used for construction activities. The beach to the north of the laydown pad widened due to the construction and remained wide through the end of 1965, at which time the sheet piles were

¹ MLLW (mean lower low water) is a tidal datum calculated as the average value of the lowest observed water level elevations each day over the National Tidal Datum Epoch, a fixed 19-yr period, currently 1983-2001. Tidal datum relationships among each other and relative to geodetic datums, like NAVD88, change with MSL.

removed. The sand in the pad was allowed to redistribute naturally along the beach, resulting in rapid decrease of beach width adjacent to the plant and more gradual adjustment over several years on beaches to the north (Flick *et al.*, 2010). The surface grade of the NIA is about 20 ft MLLW. The top of the permanent tsunami and wave protection seawall fronting the plant at Unit 1 is at an elevation of 28.2 ft MLLW.

SONGS Units 2 and 3 each had an operational capacity of about 1,200 megawatts (MW). The once-through cooling water system for each unit had a flow rate of 830,000 gallons per minute (GPM) and a normal operating temperature increase across the condensers of about 19°F. The single-port intakes of Units 2 and 3 are located about 3,300 ft offshore in 32-ft water depth. The Units 2 and 3 intakes are fitted with velocity caps to minimize entrainment of marine organisms. Large organism exclusion devices have been installed around the intake structures beneath the velocity caps to prevent marine mammals or sea turtles from entering the conduits.

Units 2 and 3 have diffuser-type discharges consisting of 63 ports, spread over a distance of approximately 2,500 ft and extending above the seafloor. The Unit 2 diffuser ports begin 5,900 ft offshore and end 8,400 ft seaward measured from the seawall, and range in water depth from 39 ft to 49 ft MLLW. The Unit 3 diffuser begins 3,600 ft offshore, extends to 6,100 ft at its terminus, and ranges in water depth from 32 ft to 38 ft MLLW (Koh *et al.*, 1974).

The top of the permanent tsunami and wave protection seawall fronting the plant at Units 2 and 3 is at an elevation of 30.0 ft MLLW. The bottom of the seawall is at 0.5 ft MLLW. The surface grade east of the seawall is about 30 ft MLLW. A walkway protected by a second lower retaining wall was constructed seaward of the main plant seawall to provide lateral beach access and transit up and downcoast of SONGS. The public beach-access walkway retaining wall is also fronted by rock riprap (revetment) to prevent scour and undermining from the ocean.

NIA was selected as the best location for storing spent fuel from Units 1, 2, and 3 in casks. There are two storage sites at the NIA (Figure 1-4). The eastern location, which was completed in 2003, is the NUHOMS ISFSI, while the western location, which was completed in 2017, is the Holtec ISFSI.

1.2 HISTORICAL CONTEXT

Grading associated with SONGS construction from 1964-1985 significantly changed the pre-existing topography, including major gully infilling north of SONGS (see existing gullies mapped on 1889 and 1934 T-Sheets, Figure 1-5) and cliff excavation at SONGS. The site contains a large seawall fronted by riprap and a lateral beach access walkway, while the cliffs to the north and south are unprotected. A narrow, sandy, and sometimes cobble beach fronts the sea cliffs. Local roads, Interstate 5, and a coastal railroad are immediately inland of SONGS. Construction of these roads and highways has altered natural drainage patterns by concentrating flow in culverts under the roads and railroad.

1.3 GEOLOGIC SETTING AND CLIFF COMPOSITION

The sea cliffs at SONGS are composed of two geologic units with an unconformable contact. The lower portion of the cliff is comprised of the 1- to 3-million-year-old San Mateo Formation, which is composed of massive, poorly cemented, dense sandstone forming a near-vertical face (Hunt, 1975). The upper unit consists of poorly to well-consolidated terrace deposits containing marine and non-marine mixtures and layers of cobbles and fine silty sand 80,000 to 120,000 years old. Both layers are subject to sub-aerial erosion, mainly from rain and associated runoff that produce cliff-face retreat, as well as deep gullies locally known as “barrancas.” The lower layer is generally more erosion resistant but is also exposed to wave action.

The Cristianitos Fault (currently inactive) intersects the coastline at the southern end of the study site, causing a change in the lower unit from the sandy San Mateo Formation in the north to landslide deposits underlain by the Monterey Formation in the south (Tan, 2001; Kennedy and Tan, 2007; Young *et al.*, 2010a, 2010b). Cliff samples of the San Mateo Formation and the terrace deposits taken in or near the study area by Young *et al.* (2010a, 2010b) consisted of about 94% sand size particles or larger.

1.4 HISTORICAL CLIFF RETREAT

Hapke and Reid (2007) present the only historical cliff retreat data for MCBCP (Marine Corps Base Camp Pendleton) using the digitized cliff-top positions from a 1934 T-Sheet and 1998 airborne LiDAR data (Figure 1-5). In total, 81 transects from Hapke and Reid (2007) are located in the present study area. For these transects, the cliff retreat from 1934-1998 ranged from 0.0-4.4 ft/yr with an average of about 1 ft/yr (Figure 1-6). The composition of the cliffs north and south of SONGS is shown in Figure 1-7.

Other cliff studies near MCBCP include USACE (1988, 1990), Everts (1991), Runyan and Griggs (2003), Young and Ashford (2006), Hapke *et al.* (2009). These studies estimate mean cliff retreat and gully erosion rates ranging from about 0.5-0.7 ft/yr, respectively. It is difficult to directly compare these studies because they use different quality data sources, time periods, coastline extents, and methods. However, most historical studies agree that over the last century, cliff retreat has generally decreased toward the south in MCBCP.

All historical studies that assess cliff and gully erosion, erosion due to land sliding, and damage to infrastructure from erosion at MCBCP have attributed this erosion to heavy rainfall. To date, no studies document the historical infrastructure damage from marine processes, such as wave action-induced failure. Complete understanding of cliff and gully erosion processes and rates is limited by the fact that spatially and/or temporally averaged histories miss the episodic nature of rapid and extreme short-term erosion events. For example, Kuhn and Shepard (1984) describe several rapid retreat events in excess of 100 ft, including 230 ft of retreat during a single storm. Additionally, retreat rates can vary widely alongshore, and local retreat rates are often several times larger than mean rates. In the MCBCP cliff section, Hapke and Reid (2007) measured a maximum local retreat rate of 5.7 ft/yr.

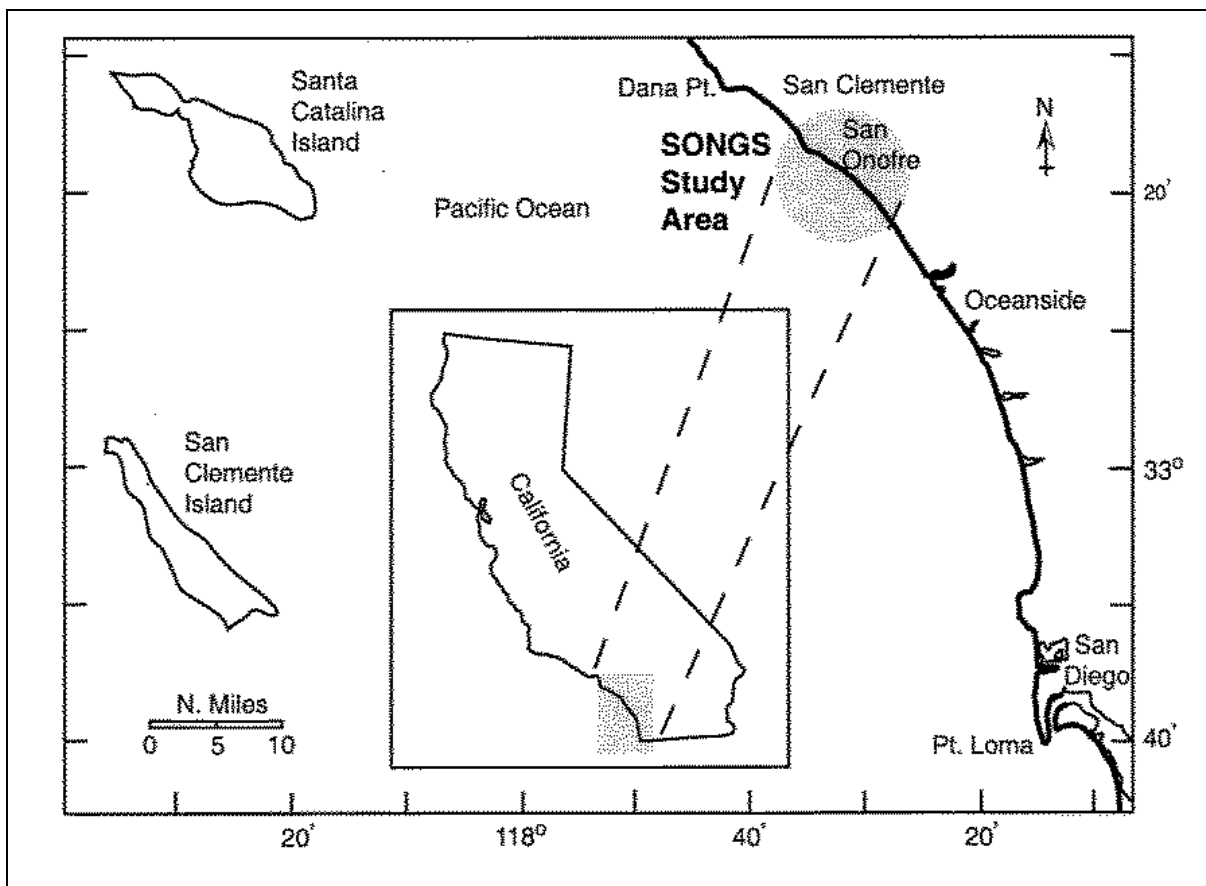


Figure 1-1. Location of SONGS. On the map scale, “N. Miles” stands for nautical miles.

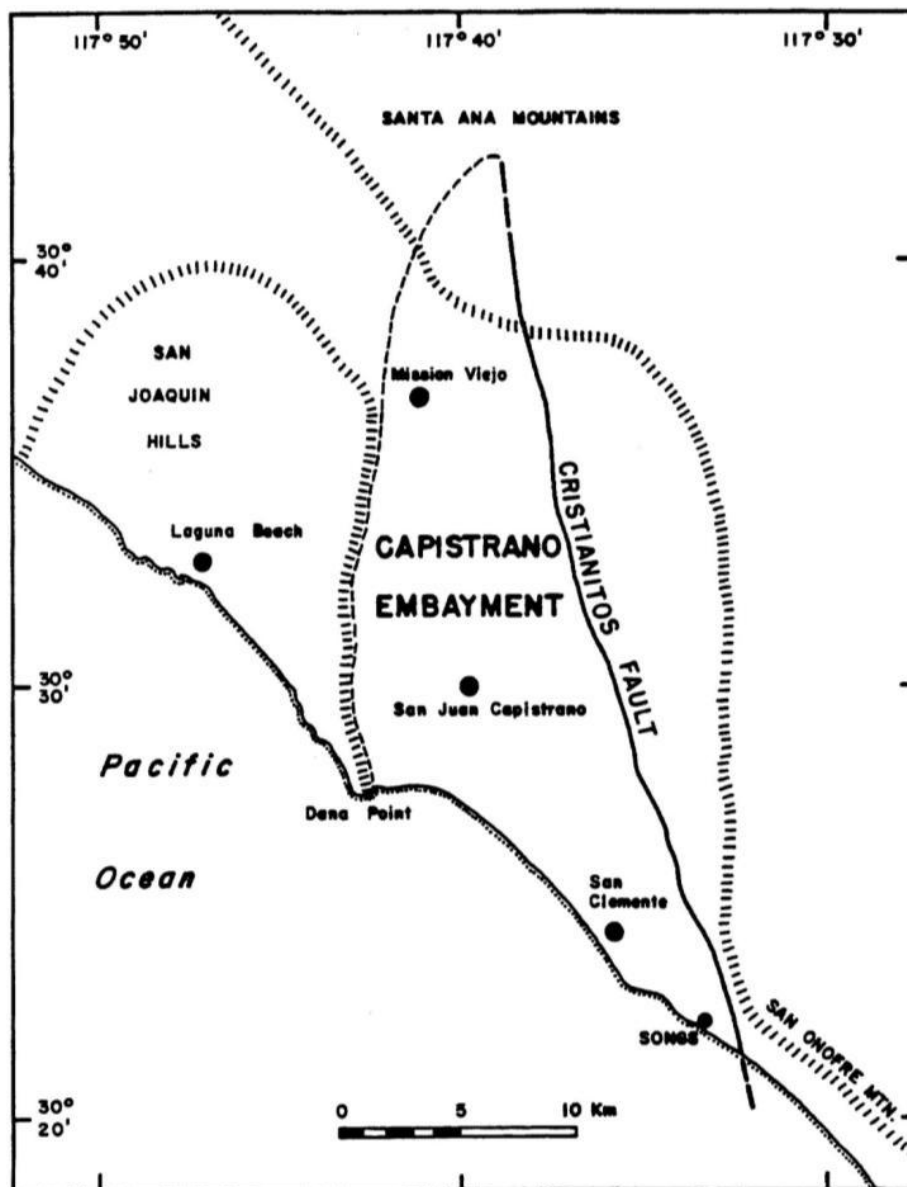


Figure 1-2. Location of Cristianitos Fault with respect to SONGS, located at the south end of the fault line.



Figure 1-3. Unit 1 (left dome), and Units 2 and 3 (right domes), prior to dismantlement of Unit 1.

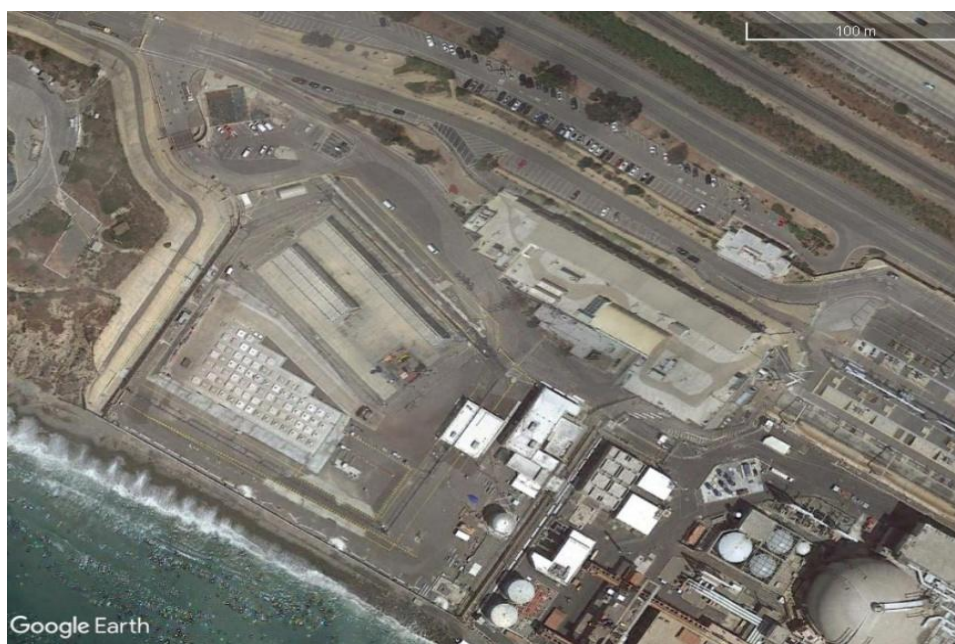


Figure 1-4. Locations of the Independent Spent Fuel Storage Installations (ISFSIs) at the North Industrial Area (NIA) where Unit 1 was previously located.

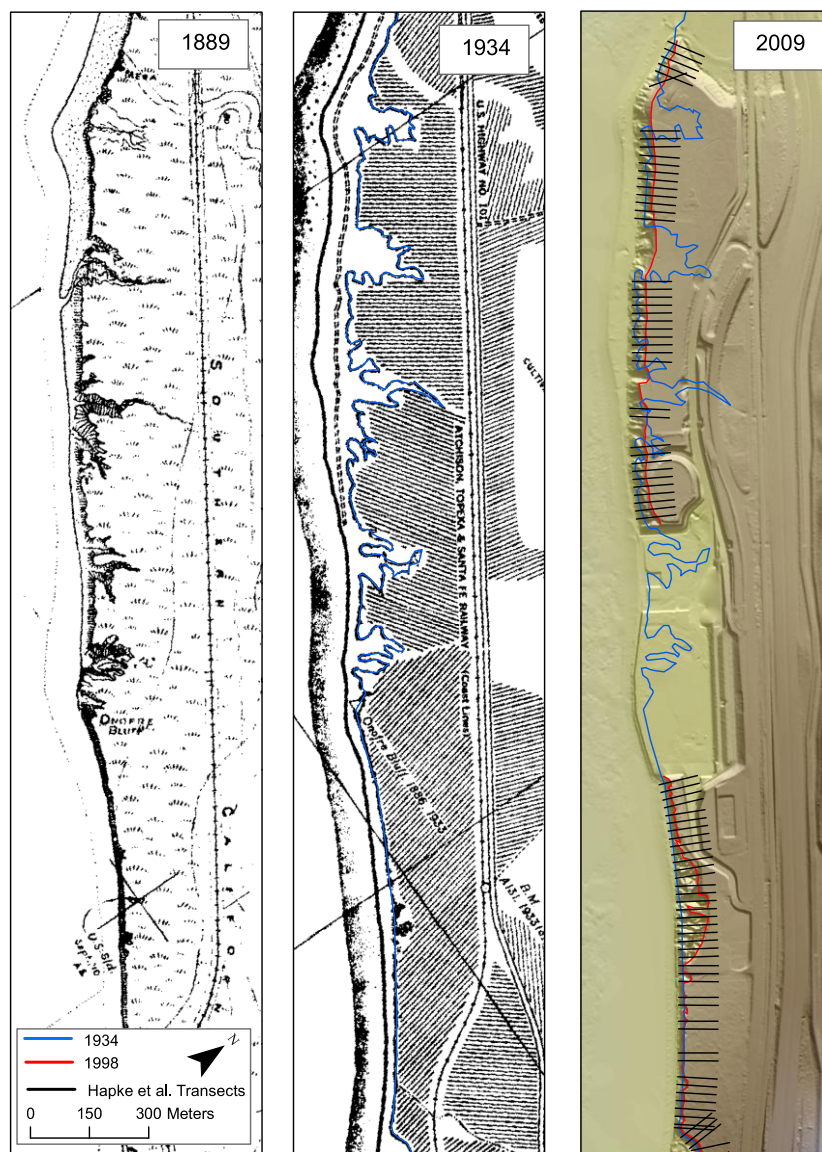


Figure 1-5. Maps of the study area showing 1889 topography (left), 1934 topography and cliff edge (center), and 2009 topography and cliff edge lines (1934 blue, 1998 red) with transects used by Hapke and Reid (2007) (right). A blue line showing the location of the previously-existing undeveloped bluffs from 1934 and a red line showing the developed site as of 1998 are included for reference in the 2009 image.

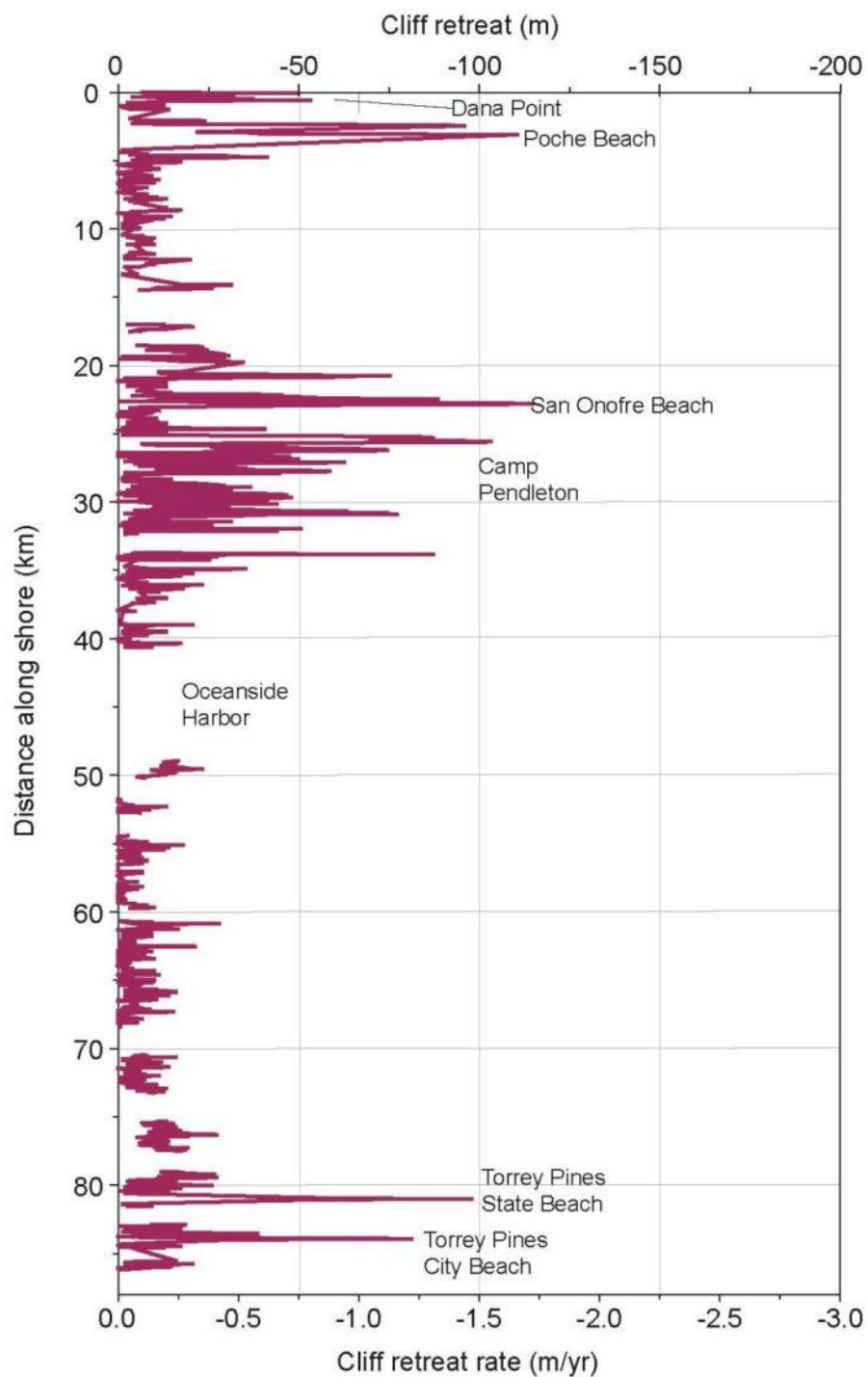


Figure 1-6. Long-term cliff retreat rates and spatial distribution for Oceanside littoral cell (Hapke and Reid, 2007).

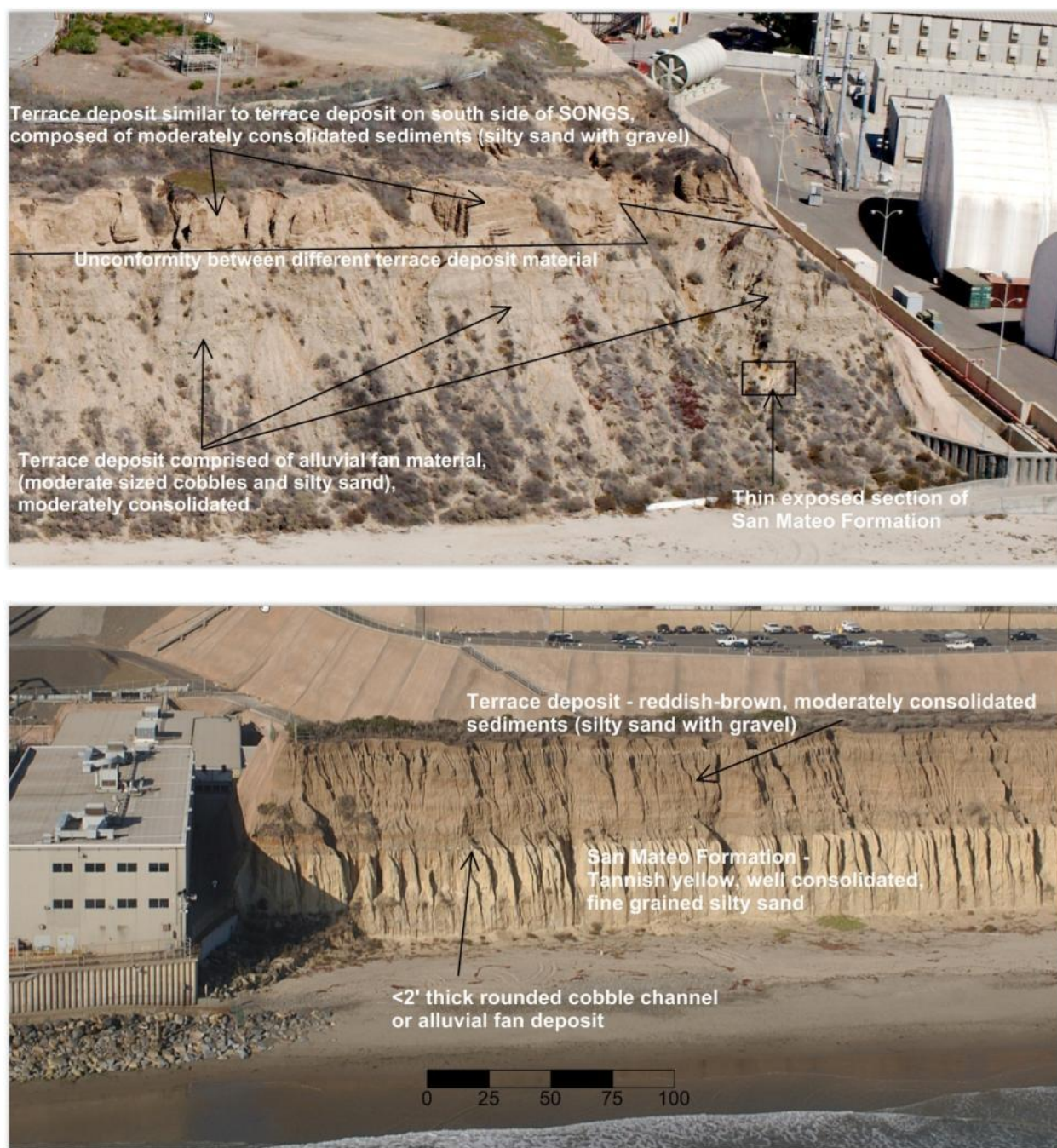


Figure 1-7. Geological description of cliffs north of SONGS (upper) and south of SONGS (lower).

2.0 MEAN SEA LEVEL RISE IMPACT ASSESSMENT

This chapter describes future MSLR scenarios that are used in the SONGS beach and cliff retreat modeling discussion in Chapter 3, and to quantify likely future extreme high-water levels, including tsunamis, to determine facility flooding and structural integrity risks. This chapter also summarizes future MSLR projections developed by the California Ocean Protection Council (OPC 2018) and adopted by the California Coastal Commission (CCC 2015, updated 2018) as official stage guidance for coastal development. The latest MSLR projections from the Intergovernmental Panel on Climate Change (IPCC), Sixth Assessment reports (AR6, IPCC 2021, 2022) are also discussed.

Sea level in this context refers to past measured and future projected mean and extreme (high) water levels, both globally and regionally. Coastal water levels in the San Diego area, including San Onofre, are well represented by data from the La Jolla tide gauge (NOAA Station 941-0230) located at the end of the UCSD/Scripps Institution of Oceanography pier. SONGS area tide and other water level fluctuations are also well represented by data from the Los Angeles (LA) tide gauge (NOAA Station 941-0660) located in Los Angeles Harbor, although the overall historical MSL upward trend is lower at LA than La Jolla.

Figure 2-1 shows the annual and monthly average water levels measured at the La Jolla tide gauge from 1925 to 2021 (black line/symbols, and grey dots, respectively), compared with the global trend (red line) reconstructed by Church and White (2011) from 1880-2009, and extended to 2021 using NASA data (Beckley *et al.*, 2010). Note that the trend of 0.67 ft/century at La Jolla is about 30% greater than the overall global trend of 0.51 ft/century. The acceleration of MSLR about 1970 is also evident, as recognized in the AR6 reports (IPCC 2021, 2022), further considered below.

Regional month-to-month, year-to-year, and decadal water level fluctuations are much larger than corresponding variations in global sea level. This is mainly due to seasonal fluctuations mainly driven by weather changes for the monthly data, as well as El Niño and large-scale oscillations in North Pacific Ocean circulation (e.g., Bromirski *et al.*, 2011, 2012; Flick, 1998, 2016) for monthly, year-to-year, and decadal variability that varies from region to region. Note for example that 2016-2021 annual levels at La Jolla show a small and likely short-term downward trend associated with large scale cooling in the North Pacific.

2.1 SONGS SEA LEVEL INFORMATION

Elwany, *et al.* (2020) introduced new California state agency documents that provide updated MSLR policy, plans, or other information potentially affecting SONGS activities. State agency advances include four reports that essentially laid out the guidance provisions still in effect as of this writing in early 2022. These reports were: Griggs *et al.* (2017) from the California Ocean Protection Council and Ocean Science Trust; Bedsworth *et al.* (2018) titled, “*California’s Fourth Climate Change Assessment, Statewide Summary Report*” from the California Governor’s Office of Planning and Research, Scripps Institution of Oceanography, California Energy Commission, and California Public Utilities Commission; OPC (2018) with update sea level rise guidance; and CCC (2015, updated 2018), which adopted the OPC (2018)

framework as its official policy. Elwany, *et al.* (2021) discusses MSLR vulnerability of the revetment fronting SONGS and an update of the sea level information presented in Elwany *et al.* (2020). This included a summary of existing State of California guidance; 2020 mean sea level (MSL) data, and California state agency documents included CCC (2020a), CCC (2020b), OPC (2020), and CNRA-CEPA (2020). Elwany *et al.* (2022) summarizes the currently existing guidelines applicable MSLR guidance and the newly issued Intergovernmental Panel on Climate Change (IPCC 2021, 2022) findings. These reports are being written to comply with California State Lands Commission Provision 14 in Lease No. PRC 6785.1

2.2 MEAN SEA LEVEL RISE GUIDANCE

Current CCC MSLR guidance (CCC 2015, updated 2018) for coastal development is based on findings from OPC. OPC (2018) developed a set of probability-of-occurrence future MSLR scenarios through 2150, relative to 2000. This study considers the extreme H++ projection scenario from this guidance, and in combination with the 1-, 2-, 10-, and 100-year return period high-water events, which include so-called “King Tides” through 2050. We compare the OPC (2018) guideline scenarios with newly published future MSLR trajectories (also made to 2150), from the latest IPCC reports (AR6, IPCC 2021, 2022). In summary, the IPCC projections are lower than those from OPC.

OPC (2018) contains MSLR projections specific to numerous California coastal areas, including La Jolla. This was part of a statewide effort to improve upon projections from IPCC AR5 (IPCC 2013, 2014) in three respects: First, to produce a low-probability but large-impact extreme high scenario (i.e., H++) that AR5 was missing because consensus could not be reached on future rates of Greenland and Antarctic ice contributions; Second, to assign likelihood probabilities for an array of future MSLR scenarios based on the IPCC AR5 “Representative Concentration Pathway” (RCP) future global socio-economic ranges considered; And finally, to make available regional projections for different parts of the California coast. The OPC (2018) scenarios were adopted by the CCC for their Sea Level Rise Policy Guidance policy document (CCC 2015, updated 2018), which must be considered when applying for a coastal development permit.

MSLR projections are continuously evolving in response to rapid data acquisition and improved scientific understanding of key climate change processes (e.g., IPCC 2021, 2022 for a full discussion). Of special concern are the possible ongoing and future ranges and rates of glacial ice loss in Greenland and Antarctica (e.g., DeConto and Pollard, 2016). Future MSLR is highly uncertain, especially after about 2050, for several reasons. The largest unknown is what mitigation strategies humans will employ to decrease the rates and amounts of greenhouse gas (GHG) emitted and ultimately resident in the atmosphere. Second, the climate sensitivity, or amount and rate of warming for a given increase in GHGs, is not precisely known. In particular, polar ice response to existing and future warming is not yet reliably predictable.

2.2.1 California OPC (2018) MSLR Projections

With one caveat concerning a potential increase in the maximum State of California MSLR guidance target value from 2.8-3.5 ft by 2050 (please see Elwany *et al.*, 2021 for details),

the currently existing guidance, so far unchanged, is summarized herein. OPC (2018) and CCC (2015, updated 2018) MSLR projections for La Jolla from 2000-2050 are listed in Table 2-1. These projections have probability ranges associated with them that originated from IPCC AR5 (2013) by calculating probabilities of each RCP scenario, as mentioned above. Each RCP has a numerical designation condensing a host of projected socio-economic factors into a final average global radiation imbalance in Watts/m² by 2100. The full range is RCP2.6 to RCP8.5, respectively from “Low” to “High.” Thus, for example, “RCP4.2” represents a “Moderate” total GHG trajectory that results in a net radiative Earth heating imbalance 4.2 Watts/m² by 2100. The probability estimates use the framework of Kopp *et al.* (2014).

From 2000-2050, only the “High” MSLR set of trajectories are considered in OPC (2018). This is based on two factors: First, there are no ambitious global GHG emissions reduction plans presently apparent, and second, even if emissions immediately dropped to net-zero, warming and MSLR would continue for at least many more decades owing to ocean warming and ice-melt inertia. In effect, both High and Low trajectories produce near-identical projections between 2000 and 2050, and only begin to differ after mid-century.

Table 2-1 shows five columns (Columns 2-6) headed with percentage probability numbers, and one (Column 7) indicated as H++. Column 2 titled “50%” indicates the median projected MSLR each year (Column 1) relative to 2000. That means, for example, there is a 50:50, or “even” chance that MSLR will be less than or greater than 0.9 ft by 2050, that is from 2.5-3.4 ft, NAVD88² relative to 2000. Columns 3-4 titled “Lo > 67% < Hi” bracket the 2/3 probability that MSLR will fall outside these numbers. In other words, it is 2/3 likely that MSLR will be above the 67% Lo trajectory (Column 3), and 2/3 likely that it will be below the 67% Hi projection (Column 4). Equivalently, it is 1/3 likely that MSL will reach between 3.2-3.7 ft by 2050, and 1/3 likely each that it will remain either below 3.2 ft, or rise above 3.7 ft. Columns 5 and 6, respectively, provide the MSLR path that has a 5%, or “1 in 20,” and a 0.5% or “1 in 200” chance of being exceeded. This means there is only a 1 in 200 chance that MSL will reach or exceed 4.5 ft by 2050. The H++ scenario (Column 7) is included in OPC (2018) to account for the for now still remote possibility that *“...rapid ice sheet loss on Antarctica could drive rates of sea level rise in California above 50 mm/year (2 inches/year) by the end of the century, leading to potential sea level rise exceeding 10 feet. This rate of sea level rise would be about 30-40 times faster than the sea level rise experienced over the last century.”* This suggests there is an unquantifiable, but small, probability that MSL will reach 5.3 ft or higher by 2050 Table 2-1, Column 7).

Figure 2-2 (upper and lower) illustrate the OPC (2018) trajectories described above along with the actual average annual and monthly MSL data measured at the La Jolla tide gauge also shown in Figure 2-1. The projections in Figure 2-2 were adjusted so their average over the 19-year epoch 1991--2009 (centered on year 2000) was 2.5 ft NAVD88 to match the corresponding

² NAVD88 – North American Vertical Datum of 1988 – A fixed geodetic reference for elevations determined by geodetic leveling of the United States, Canada, and Mexico. NAVD88 is currently the official national reference used by engineers and surveyors and supported by NOAA-National Geodetic Service. Geodetic reference elevations do not change with MSL, as opposed to tidal datums, which do.

average value of the observations over the same epoch.³ Figure 2-2 (upper) shows the entire measured water level record from 1925-2021, along with the projections from 2000-2050. Figure 2-2 (lower) is the same information but focused from 2000-2050 to facilitate comparison between data and projections. This shows that all annual average except 2015 so far fall close to or below the 50-50 trajectory (blue broken line). This could be interpreted to mean that the OPC (2018) projections since 2000 overestimate actual MSLR. However, as Figure 2-1 indicates, the natural inter-annual variability range is about 0.5 ft, while the seasonal and other variations in monthly means ranges about 1.2 ft, which is larger than the current difference between the highest and lowest scenarios (~0.4 ft). Which trajectory MSLR is actually on should become more apparent approaching mid-century (2035-2050), when projected values increase significantly and their range broadens to 1-2 ft.

2.2.2 IPCC (2021) MSLR Projections

Following the IPCC (2013, 2014) AR5 reports, and in accord with its approximately -seven-year cycle, the IPCC has prepared the Sixth Assessment Report (AR6, IPCC 2022) scheduled for release in September 2022. Three specialized working groups have contributed to this undertaking, including Working Group I (WGI), which published its findings concerning the “*Physical Science Basis*” in IPCC (2021). The topics assessed by WGI cover: atmospheric GHGs and aerosols; air, land, and ocean temperature changes; climate sensitivity; extreme weather; and hydrological, glacier, ice sheet, ocean, sea level, carbon cycle, and biogeochemical processes. WGI combined modern observations, paleoclimate data, and extensive, international, inter-comparison data-adaptive modeling to build a more robust picture of Earth’s climate and its rapid changes.

The primary conclusion of the WGI (IPCC 2021) report is:

A.1 *It is unequivocal that human influence has warmed the atmosphere, ocean and land. Widespread and rapid changes in the atmosphere, ocean, cryosphere and biosphere have occurred.*

Specific to sea level rise, key findings include:⁴

A.1.7 *Global mean sea level increased by 0.20 m between 1901 and 2018. The average rate of sea level rise was 1.3 mm yr⁻¹ between 1901 and 1971, increasing to 1.9 mm yr⁻¹ between 1971 and 2006, and further increasing to 3.7 mm yr⁻¹ between 2006 and 2018. Human influence was very likely the main driver of these increases since at least 1971.*

A.2.4 *Global mean sea level has risen faster since 1900 than over any preceding century in at least the last 3,000 years. The global ocean has warmed faster over the past century than since the end of the last deglacial transition (around 11,000 years ago).*

³ For details concerning datum adjustments for these purposes please see Flick *et al.* (2013).

⁴ Some conclusions edited or shortened for clarity and brevity. Original report heading numbers retained.

B.5 Many changes due to past and future greenhouse gas emissions are irreversible for centuries to millennia, especially changes in the ocean, ice sheets and global sea level.

B.5.4 Sea level is committed to rise for centuries to millennia due to continuing deep ocean warming and ice-sheet melt and will remain elevated for thousands of years. Over the next 2,000 years, global mean sea level will rise by about 2-3 m if warming is limited to 1.5°C, 2-6 m if limited to 2°C and 19-22 m with 5°C of warming, and it will continue to rise over subsequent millennia (low confidence). Projections of multi-millennial global mean sea level rise are consistent with reconstructed levels during past warm climate periods: likely 5-10 m higher than today around 125,000 years ago, when global temperatures were very likely 0.5°C-1.5°C higher than 1850-1900; and very likely 5-25 m higher roughly 3 million years ago, when global temperatures were 2.5°C-4°C higher.

A vital part of the massive 3,949-page WGI “*The Physical Science Basis*” document (IPCC 2021) is the development of new MSLR projections, both for the global mean trajectory, and for regional trajectories at hundreds of coastal and island locations around the world. Projection data are publicly available, through a creative commons international license, from NASA⁵ (Fox-Kemper *et al.*, 2021, Garner *et al.*, 2021). Inexplicably, only projections from San Diego Bay Quarantine Station and LA are available nearest San Onofre, while La Jolla is absent. While the LA tide regime closely matches that at La Jolla, the overall historical upward MSLR trend at LA (1 mm/yr) is half that at La Jolla (2 mm/yr), over the period of 1925–2020. However, the trends are much more similar from 1975–2021, with 1.6 mm/yr at LA and 1.8 mm/yr at La Jolla. In addition, IPCC (2021) projection trends at other southern California locations and Ensenada, Mexico available on the NASA website suggest that these are at least similar or nearly identical to LA. It is therefore assumed that projections at La Jolla, if they had been made, would be the same as those at LA, so these are utilized in this report.

IPCC uses two conditional descriptors, “*likelihood*,” and “*confidence*” to characterize their conclusions and projections, including, MSLR. “*Likelihood*” gauges the probability spread that a projection will fall in a specified numerical range. Likelihood is quantifiable, and spans high to low (probability) from, “*virtually certain*” (99-100%); “*very likely*” (90-100%); “*likely*” (66-100%); “*about as likely as not*” (33-66%); “*unlikely*” (0-33%); “*very unlikely*” (0-10%); to “*exceptionally unlikely*” (0-1%). “*Confidence*,” on the other hand, is not quantitative or statistical, but a more subjective assessment of how reliable a particular result may be. Confidence levels range from “*very low*,” “*low*,” “*medium*,” “*high*,” to “*very high*.” These terms are based on IPCC “*author teams’ judgments about the validity of findings as determined through evaluation of evidence and agreement*” (Mastrandrea *et al.*, 2010).

Like OPC (2018), the IPCC (2021) MSLR projections are based on an intricate analysis of a wide range of possible future Earth warming scenarios and the processes that contribute to

⁵ <https://sealevel.nasa.gov/ipcc-ar6-sea-level-projection-tool>

MSLR. These include ocean warming and resulting expansion, addition of water from land-based ice melt, changes in freshwater runoff due to global groundwater pumping and dam construction, changes in ocean circulation that affect the dynamical water height at coasts, and land movement such as uplift from glacial unweighting, among others.

AR6 (IPCC 2021) produced future MSLR projections that could be made with at least “*medium confidence*,” or somewhere near the middle of the “confidence” range. The projections were based on five possible future climate evolutions termed “*Shared Socioeconomic Pathway*” (SSP) scenarios that are analogous to, but broader than, the “Representative Concentration Pathway” (RCP) trajectories used in AR5 (IPCC 2013). The MSLR projections are assessed based on the combination of uncertainty in temperature change associated with emissions scenarios, and uncertainty in the relationships between global temperature and processes responsible for projected MSLR. In this context, “*likely*” means a probability of occurrence at least 66%. Each scenario has a low, median, and high MSLR amount associated with it for 2030, 2050, and additional years through 2150 relative to 2004-2005 (adjusted to 2000).

The five IPCC (2021) scenarios are described as follows and involving “*very likely*” (i.e., at least 90% probable) global temperature increases by 2100 above the 1850-1900 median:

- **SSP1-1.9** – Low emissions scenario with net-zero CO₂ by mid-century (~2050). Temperature warming projected as 1.0°-1.8°C by 2100, after a slight overshoot.
- **SSP1-2.6** – Low to moderate pathway with net zero emissions in second half of century (2050-2100). Warming 1.3°-2.4°C.
- **SSP2-4.5** – Moderate scenario in line with upper end of aggregate “Nationally Determined Contribution” emission by 2030. Warming 2.1-3.5°C.
- **SSP3-7.0** – Medium to high “reference” scenario with no additional climate policy (i.e., “business as usual”), resulting in particularly high non-CO₂ emissions, including high aerosols. Warming 2.8°-4.6°C.
- **SSP5-8.5** – High “reference” scenario with no additional climate policy. Emission levels from fossil fueled SSP5 socioeconomic development pathway. Warming 3.3-5.7°C.

A sixth “*low confidence*” but high potential impact scenario projection (“**SSP5-8.5Lo**” herein, where “Lo” stands for “Low Confidence”) added for the first time by IPCC in AR6 indicates the possible, but as yet unlikely, effects of deeply uncertain ice sheet processes supported by limited evidence and little current agreement among experts. The projection uses Greenland and Antarctic findings from a “Structured Expert Judgement” study by Bamber *et al.* (2019), and results from Antarctic marine ice cliff instability simulations by DeConto *et al.* (2021). This scenario is roughly comparable to the OPC (2018) H++ trajectory, albeit with a considerably lower upper range of MSLR.

The IPCC (2021) projections use the 20-yr period 1995-2014 (center years 2004-2005) as their base with MSLR reckoned from there. This is slightly different from the OPC projections, which used a 19-yr base of 1991-2009 (center year 2000). However, the adjustment for the LA

MSLR projections to make their start year 2000 is small, about 0.014 ft, which has been applied in what follows.

This report concerns projected MSLR through 2050. The relevant IPCC (2021) values are summarized in Tables 2-2 and 2-3 and plotted in Figure 2-3. Table 2-2 shows the median MSLR value for each SSP scenario for 2000, 2030, and 2050 in ft, NAVD88. Table 2-3 shows the range low to high for each scenario. Comparison with the OPC (2018) scenarios (Table 2-1, Column 7) shows that the IPCC (2021) SP5-8.5Lo values in 2030 and 2050 (Column 7) are 0.7 ft and 1.9 ft lower, respectively, than the OPC (2018) H++ numbers. Furthermore, Tables 2-2 and 2-3 (Columns 7) suggest that the range from 2000-2050 of the SSP5-8.5Lo scenario is fairly small, with the median value rising 0.8 ft (2.5-3.3 ft), and a low to high range change of 0.6-1.4 ft (2.5-3.1 ft and 2.5-3.9 ft, respectively). Except for the H++ and SSP5-8.5Lo scenarios, the (respective) OPC (2018) and IPCC (2021) trajectories in Tables 2-1 to 2-3 are not directly comparable, since the IPCC SSP scenarios do not have associated probabilities of occurrence, only that they are “*very likely*.” However, the overall results suggest that all IPCC scenarios produce mostly lower, or at most equal, projected MSLR by 2050 than all OPC trajectories, including H++.

Figure 2-3 illustrates the narrow range of likely MSLR from IPCC (2021) between now and 2050. The high, median, and low SSP5-8.5Lo MSLR scenarios are shown with solid red lines. The spread between high and low in 2050 is 0.8 ft (i.e., 3.1-3.9 ft, Column 7). The remaining SSP scenario median value trajectories (broken lines) are labelled only with their numerical value range, and “Conf” indicating “*medium confidence*,” and “Mid” meaning “*median*” values (Table 2-2), as opposed to the “low” to “high” range (Table 2-3). All median values of the lowest five SSP trajectories (Table 2-2, Columns 2-6) fall between the median and low SSP5-8.5Lo projections. Finally, it is apparent that the IPCC (2021) projections more closely fit the actual MSLR data from 2000-2021 compared to the OPC (2018) scenarios.

2.3 SONGS SEA LEVEL EXTREMES

It is important to recognize that water elevation at or around MSL generally does not cause flooding, erosion, or infrastructure damage. Damages almost always occur during times of extreme high water levels that, on the California coast, are driven mainly by coincidence of peak high tides and large storm waves. Elevated water levels due to El Niño and other large-scale oceanographic phenomenon also raise maximum water levels for months to several years. Of course, a continued and likely accelerated MSLR will continuously worsen these effects causing them to become more severe and last longer. For further details, see Elwany *et al.* (2020).

Observed maximum monthly water levels (in ft, NAVD88) published by NOAA for the La Jolla tide gauge are plotted in Figure 2-4, which is updated from Elwany *et al.* (2020). It is apparent that monthly maxima are increasing as sea level rises, which is expected to continue in the future. Table 2-4 lists the six highest maximum monthly water levels observed at La Jolla relative to NAVD88 and NGVD.⁶ The legacy NGVD was useful since it regionally lay close to

⁶ NGVD – National Geodetic Vertical Datum - A fixed geodetic reference for elevations determined by leveling in the United States and Canada. Also known as “NGVD29” or “MSL29.” This is a legacy datum no longer supported

MSL in the past. While NGVD is no longer supported by NGS or routinely employed by surveyors and engineers, it is still beneficial because of its extensive and long use for coastal measurements and studies, including many at SONGS. NGVD lies 0.43 ft below current MSL (as defined by the 1983-2001 epoch), and 2.11 ft below NAVD88.).

The all-time maximum reading occurred on 25 November 2015 during the 2015-16 El Niño warming event, which also produced the highest-ever annual average level observed at La Jolla. Note that the four highest events exceeding the previous record elevation of 1983 occurred in only 18 years, from 1997-2015.

NOAA-NOS also provides statistics of extreme sea levels based on the observations discussed. Their current estimates of “return period,” or the probability of exceeding a given value in any year, are summarized in Table 2-5 relative to NAVD88 and NGVD. Note the relatively small spread of less than 1 ft between the 1% (100-yr) and 99% (1-yr) extreme high water level events. This illustrates the dominant influence of the astronomical tide on extreme water levels along the California coast. The highest tide is about 7 ft above NAVD88, less than about 0.5 ft below the 100-yr return event. It also illustrates the exceedingly rare coincidence of peak high tides with extraordinary storm surges or other water level enhancing processes, such as El Niño, which can raise MSL up to about 1.5 ft over time scales of days to a year (Flick, 2016).

Table 2-1. OPC (2018) MSLR Projections, La Jolla (ft NAVD88).

| 1 | 2 | 3 | 4 | 5 | 6 | 7 |
|-------------|------------|----------------------------|----------|-----------|-------------|------------|
| Year | 50% | Lo > 67% < Hi | | 5% | 0.5% | H++ |
| 2000 | 2.5 | 2.5 | 2.5 | 2.5 | 2.5 | 2.5 |
| 2030 | 3.0 | 2.9 | 3.1 | 3.2 | 3.4 | 3.6 |
| 2040 | 3.2 | 3.0 | 3.4 | 3.5 | 3.8 | 4.3 |
| 2050 | 3.4 | 3.2 | 3.7 | 3.9 | 4.5 | 5.3 |

Table 2-2. IPCC (2021) Mid-Range MSLR Projections, Los Angeles (ft NAVD88).

| 1 | 2 | 3 | 4 | 5 | 6 | 7 |
|-------------------------|-----------------|-----------------|-----------------|-----------------|-----------------|-----------------------------|
| Year⁷ | SSP1-1.9 | SSP1-2.6 | SSP2-4.5 | SSP3-7.0 | SSP5-8.5 | SSP5-8.5⁸ |
| 2000 | 2.5 | 2.5 | 2.5 | 2.5 | 2.5 | 2.5 |
| 2030 | 2.8 | 2.9 | 2.9 | 2.9 | 2.9 | 2.9 |
| 2050 | 3.1 | 3.2 | 3.2 | 3.2 | 3.3 | 3.3 |

Table 2-3. IPCC (2021) Low-High Range MSLR Projections, Los Angeles (ft NAVD88).

| 1 | 2 | 3 | 4 | 5 | 6 | 7 |
|-------------------------|-----------------|-----------------|-----------------|-----------------|-----------------|-----------------------------|
| Year⁸ | SSP1-1.9 | SSP1-2.6 | SSP2-4.5 | SSP3-7.0 | SSP5-8.5 | SSP5-8.5⁹ |
| 2000 | 2.5 | 2.5 | 2.5 | 2.5 | 2.5 | 2.5 |
| 2030 | 2.7-3.0 | 2.7-3.0 | 2.7-3.0 | 2.7-3.0 | 2.8-3.0 | 2.8-3.1 |
| 2050 | 2.9-3.4 | 3.0-3.5 | 3.0-3.5 | 3.0-3.5 | 3.1-3.6 | 3.1-3.9 |

⁷ IPCC (2021) 2004-2005 base year projections adjusted to base year 2000 (see text).⁸ SSP5-8.5 “low confidence” projection conceptually equivalent to OPC (2018) H++ scenario (see text).

Table 2-4. Highest Maximum Observed Total Water Levels, La Jolla (ft).

| Year Month | NAVD88 | NGVD |
|-------------------|---------------|-------------|
| 2015 Nov | 7.62 | 5.51 |
| 2005 Jan | 7.47 | 5.36 |
| 1997 Nov | 7.46 | 5.35 |
| 2012 Dec | 7.42 | 5.31 |
| 1983 Aug | 7.36 | 5.25 |
| 1983 Jan | 7.26 | 5.15 |

Table 2-5. NOAA La Jolla Extreme Water Level Statistics (ft).

| Percent/Yr | Return (Yrs) | NAVD88 | NGVD |
|-------------------|---------------------|---------------|-------------|
| 1% | 100 | 7.43 | 5.32 |
| 10% | 10 | 7.20 | 5.09 |
| 50% | 2 | 6.94 | 4.82 |
| 99% | 1 | 6.51 | 4.40 |

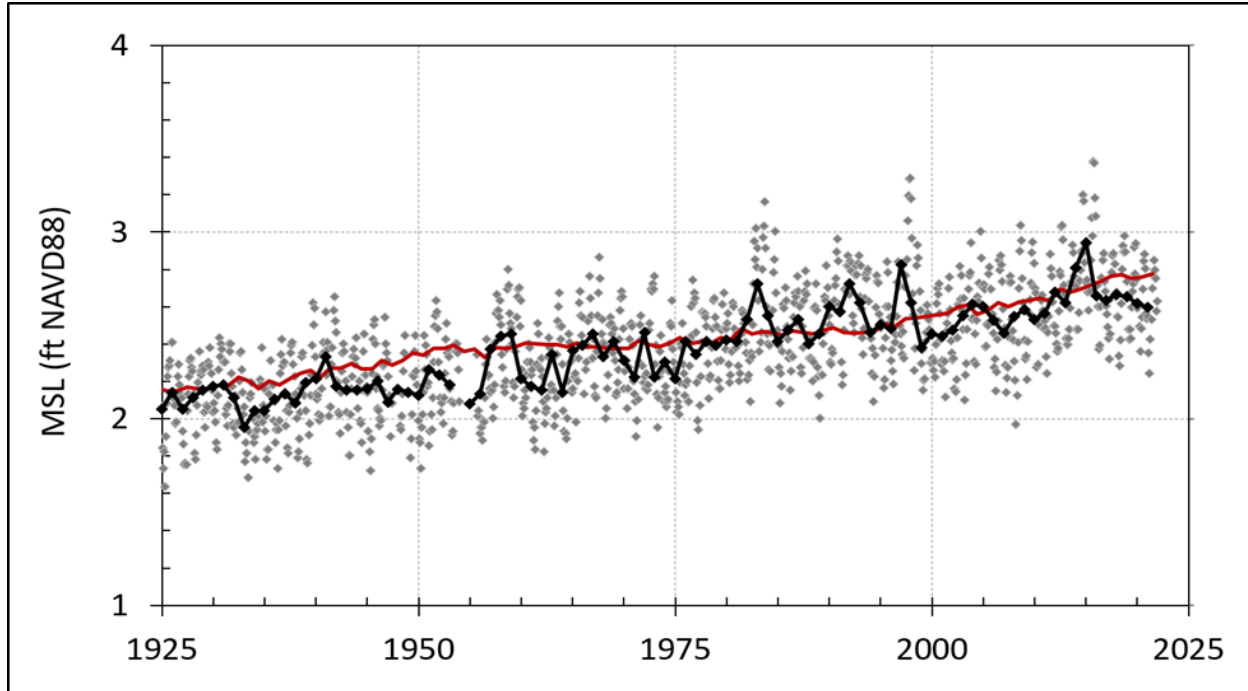


Figure 2-1. Annual and monthly average water level relative to NAVD88 at La Jolla, 1925-2021 (black line/symbols, grey symbols, respectively), and annual global MSL reconstruction (red line).

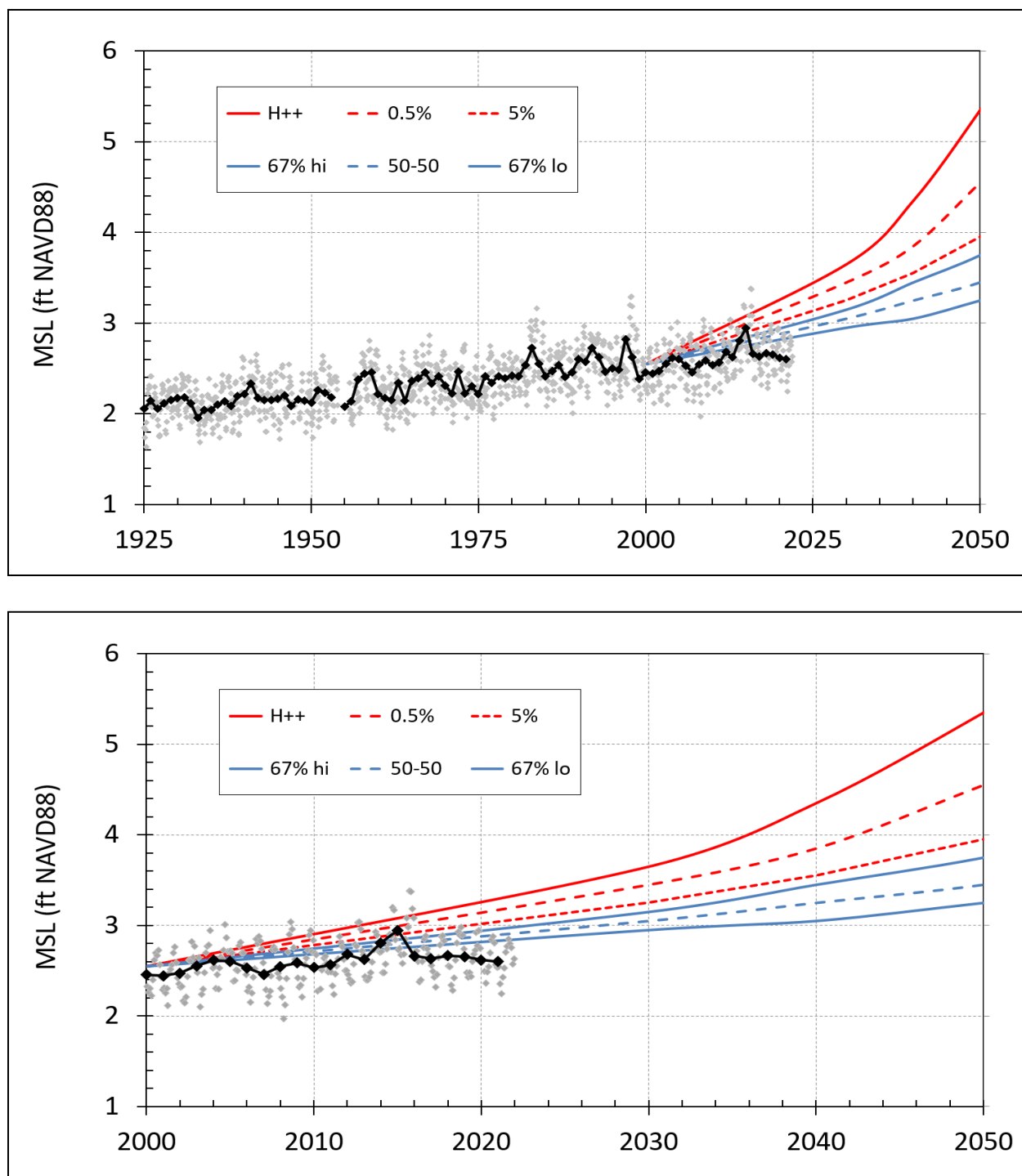


Figure 2-2. La Jolla average MSL data, 1925-2021, annual (black), monthly (grey) (upper). Same for 2000-2021 (lower). Both with OPC (2018) La Jolla MSLR projections, 2000-2050 (see legend and text).

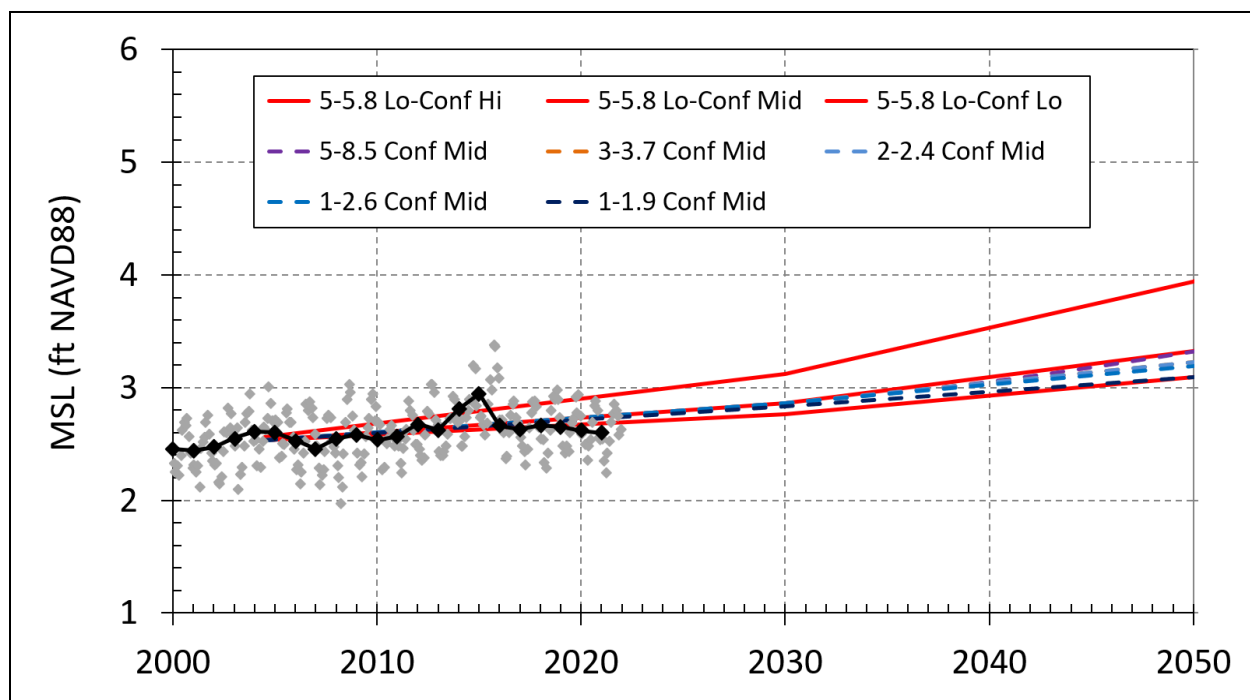


Figure 2-3. La Jolla average MSL data, 1925-2021, annual (black), monthly (grey), with IPCC (2021) LA MSLR projections, 2004.5-2050 (see legend and text).

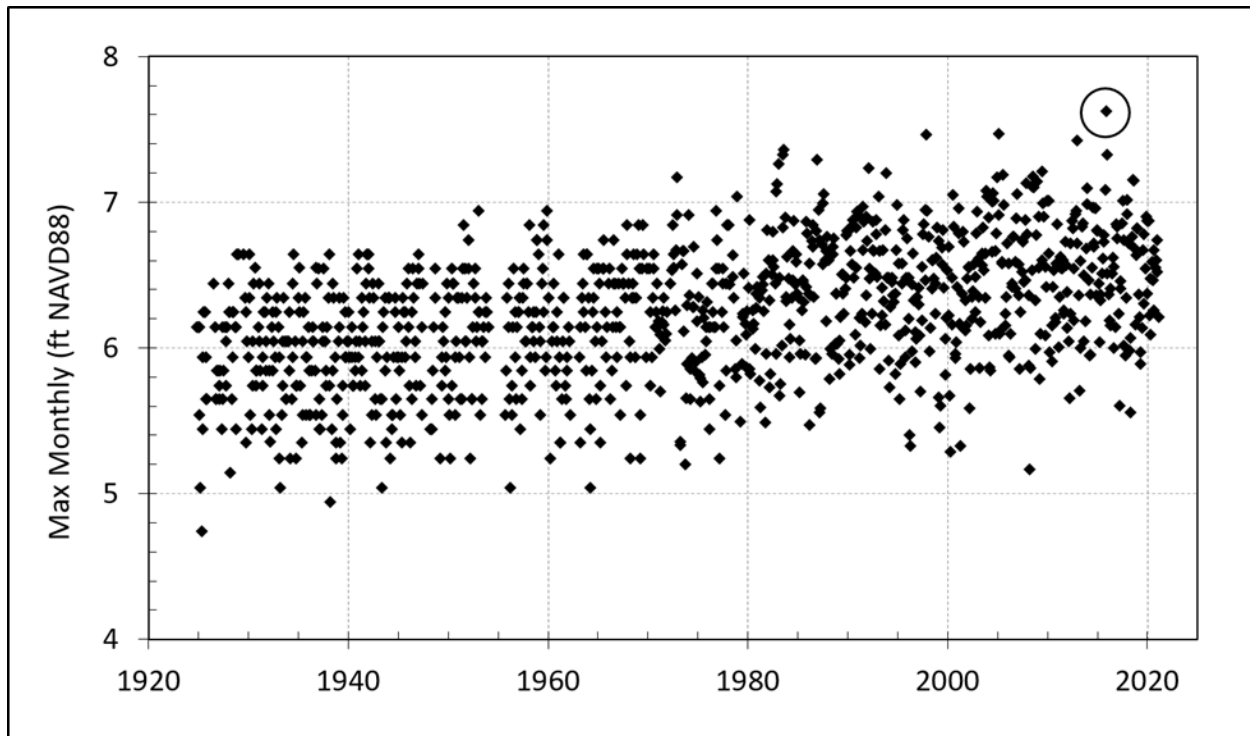


Figure 2-4. Monthly maximum sea level at La Jolla relative to NAVD88 datum, 1925-2021 (black symbols). Maximum observed 7.62 ft height (circled) on 25 November 2015 during 2015-16 El Niño. Note 2020-2021 well below historical maxima (1983-2015).

3.0 BEACH AND CLIFF RETREAT MODEL

We employed the “conditionally decoupled profile model” of Young *et al.* (2014) to project the long-term (2010-2050) sea level rise-driven coastal retreat. The model draws on aspects of complex and sand equilibrium modeling (Wolinsky and Murray, 2009; Ashton *et al.*, 2011) and incorporates these results into a sand balance model specifically adapted for coastal cliffs fronted by beaches subjected to marine and subaerial erosional processes. The model was originally developed with Space and Naval Warfare (SPAWAR) Systems Center Pacific to estimate cliff retreat at MCBCP. Subsequently, the model was also selected and applied to Naval Base Coronado (Chadwick *et al.*, 2014) and along the Los Angeles coast as part of regional efforts to quantify future land loss (USC, 2013).⁹

Coastal recession associated with MSLR is often estimated using “Bruun rule” concepts of equilibrium profile and volume conservation (e.g., Bruun, 1962). The original Bruun rule, designed for low-lying sandy coasts, assumes a fixed, active beach profile during coastal recession, homogeneous coastal material, and no external sand sources or sinks. Although commonly applied (e.g., Zhang *et al.*, 2004), the Bruun rule assumptions are often ignored or not satisfied, prompting criticism (e.g., Cooper and Pilkey, 2004; Pilkey and Cooper, 2004; Woodroffe and Murray-Wallace, 2012). Clifed coasts rarely (if ever) satisfy the original Bruun rule assumptions, leading to the use of modifications, including heterogeneous coastal material, external sand sources and sinks, and variable inland topography (Dean and Maurmeyer, 1983; Hands, 1983; Dean, 1991; Bray and Hooke, 1997; Wolinsky and Murray, 2009).

Young *et al.* (2014) built upon these Bruun rule modifications, recent equilibrium profile cliff modeling (Wolinsky and Murray, 2009; Ashton *et al.*, 2011), and established rock coast concepts to estimate cliff retreat based on coastal system sand balance, process-based relationships, and conditionally decoupled active beach and cliff profiles. The model is specifically adapted for clifed coasts fronted by beaches, but applicable to other coasts where sand balance is important. A primary assumption of sand balance models is attainable sand balance. For cliffs resistant to erosion, these models may force retreat rate results potentially exceeding the maximum physically possible. For cliffs that contain little or no coarse sand, the model is forced to produce unrealistically large or even infinite coastal retreat in the effort to produce adequate sand.

The crucial assumption underlying the Bruun model is that as sea level rises, the geometric relationship between the beach profile and sea level remains constant, all other variables (i.e., wave climate, sand grain size and availability) being equal. In other words, as sea level goes up, the beach cross-section moves upward at the same rate, but also migrates landward, eroding the upland at a rate sufficient to provide just enough sand to maintain the upward shifting profile. The idea is that beaches look essentially the same relative to sea level no matter what the actual sea level. Over long time scales, centuries to millennia, this is a reasonable assumption. Over shorter timescales such as years to decades, the model also assumes that the upland can erode fast enough and contains sufficient sand to maintain the profile. This criterion is readily met in the case of wide beaches where sand from the upper profile moves

⁹ <http://dornsife.usc.edu/uscseagrant/adaptla/>

offshore to raise the active profile, as sea level rises. For narrow beaches backed by sea cliffs, the model also considers the percentage of beach-size sand in the cliffs, and their erodibility.

For each model time step, the active beach profile (defined as extending from the upper active beach limit to the offshore closure depth where no change in profile occurs) shifts vertically by the amount of projected sea level rise, and the sand needed to accommodate the shift is calculated (Figure 3-1). As long as the upper beach is sufficiently wide to provide the needed sand, the beach is “decoupled” from the upland, i.e., the cliff, and marine erosion does not affect it. Marine-driven cliff erosion occurs when the beach retreats landward sufficiently for the active profile to reach the cliff.

Decoupling the active beach and cliff profiles in the Young *et al.* (2014) model allows the beach and cliff to conditionally retreat at different rates. Typical profile adjustments show that initial beach landward shifts can obtain sand balance without marine-driven cliff erosion. When the beach buffer width vanishes, waves begin to erode the cliff base and (ignoring possible lag time) the active beach and cliff profile become coupled, thereafter retreating at the same rate.

Young *et al.* (2014) tested the model by simulating measured historical cliff retreat at Marine Corps Base Camp Pendleton from 1934 to 1998 (Hapke and Reid, 2007) using the associated historical MSLR of (2.5 mm/yr) from the La Jolla tide gauge, and historical sand budgets (Inman and Masters, 1991). Minimum, mean, and maximum historical modeled retreat rates of 0.3, 0.9, and 4.3 ft/yr, respectively, were closely similar to the observed corresponding values of 0.0, 0.7, and 4.4 ft/yr from Hapke and Reid (2007), and well within the observed data error range of ± 0.7 ft/yr. These results suggest that the model and its assumptions are valid for use at San Onofre.

The Young *et al.* (2014) model and other sand-balance-based models predict that cliff retreat increases with decreasing cliff height because taller cliffs provide more beach sand per unit of retreat (holding other variables equal), therefore reducing the amount of retreat needed to reach the modeled sand balance. Highly variable retreat is also an artifact of the modeling approach, which does not include local beach-width smoothing from alongshore sand transport (equilibrium shoreline straightening). A key modification used in this study was to allow sand exchange between profiles to maintain the initial plan-view shoreline configuration, except where seawalls are fixing the shoreline position. Other modifications for this study include enforcing no cliff retreat behind seawalls and allowing the beach profile to shorten (from the landward end) when encountering a seawall, thus deviating from the initial equilibrium profile and causing beach profile submergence in front of seawalls. After the seawalls are removed, the initial active beach equilibrium profile reemerges, presumably very quickly.

3.1 MODEL SCENARIO

The model was run for H++ OPC (2018) MSLR projection, and two seawall scenarios, A and B. Each model run used the same 27 starting profiles. In scenario A, the revetment and seawall remain through 2050. In Scenario B, for theoretical modeling and for purposes of a conservative analysis, the revetment and seawall are assumed to be removed in 2030, and the area behind the walls backfilled. Backfilling is specified to elevation 20 ft NAVD88 for Unit 1

(Transects 223-224), and 30 ft NAVD88 for Units 2 and 3 (Transects 219-222). Seawalls are assumed non-erodible while in place. In Scenario A, beach erosion occurs in front of SONGS, but cliff erosion is limited to adjacent areas north and south, since the revetment and main seawall are assumed to remain unchanged. Scenario B is the same as Scenario A until 2030, when the revetment and seawall are theoretically removed in this hypothetical conservative analysis.

3.2 MODEL INPUTS AND PARAMETERS

The following list contains the key model inputs and parameters applied in our approach:

- 2009 topo-bathy bare earth digital elevation model
- Twenty-seven transect profiles spaced 328 ft (100 m) apart
- One sea level rise curve
- Estimated closure depth of -23 ft NAVD88
- Back shore/cliff sand content 80% based on samples from Young *et al.* (2010)
- Estimated upper active beach elevation of MHHW¹⁰ plus 1.6 ft
- Model shoreline retreat step of 1 ft
- Long-term shoreline retreat projected annually
- Output in (x,y,z) UTM, NAVD88 meters (reported here in feet)
- Enforcement of equal plan shape shoreline retreat across profiles
- Backshore erosion is initiated when waves reach backshore
- Armoring considered 100% effective when in place
- Material behind the seawall is of similar sand content and erodibility as adjacent cliffs
- Back shore sand content does not change as cliff retreat occurs

The model was used to project shoreline and cliff change annually from 2010-2050 on transects spaced 328 ft (100 m) alongshore perpendicular to the shoreline (Figure 3-2). Topographic and bathymetric profiles were obtained at each transect using 6.6-ft (2-m) resolution bare earth digital topo/bathy elevation model from NOAA's Ocean Service (NOS) Office for Coastal Management (OCM, 2013). The primary data source for this elevation at SONGS was topo/bathy airborne LiDAR collected in 2009. The vertical and horizontal accuracy of the elevation is estimated at 0.5 ft and 0.33 ft, respectively.

The initial 2009 topography was assumed to represent an equilibrium shoreline and cliff configuration. Future net alongshore and cross-shore sand movement into and out of the study area was assumed negligible. Future blockage of alongshore sand transport, natural or anthropogenic, will negate this assumption. Future beach replenishment in the study area was not considered. The San Onofre State Beach dirt parking lot to the north of SONGS was assumed erodible and unprotected in future conditions.

¹⁰ MHHW (mean higher high water) is a tidal datum calculated as the average value of the highest observed water level elevations each day over the National Tidal Datum Epoch, a fixed 19-yr period, currently 1983-2001. Tidal datum relationships among each other and relative to geodetic datums, like NAVD88, change with MSL.

Cliff base and cliff top locations at each transect were identified and defined manually. The upper active beach profile elevation subject to regular wave action was assumed to be 7 ft, NAVD88, which includes 1.6 ft of run-up above MHHW. The lower active beach profile offshore extent (closure depth) subject to regular wave action was assumed to be -23 ft NAVD88 (Hallermeier, 1978). The model was run permitting sand exchange between profiles to enforce uniform beach shoreline retreat across all transects within the study area. This constraint preserves the overall shoreline plan shape after the seawalls are removed. This assumption is consistent with the SONGS setting and experience.

A key model assumption is that the areas behind seawalls are assumed backfilled with material similar in beach sand content (80%; Young *et al.*, 2010) and erodibility compared to the *in-situ* cliff material to the north and south of the seawalls, consisting of the San Mateo Formation. The model also assumes removal of all surface and subsurface concrete and other infrastructure. Any deviation from these assumptions could cause notably different model results.

3.3 MODEL RESULTS

Modeled beach profile retreat was 102 ft and 100 ft, while mean cliff retreat was 30.6 ft and 38.2 ft by 2050, for Scenarios A and B, respectively (Table 3-1, Figure 3-3). In Scenario A, where seawalls remain in place, beach retreat at profiles crossing SONGS (Transects 219-221) caused beach submergence. Modeled cliff retreat ranged from 0-84 ft. Modeled cliff retreat varied widely because of differences in initial beach width between transects, and cliff topography (Figure 3-4). Modeled cliff retreat north of SONGS was generally smaller than to the south because of a mostly larger initial beach width. Figures 3-5 and 3-6 show the modeled H++ extreme-scenario cliff retreat for Scenarios A and B at two transects that are representative of the natural formations around the SONGS site: transect 227 located north of SONGS (Figure 3-5) and transect 217 located south of SONGS (Figure 3-6).

Modeled cliff retreat rates near the SONGS site under the H++ extreme-scenario ranged from 0-3 ft/yr from 2010-2050, for both Scenario A and Scenario B. This maximum retreat rate is less than the maximum historical cliff erosion rates of 4.3 ft/yr +/-0.7 ft/yr from Hapke and Reid (2007). In addition, rapid and considerable cliff erosion at MCBCP was documented by Kuhn and Shepard (1984). Taken together, this suggests the modeled maximum rates are locally attainable. Appendix A shows the modeled H++ extreme scenario cliff retreat profiles for Scenario A and Scenario B, respectively. No bluff retreat occurs fronting SONGS while the seawall remains in place, and the two scenarios are remarkably similar, suggesting little difference in erosion between 2030 and 2050.

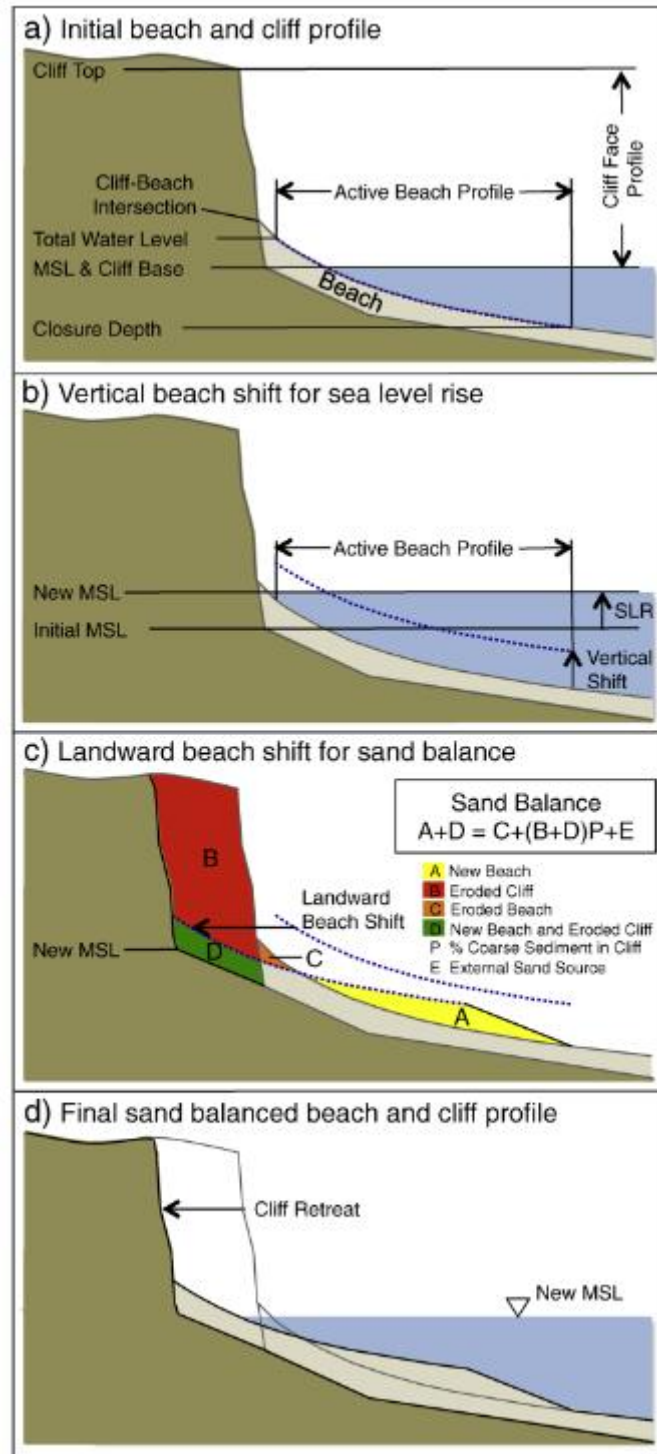


Figure 3-1. Model profile adjustments and erosion from MSLR. (a) Initial profile and active beach bounded by total water level and closure depth. (b) Active beach profile shifts vertically equal to the amount of sea level rise, and (c) landward by maintaining sand balance (d). Figure from Young *et al.* (2014).

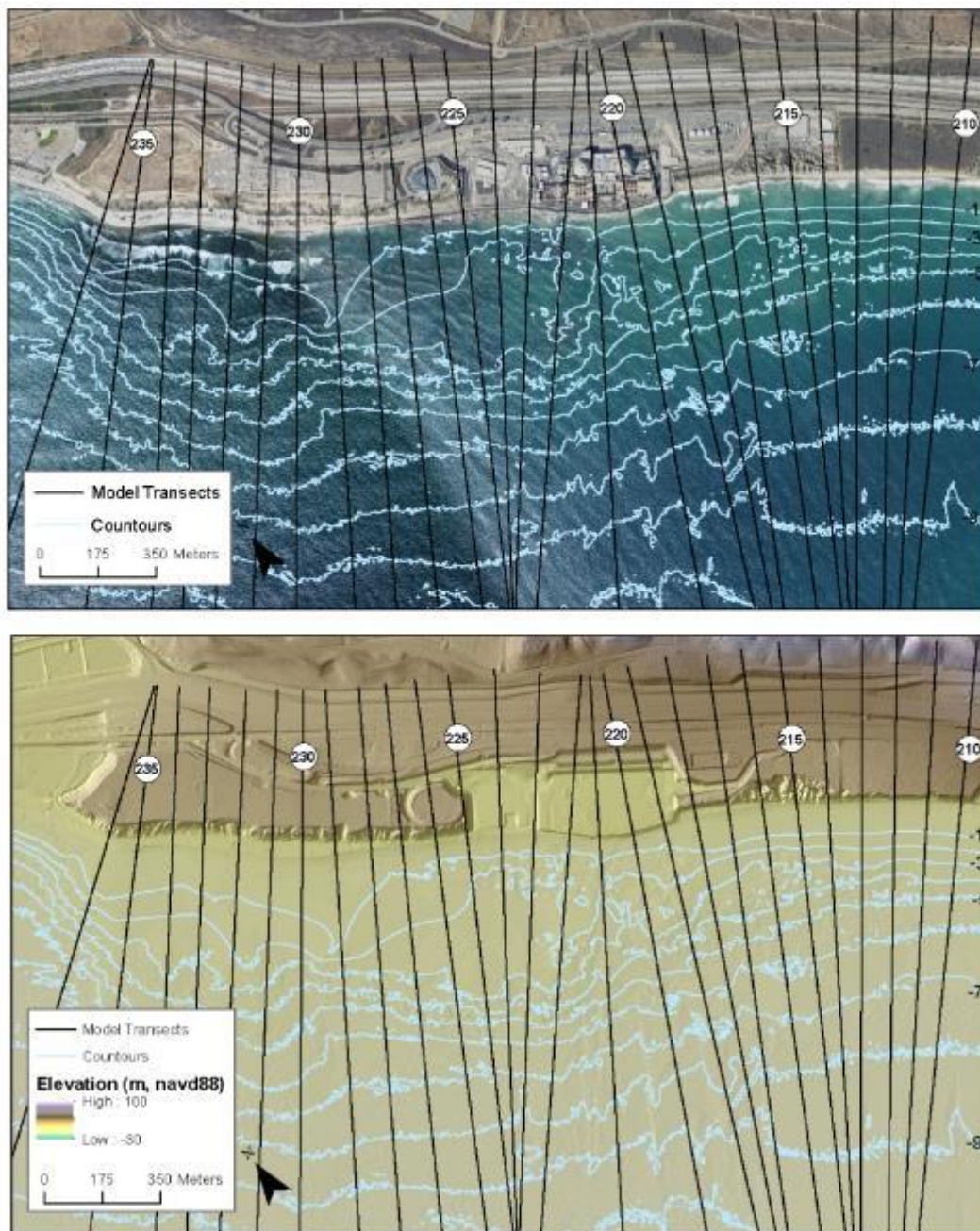


Figure 3-2. Map showing model transects and contours displayed over aerial photograph (top) and the 2009 bare earth digital elevation model (bottom).

Table 3-1. Beach and cliff retreat 2010-2050 (ft).

| Beach/Cliff Retreat (ft) | Scenario A Seawalls Remain | Scenario B Seawalls Removed 2030 |
|---------------------------------|---------------------------------------|---|
| Beach Profile Retreat | 102 | 100 |
| Cliff Retreat Min ^a | 0.0 | 0.0 |
| Cliff Retreat Mean ^b | 30.6 | 38.2 |
| Cliff Retreat Max ^c | 83.6 | 81.6 |

^a Minimum cliff retreat, 2010-2050 at 27 modeled profiles.

^b Mean cliff retreat, 2010-2050 at 27 modeled profiles.

^c Maximum cliff retreat, 2010-2050 at the 27 modeled profiles.

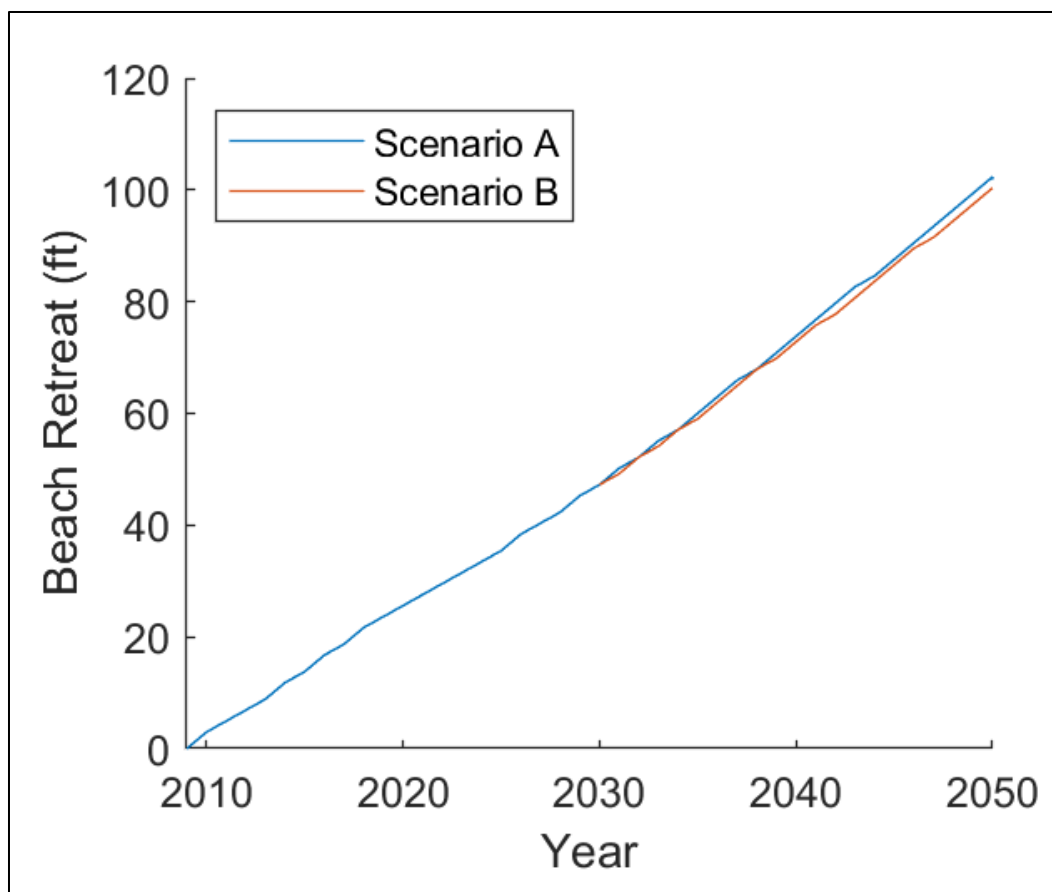


Figure 3-3. Modeled beach retreat on all 27 modeled profiles at SONGS for each scenario.

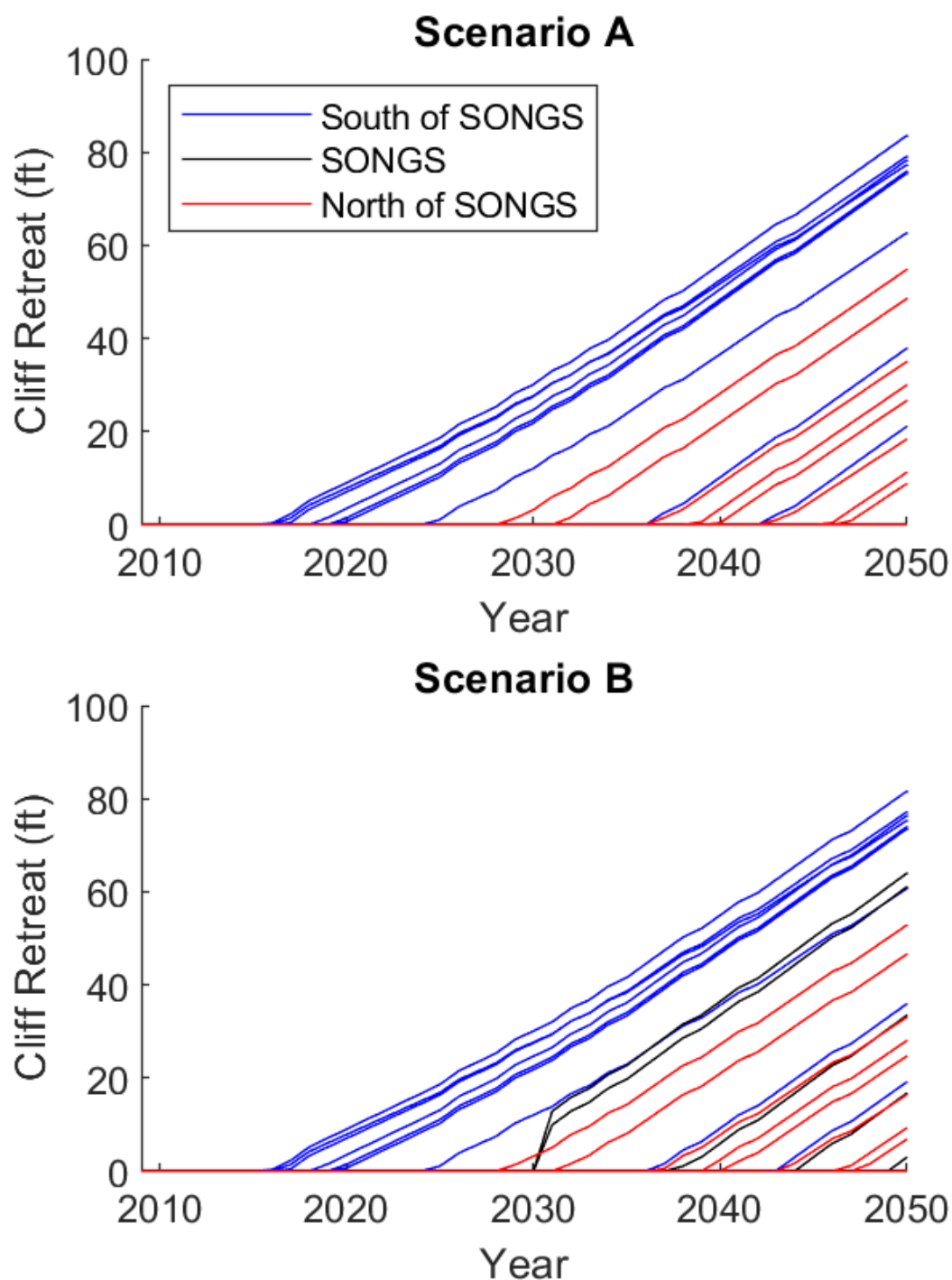


Figure 3-4. Modeled cliff retreat for profiles south of SONGS (blue lines), intersecting SONGS (black lines), and north of SONGS (red lines) for each scenario.

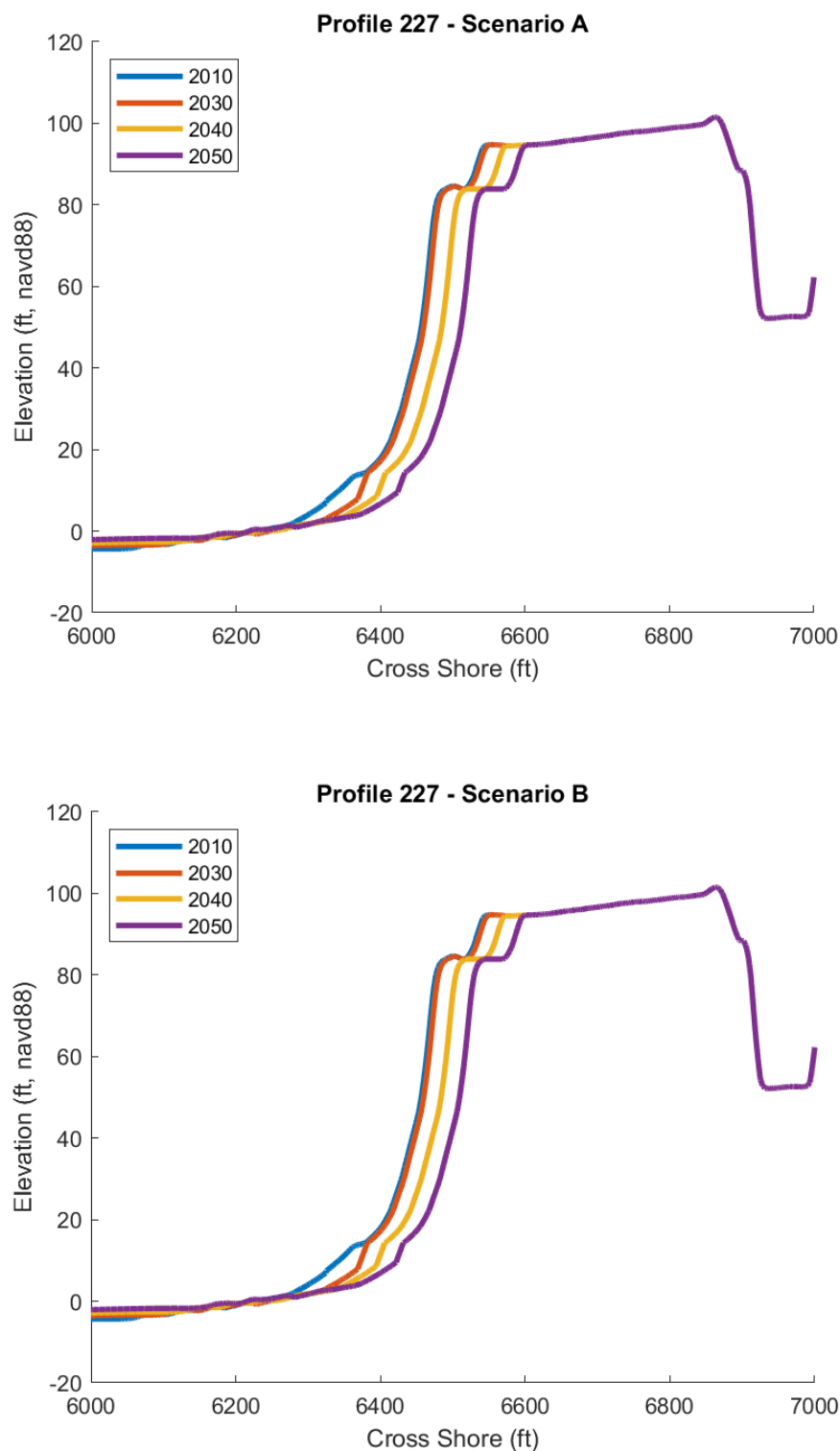


Figure 3-5. Modeled H++ extreme-scenario cliff retreat for Scenarios A and B at transect 227 located north of SONGS. Transect location is shown in Figure 3-2.

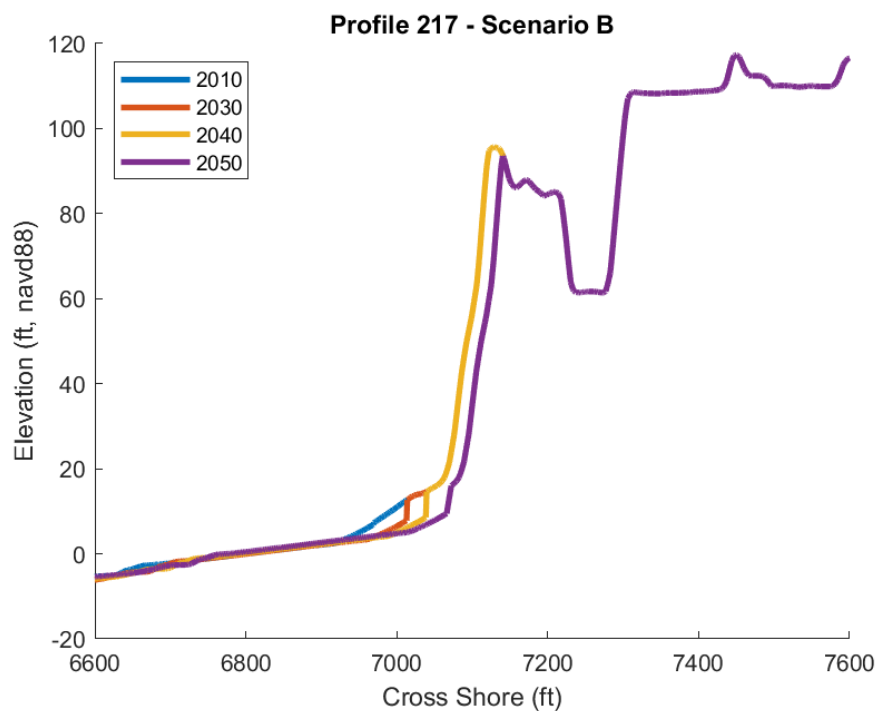
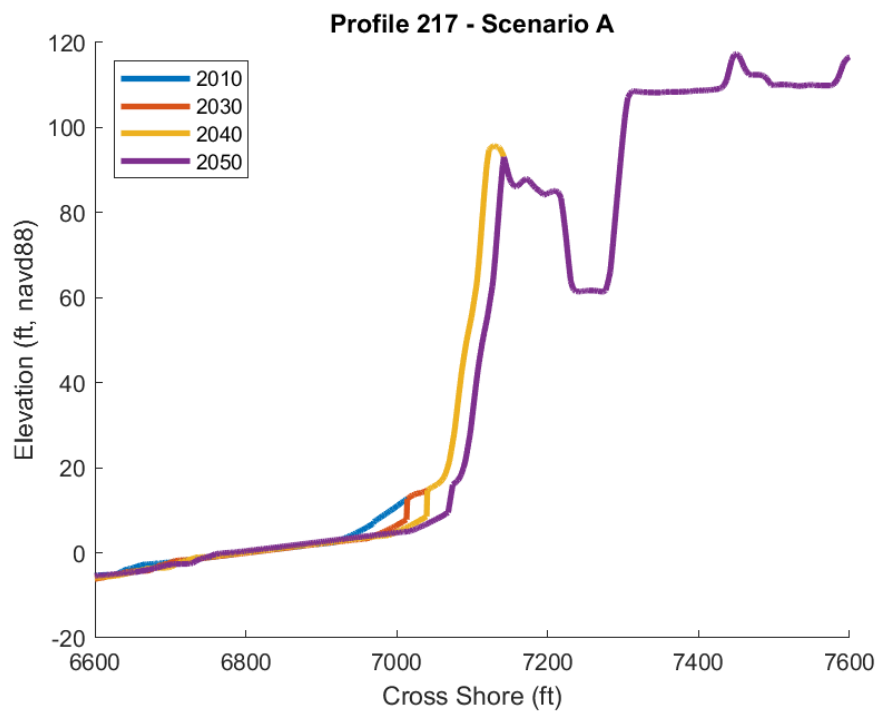


Figure 3-6. Modeled H++ extreme-scenario cliff retreat for Scenarios A and B at transect 217 located south of SONGS. Transect location is shown in Figure 3-2.

4.0 SONGS REVETMENT

4.1 DESCRIPTION OF THE SONGS REVETMENT

The SONGS revetment provides partial front-line protection for the SONGS seawall. It is also essential to maintaining the walkway that enables safe lateral access for beach users. The revetment shelters the walkway from most wave run-up and overtopping, thus preventing or reducing negative impact to lateral beach access due to flooding and other hazards from high water levels and waves, as well preventing direct wave attack on the seawall.

Figure 4-1 is an aerial photograph showing the revetment, which extends about 2,200 ft along the entire length of SONGS, on the beach fronting the walkway. Figure 4-2 is a close-up of the revetment at its southern end. The revetment is constructed of multiple layers of placed riprap of quarry rock “rubble.” A well-known and desirable characteristic of placed rubble structures is their ability to adjust and resettle under wave attack. The advantage of using rock riprap is that it is highly durable and readily available in southern California. Furthermore, due to their rough surface, rock revetments produce less wave run-up and overtopping as opposed to smoothed-faced structures.

4.1.1 Revetment and Walkway Maintenance 2018-2019

Maintenance repairs of the SONGS revetment were done in two phases, with Phase 1 extending from 7 May to 10 October 2018, and Phase 2 from 15 October to 16 December 2019. No substantial maintenance was conducted in 2020 or 2021. During the Phase 1 repairs, SCE first placed additional riprap along 500 linear feet at the southern portion of the public access walkway (Figure 4-3), and then elevated the access ramp to this walkway using imported cobbles and sand. Elevating the south access ramp compensated for sand losses due to wave action that had resulted in an approximately 10-ft lowering of the beach at that location, as well as scouring of the revetment.

During Phase 2 repairs, SCE placed an additional 150 linear feet of imported riprap north of the riprap placed in Phase 1, for a total of 650 linear ft of revetment repair. SCE also added 70 linear feet of riprap in front of the sheet pile seawall closure section at the south end of the public walkway and reinstalled the Vehicle Barrier System at the south end of the walkway. Figure 4-4 shows the south end of the walkway before and after the repair.

4.2 SITE VISIT

Inspection of the SONGS revetment was made by CE on 25-26 February 2021. During this visit, we took photos fronting the revetment at the 21 transects shown in Figure 4-9, and a laser scan survey to construct a digital elevation model (DEM) of the revetment shown in Figures 4-10, 4-11, and 4-12.

4.2.1 Rock Measurement Discussion

Rock revetments, including the one at SONGS, are constructed of rubble of varying sizes that in southern California is generally quarried from the southern end of Catalina Island. The size of individual rocks is expressed by the dimensions of their three axes. The long axis, ‘a’, is the maximum length of the stone (Figure 4-5); the intermediate axis, ‘b’, is the maximum width perpendicular to the long axis; and the short axis, ‘c’, is the height of the stone perpendicular to the plane of the a-axis and b-axis. The size of an individual rock is usually expressed as its b-axis dimension, or alternatively by its calculated or actual weight. Rock weight estimates, which are needed to evaluate riprap stability, are discussed in Section 4.3 below. Histograms of the lengths, widths, and heights of the 80 sample rocks measured at SONGS are presented in Figure 4-6, and their cumulative distributions in percentage are shown in Figure 4-7.

4.2.2 Revetment Laser Scanner Survey

A laser scanner survey was carried out using a Trimble SX10 scanning total station (Figure 4-8) for the purpose of creating a digital elevation model (DEM) to visualize the spatial characteristics of the revetment. Control points were established to aid in subsequent station setups. The revetment was scanned from the beach and the scanner location was determined from the control points. The system scanned in a vertical direction and slowly rotated horizontally to cover the areas of the revetment at a high resolution. A total of 14 scans were carried out to capture the entire SONGS revetment.

The survey on 25-26 February 2021 acquired over 47 million data points, assembled in a “point cloud.” The data set was pre-processed using “Global Mapper” software, which enables the outlier points, and those points likely reflected from the walkway wall, to be removed. The pre-processed data were then graphically presented to show the revetment and adjacent beach. The model results at each of the transects are presented in Appendix B. High water levels from the tide was a limiting factor in obtaining complete coverage from the beach at the southern portion of the revetment. Therefore, some scans were carried out from the top of the revetment near the walkway to fill data gaps.

An advantage of creating a DEM is that the model can be “sampled” to show cross sections and contour maps that would otherwise be difficult or impossible to derive in a reliable way. Twenty-one cross section transects were generated from the DEM at locations shown in Figure 4-9. Results of the revetment laser scanner survey are shown in Figures 4-10 through 4-12 for the 21 transects. For clarity, Appendix B shows the DEM comparison between 2021 and 2020 for each transect. Representative cross sections are shown in Figure 4-13; all 21 transect cross sections are presented in Appendix C. Table 4-1 provides riprap height, walkway wall height, and the revetment slope β for each transect.

The DEM was also used to determine the height of the revetment along its upper edge adjacent to the walkway retaining wall (Figure 4-14). The height of this upper edge varies from about 8 ft to 12 ft (NGVD), a few feet lower than the upper edge of the retaining wall, which lies at about 14 ft. The laser scanner survey clearly described the rock shapes and sizes while the

photographs highlighted the sand and cobble areas on the beach. Aerial photographs of the revetment for the period from 2003 to 2020 are presented in Appendix D.

4.3 RIPRAP ROCK UNIT WEIGHT

Riprap rock unit weights and their variations are essential to estimating the stability of a revetment. Individual rock weight is proportional to volume and specific weight (density) of the stone. The estimation of weight is complicated by the fact that each rock unit is not a simple geometric form, such as a sphere or rectangular shape, like a brick.

Individual rock weight, $W(x)$, was estimated from Equation 4-1, which assumes each rock (x) is equivalent to a sphere with diameter $D(x) = b(x)$, the maximum width perpendicular to the long axis, as described in Section 4.1 above. Dimension ‘b’ is often referred to as rock “diameter.” Then:

$$W_x = \frac{\pi \gamma_s D(x)^3}{6}, \quad (4-1)$$

where γ_s = Specific weight of revetment rock.

Table 4-2 gives the dimensions and weights of each sampled rock. The mean and standard deviations for the length, width, and weight of the rocks are presented in Table 4-3. Percent distribution of rock weights and the cumulative distribution of estimated rock weights are shown in Figure 4-15.

A key design parameter for any revetment is the median rock weight, designated W_{50} . Half of the rocks are heavier, and the other half are lighter than W_{50} . We estimated W_{50} in two different ways using standard coastal engineering practice from the U.S. Army Corps of Engineers (USACE 1994a, 1994b). First, we determined the individual rock weight estimates from each rock diameter, $D(x)$, as described in Equation 4-1. The result was $W_{50} = 600$ kg. Second, we calculated the median diameter of the 80 sampled rocks, which was $D_{50} = 2.5$ ft. We then used this number in place of $D(x)$ in Equation 3-1, which resulted in $W_{50} = 580$ kg, a nearly identical result.

4.4 DESIGN WATER LEVEL

Water surface elevation is dependent on tides, storm surge, and other factors described in Chapter 2. Future water levels also depend on MSLR. These factors are discussed in Section 2.3, and the values of current extreme water levels are given in Table 2-5. Table 2-5 gives the NOAA estimates for the extreme water level for various return estimates. The 100-year return period for surface water elevation at La Jolla is 7.43 ft NAVD88 (5.32 ft, NGVD), while the maximum observed water surface elevation of 7.62 ft NAVD88 (5.51 ft NGVD) occurred on 25 November 2015 during the 2015-16 El Niño warming event.

These estimations include astronomical tide, storm surge, and sea level fluctuations due to normal seasonal heating and cooling, as well as El Niño condition enhancements. They do not include wave setup caused by breaking waves, since tide gauges are located offshore of the surf

zone, and their water level sampling system filters out relatively high-frequency fluctuations such as wave surges. The design water level used for this study is the extreme thus far observed: 5.5 ft (1.7 m) NGVD, or 7.6 ft (2.3 m) NAVD88 (rounded to one significant figure).

4.5 DESIGN WAVE ESTIMATION

Wave run-up can be the dominant contribution to high water levels on beaches, depending on the state of the tide, and the height, direction, and period of the waves, especially during storms. A typical wave storm on the southern California coast has a wave height of about 6.9 ft. The wave record for San Onofre, estimated from measurements at SONGS and a comparison with the Oceanside wave array data between 1978 through 1994, were used to calculate wave height return periods for San Onofre.

The Seasonal Maxima Distribution Model (SMDM), developed by Borgmann (USACE 1988), was selected as the appropriate analysis method to estimate the design wave height at a range of return periods. Monthly wave maxima were extracted from the wave data and split into seasonal sets. The seasonal maximum wave-height distribution functions were calculated for each season and then multiplied together to produce the annual maximum distribution. This distribution function was used to estimate extreme wave-height return periods.

The design wave analysis shown in Figure 4-16 was used to identify the significant wave heights associated with a range of return periods at San Onofre. Wave spectra matching those wave heights were extracted from the UCSD Scripps Institution of Oceanography Coastal Data Information Program (CDIP) database.¹¹ The wave spectra from the selected storms (Figure 4-17) were used to estimate the peak period associated with wave-heights for 5-, 10-, 25-, 50-, and 100-year return periods. The extreme wave height and period information is summarized in Table 4-4.

The largest storm on record between 1980 and 2016 occurred on 18 January 1988. The deepwater wave height was 16 ft with a period of 17 sec (as measured at the CDIP Oceanside buoy). The corresponding wave height at San Onofre was about 12.5 ft approaching the shore from the west. Table 4-5 represents the highest significant wave heights at San Onofre in descending order estimated from the Oceanside buoy wave measurements for summer, winter, and all data.

4.6 SONGS REVETMENT STABILITY ESTIMATION

As outlined above, the median rock weight W_{50} is a key parameter in assessing the stability of a revetment. Hudson's formula (Ahrens, 1981a, Ahrens 1981b; USACE 1984, 1994a,b; BCMELP, 2000) is the standard practice method used to estimate W_{50} necessary for revetment stability:

¹¹ <https://cdip.ucsd.edu>

$$W_{50} = \frac{\gamma_r H^3}{K_D \frac{\gamma_r}{\gamma_w} - 1} \cot \alpha \quad (4-2)$$

Where:

W_{50} = required median armor unit weight,
 γ_r = specific weight of the rock unit, Kg/m³,
 H = wave height at the toe of the revetment,
 K_D = stability coefficient,
 γ_w = specific weight of water at the site,
 α = revetment slope angle from horizontal.

K_D values vary primarily with the shape of the rocks, surface roughness, sharpness of edges, and degree of interlocking. Typically, $K_D = 2.1$. Wave height H at the structure is estimated by shoaling the design waves to the breaking point (H_b). If H_b is less than the wave height at the toe, H_{toe} , of the revetment, we use H_b ; otherwise, H_{toe} is used.

The height of the wave at the toe of the revetment is depth limited. The highest estimated water depth at the toe of the SONGS revetment (D_s) is 5.5 ft + 2.29 ft = 7.79 ft, MLLW, where 5.5 ft, NGVD is extreme water level (Section 4.4) and 2.29 is the difference in elevation between datums NGVD and MLLW.

The water depth at the toe of the structure (D_s) varies as the sea level rises. In 2050, the water depth at the toe of the structure is projected to be 9.79 ft, MLLW (OPC, 2018, Medium-High Scenario) and 10.59 ft, MLLW (OPC, 2018 H++ Scenario). A calculation of the wave height (H) was made from the equation $H = 0.56 \times D_s$ (Thornton and Guza, 1982 and 1983).

Equation 4-2 is used to compute the W_{50} for stable revetment. Table 4-6 gives the values of W_{50} for the MSLR projections (medium-high and H++ at 2020 and 2050).

4.7 ASSESSMENT OF SAN ONOFRE BEACH

The condition of the beach fronting SONGS is significant since it prevents or buffers wave attack of the revetment and retaining wall, which in turn protect the walkway required for lateral beach access. The stability of the SONGS revetment depends on the condition of the beach. Presence of a healthy beach causes waves to break farther seaward of the revetment, thus reducing wave run-up, splashing, and overtopping. The beach also prevents toe scouring that can undermine the revetment and cause rock units to settle. When the beach is narrow, or water level unusually high, or both, waves breaking on the revetment can cause dislocation of individual rocks, which contributes to revetment instability.

Recent beach conditions are defined by the 2017-2020 quarterly profile measurements, which characterize the beach configuration in autumn, winter, spring, and summer seasons. Comparisons with earlier beach profiles dating back as early as 1964 show long-term erosion or accretion tendencies. The main factors controlling erosion or accretion are waves and sand supply. Other contributing factors are the nearshore and offshore bathymetry of the region, particularly any wide, flat shelf areas, and the presence of reefs, all of which limit wave height.

Structures, particularly the SONGS temporary laydown pads used for Units 1, 2, and 3 construction, also influence beach width and stability. In the future, MSLR will cause beaches worldwide to migrate landward and upward. Depending on the state of the backshore, especially its erodibility, beaches may or may not continue to exist. The study documents the complex changes of beach conditions at SONGS and puts these into their Southern California context.

Four beach profile surveys were carried out each year from 2017 through 2021 at SONGS. The results of each survey have been presented in reports by Elwany *et al.* (2021a). Longer-term beach change patterns are characterized by comparing beach widths from these recent surveys to comparable measurements from 1985-1993 sponsored by SCE. The earliest directly comparable data were taken in May 1985, just after the sand release of the SONGS Units 2 and 3 laydown pad (Flick and Wanetick, 1989), and from 1990-1993 (Elwany *et al.*, 1994), 2000 (Elwany *et al.*, 2000), and 2017-2020 (Elwany *et al.*, 2021a). Figures 4-18 and 4-19, and Table 4-7 show the long-term changes of beach width.

The beach profile surveys, and photography programs sponsored by SCE since 1964 have provided valuable information and understanding of the response at San Onofre to beach filling and the construction of stabilizing structures (Flick and Wanetick, 1989; Flick *et al.*, 2010). This insight will be valuable as MSLR accelerates in the future.

4.8 EVALUATION CRITERIA

A “stable” rock revetment must perform satisfactorily in the sense that it functions as designed even though individual rocks may move such that portions or the entire revetment settles or changes slope. Such changes are expected in rock revetments, and as previously noted, and are accounted for in the original design. In short, a revetment is functioning properly if it provides protection as designed and is considered stable if no damage exceeds ordinary maintenance needs. At a minimum, the design must withstand conditions that have a 50% probability of being exceeded during the revetment’s economic life.

Revetment failure can be caused by large dislocation of individual rocks such that they become sufficiently separated to no longer function as a unit to dampen wave attack; or extreme settlement where the height is no longer sufficient to prevent excessive overtopping. In addition, failure of a protective revetment during maximum design conditions, should not result in loss of life or unreasonable repair expenses.

4.9 REVETMENT STABILITY FROM FEBRUARY 2020 TO FEBRUARY 2021

Wave data (wave height, period, and direction) from wave buoy number 46224, located offshore of the City of Oceanside in 238 m water depth, were used to estimate the wave heights and periods in front of the SONGS revetment in 10 m water depth for the period from 1 January 2020 through 28 February 2021. These computed wave heights and periods are shown in Figure 4-20. The wave heights during this period were generally calm except for the periods from 7-9 November 2020 and from 25 January-21 February 2021 (Figure 4-20).

During November 2020 and between 25 January and 21 February 2021, the revetment was subject to large waves with heights varying between 6.6 ft and 14 ft, and with short periods of about 8 seconds. The observed 14-ft waves were higher than the previously estimated wave height for the 100-year-return period of 12.5 ft. Despite the height and duration of these waves, the damage to the revetment and walkway was minimal.

The November 2020 wave event lasted three days and had an average wave height of about 11.3 ft (Figure 4-21). The period from 1 January-28 February 2021 (Figure 4-22) was characterized by a series of large wave storms having an average wave height of about 6.6 ft with maximum wave height of 14.2 ft observed between 25-26 January 2021 as shown in Figure 4-23. The wave period during the wave storms varied between 8 and 12 secs. These wave events offered a good opportunity to examine the stability of the revetment using actual wave storm events.

The damage to the revetment was minor, occurring at two locations, Transects 1 and 10. The revetment damage at Transect 1 occurred at the drainage structure. These wave events impacted the beach fronting SONGS by removing the thin layer of sand covering the cobbles. Some of the cobbles were pushed inshore to the toe of the revetment and between the rocks at even higher elevations. Cobble was thrown onto the walkway in few locations near Transect 10 by waves splashing over the revetment. No damages were observed in the walkway, indicating that the revetment protected the walkway from wave run-up and overtopping.

It is notable from the DEM (Appendix B) that most of the storm-caused rock movement in the revetment occurred at the toe. These changes included movement of a limited number of small rocks by a few feet, exposure of some rocks previously under the sand, and pushing cobbles inshore towards and over the revetment. The changes of large rock locations that constitute the main revetment were insignificant and did not negatively impact revetment stability.

In February 2020, the north portion of the revetment was covered by beach sand. Large waves in early 2021 removed this sand, exposing cobble and more of the revetment rocks that were under the sand (Figure 4-24). The beach changes at San Onofre caused by the January and February 2021 large wave storms were normal and expected. They were typical of what has been observed at other southern California beaches, such as Camp Pendleton, Oceanside, and the City of Del Mar.

4.10 MAINTENANCE AND ADAPTIVE CAPACITY

As described in Section 4.9, the SONGS revetment is currently in good condition and can likely provide wave protection to the retaining wall and walkway through at least 2050. The major threats to revetment stability in the future include wave storms, or clusters of wave storms. As described above, revetment damages depend on the height of waves and the duration of wave attack. Large waves can cause dramatic narrowing and lowering of the beach fronting the revetment, leading to rock settlement and displacement, wave run-up, and overtopping.

Section 4.9 of this study showed that the revetment was capable of withstanding both a single large wave event of 2-4 days and a series of large wave storms. It should be pointed out that the revetment is expected to occasionally sustain future damages larger than were observed during January and February 2021, and therefore the revetment will require occasional maintenance in the future. It is not expected to collapse or fail in a way that would prevent its function if properly maintained. Such damages are expected in rock revetments, as previously noted, and accounted for in the original design such that no damage exceeds ordinary maintenance needs. In this respect, the revetment's adaptive capacity to MSLR is high in the sense that it is currently in a stable condition and has recently been tested by the January-February 2021 wave storms.

For these reasons, it is important to continue monitoring the cross-sections of the revetment at various locations by surveys and photographs (Sections 4.2.1 and 4.2.2), especially before and after large wave storms. It is also important to monitor the beach fronting the revetment and at the north and south of it as described in Section 4.7. In addition to crucial public lateral beach access, the revetment, retaining wall, and walkway also provide additional protection to the main SONGS seawall. It is crucial that these structures remain in place at least until the deconstruction efforts of Units 2 and 3 are completed.

4.11 GROUNDWATER

Groundwater elevation under the ISFSI in 2020 based on quarterly data from nine coastal wells located near the ISFSI, was 2.43 ft NGVD (Elwany *et al.*, 2021). Projections of future groundwater elevations estimated from OPC (2018) medium-high 0.5% (1:200) and extreme H++ MSLR scenarios through 2050, are 4.43 ft and 5.23 ft NGVD, respectively. These elevations are respectively 1.54 ft and 0.74 ft lower, than the bottom of the ISFSI support foundation, which is 3 ft thick, as illustrated in Figure 4-25.



Figure 4-1. Photo of SONGS revetment, 20 August 2018. Northern part of revetment (left) is covered by beach sand.



Figure 4-2. Photo of southern end of SONGS revetment.

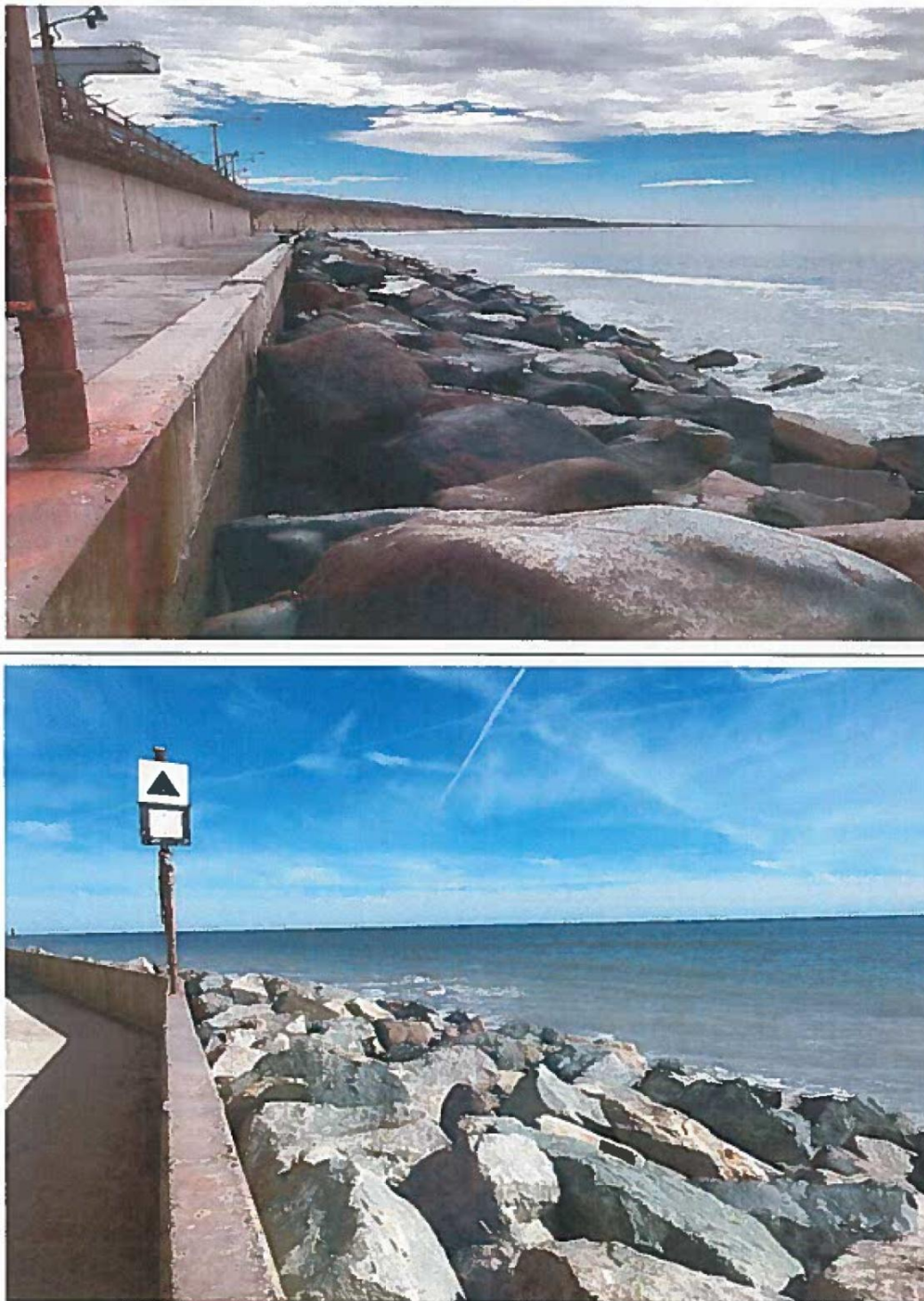


Figure 4-3. Photo of riprap revetment toward south on 20 March 2018 before placement of additional rock (upper). Photo on 17 December 2019 after placement of rock in gaps and settled areas.

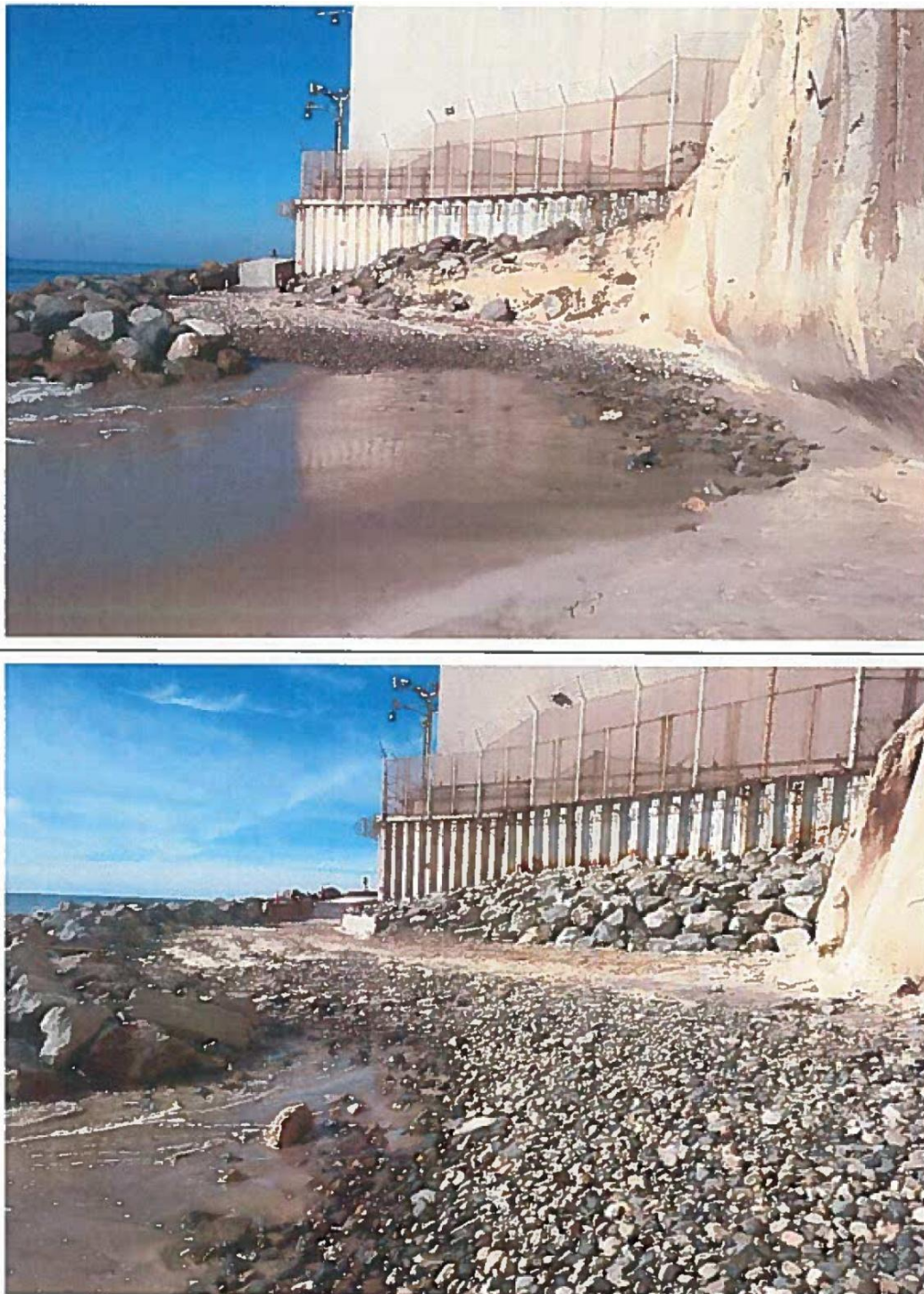


Figure 4-4. Photo of south end of riprap and access walkway on 15 October 2019 before repairs (upper). Photo on 17 December 2019 after repairs (lower).



Figure 4-5. Measurement of long axis (length) of riprap rock.

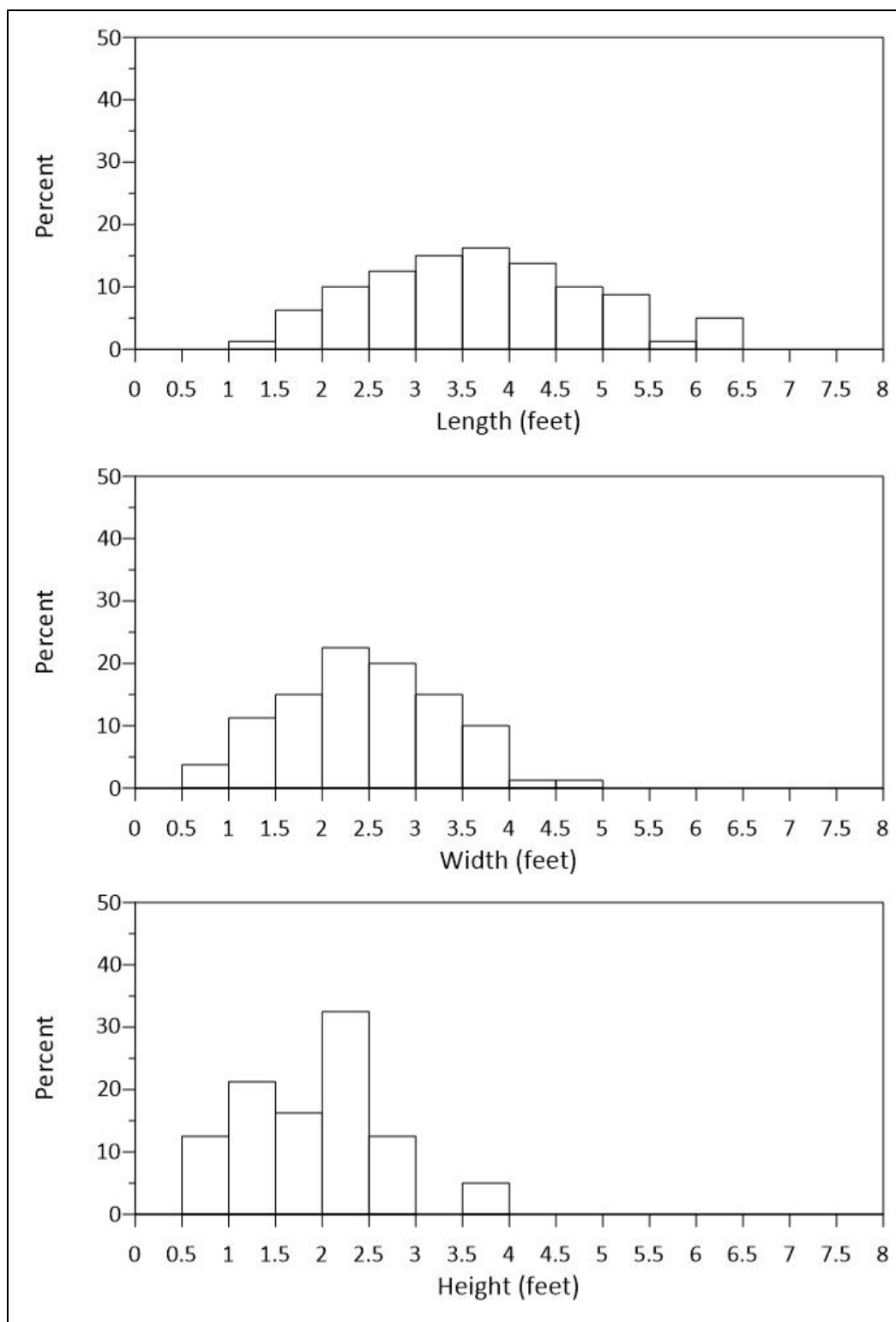


Figure 4-6. Histograms of rock length, width, and height.

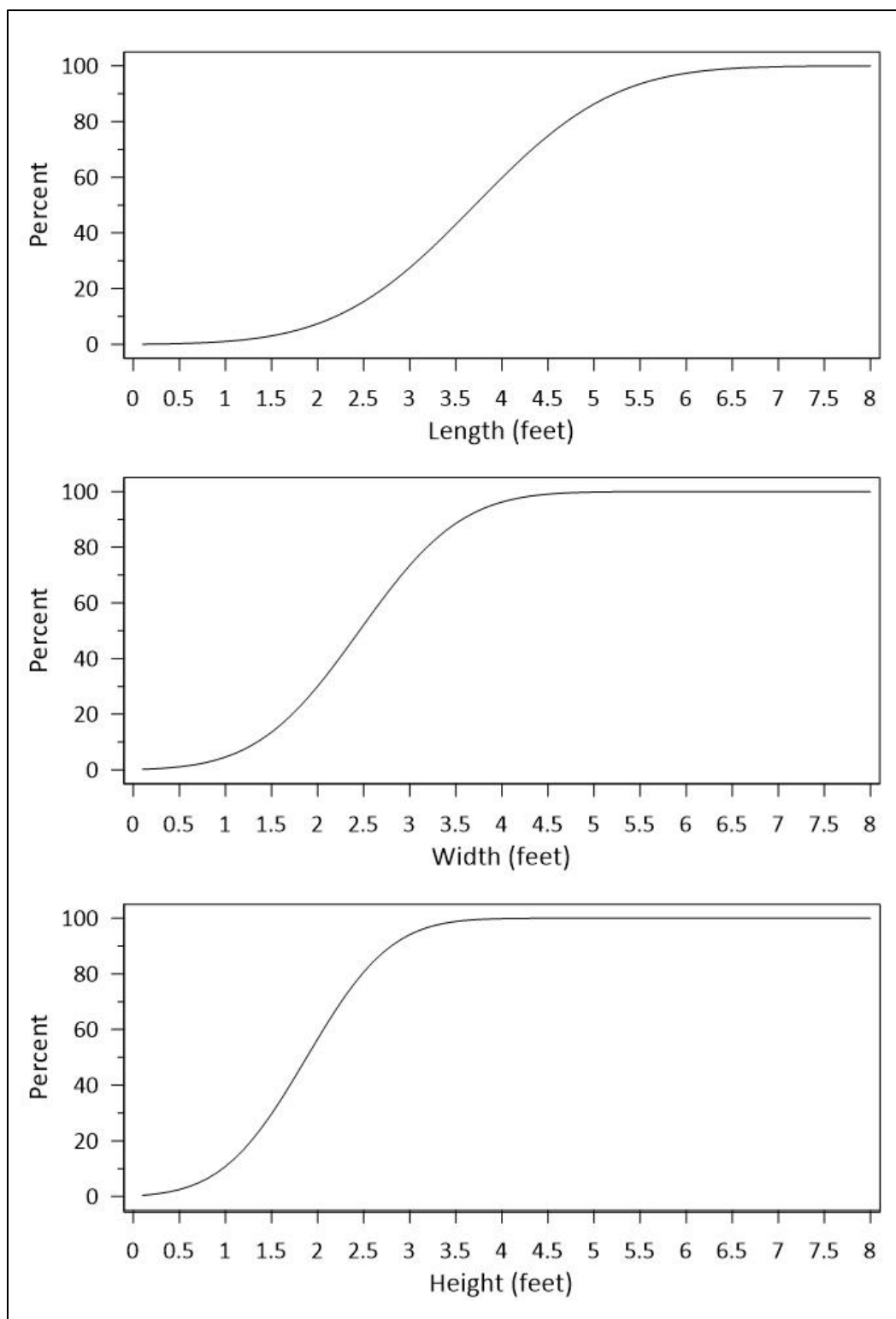


Figure 4-7. Cumulative distributions of rock length, width, and height.



Figure 4-8. Photo of Trimble SX10 scanning total station used by Coastal Environments for SONGS topographic surveys.



Figure 4-9. Location of 21 transects along the revetment, spaced 100 ft apart.

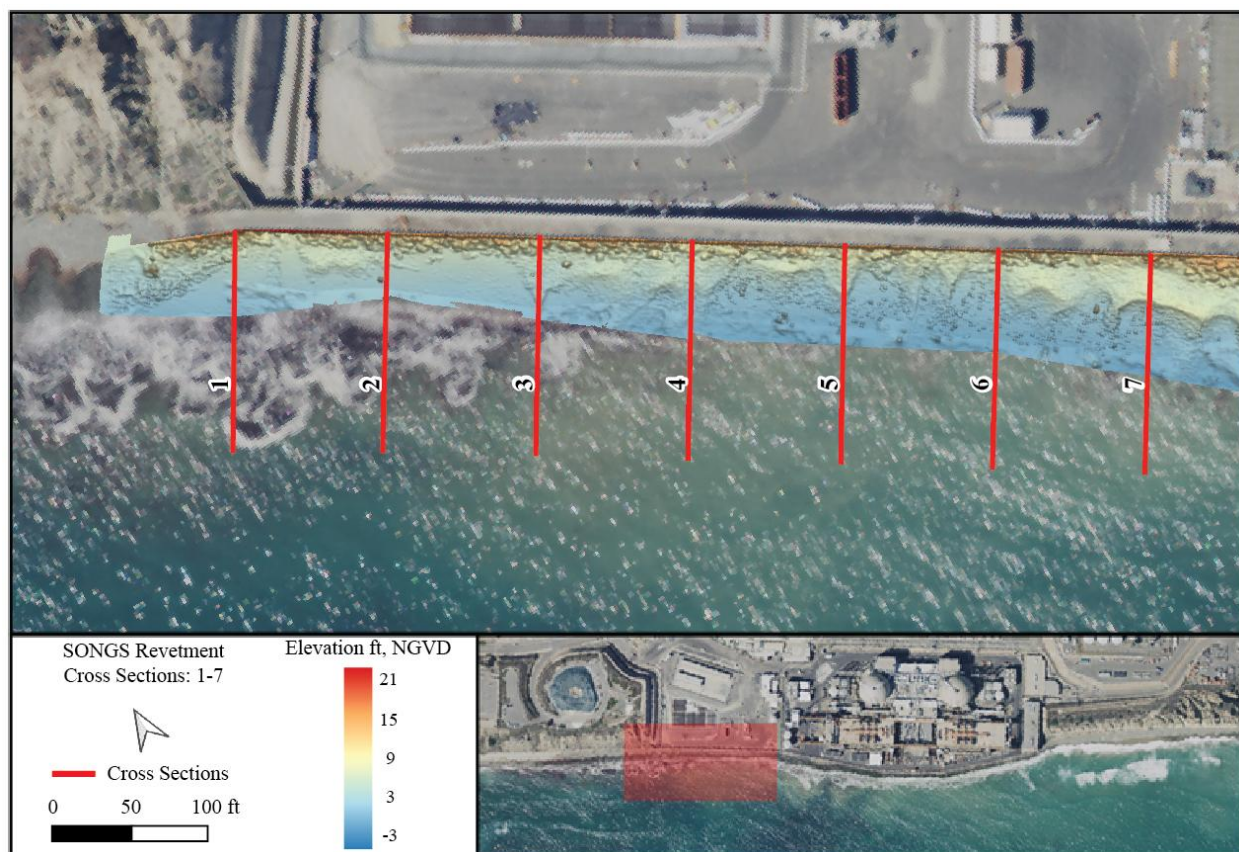


Figure 4-10. Elevation model of SONGS revetment from laser scanner, Transects 1-7.

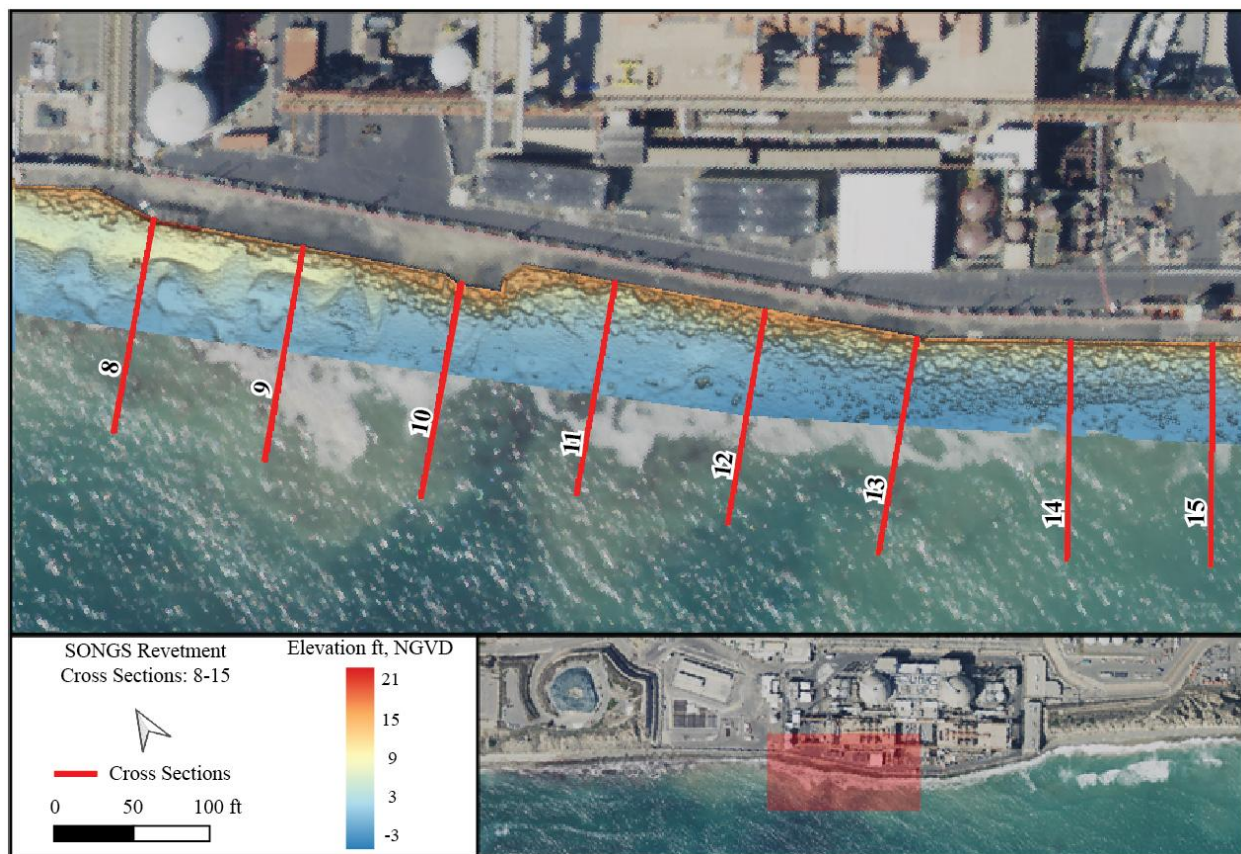


Figure 4-11. Elevation model of SONGS revetment from laser scanner, Transects 8-15.

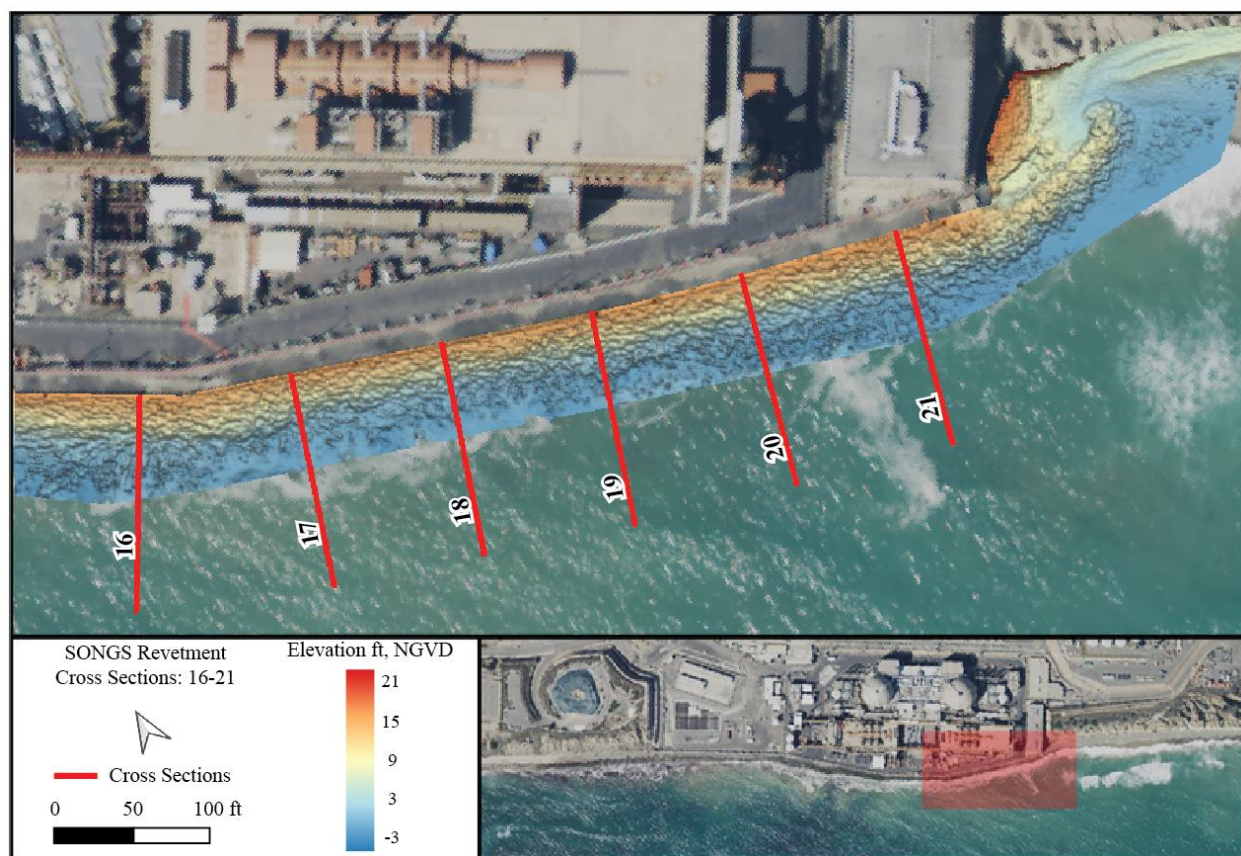


Figure 4-12. Elevation model of SONGS revetment from laser scanner, Transects 16-21.

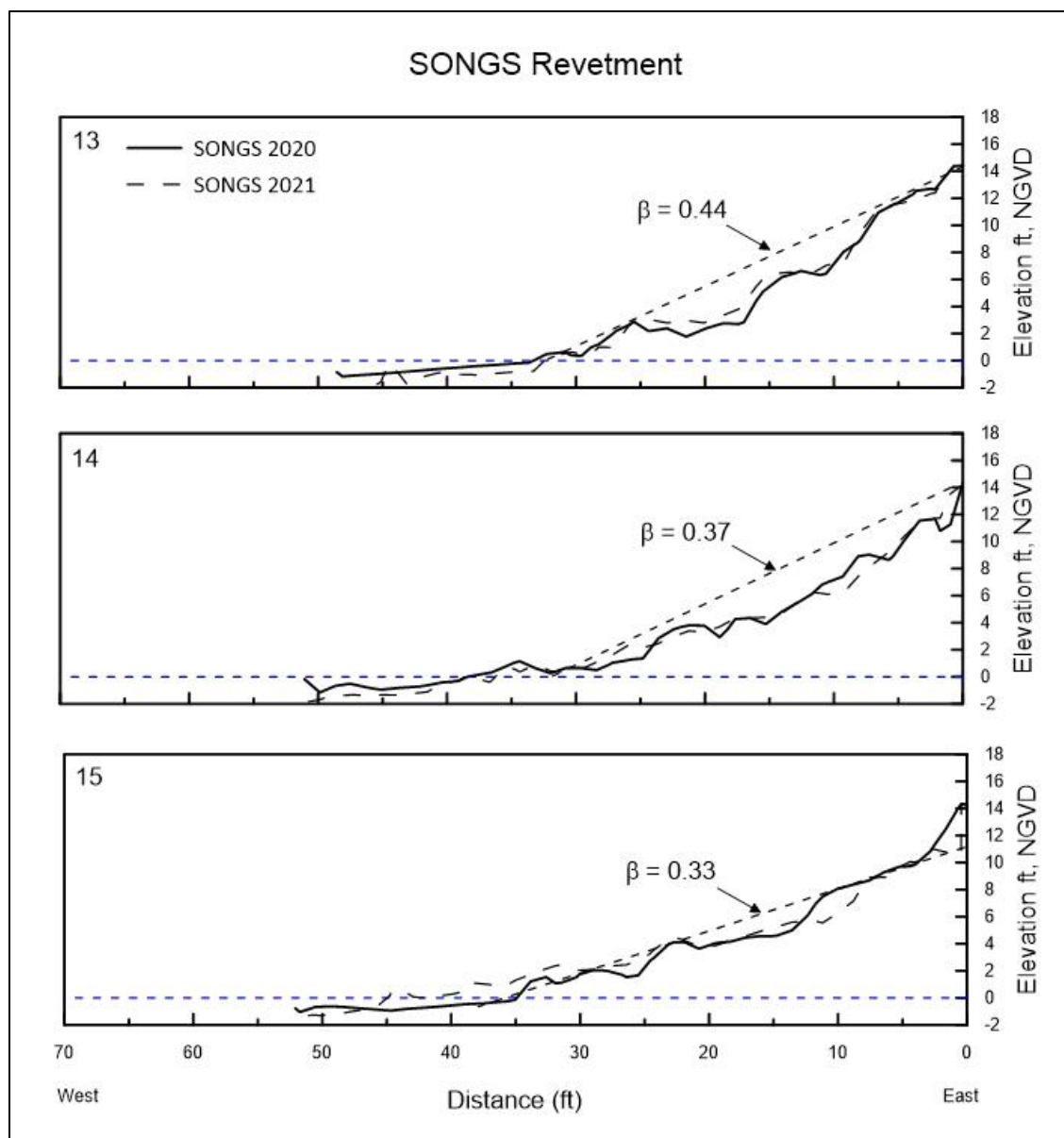


Figure 4-13. Typical revetment cross sections showing slope β at the indicated section.

Table 4-1. Riprap and walkway wall elevations and revetment slope β .

| Transect # | Riprap Elevation (ft NGVD) | Wall Elevation (ft NGVD) | Slope (β) |
|-------------------|---------------------------------------|-------------------------------------|-----------------------------------|
| 1 | 12.89 | 16.79 | 0.90 |
| 2 | 12.27 | 14.27 | 0.66 |
| 3 | 12.15 | 14.27 | 1.52 |
| 4 | 9.22 | 14.32 | 1.13 |
| 5 | 9.44 | 14.27 | 0.35 |
| 6 | 10.13 | 14.2 | 0.43 |
| 7 | 12.48 | 14.34 | 0.67 |
| 8 | 9.55 | 14.39 | 0.20 |
| 9 | 10.59 | 14.29 | 0.38 |
| 10 | 15.12 | 14.39 | 0.46 |
| 11 | 13.69 | 14.34 | 0.40 |
| 12 | 13.63 | 14.39 | 0.54 |
| 13 | 12.37 | 14.39 | 0.44 |
| 14 | 12.34 | 14.37 | 0.37 |
| 15 | 10.34 | 14.34 | 0.33 |
| 16 | 14.24 | 14.21 | 0.42 |
| 17 | 12.98 | 14.27 | 0.38 |
| 18 | 13.58 | 14.22 | 0.39 |
| 19 | 14 | 14.31 | 0.40 |
| 20 | 13.49 | 14.32 | 0.37 |
| 21 | 14.4 | 14.32 | 0.35 |

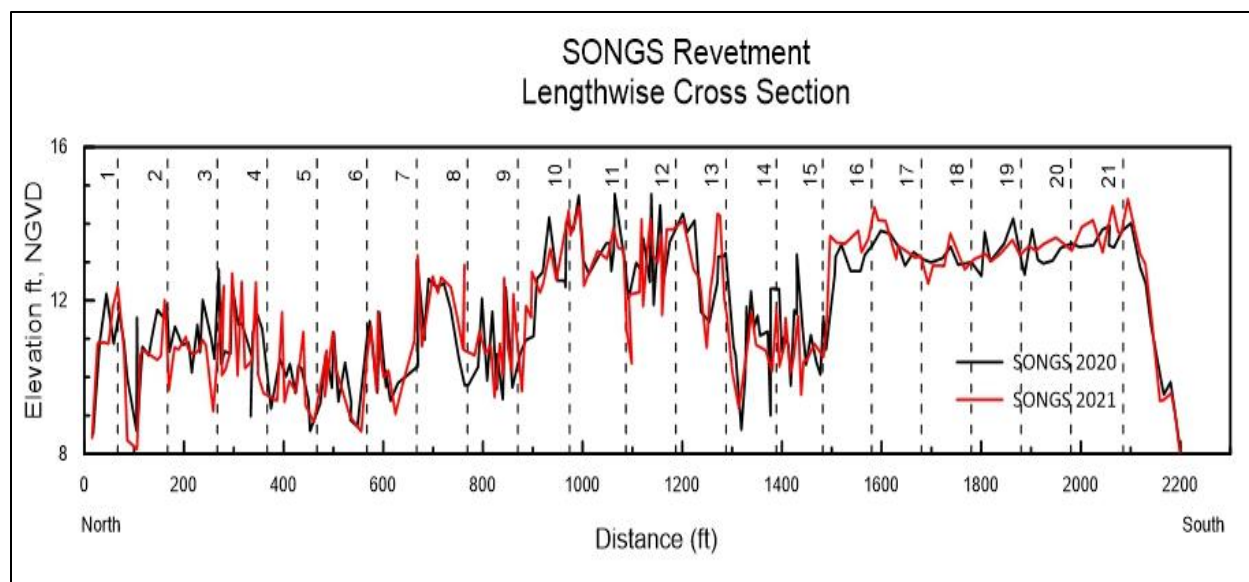


Figure 4-14. Elevation of revetment top at the 21 transects in Figure 4-9.

Table 4-2. Length, width, height, and estimated weight of the measured rocks.

| Rock # | Length (ft) | Width (ft) | Height (ft) | Weight (kg) | Rock # | Length (ft) | Width (ft) | Height (ft) | Weight (kg) |
|---------------|--------------------|-------------------|--------------------|--------------------|---------------|--------------------|-------------------|--------------------|--------------------|
| 1 | 2.6 | 2.1 | 2.0 | 369 | 43 | 3.6 | 2.1 | 2.1 | 369 |
| 2 | 3.3 | 2.4 | 2.7 | 551 | 44 | 4.0 | 2.4 | 2.6 | 551 |
| 3 | 3.3 | 2.9 | 2.1 | 973 | 45 | 4.3 | 2.7 | 3.6 | 785 |
| 4 | 2.0 | 1.8 | 1.4 | 233 | 46 | 3.8 | 2.2 | 3.6 | 425 |
| 5 | 4.8 | 3.9 | 1.8 | 2,366 | 47 | 4.1 | 3.3 | 2.1 | 1,433 |
| 6 | 3.5 | 1.7 | 1.2 | 196 | 48 | 3.6 | 2.5 | 1.5 | 623 |
| 7 | 3.2 | 2.6 | 2.5 | 701 | 49 | 3.9 | 2.4 | 1.2 | 551 |
| 8 | 2.8 | 1.6 | 1.0 | 163 | 50 | 6.3 | 3.4 | 2.3 | 1,568 |
| 9 | 3.2 | 2.4 | 1.7 | 551 | 51 | 5.1 | 2.9 | 2.2 | 973 |
| 10 | 1.9 | 1.0 | 1.0 | 40 | 52 | 2.2 | 1.5 | 1.1 | 135 |
| 11 | 3.5 | 1.9 | 2.0 | 274 | 53 | 2.0 | 1.2 | 0.9 | 69 |
| 12 | 2.0 | 1.5 | 0.9 | 135 | 54 | 2.3 | 1.6 | 1.6 | 163 |
| 13 | 2.6 | 2.3 | 1.1 | 485 | 55 | 4.4 | 2.7 | 2.1 | 785 |
| 14 | 4.3 | 3.5 | 2.5 | 1,710 | 56 | 3.3 | 2.6 | 1.2 | 701 |
| 15 | 3.8 | 2.6 | 1.3 | 701 | 57 | 2.4 | 2.1 | 1.1 | 369 |
| 16 | 2.3 | 1.7 | 1.0 | 196 | 58 | 2.5 | 2.1 | 2.1 | 369 |
| 17 | 5.2 | 3.0 | 1.4 | 1,077 | 59 | 5.5 | 3.7 | 2.7 | 2,020 |
| 18 | 4.3 | 3.9 | 1.2 | 2,366 | 60 | 3.4 | 1.9 | 2.2 | 274 |
| 19 | 5.3 | 3.6 | 3.0 | 1,861 | 61 | 4.2 | 1.7 | 1.9 | 196 |
| 20 | 4.4 | 3.2 | 2.1 | 1,307 | 62 | 2.9 | 1.4 | 2.1 | 109 |
| 21 | 4.3 | 3.5 | 2.7 | 1,710 | 63 | 5.4 | 4.2 | 2.8 | 2,955 |
| 22 | 4.7 | 3.0 | 2.6 | 1,077 | 64 | 2.9 | 1.9 | 2.3 | 274 |
| 23 | 2.6 | 1.4 | 1.5 | 109 | 65 | 5.0 | 3.2 | 1.6 | 1,307 |
| 24 | 4.8 | 3.2 | 1.8 | 1,307 | 66 | 5.8 | 3.3 | 2.0 | 1,433 |
| 25 | 5.2 | 2.9 | 2.3 | 973 | 67 | 6.1 | 3.4 | 3.7 | 1,568 |
| 26 | 3.7 | 2.5 | 2.5 | 623 | 68 | 6.4 | 4.0 | 2.8 | 2,553 |
| 27 | 3.4 | 1.9 | 1.6 | 274 | 69 | 4.2 | 3.7 | 2.9 | 2,020 |
| 28 | 4.6 | 2.2 | 2.1 | 425 | 70 | 6.3 | 3.2 | 2.2 | 1,307 |
| 29 | 4.0 | 3.4 | 2.1 | 1,568 | 71 | 3.0 | 1.1 | 2.2 | 53 |
| 30 | 3.4 | 1.9 | 1.3 | 274 | 72 | 3.4 | 2.2 | 1.3 | 425 |
| 31 | 3.8 | 2.7 | 2.1 | 785 | 73 | 2.2 | 1.1 | 1.3 | 53 |
| 32 | 4.6 | 3.9 | 0.9 | 2,366 | 74 | 1.3 | 1.1 | 0.6 | 53 |
| 33 | 4.3 | 3.2 | 2.3 | 1,307 | 75 | 1.6 | 1.0 | 0.8 | 40 |
| 34 | 4.9 | 2.4 | 2.3 | 551 | 76 | 3.8 | 2.7 | 2.7 | 785 |
| 35 | 3.5 | 2.7 | 2.2 | 785 | 77 | 5.4 | 2.4 | 2.1 | 551 |
| 36 | 2.8 | 2.8 | 1.5 | 876 | 78 | 2.3 | 1.2 | 0.7 | 69 |
| 37 | 3.0 | 2.2 | 1.6 | 425 | 79 | 2.1 | 0.7 | 1.4 | 14 |
| 38 | 3.6 | 1.8 | 0.9 | 233 | 80 | 3.8 | 2.9 | 2.0 | 973 |
| 39 | 4.5 | 3.8 | 3.7 | 2,189 | | | | | |
| 40 | 3.8 | 2.2 | 2.0 | 425 | | | | | |
| 41 | 4.9 | 4.6 | 2.4 | 3,883 | | | | | |
| 42 | 2.9 | 2.7 | 2.4 | 785 | | | | | |

Table 4-3. Mean and standard deviation for rock parameters.

| Rock Parameters | Length (ft) | Width (ft) | Height (ft) | Calculated weight (kg) |
|------------------------|------------------------|-----------------------|------------------------|-----------------------------------|
| Mean | 3.8 | 2.5 | 1.9 | 849 |
| Minimum | 1.3 | 0.7 | 0.6 | 14 |
| Maximum | 6.4 | 4.6 | 3.7 | 3,882 |
| Std Dev | 1.2 | 0.9 | 0.7 | 779 |

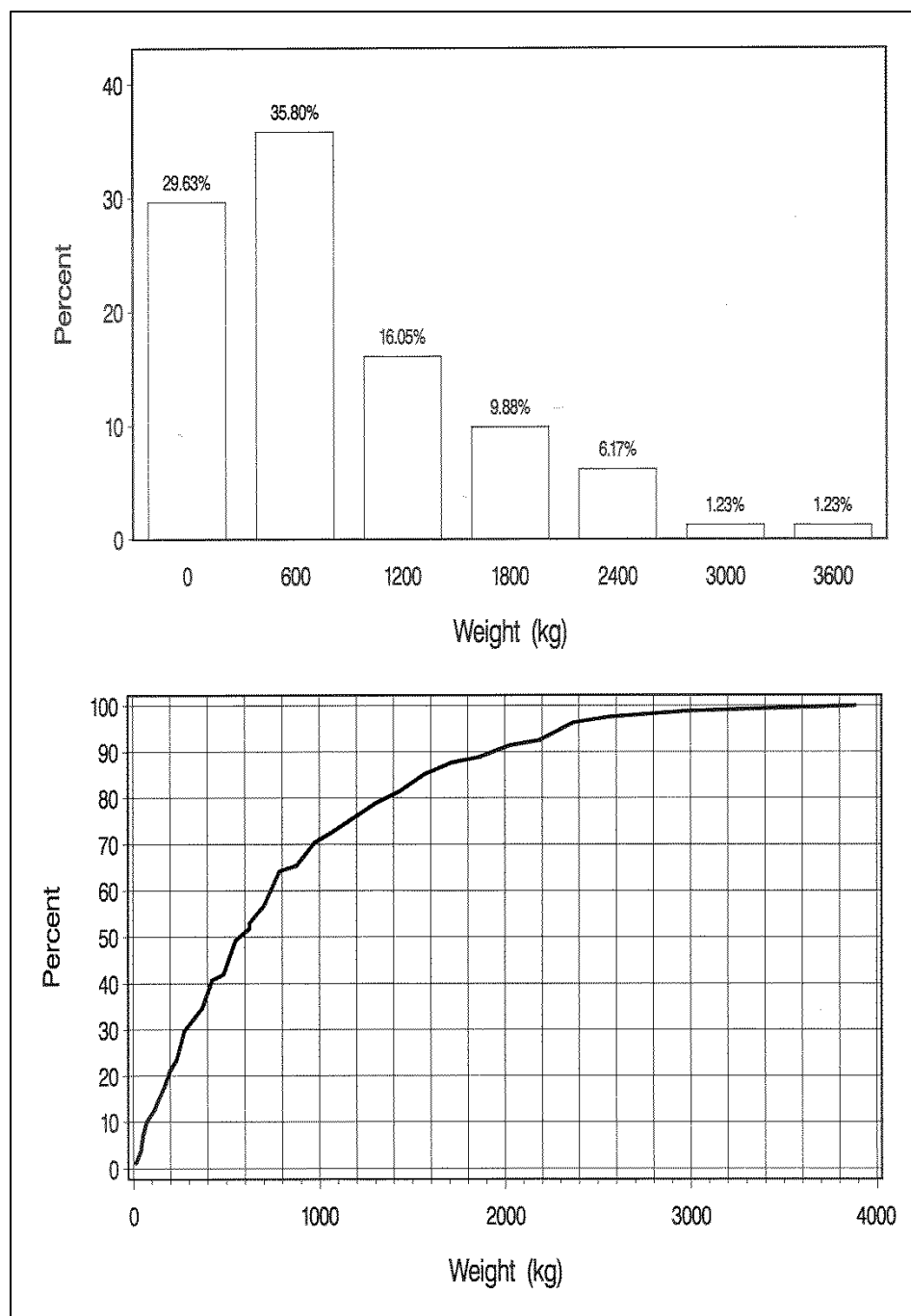


Figure 4-15. Weight distribution of existing SONGS revetment rocks.

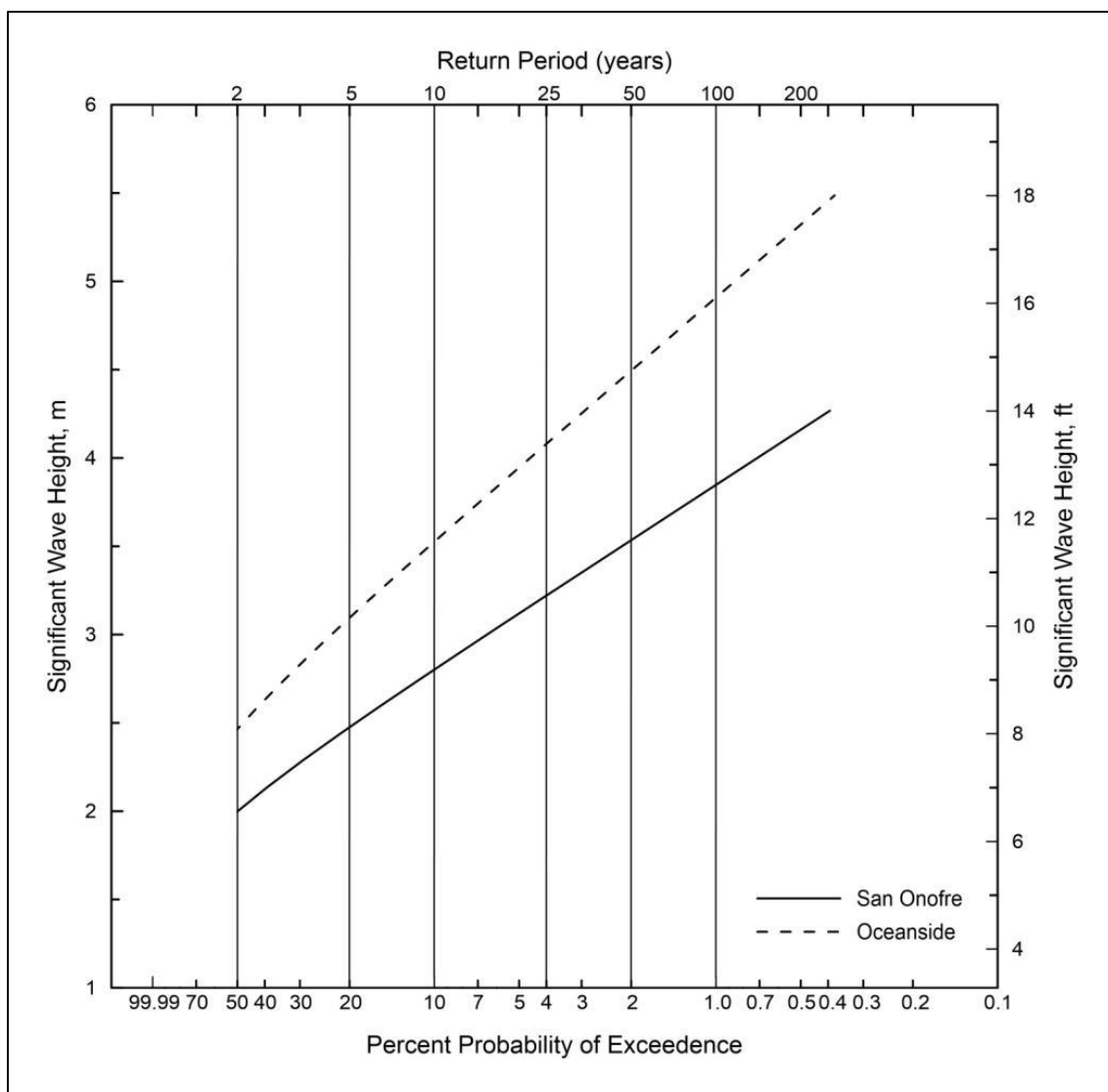


Figure 4-16. Design wave heights for various return periods at San Onofre.

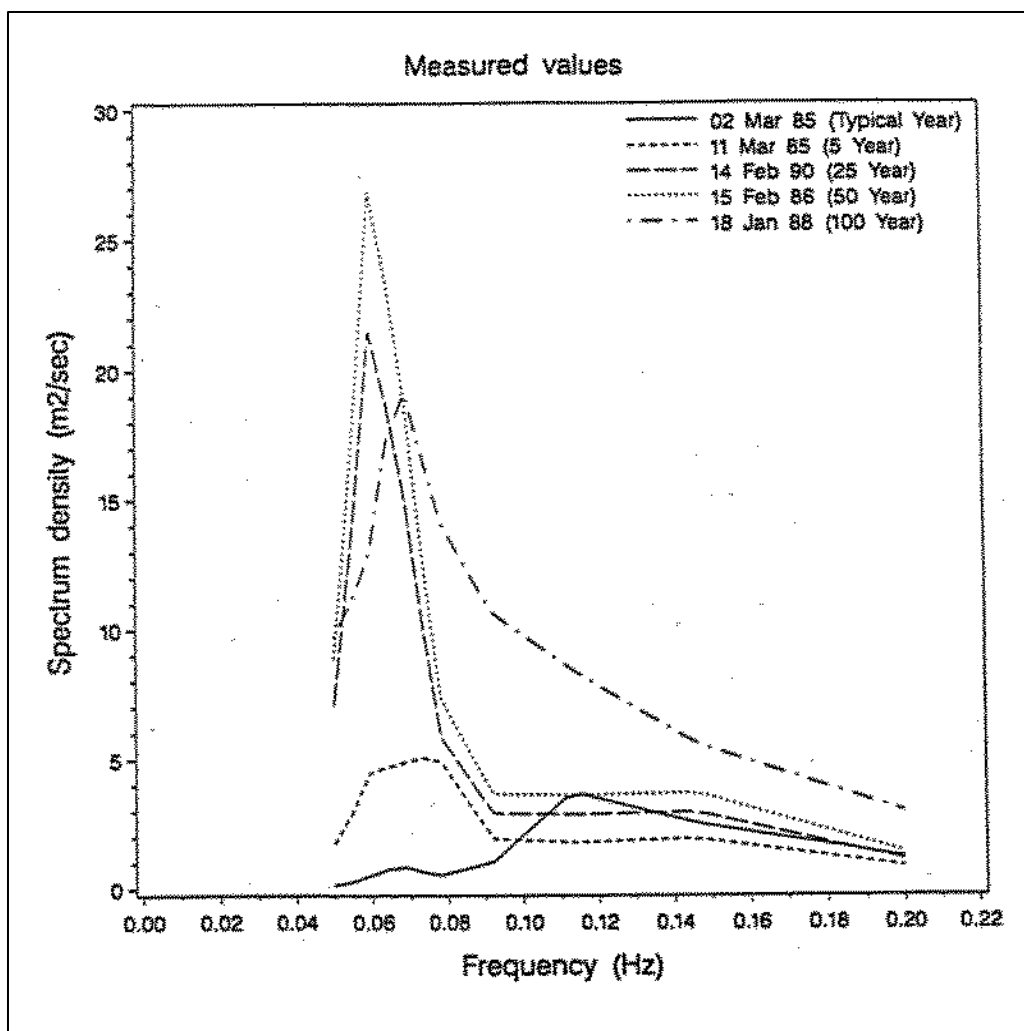


Figure 4-17. Measured wave spectral density for various storms.

Table 4-4. Design wave characteristics at San Onofre.

| Storm Return Period (yrs) | Significant Wave Height Hs (ft) | Peak Period Tp (sec) |
|--------------------------------------|--|---------------------------------|
| 2 | 6.6 | 9 |
| 5 | 7.9 | 12 |
| 10 | 9.2 | 12 |
| 25 | 10.5 | 17 |
| 50 | 11.5 | 17 |
| 100 | 12.5 | 16 |

Table 4-5. Largest 20 waves at San Onofre ranked in descending order (1976-1994).

| Rank | Winter | | Summer | | All | |
|------|---------|-----------|---------|-----------|---------|-----------|
| | Hs (ft) | Tp (secs) | Hs (ft) | Tp (secs) | Hs (ft) | Tp (secs) |
| 1 | 12.63 | 14.2 | 6.59 | 8.0 | 12.63 | 14.2 |
| 2 | 10.76 | 12.8 | 5.77 | 8.5 | 10.76 | 12.8 |
| 3 | 9.45 | 14.2 | 5.68 | 7.1 | 9.45 | 14.2 |
| 4 | 9.45 | 8.5 | 5.58 | 8.5 | 9.45 | 8.5 |
| 5 | 8.27 | 12.8 | 5.38 | 16.0 | 8.27 | 12.8 |
| 6 | 7.91 | 8.5 | 5.38 | 8.3 | 7.91 | 8.5 |
| 7 | 7.74 | 8.5 | 5.25 | 7.5 | 7.74 | 8.5 |
| 8 | 7.58 | 7.5 | 5.22 | 7.1 | 7.58 | 7.5 |
| 9 | 7.42 | 6.7 | 4.99 | 8.5 | 7.42 | 6.7 |
| 10 | 7.38 | 12.8 | 4.92 | 7.5 | 7.38 | 12.8 |
| 11 | 7.38 | 12.8 | 4.82 | 8.0 | 7.38 | 12.8 |
| 12 | 6.96 | 12.8 | 4.82 | 9.5 | 6.96 | 12.8 |
| 13 | 6.76 | 7.5 | 4.72 | 14.2 | 6.76 | 7.5 |
| 14 | 6.76 | 14.2 | 4.72 | 7.5 | 6.76 | 14.2 |
| 15 | 6.76 | 12.8 | 4.66 | 7.5 | 6.76 | 12.8 |
| 16 | 6.73 | 14.2 | 4.66 | 7.5 | 6.73 | 14.2 |
| 17 | 6.69 | 7.5 | 4.66 | 16.0 | 6.69 | 7.5 |
| 18 | 6.66 | 9.1 | 4.63 | 6.7 | 6.66 | 9.1 |
| 19 | 6.66 | 7.5 | 4.63 | 9.8 | 6.66 | 7.5 |
| 20 | 6.66 | 14.2 | 4.63 | 16.0 | 6.66 | 14.2 |

Table 4-6. Rock weights (W_{50}) needed for revetment stability, 2020 and 2050.

| Year | MSLR Scenario | Water Depth (ft) | Design Wave Height (ft) | Rock Weight W_{50} (kg) |
|-------------|----------------------|-------------------------|--------------------------------|---|
| 2020 | -- | 7.8 | 4.4 | 276 |
| 2050 | 1:200 (0.5%) | 9.8 | 5.5 | 548 |
| 2050 | H++ | 10.6 | 5.9 | 685 |

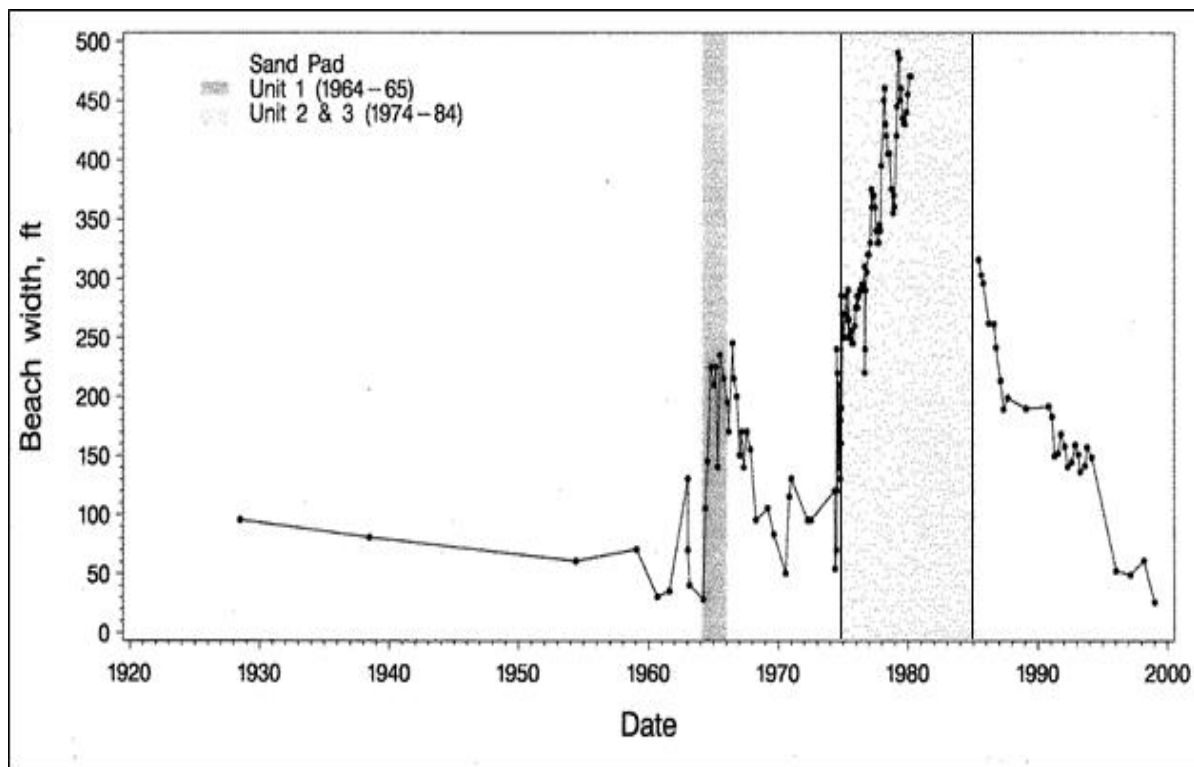


Figure 4-18. Historical beach width adjacent to Unit 1, 1928-2000. Vertical columns show periods when laydown pads were in place.

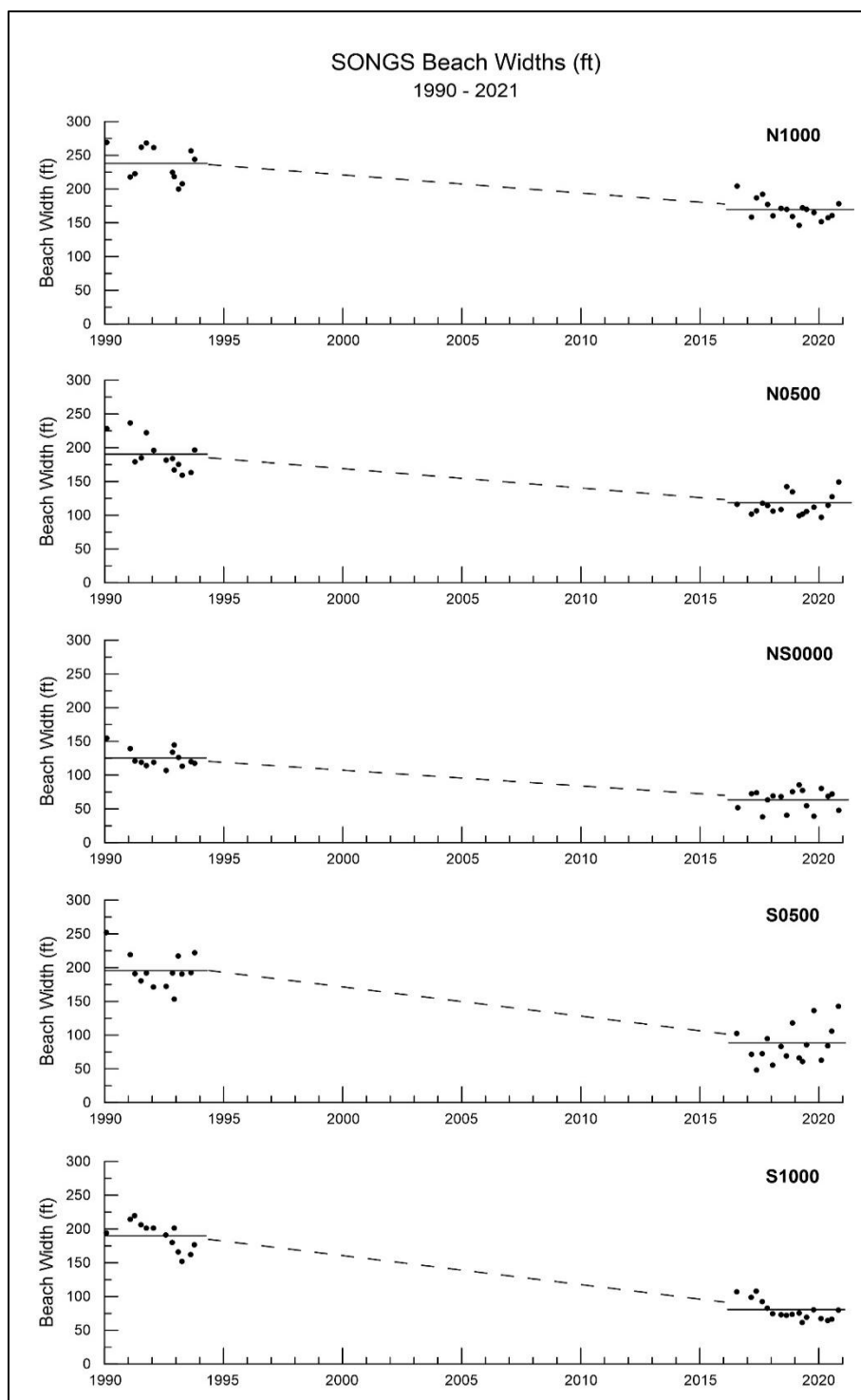


Figure 4-19. Beach width fronting SONGS, 1991-1993 and 2016-2020. Solid lines are mean beach width for each period. Dotted lines suggest long-term narrowing over years with no data.

Table 4-7. Mean beach widths (ft) at San Onofre, 1990-1993 vs 2017-2020.

| Profile | 1990-1993 | | 2017-2020 | | Difference in mean | p-value |
|---------|-----------|----------|-----------|----------|-----------------------|----------|
| | Mean | Std. Dev | Mean | Std. Dev | | |
| N1000 | 237.9 | 25.1 | 167.4 | 12.4 | 70.5 | 2.09E-07 |
| N0500 | 190.4 | 25.0 | 114.9 | 15.6 | 75.5 | 1.19E-08 |
| NS0000 | 125.4 | 13.9 | 64.3 | 15.3 | 61.1 | 1.02E-11 |
| S0500 | 195.8 | 26.0 | 84.9 | 28.0 | 110.9 | 2.64E-11 |
| S1000 | 189.8 | 20.9 | 77.5 | 12.8 | 112.3 | 6.05E-13 |

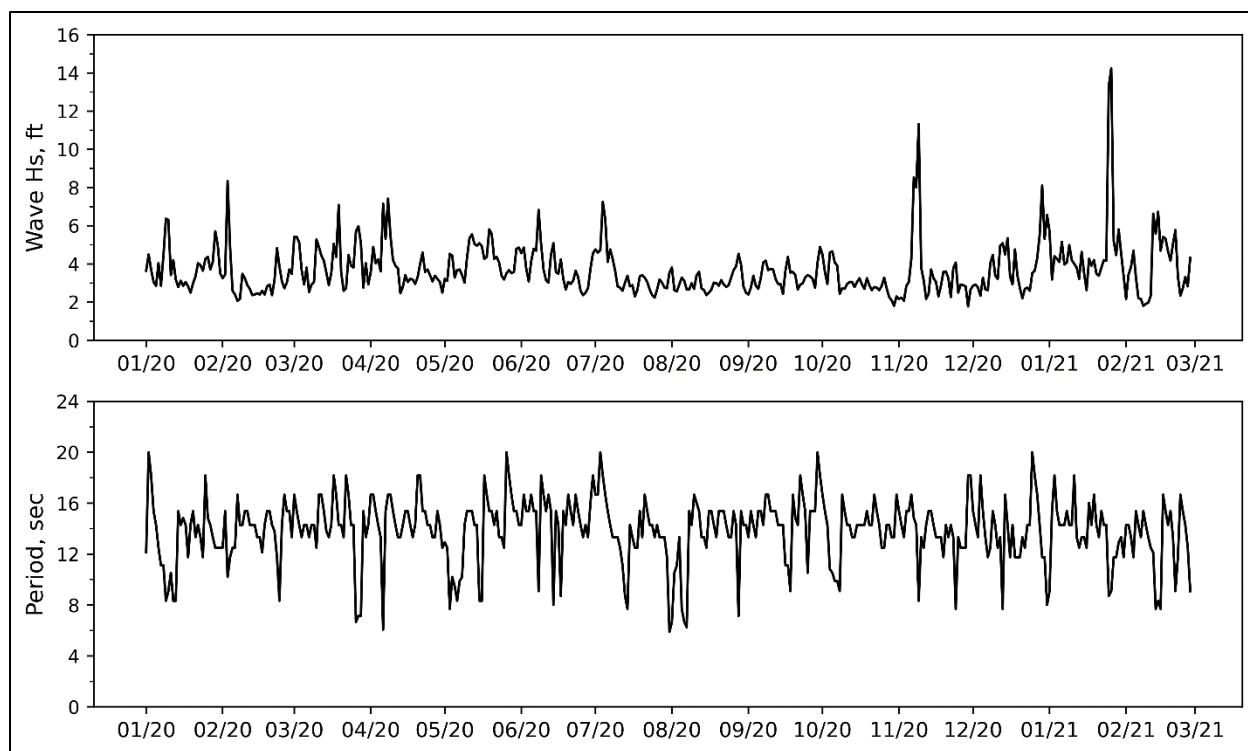


Figure 4-20. Wave height and period at SONGS, 1 January 2020 to 28 February 2021.

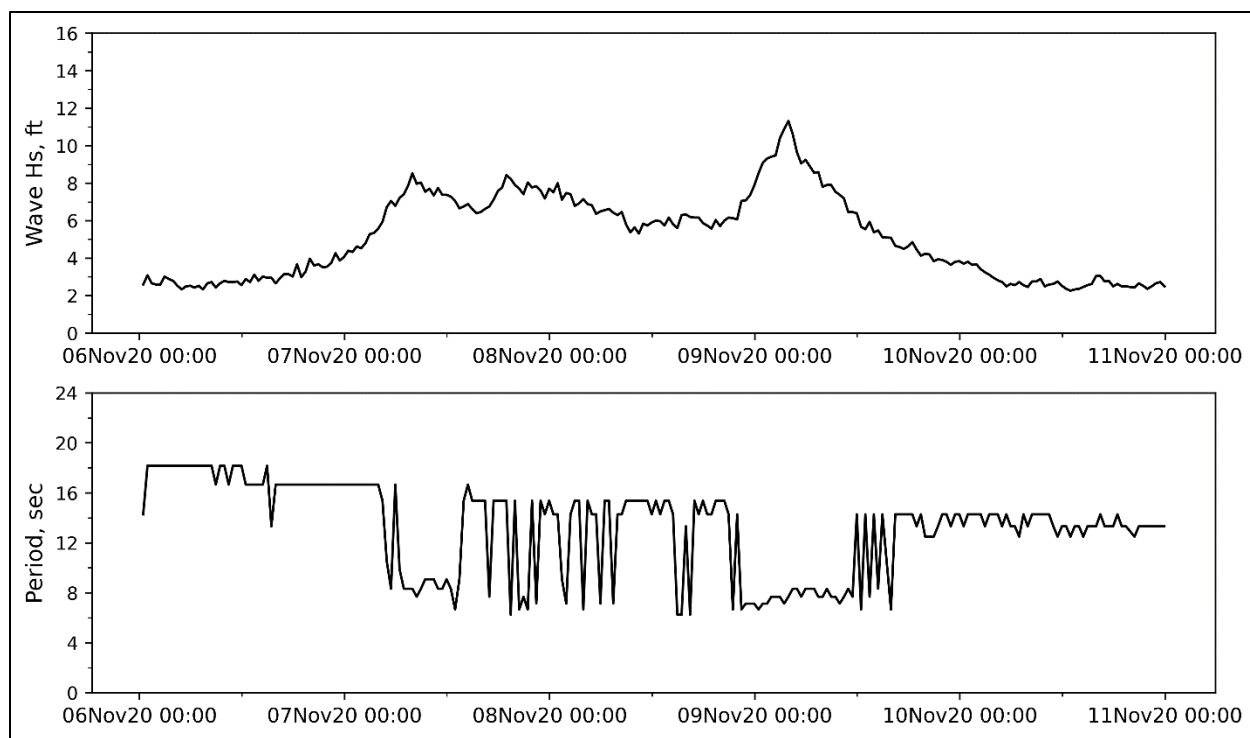


Figure 4-21. Wave height and period at SONGS, 6-11 November 2020.

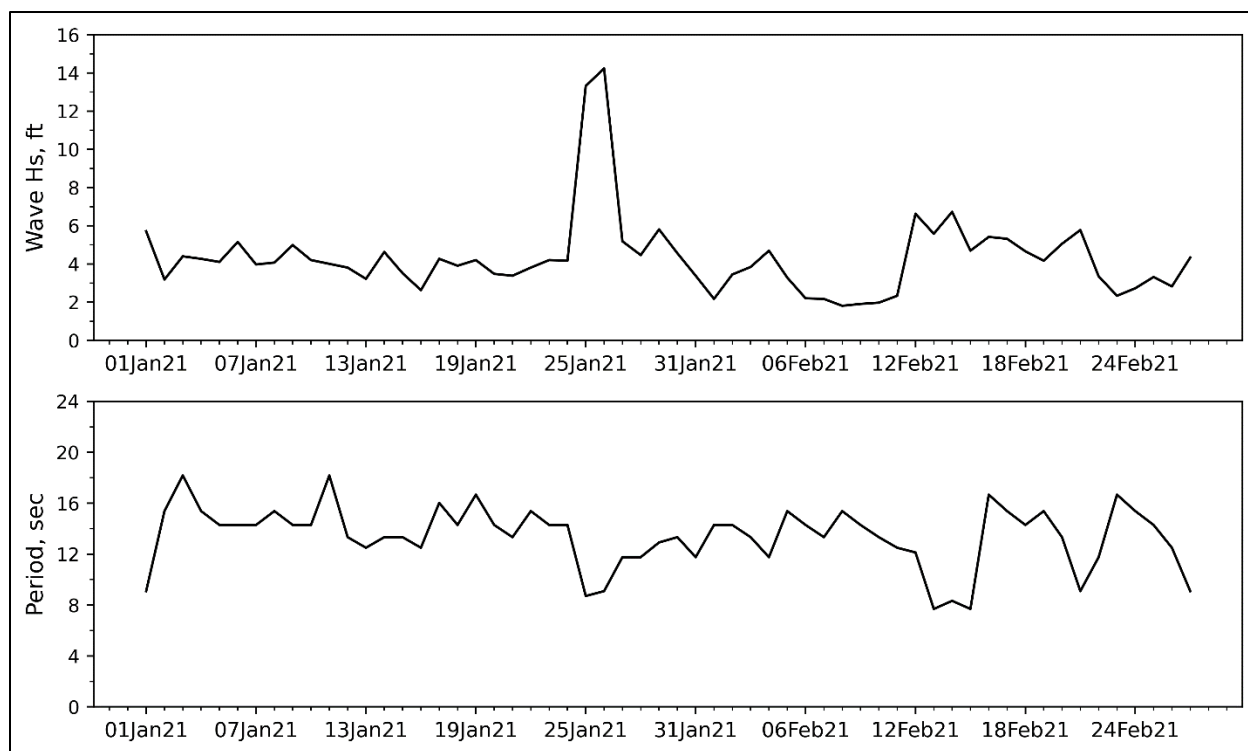


Figure 4-22. Wave height and period at SONGS, 1 January to 28 February 2021.

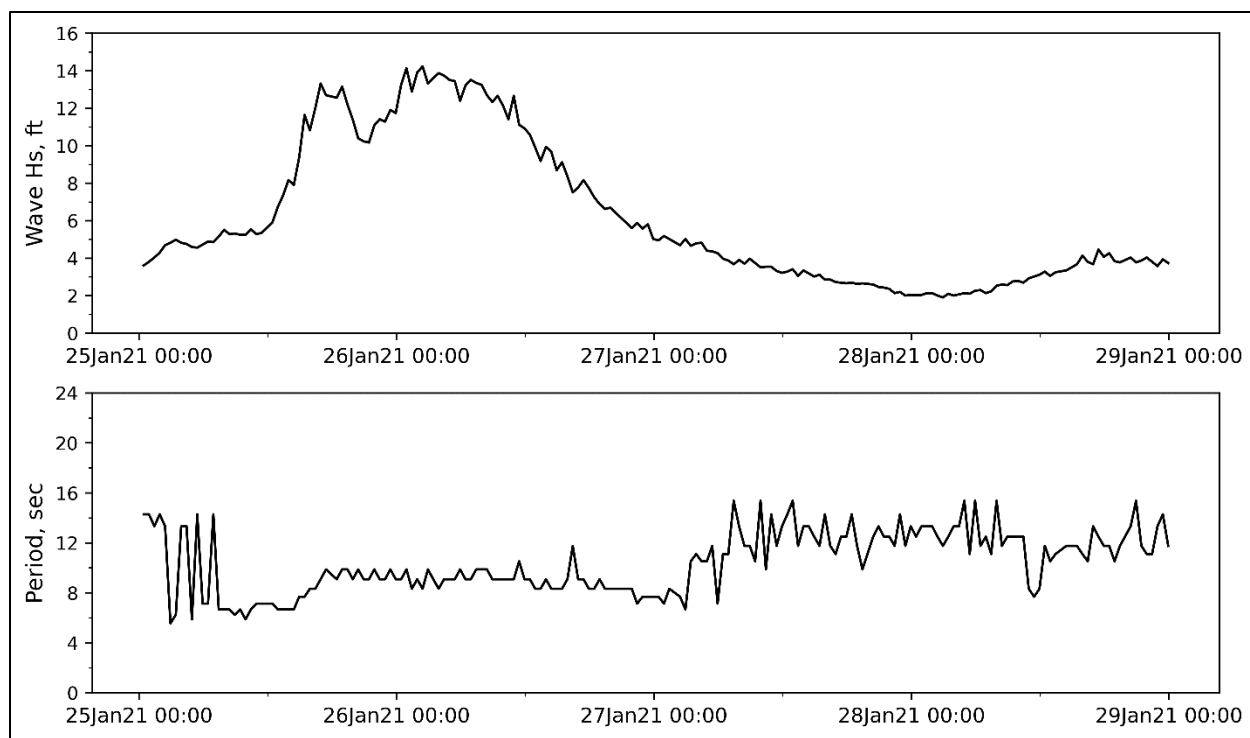


Figure 4-23. Wave height and period at SONGS, 25-29 January 2021.

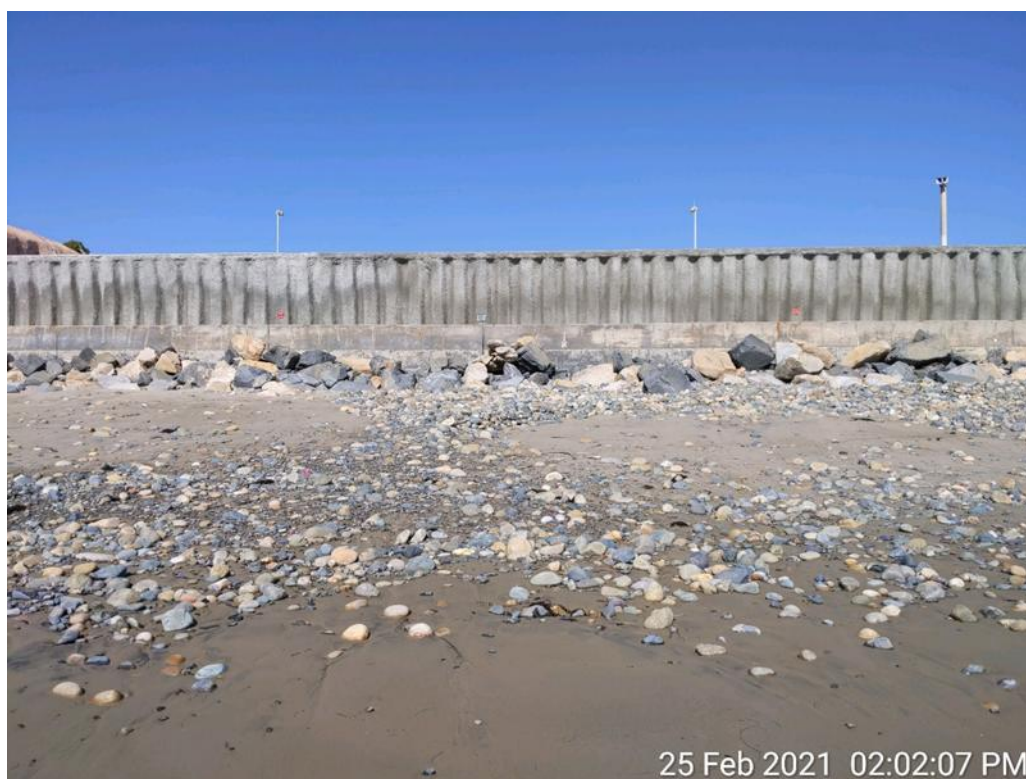


Figure 4-24. Photos of north portion of SONGS revetment covered by beach sand, spring 2020 (upper), but covered with cobble, winter 2021 (lower).

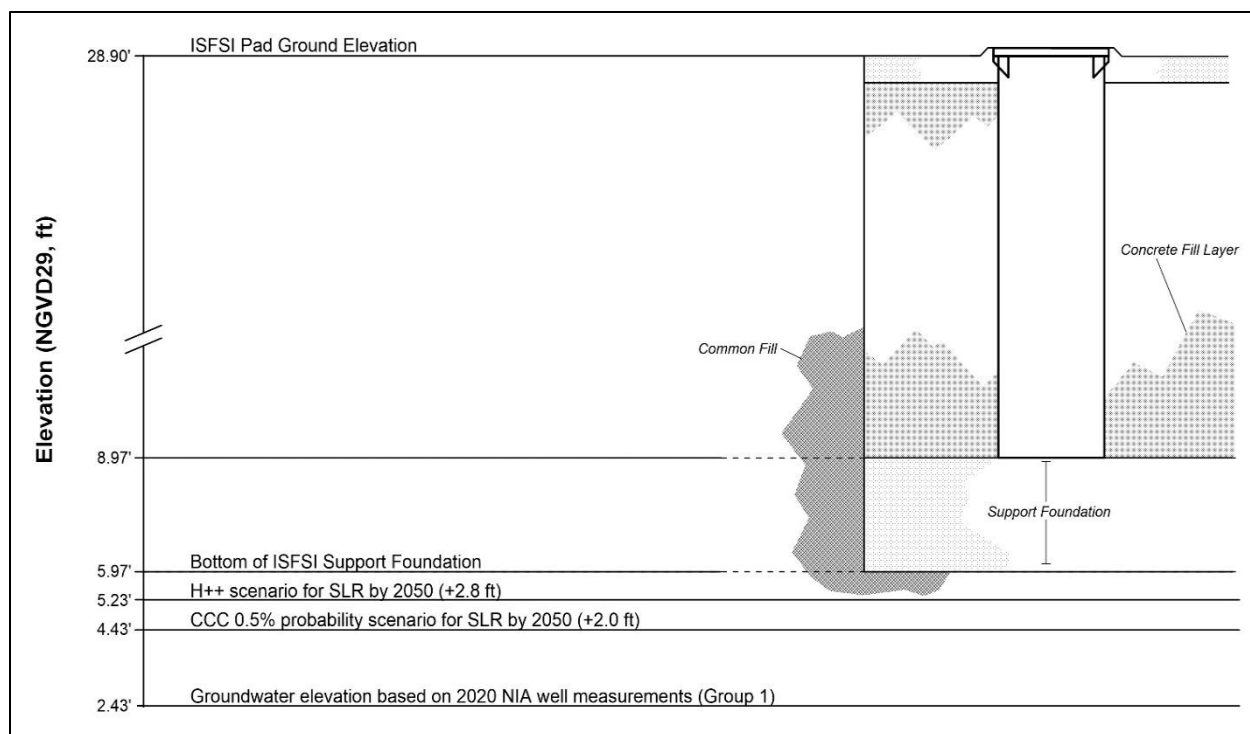


Figure 4-25. Groundwater elevations in 2020, and for OPC (2018) 0.5% and H++ MSLR projections by 2050. From Coastal Environments (2021).

5.0 RUN-UP AND OVERTOPPING ANALYSIS

Wave run-up is defined as the rush of water up a beach or coastal structure caused by, or associated with, wave-breaking. The run-up elevation, designated R (Figure 5-1), is the maximum vertical height above still water level that the run-up will reach. If the run-up elevation is higher than the back of the beach berm, the excess constitutes overtopping. Run-up elevation is dependent on the incident wave characteristics, beach slope and porosity, and if a structure is present, on that structure's shape, slope, roughness, permeability, and water depth at the toe. Run-up analysis is important to assess possible flooding and damage to the SONGS revetment, walkway, and seawall. The amount and type of possible damage depends on run-up elevation and amount of overtopping, as well as on storm wave duration. The SONGS revetment reduces wave run-up by a factor varying from 0.5-0.6 (USACE 1994b, Table 7-2) due to rock roughness and interstitial permeability.

5.1 RANDOM WAVE METHOD

Wave run-up (R) is composed of wave setup and swash run-up. The swash run-up is defined as a super elevation of the mean water level and fluctuation about that mean (S). R is given by the equation:

$$R = \eta + S/2 \quad (5-1)$$

where η is the setup and S is swash run-up.

Many small- and large-scale laboratory studies have been conducted to measure run-up on model beaches, sloped dikes, and seawalls (e.g., Hunt, 1959; Van der Meer and Jenssen, 1995; Hedges and Reis, 1998). Based on laboratory experiments, Hunt (1959) proposed various formulas for estimating wave run-up on a smooth slope as a function of offshore wave height, H , and the Iribarren number, ζ , such that:

$$R = k H \zeta, \quad (5-2)$$

where k is a constant and ζ is the Iribarren number defined as:

$$\zeta = \frac{\tan\beta}{H_o/L_o} \quad (5-3)$$

where $\tan\beta$ is beach slope, H_o is deepwater wave height, and L_o is deepwater wavelength.

Fewer studies have centered on run-up on beaches (Holland and Holman 1993; Raubenheimer *et al.*, 1995; Ruggiero *et al.*, 2004; Stockdon *et al.*, 2006). Stockdon *et al.* (2006) considered the contribution from both incident and infra gravity waves, using data from 10 field experiments with varying bathymetries and wave heights. They empirically estimated the highest 2% run-up exceedance elevation, $R_{2\%}$ with,

$$R_2 = A \left[0.35 \beta_f H_o L_o \right]^{1/2} + \frac{H_o L_o \left[0.563 \beta_f^2 + 0.004 \right]^{1/2}}{2}, \quad (5-4)$$

where β_f is the foreshore beach slope, H_o is the deepwater significant wave height, A is a coefficient equal to 1.1, as estimated by Stockdon *et al.* (2006), and the units are in meters.

5.2 OVERTOPPING

The overtopping rate, Q is defined as the volume of water that overtops a coastal structure or beach berm per unit time and unit length. Resulting units of Q are volume per second per unit length, or ft³/sec-ft. Overtopping empirical models are based on laboratory studies of structure overtopping. These models are used to test design specifications intended to limit the overtopping of levees and dikes, and they therefore give conservative values. A beach berm can act in the same manner as these structures to protect backshore development from wave attack and flooding.

Wave overtopping depends on the difference of freeboard height and wave run-up height. Freeboard, R_c , is defined as the height of the berm crest above mean water level. In order for waves to overtop a berm, the run-up heights must be greater than the freeboard height. Overtopping is dependent on run-up height and, therefore, dependent on incident wave height and period, and beach slope.

Hedges and Reis (1998) introduced a semi-empirical model (H&R model) based on an overtopping theory for regular waves developed by Kikkawa *et al.* (1968), which assumed that a seawall or beach berm acted as a weir whenever the incident water level exceeded the seawall level and the described instantaneous discharge by the weir formula. The H&R model extended the concept to random waves and had good agreement with data.

The H&R model can be written as:

$$\frac{Q}{gR_{\max}} = A \left[1 - \frac{R_c}{\gamma r R_{\max}} \right]^B \quad \text{for } 0 \leq \frac{R_c}{\gamma r R_{\max}} < 1 \quad (5-5)$$

and

$$\frac{Q}{gR_{\max}} = 0 \quad \text{for } \frac{R_c}{\gamma r R_{\max}} \geq 1, \quad (5-6)$$

where g is gravitational acceleration, R_{\max} is the maximum run-up on smooth slope, and γr is a reduction factor to account for rough slope. R_{\max} is estimated by Equation 9 in Reis *et al.* (2008). Additionally, the coefficients of the HR model were given by Reis *et al.* (2008) as:

$$A = \begin{cases} 0.0033 + 0.0025 \frac{1}{\beta} & \text{for } 0.08 \leq \beta \leq 1 \\ 0.0333 & \text{for } 0.05 \leq \beta < 0.083 \end{cases} \quad (5-7)$$

$$B = \begin{cases} 2.8 + 0.65 \frac{1}{\beta} & \text{for } 0.13 \leq \beta \leq 1 \\ 10.2 - 0.275 \frac{1}{\beta} & \text{for } 0.05 \leq \beta < 0.13 \end{cases} \quad (5-8)$$

where β is the beach slope.

Reis *et al.* (2008) compared the H&R model with three other methods used to estimate the overtopping rate for various structures subject to random wave action. The slopes of these structures varied from 1:1 to 1:20, and wave steepness varied from 0.01 to 0.3. The models were: (1) Owen (1980); (2) Van der Meer Janssen (1995); and (3) the AMAZON Numerical Model (Hu, 2000). There was general agreement between the H&R and AMAZON models, while Owen (1980) systematically over-predicted the discharges. Van der Meer and Janssen (1995) gave similar results to the H&R model, except that they over-predicted discharges for some conditions that are outside the ranges of applicability.

5.3 RESULTS

Figure 4-13 shows typical cross sections of the SONGS revetment. The locations of these profiles are shown in Figure 4-9. The slope, β , of the revetment varies from 0.33-0.44. The height of the walkway is about 14 ft (NGVD). The design water level is estimated as 5.5 ft (NGVD). Table 5-1 provides run-up and overtopping results for all design wave and water level conditions, including MSLR under the medium-high scenario for 2020, 2030, 2040, and 2050. Table 5-2 shows these results for the extreme H++ MSLR projection. Tables 5-1 and 5-2 suggest that wave overtopping of the revetment already occurs for storm wave conditions meeting or exceeding a 10-year return period (i.e., 10% probability of occurrence in a given year), which is consistent with observations (e.g., 2020).

As MSLR progresses, overtopping rates are expected to increase. For large storms, rates are projected to reach 0.5 ft³/sec-ft by 2030 and 1-1.6 ft³/sec-ft by 2050. There is a short segment in the walkway where the concrete wall has been replaced by rails to provide a flow path for the saltwater cooling system during plant operations. This opening in the wall will increase overtopping on the walkway (Figure 5-2). However, it does not represent a significant hazard to pedestrians since the walkway will be closed during storms and there are no more discharges from the system.

5.4 PROBABILITY ANALYSIS

The probability associated with run-up and overtopping is considered in quantitative terms. This risk is defined as the probability that a “T-year” return-period event will occur at least once during a given “n-year” long time period. The run-up results in Tables 5-1 and 5-2 can be used to estimate the risk for any selected “n-year” long time period. The results can also be used to estimate the probability of run-up of a given size during a specified time period. The probability of a T-year run-up in any one year is $P = 1/T$.

In other words, there is a one-percent chance that the 100-year run-up will occur during a given year. The probability is equal to the sum of the probabilities of having one run-up, two

run-ups, or n run-up events occurring during n years of interest, or to 1 minus the probability of having no run-ups. The risk can be calculated from Equation 5-9:

$$P = 1 - (1 - 1/T)^n \quad (5-9)$$

Equation 5-9 indicates that there is a 63% chance that the 100-year magnitude run-up will occur at least once during any 100-year time interval. Similarly, Equation 5-9 can be used to calculate the risk associated with any T -year run-up during any time period. Figure 5-3 gives the probability of occurrence of $T = 25$ -year, 50-year and 100-year run-ups in an n -year period based on Equation 5-9.

5.5 SUMMARY

Observations suggest that over the last decade or longer, the SONGS revetment has adjusted to reach an equilibrium configuration. Under its current condition, the revetment is expected to withstand projected wave forces with acceptable minimum rock displacement and settling that will not impact the integrity of the revetment as a whole.

The walkway elevation at 14 ft (NGVD) is relatively low and will continue to flood under large wave conditions that overtop the revetment. However, it should be noted that the results of run-up and overtopping presented in this study are conservative for the following reasons:

1. The results are based on an extreme high water level of 5.3 ft (NGVD) that includes king tides, El Niño enhancements, and 1-ft storm surges. Observations suggest that it is exceedingly unlikely for large storm waves to occur precisely at the time of peak high (King) tides (e.g., Elwany and Flick, 1999; Flick, 1998, 2016; Young *et al.*, 2018).
2. Figure 5-4 illustrates the joint probability distribution between significant wave height and water level between 1976-1994, a period characterized by large wave events occurring between 1981 and 1984. Figure 5-3 shows that the probability of 50-year and 100-year waves occurring in the next 30 years is 0.45 and 0.28, respectively. Multiplying these probabilities by the probability of larger waves occurring at high tides will lead to an extremely low probability of co-occurrence.

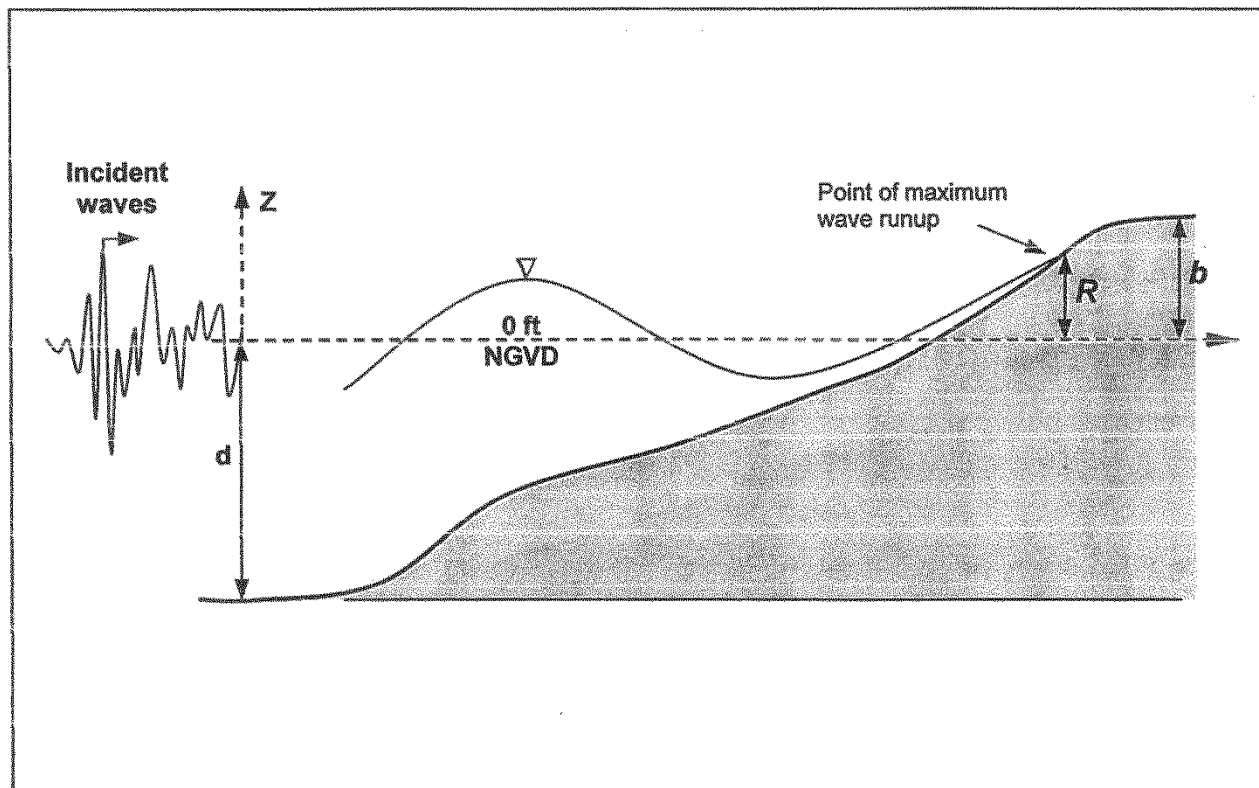


Figure 5-1. Wave run-up on a slope. R is the run-up elevation; b is the height of the beach berm. If $R > b$, then overtopping will occur.

Table 5-1. Run-up and overtopping summary for 0.5 % (1:200) scenario.

| Year | Return Period (yr) | Hs (ft) | Tp (sec) | MSLR (ft) | Run-up (ft) | Run-up Elevation (ft NGVD) | Overtopping Rate (ft³/sec-ft) |
|-------------|---------------------------|----------------|-----------------|------------------|--------------------|-----------------------------------|---|
| 2020 | 2 | 2.0 | 9 | 0.0 | 5.27 | 10.77 | 0.00 |
| | 5 | 2.4 | 12 | 0.0 | 7.23 | 12.73 | 0.00 |
| | 10 | 2.8 | 12 | 0.0 | 7.81 | 13.31 | 0.01 |
| | 25 | 3.2 | 17 | 0.0 | 10.58 | 16.08 | 0.18 |
| | 50 | 3.5 | 17 | 0.0 | 11.06 | 16.56 | 0.28 |
| | 100 | 3.8 | 16 | 0.0 | 11.09 | 16.59 | 0.32 |
| 2030 | 2 | 2.0 | 9 | 0.9 | 5.27 | 11.67 | 0.00 |
| | 5 | 2.4 | 12 | 0.9 | 7.23 | 13.63 | 0.01 |
| | 10 | 2.8 | 12 | 0.9 | 7.81 | 14.21 | 0.04 |
| | 25 | 3.2 | 17 | 0.9 | 10.58 | 16.98 | 0.34 |
| | 50 | 3.5 | 17 | 0.9 | 11.06 | 17.46 | 0.49 |
| | 100 | 3.8 | 16 | 0.9 | 11.09 | 17.49 | 0.56 |
| 2040 | 2 | 2.0 | 9 | 1.3 | 5.27 | 12.07 | 0.00 |
| | 5 | 2.4 | 12 | 1.3 | 7.23 | 14.03 | 0.02 |
| | 10 | 2.8 | 12 | 1.3 | 7.81 | 14.61 | 0.06 |
| | 25 | 3.2 | 17 | 1.3 | 10.58 | 17.38 | 0.44 |
| | 50 | 3.5 | 17 | 1.3 | 11.06 | 17.86 | 0.62 |
| | 100 | 3.8 | 16 | 1.3 | 11.09 | 17.89 | 0.71 |
| 2050 | 2 | 2.0 | 9 | 2.0 | 5.27 | 12.77 | 0.00 |
| | 5 | 2.4 | 12 | 2.0 | 7.23 | 14.73 | 0.05 |
| | 10 | 2.8 | 12 | 2.0 | 7.81 | 15.31 | 0.12 |
| | 25 | 3.2 | 17 | 2.0 | 10.58 | 18.08 | 0.69 |
| | 50 | 3.5 | 17 | 2.0 | 11.06 | 18.56 | 0.94 |
| | 100 | 3.8 | 16 | 2.0 | 11.09 | 18.59 | 1.05 |

Table 5-2. Run-up and overtopping summary for OPC (2018) H++ scenario.

| Year | Return Period (yr) | Hs (ft) | Tp (Sec) | MSLR (ft) | Run-up (ft) | Run-up Elevation (ft NGVD) | Overtopping Rate (ft³/sec-ft) |
|-------------|---------------------------|----------------|-----------------|------------------|--------------------|-----------------------------------|---|
| 2020 | 2 | 2.0 | 9 | 0.0 | 5.27 | 10.77 | 0.00 |
| | 5 | 2.4 | 12 | 0.0 | 7.23 | 12.73 | 0.00 |
| | 10 | 2.8 | 12 | 0.0 | 7.81 | 13.31 | 0.01 |
| | 25 | 3.2 | 17 | 0.0 | 10.58 | 16.08 | 0.18 |
| | 50 | 3.5 | 17 | 0.0 | 11.06 | 16.56 | 0.28 |
| | 100 | 3.8 | 16 | 0.0 | 11.09 | 16.59 | 0.32 |
| 2030 | 2 | 2.0 | 9 | 1.1 | 5.27 | 11.87 | 0.00 |
| | 5 | 2.4 | 12 | 1.1 | 7.23 | 13.83 | 0.02 |
| | 10 | 2.8 | 12 | 1.1 | 7.81 | 14.41 | 0.05 |
| | 25 | 3.2 | 17 | 1.1 | 10.58 | 17.18 | 0.39 |
| | 50 | 3.5 | 17 | 1.1 | 11.06 | 17.66 | 0.55 |
| | 100 | 3.8 | 16 | 1.1 | 11.09 | 17.69 | 0.63 |
| 2040 | 2 | 2.0 | 9 | 1.8 | 5.27 | 12.57 | 0.00 |
| | 5 | 2.4 | 12 | 1.8 | 7.23 | 14.53 | 0.04 |
| | 10 | 2.8 | 12 | 1.8 | 7.81 | 15.11 | 0.10 |
| | 25 | 3.2 | 17 | 1.8 | 10.58 | 17.88 | 0.61 |
| | 50 | 3.5 | 17 | 1.8 | 11.06 | 18.36 | 0.84 |
| | 100 | 3.8 | 16 | 1.8 | 11.09 | 18.39 | 0.94 |
| 2050 | 2 | 2.0 | 9 | 2.8 | 5.27 | 13.57 | 0.01 |
| | 5 | 2.4 | 12 | 2.8 | 7.23 | 15.53 | 0.12 |
| | 10 | 2.8 | 12 | 2.8 | 7.81 | 16.11 | 0.24 |
| | 25 | 3.2 | 17 | 2.8 | 10.58 | 18.88 | 1.12 |
| | 50 | 3.5 | 17 | 2.8 | 11.06 | 19.36 | 1.47 |
| | 100 | 3.8 | 16 | 2.8 | 11.09 | 19.39 | 1.62 |



Figure 5-2. Exposed area in the walkway wall.

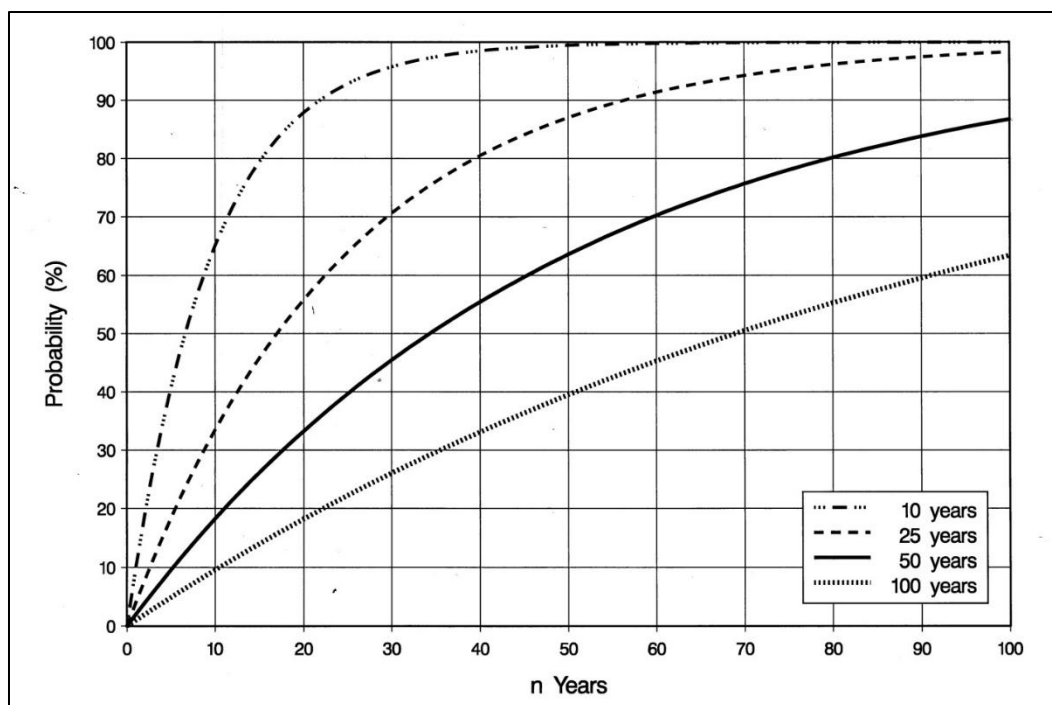


Figure 5-3. Probability of 10-, 25-, 50-, and 100-year waves return period to occur in the next 100 years.

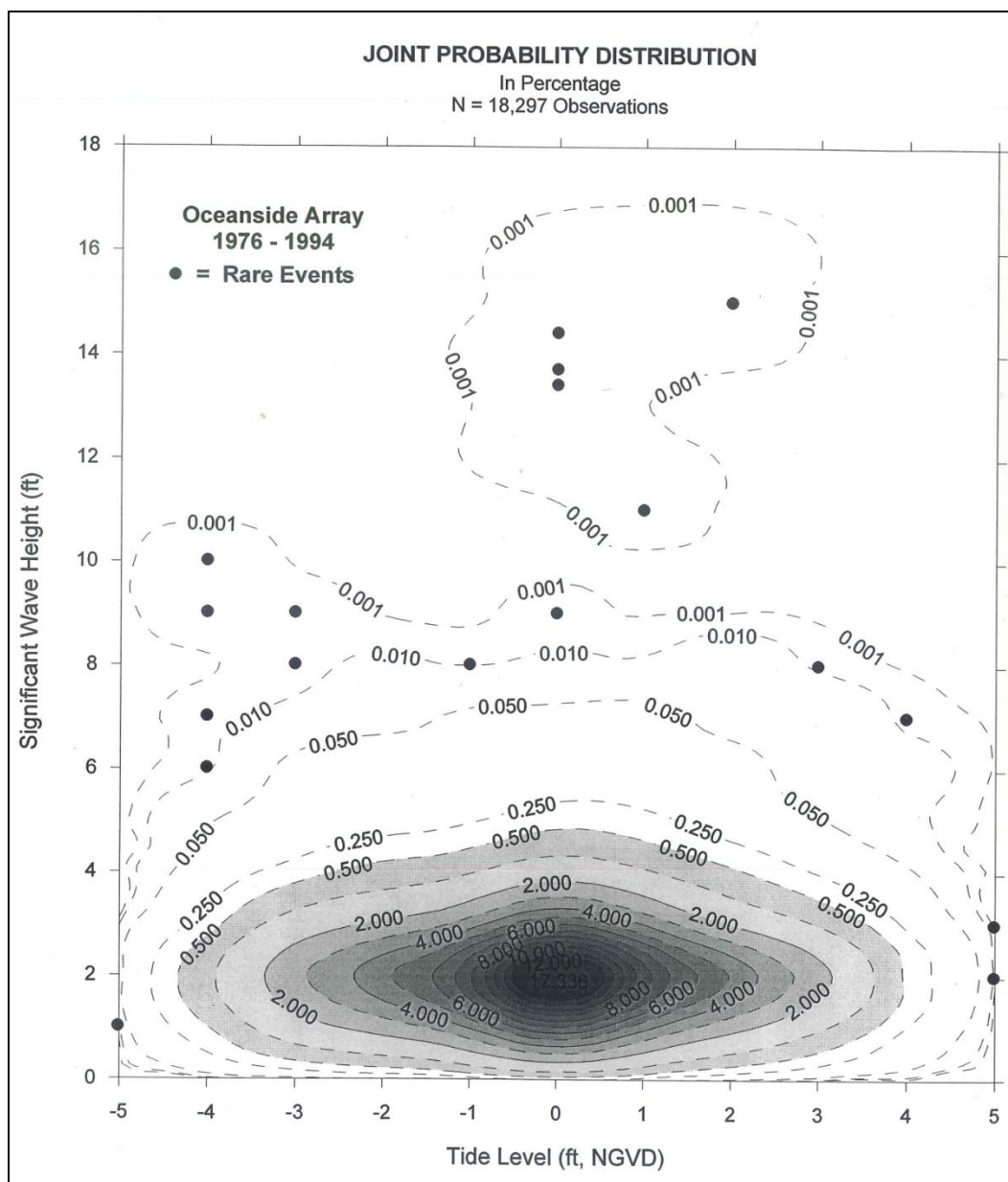


Figure 5-4. Joint Probability distribution between significant wave height and tide level. From Elwany and Flick (1999).

6.0 SUMMARY AND CONCLUSIONS

The objective of this study is to describe coastal hazards at SONGS in order to evaluate impacts of sea level rise for H++ sea level rise scenario up to 2050, waves, and wave run-up on the beach, nearshore zone, and SONGS facilities, including protective and coastal structures, particularly the revetment, access walkway and seawall. The report considers the possible future effects of sea level rise on the ongoing and long-term influences of waves on the beach, cliffs, protective structures, and wave run-up and overtopping under extreme conditions.

The findings and conclusions of our investigation are summarized as follows:

1. Waves and sand supply from offshore areas, rivers, and cliffs are the major factors controlling the cyclic erosion and accretion of the beach at SONGS. These factors together with MSLR determine long-term beach retreat. When the beaches become narrow enough for waves to impact the sea cliffs, these erode from wave action at the base, as well as from rainfall and inland drainage.
2. SONGS is fronted by a riprap rock revetment on the ocean front backed by a low retaining wall and a walkway that provides public lateral beach access. The main seawall, 28-30 ft, MLLW in elevation, backs the walkway and provides plant security and protection from erosion, and wave and tsunami overtopping.
3. Projections of future sea level rise are evolving as the understanding of key climate change processes improves. Currently applicable OPC (2018) and CCC (2015, updated 2018) State of California MSLR guidance projections through 2050 that could impact SONGS are reviewed. New IPCC (2021, 2022) projections are also discussed. Overall, the IPCC (2021, 2022) MSLR trajectories through 2050 are lower than existing guidance.
4. The relatively narrow beaches fronting and adjacent to SONGS are subject to normal seasonal fluctuations, as well as longer-term erosion and accretion. Measurements since 1991 suggest slow erosion to the present. Cliffs north and south of SONGS are exposed to marine erosion when beaches are sufficiently narrow. Beaches and cliffs are vulnerable to long-term retreat from MSLR. Beach retreat of up to 100 ft, and widely varying cliff retreat up to 84 ft by 2050 with mean value about 30 ft, is projected to occur for the highest extreme H++ MSLR scenario. (Table 3-1).
5. During winter 2020-2021, SONGS was subjected to a series of large wave events with heights up to 14 ft, which were higher than the previously estimated 100-year wave event. Despite the height and duration of these waves, damage to the revetment was minimal, being limited to normal rock settling and displacement, with expected water overtopping.
6. The integrity of the revetment as a whole was unaffected by the 2020-2021 storm waves. Stability and adaptive capacity analyses suggest that the revetment and adjacent walkway should withstand wave forces over the next 30 years, assuming regular monitoring of revetment condition, and with normal maintenance, repair, and small adjustment that may be required as MSLR proceeds.

7. Projections of future groundwater elevations estimated from the OPC (2018) 0.5% (1:200) and H++ MSLR scenarios through 2050, suggest that these will be (respectively) 1.54 ft and 0.74 ft lower than the bottom of the ISFSI support foundation, which is 3 ft thick.

7.0 REFERENCES

- Ahrens, J. P., 1981a. Irregular Wave Runup on Smooth Slopes. Coastal Engineering Technical Aid No. 81-17, USACE, 26 pp.
- Ahrens, J. P., 1981b. Design of Riprap Revetments for Protection Against Wave Attack. Technical Paper No. 81-5, USACE, 31 pp.
- Ashton, A.D., M.J.A. Walkden, and M.E. Dickson, 2011. Equilibrium responses of cliffed coasts to changes in the rate of sea level rise. *Mar. Geol.*, 284 (1-4), 217-229.
- Bamber, J.L., M. Oppenheimer, R.E. Kopp, W.P. Aspinall, and R.M. Cooke, 2019. Ice sheet contributions to future sea-level rise from structured expert judgment. *Proc. Nat. Acad. Sci.*, 116 (23), 11195-11200.
- Bedsworth, L., D. Cayan, G. Franco, L. Fisher, and S. Ziaja, 2018. Statewide Summary Report, California's Fourth Climate Change Assessment. California Governor's Office of Planning and Research, Scripps Institution of Oceanography, California Energy Commission, and California Public Utilities Commission. Publication Number SUM-CCCA4-2018-013, 133 pp.
- Beckley, B.D., N.P. Zelensky, S.A. Holmes, F.G. Lemoine, R.D. Ray, G.T. Mitchum, S.D. Desai, and S.T. Brown, 2010. Assessment of the Jason-2 Extension to the TOPEX/Poseidon, Jason-1 Sea-Surface Height Time Series for Global Mean Sea Level Monitoring. *Marine Geodesy*, 33(1).
- Bray, M.J., and J.M. Hooke, 1997. Prediction of soft-cliff retreat with accelerating sea level rise. *J. Coast. Res.*, 13, 453-467.
- British Columbia Ministry of Environment, Lands and Parks (BCMELP), 2000. Riprap Design and Construction Guide. Public Safety Section, Water Management Branch, 12 pp.
- Bromirski, P.D., A.J. Miller, R.E. Flick, and G. Auad, 2011. Dynamical Suppression of Sea Level Rise Along the Pacific Coast of North America: Indications for Imminent Acceleration. *J. Geophys. Res.*, 116(C7).
- Bromirski, P.D., A.J. Miller, and R.E. Flick, 2012. North Pacific Sea Level Trends. *Eos Trans. AGU*, 93(27), 249-256.
- Bruun, P., 1962. Sea level rise as cause of shore erosion. *J. Waterways Harbors Div., Amer. Soc. Civil Eng.*, 88, 117-130.
- California Coastal Commission (CCC), 2001. Construction of San Onofre Nuclear Generating Station (SONGS) Units 2 and 3 Temporary Spent Nuclear Fuel Storage Facility. Southern California Edison Company, San Diego Gas and Electric Company, City of

- Anaheim, and City of Riverside. Staff Report, Regular Calendar, Application File No. E-00-014, 114 pp.
- California Coastal Commission (CCC), 2015. California Coastal Commission Sea Level Rise Policy Guidance: Interpretive Guidelines for Addressing Sea Level Rise in Local Coastal Programs and Coastal Development Permits, 293 pp.
<http://www.coastal.ca.gov/climate/slrguidance.html>
- California Coastal Commission (CCC), 2015 (updated 2018). California Coastal Commission Sea Level Rise Policy Guidance, Interpretive Guidelines for Addressing Sea Level Rise in Local Coastal Programs and Coastal Development Permits. San Francisco, CA, 307 pp.
- California Coastal Commission (CCC), 2020a. Protecting California's Coast for Present and Future Generations, 2021-2025. San Francisco, CA, 56 pp.
<https://www.coastal.ca.gov/strategicplan/spindex.html>.
- California Coastal Commission (CCC), 2020b. Sea Level Rise in California: Planning for the Future. San Francisco, CA, 17 pp.
<https://storymaps.arcgis.com/stories/d0c1df224a97418bb4dad129ea4c6d17>.
- California Natural Resources Agency (CNRA) and California Environmental Protection Agency (CEPA), 2020. Making California's Coast Resilient to Sea Level Rise: Principles for Aligned State Action. Sacramento, CA, 29 April 2020, 6 pp.
<https://www.adaptationclearinghouse.org/resources/making-california-eyes-coast-resilient-to-sea-level-rise-principles-for-aligned-state-action.html>.
- Cayan, D.R., J. Kalinsky, S. Iacobellis, and D. Pierce (with R. Kopp), 2016. Creating Probabilistic Sea Level Rise Projections. Unpublished White Paper, Division of Climate, Atmospheric Sciences, and Physical Oceanography, Scripps Institution of Oceanography, La Jolla, CA, 16 pp.
- Chadwick, D.B., P.F. Wang, M. Brand, R.E. Flick, A.P. Young, W.C. O'Reilly, P.D. Bromirski, W.A. Crampton, R.T. Guza, J.J. Helly, T. Nishikawa, S. Boyce, M. Landon, M. Martinez, I. Canner, and B. Leslie, 2014. A Methodology for Assessing the Impact of Sea Level Rise on Representative Military Installations in the Southwestern United States (RC-1703). Final report submitted to The Strategic Environmental Research and Development Program, Alexandria, VA, 688 pp.
<http://www.serdp.org/Program-Areas/Resource-Conservation-and-Climate-Change/Climate-Change/Vulnerability-and-Impact-Assessment/RC-1703>
- Coastal Environments, 2000. SONGS Unit 1 Deconstruction Marine Impacts Study, Phase I. Unpublished report submitted to Southern California Edison Company, 24 January 2000, CE Ref. No. 2000-03, 44 pp. and 2 appendices.

- Coastal Environments, Inc., 2021. 2020 Groundwater Levels at San Onofre Nuclear Generating Station, San Onofre, CA. Report submitted to Southern California Edison, Rosemead, CA 91770, 8 March 2021, CE Ref No. 21-05, 14 pp. and 1 appendix.
- Cooper, J.A.G. and O.H. Pilkey, 2004. Sea level rise and shoreline retreat: Time to abandon the Bruun Rule. *Global and Planetary Change*, 43, 157-171.
- Church, J.A. and N.J. White, 2011. Sea-Level Rise from the Late 19th to the Early 21st Century. *Surv. Geophys.*, 32, 585–602.
- Dean, R.G., 1991. Equilibrium beach profiles: Characteristics and applications. *J. Coast. Res.* 7 (1), 53-84.
- Dean, R.G. and E.M. Maurmeyer, 1983. Models for beach profile response. In *CRC Handbook of Coastal Processes and Erosion*, CRC Press, Boca Raton, FL.
- DeConto, R., and D. Pollard, 2016. Contribution of Antarctica to past and future sea level rise. *Nature* 531, 591-597.
- DeConto, R.M., D. Pollard, R.B. Alley, I. Velicogna, E. Gasson, N. Gomez, S. Sadai, A. Condrón, D.M. Gilford, E.L. Ashe, R.E. Kopp, D. Li, and A. Dutton, 2021. The Paris Climate Agreement and future sea-level rise from Antarctica. *Nature* 593, 83-89.
- Elwany, H., R. Flick and S. Aijaz, 1994. 1993 Beach Profile Surveys at San Onofre, Final Report. Submitted to Southern California Edison, Rosemead, CA 91770, CE Ref. No. 94-07, 32 pp. and 2 appendices.
- Elwany, H., and R. E. Flick, 1999. Coastal and Oceanographic Conditions in the Vicinity of the Proposed Manchester Resort Development Oceanside, California. Coastal Environments Reference No. 99 03, prepared for Manchester Resort, 1 Market Place, San Diego, CA, 61 pp. and 4 appendices.
- Elwany, H., R.E. Flick, and F. Scarelli, 2020. SONGS Mean Sea Level Impact Assessment, Provision 14 In Lease NO. Prc 6785.1. Report prepared for Southern California Edison, Rosemead CA 91770, 30 March 2020, CE Ref No. 20-08, 64 pp. and 6 appendices.
- Elwany, H., R.E. Flick, and F. Scarelli, 2021. SONGS Mean Sea Level Impact Assessment, Provision 14 In Lease NO. Prc 6785.1. Report prepared for Southern California Edison, Rosemead CA 91770, 25 March 2021, CE Ref No. 21-07, 76 pp. and 6 appendices.
- Elwany, H., R.E. Flick, and F. Scarelli, 2022 SONGS Mean Sea Level Impact Assessment, Provision 14 In Lease NO. Prc 6785.1. Report prepared for Southern California Edison, Rosemead CA 91770, 30 March 2020, CE Ref No. 22-07, 77 pp. and 6 appendices.

- Elwany, H., R.E. Flick, and F. Scarelli, 2021a. Beach Profile Surveys at San Onofre Nuclear Generating Station (SONGS), Units 2 and 3 Decommissioning Project. Report prepared for Southern California Edison, Rosemead CA 91770, 20 December 2021, CE Ref No. 21-22, 49 pp. and 2 appendices.
- Everts, C.H., 1991. Seacliff retreat and coarse sediment yields in southern California. In *Proceedings of Coastal Sediments '91*, Vol. 2, pp. 1586–1598, American Society of Civil Engineers, Seattle, WA.
- Flick, R.E. (ed.), 1994. *Shoreline Erosion Assessment and Atlas of the San Diego Region* (2 volumes). Sacramento, CA: California Department of Boating and Waterways and San Diego Association of Governments.
- Flick, R. E., 1998. Comparison of California Tides, Storm Surges, and Sea Level During the El Niño Winters of 1982-83 and 1997-98. *Shore & Beach*, 66(3), 7-11.
- Flick, R. E., 2016. California tides, sea level, and waves. *Shore & Beach*, Winter 2015-2016, 84(2), 25-30.
- Flick, R.E., and J.R. Wanetick, 1989. San Onofre Beach Study. Unpublished report submitted to Southern California Edison Co., Rosemead, CA, October 1989, SIO Ref. No 89-20, 26 pp. and 25 figures.
- Flick, R.E., J.R. Wanetick, M.H. Elwany, R.S. Grove, and B.W. Waldorf, 2010. Beach changes from construction of San Onofre Nuclear Generating Station, 1964-1989. *Shore & Beach*, 78(4), 12-25.
- Fox-Kemper, B., H.T. Hewitt, C. Xiao, G. Aðalgeirsdóttir, S.S. Drijfhout, T.L. Edwards, N.R. Golledge, M. Hemer, R.E. Kopp, G. Krinner, A. Mix, D. Notz, S. Nowicki, I.S. Nurhati, L. Ruiz, J-B. Sallée, A.B.A. Slangen, and Y. Yu, 2021. Ocean, Cryosphere and Sea Level Change. In *Climate Change 2021: The Physical Science Basis. Contribution of Working Group I to the Sixth Assessment Report of the Intergovernmental Panel on Climate Change*. Masson-Delmotte, V., P. Zhai, A. Pirani, S.L. Connors, C. Péan, S. Berger, N. Caud, Y. Chen, L. Goldfarb, M.I. Gomis, M. Huang, K. Leitzell, E. Lonnoy, J.B.R. Matthews, T.K. Maycock, T. Waterfield, O. Yelekçi, R. Yu, and B. Zhou (eds.), Cambridge University Press.
- Garner, G.G., T. Hermans, R.E. Kopp, A.B.A. Slangen, T. L. Edwards, A. Levermann, S. Nowicki, M.D. Palmer, C. Smith, B. Fox-Kemper, H.T. Hewitt, C. Xiao, G. Aðalgeirsdóttir, S.S. Drijfhout, T.L. Edwards, N.R. Golledge, M. Hemer, R.E. Kopp, G. Krinner, A. Mix, D. Notz, S. Nowicki, I.S. Nurhati, L. Ruiz, J-B. Sallée, Y. Yu, L. Hua, T. Palmer, B. Pearson, 2021. *IPCC AR6 Sea-Level Rise Projections, Version 20210809*. PO.DAAC, CA, USA.

- Griggs, G., J. Arvai, D. Cayan, R. DeConto, J. Fox, H.A. Fricker, R.E. Kopp, C. Tebaldi, and E.A. Whiteman, 2017. Rising Seas in California: An Update on Sea Level Rise Science. California Ocean Protection Council Science Advisory Team Working Group, California Ocean Science Trust, 71 pp.
- Hallermeier, R.J., 1978. Uses for a calculated limit depth to beach erosion. Proceedings, 16th Coastal Engineering Conference, American Society of Civil Engineers, 1493-1512.
- Hands, E.B., 1983. The Great Lakes as a test model for profile responses to sea level changes. In Komar, P.D. (ed.), Handbook of Coastal Processes and Erosion. CRC Press, Boca Raton, Florida, pp. 176-189.
- Hapke, C.J. and D. Reid, 2007. National Assessment of Shoreline Change, Part 4: Historical Coastal Cliff Retreat Along the CA Coast. USGS Report 2007-1133.
- Hapke, C.J., D. Reid, and B. Richmond, 2009. Rates and trends of coastal change in California and the regional behavior of the beach and cliff system. J. Coast. Res., 25(3), 603-615.
- Hedges, T.S., and M.T., Reis, 1998. Random wave overtopping of simple sea walls: A new regression model. Proc. Inst. Civ. Eng., Water Maritime Energy, 130(1), 1-10.
- Holland, K.T. and R.A. Holman, 1993. Statistical distribution of swash maxima on natural beaches. J. Geophys. Res., v. 98, no. C6, 10271-10278.
- Hu, K., C.G. Mingham, and D.M. Causon, 2000. Numerical simulation of wave overtopping of coastal structures using the non-linear shallow water equations. Coastal Engineering, 41(4), 433-465.
- Hunt, G.S., 1975. Geology of the San Onofre area and parts of the Cristianitos Fault. In Studies on the Geology of Camp Pendleton and Western San Diego County, California, S. Ross and R.J. Dowlen (ed). San Diego, CA: San Diego Association of Geologists, 90 pp.
- Hunt, I.A., 1959. Design of seawalls and breakwaters. J. Waterways and Harbors Div., ASCE, Vol. 85, No. WW3.
- Inman, D.L., and P.M. Masters, 1991. Budget of sediment and prediction of the future state of the coast. In California Storm and Tidal Waves Study, State of the Coast Report, Chapter 9. U.S. Army Corps of Engineers, Los Angeles District, 111 pp.
- Intergovernmental Panel on Climate Change (IPCC), 2013. Climate Change 2013: The Physical Science Basis, Contribution of Working Group I to the Fifth Assessment Report of the Intergovernmental Panel on Climate Change. Cambridge University Press, Cambridge, United Kingdom and New York, NY, 1535 pp.
- Intergovernmental Panel on Climate Change (IPCC), 2014. Climate Change 2014: Synthesis Report, Contribution of Working Groups I, II and III to the Fifth Assessment Report of the Intergovernmental Panel on Climate Change. Geneva, Switzerland, 151 pp.

- Intergovernmental Panel on Climate Change (IPCC), 2021. Climate Change 2021: The Physical Science Basis, Contribution of Working Group I to the Sixth Assessment Report of the Intergovernmental Panel on Climate Change. Cambridge University Press, 3949 pp.
- Intergovernmental Panel on Climate Change (IPCC), 2022. AR6 Synthesis Report: Climate Change 2022, Sixth Assessment Report of the Intergovernmental Panel on Climate Change. Cambridge University Press, in press.
- Kennedy, M.P., and S.S. Tan, 2007. Geologic map of the Oceanside 30'×60'quadrangle, California, California Department of Conservation, Division of Mines and Geology, scale 1:100,000, 1 plate.
- Kikkawa, H., H. Shiigaki, and T. Kono, 1968. Fundamental study of wave over-topping on levees. Coastal Eng. Japan, 11, 107-115.
- Kirk, R.M., P.D. Komar, J.C. Allen, and W.J. Stephenson, 2000. Shoreline erosion on 473 Lake Hawea, New Zealand, caused by high lake levels and storm-wave runoff. J. Coastal Res., 16 (2): 346-356.
- Koh, R.C.Y., N.H. Brooks, and E.J. List, 1974. Hydraulic Modeling of Thermal Outfall Diffusers for the San Onofre Nuclear Power Plant. Unpublished report, California Institute of Technology, Pasadena, CA. <http://resolver.caltech.edu/CaltechKHR:KH-R-30>
- Kopp, R.E., R.M. Horton, C.M. Little, J.X. Mitrovica, M. Oppenheimer, D.J. Rasmussen, B.H. Strauss, and C. Tebaldi, 2014. Probabilistic 21st and 22nd century sea-level projections at a global network of tide-gauge sites. Earth's Future, 2, 383-406.
- Kuhn, G.G., and F.P. Shepard, 1984. Seacliffs, Beaches, and Coastal Valleys of San Diego County. Berkeley, California: University of California Press.
- NOAA's Ocean Service (NOS), Office for Coastal Management (OCM), 2013. 2013 NOAA Coastal California TopoBathy Merge Project. <https://coast.noaa.gov>
- Mastrandrea, M.D., C.B. Field, T.F. Stocker, O. Edenhofer, K.L. Ebi, D.J. Frame, H. Held, E. Kriegler, K.J. Mach, P.R. Matschoss, G.-K. Plattner, G.W. Yohe, and F.W. Zwiers, 2010. Guidance Note for Lead Authors of the IPCC Fifth Assessment Report on Consistent Treatment of Uncertainties. Intergovernmental Panel on Climate Change (IPCC), 6 pp. <http://www.ipcc.ch>.
- National Research Council (NRC), 2012. Sea-Level Rise for the Coasts of California, Oregon, and Washington: Past, Present, and Future. National Academy Press, Washington, D.C., 201 pp.
- Ocean Protection Council (OPC), 2018. State of California Sea Level Rise Guidance, 2018 Update (California Natural Resources Agency Ocean Protection Council), 84 pp.

- Ocean Protection Council (OPC), 2020. Strategic Plan to Protect California's Coast and Ocean 2020–2025. California Natural Resources Agency Ocean Protection Council, 64 pp.
<https://www.opc.ca.gov/webmaster/ftp/pdf/2020-2025-strategic-plan/OPC-2020-2025-Strategic-Plan-FINAL-20200228.pdf>.
- Owen, M.W., 1980. Design of Seawalls Allowing for Wave Overtopping. Report EX924, Hydraulics Research Station, Wallingford, U.K.
- Pawka, S.S., 1983. Island shadows in wave directional spectra. *Jour. Geophys. Res.*, 88(C4), 2579-2591.
- Pilkey, O.H., and J.A.G. Cooper, 2004. Society and sea level rise. *Science*, 303 (5665), 1781-1782.
- Raubenheimer, B., R.T. Guza, S. Elgar, and N. Kobayashi, 1995. Swash on a gently sloping beach. *J. Geophys. Res.*, 100, 8751-8760.
- Raubenheimer, B., and R.T. Guza, 1996. Observations and predictions of run-up. *J. Geophys. Res.* 101 (C10), 25575-25587.
- Reis, M.T., K. Hu, T.S. Hedges, and H. Mase, 2008. A comparison of empirical, empirical, and numerical wave overtopping models. *J. Coastal Res.*, 24(2A), 250-262.
- Ruggiero, P., P.D. Komar, J.J. Marra, W.G. McDougal, and R.A. Beach, 2001. Wave runup, extreme water levels, and the erosion of properties backing beaches. *J. Coastal Res.*, 17, 407-419.
- Ruggiero, P., R.A. Holman, and R.A. Beach, 2004. Wave run-up on a high-energy dissipative beach. *J. Geophys. Res.*, 109, no. C6, 12 pp.
- Runyan, K., and G.B. Griggs, 2003. The effects of armoring seacliffs on the natural sand supply to the beaches of California. *J. Coast. Res.* 19 (2), 336-347.
- Shepard, F.P., 1950. Beach cycles in southern California. U.S. Army Corps of Engineers, Beach Erosion Board, Tech. Memo. No. 20, 26 pp.
- Shih, S.M., P.D. Komar, K.J. Tillotson, W.G. McDougal, and P. Ruggiero, 1994. Wave 517 run up and sea-cliff erosion. In *Coastal Engineering 1994 Proceedings*, 24th International 518 Conference, American Society of Civil Engineers, 2170-2184.
- Stockdon, H. F., Holman, R. A., Howd, P. A., and Sallenger, A. H., 2006. Empirical parameterization of setup, swash, and runup. *Coastal Engineering*, 53, 573-588.
- Tan, S.S., 2001. Geologic map of the San Onofre Bluff 7.5' quadrangle, San Diego County, California: A digital database, version 1.0. California Department of Conservation, Division of Mines and Geology, scale 1:24000, 1 plate.

- Thornton, E. B. and Guza, R. T., 1982. Energy Saturation and Phase Speeds Measured on a Natural Beach. *Journal of Geophysical Research*, 87(C12), 9499-9508.
- Thornton, E. B. and Guza, R. T., 1983. Transformation of Wave Height Distribution. *Journal of Geophysical Research*, 88 (C10), 5925-5938.
- United States Army Corps of Engineers (USACE), 1984. Shore Protection Manual. Waterways Experiment Station, Coastal Engineering Research Center, Vicksburg, MS, 2 vols.
- United States Army Corps of Engineers (USACE), 1988. Historic Wave and Sea Level Data Report: San Diego Region. Coast of California Storm and Tidal Wave Study, Reference No. 88-6.
- United States Army Corps of Engineers (USACE), 1994a. Hydraulic Design of Flood Control Channels. Department of the Army. CECW-EH-D, Engineer Manual 1110-2-1601.
- United States Army Corps of Engineers (USACE), 1994b. Shore Protection Manual, Volume II. Department of the Army. Coastal Engineering Research Center.
- United States Army Corps of Engineers (USACE), 1990. Sediment Budget Report, Oceanside Littoral Cell, Coast of California Storm and Tidal Wave Study. Reference No. 90-2.
- University of Southern California (USC) Sea Grant Program, 2013. Sea Level Rise Vulnerability Study for the City of Los Angeles. Report prepared for the Mayor of Los Angeles, 85 pp.
- Van der Meer, J.W. and J.P.F.M. Janssen, 1995. Wave runup and wave overtopping at dikes. In *Wave Forces on Inclined and Vertical Wall Structures*. Ed. N. Kobayashi and Z. Demirbilek, ASCE, Ch. 1, pp. 1-27.
- Wolinsky, M.A., and A.B. Murray, 2009. A unifying framework for shoreline migration: Application to wave-dominated coasts. *J. Geophys. Res.*, 114 (F1), F01009.
- Woodroffe, C.D., and C.V. Murray-Wallace, 2012. Sea level rise and coastal change: The past as a guide to the future. *Quaternary Science Reviews*, 54, 4-11.
- Yates, M.L., R.T. Guza, and W.C. O'Reilly, 2009. Equilibrium shoreline response: Observations and modeling. *J. Geophys. Res.* C, 114, C0910.
- Yates, M.L., R.T. Guza, W.C. O'Reilly, J.E. Hansen, and P.L. Barnard, 2011. Equilibrium shoreline response of a high wave energy beach. *J. Geophys. Res.*, 116, C04014, 13 pp.
- Young, A.P., and S.A. Ashford, 2006. Application of airborne LiDAR for seacliff volumetric change and beach sediment budget contributions. *J. Coast. Res.*, 22, 307-318.

- Young, A.P., J.H. Raymond, J. Sorenson, E.A. Johnstone, N.W. Driscoll, R.E. Flick, and R.T. Guza, 2010a. Coarse sediment yields from seacliff erosion in the Oceanside Littoral Cell. *J. Coast. Res.*, 26, 580-585.
- Young, A.P., M.J. Olsen, N. Driscoll, R.E. Flick, R. Gutierrez, R.T. Guza, E. Johnstone, and F. Kuester, 2010b. Comparison of airborne and terrestrial LiDAR estimates of seacliff erosion in southern California. *Photogrammetric Engineering and Remote Sensing* 76, 421-427.
- Young, A.P., R.E. Flick, W.C. O'Reilly, D.B. Chadwick, R.T. Guza, W.C. Crampton, and J.J. Helly, 2014. Estimating cliff retreat in southern California considering sea level rise using a sand balance approach. *Mar. Geology*, 348, 15-2.
- Young, A.P., R. E. Flick, T.W. Gallien, S. N. Giddings, R.T. Guza, M. Harvey, L. Lenain, B.C. Ludka, W. K. Melville, and W. C. O'Reilly, 2018. Southern California coastal response to the 2015-2016 El Niño, *J. Geophys. Res: Earth Surface*, 123.
- Zhang, K., Douglas, B.C., and S.P. Leatherman, 2004. Global warming and coastal erosion. *Climatic Change*, 64 (1), 41-58.

APPENDIX A

**MODELED BEACH AND CLIFF PROFILE CHANGES
BY 2050 DUE TO MSLR**

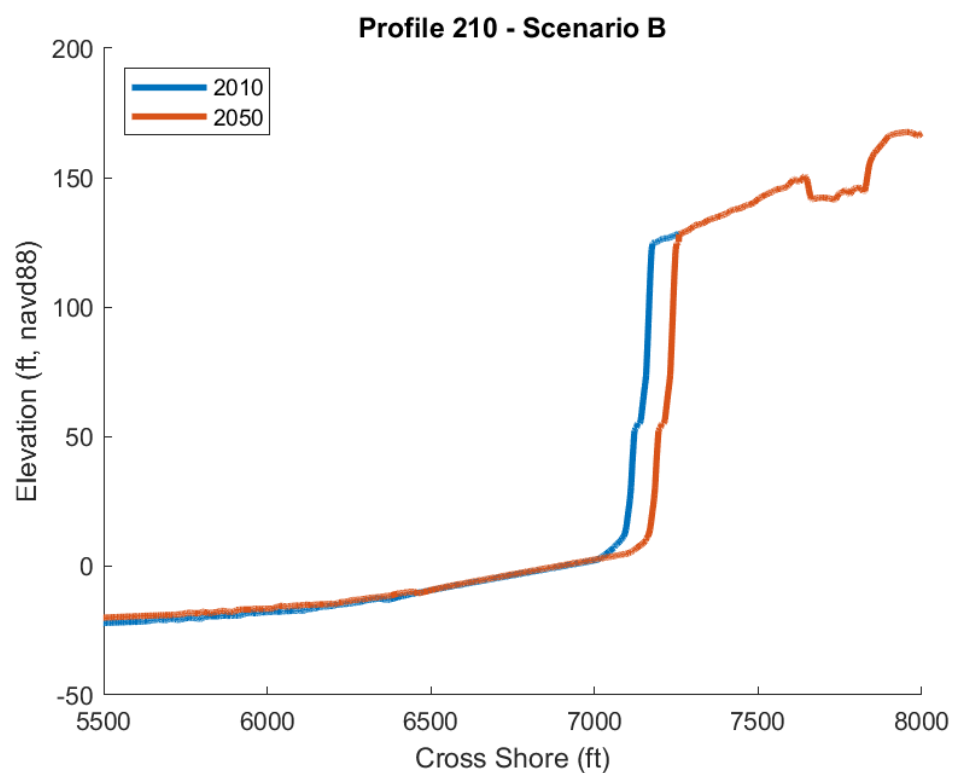
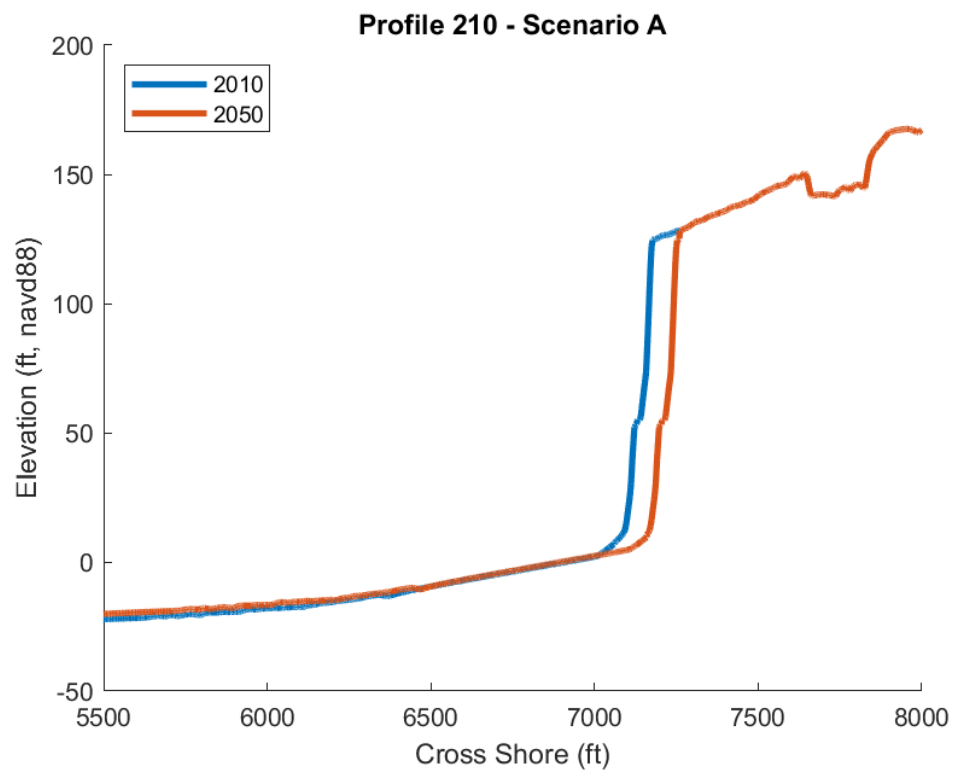


Figure A-1. Observed 2010 and modeled 2050 Profile 210.

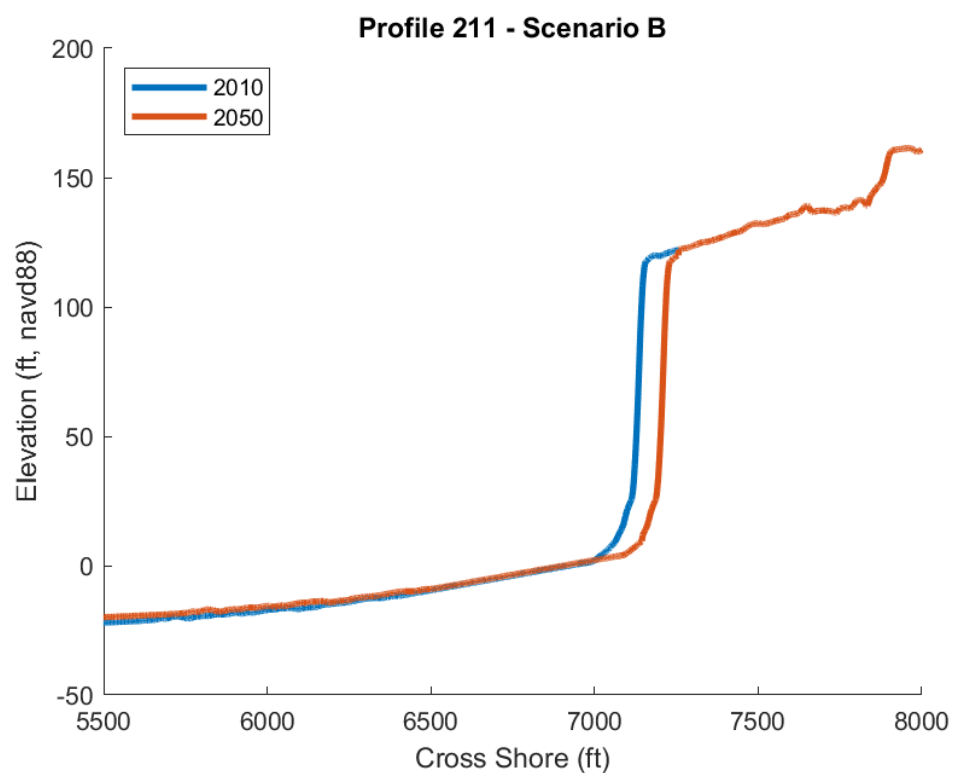
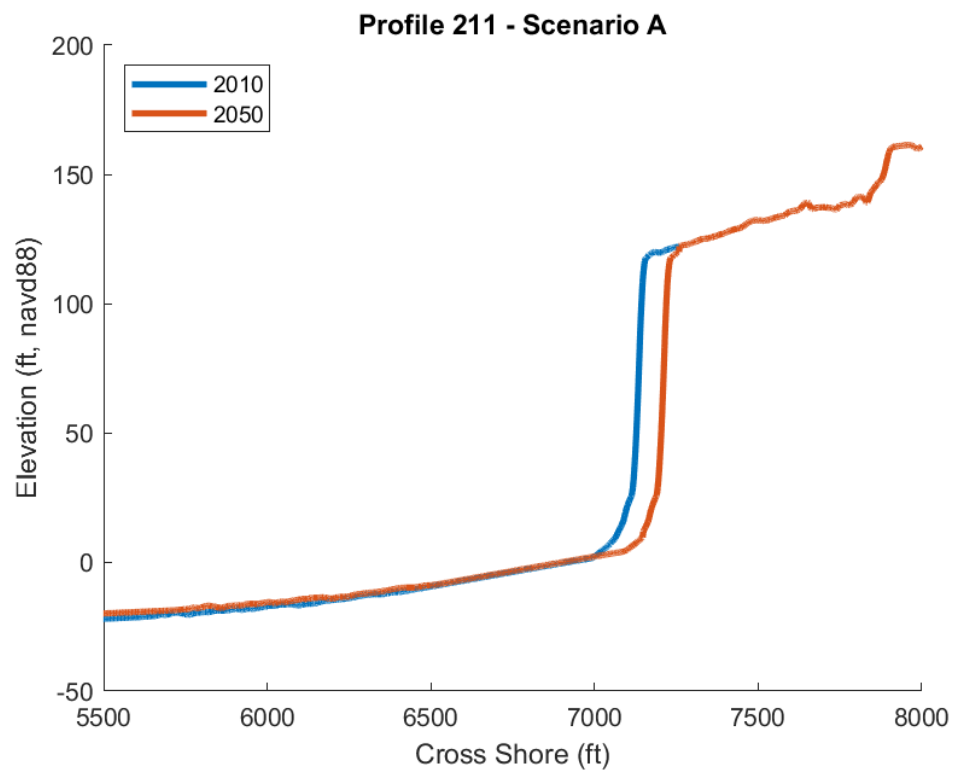


Figure A-2. Observed 2010 and modeled 2050 Profile 211.

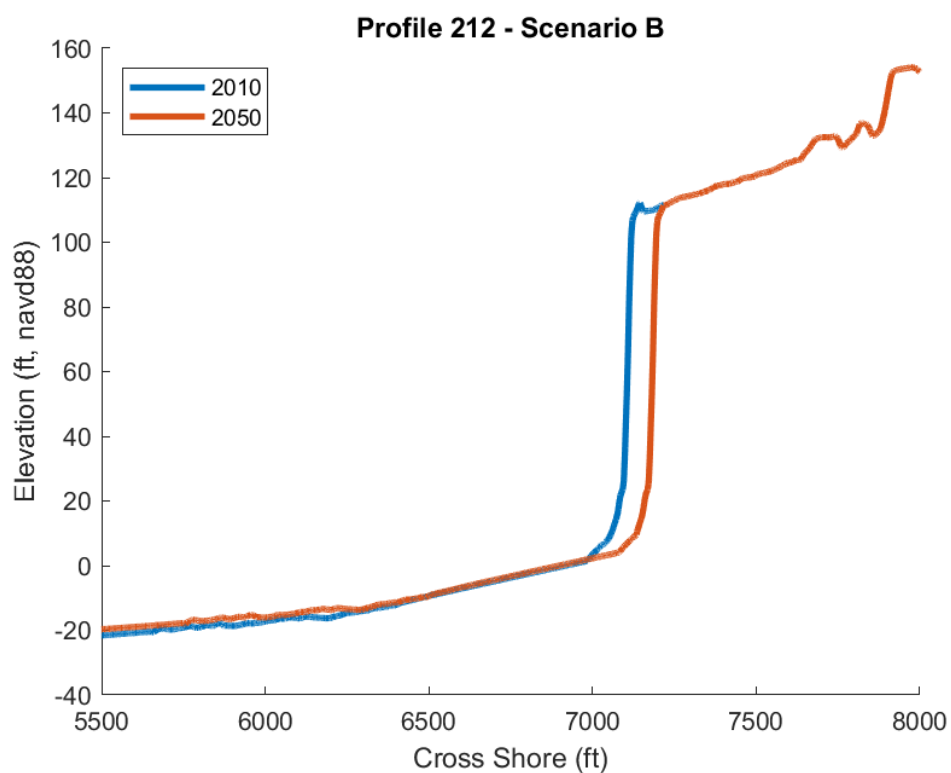
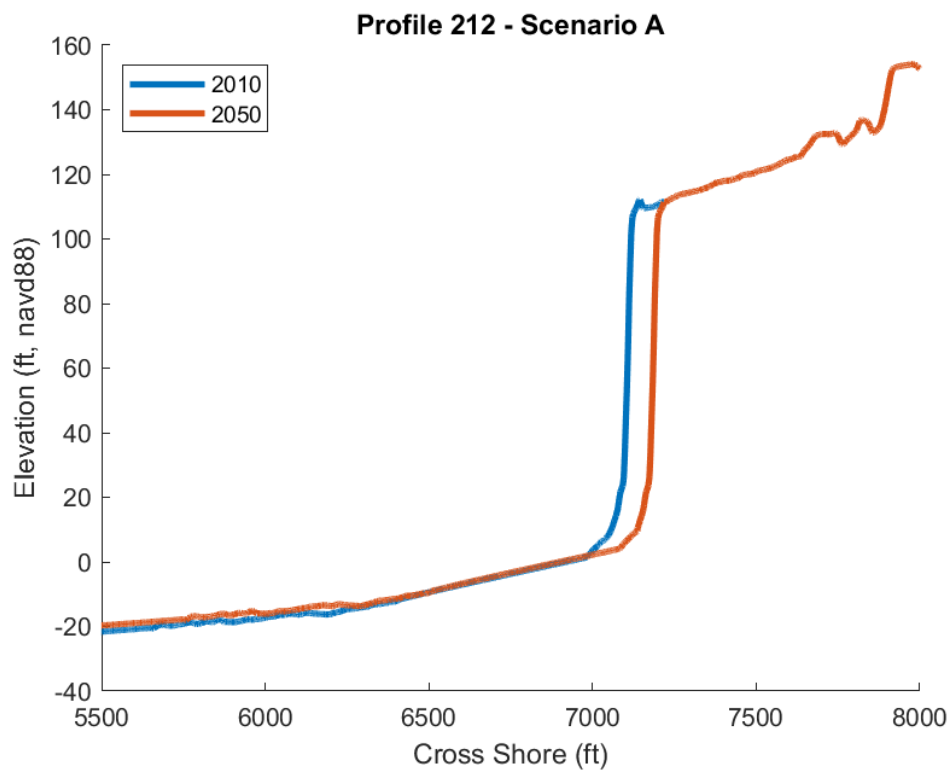


Figure A-3. Observed 2010 and modeled 2050 Profile 212.

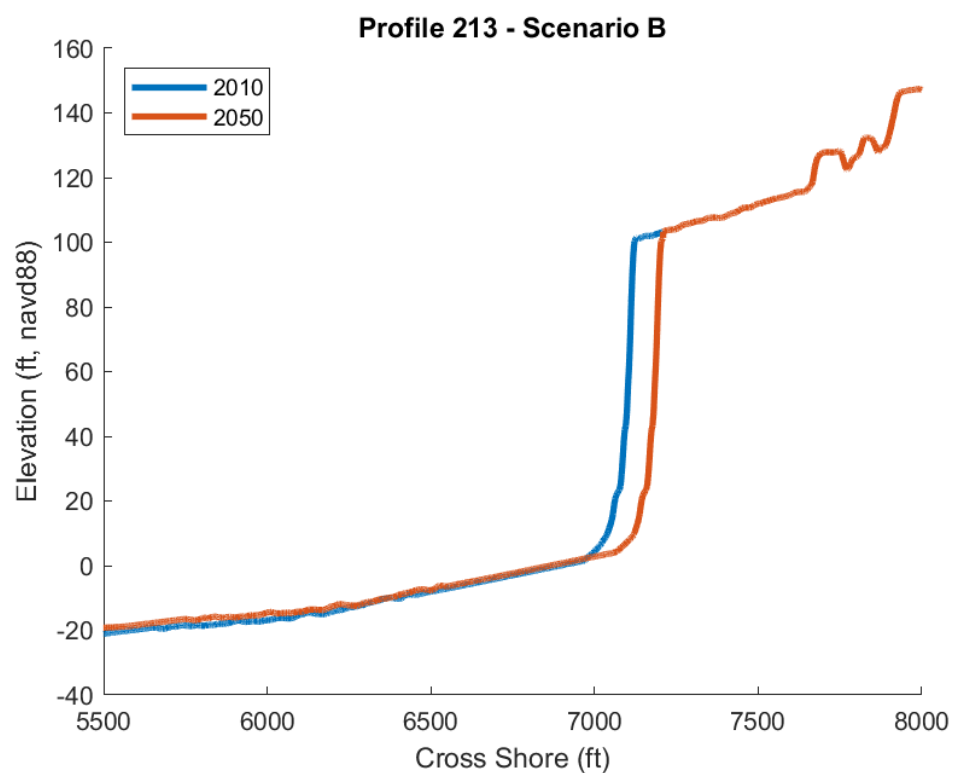
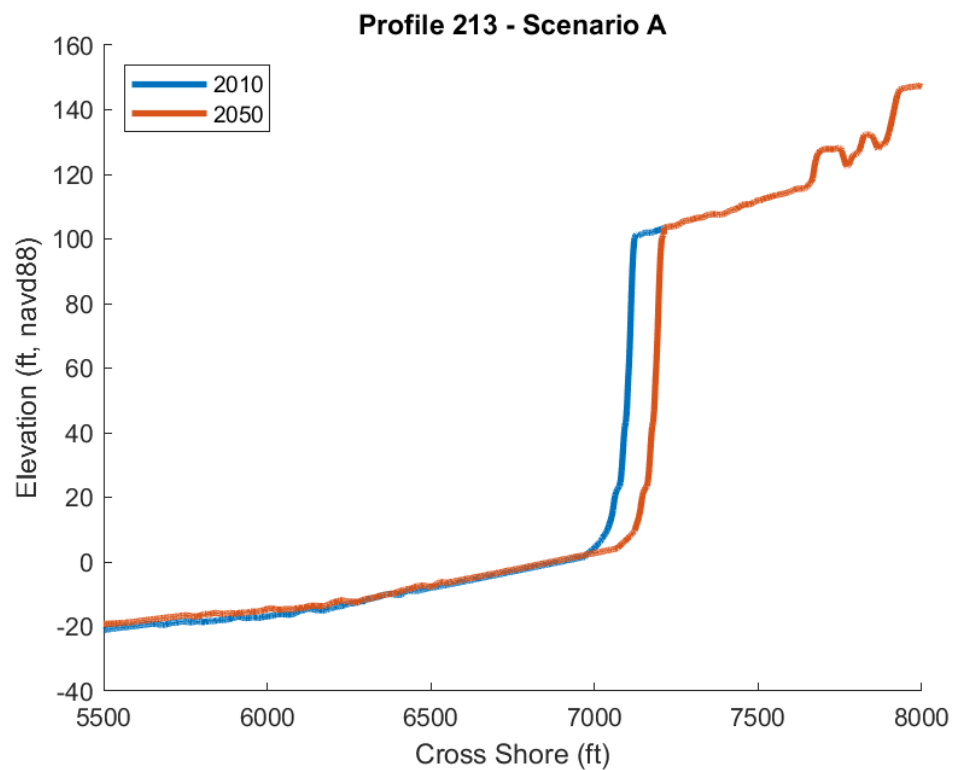


Figure A-4. Observed 2010 and modeled 2050 Profile 213.

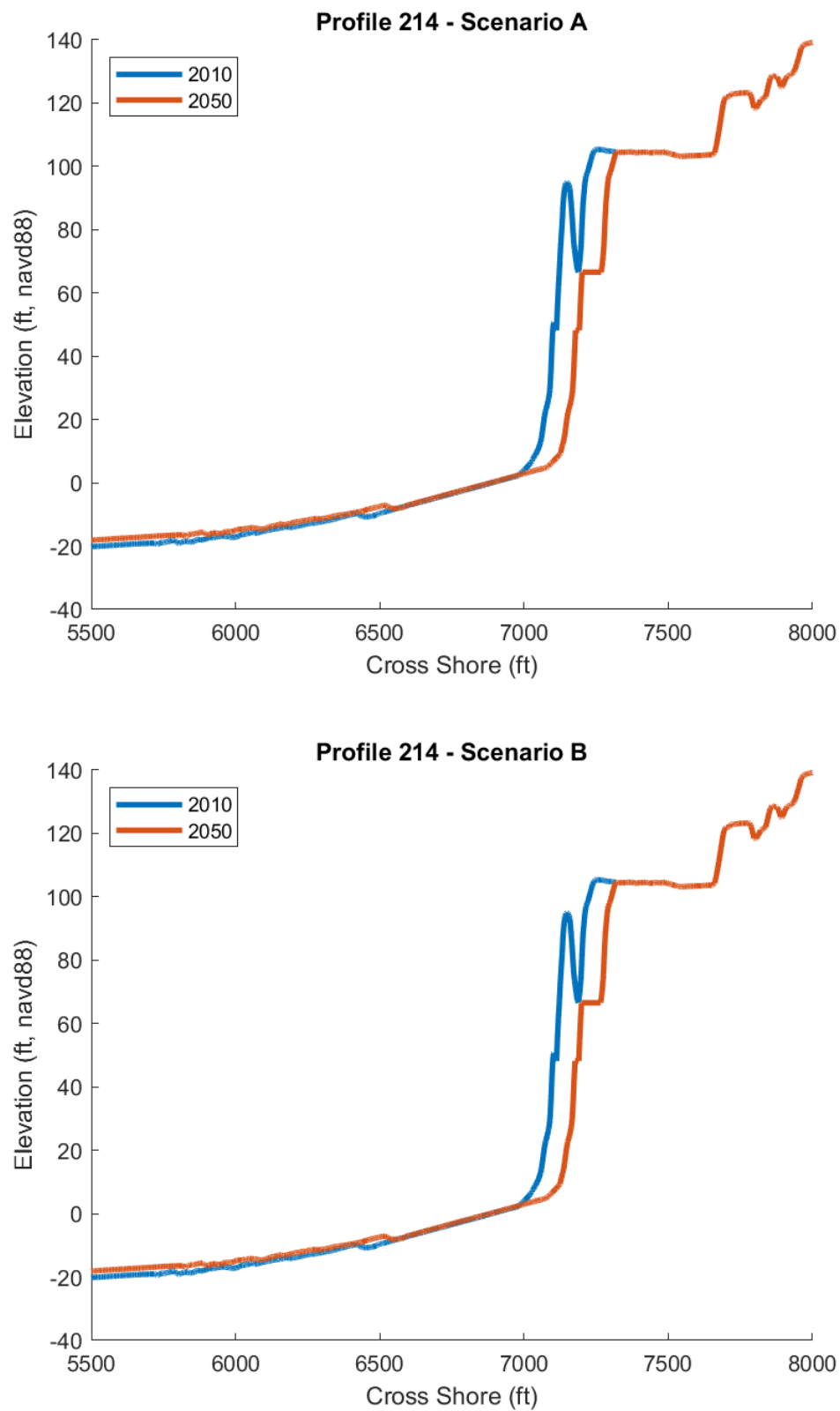


Figure A-5. Observed 2010 and modeled 2050 Profile 214.

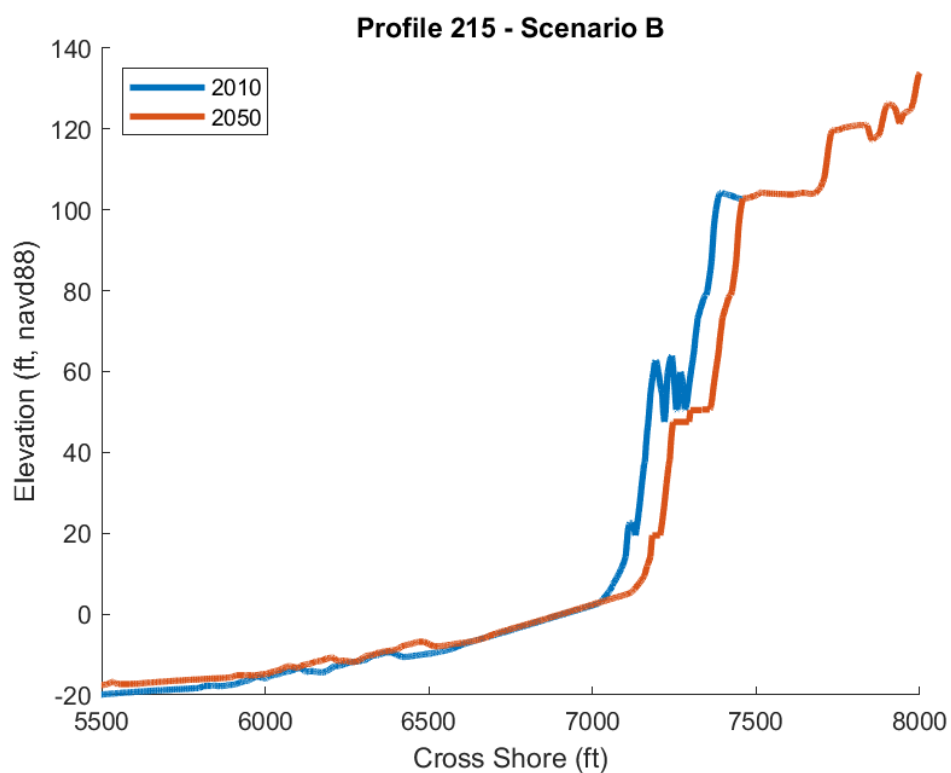
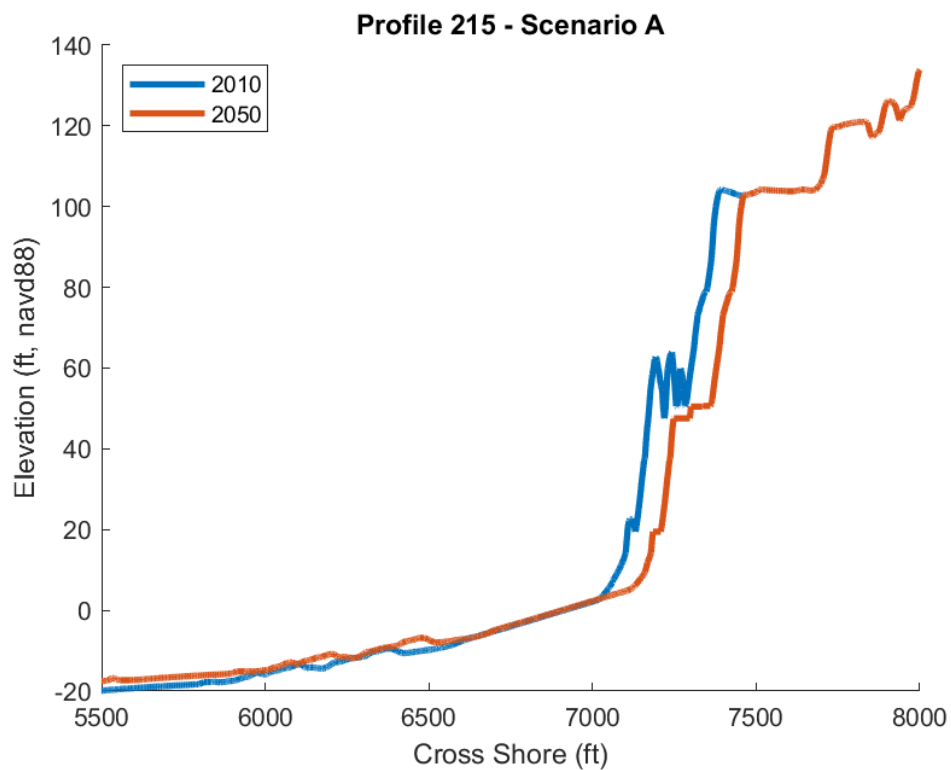


Figure A-6. Observed 2010 and modeled 2050 Profile 215.

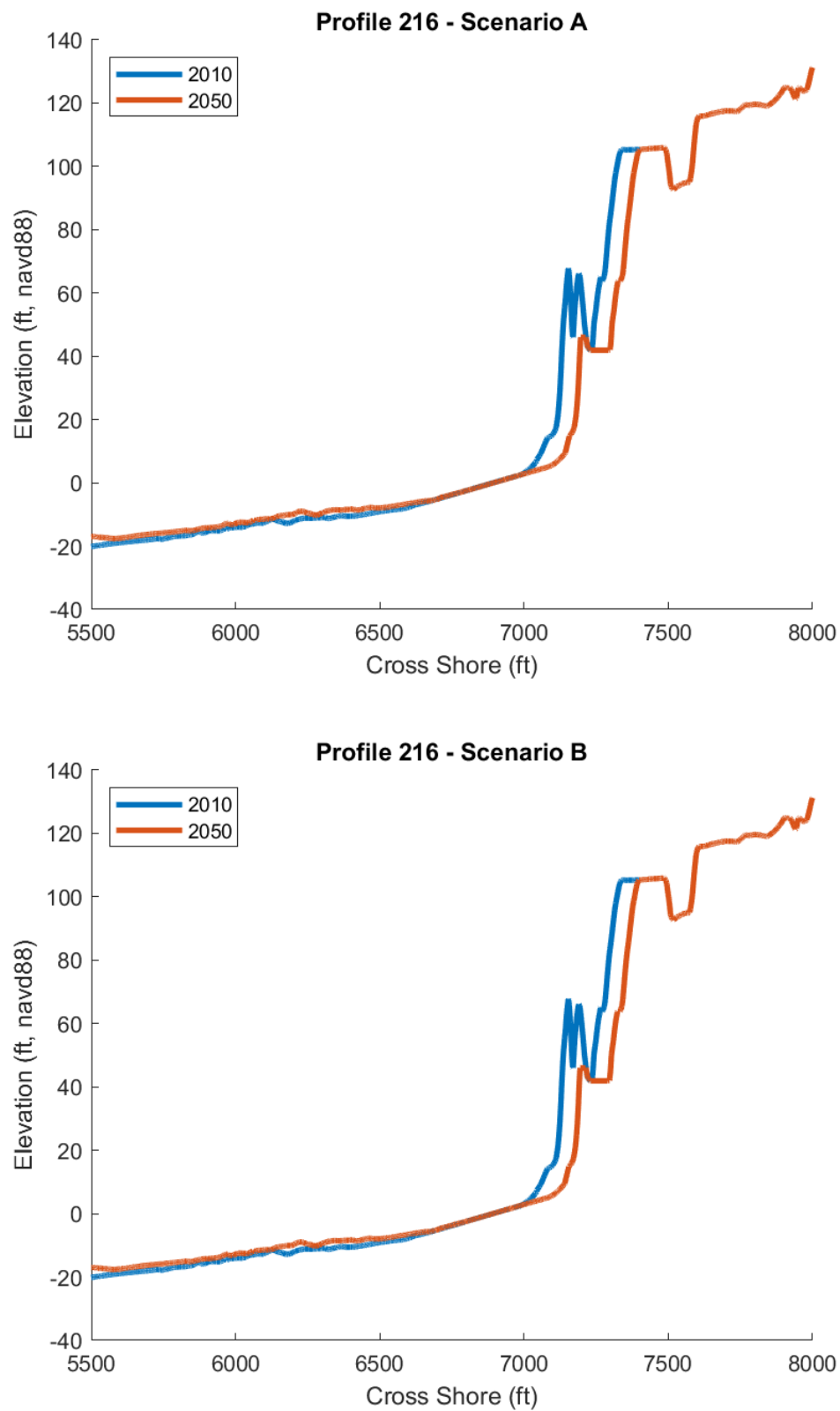


Figure A-7. Observed 2010 and modeled 2050 Profile 216.

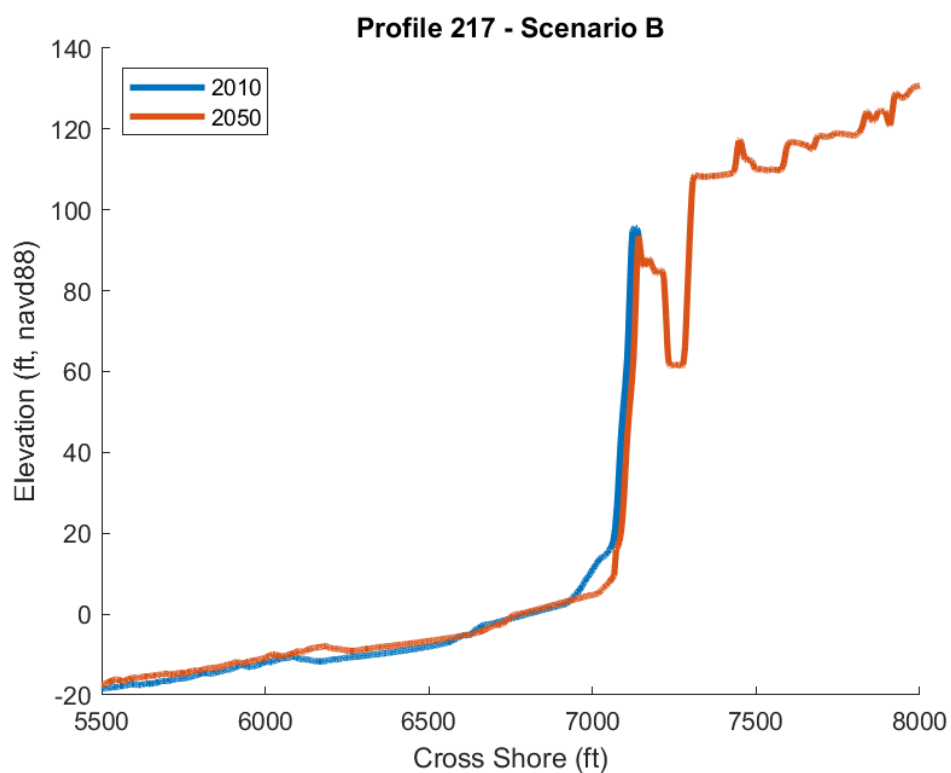
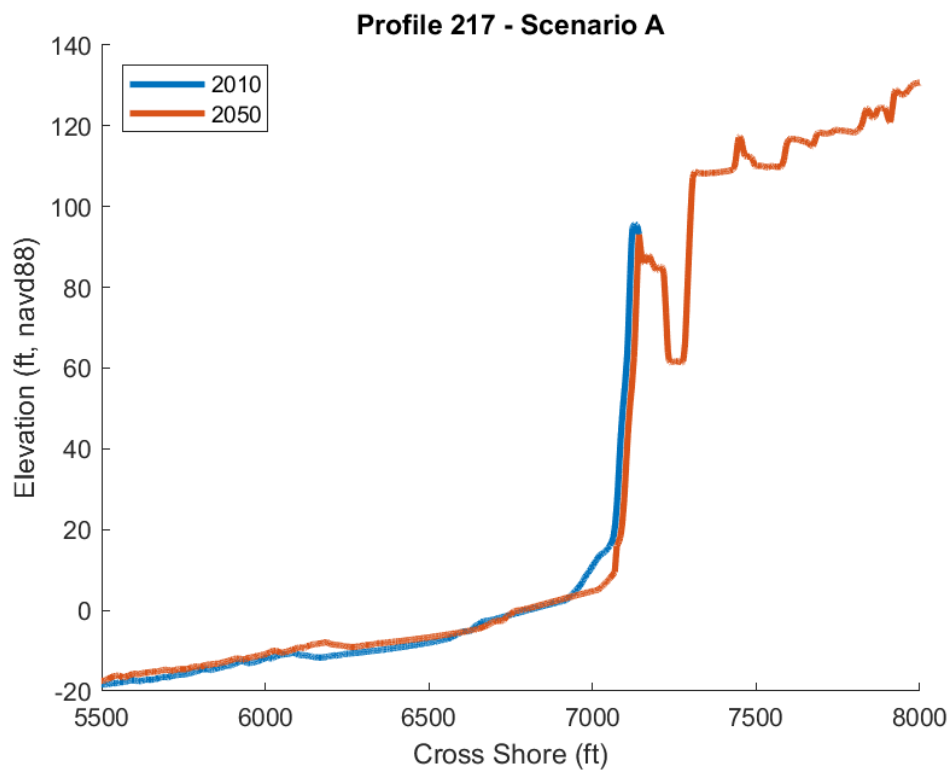


Figure A-8. Observed 2010 and modeled 2050 Profile 217.

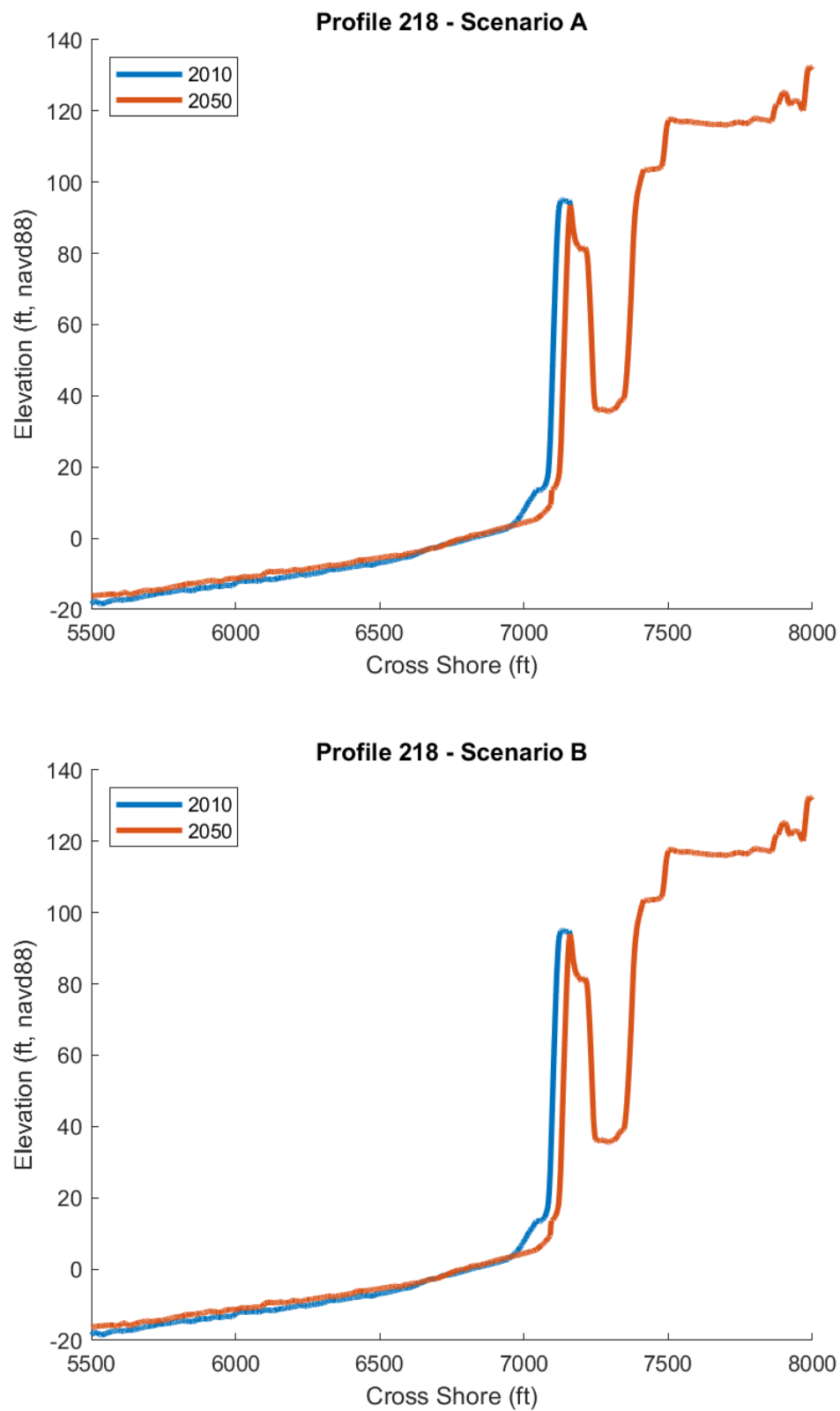


Figure A-9. Observed 2010 and modeled 2050 Profile 218.

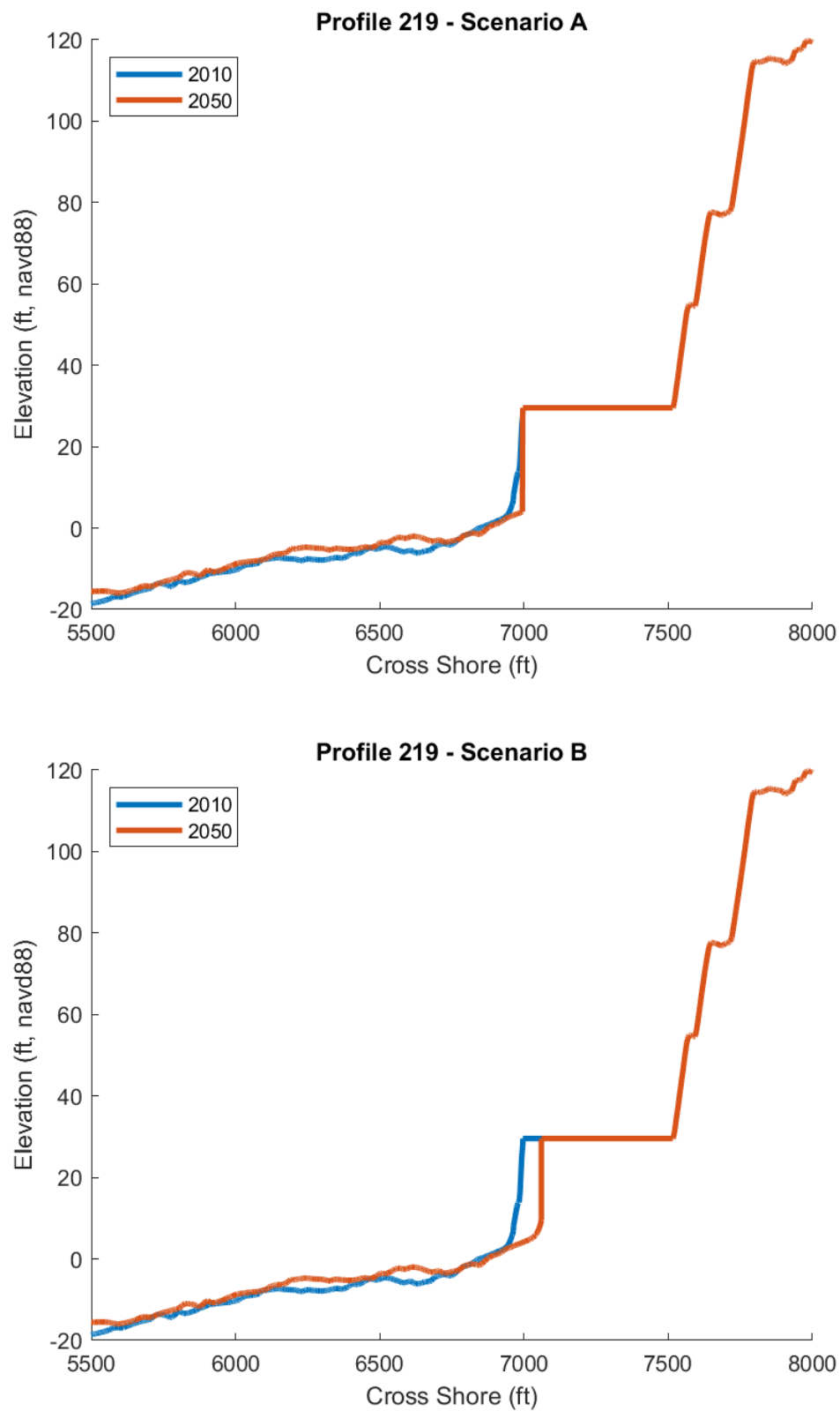


Figure A-10. Observed 2010 and modeled 2050 Profile 219.

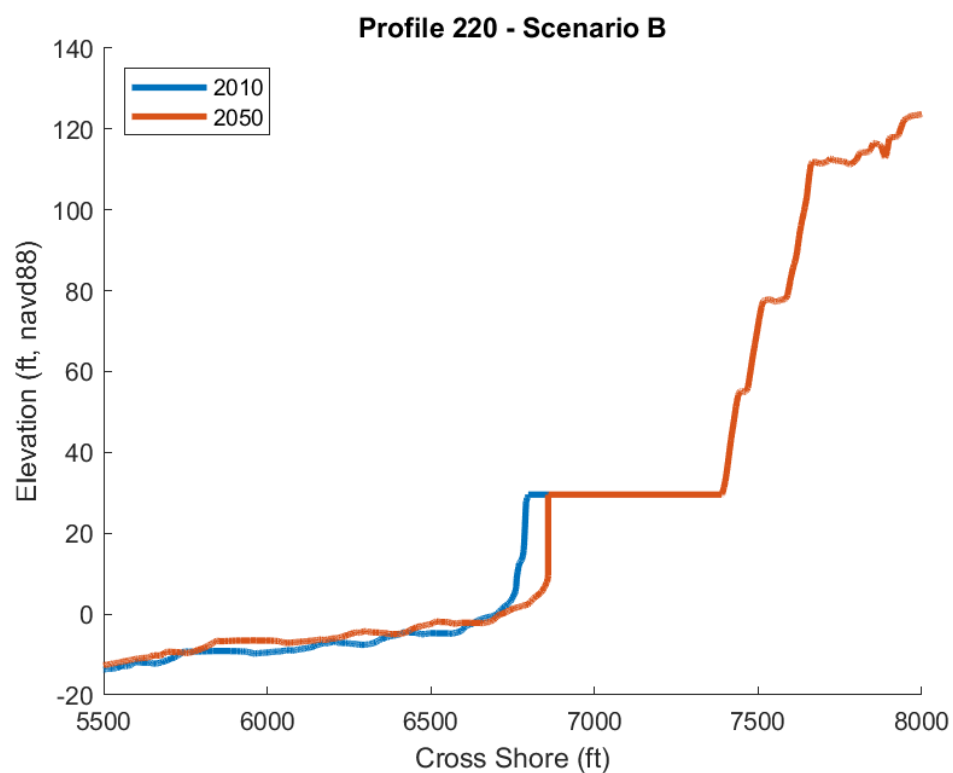
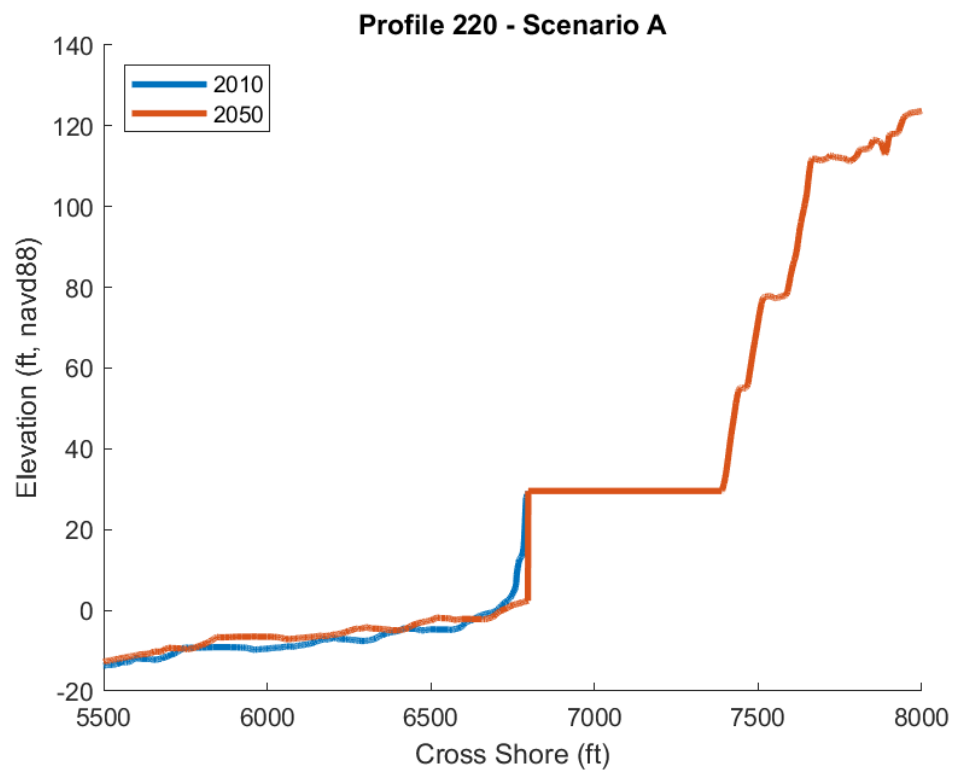


Figure A-11. Observed 2010 and modeled 2050 Profile 220.

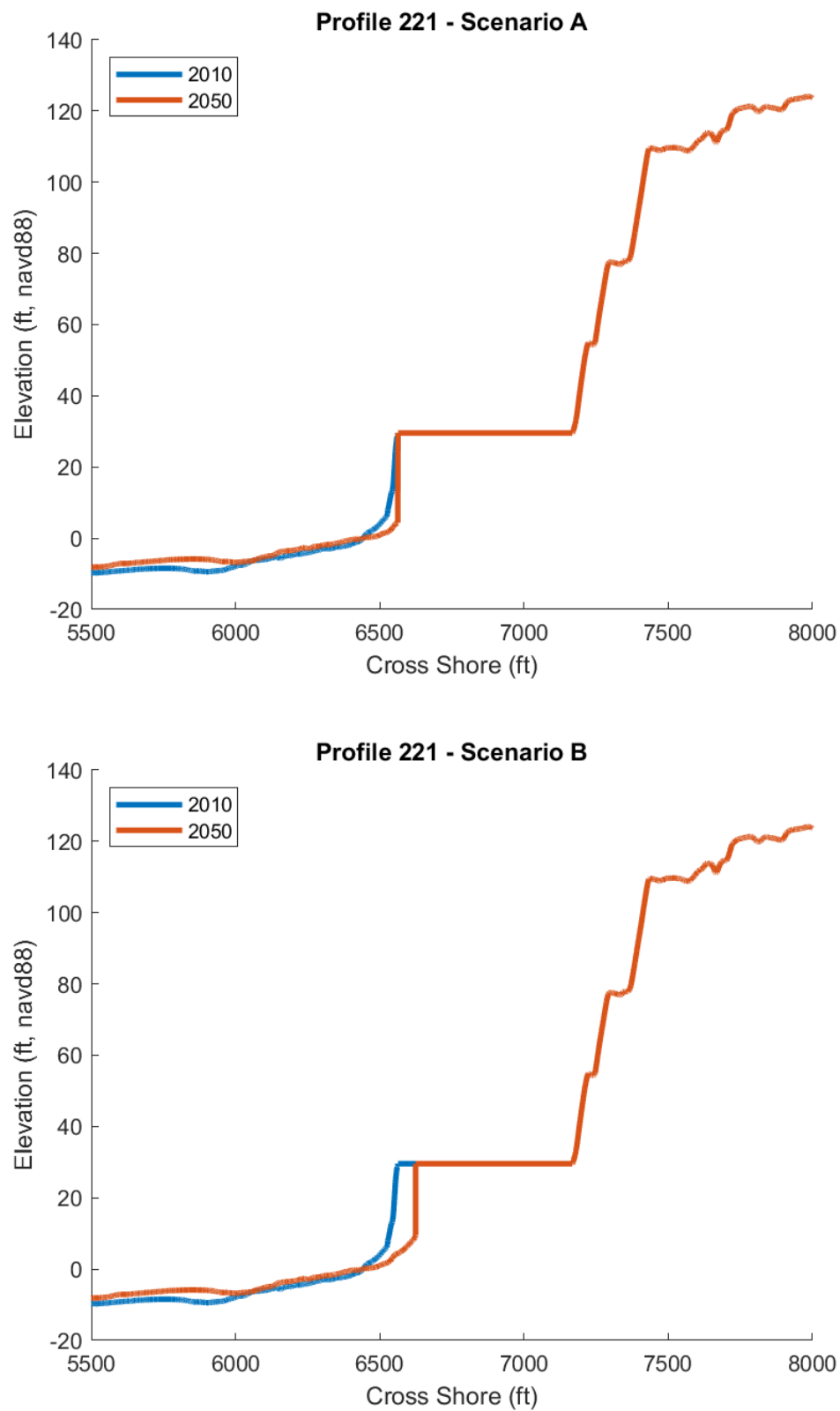


Figure A-12. Observed 2010 and modeled 2050 Profile 221.

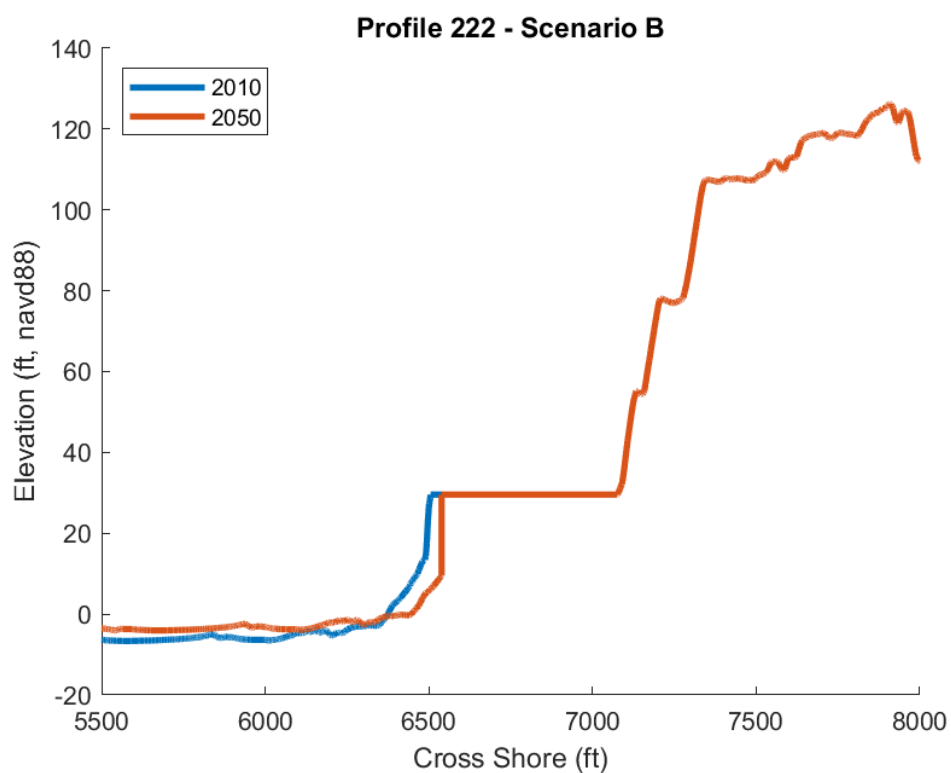
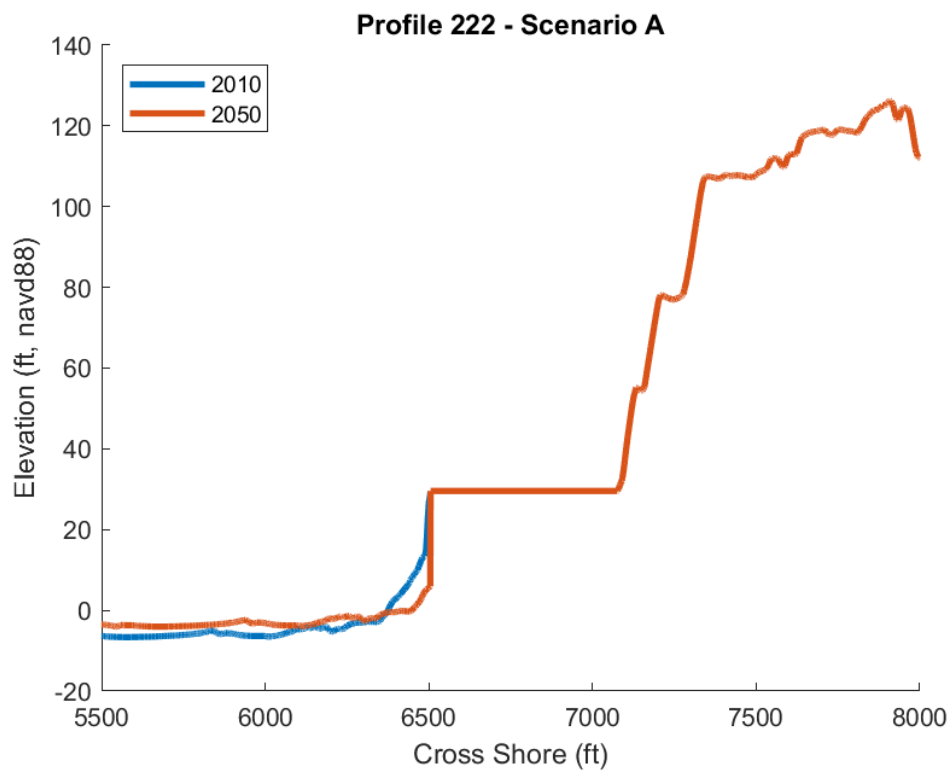


Figure A-13. Observed 2010 and modeled 2050 Profile 222.

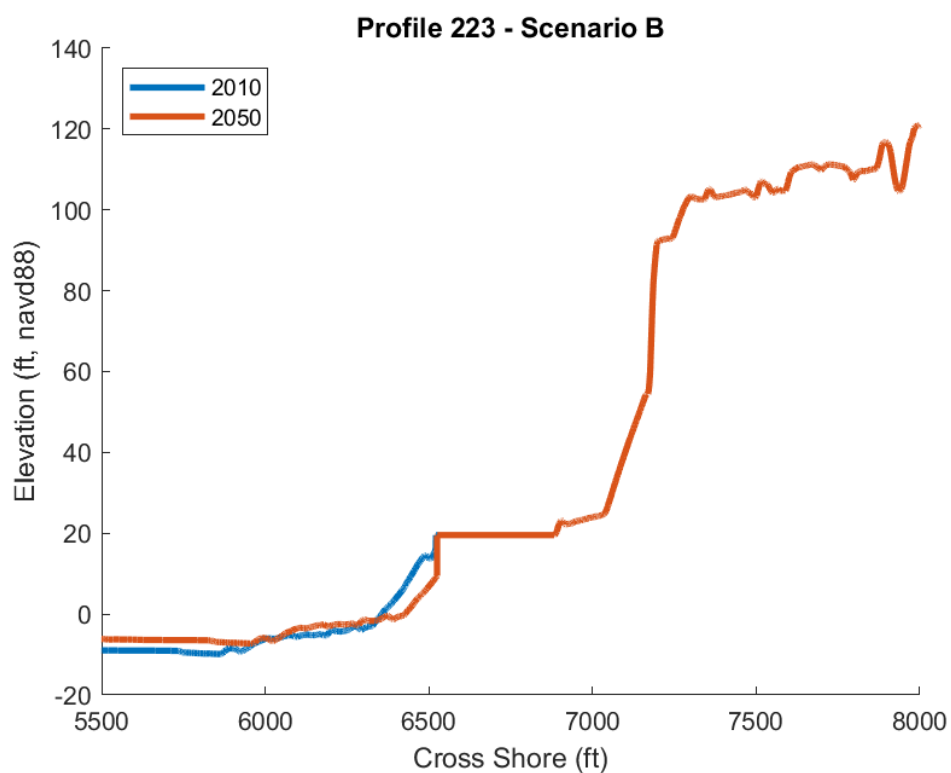
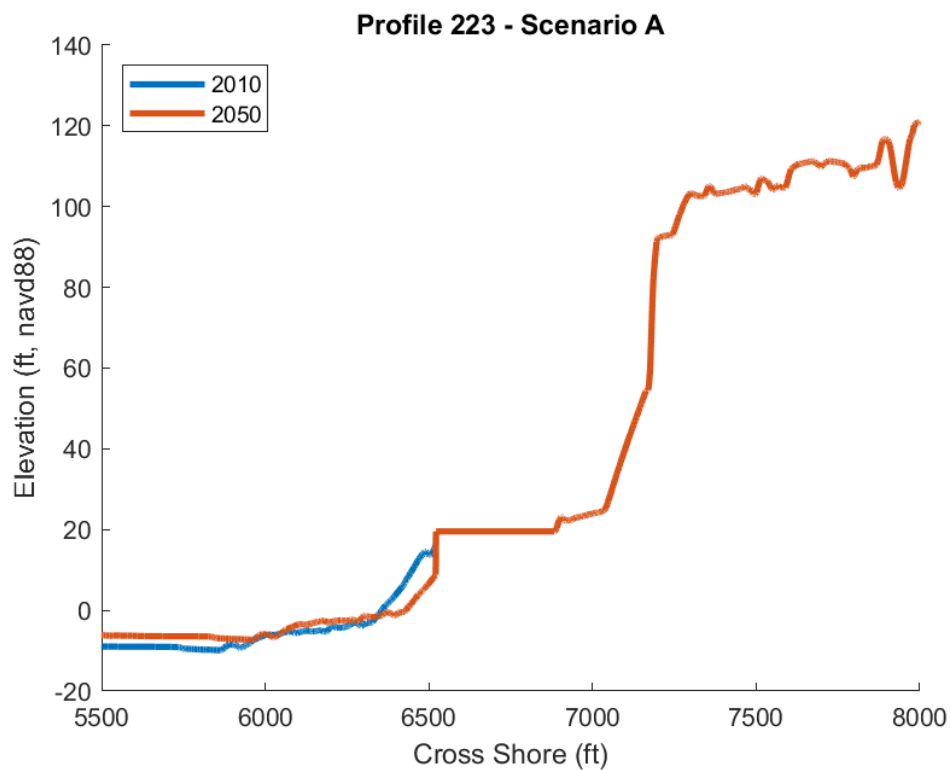


Figure A-14. Observed 2010 and modeled 2050 Profile 223.

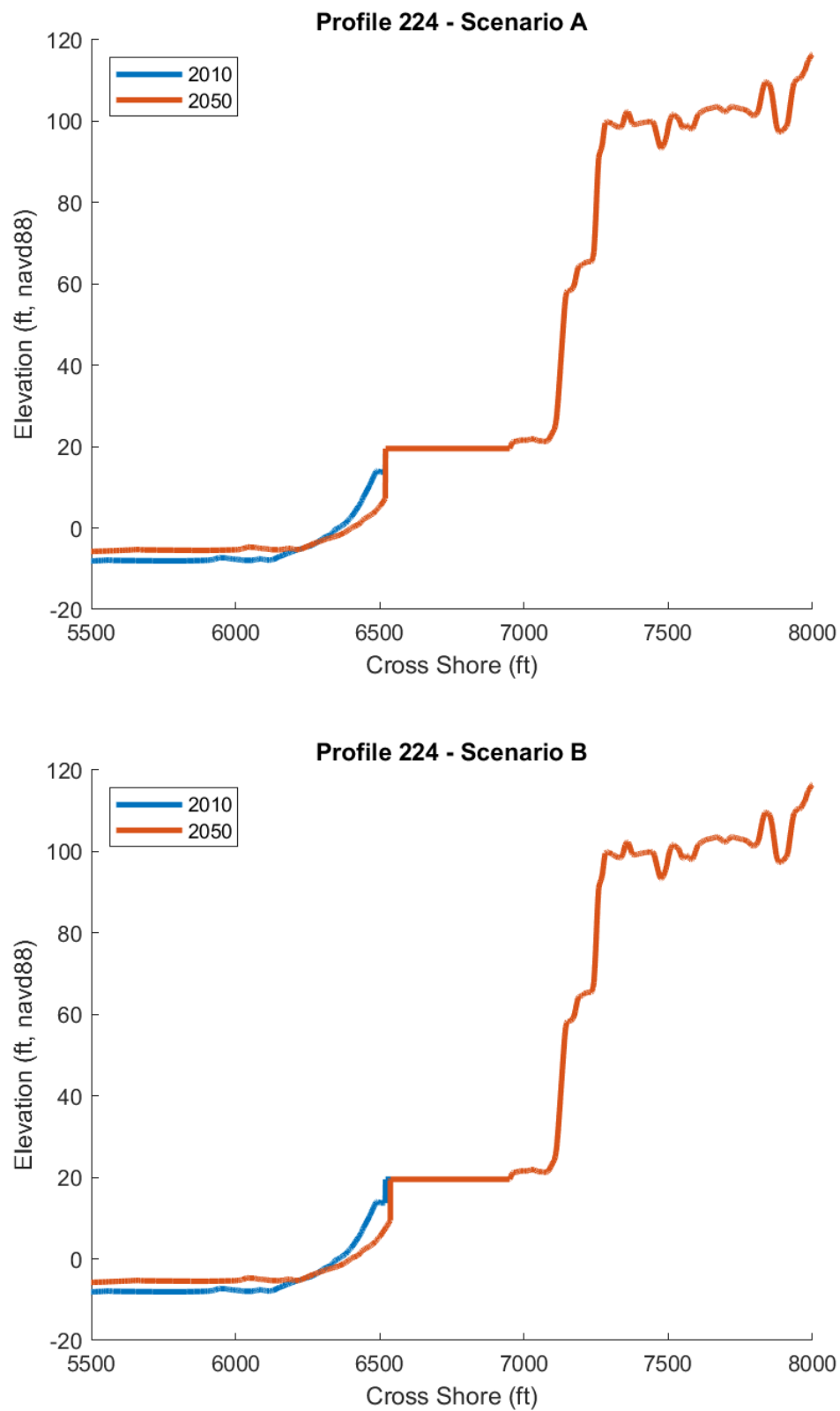


Figure A-15. Observed 2010 and modeled 2050 Profile 224.

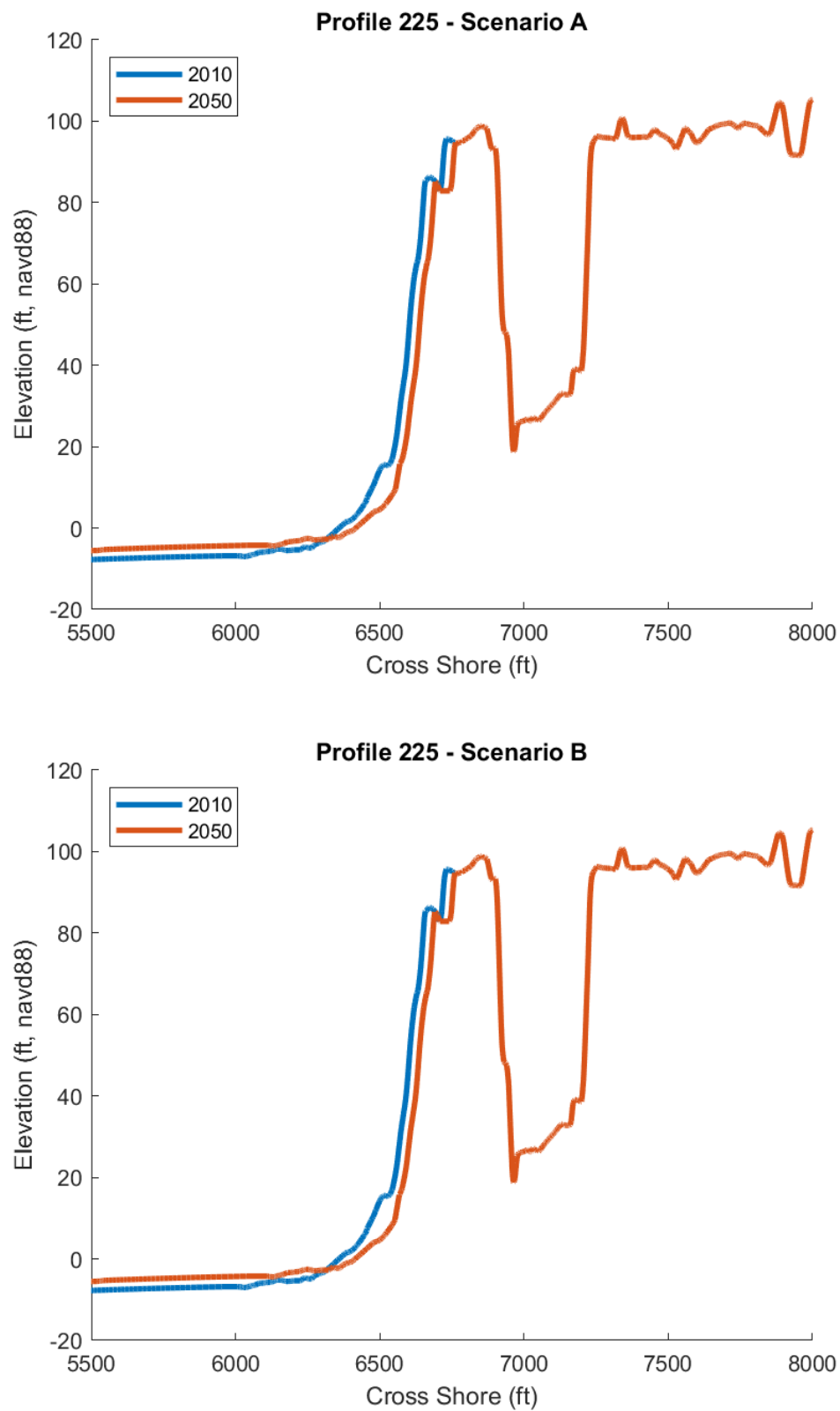


Figure A-16. Observed 2010 and modeled 2050 Profile 225.

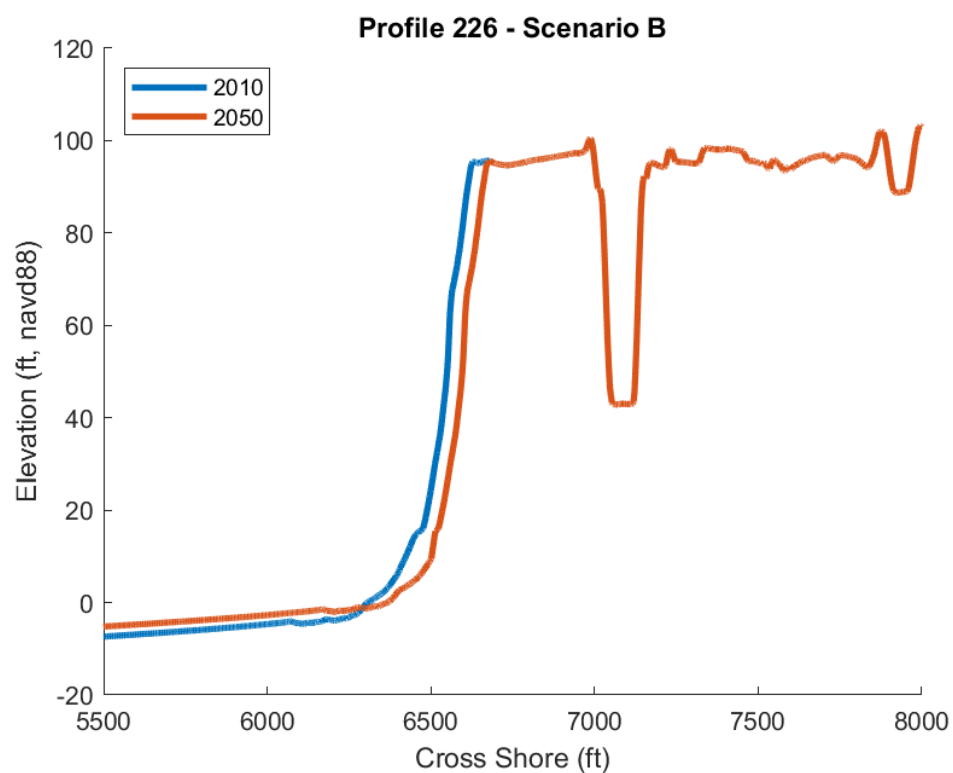
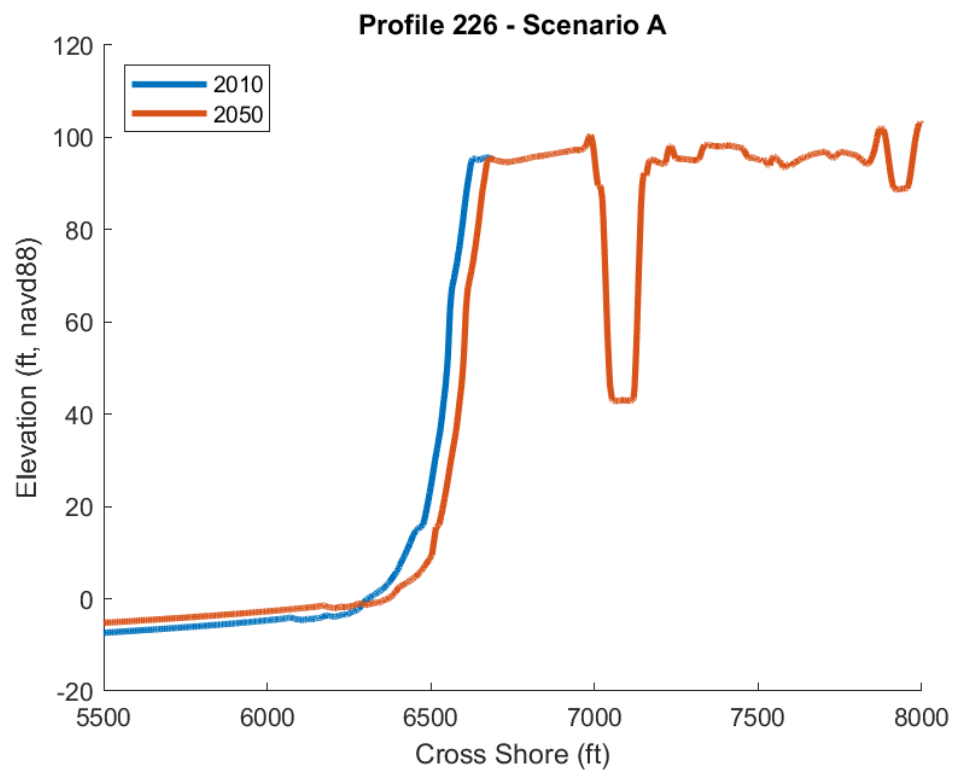


Figure A-17. Observed 2010 and modeled 2050 Profile 226.

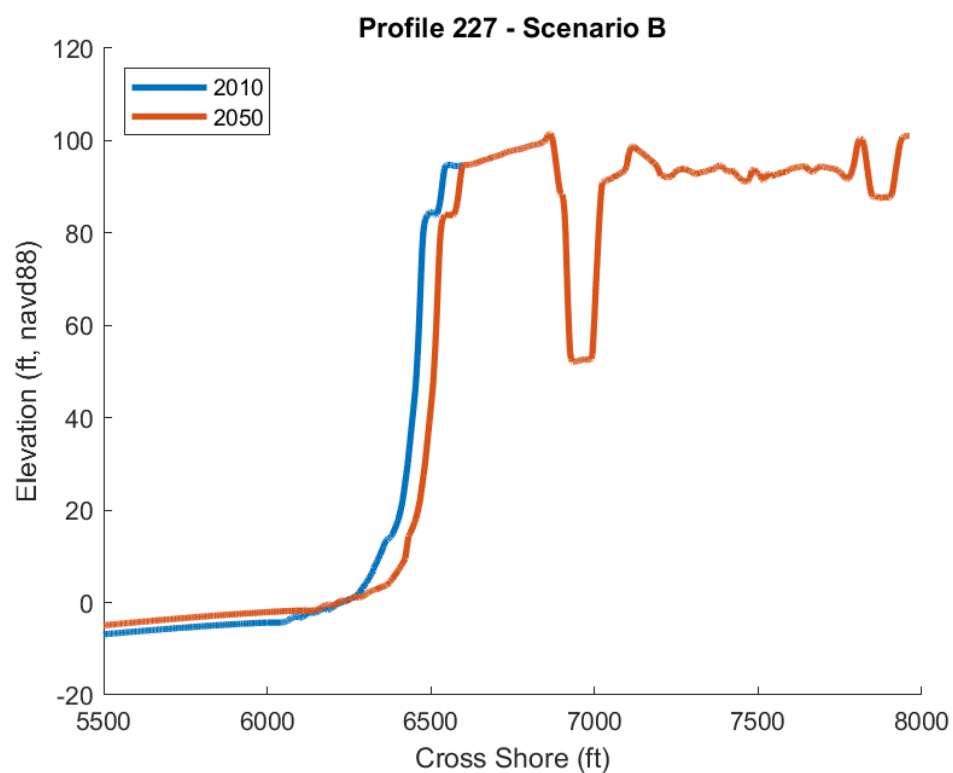
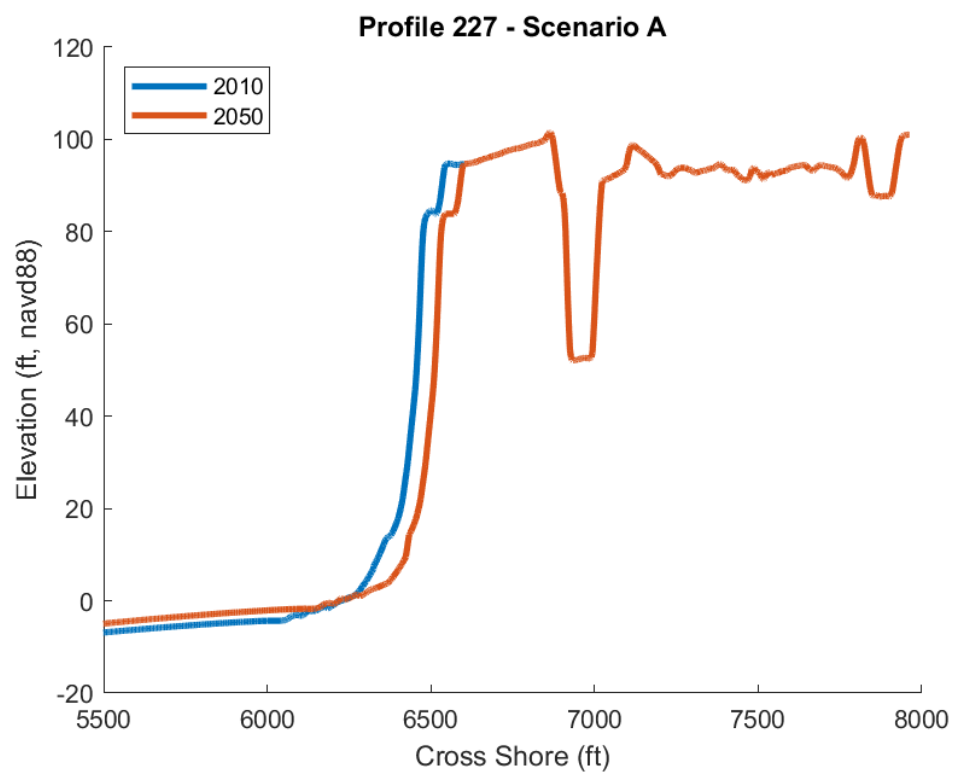


Figure A-18. Observed 2010 and modeled 2050 Profile 227.

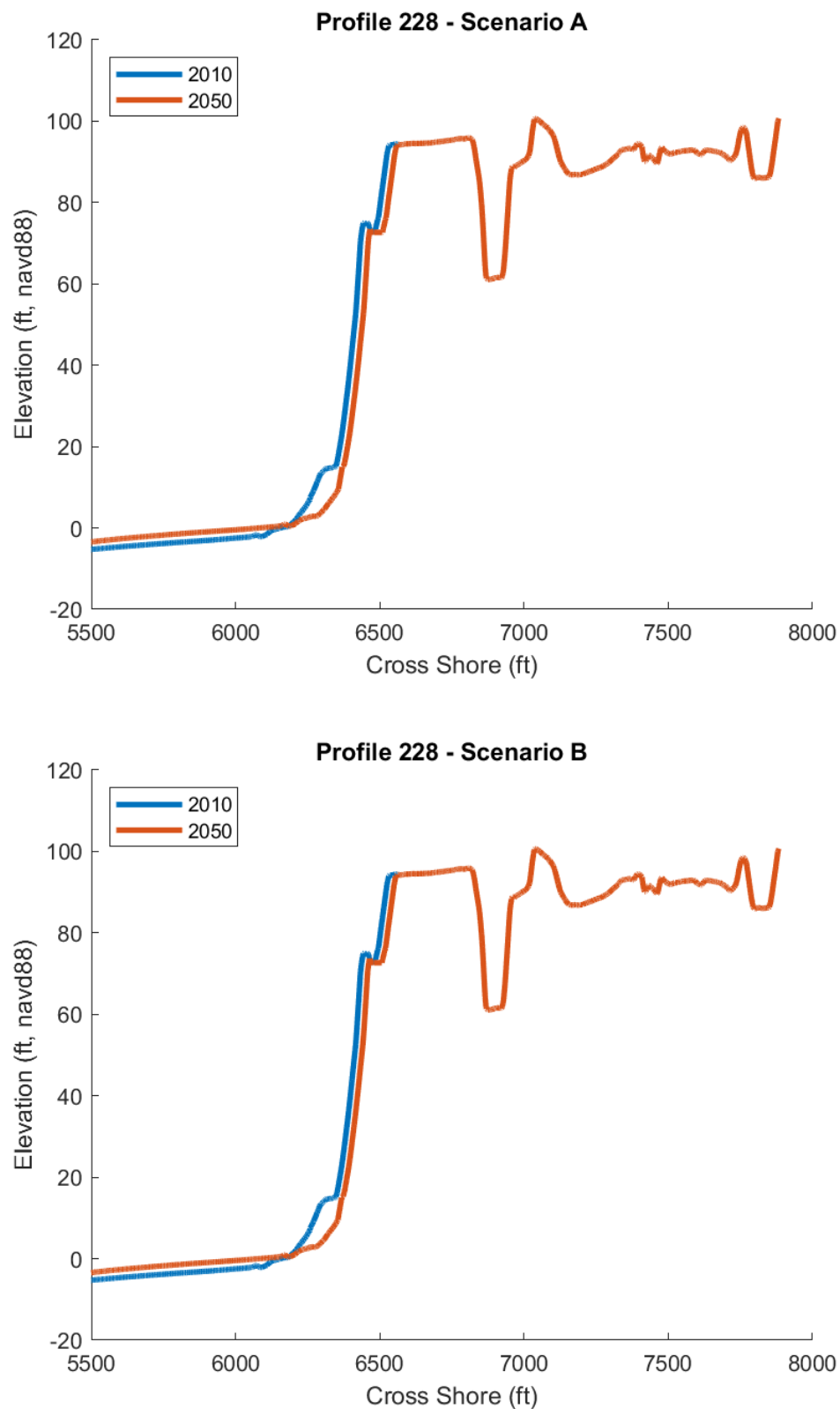


Figure A-19. Observed 2010 and modeled 2050 Profile 228.

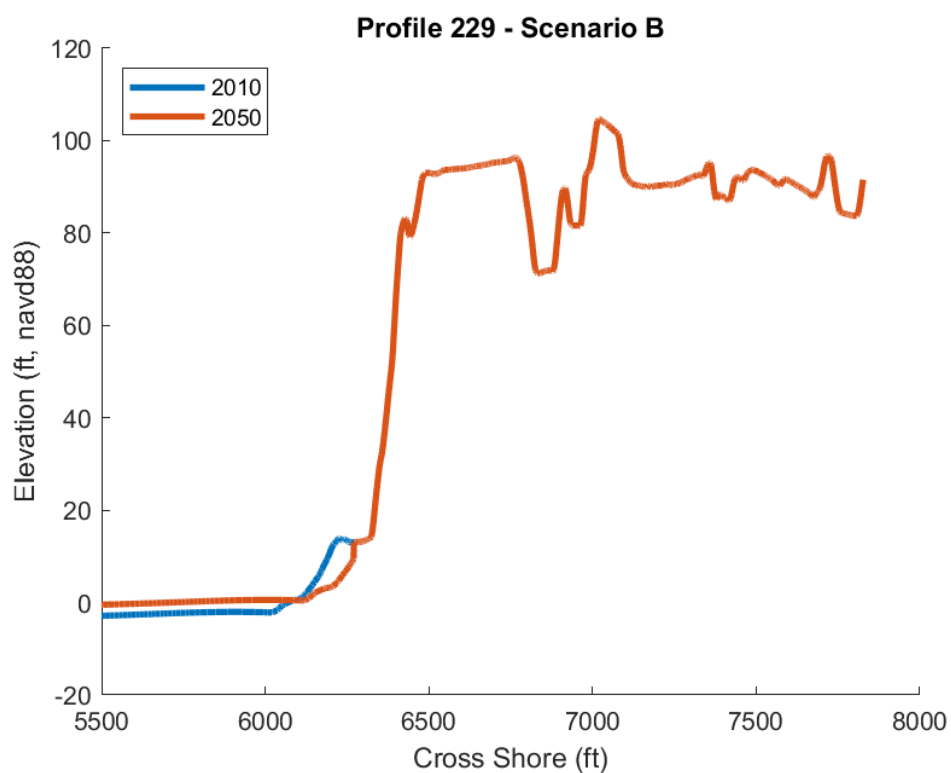
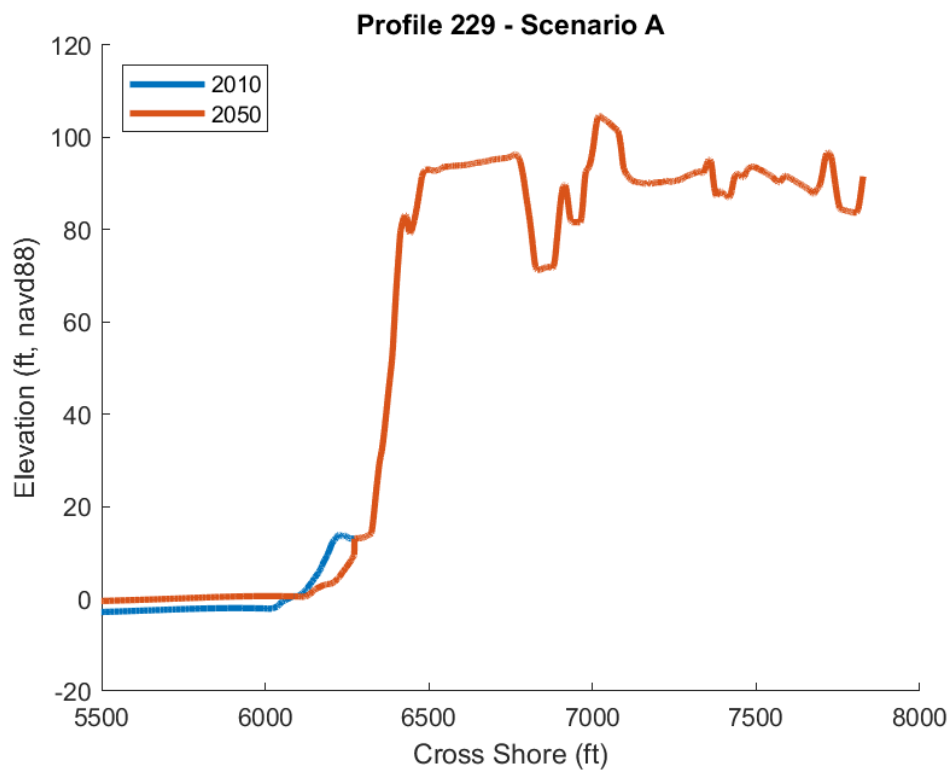


Figure A-20. Observed 2010 and modeled 2050 Profile 229.

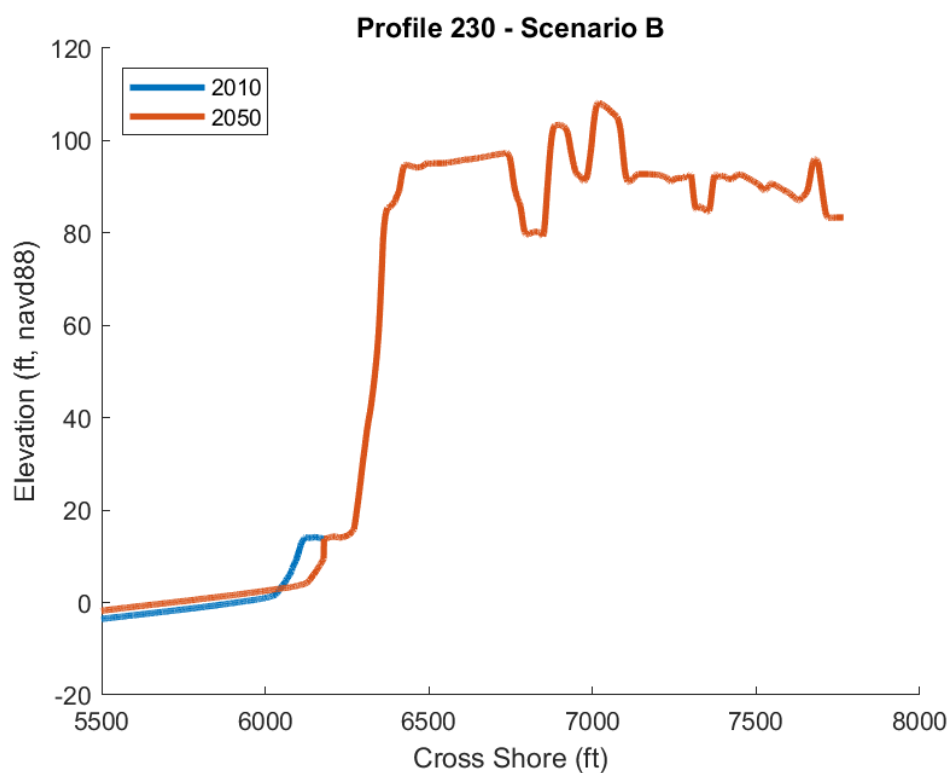
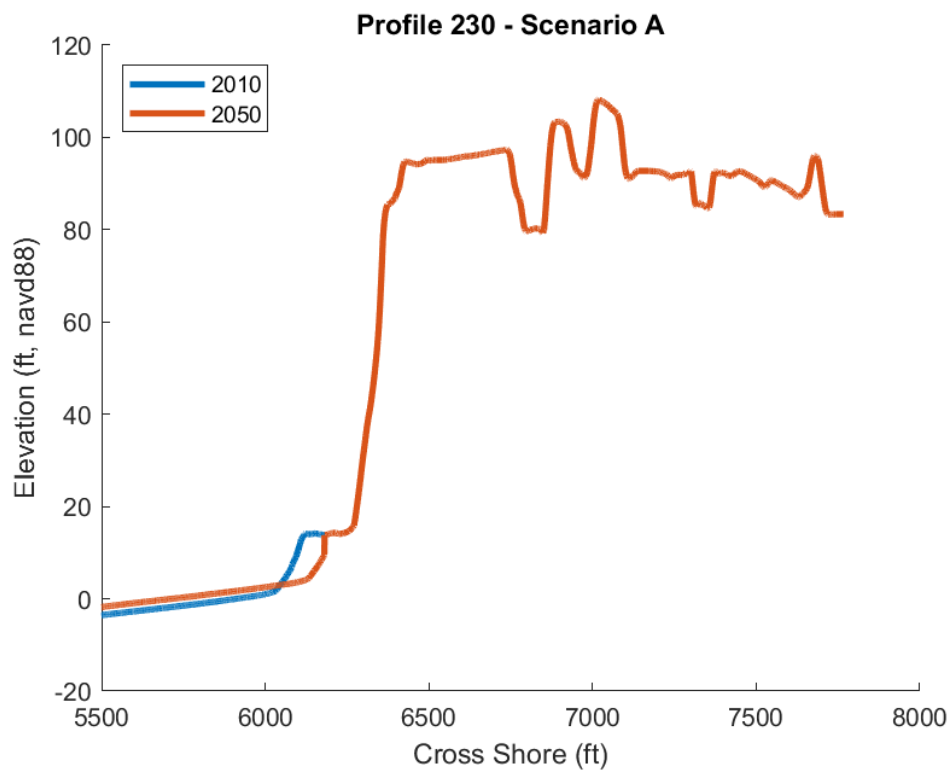


Figure A-21. Observed 2010 and modeled 2050 Profile 230.

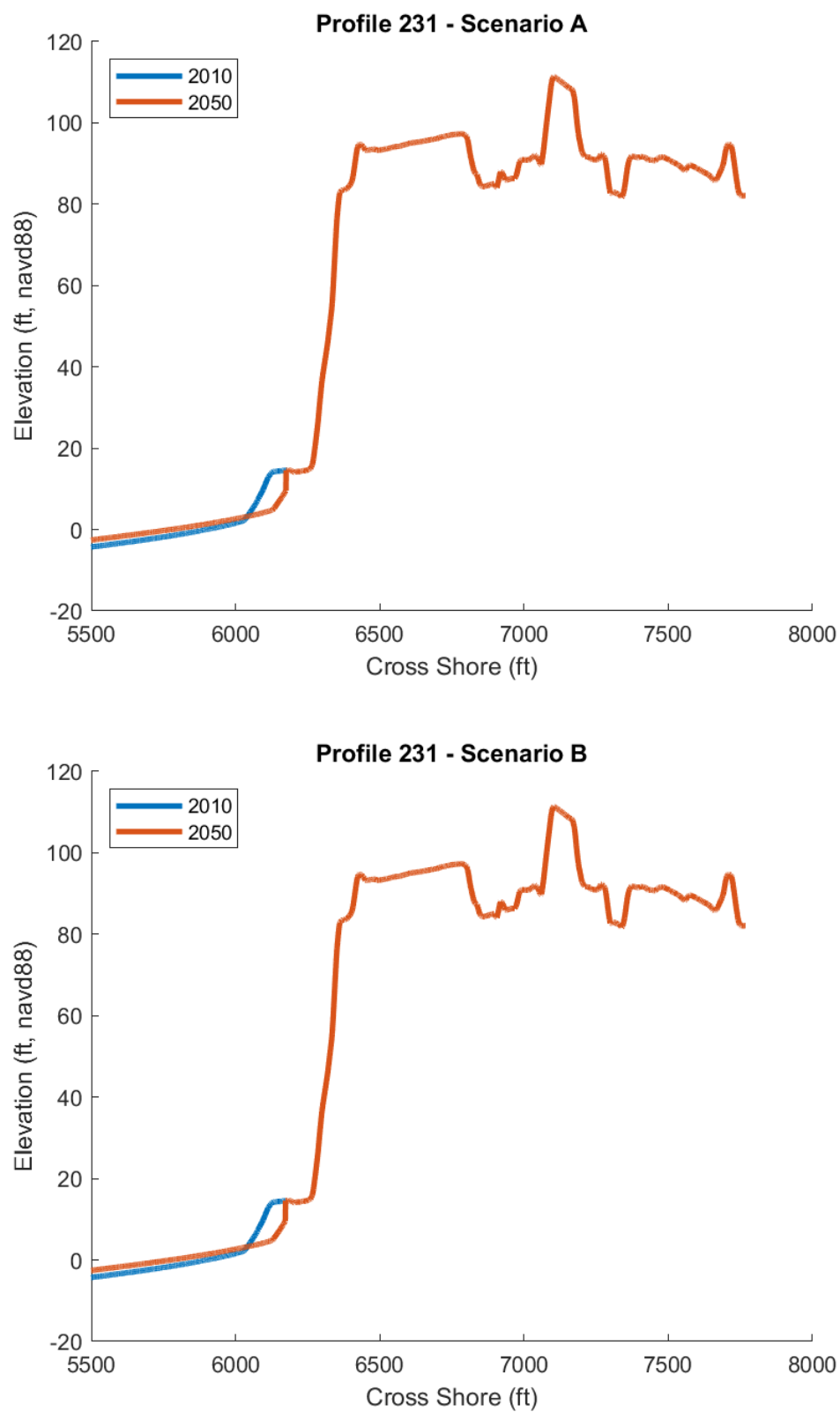


Figure A-22. Observed 2010 and modeled 2050 Profile 231.

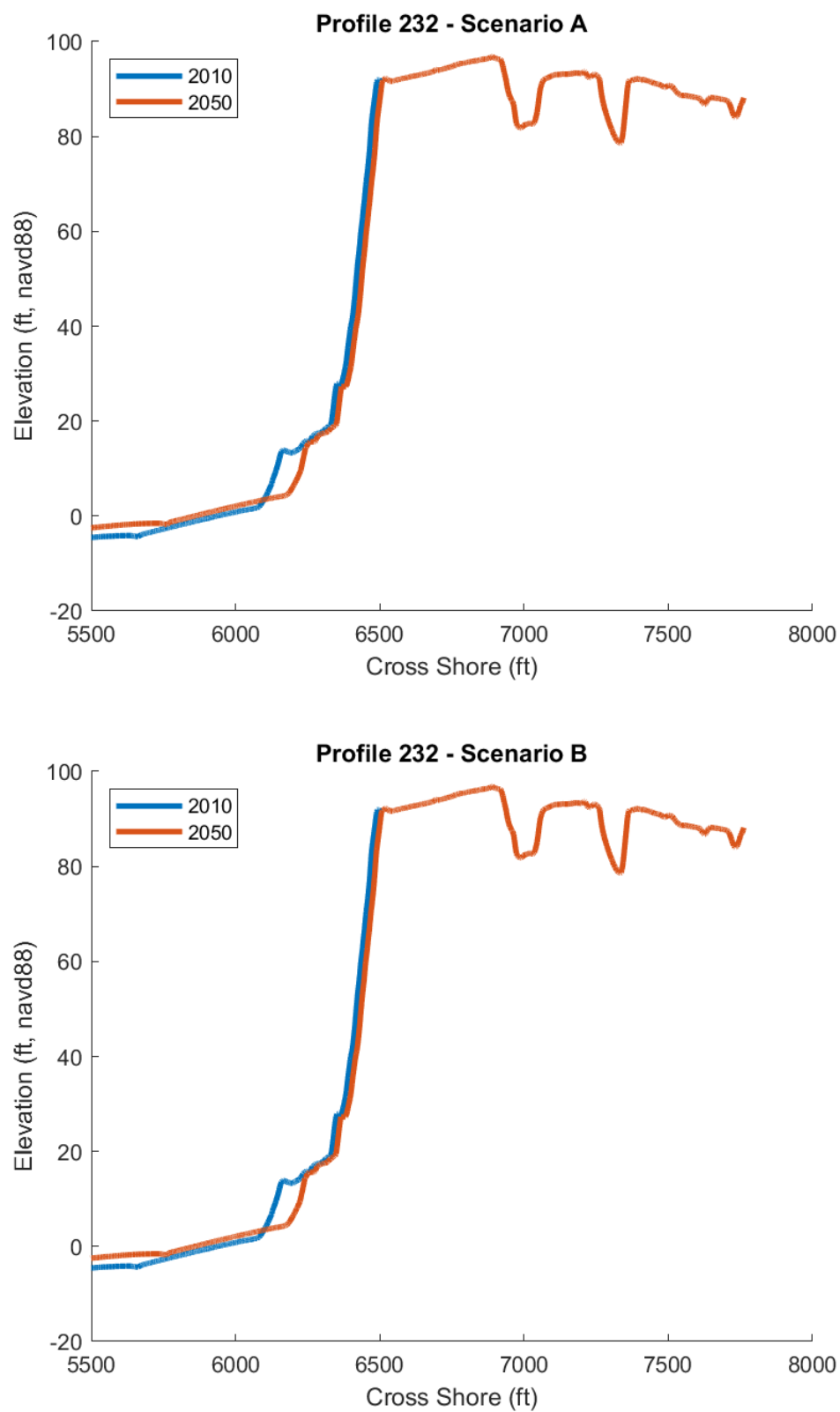


Figure A-23. Observed 2010 and modeled 2050 Profile 232.

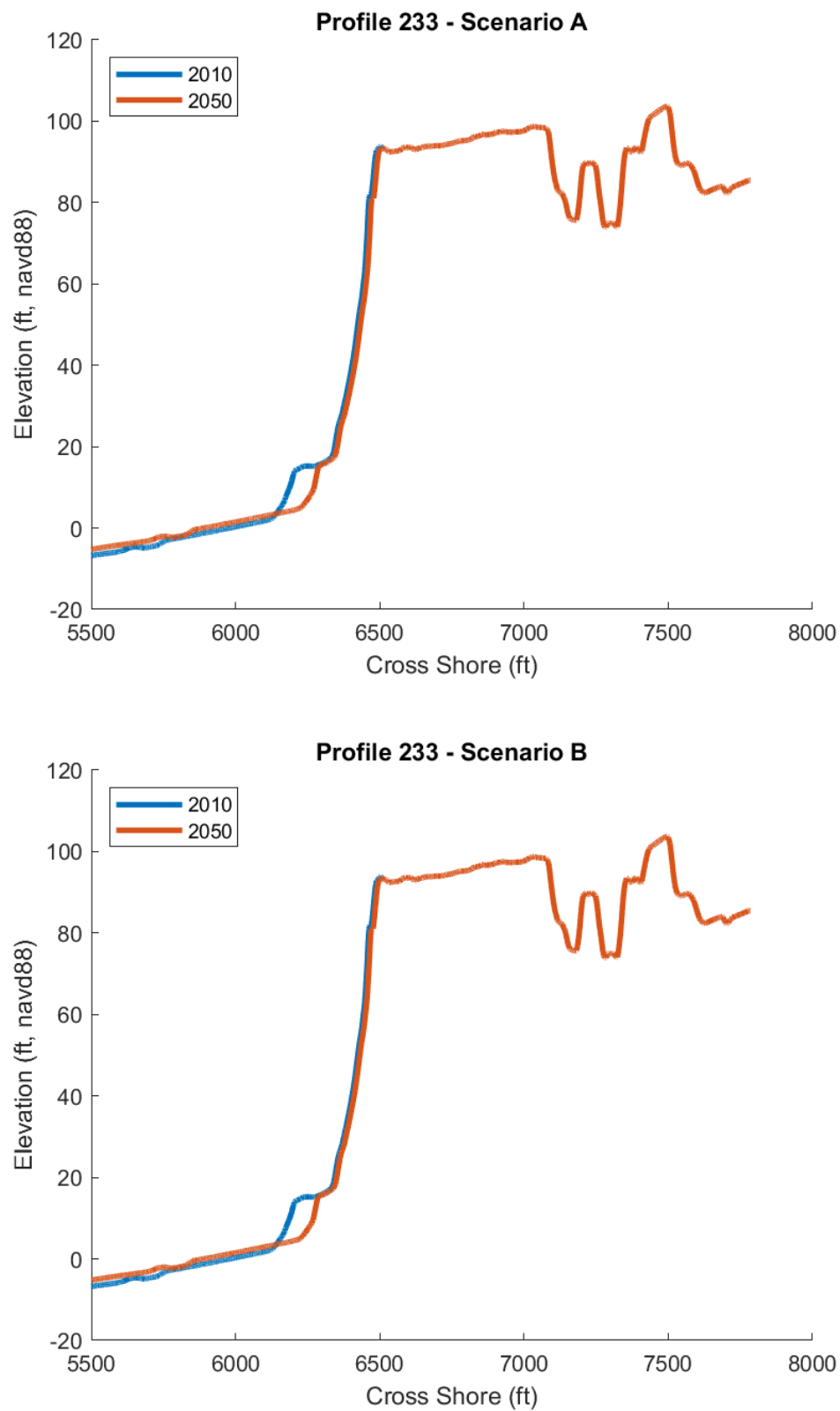


Figure A-24. Observed 2010 and modeled 2050 Profile 233.

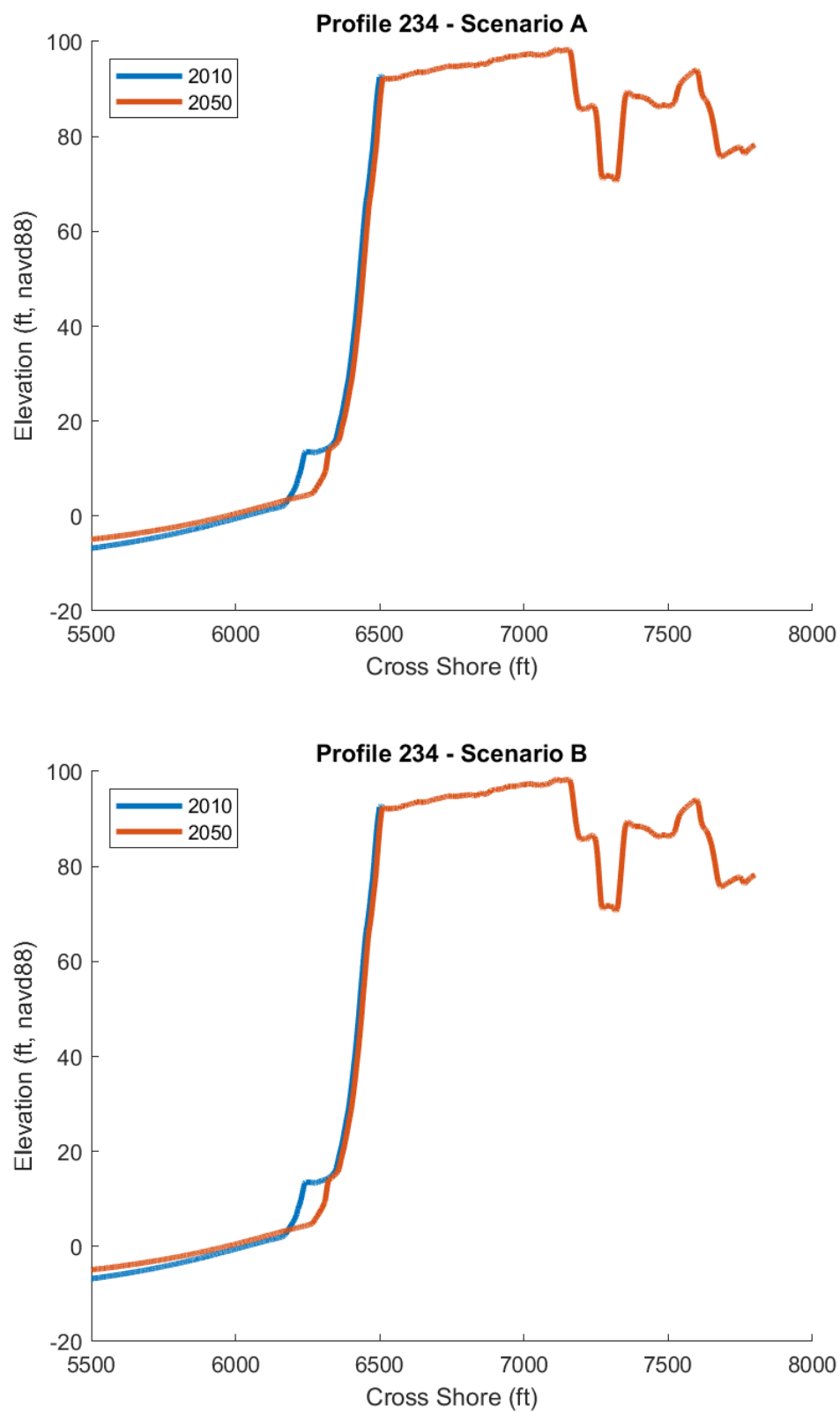


Figure A-25. Observed 2010 and modeled 2050 Profile 234.

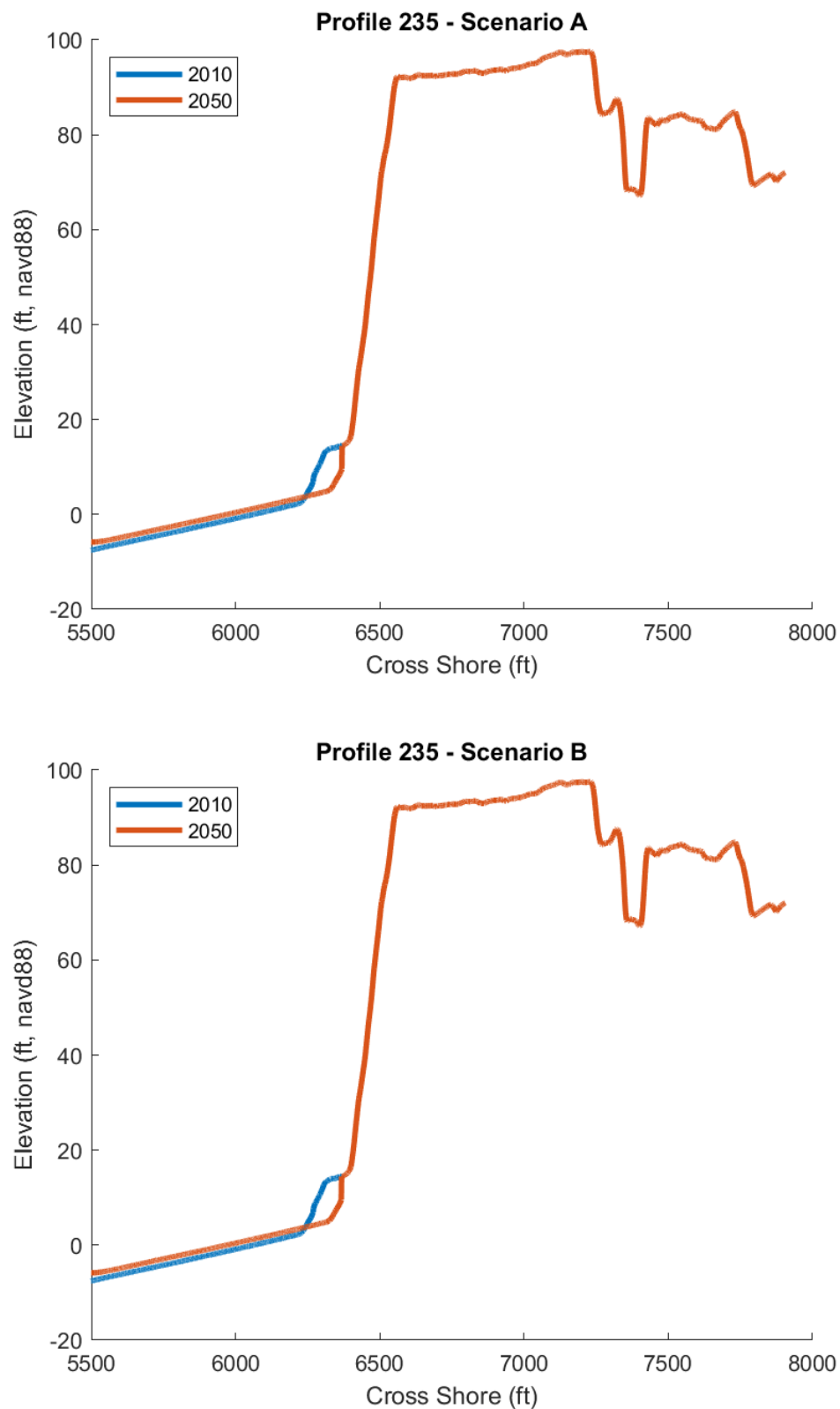


Figure A-26. Observed 2010 and modeled 2050 Profile 235.

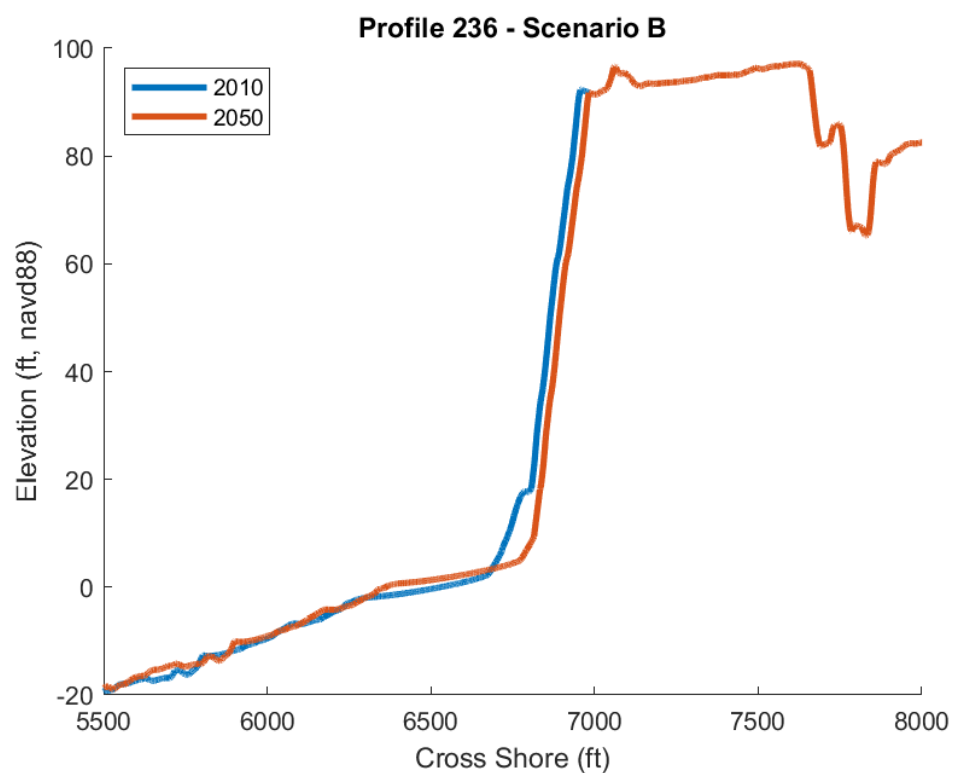
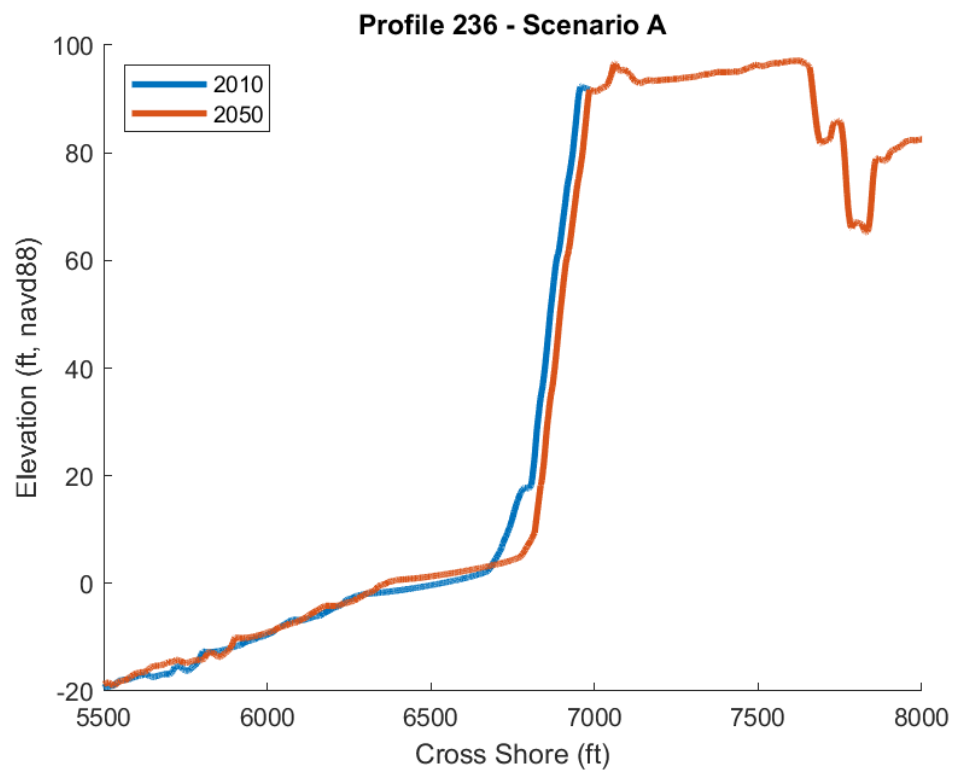


Figure A-27. Observed 2010 and modeled 2050 Profile 236.

APPENDIX B

DIGITAL ELEVATION MODELS (DEM)
FROM 2020 AND 2021 REVETMENT SURVEYS



Figure B-1. Locations of 21 transects along the revetment, spaced 100 ft apart.

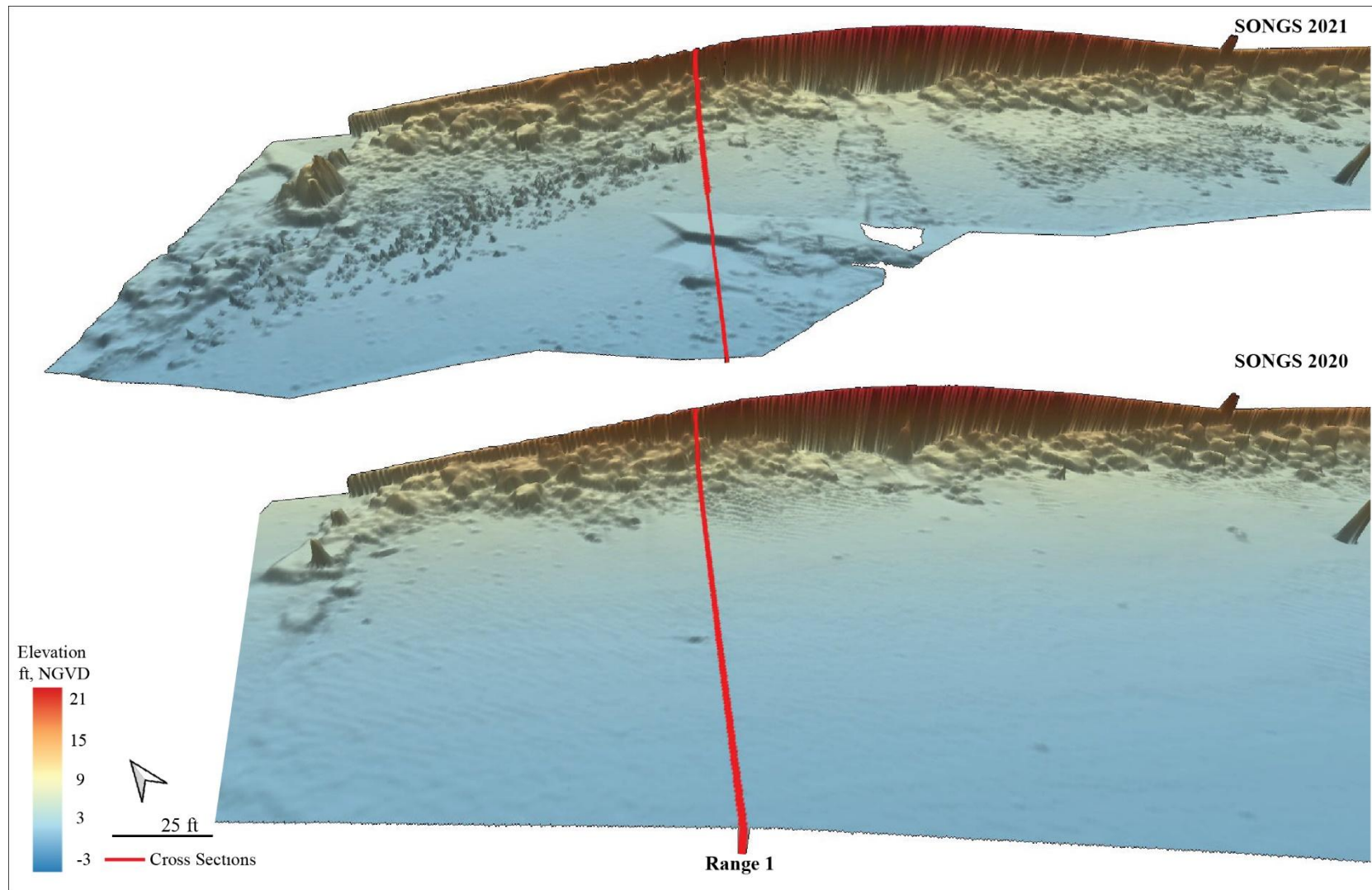


Figure B-2. DEM comparison between 2021 (top) and 2020 (bottom) showing Transect 1 along the SONGS revetment. Notice the increased presence of cobbles in 2021 on either side of Transect 1. There is no noticeable movement of the larger rocks against the wall of the walkway.

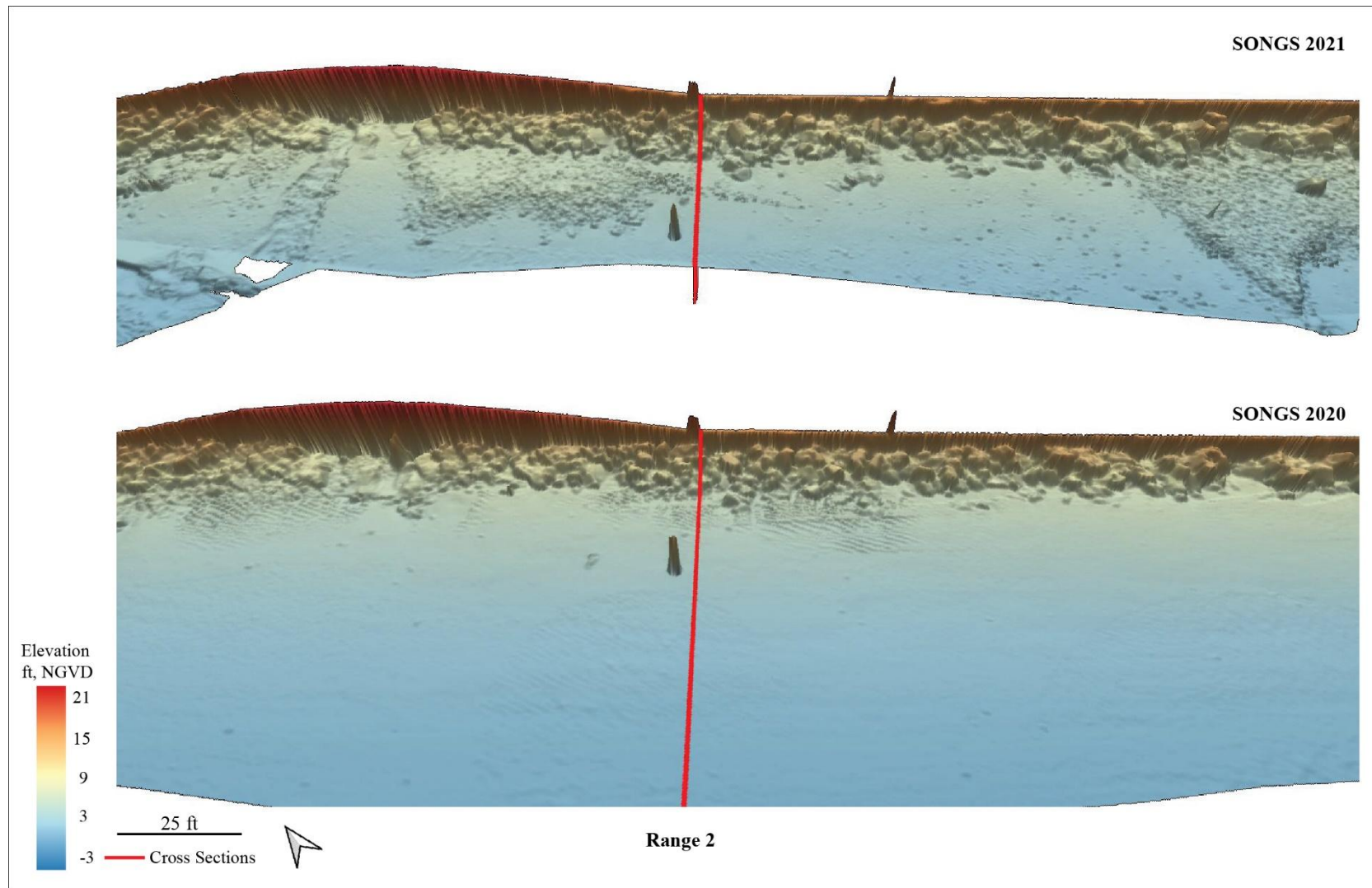


Figure B-3. DEM comparison between 2021 (top) and 2020 (bottom) showing Transect 2 along the SONGS revetment. Notice the increased presence of cobbles in 2021 just north of Transect 2. There is no noticeable movement of the larger rocks against the seawall.

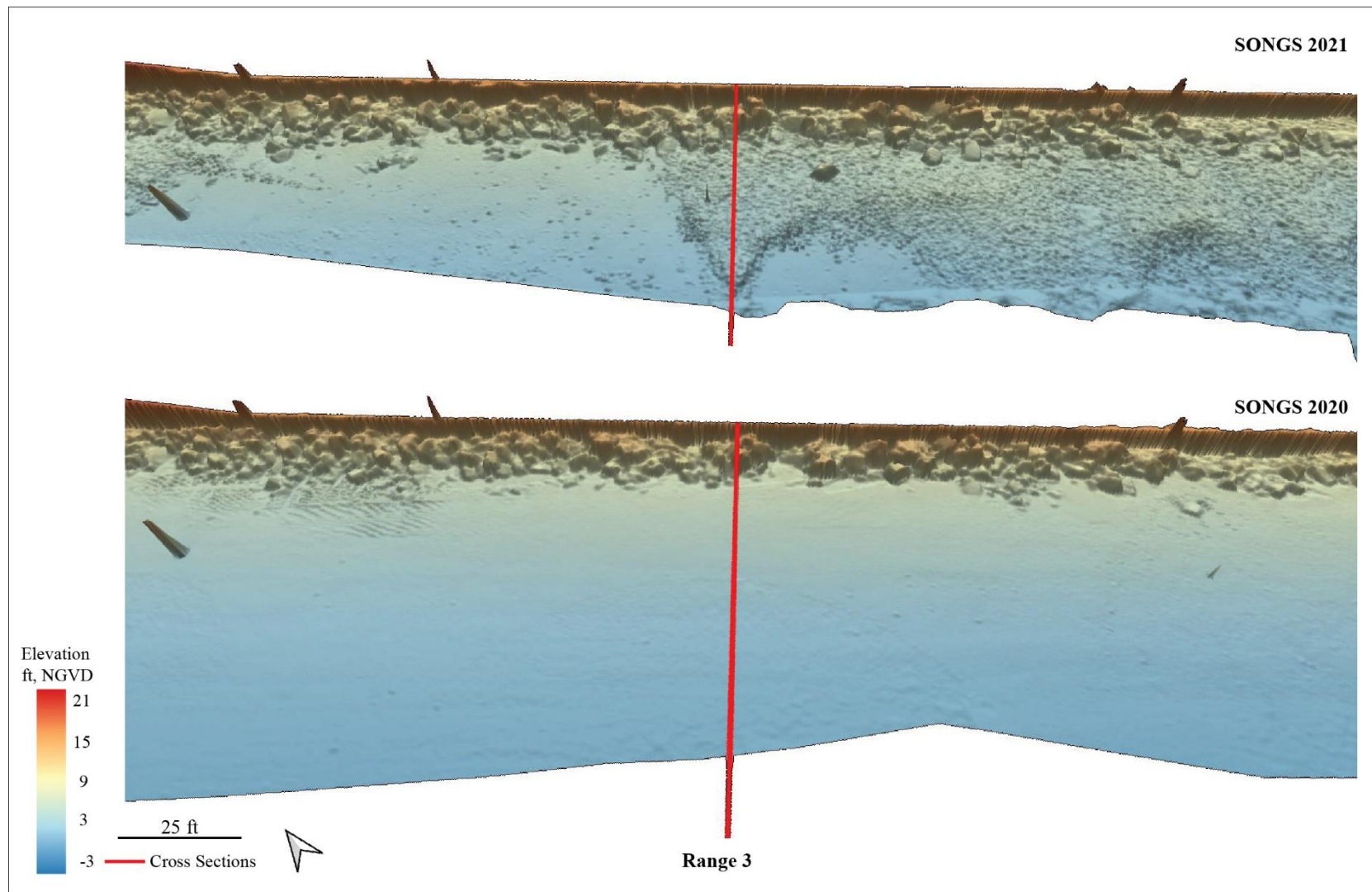


Figure B-4. DEM comparison between 2021 (top) and 2020 (bottom) showing Transect 3 along the SONGS revetment. Notice the increased presence of cobbles in the 2021 survey along and south of Transect 3. There is no noticeable movement of the larger rocks against the walkway wall.

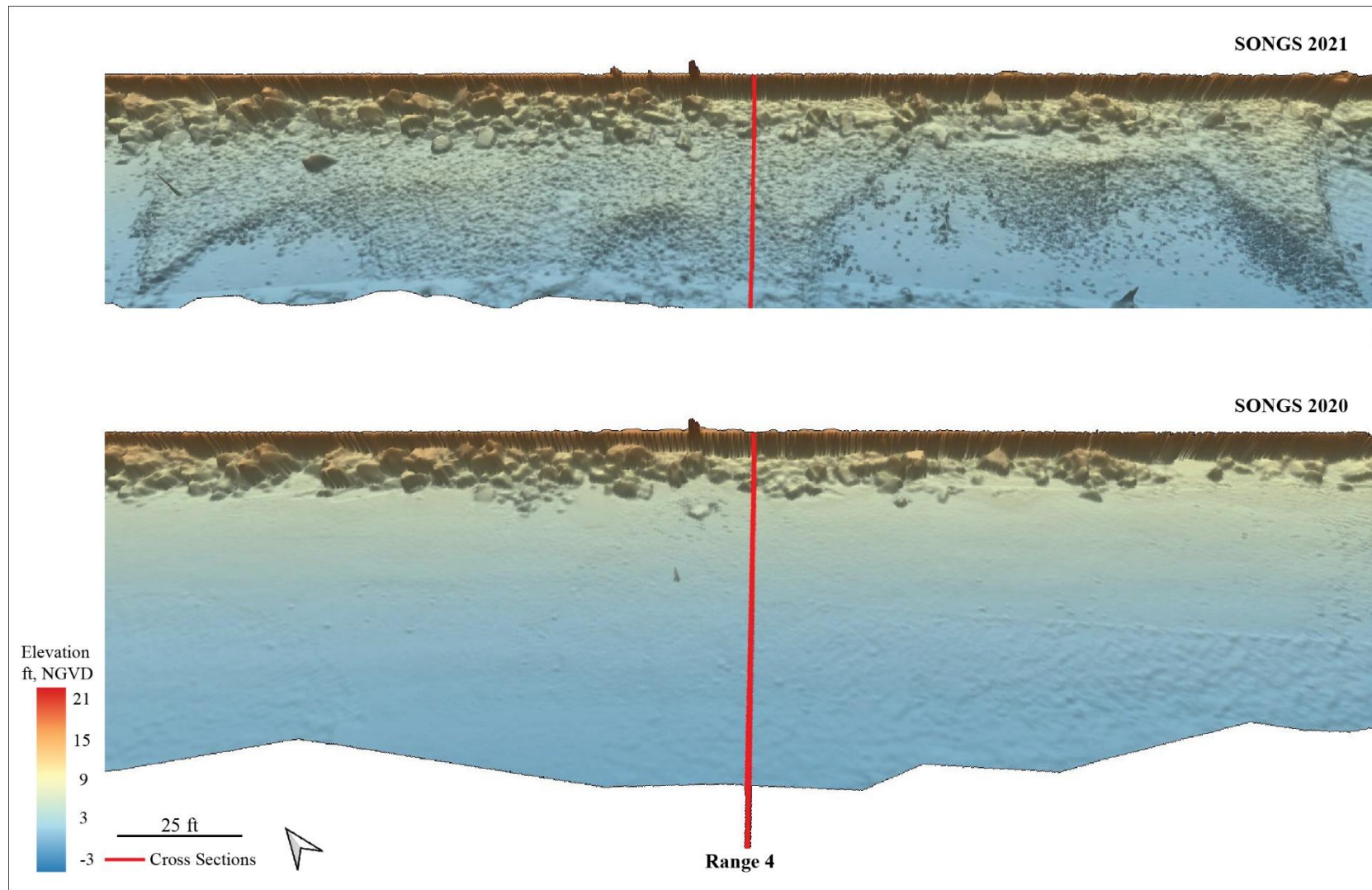


Figure B-5. DEM comparison between 2021 (top) and 2020 (bottom) showing Transect 4 along the SONGS revetment. Notice the increased presence of cobbles along the entire beach in 2021. There is no noticeable movement of the larger rocks against the walkway wall.

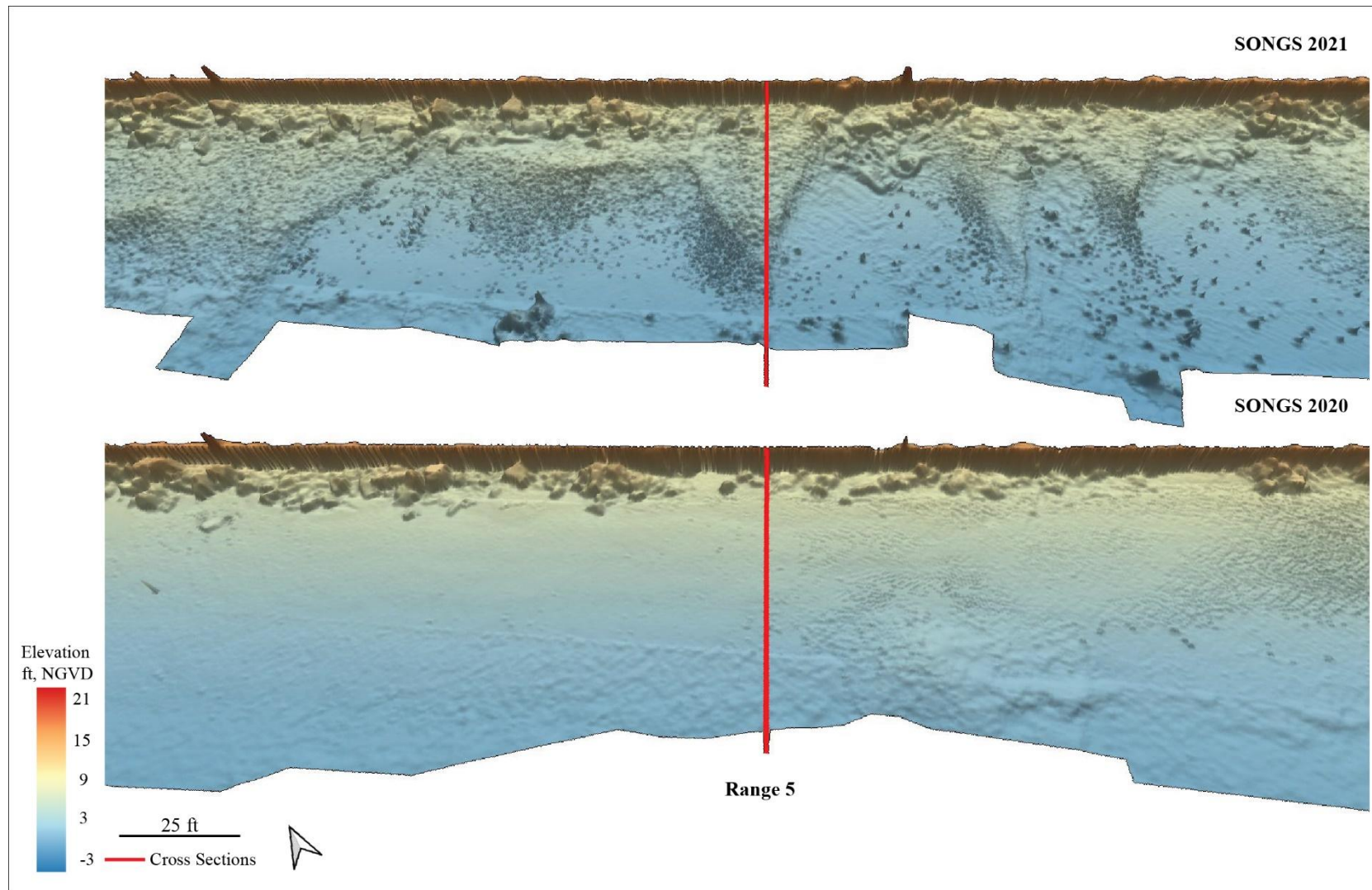


Figure B-6. DEM comparison between 2021 (top) and 2020 (bottom) showing Transect 5 along the SONGS revetment. Notice the increased exposure of cobbles along the beach and larger rocks against the walkway wall just south of Transect 5 in 2021 due to erosion.

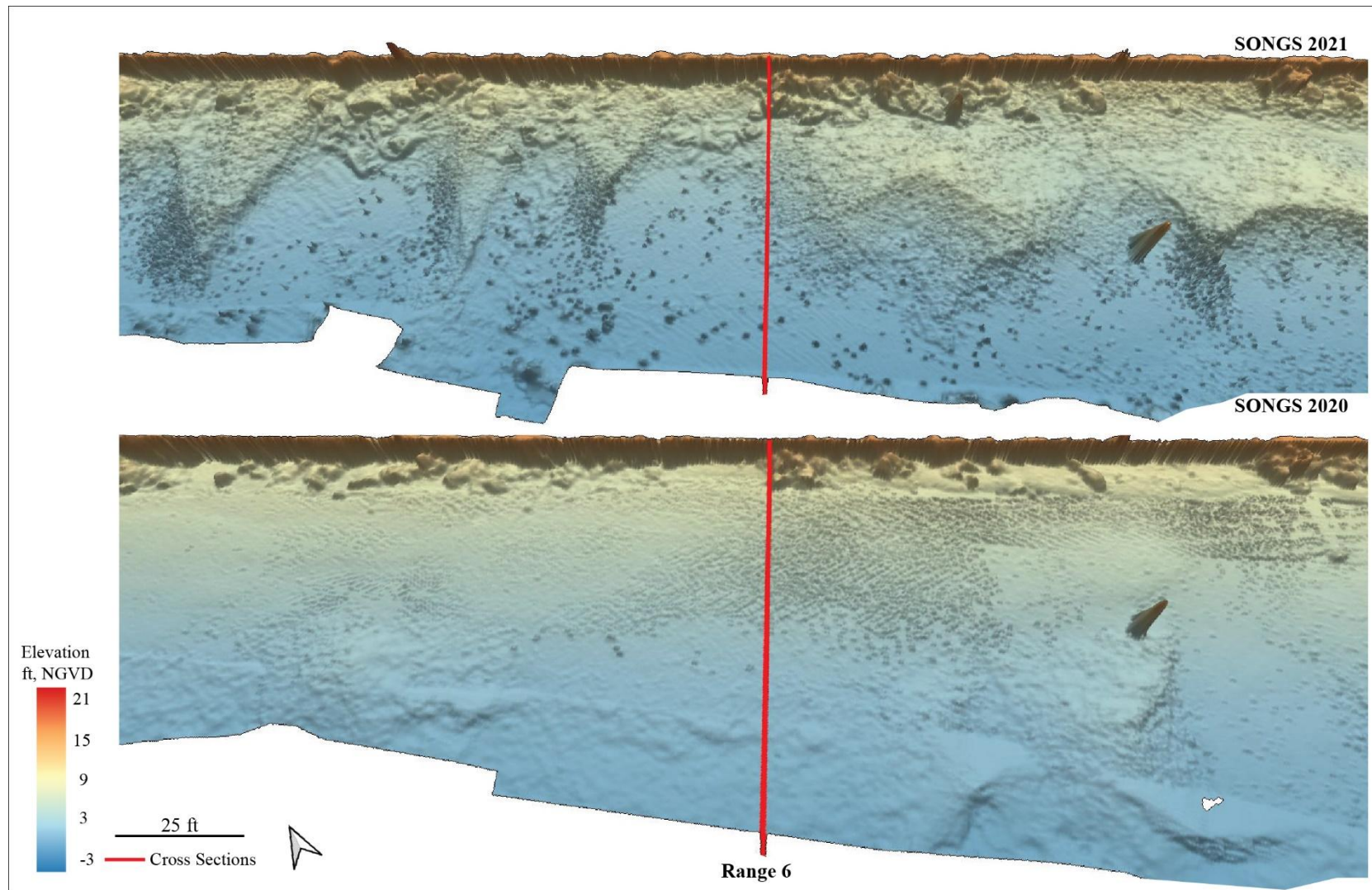


Figure B-7. DEM comparison between 2021 (top) and 2020 (bottom) showing Transect 6 along the SONGS revetment. Notice the increased exposure of cobbles along the beach and larger rocks against the walkway wall just south of Transect 6 in 2021 due to erosion.

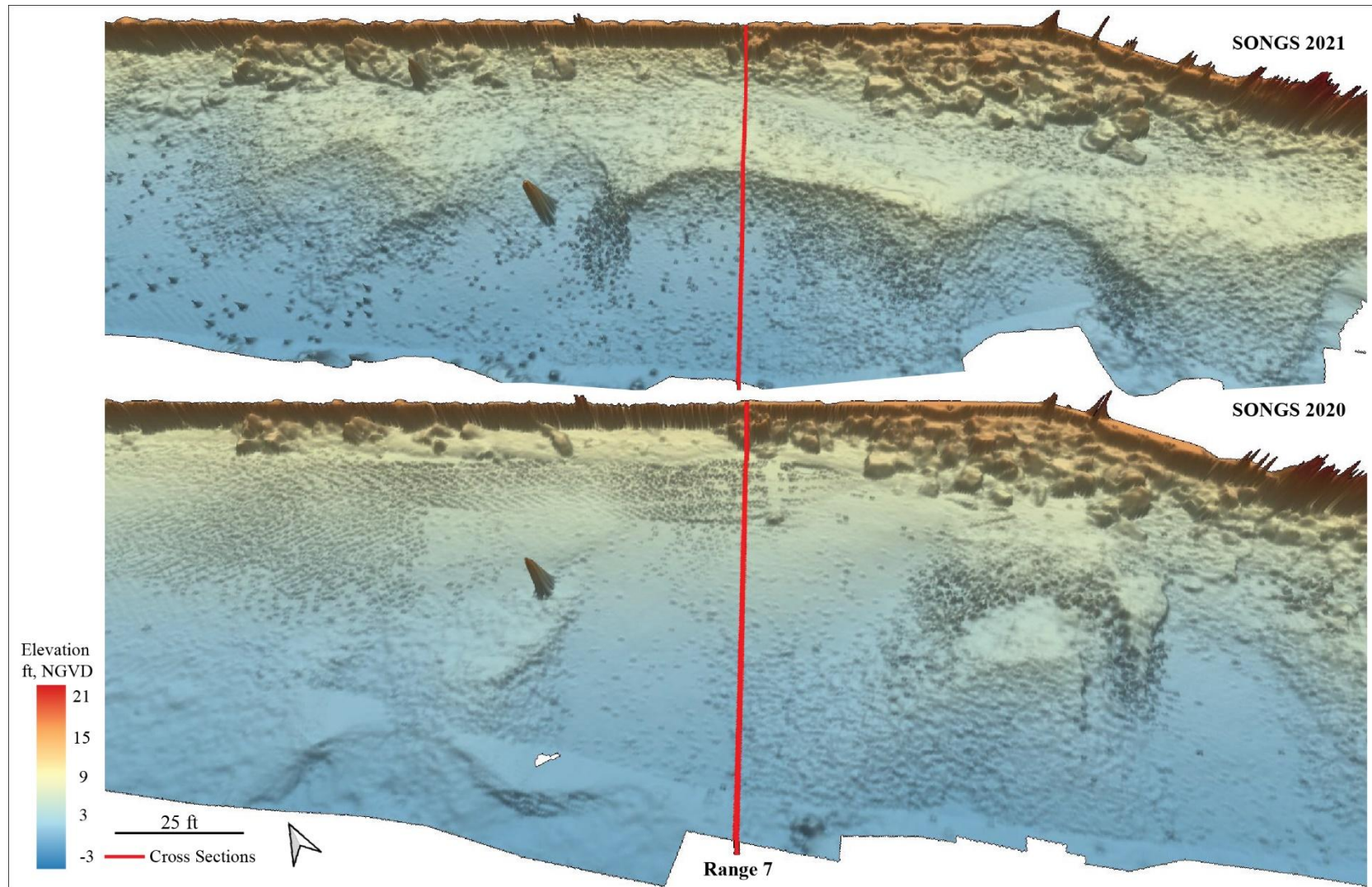


Figure B-8. DEM comparison between 2021 (top) and 2020 (bottom) showing Transect 7 along the SONGS revetment. Notice the presence of both an elevated berm and exposed cobbles along Transect 7 in 2021. There is no noticeable change in the larger rocks against the walkway wall along Transect 7.

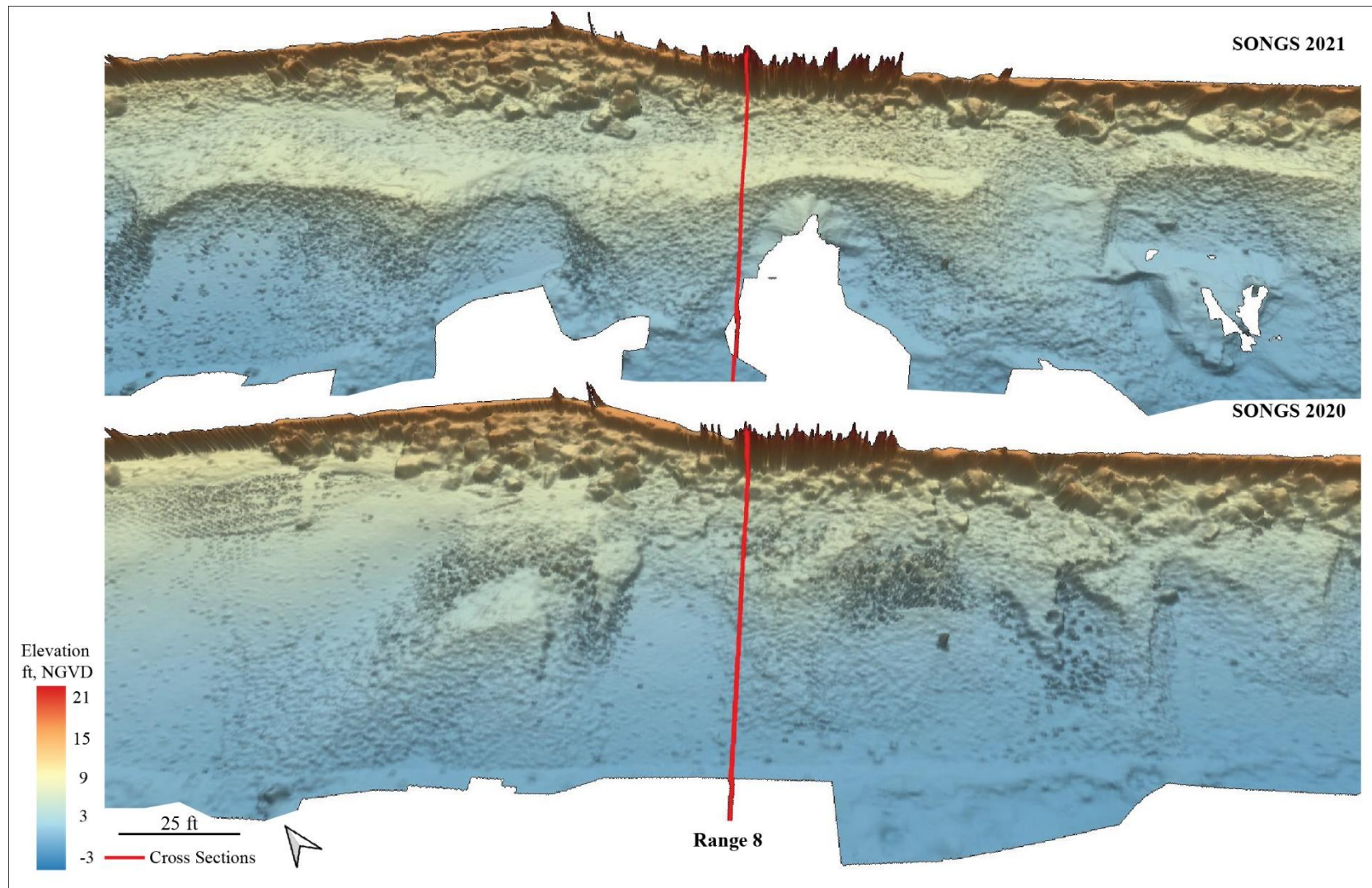


Figure B-9. DEM comparison between 2021 (top) and 2020 (bottom) showing Transect 8 along the SONGS revetment. Notice the elevated sand berm and partial coverage of larger rocks against the walkway wall due to accretion in 2021.

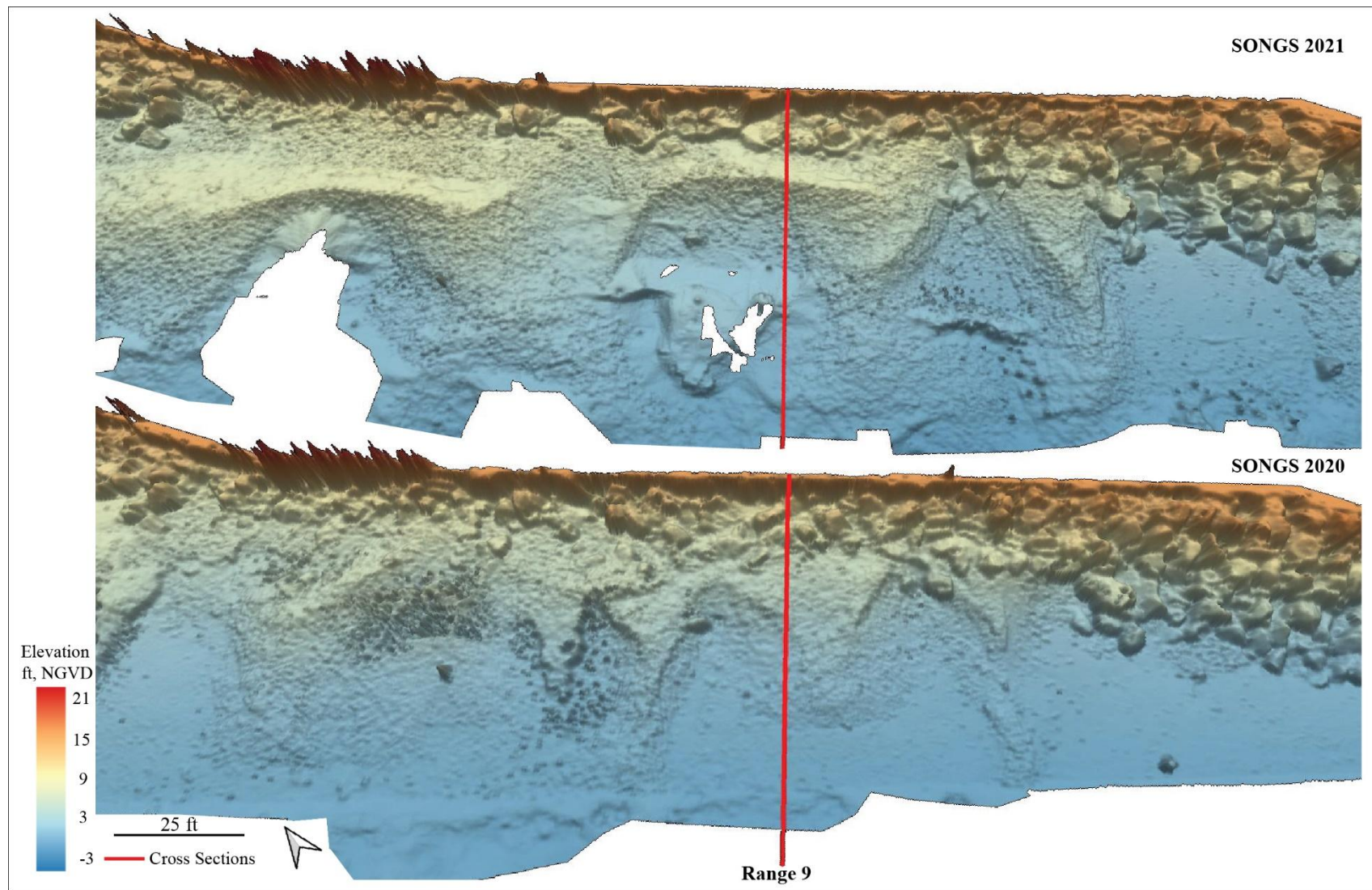


Figure B-10. DEM comparison between 2021 (top) and 2020 (bottom) showing Transect 9 along the SONGS revetment. Notice the elevated berm and partial coverage of larger rocks against the walkway wall due to accretion in 2021.

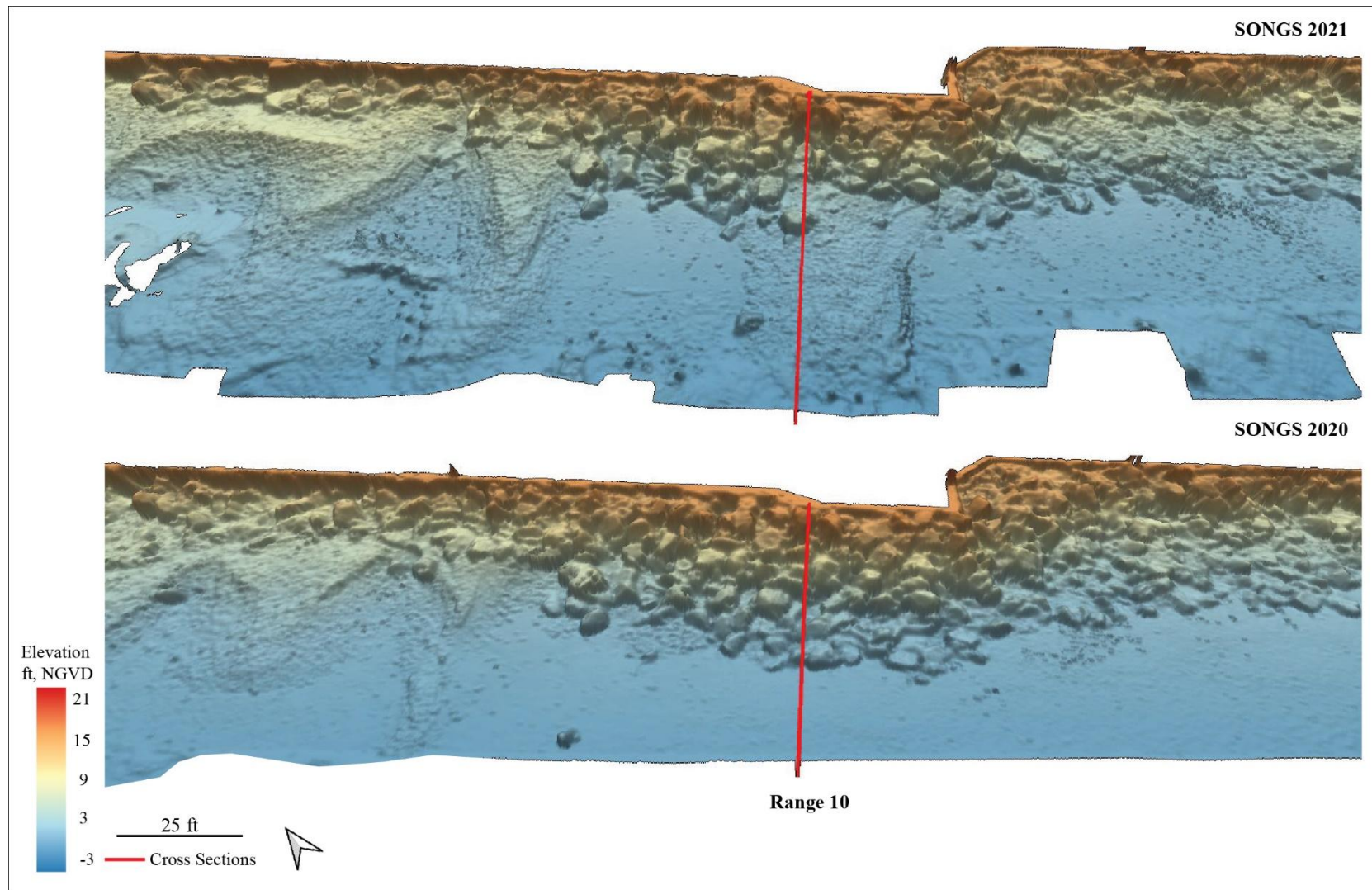


Figure B-11. DEM comparison between 2021 (top) and 2020 (bottom) showing Transect 10 along the SONGS revetment. Notice the movement of large rocks at the midpoint of the revetment along Transect 10 and increased presence of cobbles in 2021.

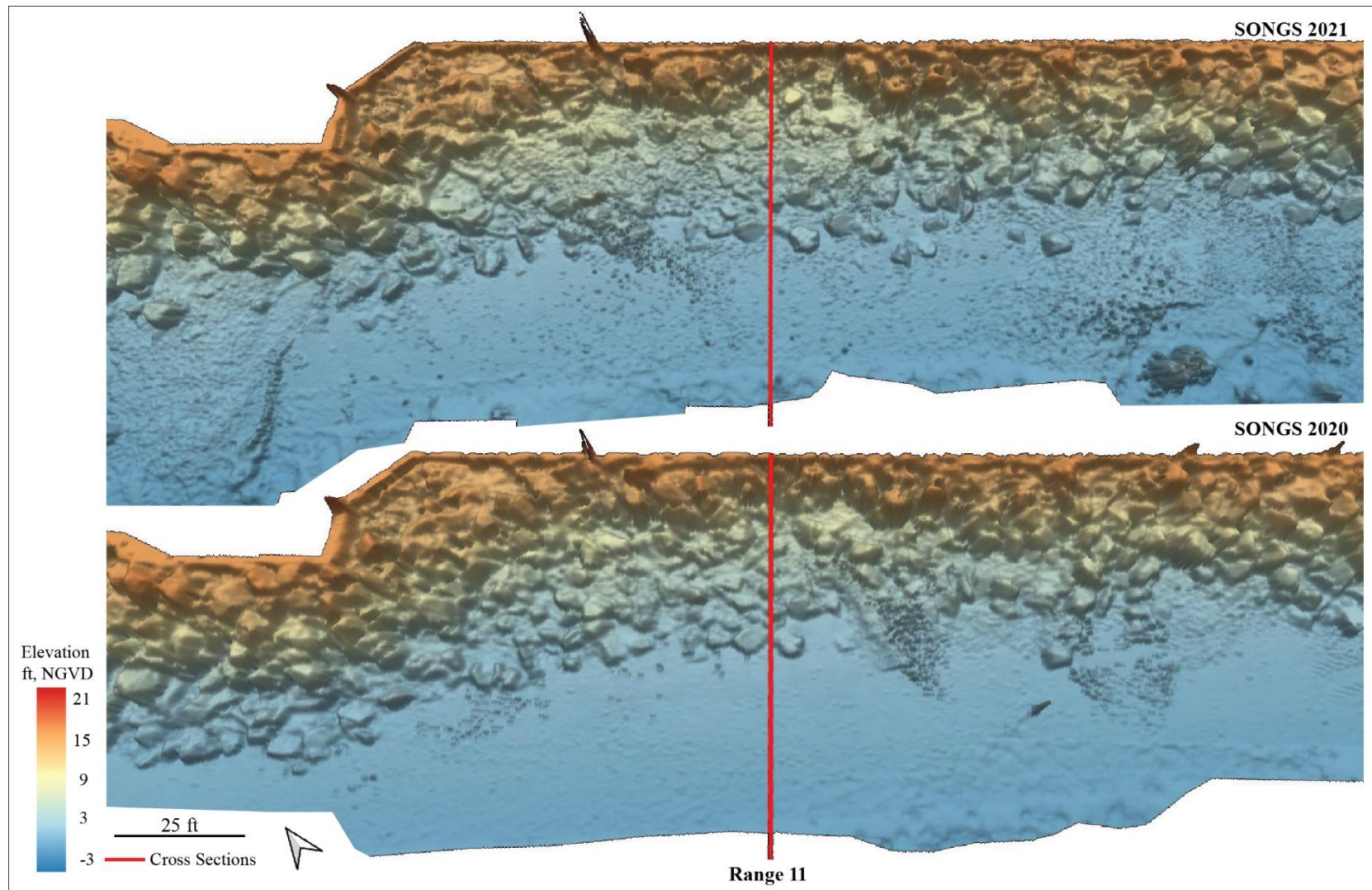


Figure B-12. DEM comparison between 2021 (top) and 2020 (bottom) showing Transect 11 along the SONGS revetment. Notice the partial burial of larger rocks in the middle of the revetment with sand and cobble in 2021.

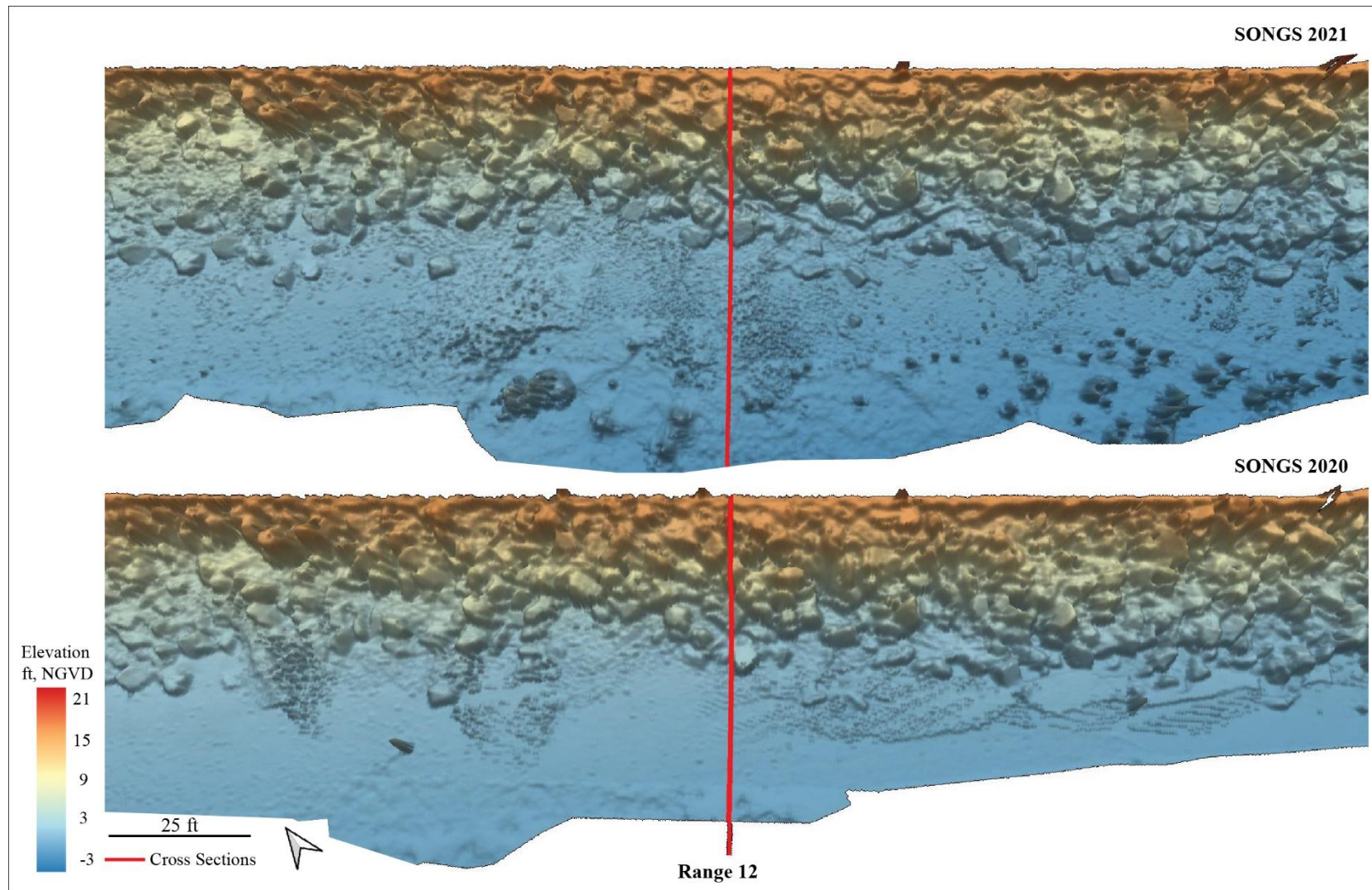


Figure B-13. DEM comparison between 2021 (top) and 2020 (bottom) showing Transect 12 along the SONGS revetment. Notice the increased presence of cobble on the beach along Transect 12 in 2021. There is no noticeable difference in the revetment rocks between the two years.

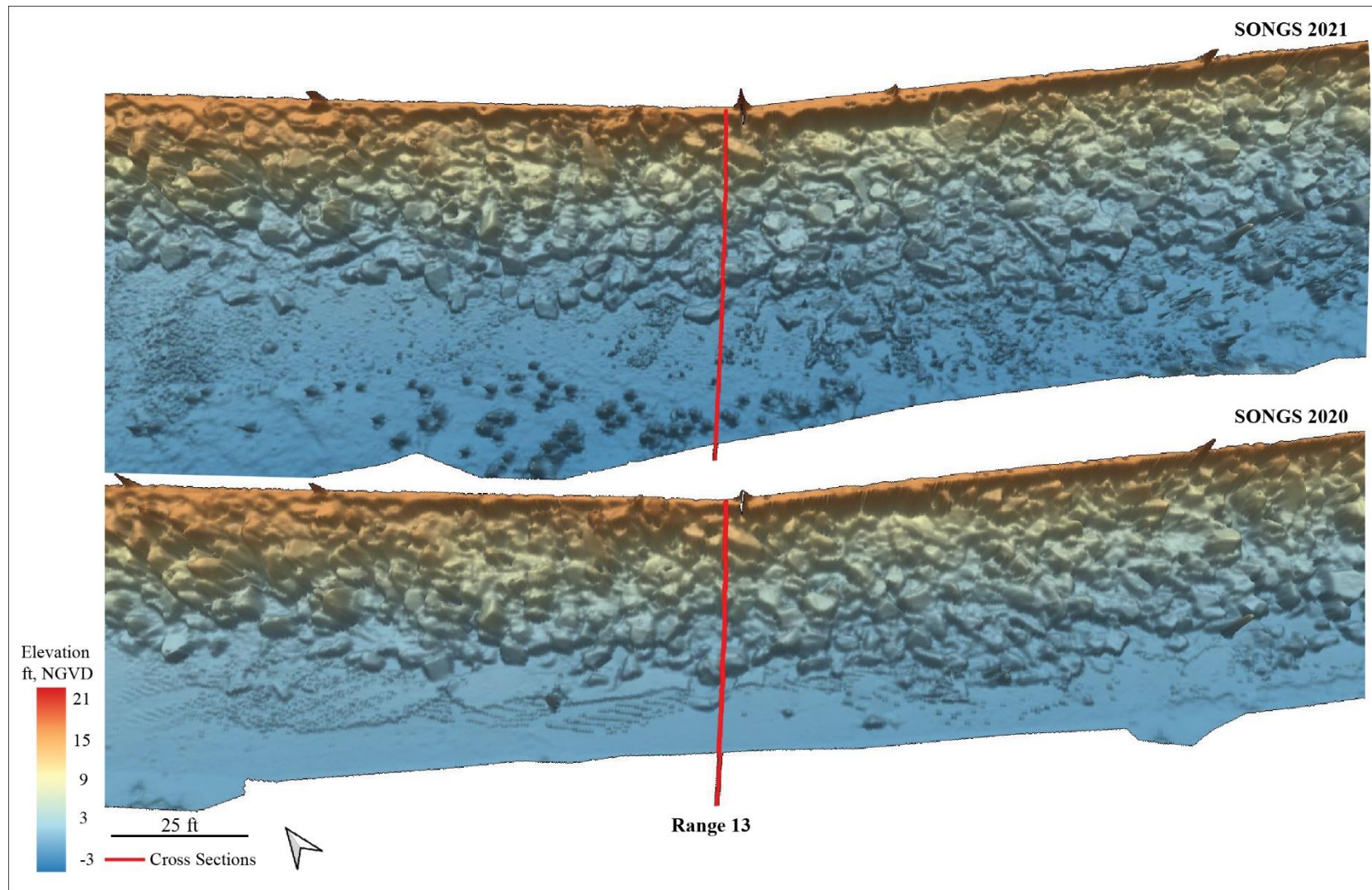


Figure B-14. DEM comparison between 2021 (top) and 2020 (bottom) showing Transect 13 along the SONGS revetment. Notice the slight erosion at the toe of the revetment in 2021. There is no noticeable difference in the revetment rocks between the two years.

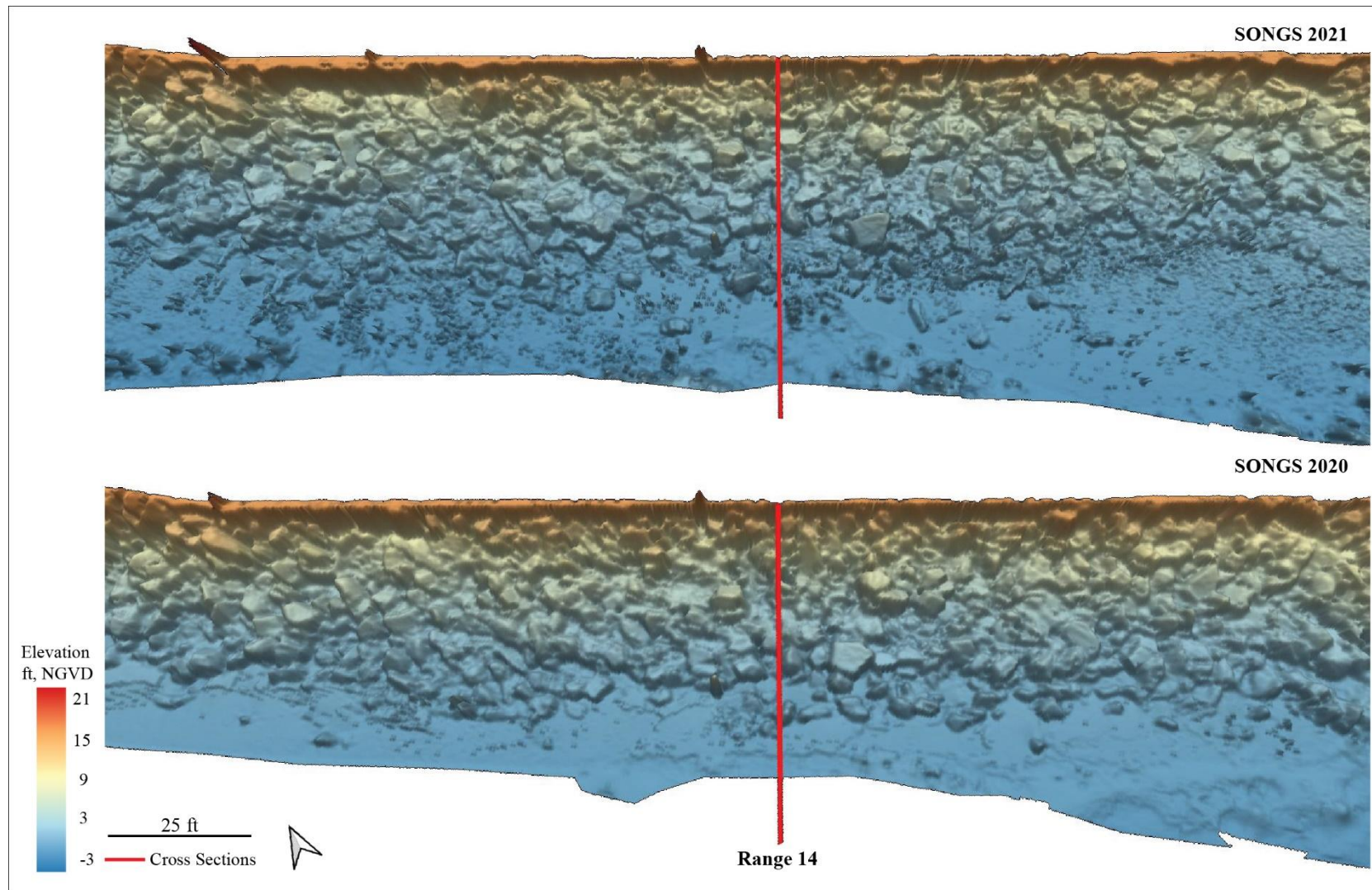


Figure B-15. DEM comparison between 2021 (top) and 2020 (bottom) showing Transect 14 along the SONGS revetment. Notice the increased cobbles, erosion, and movement of some larger rocks at the toe of the revetment in 2021.

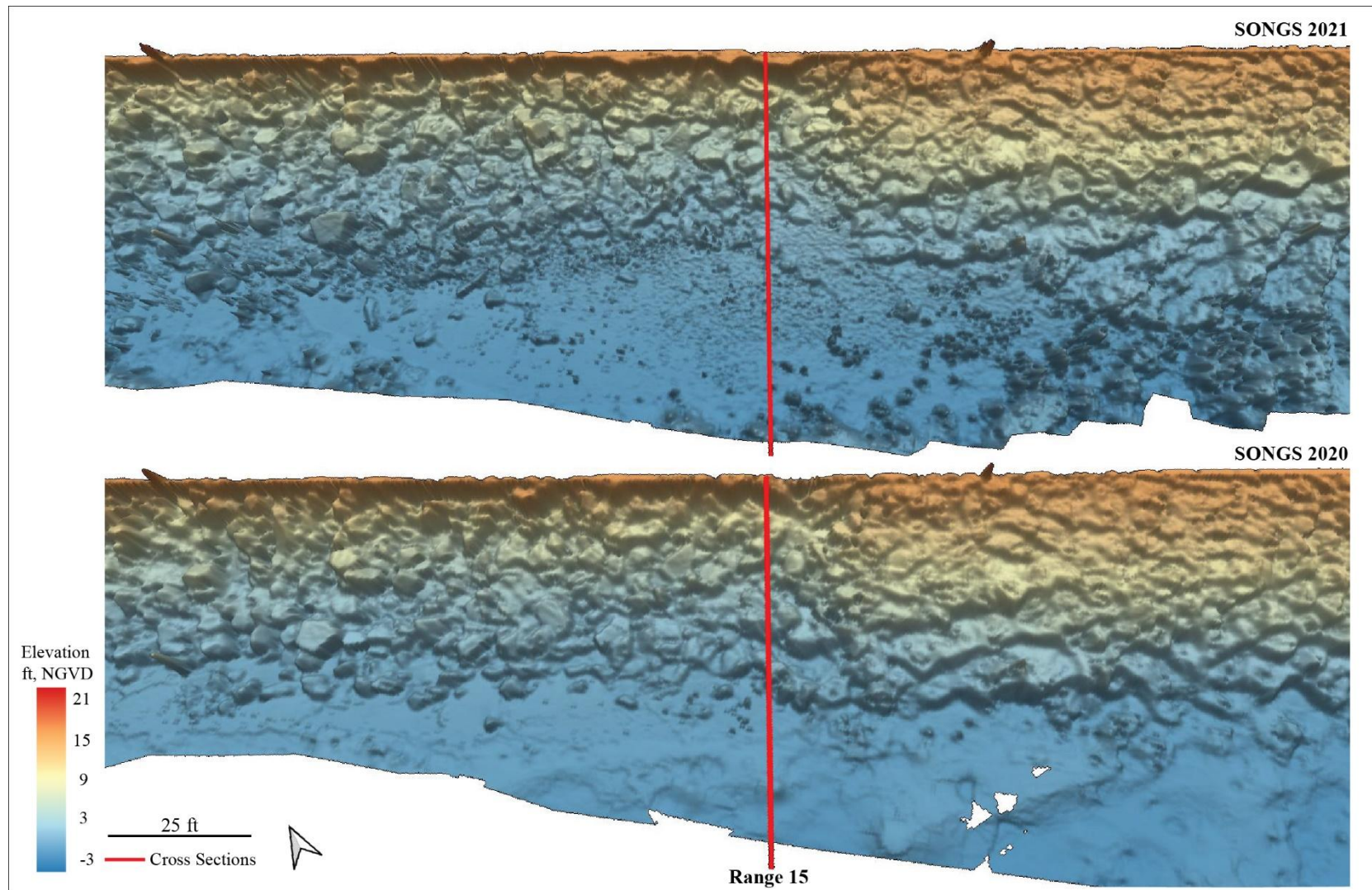


Figure B-16. DEM comparison between 2021 (top) and 2020 (bottom) showing Transect 15 along the SONGS revetment. Notice the increased cobbles and partial coverage of large rocks at the toe of the revetment due to accretion in 2021.

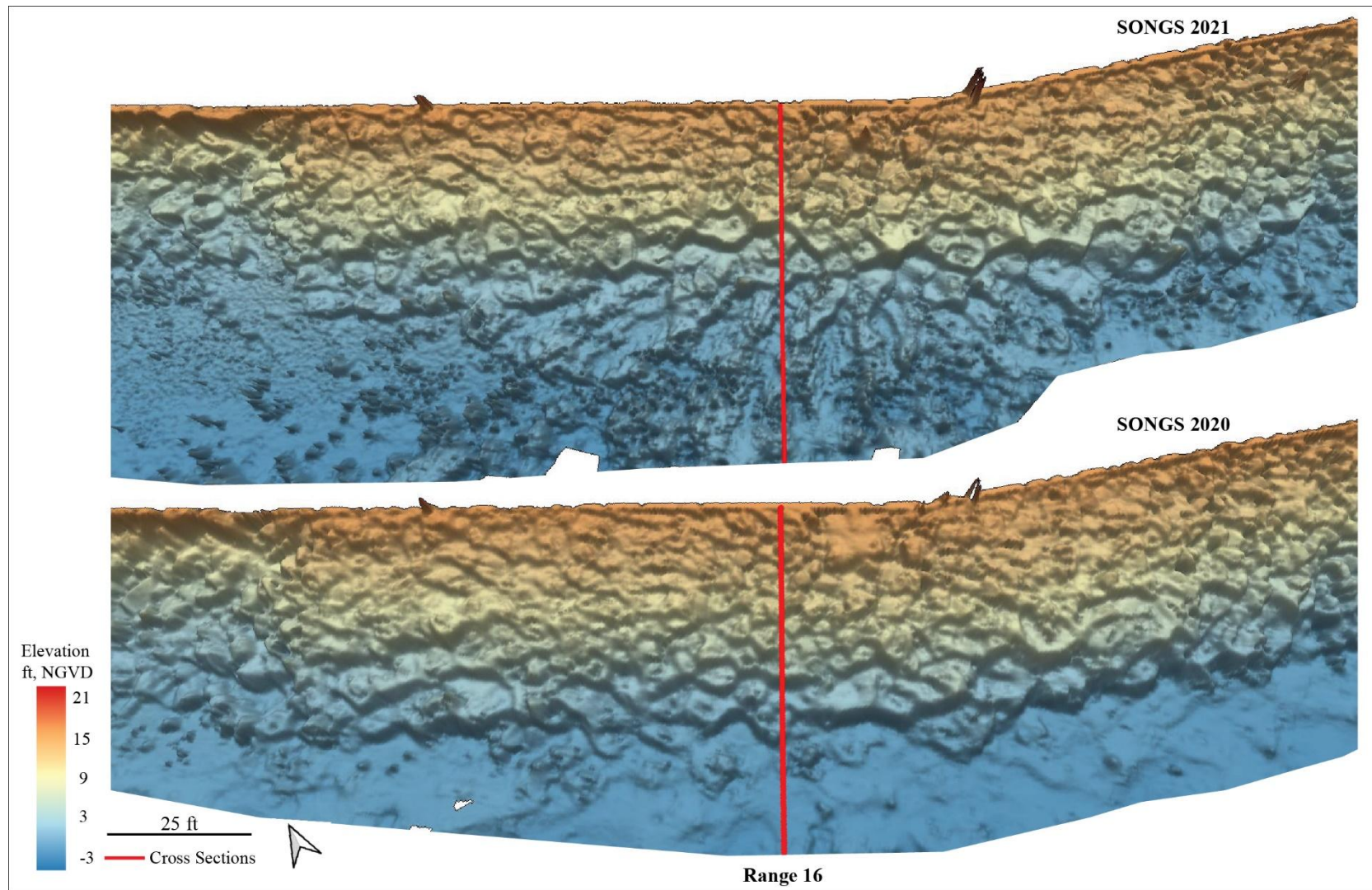


Figure B-17. DEM comparison between 2021 (top) and 2020 (bottom) showing Transect 16 along the SONGS revetment. Notice the increased amount of cobble at the toe of the revetment in 2021.

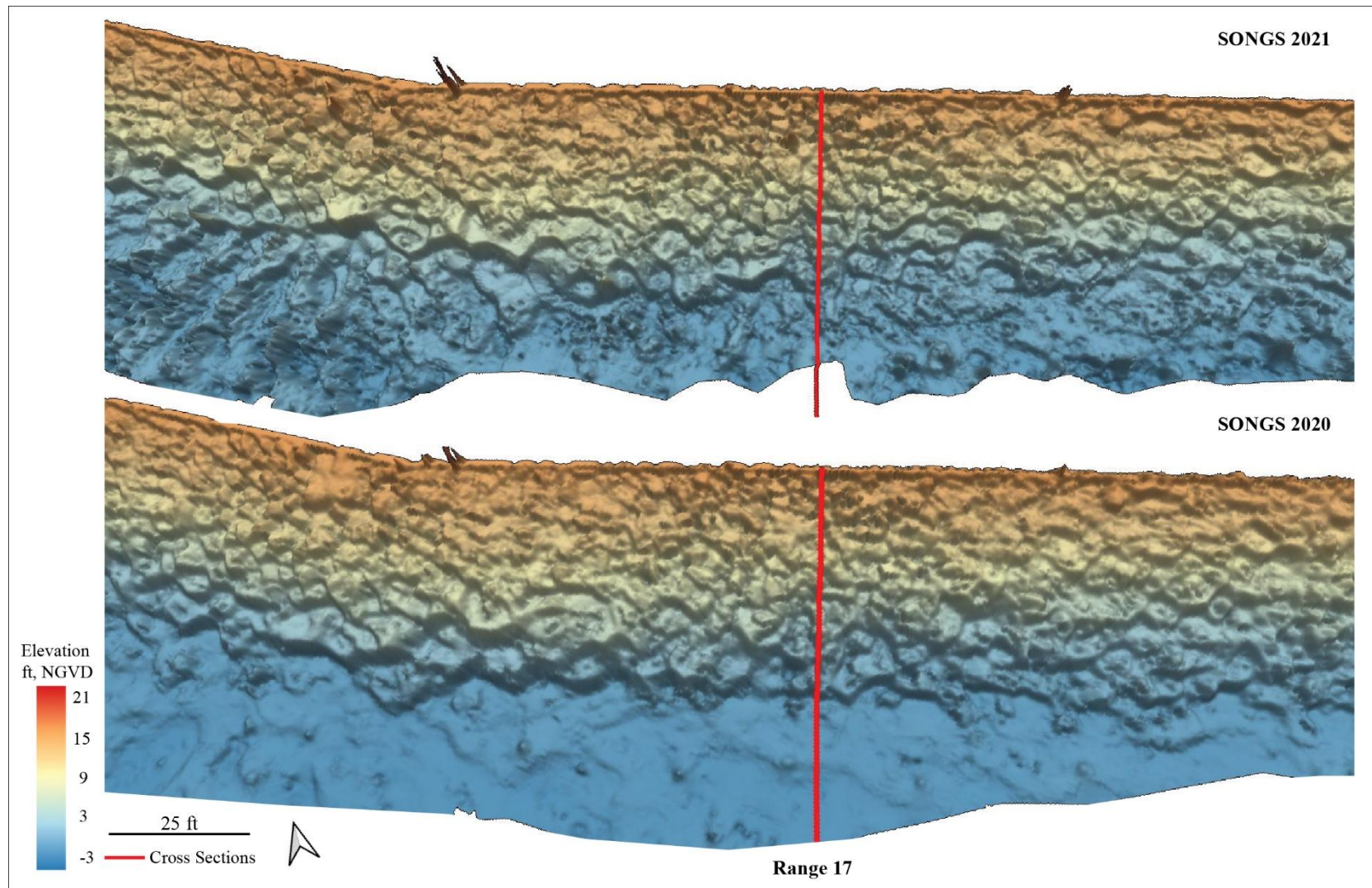


Figure B-18. DEM comparison between 2021 (top) and 2020 (bottom) showing Transect 17 along the SONGS revetment. Notice the increased amount of cobble at the toe of the revetment in 2021.

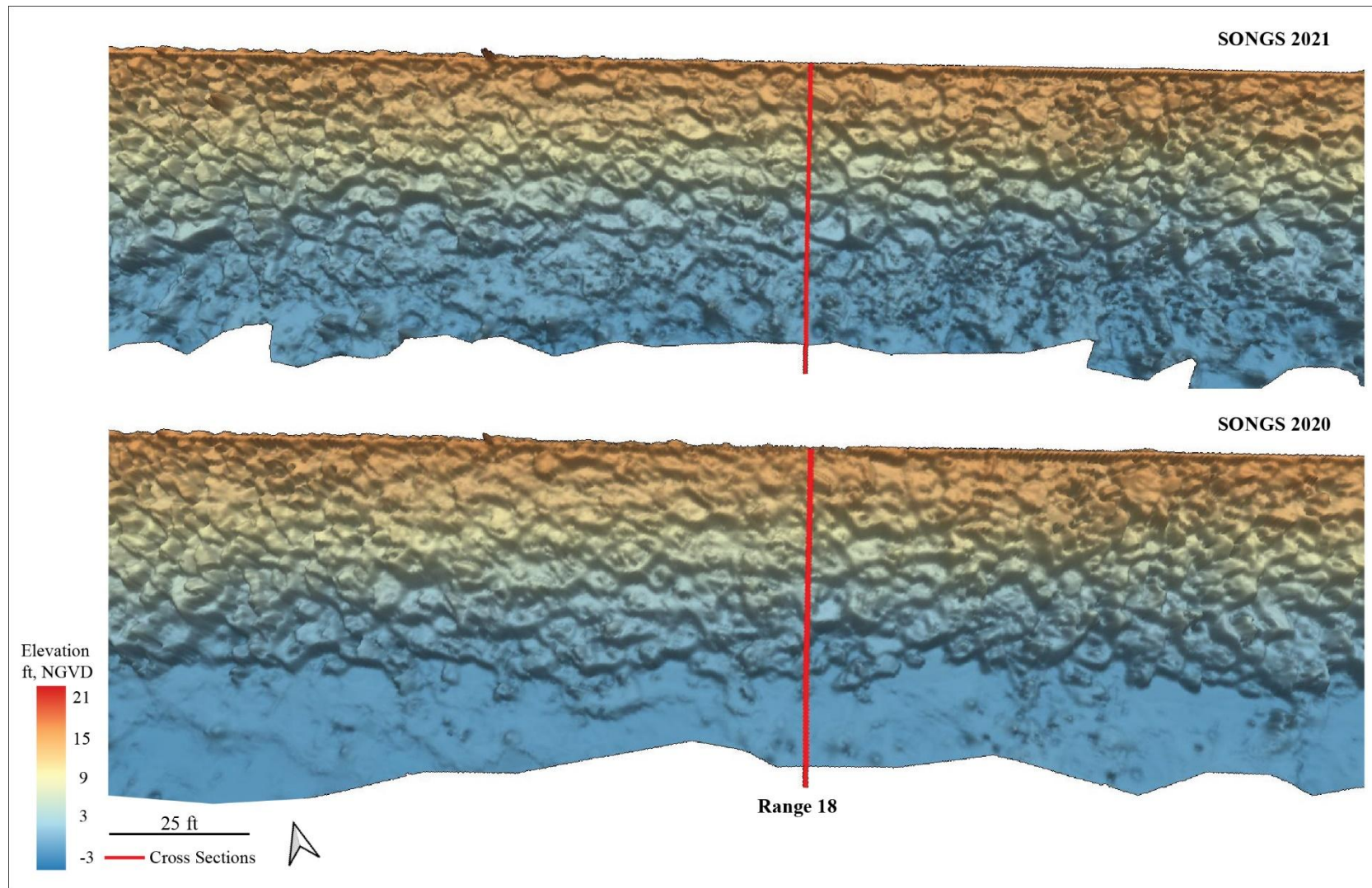


Figure B-19. DEM comparison between 2021 (top) and 2020 (bottom) showing Transect 18 along the SONGS revetment. Notice the increased amount of cobble at the toe of the revetment in 2021.

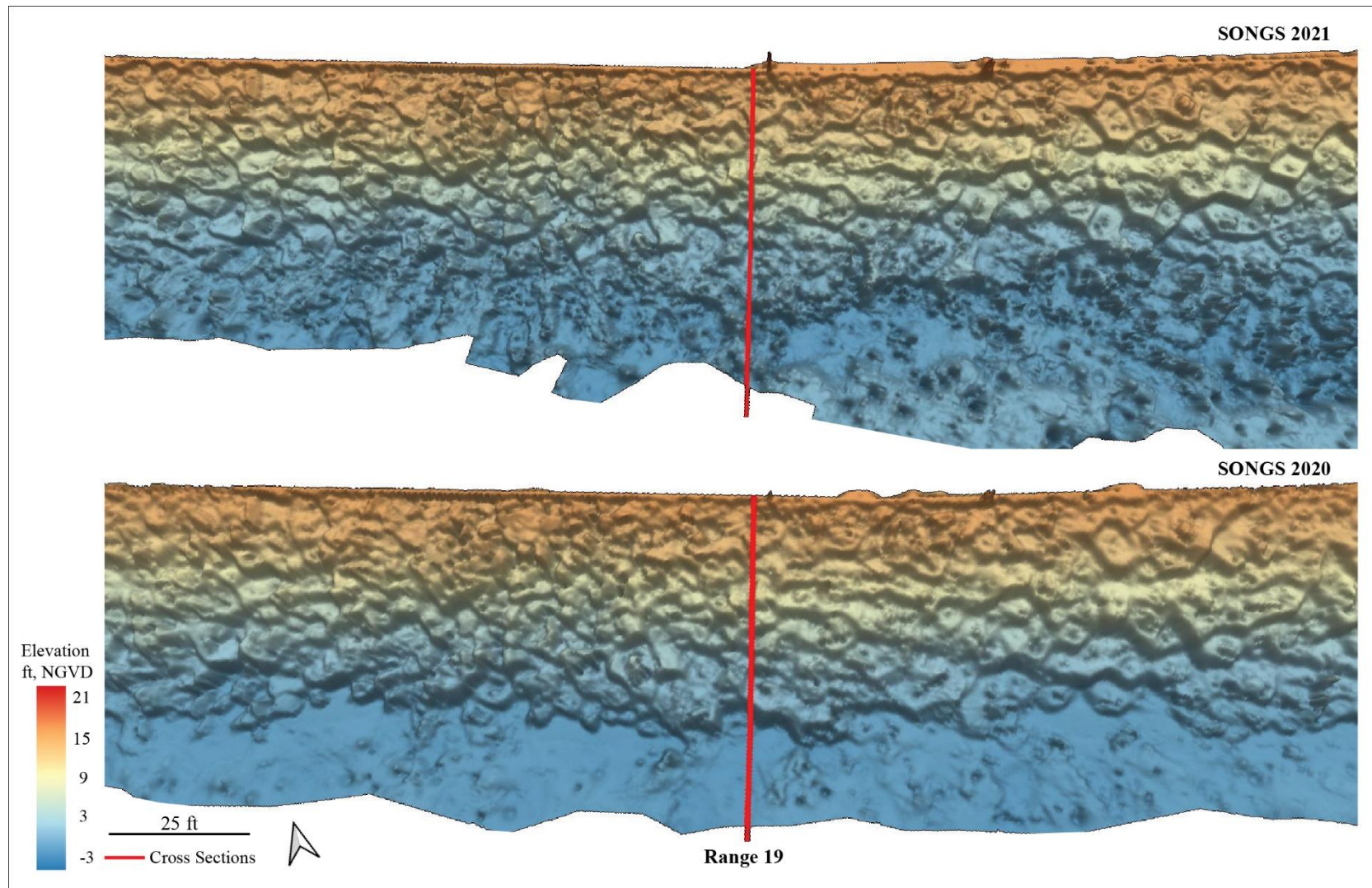


Figure B-20. DEM comparison between 2021 (top) and 2020 (bottom) showing Transect 19 along the SONGS revetment. Notice the increased amount of cobble at the toe of the revetment in 2021.

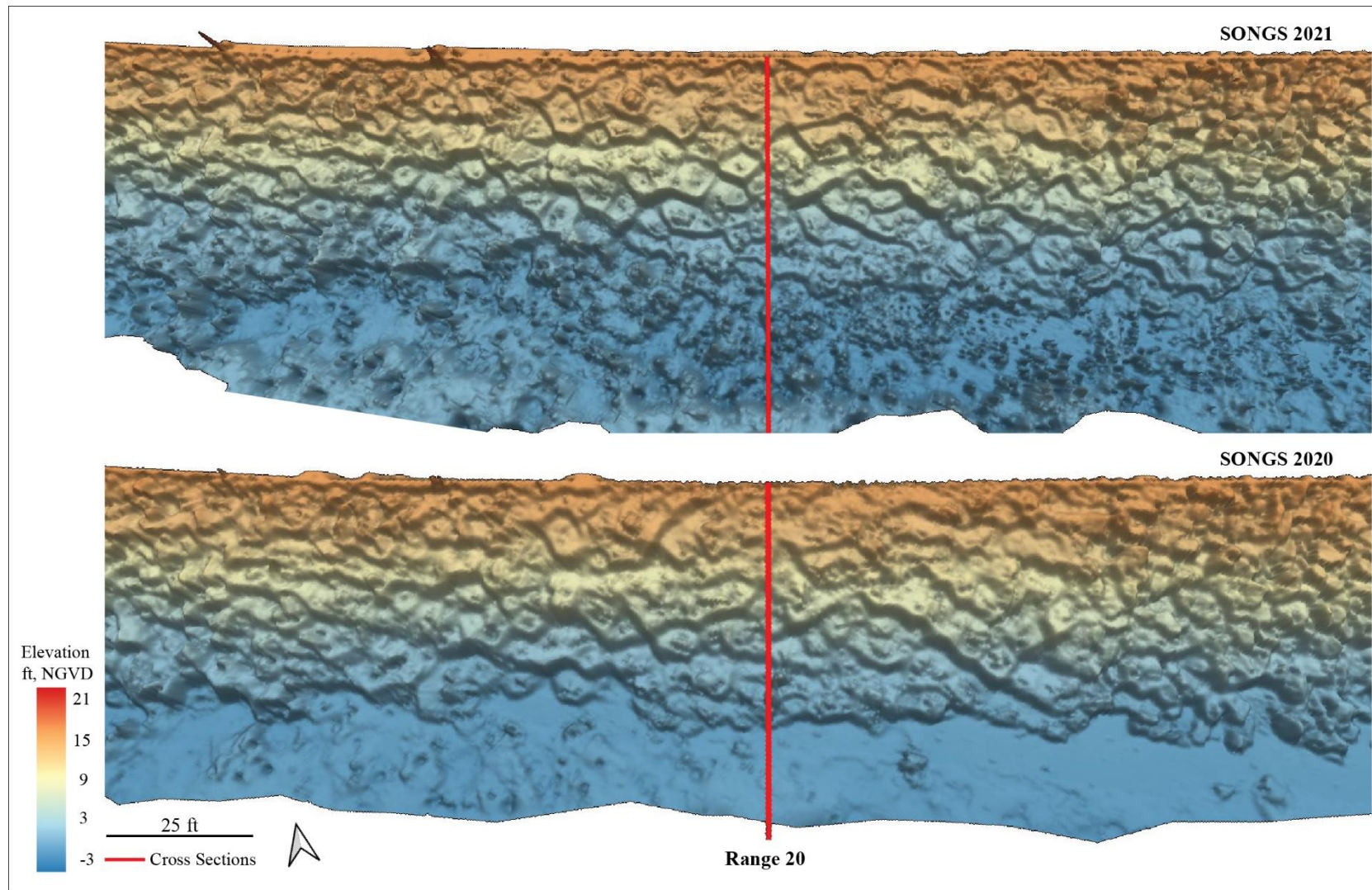


Figure B-21. DEM comparison between 2021 (top) and 2020 (bottom) showing Transect 20 along the SONGS revetment. Notice the increased amount of cobble at the toe of the revetment in 2021.

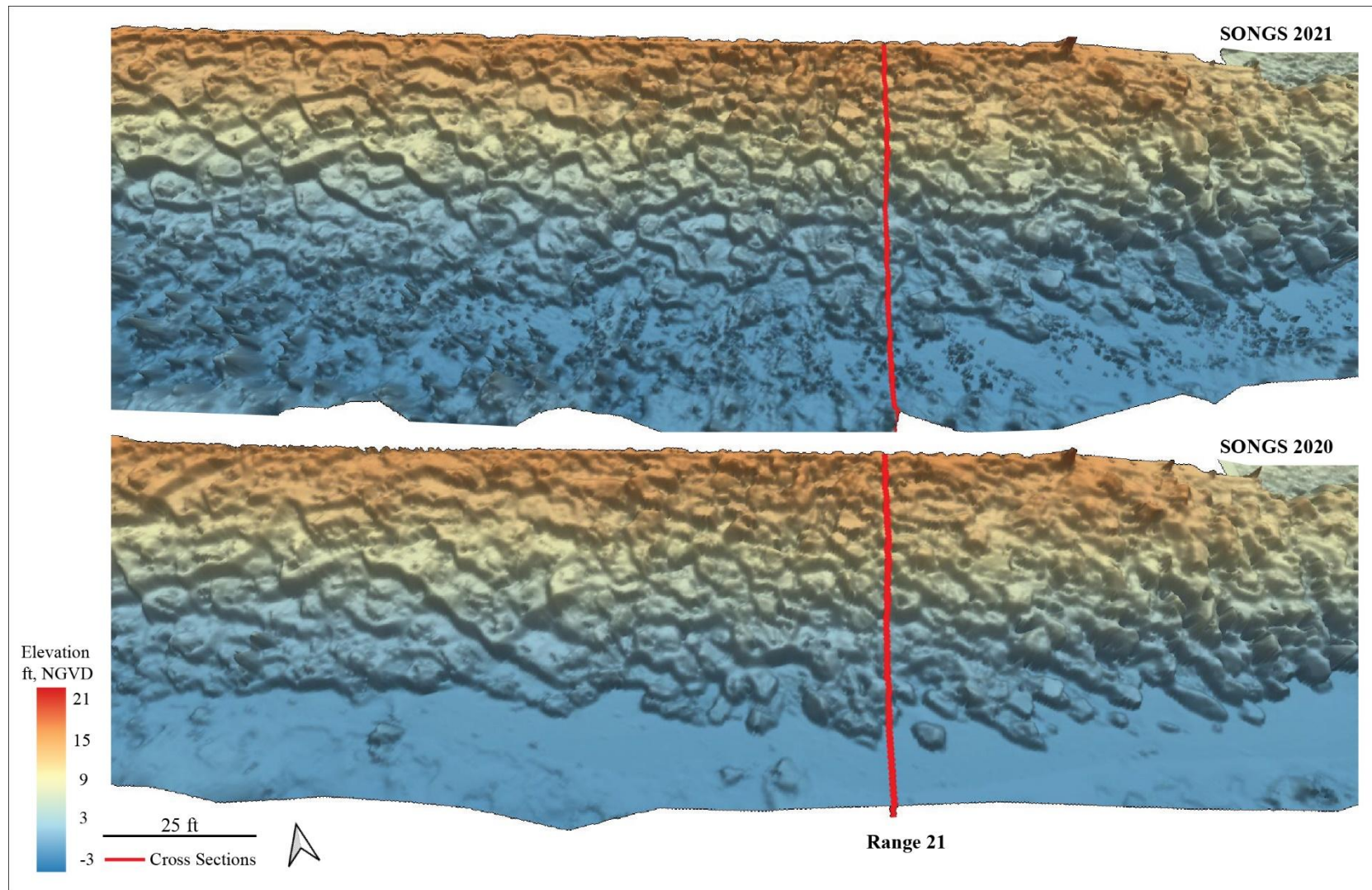


Figure B-22. DEM comparison between 2021 (top) and 2020 (bottom) showing Transect 21 along the SONGS revetment. Notice the increased amount of cobble at the toe of the revetment in 2021.

APPENDIX C

**CROSS SECTION ELEVATIONS
OF SONGS REVETMENT**

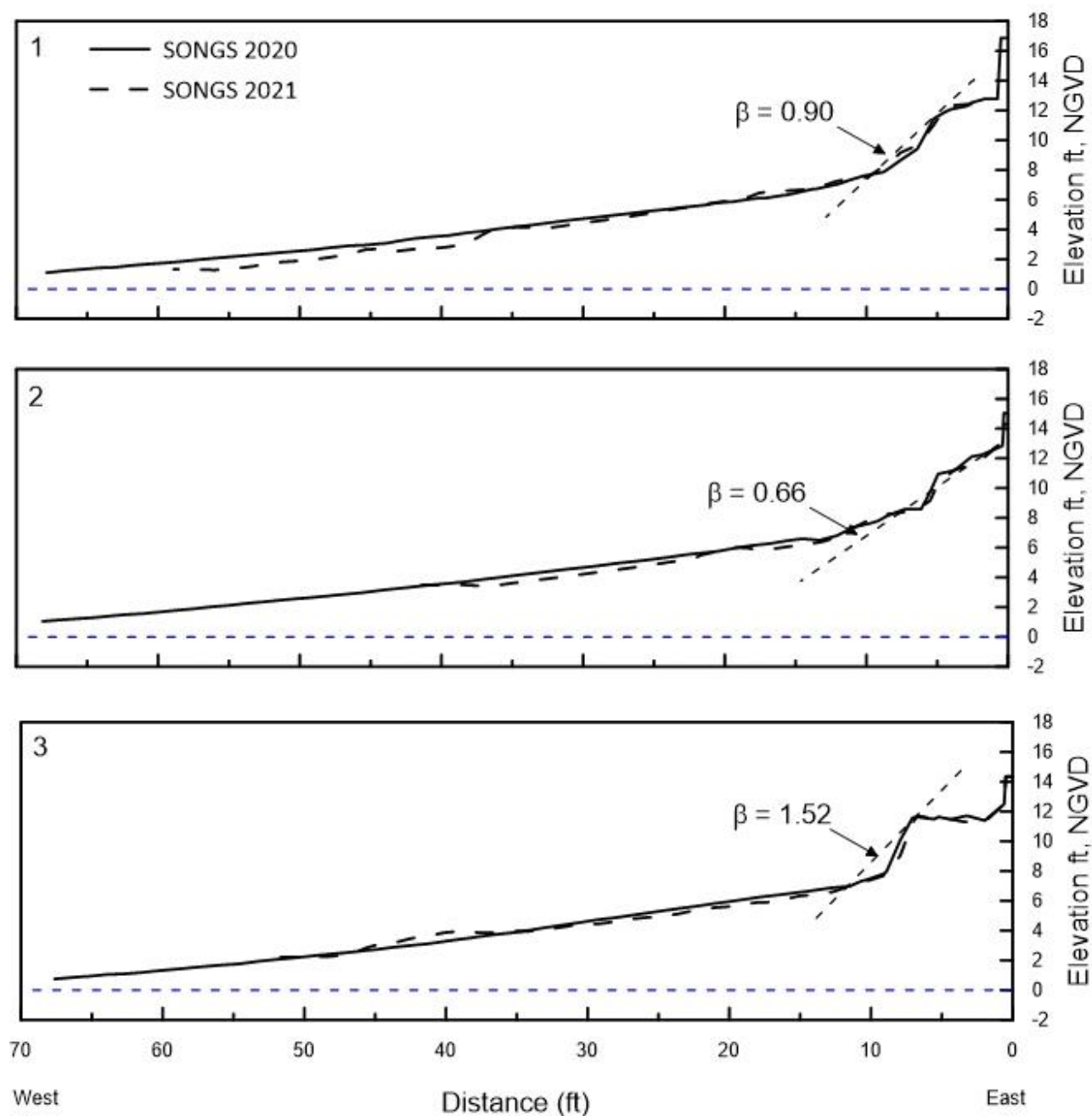


Figure C-1. Cross sections of SONGS revetment along transects 1-3, surveyed on 25 February 2021 and 5 March 2020. β represents the revetment slope.

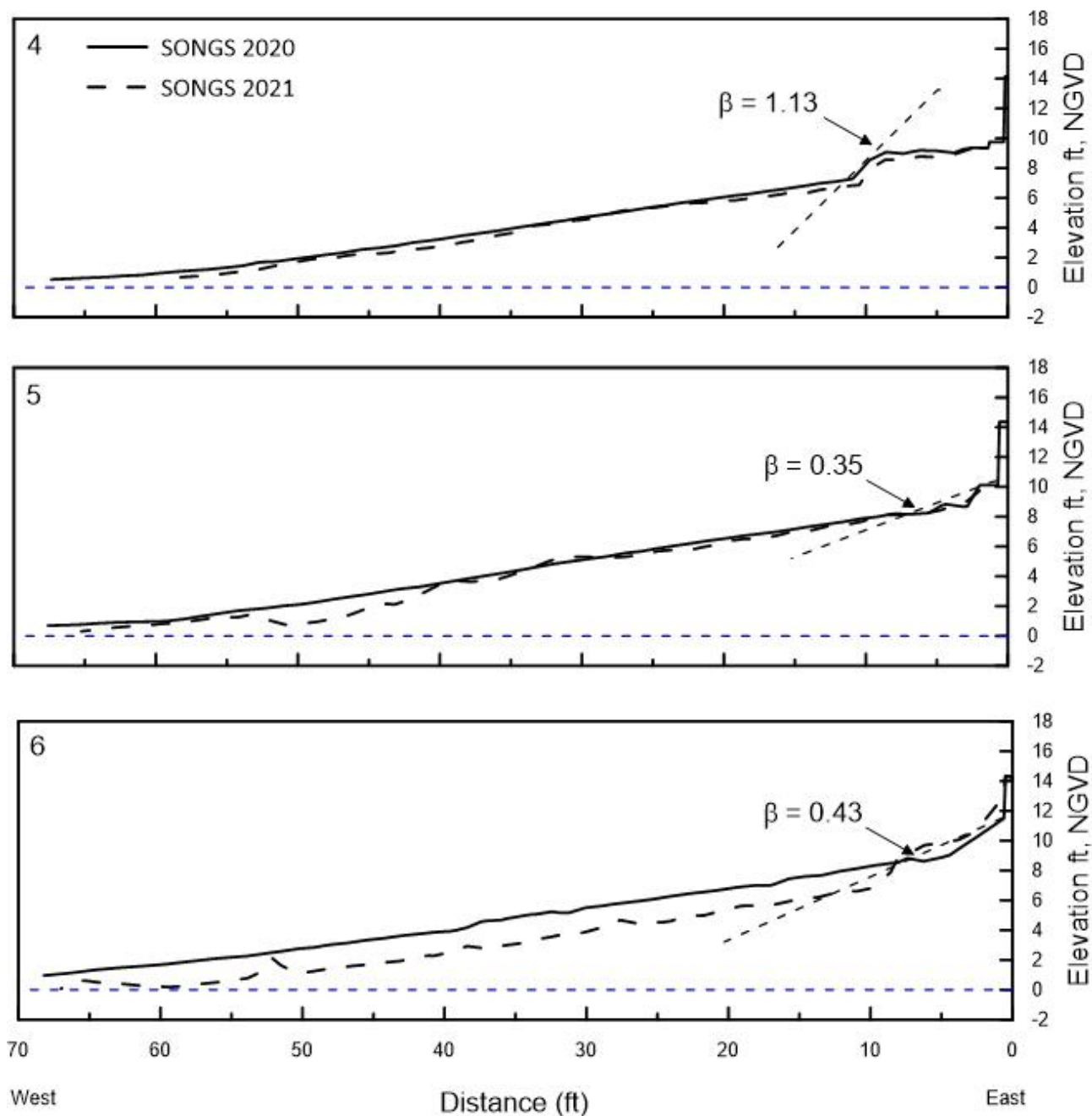


Figure C-2. Cross sections of SONGS revetment along transects 4-6, surveyed on 25 February 2021 and 5 March 2020. β represents the revetment slope.

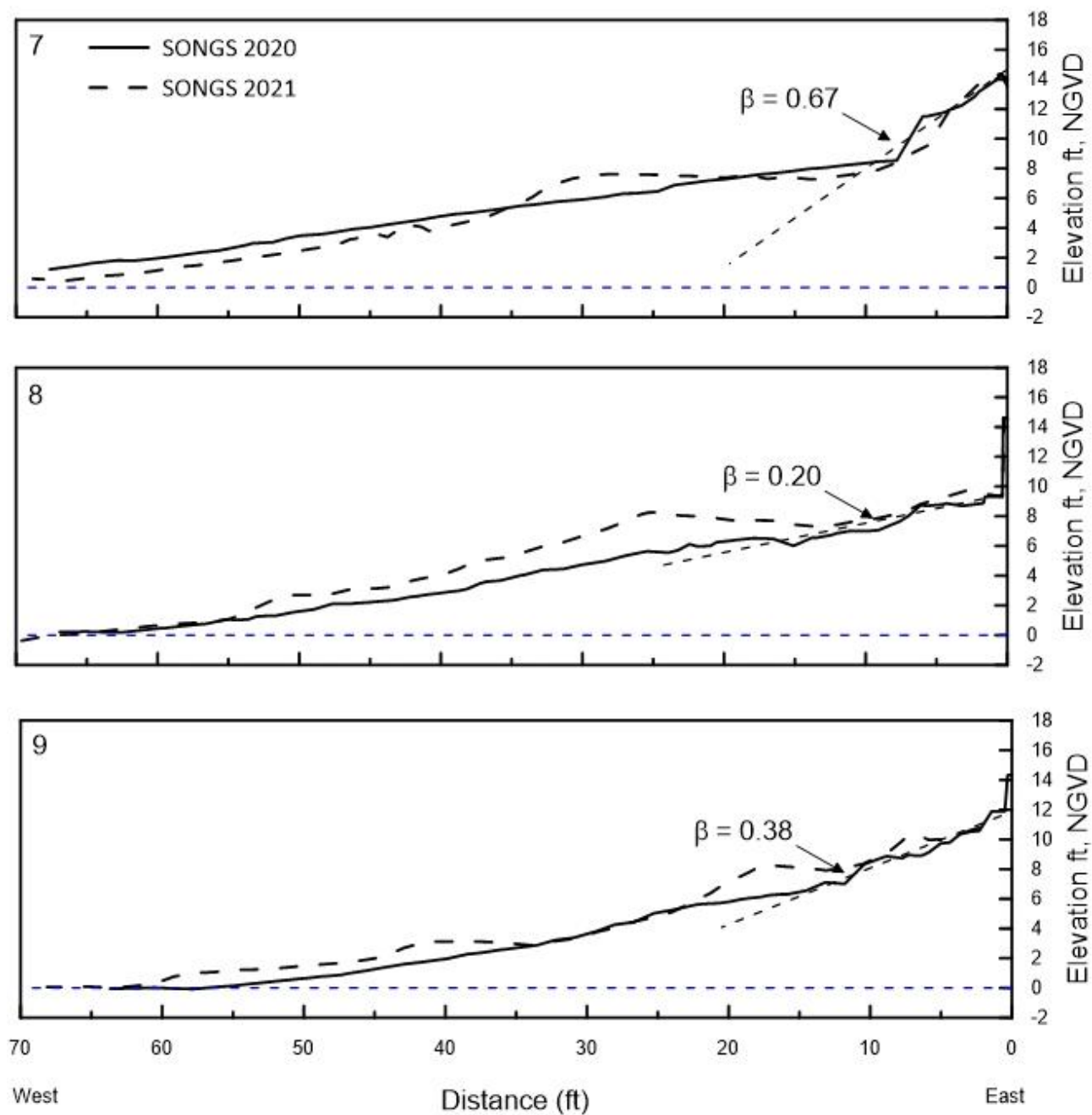


Figure C-3. Cross sections of SONGS revetment along transects 7-9, surveyed on 25 February 2021 and 5 March 2020. β represents the revetment slope.

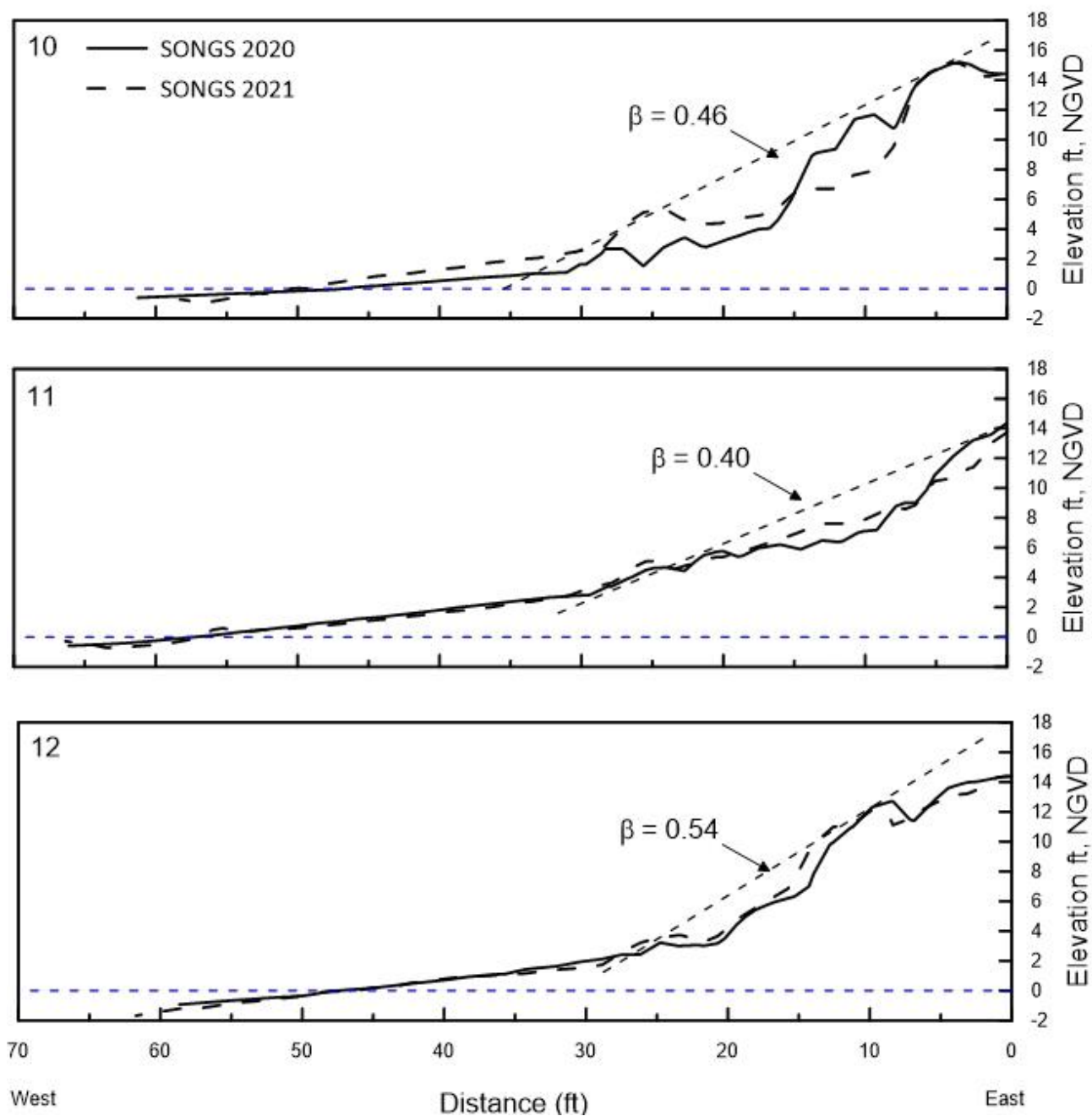


Figure C-4. Cross sections of SONGS revetment along transects 10-12, surveyed on 25 February 2021 and 5 March 2020. β represents the revetment slope.

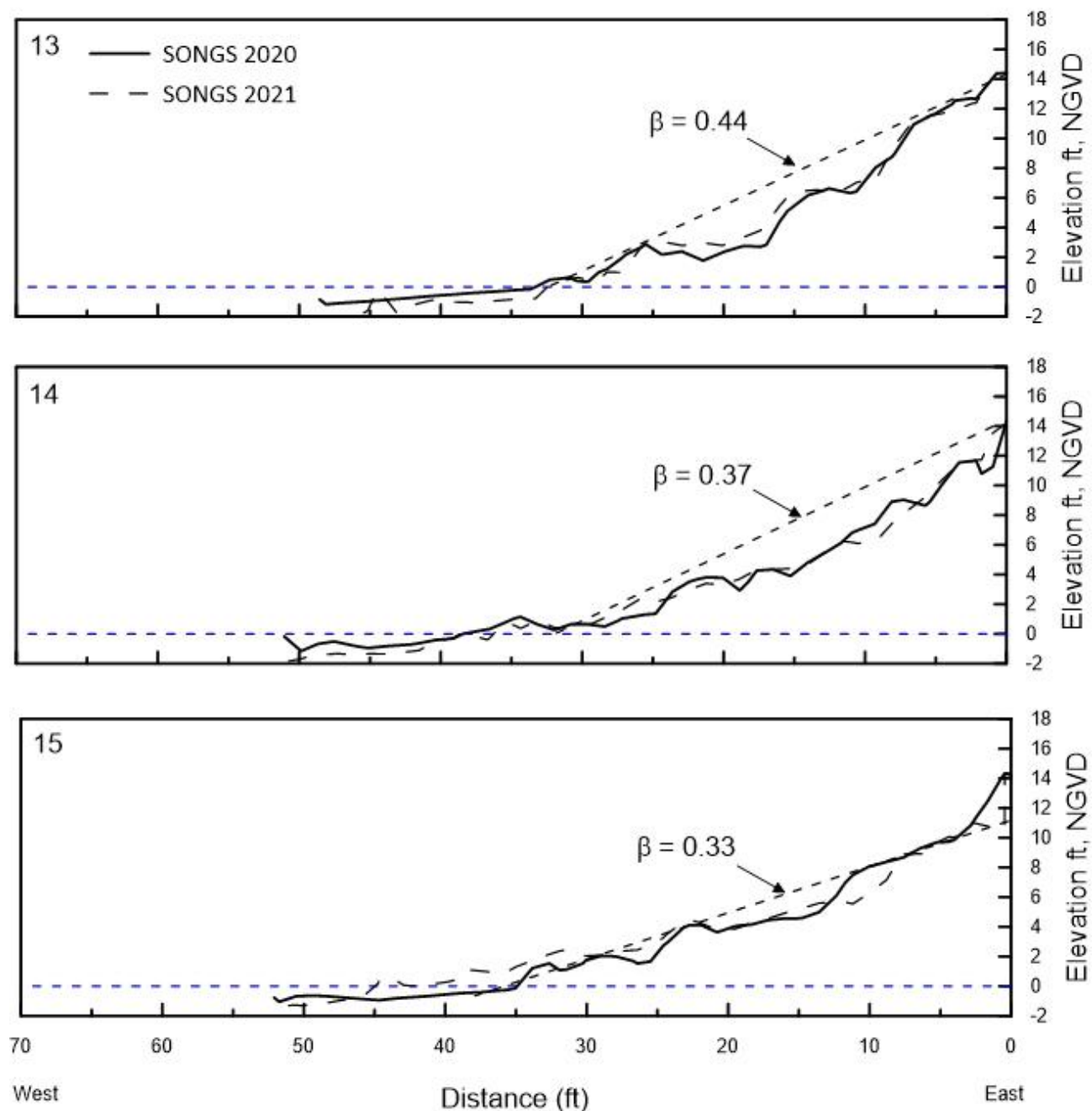


Figure C-5. Cross sections of SONGS revetment along transects 13-15, surveyed on 25 February 2021 and 5 March 2020. β represents the revetment slope.

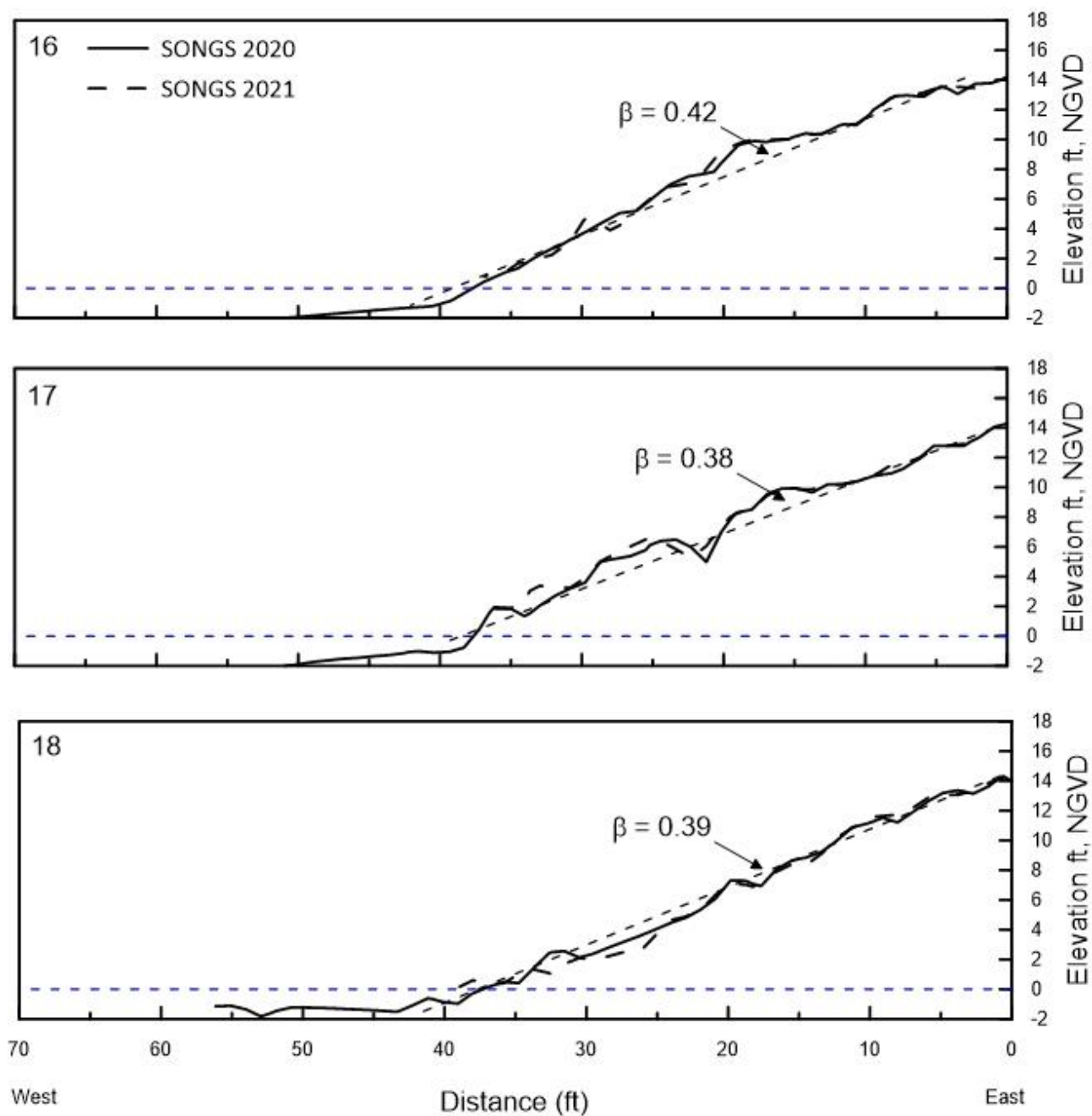


Figure C-6. Cross sections of SONGS revetment along transects 16-18, surveyed on 25 February 2021 and 5 March 2020. β represents the revetment slope.

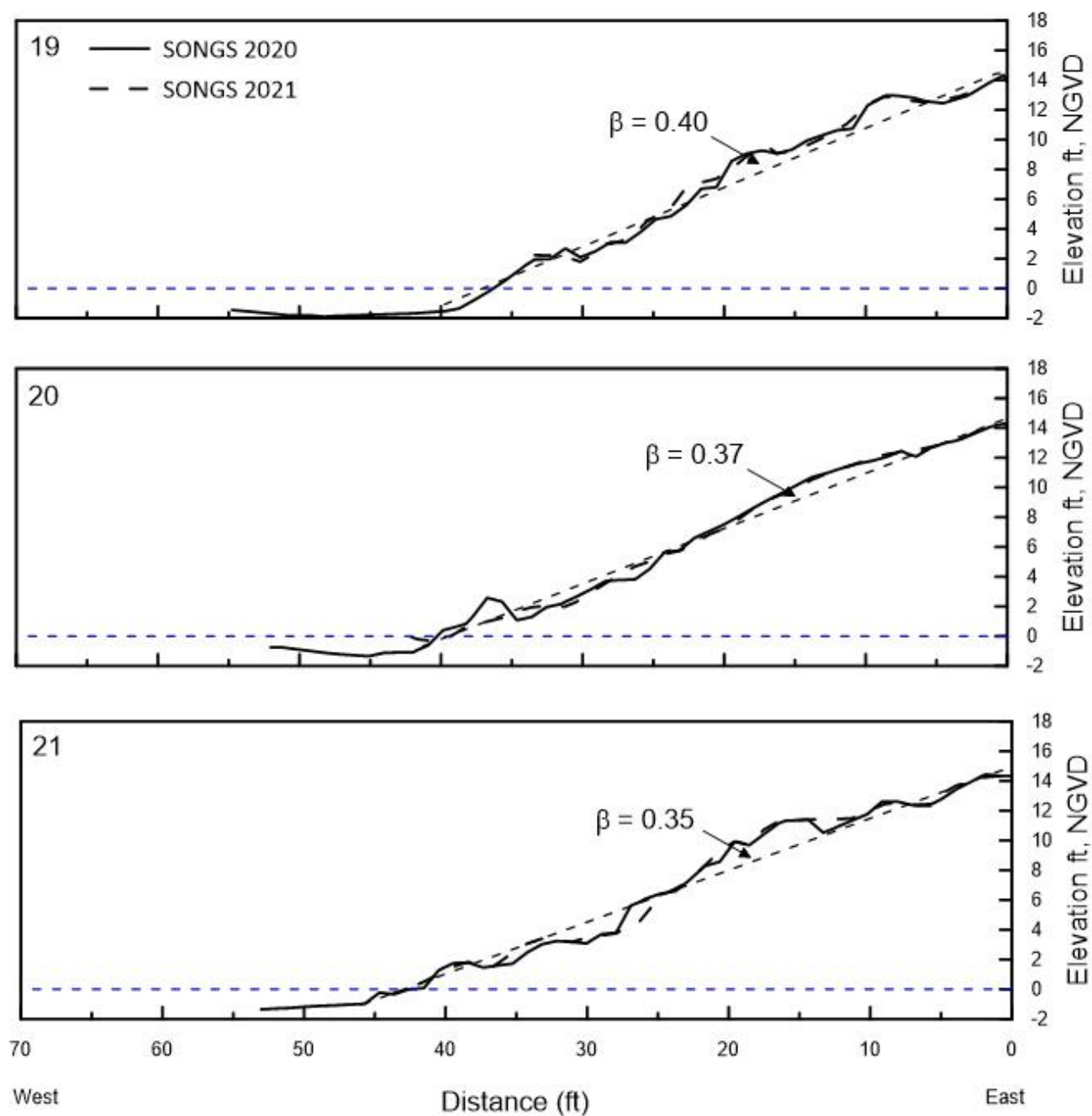


Figure C-7. Cross sections of SONGS revetment along transects 19-21, surveyed on 25 February 2021 and 5 March 2020. β represents the revetment slope.

APPENDIX D

AERIAL PHOTOGRAPHS

NORTH AND SOUTH SONGS, 2003-2020



Photo D-1. Photograph showing revetment covered by sand and fronted by a wide beach at the northern end of SONGS (10 March 2003).



Photo D-2. Photograph showing waves from north swell attacking SONGS revetment at the southern end of SONGS (10 March 2003).



Photo D-3. Photograph showing waves attacking the revetment and the presence of a sand beach at the northern end of SONGS (26 November 2003).



Photo D-4. Photograph showing waves attacking SONGS revetment at the southern end of SONGS (26 November 2003).



Photo D-5. Photograph showing revetment covered by sand and fronted by a wide beach at the northern end of SONGS (2 August 2006).

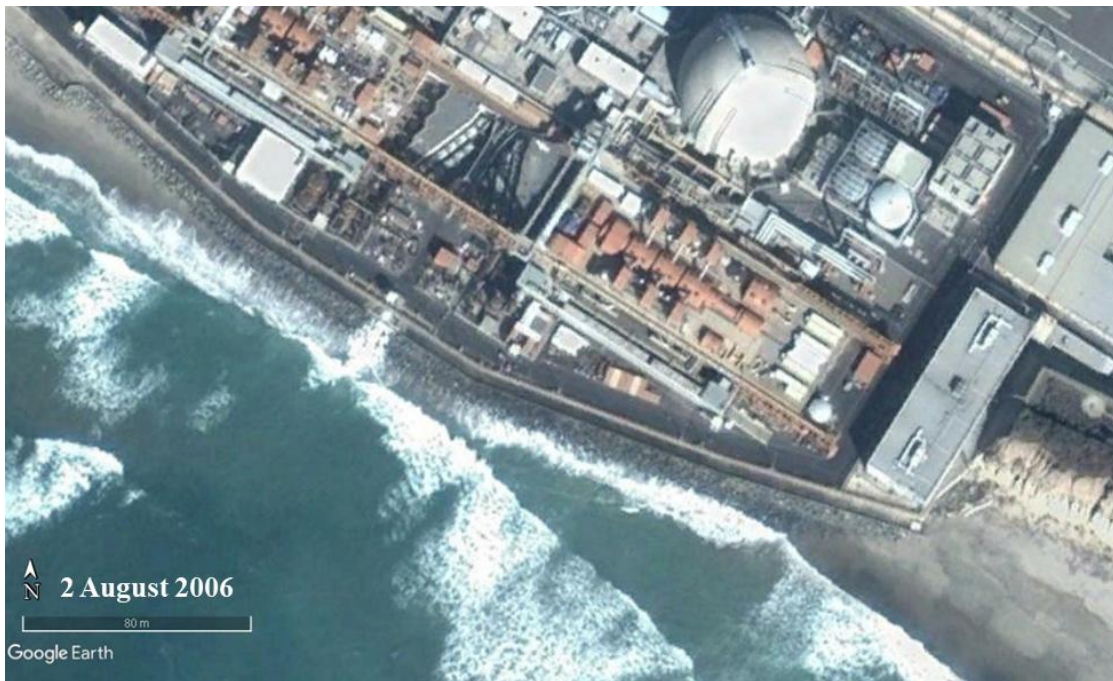


Photo D-6. Photograph showing waves from north swell attacking SONGS revetment at the southern end of SONGS (2 August 2006).



Photo D-7. Photograph showing revetment covered by sand and fronted by a wide beach at the northern end of SONGS (31 January 2006).



Photo D-8. Photograph showing waves from north swell attacking SONGS revetment and refracting towards south at the southern end of SONGS (31 January 2006).

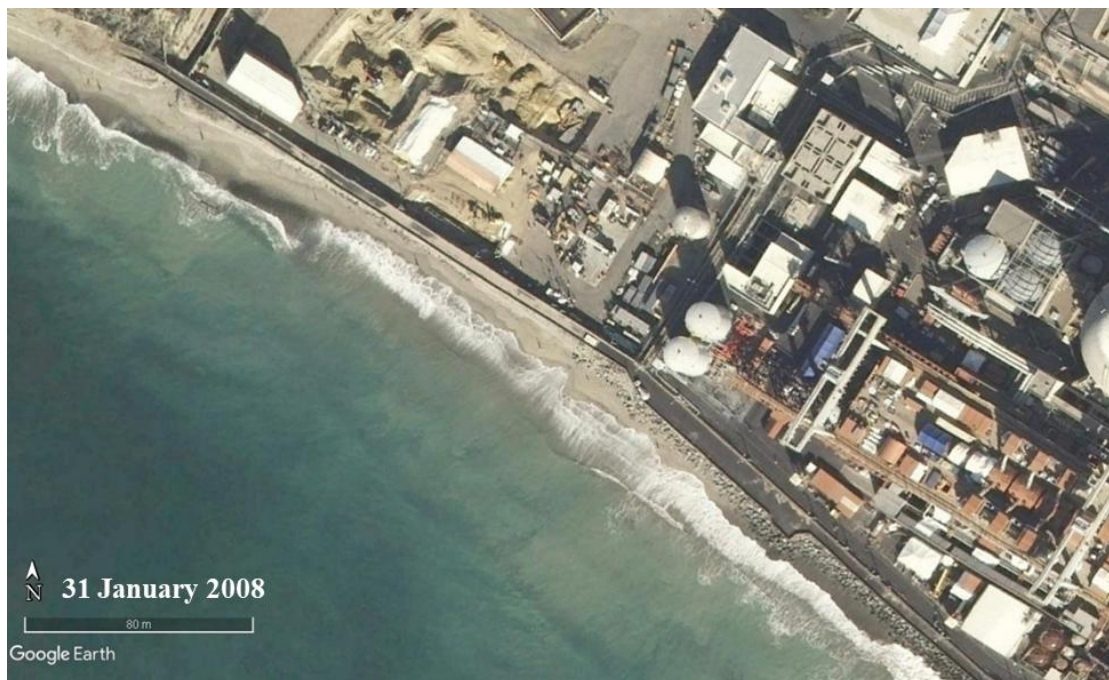


Photo D-9. Photograph showing revetment covered by sand and fronted by a wide beach at the northern end of SONGS (31 January 2008).

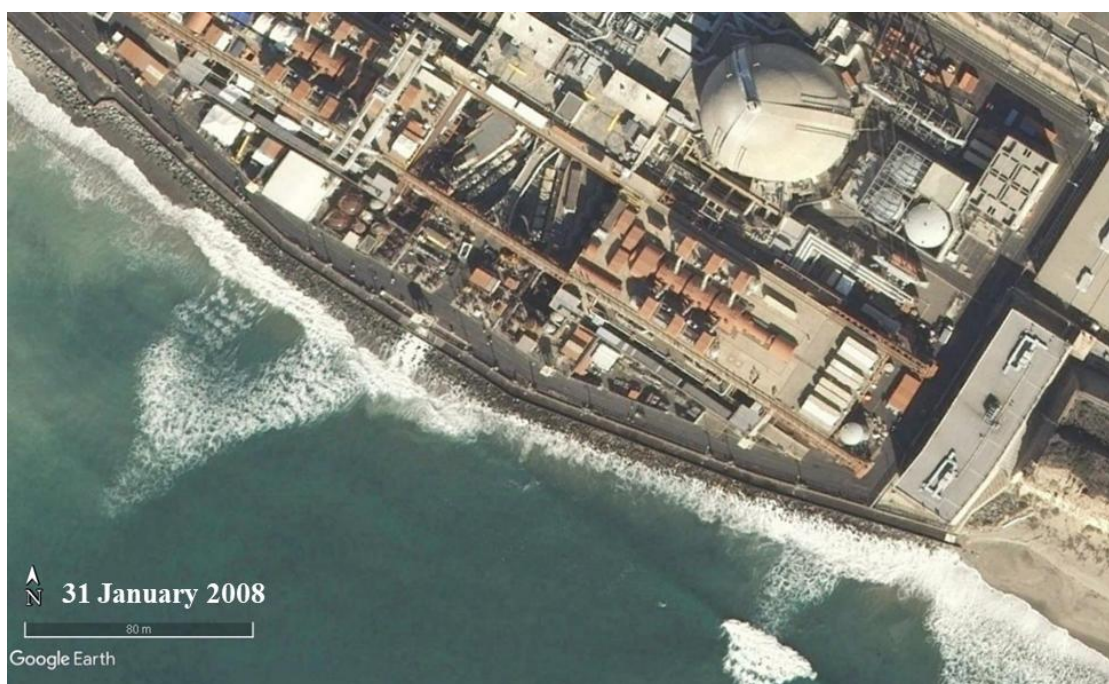


Photo D-10. Photograph showing waves attacking SONGS revetment at the southern end of SONGS (31 January 2008).



Photo D-11. Photograph showing revetment covered by sand and fronted by a wide beach at the northern end of SONGS (12 November 2013).



Photo D-12. Photograph showing waves attacking SONGS revetment and refracting towards south at the southern end of SONGS (12 November 2013).

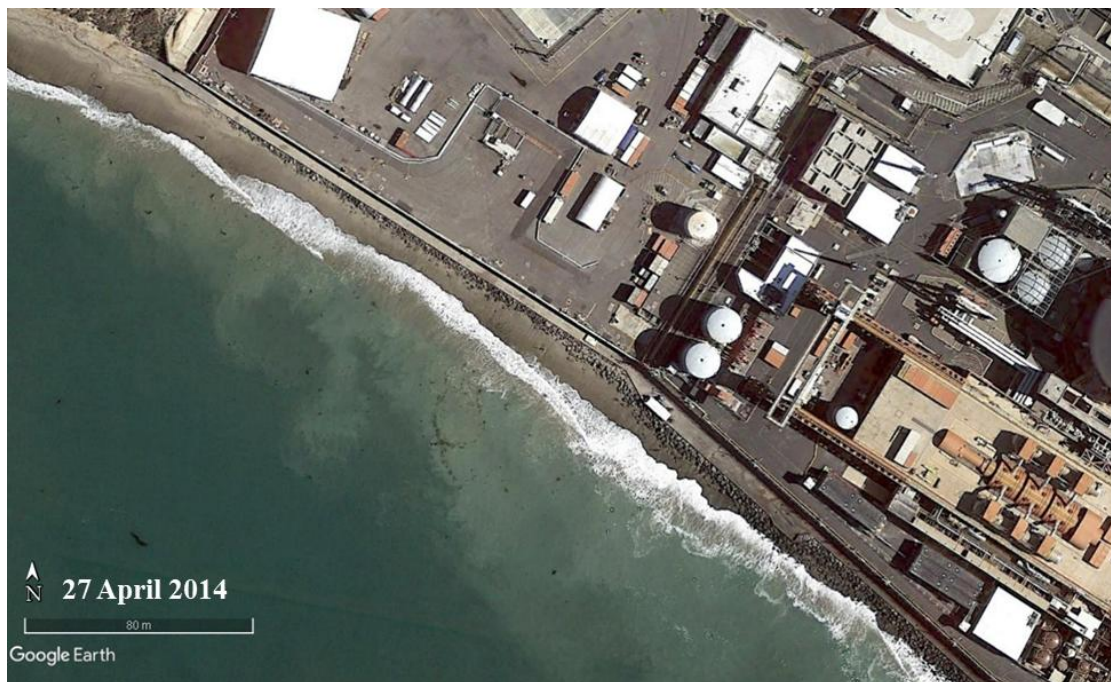


Photo D-13. Photograph showing revetment exposed and fronted by a wide beach at the northern end of SONGS (27 April 2014).

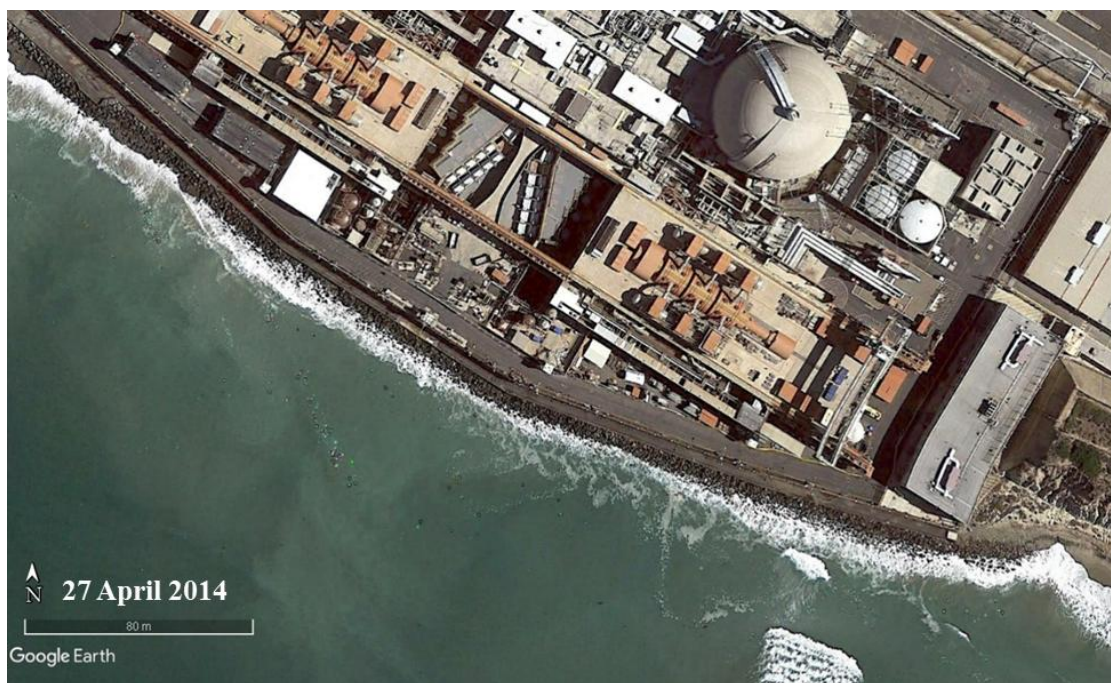


Photo D-14. Photograph showing waves attacking SONGS revetment and refracting towards south at the southern end of SONGS (27 April 2014).

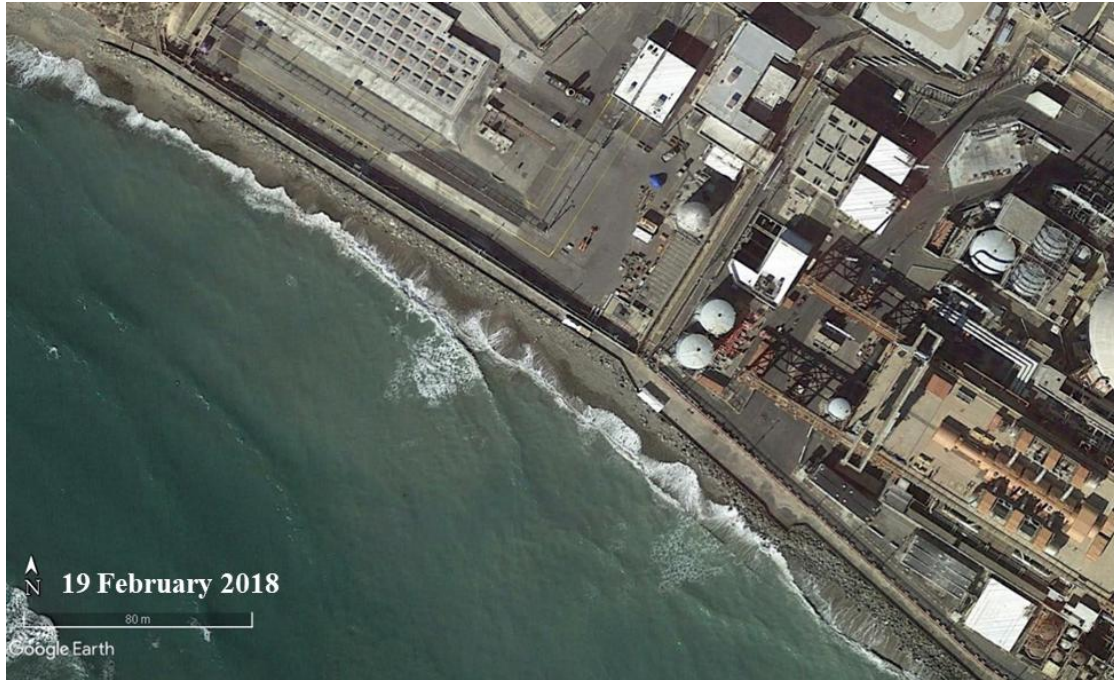


Photo D-15. Photograph showing revetment exposed and fronted by a sand beach at the northern end of SONGS (19 February 2018).

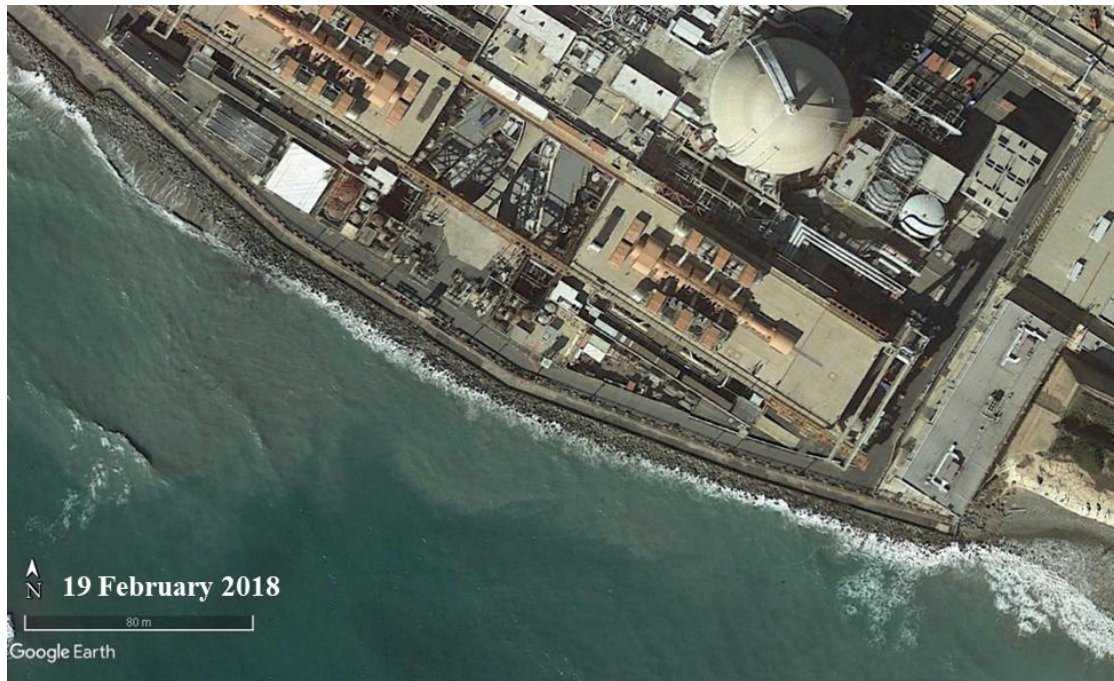


Photo D-16. Photograph showing waves from north swell attacking SONGS revetment and refracting towards south at the southern end of SONGS (19 February 2018).

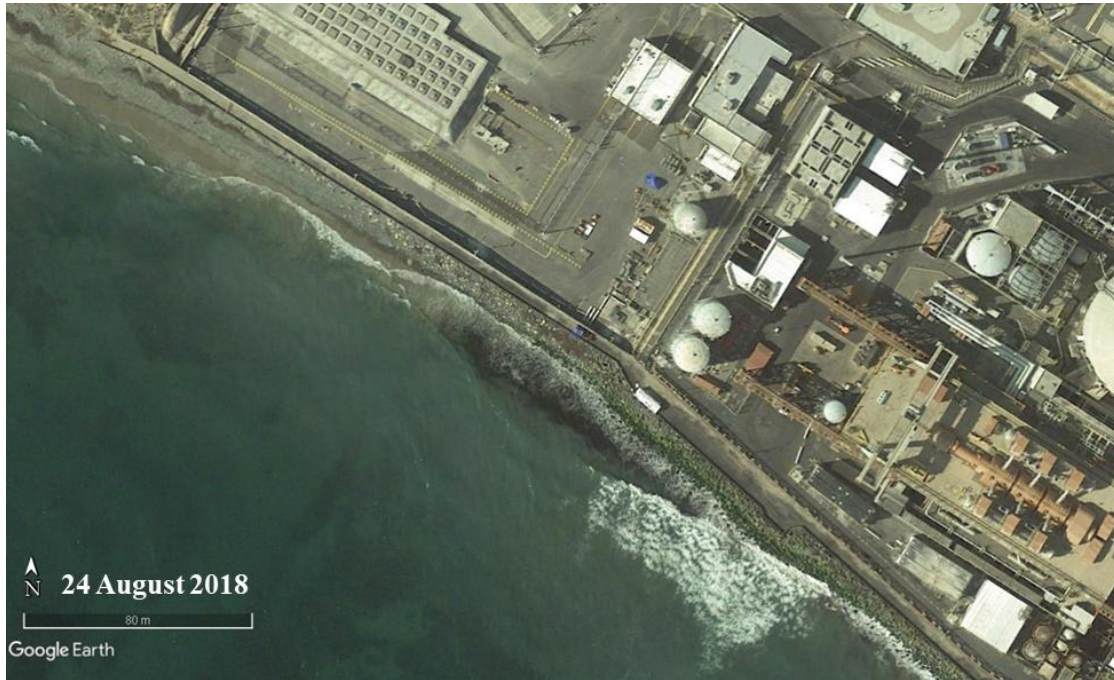


Photo D-17. Photograph showing revetment exposed and fronted by a wide beach at the northern end of SONGS (24 August 2018).



Photo D-18. Photograph showing waves from north swell attacking SONGS revetment and refracting towards south at the southern end of SONGS (24 August 2018).

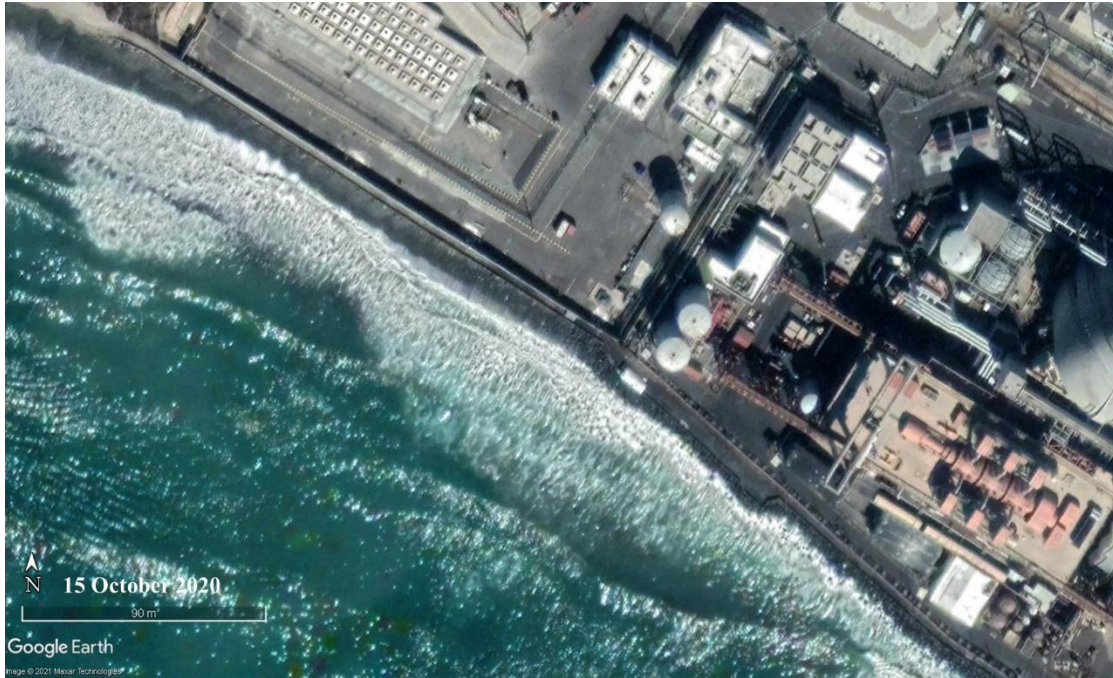


Photo D-19. Photograph showing revetment exposed and fronted by a wide beach at the northern end of SONGS (15 October 2020).



Photo D-20. Photograph showing waves attacking SONGS revetment and refracting towards south at the southern end of SONGS (15 October 2020).

Commercial Nuclear Waste

State-Fed Fight Heats Up Over Building Private Nuclear Disposal Sites



Proposed site project, estimated at \$350M to build and \$2.3B to operate over 40 years, has a federal license but state officials are fighting it in court. Image: US Nuclear Regulatory Commission

July 17, 2022

Mary B. Powers and Debra K. Rubin

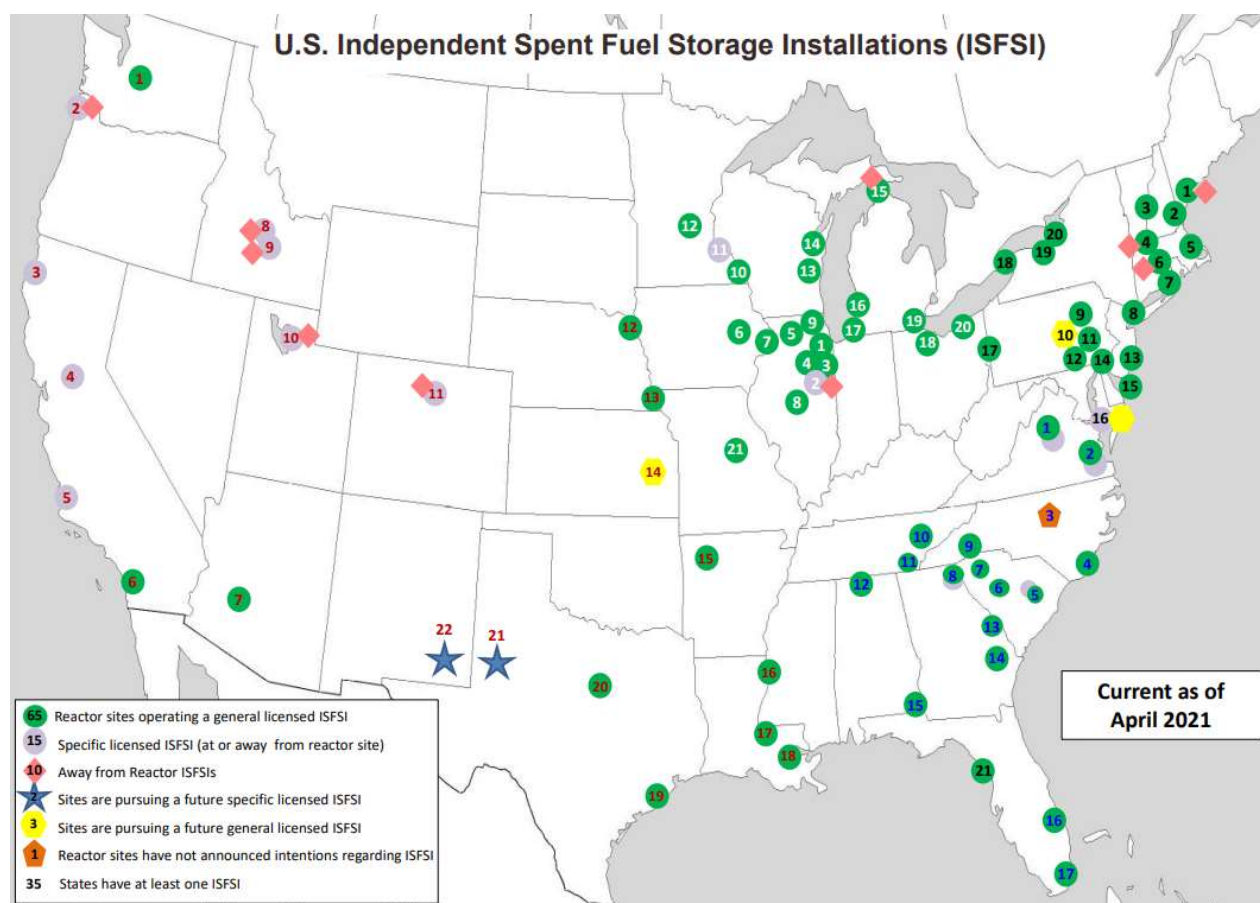
The U.S. Nuclear Regulatory Commission and Interim Storage Partners, a joint venture that gained a federal license last year to build an interim storage facility for spent commercial nuclear fuel at a Texas site, have until Aug. 3 to answer a federal lawsuit claim by state officials that a new U.S. Supreme Court decision eliminates the federal agency's licensing authority.

The state challenge now is before the U.S. appellate court in New Orleans.

NRC issued a license to the JV team of Waste Control Specialists and Orano USA to store for 40 years up to 5,000 metric tons of spent nuclear power plant fuel and 231 metric tons of low-level radioactive waste at the proposed site northwest of Midland, near the New Mexico border.

The proposed facility is estimated to cost \$350 million to build, with total expenses nearing \$2.3 billion by the end of its 40-year lifespan, says an NRC final environmental review issued in July 2021.

Interim Storage Partners said it could also enlarge the site to hold 40,000 metric tons of spent fuel, but NRC said that would require a license amendment with added review.



Map: US Nuclear Regulatory Commission

**Click the image for greater detail*

The facility would be located adjacent to a separately operated existing low-level nuclear materials disposal facility in Andrews County, Texas, with other locations in the state now storing spent fuel from two nuclear power plants.

Texas Attorney General Kenneth Paxton originally challenged the proposed site's license, claiming it violated the federal Nuclear Waste Policy Act and NEPA.

He now argues that NRC lacks statutory authority to issue the interim storage license, following the U.S. Supreme Court's June 30 [decision in *West Virginia v. EPA*](#)—which placed limits on the U.S. Environmental Protection Agency's regulation of power plant greenhouse gas emissions—and could set other federal regulatory curbs, some observers speculate.

While NRC bases its authority on the 1954 Atomic Energy Act to license waste storage at a private site without a state's consent, the law does not specifically refer to the storage or disposal of spent nuclear fuel, Texas claims. Following state enactment of a new law last year that bans interim commercial waste storage, Texas wants the federal court to vacate the Interim Storage Partners site license.

That NRC was not given explicit authority by Congress raises issues under the “major questions doctrine,” Texas Assistant Solicitor General Michael Abrams [said](#) in a July 6 letter to the court.

The Supreme Court said that the doctrine applies when Congress has consistently rejected proposals to amend the law to give an agency an authority. Texas argues that Congress has considered multiple bills to explicitly authorize the U.S. Energy Dept. to contract with privately owned spent fuel storage facilities but none are enacted.

“Difficult and even intractable problems do not give an agency a blue pencil to rewrite its governing statute,” said the state. Texas accused the federal government of committing a “massive breach” of its obligation to provide permanent storage for spent nuclear fuel at Yucca Mountain in Nevada, a now mothballed project.

The suit is playing out as new legislation floated by Sen. Joe Manchin, (D-W. Va.), would create a new federal agency separate from DOE to find a community willing to house a new permanent site. It would also authorize that agency to operate one or more federally-owned interim storage sites and one or more with a private partner. The bill is set for a hearing this month in the Energy and Natural Resources Committee, which he chairs.

NRC, Interim Storage Partners and the U.S. Justice Dept asked the court to allow case participants to file new briefs on the issues, due Aug. 3, with oral arguments set for the week of Aug. 29.

New Mexico Storage Site Also Contentious

Meanwhile, New Mexico also is challenging NRC in U.S. appellate court in Denver over plans to site an interim storage facility in that state proposed by Holtec International.

The agency on July 13 issued the final environmental impact review for the first \$230-million project phase, with agency staff recommending that the facility license be issued.

The site would initially store about 8,680 metric tons of spent nuclear fuel in 500 canisters. The agency review also considered the environmental effects of an expanded site holding 10,000 canisters. The project, if fully built, would cover 1,000 acres in southeastern New Mexico and cost up to \$2.4 billion

The agency expects to decide in January whether to issue the license.

In a statement, Holtec said that the final NRC review “confirms that there are no adverse impacts to other enterprises in the area including oil and gas, ranching and farming.”

It added that “the completely welded and hermetically closed canisters that will be safely stored at the facility are designed, qualified and tested to maintain their integrity and prevent the release of radioactive material under the most adverse accident scenarios postulated by NRC regulations for both storage and transportation.”

The [statement](#) also includes comments from local officials that support building the facility.

Gov. Michelle Lujan Grisham said, in a statement, that “while NRC and Holtec International say that the proposal is ‘temporary,’ a 40-year license with the opportunity for renewal will threaten the health and safety of generations of New Mexicans.”

However, the New Mexico legislature this year did not pass a bill that would have prevented state regulators from issuing Holtec permits for industrial wastewater and construction work at the site..

While Energy Secretary Jennifer Granholm has said the U.S. Energy Dept. is making progress to obtain interest from U.S. communities to locate interim private storage sites for spent nuclear fuel, bills also are pending in the U.S. Congress to block use of federal funds to support activity at such sites.

Recent Articles By Mary B. Powers

Biden Boosts Resilient Infrastructure, Offshore Wind as Climate Actions

US LNG Export Projects Ramp Up in Gap of Closed Freeport Site in Texas



Mary B. Powers has reported on engineering and construction issues in the global energy and environmental sectors for more than 30 years from Washington, D.C. and Birmingham, Ala. She formerly wrote for the Platt's group of energy sector publications under McGraw Hill and S&P Global that included *Inside Energy* and *Megawatt Daily*, and was state editor for the Lexington, Ky., *Herald Leader*. Mary has a master's degree in journalism from The American University.



As ENR Editor-at-Large for Management, Business and Workforce, Debra K. Rubin has a broad vantage for news, issues and trends in global engineering, architecture and construction—from corporate finance and executive management to regulation and risk, next-generation workforce and developing markets such as offshore wind energy.

Debra also launched and manages ENR's Top 200 Environmental Firms ranking, which defines a \$51-billion global market; and is editor of *ENR WorkforceToday* e-newsletter on industry talent management; She also is a key organizer of ENR's annual **Groundbreaking Women in Construction** conference, a major AEC industry forum for talent management and women's career advancement.

[Click here](#) for more detail on plans in formation for the 2022 live event.

The latest news and information

#1 Source for Construction News, Data, Rankings, Analysis, and Commentary

JOIN ENR UNLIMITED

Copyright ©2022. All Rights Reserved BNP Media.

Design, CMS, Hosting & Web Development :: ePublishing

SCE Responses to August 18 Questions from Coastal Commission Staff

September 9, 2022

Coastal Hazards

- 1) Please provide one or more representative cross sections of the existing coastal armoring at the site, going back across the bluff past the NUHOMS ISFSI. The representative cross sections would ideally include the elevations of key aspects of the armoring infrastructure e.g., crest and toe elevations of seawall, crest and toe elevation of revetment, various widths of each component, extent and material type of any sub-grade infrastructure etc. It would also be helpful to get a version of this cross section with high, average, and low groundwater levels marked.

Please see attached cross-section showing the existing coastal armoring at the site (Attachment A). As noted in the attachment, SONGS site elevation is referenced to the Mean Lower Low Water (MLLW) tidal datum (EPOCH 1941 – 1959). To convert from an elevation in MLLW to NAVD88, subtract 0.62 feet.

For additional details regarding the revetment and seawall, see Figures 1 and 2 below.

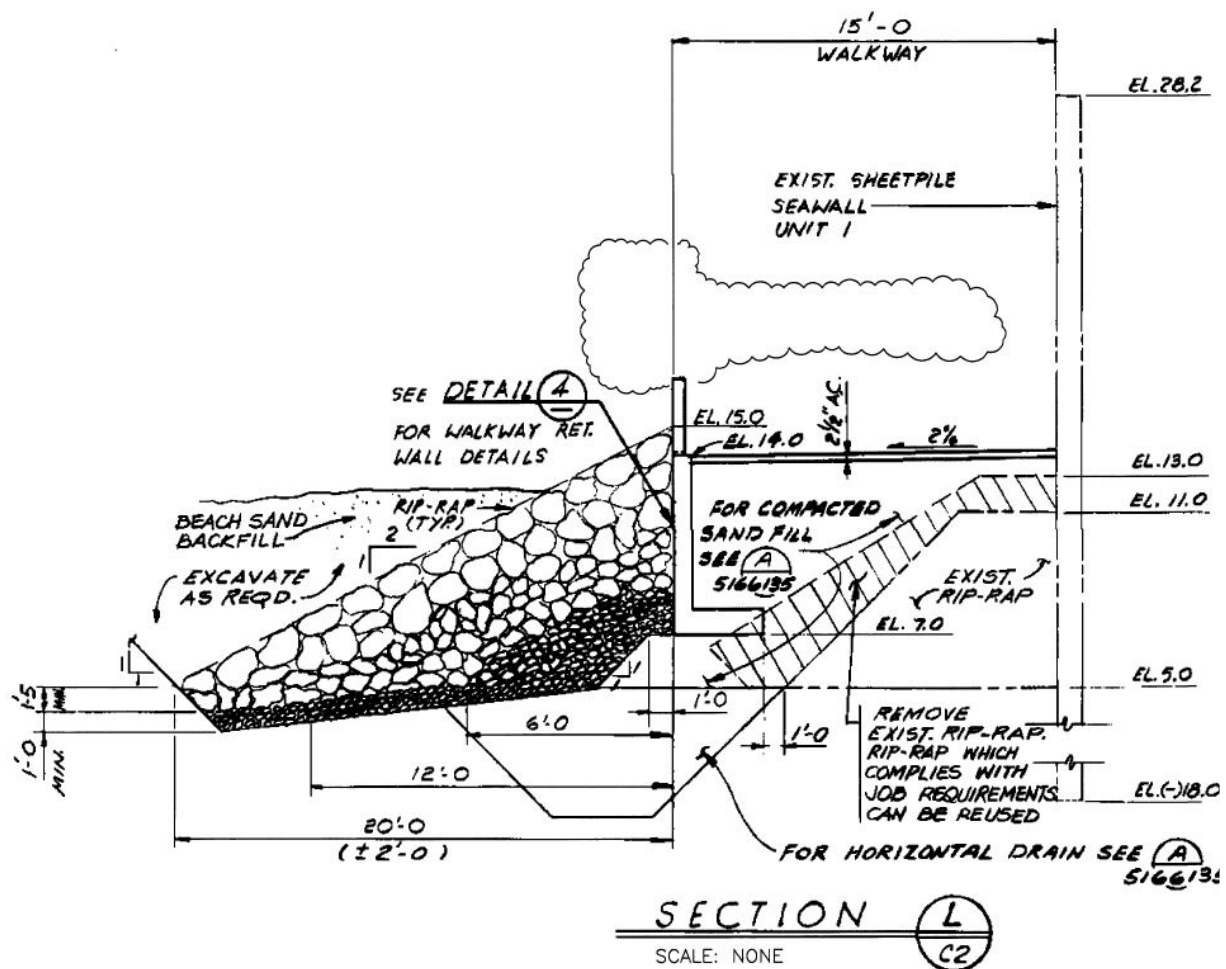


Figure 1. Cross-section showing elevation and dimensional information.

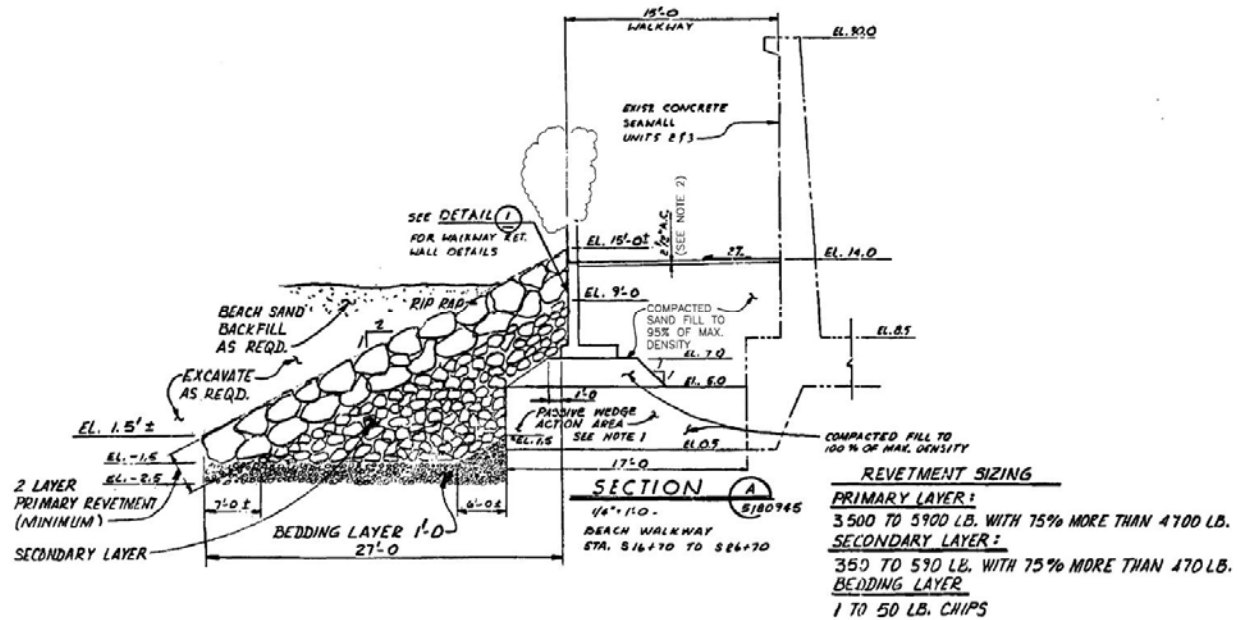


Figure 2. Cross-section showing revetment sizing.

- 2) Please provide a narrative describing the state of repair of the existing seawall and an assessment of its remaining useful life or anticipated repairs.

The North Industrial Area (NIA) seawall is on the plant side of the pedestrian walkway at SONGS, between the pedestrian walkway and the plant. The pedestrian walkway and seawall are protected by the riprap.

The seawall is in good condition. SCE regularly inspects and maintains the seawall. The only repair that has been made to the seawall since 2015 was replacement of the corroded beam along the top of the seawall in 2017.

Some vertical cracks in the nonstructural gunite protective cover were identified during a 2022 inspection, and maintenance is planned to seal these cracks to inhibit possible long-term corrosion of the steel sheet pile structural members. A walk-down of the planned work with a prospective vendor was performed in August 2022 and a proposal for sealing the cracks is pending. With routine maintenance, the seawall will remain in good condition through at least 2050.

SCE provides an annual report to the California State Lands Commission summarizing the condition of the shoreline facilities that protect the seawall and plant (i.e., the riprap). The latest annual report (Coastal Environments 2021) found that the revetment, in its present condition, is likely to tolerate wave forces with acceptable rock movement that will not affect the integrity of the revetment through 2050. The condition of the revetment is important because it, along with the retaining wall and walkway, provides protection to the SONGS seawall against scouring and erosion.

- 3) Please supplement the analysis of the adequacy of the riprap sizing to withstand wave forces through 2050; the analysis included with the materials was incomplete – the results of the exercise were not presented or discussed. (We realize that the seawall and riprap are not a part of the proposed permit amendment, but we expect to get questions on their condition, and we want to be prepared with responses.)

The SONGS revetment provides partial front-line protection for the SONGS seawall. It is also essential to maintaining the walkway that enables consistently safe lateral access for beach users. The revetment shelters the walkway from most wave run-up and overtopping, thus preventing or reducing impacts to access due to flooding or waves, as well as preventing direct wave attack on the seawall.

SCE provide the report titled “SONGS Mean Sea Level Rise Impact Assessment” to Coastal Commission staff in May 2022 in connection with this CDP application (MSL Vulnerability Report). This report contains a thorough discussion of the condition of the SONGS revetment, including information about the size of the riprap and figures showing the riprap.

Revetment stability is a function of rock size and wave conditions. It depends on water level (and thus mean sea level rise), since deeper water at the toe of the structure permits higher (depth limited) wave heights to impact the structure. The MSL Vulnerability Report provided a stability analysis for the revetment based on standard coastal engineering practices (US Army Corps of Engineers 1994a, 1994b), and determined, “...that with routine maintenance, the revetment can continue to function as intended until at least 2050.” This means that rock sizing and other revetment specifications are adequate through 2050.

The median rock weight W_{50} is a key parameter in assessing the stability of a revetment. Hudson’s formula (Ahrens, 1981a,b; USACOE 1984, 1994a,b; BCMELP, 2000) is the standard practice method used to estimate W_{50} necessary for revetment stability:

$$W_{50} = \frac{\gamma_r H^3}{K_D \frac{\gamma_r - 1}{\gamma_w} \cot \alpha} \quad (3-2)$$

Where:

W_{50} = required median armor unit weight,
 γ_r = specific weight of the rock unit, Kg/m³,
 H = wave height at the toe of the revetment,
 K_D = stability coefficient,
 γ_w = specific weight of water at the site, and
 α = revetment slope angle from horizontal.

The following values were used for the assessment of the revetment in the MSL Vulnerability Report:

- A value of 2,670 kg/m³ was used for the specific weight of the rock unit.
- The height of the wave at the toe of the revetment is depth limited. The extreme water depth at the toe of the SONGS revetment (D_s) is 5.5 ft + 2.29 = 7.79 ft, MLLW, where 5.5 ft, NGVD is extreme water level (Section 3.4) and 2.29 is the difference in elevation between datums NGVD and MLLW.
- The water depth at the toe of the structure (D_s) varies as the sea level rises. In 2050, the water depth at the toe of the structure is projected to be 9.79 ft, MLLW (OPC, 2018, Medium-High Scenario) and 10.59 ft, MLLW (OPC, 2018 H++ Scenario). A calculation of the wave height (H) was made from the equation $H = 0.56 \times D_s$ (Thornton and Guza, 1982 and 1983).

- K_D values vary primarily with the shape of the rocks, surface roughness, sharpness of edges, and degree of interlocking. A value of $K_D = 2.1$ was used in the computations.
- A value of 1,026 kg/m³ was used for the specific weight of sea water.
- A value of 20.8 degrees was used for revetment slope angle from horizontal.

The average weight of the existing revetment rocks is computed to be between 600-840 kg. This range is based on the fact that a relatively small difference in the measured average rock width (which was estimated to be between 2.5 and 2.8 ft) results in an estimated average weight of between 600 and 840 kg. Table 3-6 of the report presented below gives the acceptable values of W_{50} at year 2020 and for the MSLR projections (medium-high and H++ in year 2050).

Table 3-6. Rock weights (W_{50}) for 2020 and 2050.

| Year | Water Depth D_s (ft) | H (ft) | H (m) | W_{50} (kg) |
|---------------|------------------------|--------|-------|---------------|
| 2020 | 7.79 | 4.4 | 1.33 | 276 |
| 2050 (P .05%) | 9.79 | 5.5 | 1.67 | 548 |
| 2050 (H++) | 10.59 | 5.9 | 1.8 | 685 |

These results show that even with the maximum projected mean sea level increase of 2.8 ft by 2050 (relative to 2000) from the H++ scenario, the revetment would be expected to protect the beach walkway and seawall, provided that regular monitoring and any necessary maintenance is completed.

In fact, during November 2020, and between late January and late February 2021, the revetment was subject to multiple 100-year wave events, ranging from 6.6 ft to 14 ft. Despite the wave heights and duration, there was no significant damage to the revetment and walkway. These events offered a good opportunity to confirm the stability of the revetment during actual wave storm episodes. No repairs were necessary after these events.

References

- Coastal Environments, 2022. *Coastal Hazard Analysis at San Onofre Nuclear Generating Station, Part 1: Coastal Processes and Structure Stability*, Report prepared for Southern California Edison, San Clemente, CA, CE Reference No. 22-02, 148 pp.
- U.S. Army Corps of Engineers, 1994a. *Hydraulic Design of Flood Control Channels*, Department of the Army, CECW-EH-D, Engineer Manual 1110-2-1601, 184 pp.
- U.S. Army Corps of Engineers, 1994b. *Shore Protection Manual, Volume II*, Department of the Army, Coastal Engineering Research Center, Vicksburg MS.

Ground Shaking Analysis

- 4) As a supplement to Section 2.2.7 (Hypothetical Mw7.6 Earthquake Scenario) of the geological hazards report, please provide a more detailed, step-by-step description of the modeling done to evaluate the potential ground-shaking intensity associated with the nine-segment, M7.6 earthquake on nearby offshore faults; if possible, please also provide the full ground motion response spectra for this analysis. This is needed to assist staff in understanding and evaluating the analysis.

Calculations of the expected Peak Horizontal Ground Acceleration (PGA) for the site were made for the nine-segment earthquake source model used in the Tsunami Hazards Analysis (Section 7.5). We have updated the hazard estimate by calculating the PGA for the ISFSI site using a 2015 set (GK15, Graizner and Kalkan, 2016) of Ground Motion Prediction Equations (GMPE) which were compiled from an expanded database of strong ground-motion records (Chiou and Youlds, 2014). The procedure requires basic earthquake source information, including closest horizontal distance to the fault plane, earthquake magnitude, and site conditions represented by the time-averaged shear-wave velocity in the upper 30 m of the ground (V_{s30}), as well as information regarding the type of faulting. A combination of strike-slip and reverse-slip faults was used for the Mw7.6 Coastal fault system analysis. The GK15 equations include additional terms and coefficients to estimate potential ground shaking more accurately than older versions. For simplicity, these equations do not include details such as rupture propagation direction or hanging wall effects, which are difficult to quantify with the available ground-motion data. Nonetheless, the additional strong ground-motion data from recent earthquakes provides a better set of GMPEs than previously available.

The primary physical parameters used for the GK15 estimation of the PGA are the same as in previous GMPEs. The distance of the site to the trace of the Newport-Inglewood-Rose Canyon fault (Maloney et al, 2016) was measured as 7.0 km using a Geographic Information System (MapInfo) and coordinates from Google Earth for the central casks (33.37019N, 117.44836W). The moment magnitude (M_w) was set at 7.62 based on the tsunami source model SRC-1. The combination of strike-slip and reverse faulting was used for the PGA calculations to account for oblique-reverse slip fault segments. The GK15 parameters and coefficients for the PGA ground motions were applied to compute the expected shaking level. The ground-motion response spectra computed by the GK15 equations represent 5% damped pseudo-accelerations (PSA). The PSAs are plotted as a function of the period in seconds; some Response Spectral plots use frequency in Hertz, which is the inverse of the time value, e.g. 10 sec period = 0.1 Hz. The shape of the PSA response spectrum is tied to the PGA, so we compare the PGA computed with the GK15 equations to actual ground-motion response spectra from recent large earthquakes. The 1999 M7.6, Chi-Chi, Taiwan event represents an earthquake with similar magnitude and reverse-slip character (Figure 3).

The GK15 equations consider anelastic attenuation to account for variations in regional geology of active tectonic regions. A regional quality factor value, $Q_0=150$ applies to active tectonic regions like California. The factor of 1.14 applies for earthquakes with both strike-slip and reverse-slip character, and is relevant for the local tsunamigenic earthquake considered. We computed the expected PGA for two soil cases: NEHRP B/C firm soil/soft rock boundary condition ($V_{s30}=760$ m/s) and for a soft soil site ($V_{s30}=180$ m/s) which is consistent with response spectral modeling done for the design of the new storage facility considering soil-structure interaction (APA Consulting, 2015). Computed GK15 PGA values were **0.46 g** for the stiff rock condition (760m/sec) and **0.67 g** for the soft soil condition (180m/sec). The PGA calculated for the NUHOMS site used the factor of 1.14 for the combination of strike-slip and reverse faulting The

Probabilistic Seismic Hazard Analysis (PSHA) prepared by GeoPentech, (20) used a site condition $V_{SH30}=500$ m/s, and our recalculated GK15 PGA for this site condition is 0.51 g. These PGA 0.51 and 0.76 values correspond to ground-motion period of about 0.03 sec (33 Hz) and are shown as red and blue boxes on the plot of Response Spectra for the GK15 analysis of the 1999 M7.6 Chi-Chi, Taiwan earthquake.

Actual ground-motion PSA values obtained from two large earthquakes, the 1979 M6.5 Imperial Valley, California, and the 1999 M7.6 Chi-Chi, Taiwan events, show a wide variation in amplitudes (gray lines in Figure 3). The bold red curve represents the expected response spectra based on the GK15 calculations for the ground-motion recordings of the earthquake. Dashed red curves represent the ± 1 sigma uncertainty bounds. The GMPEs compute the median value of the expected ground-motions, and the black curve provides the mean (average) of the actual ground-motion data from each earthquake. Pure strike-slip is the reference factor at 1.0 and reverse faulting has a factor of 1.28. Consequently, the Chi-Chi M7.6 earthquake response spectra are conservative with respect to the San Onofre site conditions. The median curve of Chi-Chi M7.6 provides a consistent estimation of the curves for the 0.51 g PGA expected at a stiff soil/soft rock site at San Onofre. In all cases, the GK15 ground-motion estimates are significantly below the 1.5 g horizontal PGAs used for the design of the storage facilities.

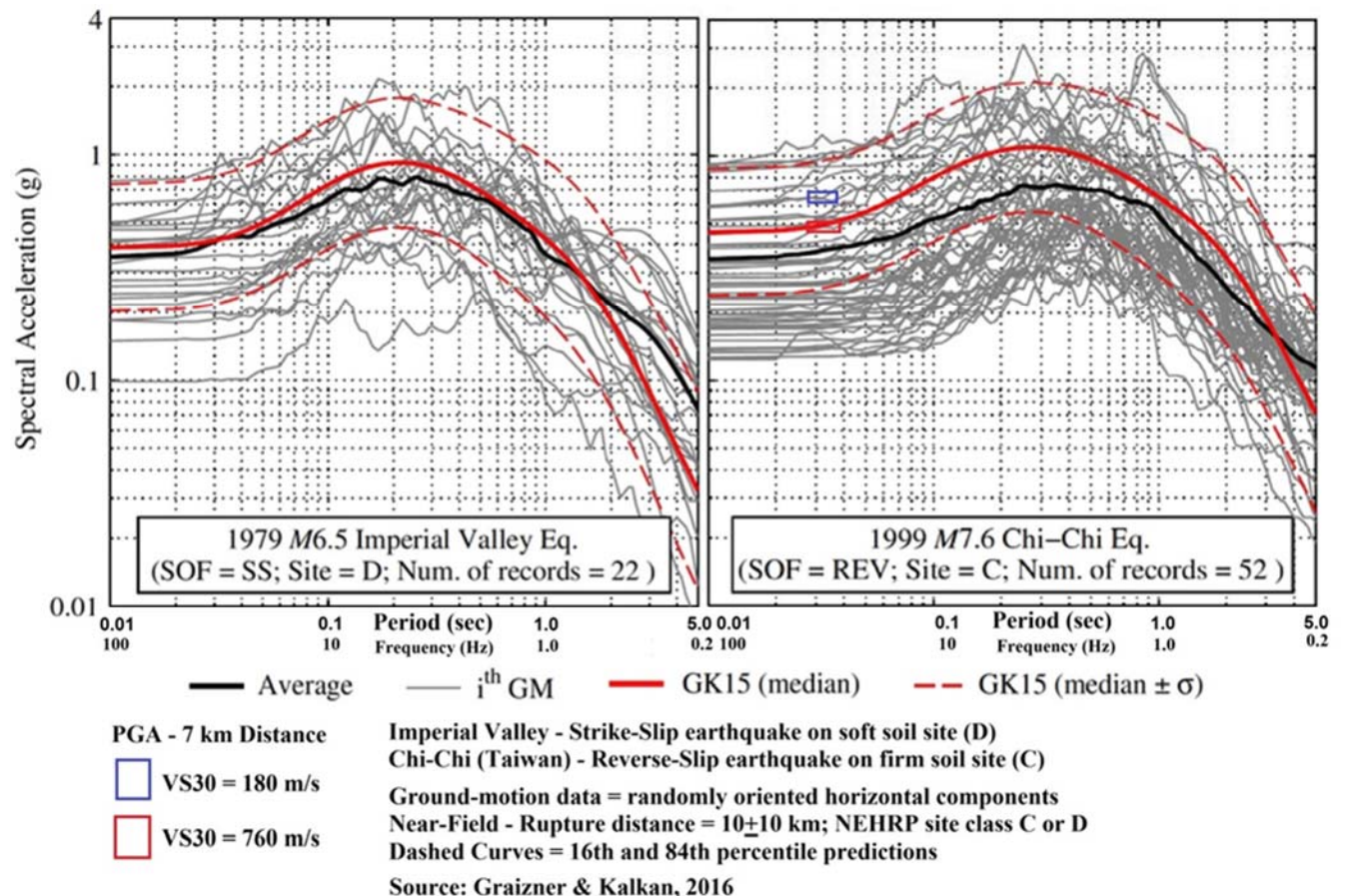


Figure 3. Comparison of GK15 predictions for 5% damped pseudo-spectral accelerations (PSA) for two earthquakes. The M6.5 Imperial Valley earthquake was a moderate strike-slip earthquake in southern California. The M7.6 Chi-Chi earthquake was a large reverse-slip earthquake in Taiwan.

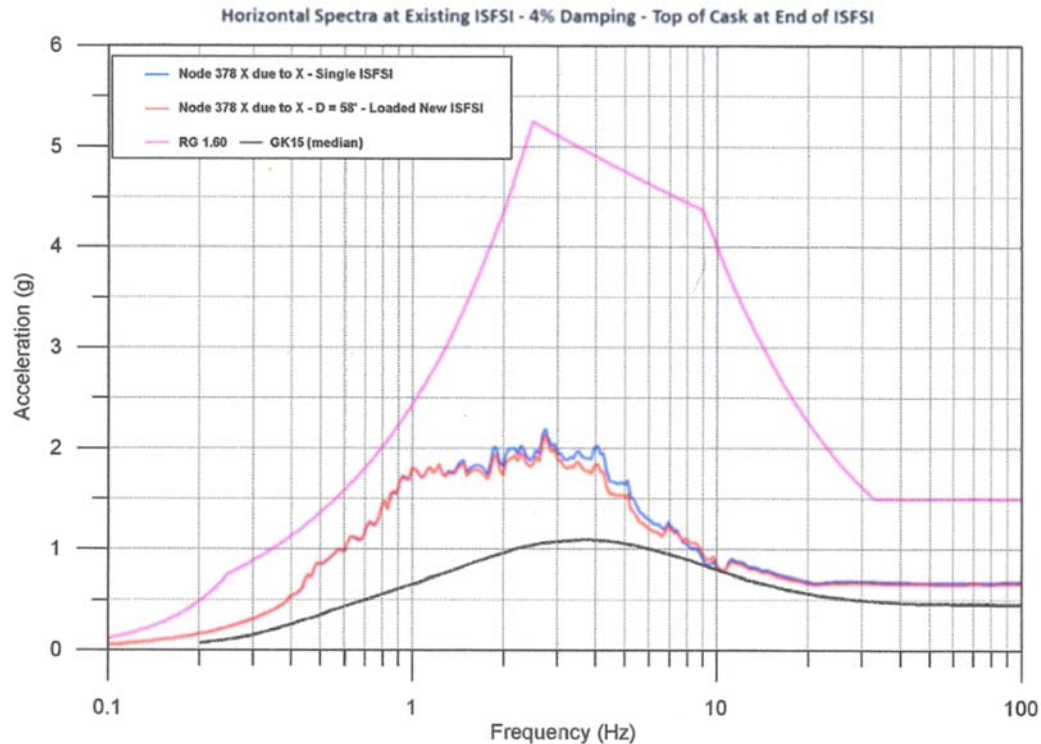


Figure 4. Near-field acceleration response spectra (GK15) computed from the Mw7.6 Chi-Chi Taiwan reverse-slip earthquake are compared to design response spectra for the ISFSI including soil-structure interaction. The median values from the updated ground motion prediction equations (Graizner and Kalkan, 2016) are below the response spectra computed for soil-structure interaction at the ISFSI (APA Consulting, 2015), and well below the allowable acceleration response spectra (RG 1.60). The scenario Mw7.62 oblique reverse-slip earthquake offshore San Onofre at 7-km distance from the ISFSI would produce similar or lower acceleration response spectra compared to the reverse-slip Chi-Chi event near-field sites (10 ±10 km fault distance).

References

- APA Consulting, 2015, Effect of a new ISFSI on the seismic response to the existing ISFSI at SONGS, Technical Report, APA Consulting, Washington, D.C., prepared for the San Onofre Nuclear Generating Station, Southern California Edison, 72 p.
- Chiou, B., and Youngs, R.R. (2014). Update of the Chiou and Youngs NGA model for the average horizontal component of peak ground motion and response spectra. *Earthquake Spectra*, v. 30, no. 3 p. 117-1153.
- Graizer, V. & Kalkan, E., (2016), Summary of the GK15 Ground-Motion Prediction Equation for horizontal PGA and 5% damped PSA from shallow crustal continental earthquakes: Bulletin Seismological Society of America, v. 106, p. 687-707. Doi: 10.1785/0120150194
- Maloney, J.M., Driscoll, N.W., Kent, G.M., Bormann, J., Duke, S. and Freeman, T. (2016), Segmentation and stepovers along strike-slip fault systems in the Inner California Borderlands: Implications for fault

architecture and basin formation, in *Applied Geology in California: Association of Environmental and Engineering Geologists, Special Publication Number 26, Chapter 36*, Anderson, R. and Ferriz, H, eds., p. 655-677, Star Publishing Company, Redwood, California.

Fault Rupture

- 5) Please provide additional explanation for the conclusion of Section 2.3.1 of the geological hazards report: “secondary fractures that could result from [blind faulting in Capo Embayment] would not adversely affect the SONGS ISFSI, given its reinforced concrete slab support foundation and rigid construction.” What are the specific reasons for thinking that the foundation design is adequate to resist the displacement that might be associated with this secondary fracturing?

Although scientific understanding regarding the possible generating mechanism for secondary fractures at the SONGS site has changed, the main conclusions reached at the time the geologic features were first identified in the mid-1970s remain valid. The secondary fractures at the SONGS site were first identified during excavation in the San Mateo sandstone formation for construction of SONGS Units 2&3 in the mid-1970s and were extensively investigated at that time, both by SCE and independently by the NRC. The reports generated at the time did not indicate any mapped geologic features extending onto the former Unit 1 site, which is the current location for the NUHOMS ISFSI. Both the geologic consultant for SCE (FUGRO) and the independent review by the NRC (performed by the USGS) concluded that no movement on the secondary fracture geologic features had occurred within the last 125,000 years and were, therefore, not classified as “capable faults” in accordance with the Atomic Energy Commission criteria at the time.

Based on field measurements by the SCE geologic consultant in the mid-1970s, displacements along the secondary fracture geologic features at SONGS were not greater than 4 inches. The function of the ISFSI foundation pad is to provide a rigid surface to support the spent fuel storage modules. In fact, the modules are designed for movement and are permitted to displace laterally on the foundation pad surface up to 10 feet during a seismic event. The foundation pad is constructed of heavily reinforced concrete with a thickness of 3-feet, with a minimum concrete compressive strength of 4,000 psi. The supporting soil subgrade is much less rigid than the reinforced concrete support pad, having an allowable bearing capacity of approximately 23,500 psf (or 163 psi).

A secondary fracture at the NUHOMS ISFSI would be extremely unlikely to occur. Even if it were to occur, the surrounding soil would almost certainly deform before there was any effect on the more rigid ISFSI foundation pad, and the effects would be well within the design capability for the spent fuel storage system.

Tsunamis

- 6) Probabilistic Tsunami Hazard Analysis (PTHA) is currently a broadly accepted approach for evaluating tsunami risk, which appears different than the approach used in the analysis provided. Please provide a discussion of why you used a deterministic approach for the analysis as opposed to a probabilistic approach.

SCE's analysis used the deterministic approach because, based on current science, the deterministic approach is better suited to the problem of estimating maximum tsunami heights and related flooding at SONGS. From geological and engineering evidence (e.g., Synolakis and Kanoglu 2015, Behrens et al, 2021), the current state of science suggests that it is more prudent to rely on worst-case scenarios instead of probabilistic tsunami hazard analysis (PTHA) estimates.

SCE's response to the next question (regarding ASCE 7 standards) contains a comparison of the results from the deterministic model to the PTHA results published at asce7tsunami.online.

References

Synolakis, C.E. and Kanoglu E., 2015, The Fukushima accident was preventable, Philosophical Transactions of The Royal Society A Mathematical Physical and Engineering Sciences 373(2053) DOI:10.1098/rsta.2014.0379.

Behrens et al, 2021. Probabilistic Tsunami Hazard and Risk Analysis: A review of Research Gaps. Frontiers in Earth Science, Article 628772, www.frontiersin.org/articles. 28 pp.

- 7) Please provide an evaluation and discussion of how the ISFSI fits within the ASCE 7 standards for tsunami loads and effects, including evaluation of ASCE 7-16 and ASCE 7-22 tsunami model results for the area (<https://asce7tsunami.online>).

In SCE's deterministic analysis, the SONGS seawall is not credited as being present. Similarly, for the PTHA analysis of tsunami run-up at SONGS and adjacent beaches, shown in Figure 5 below, the seawall is also not present. Figure 6 below shows run-up elevation data from the PTHA analysis. Figure 7 shows the results of the tsunami amplitudes at 100 m for PTHA data.

Table 1 below presents the comparison between the results of SCE's deterministic analysis (CE, 2022 Table 9-1) and the PTHA analysis from <https://asce7tsunami.online>. There is a good agreement between the Coastal Environments deterministic model results and PTHA data from <https://asce7tsunami.online>.

Table 2 gives the range and the mean of the two results. The difference of the mean comparison is about 1 ft, showing that the deterministic model results bound the PTHA model results.

References

Synolakis, C.E. and Kanoglu E., 2015, The Fukushima accident was preventable, Philosophical Transactions of The Royal Society A Mathematical Physical and Engineering Sciences 373(2053) DOI:10.1098/rsta.2014.0379.

Behrens et al, 2021. Probabilistic Tsunami Hazard and Risk Analysis: A review of Research Gaps. Frontiers in Earth Science, Article 628772, www.frontiersin.org/articles. 28 pp.

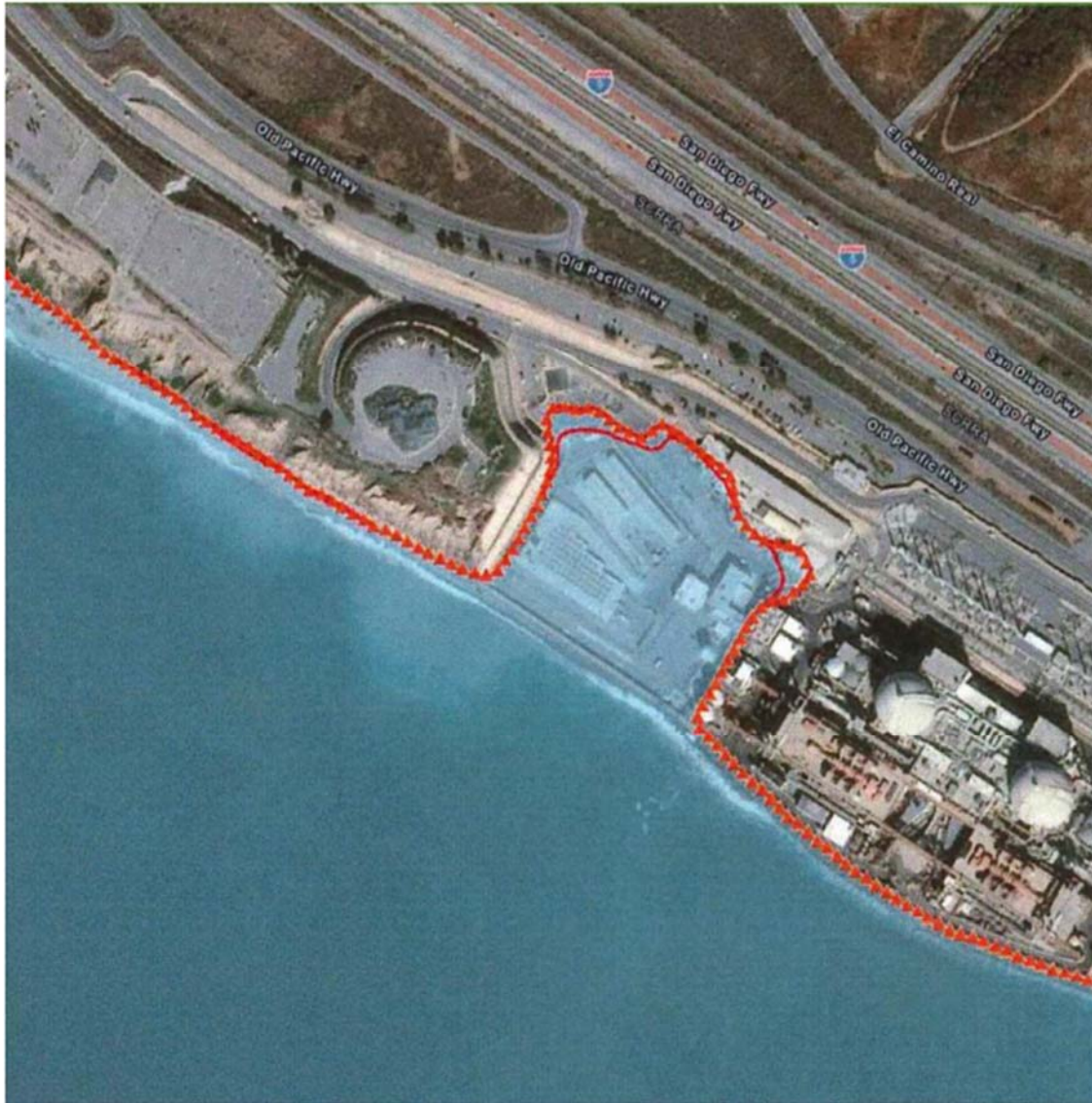


Figure 5. Inundation map taken from <https://ASCE7tsunami.online>.



Figure 6. SONGS aerial view showing tsunami run-up data, taken from <https://ASCE7tsunami.online>.



Figure 7. Tsunami wave amplitudes at 100 m water depth, taken from <https://ASCE7tsunami.online>.

Table 1. Comparison between run-up elevations (MLLW, Epoc 1941-1959)) between CE (2022, worse case at Table 9-1) and PTHA data at 2050 for Sea level rise Scenario H++ (2.8 ft).

| Site | CE (2022) | | PTHA | |
|------------------------------------|-----------------------|--|-----------------------|--|
| | Elevation ft, MLLW | Depth of run-up above grade (ft) | Elevation Ft, MLLW | Depth of run-up above grade (ft) |
| Unit 1 Grade 20 ft, MLLW | 29.8 | 9.8 | 29.7 ^a | 9.7 |
| Units 2 &3 Grade 30 ft, MLLW | 28.4 | 0 | 28.7 ^a | 0 |

^a Values from Figure 2 corrected from NAVD88 to MLLW (Epoch 1941-1959) by adding 0.62 ft plus 2.8 ft.

^b For Unit 1 we used average value Of 26.52, 25.79, 26.54 ft, NAVD and for Unit 2 & 3 we used 25.3 ft, NAVD. Data From Figure 2

Table 2. Tsunami Wave amplitude at 100 m water depth

| Parameter | CE (2022) | | PTHA | |
|----------------------------------|-------------|------------|------------------|------------------|
| | Range ft | Mean ft | Range ft | Mean ft |
| Tsunami Amplitude at 100 m | 7- 8.5 | 7.75 | 6-7 ^a | 6.5 ^a |

^a Values from Figure 3.

- 8) The tsunami hazard analysis looked only at inundation depths of the ISFSI, it didn't include the impacts of flow velocity. Please provide information on why flow velocity wasn't included in the analysis.

The NUHOMS spent fuel storage system is a hardened structure designed against extreme environmental hazards including tornado generated missiles, wind loads, and flooding that might result in complete submergence of the structure and water velocity up to 4.6 m/s (15 fps). In addition, although the protection by the seawall in the tsunami hazard analysis is not credited so that the site inundation can be determined, the seawall is in fact present and would provide some level of protection; so flow velocity during a tsunami event is not likely to be a significant consideration.

The flow velocity data was retrieved from the tsunami hazard analysis and is shown in figure 8 below. The flow velocity in the vicinity of the NUHOMS ISFSI is generally less than 3 m/s (10 fps) and does not exceed 4 m/s (13 fps). This is bounded by the NUHOMS ISFSI design value of 4.6 m/s (15 fps).

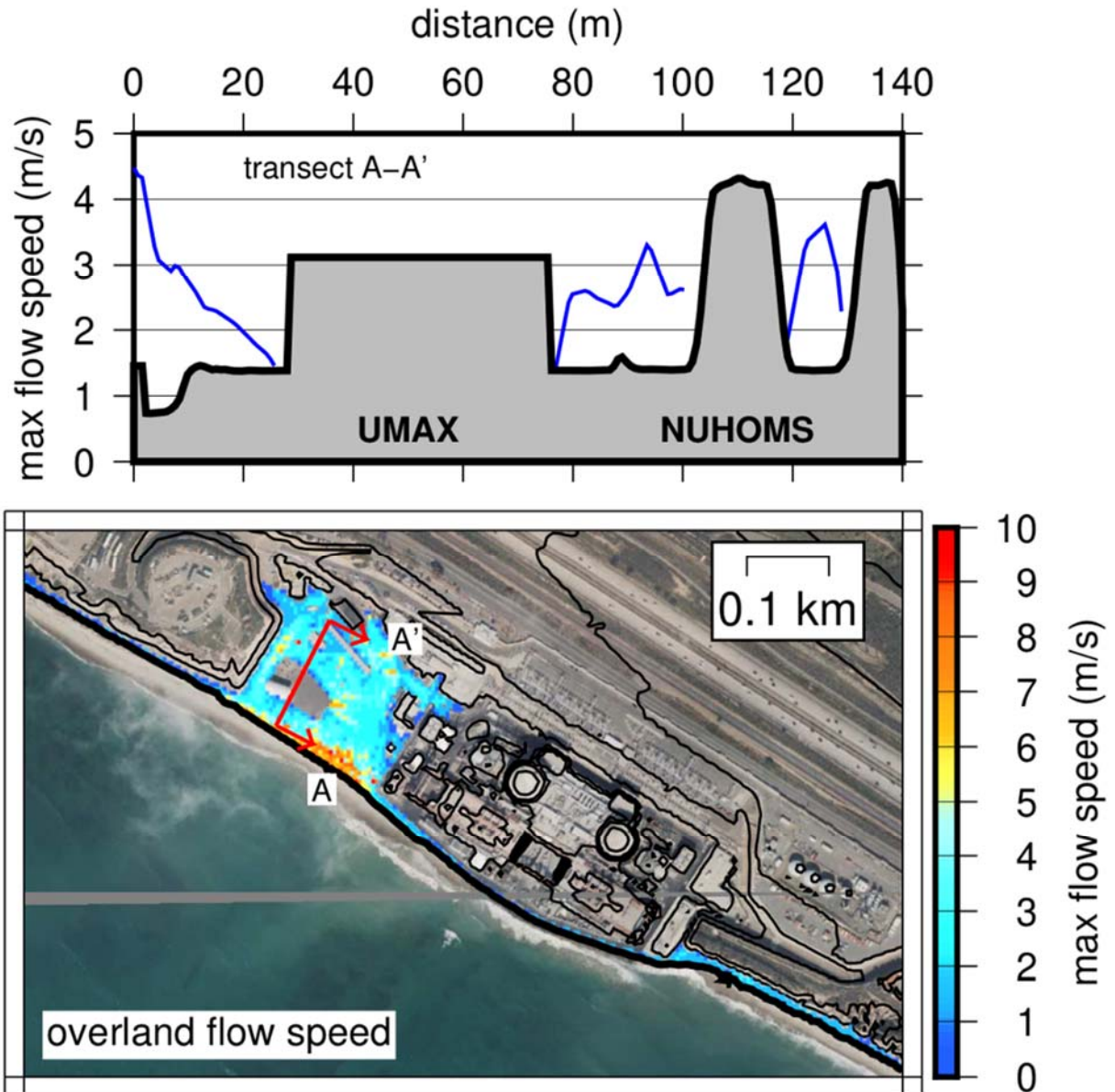
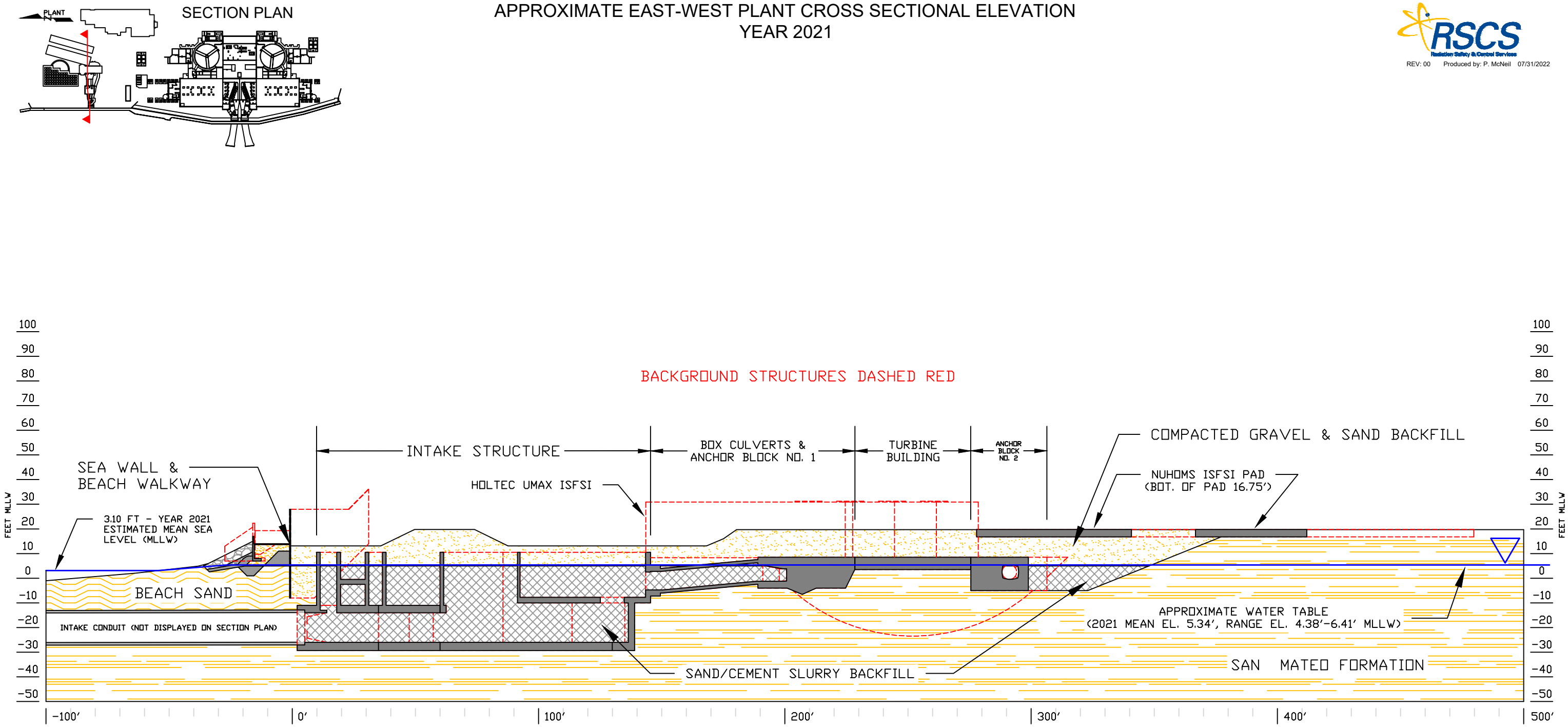


Figure 8. Flow velocity data from the tsunami hazard analysis.

Attachment A

APPROXIMATE EAST-WEST PLANT CROSS SECTIONAL ELEVATION
YEAR 2021



- NOTES
- Sections are combined interpretations of the following data sources:
 - Plant Drawings #: U1-C-0014 (2003), U1-C-0014 (2010)
 - Technical Design Guide for Unit 1 Foundations to Remain at the SONGS Unit 1 Site, Rev 00
 - San Onofre Generating Station Unit 1, Updated Final Safety Analysis Report figures 2.12, 3.1, 3.2, 3.3, 3.4, 3.5
 - Bathymetry data provided by Coastal Environments, Sept. 2016
 - Department of Commerce (DOC), National Oceanic and Atmospheric Administration (NOAA), National Ocean Service (NOS), Office for Coastal Management (OCM), 2009 - 2011 CA Coastal Conservancy Coastal Lidar Project: Hydro-flattened Bare Earth DEM
 - San Mateo Formation: Historical boring log data provided by Ransom Consulting
 - Groundwater elevation provided by site staff; based on 2021 level measurements
 - SONGS site elevations are referenced to the Mean Lower Low Water (MLLW) tidal datum (EPOCH 1941-1959). The MLLW is lower than the NAVD88 by 0.62 feet. To convert an elevation MLLW to NAVD88, Subtract 0.62 feet.
 - Horizontal origin (0') = Sta. W 7+27